BrJAC

Brazilian Journal of Analytical Chemistry

an International Scientific Journal

Women in (Bio)Analytical Chemistry:

Moving Towards Equily and Inclusion

Special Edition of BrJAC on Women in (Bio)Analytical Chemistry

July – September 2023 Volume 10 Number 40

XV Latin American Symposium on Environmental Analytical Chemistry (LASEAC) and X National Meeting on Environmental Chemistry (ENQAmb)

From September 18 to 21, 2023

The XV LASEAC and X ENQAmb will be held simultaneously at the the Center for Arts and Conventions of the Federal University of Ouro Preto, at the Augusto Barbosa Metalworking Park, Ouro Preto, MG, Brazil, from September 18 to 21, 2023.

The organization is in charge of the UFOP and the Federal University of Minas Gerais (UFMG), MG, Brazil, with the support of the “Red para el Análisis de la Calidad Ambiental en América Latina” (RACAL) and the Brazilian Chemical Society / Division of Environmental Chemistry (SBQ/DAMB).

Thematic Areas

Inorganic species and speciation analysis; New trends in sample preparation; Green analytical chemistry methods; Instrumental and environmental analysis; Biosensors and electroanalysis; Ecotoxicology; Quimometry; Environmental biotechnology and remediation; Regulations on environmental pollution control; Climate change; Emerging contaminants and Pesticides; Atmospheric chemistry and air pollution.

SUBSCRIBE

Brazilian Journal of Analytical Chemistry

VISÃO FOKKA - COMMUNICATION AGENCY

Aims & Scope

BrJAC is a double-blind peer-reviewed research journal, dedicated to the diffusion of significant and original knowledge in all branches of Analytical Chemistry and Bioanalytical Chemistry. It is addressed to professionals involved in science, technology, and innovation projects at universities, research centers and in industry. The **BrJAC welcomes** the submission of research papers reporting studies devoted to new and significant analytical methodologies, putting in evidence the scientific novelty, impact of the research, and demonstrated analytical or bioanalytical applicability. BrJAC **strongly discourages** those simple applications of routine analytical methodologies, or the extension of these methods to new sample matrices, unless the proposal contains substantial novelty and unpublished data, clearly demonstrating advantages over existing ones.

BrJAC is a quarterly journal that publishes original, unpublished scientific articles, reviews and technical notes. In addition, it publishes interviews, points of view, letters, sponsor reports, and features related to analytical chemistry.

For complete information on ethics and policies on conflicts of interest, copyright, reproduction of already published material and preprints, in addition to the manuscript submission and peer review system, please visit 'About us' and 'Author Guidelines' at www.brjac.com.br

ISSN 2179-3425 printed

ISSN 2179-3433 eletronic

Indexing Sources

Scopus

CiteScore 2022: 1.0; SJR: 0.165; SNIP: 0.242; CiteScore Tracker 2023: 1.5 **Access source details**

CiteScore trend

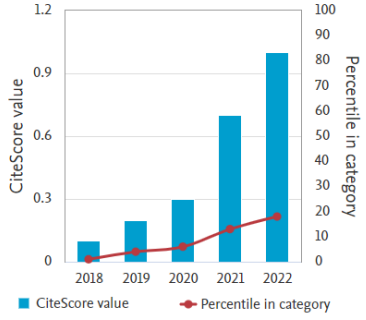

CLARIVATE ANALYTICS
EMERGING SOURCES CITATION INDEX
INDEXED

CAPES
QUALIS

BrJAC is in the Qualis B3 stratum according to preliminary list published on 2022/12/29

Google scholar

Cited by

	All	Since 2018
Citations	491	401
h-index	9	9
i10-index	9	7

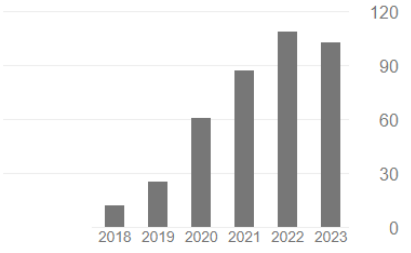

Production Editor
Silvana Odete Pisani, PhD

Publisher
Lilian Freitas
MTB: 0076693/ SP
lilian.freitas@visaofokka.com.br

Advertisement
Luciene Campos
luciene.campos@visaofokka.com.br

Art Director: Adriana Garcia

WebMaster: Daniel Letieri

BrJAC's website: www.brjac.com.br / Contact: brjac@brjac.com.br
Like BrJAC on Facebook: https://www.facebook.com/brjachem

ABEC BRASIL
BrJAC is associated to the Brazilian Association of Scientific Editors

VISÃO FOKKA
BrJAC is published quarterly by:
Visão Fokka Communication Agency
Av. Washington Luiz, 4300 - Bloco G - 43
13042-105 – Campinas, SP, Brazil
contato@visaofokka.com.br
www.visaofokka.com.br

EDITORIAL BOARD

EDITORIAL ADVISORY BOARD

EDITORIAL ADVISORY BOARD (Continuation)

CONTENTS

CONTENTS (Continuation)

Articles

Technical Notes

Feature

Sponsor Reports

Sponsor Releases

CONTENTS (Continuation)

Sponsor Releases

Releases

Brazilian Journal of Analytical Chemistry
2023, Volume 10, Issue 40, pp 1-2
doi: 10.30744/brjac.2179-3425.editorial.women.chem.N40

BrJAC

EDITORIAL

Women in (Bio)Analytical Chemistry: *Moving Towards Equity and Inclusion*

Márcia Andreia Mesquita Silva da Veiga

Guest Editor of this BrJAC special edition on Women in (Bio)Analytical Chemistry
Associate Professor in the Department of Chemistry at the Faculty of Philosophy, Sciences, and Letters of Ribeirão Preto, University of São Paulo, SP, Brazil

Maria das Graças Andrade Korn

Guest Editor of this BrJAC special edition on Women in (Bio)Analytical Chemistry
Full Professor at the Institute of Chemistry, Federal University of Bahia, BA, Brazil

Women's participation in science has been an increasingly relevant and discussed topic in recent decades. Throughout history, women have faced numerous barriers and challenges to enter and stand out in this field of knowledge. However, despite the difficulties, women have contributed significantly to scientific advancement in all areas. In Brazil, the discussion about the participation of women in science has been highlighted in national events around analytical chemistry and academia. Thus, some changes have been implemented to minimize the differences discussed herein.

Today we see more and more women engaged in science, holding prominent positions as researchers, professors, and leaders in their fields. They exist in many scientific disciplines, including physics, chemistry, biology, mathematics, engineering, and technology. In addition, women have also been involved in emerging and interdisciplinary areas such as computer science, artificial intelligence, and biotechnology.

It is crucial to promote gender equality in chemistry by providing an inclusive environment and encouraging the active participation of women. This can be achieved by implementing policies that promote equal opportunities, encouraging female role models and mentors, supporting women chemists' training and professional development, and valuing and recognizing their contributions.

Women's participation in chemistry is essential to scientific advancement in this field. We bring unique perspectives, creativity, and skills to address chemical challenges and contribute to a more comprehensive understanding of chemical processes and their practical applications. Gender diversity in chemistry drives innovation and promotes a more prosperous and inclusive scientific environment. It is essential to provide equal opportunities, support, and encouragement for women to enter and thrive in academic careers in the exact sciences, thus strengthening female representation in this field and boosting scientific excellence.

In this context, the BrJAC journal worked on organizing an issue dedicated to women researchers in the field of (bio)analytical chemistry. The central idea is to celebrate those female researchers who have worked hard and dedicatedly in analytical chemistry. The interview was with Dr. Joanna Szpunar from the National Research Council of France (CNRS). She talked about her career and experience as a prominent researcher in the spectroanalytical chemistry field. The point of view was with Dr. Maria Valnice Boldrin Zanoni from UNESP, who excels in electroanalytical chemistry and shares a new perspective on artificial photosynthesis technology. The Letter written by Dr. Quezia Cass from UFSCar presented us with text on separation techniques highlighting affinity selection mass spectrometry.

Cite: da Veiga, M. A. M. S.; Korn, M. G. A. Women in (Bio)Analytical Chemistry: *Moving Towards Equity and Inclusion*. *Braz. J. Anal. Chem.* 2023, *10* (40), pp 1-2. http://dx.doi.org/10.30744/brjac.2179-3425.editorial.women.chem.N40

The issue will also feature three reviews, eight articles, and three technical notes, all led by women in (bio)analytical chemistry. It is imperative to thank all the reviewers who participated in this process by giving their time and expertise in evaluating the manuscripts. Many thanks!

We hope you enjoy the reading and learn some of the work these researchers have been developing in (bio)analytical chemistry.

Márcia Andreia Mesquita Silva da Veiga is an Associate Professor in the Department of Chemistry at the Faculty of Philosophy, Sciences, and Letters of Ribeirão Preto, University of São Paulo, Brazil. She has a degree in chemistry (Federal University of Amazonas, 1991), a master's degree in physical chemistry, and a doctorate in analytical chemistry (Federal University of Santa Catarina, 1996 and 2000), with postdoctoral work in analytical chemistry at the Institute of Chemistry, University of São Paulo (2005). She currently leads the research group L.Q.A.I.A. (Laboratory of Applied Instrumentation and Analytical Chemistry) and is Vice President of the Brazilian Society of Forensic Sciences. She works mainly with optical techniques for trace and isotopic analysis. Her current research focus is on sample preparation procedures, the detection and quantification of nanomaterials and their application, bioaccessibility assays in foods and soils, the potential of high-resolution graphite furnace molecular absorption spectrometry for elemental and isotopic analysis, micro trace (evidence) analysis and detection for forensic purposes, and new technological approaches to chemistry teaching. CV

Maria das Graças Andrade Korn is a Full Professor at the Institute of Chemistry of the University of Bahia (UFBA), with a master's degree in chemistry (Inorganic Analytical Chemistry, 1987) from the Pontifical Catholic University of Rio de Janeiro and a doctorate in chemical sciences from the University of São Paulo (USP) (1997). She was Director of the Analytical Chemistry Division of the Brazilian Chemical Society (2014-2016) and is currently a full member of the Bahia Academy of Sciences. She is the author of more than 144 articles and has supervised 75 undergraduate students, 29 doctoral theses, 41 master's dissertations and 6 postdoctoral fellows. She has always worked in the area of analytical chemistry, developing studies related to the use of molecular and atomic spectroscopic techniques and sample preparation procedures, applied to different types of samples of food, environment, fuels, and medicines, among others. The main focus of her research has been to obtain reliable chemical information through the development of fast methods, with greater detectability, are ecologically friendly, and especially target more complex systems, in order to meet society's demand. CV

Brazilian Journal of Analytical Chemistry
2023, Volume 10, Issue 40, pp 3-9
doi: 10.30744/brjac.2179-3425.interview.jszpunar

BrJAC

INTERVIEW

Joanna Szpunar, an outstanding chemical researcher in the chemistry of metal-biomolecule interactions, shares her experience as a woman scientist with BrJAC

Joanna Szpunar graduated from the Warsaw University of Technology in 1986 and obtained her Ph.D. (1992) and D.Sc. (Habilitation) (2000) from the University of Warsaw. Since 1997, she works at the National Research Council of France (CNRS). In 2007, she obtained in Poland the title of professor of chemistry. She has broad experience in the field of mass spectrometry-based bio-inorganic speciation analysis and metallomics with a focus on the identification and quantification of trace element species in biological systems and in the chemistry of metal-biomolecule interactions. She is the co-author of a book and approximately 250 scientific publications in peer-reviewed international journals.

Joanna Szpunar is a fellow of the Royal Society of Chemistry (UK) and has been, for many years, a member of the boards of *Journal of Analytical Atomic Spectrometry* and *Metallomics*. She regularly gives invited lectures at international analytical chemistry meetings and was the chairperson of the European Winter Conference on Plasma Spectrochemistry (Kraków, Poland) in 2013.

The investigations carried out under her supervision and/or with her active participation resulted in the identification of a number of molecular targets of metals in biological systems, as well as contribute to selenometabolomics and selenoproteomics studies in bacteria and plants. In recent years, her interests were broadened to the environmental fate of metal-containing nanoparticles and nanoplastics. She has supervised 12 Ph.D. theses and several post-doctoral fellows.

Joanna Szpunar is the laureate of the 2013 Jerzy Fijalkowski Award of the Committee of Analytical Chemistry of the Polish Academy of Sciences and the 2017 European Award for Plasma Spectrochemistry.

In recent years, Joanna Szpunar has been involved in collaboration with analytical chemists in Brazil, hosting graduate students from the University of Campinas and the Federal University of Pelotas in the laboratory at the Institute of Analytical Sciences (IPREM) in Pau afiliated with the CNRS, lecturing at the Federal University of Santa Maria and co-supervising a Ph.D. student with work carried out at the University of Pau and the Federal University of Pelotas.

Cite: Joanna Szpunar, an outstanding chemical researcher in the chemistry of metal-biomolecule interactions, shares her experience as a woman scientist with BrJAC. *Braz. J. Anal. Chem.* 2023, *10* (40), pp 3-9. http://dx.doi.org/10.30744/brjac.2179-3425.interview.jszpunar

BrJAC: Which factors influenced your education? When did you decide to study chemistry? What motivated you? How was the beginning of your career?

Dr. Szpunar: Chemistry has been present in my life since the very beginning. My mother was a high school chemistry teacher and my father a researcher and university professor in materials science, so I was exposed to different notions of chemistry very early. So, in my case, there was no sudden light bulb revelation but rather a gradual process of subconscious learning. Quite naturally, maybe because I was an only child, I was intrigued by what my parents were doing and step by step it led me to getting closer to this field and finally choosing it for my personal career.

At the same time, I must confess that for quite a period I was inclined to go towards literary studies (I have always been an avid reader) but finally opted for a technical university. My *Alma Mater* is Politechnika Warszawska (the Warsaw University of Technology) which is considered the leading technical university in Poland. My first choice was materials science and my M.Sc. work was focused on the synthesis of a particular group of spinels. Nevertheless, already at that time, I was also carrying out my first analytical activities necessary to characterize the products of my experiments.

My real adventure with analytical chemistry started at the University of Warsaw with a Ph.D. project focused on flow-injection analysis (FIA) which was, at that time, a new technique introduced in Poland by Prof. Marek Trojanowicz. My Ph.D. project dealt with the development of a flow injection system with a multi-LED detector for photometric measurements. I was quickly enchanted by the elegance of this concept that, in a way, even now still stays with me - peaks, not FIA but chromatographic ones, have been accompanying me for the rest of my career. After my Ph.D., I have had an extraordinary opportunity to be a part of the beginnings of an emerging field of analytical chemistry - speciation analysis. I started at the University of Antwerp, in the group of Prof. Freddy Adams, where I participated in method development for environmental projects dealing with the long-distance transport of organolead compounds from leaded gasoline (which was still in use at that time) and with organotin cycling in the marine environment. I continued and expanded the latter in the frame of my post-doctoral fellowship with the European Environmental Research Organization at the University of Bordeaux. At that time, in that part of France, there were still fresh memories of the problems in oyster farming in the Bay of Arcachon related to the use of antifouling paints containing tributyltin. Therefore, there was a need for analytical methodologies able to follow the release of butyltin compounds into seawater, their uptake by marine biota and incorporation into sediments. Looking back at these two post-doctoral stays I realize that they shaped my final research interests and my whole career up to now.

During PhD at the Laboratory of Flow Analysis and Chromatography at the Faculty of Chemistry, University of Warsaw, Poland (1990).

BrJAC: What has changed in the student profile, ambitions, and performance since the beginning of your career?

Dr. Szpunar: It is certain that many changes have occurred since I was a university student. The most striking one, and here I am speaking from the European perspective, is the increase in the number of students and the trivialization of certain university studies. It seems now to be a natural continuation of high school and, in some places, there is even no selection for enrollment. As a consequence, some choices are not well thought through, and many students resign during the first or second year. It is a terrible waste of resources and a source of disappointment and stress for both students and university teachers. At the same time, there is less personal contact between students and professors who have no chance to get to know each other and to interact. This situation was further aggravated by the COVID-19 crisis and on-line teaching. Another issue is a change in the very concept of higher education with universities sometimes considered as providers of services and diplomas. I see more and more business-like relationships with students paying a certain price and expecting a service in exchange. I also have an impression that today's students are much more focused on their career paths and have no time (or desire) for exploration of the broader context of their work. This situation makes me uneasy. A recent *Nature* paper (https://doi.org/10.1038/s41586-022-05543-x) claims that scientific papers and patents are becoming less disruptive over time which might result from "a tunnel perspective" without a general overview. And if that is lost, we will be heading towards smaller and smaller research compartments, or bubbles, isolated and not communicating with each other and thus blocking progress in each of them.

BrJAC: What are your lines of research? What work are you currently developing?

Dr. Szpunar: As I have already mentioned, during the last 30 years I have been developing an analytical methodology for species-selective studies. The concept of chemical speciation emerged gradually from the work of biologists, medical doctors and nutritionists dating back many years, certainly to the middle of the previous century. The realization that the information on total element content was insufficient resulted from the observations that the essentiality of a trace element in biology depends on the species, for example, for hemoglobin or cobalamin. In addition, the toxicity of a trace element in the environment is species-dependent, therefore there is no point in determining total tin if the toxic compound is tributyltin. Then come the metabolic pathways of metals and metalloids that can only be understood if we determine species and not the total element content as it is the case for arsenic, whose poisonous notoriety results from essentially one chemical form (arsenic(III)). During these early days, the analytical procedures were tedious, focused on single species and originally did not refer to speciation at all! In fact, the term "speciation" was mainly used in biology and not in chemistry.

A breakthrough came with the concept of coupling chromatographic separation techniques with element-selective detectors allowing clear visualization of the trace element distribution among different species in the form of multiple peaks in the chromatograms. To cut a long story short, the improvements in analytical methodologies, especially related to the introduction of highly sensitive inductively coupled plasma mass spectrometric detection, resulted in discovery of more and more element species in the studied samples. It led to the possibility of studies of previously unknown endogenous species. However, analytical chemists are faced with the problem of the identification and quantification of tens and hundreds of species for which no analytical standards exist. Indeed, with time and increase in sensitivity, the chromatograms started to show dense forests of peaks to the point that we had to employ multidimensional chromatographic schemes to improve species separation. Despite that, the chromatographic peak capacity still proved insufficient, and the paradigm had to be changed to the peak capacity in high resolution mass spectra.

My work, carried out in close collaboration with Prof. Ryszard Lobinski, addresses these challenges by taking advantage of high-resolution high accuracy molecular mass spectroscopy, mainly electrospray ionization mass spectrometry. At the Institute of Analytical and Physical Chemistry for the Environment and Materials (IPREM), which is affiliated with the National Research Center of France (CNRS) in Pau, France, our group has pioneered and developed a concept of the parallel element- and molecule-specific detection

At the 2019 Rio Symposium on Atomic Spectrometry in Mendoza, Argentina with Prof. Érico Flores (left) and Prof. Ryszard Lobinski (right).

in liquid chromatography for speciation analysis. This approach allowed us to characterize seleno-, arseno- and metal-metabollomes of many complex biological systems. Our findings allow better understanding of the uptake and metabolization of metals and metalloids by microorganisms and plants in the environment and biotechnological processes aimed at the development of food and feed supplements. The recent projects concerned characterization of selenometabolites in selenium-enriched probiotic *Bifidobacterium longum* and different yeast stains, species involved in translocation of Zn and Cu in indigenous plants from post-mining areas in Peru, and iron complexes with metallophores excreted by bacteria present in peat from the neighboring Pyrenees area. Our research resulted in the identification of molecular targets of metals in biological systems including, among others, Bi-binding proteins in *Helicobacter pylori*, tumor-related polypeptide in human epidermal keratinocytes upon exposure to Ni nanoparticles, Cd-metallothionein complexes in kidney cell lines upon exposure to CdS nanoparticles, I-containing proteins in algae, as well as selenoproteins in bacteria and plants.

We have been making constant progress towards the detection, identification and characterization of metal species in biological systems. The currently available techniques allow us to identify many metal compounds and rapidly get multispecies distribution patterns in complex matrices. But we aspire to go a step further beyond pure observation and to understand why and how metal species are synthesized. What are the mechanisms making an organism facing an excess or a deficit of metal to synthetize a particular species? Metal ions are part of a global biochemical network including genes, proteins and metabolites and their complexes appear because there is a ligand produced by an enzyme and there is gene expression of the enzyme triggered by the presence or absence of a metal. This brings us to metallomics, a field of research largely influenced, if not created, by the progress of trace metal speciation analysis. The term was originally proposed by Prof. Haraguchi from the University of Nagoya who defined “metallomics” as metal-assisted functional biochemistry and postulated it to be considered at the same level of scientific significance as genomics or proteomics. Our group has been active in the field of metallomics from the very beginning working in close collaboration with molecular biologists. Indeed, information delivered by the novel speciation analytical tools has reached the level where it is attractive for genetic and molecular biology studies aimed at elucidation of biological mechanisms involving essential, toxic, and therapeutic metals and metalloids and their compounds.

This new broad understanding of metal/metalloid-related research led me to get familiar with the basics of life sciences in order to grasp the context of interdisciplinary projects and to be able to creatively contribute to their realization.

BrJAC: For you, what have been the most important achievements in the analytical research field recently? Could you briefly comment on recent advances and challenges in analytical chemistry considering your contributions?

Dr. Szpunar: From my point of view the most important are amazing developments in high-precision high-resolution mass spectrometry allowing access to the isotopic fine structure corresponding to the combination of all the isotopes constituting molecules. It opens the door to the experimental determination

of molecular formulas that can serve as a basis for the identification of unknown species. This capability, combined with multistage fragmentation of molecular ions for their structural characterization, has become an indispensable tool in modern speciation analysis and metallomics studies. At the same time, the progress in inductively coupled plasma mass spectrometry (ICP-MS) made it easier to follow elements (such as, sulfur or phosphorus) offering complementary information about the metal-containing species detected. Also, the introduction of single-particle ICP-MS helped to account for nanoparticles, another form of the chemical species present in some biological systems. Also, on this basis, studies could be developed for the metabolization of metal-containing nanoparticles with possible formation of new species.

BrJAC: There are several meetings of chemistry experts that take place around the world. What is the importance of these meetings to the development of the area?
Dr. Szpunar: I strongly believe in the importance of personal contacts. The nature of research work is very closely linked to the personal qualities of people, their intelligence, curiosity and vision and can only flourish when exposed to ideas of fellow scientists. It is especially true nowadays after the pandemic when many pre-crisis collaborations were weakened or abandoned. Also, interdisciplinary contacts are a must and are much more difficult to develop without a direct face-to-face discussion. I am a regular participant of several analytical chemistry meetings, including the Winter Plasma Spectrochemistry Conference, the Colloquium Spectroscopicum Internationale, the Instrumental Methods of Analysis conference as well as the International Metallomics Symposium and some other interdisciplinary ones related to current projects of our group. It is evident that staying in one's bubble means missing opportunities and narrowing horizons. In addition growing specialization and partitioning of research disciplines make reaching out to colleagues from other disciplines more and more challenging. New ideas are often born not only while listening to the presentations but during informal contacts during coffee breaks, dinners or even conference excursions.

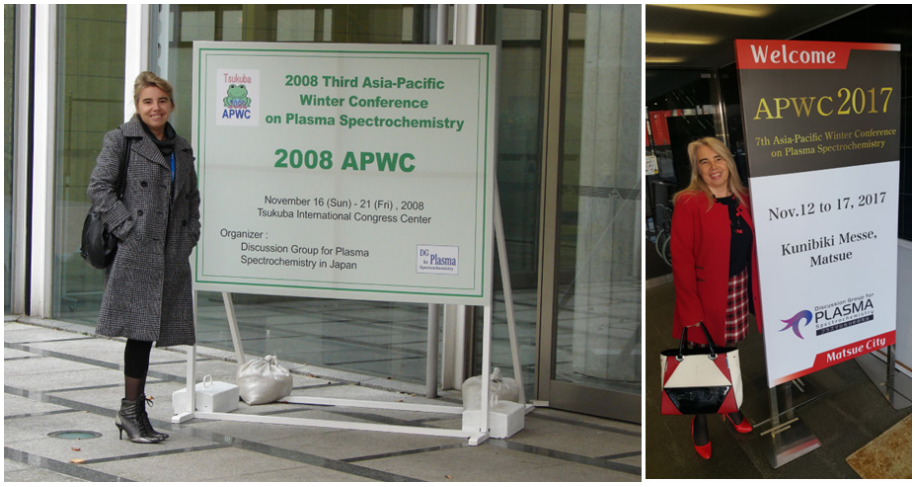

At the Asia-Pacific Winter Conferences on Plasma Spectrochemistry: 2008 in Tsukuba and 2017 in Matsue, Japan.

BrJAC: Do you believe that the current graduate programs produce quality researchers in the field of analytical chemistry? Is there a need for further integration?
Dr. Szpunar: This question is a little difficult for me because I do not teach on a regular basis so - not being personally involved in the process - I do not feel comfortable criticizing. Nevertheless, I do have contact with students coming to our lab to carry out their Master internships and I supervise Ph.D. projects. What I observe is a large variation in the competencies among students coming to our laboratory. From my experience it comes from the possibility of choosing an individual path in terms of the modules studied; although attractive *per se*, it sometimes results in the lack of very basic skills and knowledge. The notion

of inclusivity, although very noble, often backfires when a student arrives at the high education level not prepared to face the challenges. Also, where Ph.D. programs are concerned, there is an enormous pressure on providing a degree within a given time frame, which might be difficult in experimental science when new concepts are tested. It sometimes leads to abandoning “high gain - high risk” ideas and choosing an already beaten path. In such situations the lesson learned by the student is not the best for his creativity and professional future.

Since the essence of analytical chemistry is the laboratory work, I believe the earliest possible integration into the experimental activities, with exposure to real life problems, is key for gaining the skills necessary for a successful career in this field. I believe such participation (with its ups and downs), the choice of a scientific method to use, the hypothesis testing followed by critical evaluation of the data and the necessity of management of time and resources is an invaluable and essential part of the training.

BrJAC: For you what is the importance of the support of funding agencies for the scientific development of the country?

Dr. Szpunar: It is evident for me that funding scientific development is an important investment in the future of any society and country. And even if it is also evident that not all funded projects can be successful, nevertheless, they offer an opportunity to explore and test new ideas and provide experience allowing researchers to face new challenges. There is a never-ending discussion about the criteria for assessment of the feasibility of proposals and a choice between “high risk-high gain” and “low risk-low gain” projects. However, it has to be remembered that asking questions for which we already know answers cannot be considered a science, so opening new horizons should be a priority. At the same time, companies should be encouraged and financially motivated to contribute to projects with more applied character thus broadening the spectrum of funding options.

BrJAC: What sort of a career could someone expect in the field of analytical chemistry? What advice would you give to a newcomer to this area?

Receiving the Award of the Committee of Analytical Chemistry of the Polish Academy of Sciences presented by Dr. Barbara Wagner, 2013.

Dr. Szpunar: Analytical chemistry is a specific field that is indispensable for and, at the same time, dependent on many other research areas. It is fascinating in a sense of its capability to describe and characterize the big and small components of the world around us as well as give information about the composition of our bodies. So, a career in analytical chemistry theoretically gives endless opportunities, including forensic and clinical analysis, environmental and food safety monitoring, as well as participation in high-profile projects ranging from space exploration to development and testing new medicines. Also, there is a place for a variety of personal and professional profiles with people preferring more regular routine work (nothing wrong with that! - we badly need high quality reliable routine data!) and others who value exploration of new paths and developing new methods for emerging analytical problems. So, my advice would be not too original - try to imagine yourself in 5 or 10 years’ time and decide what position and work profile would suit best your abilities, ambition, temperament and, the last but not least, personal plans.

BrJAC: How would you like to be remembered?
Dr. Szpunar: Well, it is a serious, I would say multidimensional, question. From a professional perspective I hope that some of the ideas presented in papers and presentations from our group may inspire young researchers, which is already a kind of positive memory. Naturally, with time, these ideas will not be considered novel anymore and the process of forgetting will start. As to the broader, personal perspective, I do hope that at least some of my colleagues with whom I shared everyday work and some collaborators from more or less distant laboratories may remember our joint efforts with a smile.

Brazilian Journal of Analytical Chemistry
2023, Volume 10, Issue 40, pp 10-12
doi: 10.30744/brjac.2179-3425.point-of-view-mvbzanoni

BrJAC

POINT OF VIEW

Artificial Photosynthesis Technology: Is it Possible?

Maria Valnice Boldrin Zanoni

Instituto de Química da Universidade Estadual Paulista (UNESP), Rua Francisco Degni, 55, Quitandinha, 14800-060, Araraquara, SP, Brazil

Instituto Nacional de Tecnologias Alternativas para Detecção, Avaliação Toxicológica e Remoção de Contaminantes Emergentes e Radioativos (INCT-DATREM), Instituto de Química da Universidade Estadual Paulista (UNESP), Araraquara, SP, Brazil

How to artificially mimic a natural process as important and complex as photosynthesis in plants? Apart from being essential for life on our planet, the phenomenon of photosynthesis is intriguing because it provides an incredible ability to capture light and energy, subsequently converting it into chemical energy with high-quantum efficiency. As a consequence of increasing economic and environmental interest, research on artificial photosynthesis has increased; an exponential growth has been seen from the 21st century onwards, with mastery of the phenomenon's mechanisms being a major challenge to stimulate further development of the subject. Since the 20th century, there have been great expectations regarding further advancing the process of artificial photosynthesis due to the clear recognition of its importance for humanity. With increasing problems in the context of climate change and energy shortages, the possibility of using the core concepts of photosynthesis to contribute to advancing our knowledge on the generation of clean energy from water splitting and hydrogen production, and the recycling of CO_2 into hydrocarbon compounds and/or fuels with ample added value has become increasingly important.

But the lingering question is how to use visible light irradiation to mimic the intricate multistep mechanism of photoexcitation produced by sunlight. The photosynthesis process involves the photooxidation of water to release oxygen and protons, concomitant to a light-independent second phase with complex chemical reactions able to convert carbon dioxide into glucose (fuel) for plants. In the last century, the use of p-type semiconductors, n-p heterojunctions, the doping process, and the combination of multiple semiconductor materials has increased our ability to design photocatalysts, contributing to the efficiency of water splitting, as well as to the reduction of carbon dioxide using solar irradiation alone. However, the materials used in this process are very different from those occurring during the natural process. The most efficient artificial photosynthesis process requires the construction of a system idealized by semiconductors and/or complex light-collecting organisms, which must be capable of capturing photons and transforming them into electrons and protons, which are then transferred to the photosynthetic chain through efficient local and spatial charge separation. In these systems, the search for semiconductors with low charge recombination and a sufficient lifetime to conduct the steps with intricate multiple electron transfer systems, formation of radical species, and surface adsorption can lead to low conversion efficiency or low selectivity regarding the formation of products.

The possibility of producing photochemical devices capable of capturing and promoting the conversion of water and CO_2 into carbohydrates from radiant energy provided by the sun was predicted in 1912. However, although photocatalytic arrays have been tested with relative success through the construction of "artificial leaves", and there have been remarkable improvements in the understanding of these reactions, there remain many controversies around the efficiency of the process.

Cite: Zanoni, M. V. B. Artificial Photosynthesis Technology: Is it Possible? *Braz. J. Anal. Chem.,* 2023, *10* (40), pp 10-12. http://dx.doi.org/10.30744/brjac.2179-3425.point-of-view-mvbzanoni

The great challenge is to find ideal semiconductor materials that can be photoexcited when exposed to sunlight, generate electron/hole charge pairs with a low recombination rate, and still present the ability to catalyze water reduction and/or conversion of CO_2 into hydrogen and hydrocarbons of economic interest, respectively. During the last 15 years, the use of photoelectrocatalysis has been proposed, to improve charge separation and consequently increase the efficiency of the photocatalytic process. This process consists of applying an external potential or current density to a semiconductor, immobilized on a conductive material, which can improve the adsorption of water/CO_2 in an aqueous medium, as well as improving the band bending of the semiconductor, subsequently increasing charge separation. Considering the latter, our research group has tested new functional semiconductor materials with the potential to be applied in both the promotion of water splitting and CO_2 reduction using solar irradiation and ultraviolet/visible irradiation.

To date, the most interesting results have been obtained using n-type and p-type semiconductors modified with thin films stemming from metallic nanoparticles, phosphorene, graphene, metal-organic frameworks (MOFs), porphyrins, copper complexes, ionic liquids, doping semiconductors, and/or coupled in heterojunctions. The use of nanostructures of semiconductors has increased the adsorption processes and surface area through the platform of nanotubes, nanospheres, nanoparticles, nanowires, bioinspired forms, and other nanoporous forms. Among all the arrangements, structures with multiple semiconductors in the form of heterojunctions of semiconductors and the modification of MOFs still deserve greater attention to achieve a higher CO_2 conversion efficiency.

Furthermore, since most of the photocatalyst can promote the formation of carbon monoxide, formic acid, methane, methanol, ethanol, formaldehyde, acetaldehyde, acetone, and other hydrocarbons as products during CO_2 reduction, another challenge concerns the selectivity of the process. This selectivity also depends on the pH, the supporting electrolyte type, the concentration, and the photocatalysis/photoelectrocatalysis time. The semiconductor material plays the most important role in the photo(electro)lytic reaction, and those based on copper oxides with different oxidation states have demonstrated very promising results. However, the low stability of the photocatalyst against self-corrosion, low efficiency to absorb solar radiant energy, low selectivity in product formation, competitiveness of parallel reactions, low solubility of CO_2 in aqueous medium, and high complexity of photocatalytic reactions has generally extended the dream of developing an efficient technological system that is economically viable for wide application in industrial systems or productive markets, with low cost. In the past year, we have been investigating new options for developing hybrid semiconductor materials modified with primitive photosynthetic bacteria or chloroplasts. The chloroplast is a promising photosynthetic material. When deposited on semiconductors, it has contributed to the construction of efficient biohybrid devices for solar energy conversion based on the thylakoid membranes (PSI, and PSII) with remarkably quantum efficiency, with potential applications in photo(bio)electrochemical sensors, as well as in solar energy conversion. However, to be practically applied at a large scale for practical application, there is still a lot to learn about the development of artificial photosynthetic systems and about water splitting, CO_2 reduction, and hydrogen production by light irradiation, which is still a dream and part of the ultimate goal: a sustainable world.

REFERENCES

Weliwatte, N. S.; Grattieri, M.; Minteer, S. D. Rational design of artificial redox-mediating systems toward upgrading photobioelectrocatalysis. *Photochem. Photobiol. Sci*. **2021**, *20*, 1333–1356. https://doi.org/10.1007/s43630-021-00099-7

Bessegato, G. G.; Guaraldo, T. T.; de Brito, J. F.; Brugnera, M. F.; Zanoni, M. V. B. Achievements and Trends in Photoelectrocatalysis: from Environmental to Energy Applications. *Electrocatalysis* **2015**, *6*, 415–441. https://doi.org/10.1007/s12678-015-0259-9

Silva, C. C. G.; Torquato, L. D. M.; Araújo, B. C.; Mantilla, H. D. R.; Zanoni, M. V. B.; Garrido, S. S. Assessment of WO_3 electrode modified with intact chloroplasts as a novel biohybrid platform for photocurrent improvement. *Bioelectrochemistry* **2022**, *147*, 10-8177. https://doi.org/10.1016/j.bioelechem.2022.108177

Maria Valnice Boldrin Zanoni is a Full Professor at the Institute of Chemistry at São Paulo State University (UNESP), Araraquara (1987), with a master's and Ph.D. degree in chemical sciences from the University of São Paulo (USP) (1985, 1989) with a focus on electroanalysis and organic electrochemistry; a member of the Brazilian Academy of Sciences (ABC); a member of the Brazilian Academy of the State of São Paulo (ACIESP); Pro-Rector of Graduate Studies at UNESP (since 2021); with postdoctoral internships in analytical chemistry at the University of Loughborough, England (1992-1994), the University of Wisconsin, Madison, USA (2002), and an academic visitor, Oxford University (2008), working on the electroanalysis of dyes, pharmaceutical compounds, and the photoelectrocatalysis oxidation of pollutants. She was awarded the Elsevier/CAPES 2014 award, which highlighted 10 Brazilian researchers whose research had more impact on the scientific community. She was honored by the Brazilian Society of Electrochemistry and Electroanalysis (SBEE) for work in the development and consolidation of electroanalysis in Brazil (2019) and was also honored by the Analytical Chemistry Society (2022). She was advisor to the Pro-Rectory of Research development at UNESP (2010-2018), coordinator of the Graduate Program in Chemistry at the Institute of Chemistry (2004-2007), and coordinator of FAPESP's thematic project in analytical chemistry of dyes (2009-2015). She was a member of the Advisory Committee on Chemistry of CNPq (03/2013 to 04/2015) and (2019-2022) and was director of the Electrochemistry and Electroanalytical division of SBQ (2016-2018). She is the coordinator of the INCT-DATREM project (National Institute of Alternative Technologies for the detection, toxicological evaluation, and removal of emerging and radioactive contaminants (2017-2024)). Her research group is interested in the development of sensors and new methods of advanced oxidative methods for water treatment and disinfection, CO_2 reduction and hydrogen generation using photoelectrochemical processes. Prof. Zanoni has supervised over 71 graduate students (MS, Ph.D.) and post-docs and has published about 292 papers, 5 books and 14 book chapters, with 7992 citations (ISI) with an *h*-index of 47 (ISI) and 13769 citations with an *h*-index of 57 (scholar google). CV

Brazilian Journal of Analytical Chemistry
2023, Volume 10, Issue 40, pp 13-16
doi: 10.30744/brjac.2179-3425.letter-almeida-cass

BrJAC

LETTER

Affinity Selection Mass Spectrometry (AS-MS) as a Tool for Prospecting Target Ligands

Fernando G. Almeida[1], Quezia B. Cass[2]*

[1]*OMass Therapeutics, Oxford, United Kingdom*

[2]*Separare, Departamento de Química, Universidade Federal de São Carlos, São Carlos, 13565-905, SP, Brazil*

Affinity selection mass spectrometry (AS-MS) has been shown to be a powerful tool for identifying bioactive molecules in synthetic and/or natural libraries. The selection provided by the formation of the target-ligand complex allows the identification of hits irrespective of their functional effect. Moreover, it precludes the use of label, since the binders are identified by their exact mass.[1] The binders are determined by an affinity or index ratio calculated through control assays.[2–4] The target protein can be used in solution or immobilized in a solid support (Figure 1). Both approaches have pros and cons.[5,6]

Unlike most conventional high-throughput screening assays, AS-MS has fewer or no limitations when it comes to target selection. It is important, however, to understand the implications of choosing membrane proteins as targets. Membrane proteins correspond to 42% of all drug targets listed in DrugBank. Moreover, they are likely to be selected as protein targets due to their participation in many disease pathways, acting as ion channels, molecular transporters, solute carriers, receptors, and anchors.[7] One of the bottlenecks in working with membrane proteins comes from the need to use a detergent for solubilization, folding, and structure maintenance. Detergents are usually used above the critical micelle concentration, which can lead to empty micelles and thus to false positive results, caused by nonspecific interactions with the detergent micelles.[8] Interference in the ionization of the binders also needs to be examined.[9]

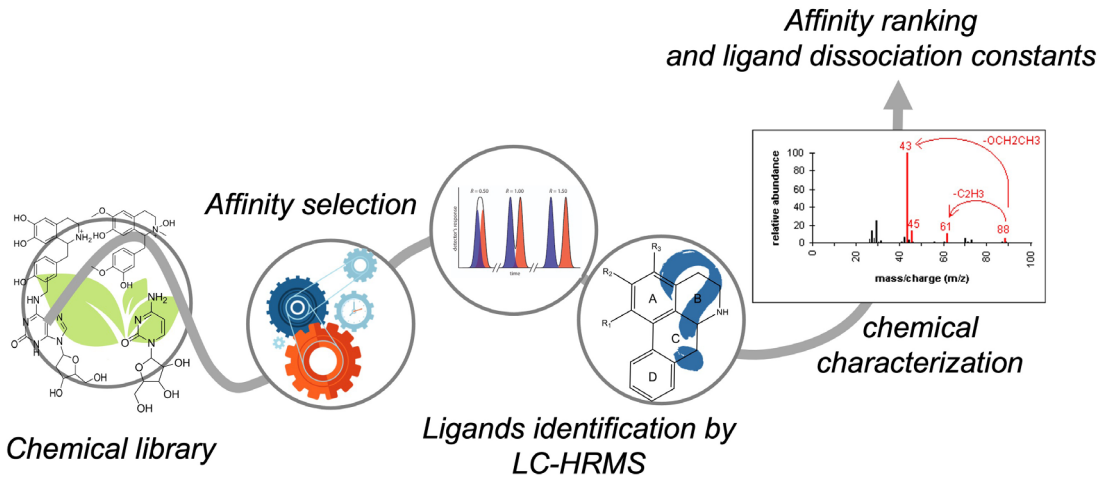

Figure 1. Schematic AS-MS for ligand screening in a chemical library.

Cite: Almeida, F. G.; Cass, Q. B. Affinity Selection Mass Spectrometry (AS-MS) as a Tool for Prospecting Target Ligands. *Braz. J. Anal. Chem.* 2023, *10* (40), pp 13-16. http://dx.doi.org/10.30744/brjac.2179-3425.letter-almeida-cass

The AS-MS technologies mainly used with protein targets in solution are size exclusion chromatography (SEC) and pulsed ultrafiltration (PUF). These approaches are used to separate the protein–ligand complexes from unbound ligands. The collected protein–ligand complexes are then denatured by a variety of experimental conditions and the ligands are thus analyzed, usually by liquid chromatography high-resolution mass spectrometry (LC-HRMS).[1,6]

Two commercial settled technologies are used for SEC: SpeedScreen (Novartis) and the Automated Ligand Identification System (ALIS) (Merck & Co.).[1] SpeedScreen uses a micro-plate for the target-ligand complex formation and SEC for the separation step,[9] while ALIS relies on continuous-flow chromatography for the isolation and dissociation of the complex.[10] PUF is carried out either with a solvent pump or a centrifuge to push the protein–ligand complex through the membrane. The pore size and chemical composition of the membranes are important parameters to consider, to minimize adsorption of the protein and/or small molecules.[1,5]

AS-MS based on a solid supported target (Figure 2) has been explored with a diversity of applications and a variety of supports.[11] The workflow comprises the same four main steps used in the solution-based assay: load, wash, ligand extraction or desorption, and LC-MS analysis.

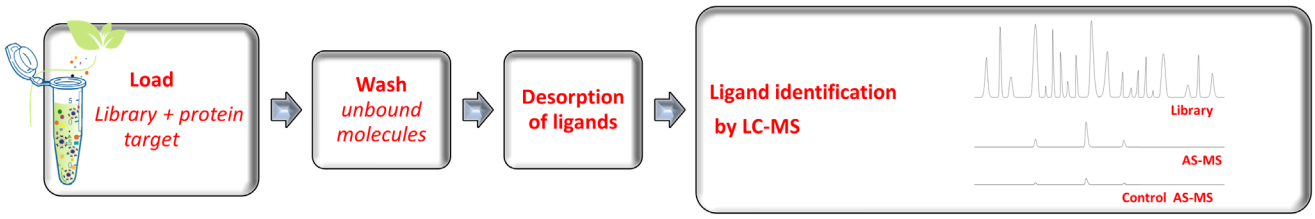

Figure 2. Workflow of AS-MS using a solid supported target.

Among the diversity of solid supports, magnetic beads have been the most used, probably because they provide large specific surfaces and can be separated rapidly and consistently by the application of external magnetic forces. The beads are composed of a magnetic material, such as iron, cobalt, nickel, and metal oxides, and a chemical moiety, which is used for target immobilization.[12] The beads' size and chemical composition are important parameters for their use in AS-MS.[13]

When screening synthetic libraries, one main advantage is that they are formed by known molecules, and the structural characterization of the identified ligands is thus made by the correlation of the exact mass, isotopic pattern, and LC retention time of each ligand present in the collection.[1] There are numerous synthetic library suppliers that provide multiple formats (96, 384, 1536 well plates), pooled compounds, and concentrations. In using a synthetic library, it is possible to design the configuration that is most suitable for the purpose. Ideally, the target should be present in molar excess relative to the pool of compounds. This avoids missing binders with lower affinity.[1] Another important aspect of synthetic libraries is that the chemical space can be covered in a more controlled fashion. Moreover, most of the compounds in these libraries have physicochemical properties that are associated with acceptable aqueous solubility and intestinal permeability, which comprise the first steps in oral bioavailability.[14] Consequently, when confirmed as binders, they have a better chance of progressing.

It is acknowledged that synthetic libraries should have a diversity of chemical scaffolds, while having synthetic availability. These requirements have recently been met by a "synthetic methodology-based natural product-like library", which enabled the identification of small molecules that cause the disruption of GIT1/β-Pix interactions.[15] Nonetheless, it has not yet been used in AS-MS.

Finally, the best benefit one can have with a synthetic library in AS-MS is the capability of validating the ligands as singlets, as the suppliers also provide any compound individually from the library.

The molecular and stereochemical complexities encoded in natural product libraries play a significant role in the drug discovery and development processes,[15,16] but hold a huge challenge in their use, and demands innovative assays method, in which AS-MS has been explored.

As an example, an AS-MS hemp screen[17] was carried out using a recombinant SARS-CoV-2 spike protein S1 subunit (~72 kDa) containing an N-terminal His-tag immobilized on Ni^{2+}-nitrilotriacetic acid-derivatized magnetic microbeads. Based on the dereplication of the ligands, and using cannabinoid standards for the equilibrium dialysis experiments, cannabigerolic acid (CBGA), tetrahydrocannabinolic acid (THCA-A), and cannabidiolic acid (CBDA) were identified as the ligands with the highest affinities. To this end, CBGA and CBDA blocked the infection of human epithelial cells by a pseudovirus expressing the spike protein.

The use of HRMS, software for data processing and curation, fragmentation experiments, spectral libraries, and molecular networks are all necessary for these collections, represented by the natural product extracts, to infer the molecular structures of the identified ligands.[2,4] It is an arduous and not always successful step in structural elucidation.[2,3] Anyhow, the clear identification of isobaric binders, either in a very compressed synthetic library or in natural products, is always a problem that requires additional deconvolution experiments.

It is important to stress that suitable biochemical and/or cellular assays are required to furnish further biological information, so as to characterize the identified ligands. Zonal or frontal bioaffinity chromatography can be used to this end. The AS-MS platform also serves to characterize target-ligand interaction mechanisms and can be used either to identify molecular targets or in phenotyping experiments. We expect to see more intensive use of AS-MS as a means of identifying low concentration binders from natural product extracts and the use of more diverse scaffold synthetic libraries.

REFERENCES

(1) Prudent, R.; Annis, D. A.; Dandliker, P. J.; Ortholand, J.-Y.; Roche, D. Exploring new targets and chemical space with affinity selection-mass spectrometry. *Nat. Rev. Chem.* **2021**, *5*, 62–71. https://doi.org/10.1038/s41570-020-00229-2

(2) Lima, J. M.; Leme, G. M.; Costa, E. V.; Cass, Q. B. LC-HRMS and acetylcholinesterase affinity assay as a workflow for profiling alkaloids in Annona salzmannii extract. *J. Chromatogr. B* **2021**, *1164*, 122493. https://doi.org/10.1016/j.jchromb.2020.122493

(3) do Amaral, B. S.; da Silva, L. R. G.; Valverde, A. L.; de Sousa, L. R. F.; Severino, R. P.; de Souza, D. H. F.; Cass, Q. B. Phosphoenolpyruvate carboxykinase from T. cruzi magnetic beads affinity-based screening assays on crude plant extracts from Brazilian Cerrado. *J. Pharm. Biomed. Anal.* **2021**, *193*, 113710. https://doi.org/10.1016/j.jpba.2020.113710

(4) Wang, Z.; Kim, U.; Liu, J.; Cheng, C.; Wu, W.; Guo, S.; Feng, Y.; Quinn, R. J.; Hou, Y.; Bai, G. Comprehensive TCM molecular networking based on MS/MS in silico spectra with integration of virtual screening and affinity MS screening for discovering functional ligands from natural herbs. *Anal. Bioanal. Chem.* **2019**, *411*, 5785–5797. https://doi.org/10.1007/s00216-019-01962-4

(5) Muchiri, R. N.; Breemen, R. B. Affinity selection–mass spectrometry for the discovery of pharmacologically active compounds from combinatorial libraries and natural products. *J. Mass Spectrom.* **2021**, *56* (5). https://doi.org/10.1002/jms.4647

(6) Ramatapa, T.; Msobo, A.; Maphari, P. W.; Ncube, E. N.; Nogemane, N.; Mhlongo, M. I. Identification of Plant-Derived Bioactive Compounds Using Affinity Mass Spectrometry and Molecular Networking. *Metabolites* **2022**, *12*, 863. https://doi.org/10.3390/metabo12090863

(7) Gong, J.; Chen, Y.; Pu, F.; Sun, P.; He, F.; Zhang, L.; Li, Y.; Ma, Z.; Wang, H. Understanding Membrane Protein Drug Targets in Computational Perspective. *Curr. Drug Targets* **2019**, *20*, 551–564. https://doi.org/10.2174/1389450120666181204164721

(8) Landreh, M.; Costeira-Paulo, J.; Gault, J.; Marklund, E. G.; Robinson, C. V. Effects of Detergent Micelles on Lipid Binding to Proteins in Electrospray Ionization Mass Spectrometry. *Anal. Chem.* **2017**, *89*, 7425–7430. https://doi.org/10.1021/acs.analchem.7b00922

(9) Zehender, H.; Mayr, L. M. Application of high-throughput affinity-selection mass spectrometry for screening of chemical compound libraries in lead discovery. *Expert Opin. Drug Discov.* **2007**, *2*, 285–294. https://doi.org/10.1517/17460441.2.2.285

(10) Zhang, T.; Liu, Y.; Yang, X.; Martin, G. E.; Yao, H.; Shang, J.; Bugianesi, R. M.; Ellsworth, K. P.; Sonatore, L. M.; Nizner, P.; et al. Definitive Metabolite Identification Coupled with Automated Ligand Identification System (ALIS) Technology: A Novel Approach to Uncover Structure–Activity Relationships and Guide Drug Design in a Factor IXa Inhibitor Program. *J. Med. Chem.* **2016**, *59*, 1818–1829. https://doi.org/10.1021/acs.jmedchem.5b01293
(11) de Moraes, M. C.; Cardoso, C. L.; Cass, Q. B. Solid-Supported Proteins in the Liquid Chromatography Domain to Probe Ligand-Target Interactions. *Front. Chem.* **2019**, *7*, 752. https://doi.org/10.3389/fchem.2019.00752
(12) Gkantzou, E.; Patila, M.; Stamatis, H. Magnetic microreactors with immobilized enzymes-From assemblage to contemporary applications. *Catalysts* **2018**, *8*, 282. https://doi.org/10.3390/catal8070282
(13) de Lima, J. M.; Furlani, I. L.; da Silva, L. R. G.; Valverde, A. L.; Cass, Q. B. Micro- and nano-sized amine-terminated magnetic beads in a ligand fishing assay. *Anal. Methods* **2020**, *12*, 4116–4122. https://doi.org/10.1039/D0AY01269F
(14) Agarwal, P.; Huckle, J.; Newman, J.; Reid, D. L. Trends in small molecule drug properties: A developability molecule assessment perspective. *Drug Discov. Today* **2022**, *27*, 103366. https://doi.org/10.1016/j.drudis.2022.103366
(15) Gu, J.; Peng, R.-K.; Guo, C.-L.; Zhang, M.; Yang, J.; Yan, X.; Zhou, Q.; Li, H.; Wang, N.; Zhu, J.; et al. Construction of a synthetic methodology-based library and its application in identifying a GIT/PIX protein–protein interaction inhibitor. *Nat. Commun.* **2022**, *13*, 7176. https://doi.org/10.1038/s41467-022-34598-7
(16) Batista, A. N. L.; dos Santos, F. M.; Batista, J. M.; Cass, Q. B. Enantiomeric Mixtures in Natural Product Chemistry: Separation and Absolute Configuration Assignment. *Molecules* **2018**, *23*, 492. https://doi.org/10.3390/molecules23020492
(17) van Breemen, R. B.; Muchiri, R. N.; Bates, T. A.; Weinstein, J. B.; Leier, H. C.; Farley, S.; Tafesse, F. G. Cannabinoids Block Cellular Entry of SARS-CoV-2 and the Emerging Variants. *J. Nat. Prod.* **2022**, *85*, 176–184. https://doi.org/10.1021/acs.jnatprod.1c00946

Quezia B. Cass is a Full Professor at the Chemistry Department of the Federal University of São Carlos. 2D-LC methods for quantifying chiral and achiral drugs in either biological fluids or environmental matrices play an important role in her research projects. Immobilized enzymes in solid support for ligand screening in natural or synthetic libraries by affinity-based assays has been one of her main research interests. She has authored more than 185 articles and supervised more than 55 graduated students, 16 research fellows, and 25 undergraduate research students. Her research group has contributed to the development of cutting-edge analytical techniques. CV

Fernando G. Almeida is Senior Scientist at OMass Therapeutics in Oxford, UK. He was a pioneer in setting up the affinity-based ligand screening platform at the company and has been successful in applying the AS-MS screening platform across different targets/projects. With more than 10 years of experience in LC-MS, it is worth mentioning his trajectory at the Research Facility (BioMass – CEFAP), Institute of Biomedical Sciences, University of São Paulo establishing the proteomics platform, followed by a post-doctoral fellowship at the Biological Chemistry and Drug Discovery, School of Life Sciences, University of Dundee, working with protein interaction and cross-linking proteomics.

Brazilian Journal of Analytical Chemistry
2023, Volume 10, Issue 40, pp 17-34
doi: 10.30744/brjac.2179-3425.RV-126-2022

BrJAC

REVIEW

Recent Developments in Green Chromatography

Bianca Furukawa de Godoi Passerine, Márcia Cristina Breitkreitz*

Instituto de Química, Universidade Estadual de Campinas (Unicamp). Rua Josué de Castro, s/n, Campinas, SP, 13083-861, Brazil

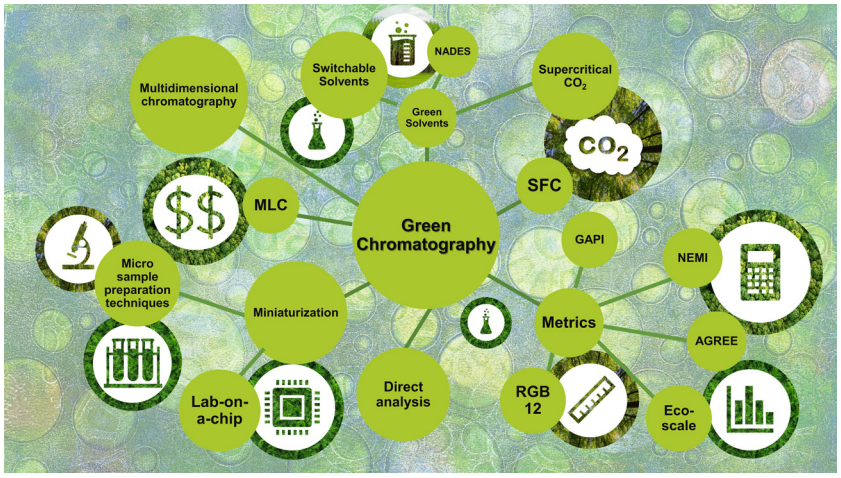

In recent decades, green analytical chemistry has received more attention due to the growing concern over environmental conservation and the use of non-renewable resources. Among the analytical techniques, liquid chromatography is the most widely used in quality control analysis of food, drugs, and clinical analysis among others, but it is also the technique that uses the largest amount of hazardous organic solvents and generates large volumes of waste. Therefore, strategies such as the miniaturization of chromatographic systems, the use of online sample preparation systems, and the replacement of hazardous organic solvents by green solvents have been applied to develop greener chromatographic methods. In this paper, strategies for greening methods and recent developments in green chromatography are presented. In addition, metrics for the proper evaluation of these methods are discussed.

Keywords: chromatography, green analytical chemistry, greenness assessment, miniaturization, sustainability

INTRODUCTION

The concept of green chemistry emerged in the early 1990s to mitigate the hazards posed by chemicals to the environment and human health.[1] To this end, Anastas and Warner proposed the 12 principles of green chemistry as guidelines for improving chemical systems, processes, materials, and products, and applied them primarily to industrial chemical processes.[2] Later, the IUPAC (International Union of Pure and Applied Chemistry) defined green chemistry as *"The invention, design, and application of chemical products and processes to reduce or to eliminate the use and generation of hazardous substances"*.[3] These principles were elaborated for synthetic chemists and at the industrial level at the first moment due to their large scale, large amount of waste produced, and therefore high impact on the environment, when compared to analytical chemistry.

However, the environmental impact generated by analytical laboratories nowadays is high considering that thousands of analyses are performed in a single day.[4] Thus, the application of green chemistry

Cite: Passerine, B. F. G.; Breitkreitz, M. C. Recent Developments in Green Chromatography. *Braz. J. Anal. Chem.* 2023, *10* (40), pp 17-34. http://dx.doi.org/10.30744/brjac.2179-3425.RV-126-2022

Submitted 25 November 2022, Resubmitted 16 February 2023, Accepted 26 February 2023, Available online 11 April 2023.

principles in analytical chemistry laboratories is fundamental to reducing the environmental impact and guarantee safety to the analysts. The application of green chemistry principles in analytical chemistry can be defined as Green Analytical Chemistry (GAC), seeking the development of new methods and techniques capable of reducing the use and generation of hazardous substances in all stages of chemical analysis. However, only four of the twelve principles of green chemistry could be applied directly to GAC once they were planned to attain the needs of industrial and synthetic chemistry.[5] In this context, in 2013, Galuska *et al*. adapt the 12 principles of green chemistry and proposed the 12 principles of the GAC which are: (1) Direct analysis techniques should be employed to avoid sample treatment; (2) The number and size of the sample should be minimal; (3) Perform in-situ measurements; (4) Integrate analytical procedures and operations to save energy and reduce reagent consumption; (5) Select automated and miniaturized methods; (6) Avoid derivatizations; (7) Avoid the generation of large volumes of waste and dispose of it properly; (8) Use multi-analyte or multi-parameter methods; (9) Energy consumption must be minimized; (10) Use reagents from renewable sources; (11) Toxic reagents must be eliminated or replaced; (12) The security of the analyst should be increased.[6]

According to the GAC principles, the development of analytical methods should cause a minimum impact on the environment and should be safe for the analyst. However, the GAC principles implementations may lead to significant challenges regarding analytical method validation. For example, the reduction of sample size or the number of samples in the sampling process may cause a loss of the method representativity, precision, trueness, selectivity, and sensibility. As a consequence, the main challenge to future applications of the GAC is to reach a compromise between the validation parameters of analytical methods and the method's sustainability.

Liquid chromatography (LC) is a powerful and widespread separation technique that has been routinely used for the determination of organic compounds in complex mixtures at very low concentrations. However, substantial sample cleanup is needed for LC procedures, and large amounts of organic solvents and reagents are used during analysis. In light of this, these features of LC methods can be enhanced by implementing strategies based on the GAC principles into practice.[7] Thus, the application of concepts of GAC in chromatographic techniques can be called green chromatography.

GREEN CHROMATOGRAPHY

Green chromatography generally aims to eliminate or reduce toxic solvent consumption, reduce analysis time, ensure analyst safety, and reduce waste generation. Several strategies can be employed to meet these objectives such as using miniaturized chromatographic techniques, performing on-site measurements, using green solvents as mobile phases, integrating multiple steps of the analytical procedure into a single step using hyphenated techniques, using automated methods, and when possible, using direct analysis.[7,8,9] As it is known, high-performance liquid chromatography (HPLC) uses large amounts of organic solvents such as acetonitrile and methanol, producing large volumes of waste. From the GAC's perspective, the simplest approach in this circumstance would be to minimize solvent consumption or replace it with less harmful or biodegradable solvents. Glycerol, for example, is derived from renewable sources and is a low-cost green solvent (biodiesel byproduct) that is non-volatile and stable under normal storage circumstances. And recently, mobile phases based on glycerol and an aqueous buffer solution were reported in the literature for detecting ascorbic acid and glutathione in pharmaceutical tablets.[10,11] On the other side, gas chromatography (GC) does not use solvents in the separation process. Hereby, the use of new technologies for temperature control and modifications to sample preparation must be carried out for the development of green methods. Other chromatographic modes that can minimize the consumption of hazardous organic solvents in the mobile phase include supercritical fluid chromatography (SFC) and enhanced fluidity liquid chromatography (EFLC). SFC is comparable to HPLC, except that the mobile phase is mostly composed of fluid at or near its critical temperature and/or pressure. These fluids are more gas-like than normal liquids, with increased solute diffusivity and decreased viscosity. As a type of normal phase chromatography, SFC uses non-polar fluids like carbon dioxide.[12] Polar organic solvents are added

to the fluid to increase the mobile phase polarity to 30 to 40%, and when the percentage of organic solvent is higher, it is referred to as EFLC.[13]

In terms of sample preparation, for example, microextraction techniques using less hazardous solvents[14] and the use of innovative sorbent materials with lower cytotoxicity and biocompatible supports are the main topics of recent studies in the development of green chromatographic procedures.[15,16] These current studies also attempt to create reusable instrumentation that ensures analytical performance equivalent to or better than the systems already in use.[15]

Green chromatography techniques are frequently cost-effective because they support protocols that require minimal or reduced solvent or reagent requirements. Therefore, the chromatographic methods have the potential to be greener in all analysis steps, from sample preparation to the separation and the final determination. Moreover, when developing a method in agreement with GAC principles, it is necessary to determine whether the strategies employed in its development have made it greener. Thus, the evaluation of method greenness is performed by qualitative, semiquantitative, and quantitative metrics, which allows us to compare different methods and choose the greenest option. In this regard, this paper discusses several ways for making GC and HPLC greener, such as direct analysis and miniaturization of sample preparation and chromatographic system, as well as the available metrics for method greenness assessment.

Tools for method greenness assessment

The first developed metric for green chemistry was the National Environmental Method Index (NEMI),[17] which judges the method greenness through a pictogram divided into four quadrants PBT (persistent, bioaccumulate, and toxic), Hazardous, Corrosive, and Waste.

The respective quadrant is filled with green color when the method meets the established criteria and the method with the most filled quadrants is the greenest one. Despite the simple representation and easy understanding, NEMI provides qualitative results and does not consider the reagent number used, the occupational hazards, and the equipment energy consumption. Therefore, according to GAC principles, this metric does not include all the parameters necessary to assess if a method is eco-friendly.

A semiquantitative evaluation can be done employing the Analytical Eco-scale (Eco-Scale)[18] metric, which is a score classification system. An ideal green method starts with 100 points and penalties are applied to this score for each parameter such as reagent amount, hazardous, energy consumption, and waste generation that diverges from GAC ideality.

The Green Analytical Procedure Index (GAPI)[19] is a tool that uses a pictogram to classify the method's greenness in each step of the analytical procedure, using a color scale with three levels of evaluation. In GAPI a specific symbol with five pentagrams is used to assess the levels of environmental impact involved in each step of the methodology, with the green color meaning low impact, yellow representing intermediate impact, and red as high impact. Each field reflects a different aspect of the analytical procedure described and it is represented by a number referring to the GAPI parameter description (Figure 1).

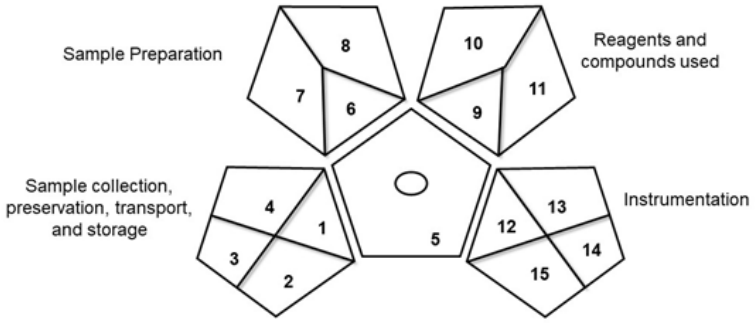

Figure 1. Representation of the GAPI pictogram. [Reprinted with permission by CCC Rights Service, from Ref. 19: Płotka-Wasylka, J. A New Tool for the Evaluation of the Analytical Procedure: Green Analytical Procedure Index. *Talanta* **2018**, *181*, 204–209. DOI: 10.1016/j.talanta.2018.01.013. Copyright© (March, 2023), Elsevier].

The Eco-scale and GAPI metrics comprehended parameters that are not included by NEMI as several reagents employed and energy consumption. However, the GAPI metric provides a more complete evaluation than Eco-scale by detailing the analytical procedure from sampling, transportation, and sample preparation until the final determination of analytes. Despite the details provided by GAPI, the pictogram obtained is complex, and qualitative and does not assess the analytical method performance.[19]

A quantitative evaluation can be realized by Analytical Greenness Calculator (AGREE),[20] a comprehensive, flexible, and direct metric that provides an informative result and is easily interpretable. In this free software, there are twelve evaluation criteria based on the twelve principles of GAC, which are converted into scores ranging from 0 to 1. The final score result is the product of each principle's assessment results. The final assessment is presented as a clock shape pictogram (Figure 2), indicating the final score and the color in the clock center.[20]

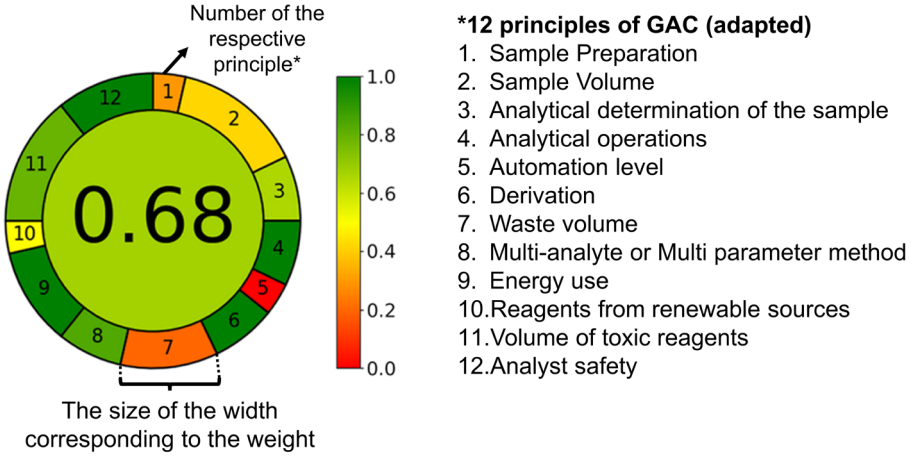

Figure 2. Representation of the AGREE pictogram. [Reprinted from Ref. 20: Pena-Pereira, F.; Wojnowski, W.; Tobiszewski, M. AGREE - Analytical GREEnness Metric Approach and Software. *Anal. Chem*. **2020**, *92* (14), 10076–10082. DOI: 10.1021/acs.analchem.0c01887, an open access article published under a CC-BY License, which permits unrestricted use, distribution and reproduction in any medium.]

Of the metrics introduced, the AGREE metric is the one that best incorporates all GAC principles. However, it does not assess the number of reagents used in the method. Besides that, the introduced metrics do not consider the analytical method performance parameters, very important to the analytical validation step, and the practical viability of the method.

Due to the lack of a tool or metric capable of performing a comprehensive analytical method evaluation together with its green aspects, Nowak and Kóscielniak proposed an original model based on the RGB additive color model that allows a global method evaluation that can be performed in an Excel spreadsheet.[21] The RGB additive model color commonly is used in electronic systems to represent and display colors and the name refers to the red, green, and blue colors, respectively. In the proposed RGB model the colors represent the primary attributes of analytical methods. The red color corresponds to the method performance assessed by analytical validation, the green color represents the GAC principles and the blue color refers to the productivity effectiveness which includes cost and time effectiveness, the complexity of methodology, trained staff, and equipment maintenance. To quantitatively assess whether the method conforms to the three main colors of the RBG model, a color score (CS) is calculated and ranges from 0 to 100%. If the evaluated method receives a CS higher than 66%, i.e., is rated as satisfactory, for all three colors the final color of the method will be white. This means that the method meets all the evaluated criteria, analytical performance, practical effectiveness, safety, and environmental friendliness. When the method

reaches CS ≥ 66.6% for only two colors and results in color with 33.3 ≤ CS ≤ 66.6%, i.e., is classified in a tolerable value range, the final color of the method is a mixture of the colors that reached the satisfactory level. The colors resulting from the mixtures are yellow, (a combination of the color green and red), cyan (blue and green), and magenta (blue and red). If the CS of a method reaches the satisfactory level for only one of the colors, the final color of the method will be red, blue, or green. If the method has 33.3 ≤ CS ≤ 66.6% for all three main colors the final color of the method will be gray (no color) and indicates that the use of the method is not recommended if a better method is available. However, if at least one CS is less than 33.3% the method gets the color black because at least one of the main attributes of the method is unacceptable.

Another parameter of the RGB model that can be used to evaluate the methods is the method brilliance (MB), which can be calculated by the geometric weighted average of the individual values achieved by the method. Thus, the method with the highest MB will be the one with the highest individual CS values. The RGB model was the first model proposed by the authors.[21]

Recently, Nowak *et al*. formulated the 12 principles of white analytical chemistry (WAC) to implement the principles of sustainable development (SD) in analytical chemistry due to the need to find an equilibrium between method greenness, its potential usefulness, and analytical performance. Just as sustainable development is based on three pillars (economic, social, and environmental), the 12 principles of the WAC were divided into three complementary areas (Figure 3). As in the RGB model, a white method contemplates the three colors and represents a balanced analytical methodology suitable for its intended use.[22]

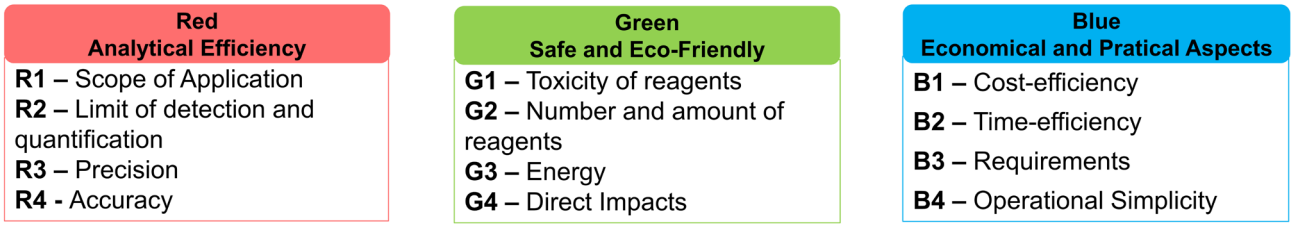

Figure 3. The 12 principles of white analytical chemistry are based on the RGB model. The 12 principles of green analytical chemistry were summarized into four main principles and complemented with four red principles and four blues principles representing analytical performance and practical/economic criteria, respectively. Adapted from Nowak *et al*.[22]

The authors also proposed a new version of the RBG model and named it RGB 12. The new model is still based on free Excel spreadsheets and has been simplified for easy and quick evaluation of a method against each of the 12 proposed WAC principles. And thus assess the level of sustainability of the method, i.e., the whiteness of the method.[22]

Strategies and current improvements to make chromatographic procedures more environmentally friendly

Green strategies applied to sample pre-treatment

Sample preparation is considered the step of the analysis with the greatest polluting potential, as it generally requires the use of organic solvents in large volumes. Sample preparation is also considered a crucial part of the analytical procedure based on quantitative determinations, identification, and chromatographic separations of a wide spectrum of analytes, especially in samples characterized by a matrix with complex composition.[7,23] There are several ways to make sample preparation greener such as eliminating or reducing the number of organic solvents and reagents used in the analysis or the application of green solvents and recovery and reuse of solvents. The main advances related to sample preparation techniques applied to chromatographic methods are concentrated in the search for greener solvents such

as ionic liquids (IL), natural eutectic solvents (NADES), and supramolecular solvents (SUPRA), to replace the organic solvents used in microextraction. In this context, a class of green solvents called switchable solvents has been used for extraction purposes.[23] Switchable solvents are defined as solvents whose properties change abruptly in response to an external *stimulus*, such as a change in temperature or by purging or removing a gas. Usually, the term switchable solvents are related to tertiary and secondary amines that can switch their hydrophilicity as their structure changes in solutions due to pH changes.[24] For example, under normal conditions, switchable hydrophilic solvents are liquids that are so hydrophobic that they are immiscible with water and form a two-phase mixture. However, when CO_2 is added to the two-phase solvent/water mixture, the hydrophobic nature of the solvent significantly changes and becomes hydrophilic, which mixes with water to form a homogeneous mixture and increases extraction efficiency.[25] After the extraction process, an alkali treatment removes the CO_2, and the system reverts to a two-phase state, allowing the analytes to be easily removed and injected into the chromatograph.[26] Other switchable properties of these solvents include polarity, ionic strength, and surface activity.[24] In a recent study, Karayaka *et al*.[25] developed a method for the determination of alkylphenols and bisphenol A at trace levels using GC-MS after preconcentration with switchable liquid-liquid microextraction (SLLME) with N, N-dimethylbenzoamine as a switchable solvent. With the SLME-GC-MS method, the detection limits of the four analytes investigated remained in the range of 0.13-0.54 ng mL^{-1}, with an increase in detection power of 86- to 113-fold as compared to the detection limits reported by direct GC-MS. Recovery studies in tap water and wastewater were used to determine the method's accuracy and applicability in real samples, and the results ranged from 87 to 106%, showing that the method could be easily applied in routine water quality analysis. Furthermore, with this sample preparation, it was possible to reduce the consumption of solvents, and the generated residues were less toxic, making the method economical and compatible with the principles of the GAC, with a score of 88 on the Eco-scale. Other studies also presented greener chromatographic methods employing switchable solvents in microextraction techniques, as shown in Table II. Although the secondary and tertiary amines required for switchable solvent extraction are more expensive than ordinary organic solvents, the extractions are carried out on a micro-scale, and the extraction process is simplified, requiring only the addition/removal of CO_2 and a subsequent centrifugation step.

Table II. Recent applications of switchable solvents in sample preparation

Analytes	Matrix	Extraction Technique	Extraction Solvent/Sorbent	Analytical Technique	Mobile Phase	Benefits	Metric Employed
BFA[25]	Plastic bottles	LLE[a]	N,N-dimethylbenzamine	GC-MS	He	Waste with low toxicity Inexpensive and non-hazardous reagents	Eco-scale 88
Methamphetamine[27]	Urine	SHS - HLLME[b]	Dipropylamine	GC-MS	He	Quick extraction Reduced analysis time	NA[g]
Polybrominated diphenyl ethers[28]	Fish oil	VALLME[c]	different DES	GC-MS	He	Environmentally friendly and economical Low toxicity substances	NA[g]
Chlorobenzenes[29]	Water	HLLME	monoethanolamine/ 4-methoxyphenol[f]	GC-MS	He	Biodegradable solvents Fast and efficient extraction	NA[g]
Non-steroidal anti-inflammatory drugs[30]	Drinking Water	D-μ-SPE -HLLME[d]	Dispersive Solid - D-μ-SPE/Dipropylamine	HPLC-UV	ACN + 0.1% acetic acid	Reduced analysis time Environmentally safe	NA[g]
Tetracyclines[31]	Urine	SP-LPME[e]	Fatty Acids[f]	HPLC-UV	Elution gradient ACN and MeOH (2:1) + 0.5% formic acid	Cheap reagents	Eco-scale 85

[a]Liquid-liquid extraction; [b]Homogeneous liquid-liquid microextraction with switchable hydrophilicity solvent; [c]Vortex-assisted liquid-liquid microextraction; [e]Membrane liquid-liquid microextraction; [f]DES; [g]Not applied.

In another study Wang *et al*. used for the first time NADES solvents as a matrix medium to replace DMSO, DMF, DMA, and water in a static headspace gas chromatography method for the determination of residue solvents in active pharmaceutical ingredients (API).[32] The validated method showed an $R^2 \geq 0.999$ and provided high sensitivity with limits of detection (LOD) between 0.06 and 0.12 μg g^{-1} for acetone, methanol, ethanol, isopropanol, n-butanol, acetonitrile, tetrahydrofuran, and 1,4-dioxane. Accuracy and precision showed acceptable results with recoveries of the tested solvents in the range of 94.3% to 105.4%, and relative standard deviations (RSD) ranged from 0.85 to 3.65 for intra-day precision and 1.51 to 4.53 for inter-day precision. The new approach was also used to successfully detect residual solvents in six APIs, sitagliptin, ramipril, imatinib mesylate, lisinopril, pramipexole dihydrochloride, and rivaroxaban.[32] The replacement of these hazardous solvents with NADES provided a more eco-friendly and safer method from the GAC point of view, while not compromising the analytical method performance. However, no metrics were used to evaluate the greenness of the method. Sereshti *et al*. developed a novel micro QuEChERS/GC-MS method for the multi-class analysis of pesticide residues in cereal flour samples. The authors synthesized a nanofiber from a polymerizable eutectic solvent composed of poly (2-hydroxyethyl methacrylate):1tetradecanol and polyamide 6 and applied it for the first time as a sorbent in micro solid phase step extraction. The proposed method reduced the amount of sample and the consumption of organic solvents (21%) needed for analysis while keeping the analytical performance similar to the methods referenced in the study. In addition, the proposed method was evaluated by two metrics, Complex GAPI, and Analytical Eco-Scale with a score of 72.[33] This method is a good example of how green strategies such as miniaturization, the use of green materials, and the reduction of solvent consumption can be combined to obtain a greener method without compromising analytical efficiency.

Miniaturization of instruments and reduction of the analytical scale of operations and increasing the efficiency of sample preparation with increased temperature and/or pressure or the use of microwaves and ultrasound techniques are also alternatives to make the process greener.[34,35]

Methods with online sample preparation have also gained prominence in recent years due to reduced analysis time, manual operations, and sample quantity compared to offline sample preparation techniques.[36] The use of analytical methods that integrate the steps of sample preparation, separation, and detection reduces the number of reagents needed for the analysis, increases analyst safety, and minimizes the migration of solvents into the environment.[37] In addition, because online methods are automated, they ensure better accuracy and sensitivity, as well as reduce analysis time, meeting at least 4 of the 12 principles of the GAC.[38] However, as underlined by RGB 12 concepts, simply implementing these measures won't be enough to convince the industry and academia to follow GAC principles. The selected solutions must also be financially viable, primarily in terms of cost and time effectiveness and operational simplicity. In addition, the GAC principles and practices must be encouraged and regulated by specific legislations to further drive the adherence of industry and academia to GAC.

In this context, Jin *et al*. performed a study comparing the liquid-liquid extraction method and liquid chromatography coupled to mass spectrometry (LLE-LC-MS/MS) with the online extraction method with supercritical fluid combined with fluid chromatography supercritical coupled to mass spectrometry (SFE-SFC-MS/MS), for the determination of lipids in rat brain tissues.[39] The authors optimized the extraction by performing only 17 experiments using the Box-Behnken experimental design and the response surface methodology. As a result, the proposed SFE-SFC-MS/MS online method provided excellent performance compared to the LLE-LC-MS/MS offline method. The use of the design of experiments in extraction contemplated the reduction in the number of experiments and consequently saved time, energy, and reagents, while the online extraction system complied with the principles of GAC by integrating sample preparation and analysis, automation, and as consequence fewer manual steps were required, increasing operator safety and saving time and energy. All requirements met according to the GAC were proven by the AGREE algorithm by comparing the score of each method 0.75 and 0.49, for the online method SFE-SFC-MS/MS and the offline method LLE- LC-MS/MS, respectively.

Zhang *et al*. also developed an automated method combining online Solid Phase Extraction (SPE) and bidimensional liquid chromatography (LC-LC) for the simultaneous determination of vitamin A, D, and 4 vitamin E homologs in foodstuffs. In this method, the target analytes were released from their lipoprotein-coated state after saponification. Then, the saponified solution was injected directly into the system built by combining SPE (PLRP-S column) online and 2D-LC for pre-concentration, purification, separation, and quantification.[40] Vitamin A and vitamin E homologs were separated in the first column with pentafluoro phenyl (PFP) stationary phase and the separation of vitamin D was performed in the second column composed of polycyclic aromatic hydrocarbons (PAH). Evaluation of the results showed that this method not only fully met the requirements of analysis of vitamins A, D, and E in fortified foods or dietary supplements, but also had significant advantages over conventional liquid chromatography methods with ultraviolet detection (LC-UV) or LC-MS/MS in terms of method repeatability and recovery. Due to the simplification of sample preparation, the analysis efficiency has been significantly improved and the analytical cost has also been reduced. In addition, it is a green method since it avoids the use of pentane or other organic reagents. Therefore, the proposed method covered the six main trends of current analytical methods which are simplification, speed, cost and waste reduction, automation, and safety. However, no metric was used to verify the green aspects of the method.

Direct chromatographic analysis

In direct chromatographic analysis, the sample is introduced into the chromatograph without sample preparation to reduce the consumption of reagents and energy. However, methodologies of direct analysis involving complex matrices can damage the chromatographic columns due to the sample components that do not elute from the column. In general, the introduction of aqueous samples in GC capillary columns is not recommended as water and polar solvents can cause column bleed and can affect the performance of the column when samples are injected in the mode on-column resulting in a negative impact on the sensibility of the detector. An alternative to circumvent these limitations is the use of injectors with programmed temperature vaporization (PTV), the application of liners filled with sorbent material, or the installation of deactivated columns before the chromatographic columns. Temperature is one of the most important parameters that can be controlled in GC and its programming is widely used to improve the detection limit or peak symmetry, and results in a significantly reduced analysis time. This parameter can have an even greater positive environmental impact with the implementation of low thermal mass (LTM) technology. This technology utilizes an LTM column module combining a fused silica capillary column with heating and temperature sensing components wrapped around the capillary. Due to the small size of the system and its low heat capacity, the increase in capillary temperature requires smaller amounts of heat and therefore less energy compared to conventional GC ovens.[4] The energy consumed using LTM technology is approximately 1% of the energy consumed by a conventional GC. In addition, it is possible to program temperatures with a rate of 1800 ºC min^{-1} heating and shorter cool-down times, resulting in reduced analysis times.[41]

Direct injection of aqueous samples can be performed in LC systems as long as the sample is filtered to prevent tube obstruction and damage to the chromatography column. As recommended by GAC, this approach involves minimal sample pre-treatment since most applications require only one dilution step with organic solvent and filtration before chromatographic analysis, ensuring less exposure of the analyst to these solvents. From this perspective, Dias *et al*. developed a fully validated ultra-high performance liquid chromatography-mass spectrometry (UHPLC-MS/MS) method for the simultaneous determination of 162 pesticides and 10 mycotoxins in wine samples with minimal sample pretreatment.[42] Another example of direct chromatographic analysis is proposed by Restrepo-Vieira *et al*., which developed and validated a UHPLC-MS/MS method with direct injection for the analysis of psychopharmaceuticals and illicit drugs in wastewater from Australia. The authors used 15 deuterated analytical standards to circumvent matrix effects and thereby reduced the analysis time, the number of consumables, and the production of residues when compared to methods using the SPE technique.[43] Nevertheless, the use of deuterated analytical

standards is not interesting from the economical point of view. According to GAC, these examples of direct chromatographic analysis provide simpler methods with less reagent consumption and less exposure of the analyst to hazardous organic solvents, as well as analytical performance comparable to methods that use pre-concentration and extraction techniques.

Replacement of toxic mobile phase solvents

The conventional mobile phase composition of Reversed Phase Liquid Chromatography (RPLC) consists of mixtures of acetonitrile or methanol in water. Both acetonitrile and methanol are toxic solvents and disposal of acetonitrile is expensive. Thus, these solvents must be replaced by greener alternatives such as water, acetone, and ethanol.[44,45] Acetone has already been explored as a solvent to replace acetonitrile as a mobile phase in RPLC for the separation of peptides without any equipment modification.[46,47] Recently, two studies on the solvation and retention properties of acetone have highlighted its potential to be employed as mobile in columns with typical octadecyl siloxane-bonded silica, octyl siloxane-bonded silica, and biphenyl siloxane-bonded silica phases.[48,49] The only disadvantage of using acetone as a mobile phase in RPLC is the UV cut-off at 330 nm which makes it impractical to use UV-based detectors. However, for liquid chromatography coupled with evaporative light scattering detection, mass spectrometry, condensation nucleation light scattering detection, and charged aerosol detection, the use of acetone is a promising alternative. Ethanol was also explored as a mobile phase in RPLC applications. Dogan *et al.* have demonstrated that the analysis of drugs such as paracetamol and famotidine can be performed by green chromatography techniques, using a mobile phase based on ethanol-water, without losing any chromatographic performance and fulfilling all the requirements of the validation process.[50] Ethanol water-based mobile phase was also used in the determination of eight water-soluble vitamins in cosmetics.[51] Organic solvents can also be replaced by supercritical fluids, and superheated water,[30] in this case, there is a change in the chromatographic technique. The analysis is performed on appropriate SFC equipment such as the ACQUITY UltraPerfornamance Convergence Chromatography (UPC²) (Waters), the 1260 Infinity II SFC/UHPLCA Hybrid System (Agilent), and the Nexera UC (Shimadzu). CO_2 is the gas most used supercritical fluid due to its properties such as non-inflammability, low critical pressure (7,38 MPa), and temperature (31 ºC).[52] Besides that, CO_2 is an industrial subproduct of renewable resources. The supercritical CO_2 as a mobile phase in SFC exhibits the advantage of having solvent properties similar to hydrocarbons derived from petrochemical products, giving a more environmentally friendly choice to commonly used normal phase solvents, e.g., hexane, heptane, or chlorinated solvents. In addition, supercritical CO_2 has low viscosity, which allows high flow rates and faster separations, and has high diffusivity resulting in more efficient separations, reduced organic solvent consumption, and reduced cost in waste disposal, since CO_2 has a low environmental impact.[53] However, because of its non-polar character, it is not possible to employ pure CO_2 in samples containing polar analytes. In such cases, the addition of organic modifiers such as methanol or ethanol is necessary. The use of CO_2 with a higher percentage of organic modifiers can be referred to as enhanced fluidity liquid chromatography (EFLC), which has similar advantages to SFC. Following this, Lu *et al*. developed a fast, efficient, and green SFC method for the separation of actinomycin D and X_2 within less than 25 minutes. The proposed method allowed a reduction in the consumption of hazardous organic solvents since CO_2 and ethanol (80:20) were used as mobile phase instead of water and acetonitrile and the analysis time was also reduced by approximately 42% compared to the reference method presented in the study.[54]

Another green alternative is micellar liquid chromatography (MLC), an RPLC mode with a mobile phase consisting of an aqueous surfactant solution above its critical micellar concentration (CMC). The idea of using aqueous pure micellar solutions as mobile phases in RPLC is very attractive due to lower cost and toxicity, and reduced environmental impact. In practice, however, the addition of a small amount of organic solvent to the micellar solution is necessary to achieve retention in practical time windows and improve peak efficiency and resolution. For this reason, MLC methods have become a trending topic in recent years when it comes to GAC.[55,56,57] As an example, Ramezani *et al*. reported an eco-friendly MLC method using

a NADES solvent as a modifier of the mobile phase for melamine analysis in milk. The developed MLC revealed that the modified mobile phase composed of sodium dodecyl sulfate, NADES, and glacial acetic acid, significantly reduced the peak broadening and the melamine retention time resulting in an increased chromatographic resolution. In addition, the matrix effects analysis shows that the proposed method has the potential for direct injection analysis of the diluted milk samples.[58] The green potential of MLC methods is further highlighted by the study of Al-Shaalan *et al*. in which a modified green MLC method was used for the determination of residues of imidocarb dipropionate in food samples employing a NADES solvent as a modifier and direct sample injection. Furthermore, this study showed a complete evaluation of the greenness of the proposed method and the obtained reference methods using the Complex GAPI, AGREE, and RGB model tools. Comparing the results of the evaluations, the proposed method was superior to all the reference methods presented, with values of 0.78 for AGREE and 90.8 for the RGB model.[59]

Multidimensional chromatography

The use of multidimensional chromatography can be considered a green strategy if used with green modulators. There are two types of multidimensional chromatography, the comprehensive one (GCxGC or LCxLC) in which all eluent from the first columns is transferred to the second column, and the heart cutting (GC-GC or LC-LC) in which only some fractions of the eluent are transferred from the first to the second column.[60] In two-dimensional chromatography, two orthogonal chromatographic columns are used, connected by a modulator, which transfers the eluent from the first to the second column.[61] Due to the presence of two columns, it is possible to obtain a better resolution and lower detection limits with analysis time and reagent consumption similar to one-dimensional chromatography.[62] Furthermore, due to the better peak capacity, the use of GCxGC or LCxLC allows for better separations even in complex samples. Although GCxGC is a relatively green technique, there is still the possibility of making it more environmentally friendly by replacing thermal modulators with flow modulators, which operate simply and cheaply and do not require the use of cryogenic gases.[63] However, the use of flow modulators leads to low sensitivity due to the limited modulation period.[44] The advantages of using the LCxLC include the prevention of sample loss and contamination and the possibility of automation. On the other hand, the volume of data generated can be large and its treatment requires chemometric tools as well as the optimization of operating conditions.[64] In addition, the cost of multidimensional chromatographic systems is frequently higher than that of one-dimensional chromatography.[65]

Miniaturization of chromatographic systems

The application of a miniaturized system is usually related to the reduction of consumables, energy, and reagents needed to perform the analysis. The reduction of column dimensions and particle size reduces mobile phase flow rate and so the solvent or gas consumption. Miniaturization results in lower costs and lower production of waste, being more cost-effective and eco-friendlier. It is also possible to perform faster analysis and improve the sensibility of the method because the analytes are less soluble in the mobile phase. This strategy is very useful in forensics sciences and biomedicine, where large sample volumes are not always available. The miniaturization of all parts of a chromatographic system can result in portable systems which can be applied online, at-line, and on-site analysis, making the method greener.

The miniaturization of GC systems enables rapid in situ analysis of volatile organic compounds (VOC) for environmental protection, industrial monitoring, and toxicology.[66] The Lab-on-a-chip is another miniaturization approach that can be applied to chromatography systems. These miniaturized systems are manufactured on a chip platform (microfluidic devices) and have unique advantages including low maintenance cost, large-scale manufacturing, fast analysis, the need for very small amounts of solvents and samples, high-resolution detection, and excellent portability.[67] Recent advances related to sustainability in GC have focused on the miniaturization of specific pieces of equipment such as the preparation of micro columns and micro detectors. This field was made possible by parallel advances in certain processes and technologies of additive manufacturing, also known as 3D printing, microelectromechanical systems

(MEMS), lithography, and etching techniques.[68] Hsieh and Kim demonstrated the separation of a pair of structural isomers (isopentane and pentane) in a μGC system with a circulatory loop consisting of two 25 cm open tubular micro columns while operating under a minimum pressure of <10 kPa available in current technology of chip-scale micropump. This demonstration was possible by extending the column length from 0.5 m (two 25 cm columns) to 12.5 meters, corresponding to 25 cycles using the circulatory column system.[69]

The achieved effective column length of 12.5 meters is the longest ever used by any μGC system and presented an alternative to the limitations of chromatography columns related to this parameter in μGC. Furthermore, the described microscale system enabled rapid and sustainable analysis of complex samples with minimal sample volume and without entailing additional energy and carrier gas consumption, comprising GAC principles 2, 5, and 7. Despite recent developments in 3D printing, the peaks showed broadening due to the 0.6 μL dead volume at the valve connections affecting the separation resolution. Thus, advances in this field are needed to develop instruments free of these limitations.

In another study employing a microfabricated gas chromatograph, Whiting *et al*. described the development and evaluation of a comprehensive two-dimensional chromatography (μGC x μGC) microsystem consisting of micro columns, a flame ionization detector (FID), and a nanoelectromechanical resonator system (NEMS) also used as a detector.[70] With this system, it was possible to separate a mixture of 29 polar compounds covering a boiling point range from 46 to 253 °C on a pair of microfabricated columns using a Staiger valve manifold in less than 7 seconds. Thus, the μGC x μGC-NEMS system allowed ultra-fast analysis with low energy and carrier gas consumption due to the use of greener modulators such as the pneumatic stop-flow modulator, showing that the two strategies employed in combination, miniaturization, and two-dimensional chromatography, made the method greener by meeting some of the principles of GAC.

To overcome the above-mentioned obstacles, Li *et al.* reported the development and characterization of a microfabricated column containing phosphonium ionic liquid (μIL) as the stationary phase and demonstrated the separation of polar and non-polar compounds using this column by analyzing alcohols, chloroalkanes, aromatics, aldehydes, fatty acid methyl esters, and alkanes.[66] The use of IL as the stationary phase provided robustness to the column concerning the presence of oxygen, humidity, and temperature, allowing the use of synthetic air as carrier gas and high temperatures during the separations. Consequently, faster and more sustainable separations were obtained without the need for additional accessories.

The reduction in analysis time is not only restricted to miniaturizations, Fialkov *et al.* obtained separations with complete analysis cycle times of less than 1 minute by employing for the first time LP-GC coupled to MS with low thermal mass resistive heating due to the use of LTM technology for the rapid increase temperature and cooling of the capillary column.[71] An example of recent advances in LC miniaturization is the study carried out by Peretzki and Belder. In this study, the authors presented a chip-integrated approach to post-column segmentation of Normal Phase Liquid Chromatography (NPLC), obtained by integrating a chiral NP-chip-HPLC column, a Flow focusing droplets, and a segmented flow channel on a single glass microfluidic chip.[72] This allowed continuous segmentation of the eluent into droplets that are collected and transported through a continuous immiscible phase. The combination of NP-chip-HPLC and droplet-based microfluidics also allowed fractionation and conservation of chromatographic runs for other picoliter-scale downstream processes. With this, the authors tested three microfluidic devices with different structural arrangements for the separation of the (R)- and (S)- trifluoro anthryl ethanol isomers under the same elution conditions (0.5 μL min^{-1} n-heptane/2-propanol 95/5 (v/v)) and continuous phase (0.10 μL min^{-1} ethylene glycol) and the sample volume inject was very low (5 μL). The separation of the isomers took less than 5 minutes and the peak widths at half height were approximately 0.17 min (isomer R) and 0.22 min (isomer S) for all three devices. Furthermore, the efficiency was in the range of 27.400 to 41.600 for the three devices tested. The proposed system combined the advantages of minimized reagent consumption, dead volume-free interconnections, high separation speed and performance, and the possibility of integrating additional processes from chip-HPLC with the benefits of droplet-based microfluidics such as avoiding

peak distortion post column. As a result, the system complies with GAC principles and allows coupling with other detectors after chromatographic separation, expanding the application of the system.

CONCLUSIONS

The use of miniaturized, online, or at-line sample preparation techniques, or the use of green solvents is essential to improve the green aspects of chromatographic methods and to conform to GAC principles, especially for GC, where few modifications in separation conditions are possible.

The advances made in the miniaturization of chromatographic techniques have sought to overcome the limitations presented by system connections, microcolumn fabrication, and micro detectors. Such advances were possible due to the development of additive manufacturing techniques, but most published works present prototypes of micro chromatographic systems with many factors to be improved, such as band broadening due to the presence of large dead volume. Within miniaturization, LOC-based chromatographs are the most promising systems due to the potential to integrate multiple functionalities on a single chip, minimal reagent and power consumption, fast separations and good performance, and the possibility of manufacturing these systems on a large scale, resulting in low manufacturing cost.

However, more methods should be developed to evaluate which applications are possible and if they are repeatable, and how durable they are as instruments, since the low cost of large-scale production may become an environmental problem if the durability of these systems is short. In addition, no metrics were applied in the miniaturization studies. The use of methods and techniques that use green solvents as a mobile phase, such as MLC and SFC, for example, should be further explored for the replacement of traditional LC methods. As these methods drastically reduce the environmental and occupational hazards related to the use of organic solvents and consequently make the method more economical.

Most papers that mentioned the development of greener methods did not evaluate the methods or evaluated the methods using qualitative metrics. It is important to consider that the green features claimed in these approaches should be supported by suitable green metrics. The AGREE algorithm is the most suitable metric for evaluating method greenness as it quantitatively covers the 12 principles of GAC. However, evaluating only the green aspect of the method is not sufficient for the method to be considered suitable for its intended use. Therefore, the developed methods must be evaluated by metrics that encompass the three pillars of sustainable development: the green aspects, analytical performance, and economic viability as proposed by the RGB 12 metric.

Conflicts of interest

The authors declare no conflict of interest of any kind.

Acknowledgements

Authors would like to thank “Instituto Nacional Ciencia e Tecnlogia de Bioanalitica” (INCT-Bio) and CAPES (Finance code 001).

REFERENCES

(1) Warner, J. C.; Cannon, A. S.; Dye, K. M. Green Chemistry. *Environmental Impact Assessment Review* **2004**, *24* (7–8), 775–799. https://doi.org/10.1016/j.eiar.2004.06.006

(2) de Marco, B. A.; Rechelo, B. S.; Tótoli, E. G.; Kogawa, A. C.; Salgado, H. R. N. Evolution of Green Chemistry and Its Multidimensional Impacts: A Review. *Saudi Pharmaceutical Journal* **2019**, *27* (1), 1–8. https://doi.org/10.1016/j.jsps.2018.07.011

(3) Tundo, P.; Anastas, P.; Black, D. S.; Breen, J.; Collins, T.; Memoli, S.; Miyamoto, J.; Polyakoff, M.; Tumas, W. Synthetic Pathways and Processes in Green Chemistry. Introductory Overview. *Pure Appl. Chem.* **2000**, *72* (7), 1207–1228. https://doi.org/10.1351/pac200072071207

(4) Płotka, J.; Tobiszewski, M.; Maria, A.; Kupska, M.; Górecki, T.; Namie, J. Green Chromatography. *J. Chromatogr. A* **2013**, *1307*, 1–20. https://doi.org/10.1016/j.chroma.2013.07.099

(5) Anastas, P. T. Green Chemistry and the Role of Analytical Methodology Development. *Crit. Rev. Anal. Chem.* **1999**, *29* (3), 167–175. https://doi.org/10.1080/10408349891199356
(6) Gałuszka, A.; Migaszewski, Z.; Namieśnik, J. The 12 Principles of Green Analytical Chemistry and the SIGNIFICANCE Mnemonic of Green Analytical Practices. *TrAC, Trends Anal. Chem.* **2013**, *50*, 78–84. https://doi.org/10.1016/j.trac.2013.04.010
(7) Armenta, S.; Guardia, M. De. Green Chromatography for the Analysis of Foods of Animal Origin. *TrAC, Trends Anal. Chem.* **2016**, *80*, 517–530. https://doi.org/10.1016/j.trac.2015.06.012
(8) Korany, M. A.; Mahgoub, H.; Haggag, R. S.; Ragab, M. A. A.; Elmallah, O. A. Green Chemistry: Analytical and Chromatography. *J. Liq. Chromatogr. Relat. Technol.* **2017**, *40* (16), 839–852. https://doi.org/10.1080/10826076.2017.1373672
(9) Welch, C. J.; Wu, N.; Biba, M.; Hartman, R.; Brkovic, T.; Gong, X.; Helmy, R.; Schafer, W.; Cuff, J.; Pirzada, Z.; Zhou, L. Greening Analytical Chromatography. *TrAC, Trends Anal. Chem.* **2010**, *29* (7), 667–680. https://doi.org/10.1016/j.trac.2010.03.008
(10) Habib, A.; Mabrouk, M. M.; Fekry, M.; Mansour, F. R. Glycerol as a Novel Green Mobile Phase Modifier for Reversed Phase Liquid Chromatography. *Microchem. J.* **2021**, *169*, 106587. https://doi.org/10.1016/j.microc.2021.106587
(11) Habib, A.; Mabrouk, M. M.; Fekry, M.; Mansour, F. R. Glycerol as a New Mobile Phase Modifier for Green Liquid Chromatographic Determination of Ascorbic Acid and Glutathione in Pharmaceutical Tablets. *J. Pharm. Biomed. Anal.* **2022**, *219*, 114870. https://doi.org/10.1016/j.jpba.2022.114870
(12) Poe, D. P. *Theory of Supercritical Fluid Chromatography*; Elsevier Inc., 2017. https://doi.org/10.1016/B978-0-12-809207-1.00002-1
(13) Losacco, G. L.; Veuthey, J. L.; Guillarme, D. Metamorphosis of Supercritical Fluid Chromatography: A Viable Tool for the Analysis of Polar Compounds? *TrAC, Trends Anal. Chem.* **2021**, *141*, 116304. https://doi.org/10.1016/j.trac.2021.116304
(14) Carasek, E.; Bernardi, G.; Morelli, D.; Merib, J. Sustainable Green Solvents for Microextraction Techniques: Recent Developments and Applications. *J. Chromatogr. A* **2021**, *1640*, 461944. https://doi.org/10.1016/j.chroma.2021.461944
(15) Pacheco-Fernández, I.; Rentero, M.; Ayala, J. H.; Pasán, J.; Pino, V. Green Solid-Phase Microextraction Fiber Coating Based on the Metal-Organic Framework CIM-80(Al): Analytical Performance Evaluation in Direct Immersion and Headspace Using Gas Chromatography and Mass Spectrometry for the Analysis of Water, Urine and Brewed. *Anal. Chim. Acta* **2020**, *1133*, 137–149. https://doi.org/10.1016/j.aca.2020.08.009
(16) Kanu, A. B. Recent Developments in Sample Preparation Techniques Combined with High-Performance Liquid Chromatography: A Critical Review. *J. Chromatogr. A* **2021**, *1654*, 462444. https://doi.org/10.1016/j.chroma.2021.462444
(17) Keith, L. H.; Gron, L. U.; Young, J. L. Green Analytical Methodologies. *Chemical Reviews* **2007**, *107* (6), 2695–2708. https://doi.org/10.1021/cr068359e
(18) Gałuszka, A.; Migaszewski, Z. M.; Konieczka, P.; Namieśnik, J. Analytical Eco-Scale for Assessing the Greenness of Analytical Procedures. *TrAC, Trends Anal. Chem*. **2012**, *37*, 61–72. https://doi.org/10.1016/j.trac.2012.03.013
(19) Płotka-Wasylka, J. A New Tool for the Evaluation of the Analytical Procedure: Green Analytical Procedure Index. *Talanta* **2018**, *181*, 204–209. https://doi.org/10.1016/j.talanta.2018.01.013
(20) Pena-Pereira, F.; Wojnowski, W.; Tobiszewski, M. AGREE - Analytical GREEnness Metric Approach and Software. *Anal. Chem.* **2020**, *92* (14), 10076–10082. https://doi.org/10.1021/acs.analchem.0c01887
(21) Nowak, P. M.; Kościelniak, P. What Color Is Your Method? Adaptation of the Rgb Additive Color Model to Analytical Method Evaluation. *Anal. Chem*. **2019**, *91* (16), 10343–10352. https://doi.org/10.1021/acs.analchem.9b01872

(22) Nowak, P. M.; Wietecha-Posłuszny, R.; Pawliszyn, J. White Analytical Chemistry: An Approach to Reconcile the Principles of Green Analytical Chemistry and Functionality. *TrAC, Trends Anal. Chem.* **2021**, *138*. https://doi.org/10.1016/j.trac.2021.116223
(23) Alampanos, V.; Samanidou, V. Current Trends in Green Sample Preparation before Liquid Chromatographic Bioanalysis. *Curr. Opin. Green Sustainable Chem.* **2021**, *31*, 100499. https://doi.org/10.1016/j.cogsc.2021.100499
(24) Bazel, Y.; Rečlo, M.; Chubirka, Y. Switchable Hydrophilicity Solvents in Analytical Chemistry. Five Years of Achievements. *Microchem. J.* **2020**, *157*, 105115. https://doi.org/10.1016/j.microc.2020.105115
(25) Karayaka, S.; Chormey, D. S.; Fırat, M.; Bakırdere, S. Determination of Endocrine Disruptive Phenolic Compounds by Gas Chromatography Mass Spectrometry after Multivariate Optimization of Switchable Liquid-Liquid Microextraction and Assessment of Green Profile. *Chemosphere* **2019**, *235*, 205–210. https://doi.org/10.1016/j.chemosphere.2019.06.079
(26) Hassan, M.; Alshana, U. Switchable-Hydrophilicity Solvent Liquid–Liquid Microextraction of Non-Steroidal Anti-Inflammatory Drugs from Biological Fluids Prior to HPLC-DAD Determination. *J. Pharm. Biomed. Anal.* **2019**, *174*, 509–517. https://doi.org/10.1016/j.jpba.2019.06.023
(27) Shahvandi, S. K.; Banitaba, M. H.; Ahmar, H. Development of a New PH Assisted Homogeneous Liquid-Liquid Microextraction by a Solvent with Switchable Hydrophilicity: Application for GC-MS Determination of Methamphetamine. *Talanta* **2018**, *184*, 103–108. https://doi.org/10.1016/j.talanta.2018.02.115
(28) Solaesa, A. G.; Fernandes, J. O.; Sanz, M. T.; Benito-Román, Ó.; Cunha, S. C. Green Determination of Brominated Flame Retardants and Organochloride Pollutants in Fish Oils by Vortex Assisted Liquid-Liquid Microextraction and Gas Chromatography-Tandem Mass Spectrometry. *Talanta* **2019**, *195*, 251–257. https://doi.org/10.1016/j.talanta.2018.11.048
(29) Nazraz, M.; Yamini, Y.; Ramezani, A. M.; Dinmohammadpour, Z. Deep Eutectic Solvent Dependent Carbon Dioxide Switching as a Homogeneous Extracting Solvent in Liquid-Liquid Microextraction. *J. Chromatogr. A* **2021**, *1636*, 461756. https://doi.org/10.1016/j.chroma.2020.461756
(30) Al-Khateeb, L. A.; Dahas, F. A. Green Method Development Approach of Superheated Water Liquid Chromatography for Separation and Trace Determination of Non-Steroidal Anti-Inflammatory Compounds in Pharmaceutical and Water Samples and Their Extraction. *Arabian J. Chem.* **2021**, *14* (7), 103226. https://doi.org/10.1016/j.arabjc.2021.103226
(31) Lebedinets, S.; Vakh, C.; Cherkashina, K.; Pochivalov, A.; Moskvin, L.; Bulatov, A. Stir Membrane Liquid Phase Microextraction of Tetracyclines Using Switchable Hydrophilicity Solvents Followed by High-Performance Liquid Chromatography. *J. Chromatogr. A* **2020**, *1615*, 460743. https://doi.org/10.1016/j.chroma.2019.460743
(32) Wang, M.; Fang, S.; Liang, X. Natural Deep Eutectic Solvents as Eco-Friendly and Sustainable Dilution Medium for the Determination of Residual Organic Solvents in Pharmaceuticals with Static Headspace-Gas Chromatography. *J. Pharm. Biomed. Anal.* **2018**, *158*, 262–268. https://doi.org/10.1016/j.jpba.2018.06.002
(33) Sereshti, H.; Mohammadi, Z.; Soltani, S.; Najarzadekan, H. A Green Miniaturized QuEChERS Based on an Electrospun Nanofibrous Polymeric Deep Eutectic Solvent Coupled to Gas Chromatography-Mass Spectrometry for Analysis of Multiclass Pesticide Residues in Cereal Flour Samples. *J. Mol. Liq.* **2022**, *364*, 120077. https://doi.org/10.1016/j.molliq.2022.120077
(34) Yuan, Y.; Han, Y.; Han, D.; Yang, C.; Yan, H. Ultrasound-Assisted Dispersive-Filter Extraction Coupled with High-Performance Liquid Chromatography: A Rapid Miniaturized Method for the Determination of Phenylurea Pesticides in Vegetables and Fruits. *Food Control* **2020**, *118*, 107417. https://doi.org/10.1016/j.foodcont.2020.107417
(35) Naccarato, A.; Tassone, A.; Moretti, S.; Elliani, R.; Sprovieri, F.; Pirrone, N.; Tagarelli, A. A Green Approach for Organophosphate Ester Determination in Airborne Particulate Matter: Microwave-Assisted Extraction Using Hydroalcoholic Mixture Coupled with Solid-Phase Microextraction Gas Chromatography-Tandem Mass Spectrometry. *Talanta* **2018**, *189*, 657–665. https://doi.org/10.1016/j.talanta.2018.07.077

(36) Zoccali, M.; Russo, M.; Rita, M.; Camillo, T.; Salafia, F.; Tranchida, P. Q.; Dugo, P.; Mondello, L. On-Line Coupling of Supercritical Fluid Extraction with Enantioselective Supercritical Fluid Chromatography-Triple Quadrupole Mass Spectrometry for the Determination of Chiral Pesticides in Hemp Seeds: A Proof-of-Principle Study. *Food Chemistry* **2021**, 131418. https://doi.org/10.1016/j.foodchem.2021.131418

(37) Cruz, J. C.; de Souza, I. D.; Grecco, C. F.; Figueiredo, E. C.; Queiroz, M. E. C. Recent Advances in Column Switching High-Performance Liquid Chromatography for Bioanalysis. *Sustainable Chem. Pharm.* **2021**, *21*. https://doi.org/10.1016/j.scp.2021.100431

(38) Wicker, A. P.; Tanaka, K.; Nishimura, M.; Chen, V.; Ogura, T.; Hedgepeth, W.; Schug, K. A. Multivariate Approach to On-Line Supercritical Fluid Extraction-Supercritical Fluid Chromatography-Mass Spectrometry Method Development. *Anal. Chim. Acta* **2020**, *1127*, 282–294. https://doi.org/10.1016/j.aca.2020.04.068

(39) Yang, J.; Liu, D.; Jin, W.; Zhong, Q.; Zhou, T. A Green and Efficient Pseudotargeted Lipidomics Method for the Study of Depression Based on Ultra-High Performance Supercritical Fluid Chromatography-Tandem Mass Spectrometry. *J. Pharm. Biomed. Anal.* **2021**, *192*, 113646. https://doi.org/10.1016/j.jpba.2020.113646

(40) Zhang, Y.; Lin, Y.; Yang, X.; Chen, G.; Li, L.; Ma, Y.; Liang-Schenkelberg, J. Fast Determination of Vitamin A, Vitamin D and Vitamin E in Food by Online SPE Combined with Heart-Cutting Two Dimensional Liquid Chromatography. *J. Food Compos. Anal.* **2021**, *101*, 103983. https://doi.org/10.1016/j.jfca.2021.103983

(41) Armenta, S.; Esteve-turrillas, F. A.; Garrigues, S.; Guardia, M. De. *Green Analytical Chemistry*; Elsevier, 2020. https://doi.org/10.1016/B978-0-08-100596-5.22800-X

(42) Dias, J. V.; Nunes, M. da G. P.; Pizzutti, I. R.; Reichert, B.; Jung, A. A.; Cardoso, C. D. Simultaneous Determination of Pesticides and Mycotoxins in Wine by Direct Injection and Liquid Chromatography-Tandem Mass Spectrometry Analysis. *Food Chemistry* **2019**, *293*, 83–91. https://doi.org/10.1016/j.foodchem.2019.04.088

(43) Restrepo-Vieira, L. H.; Busetti, F.; Linge, K. L.; Joll, C. A. Development and Validation of a Direct Injection Liquid Chromatography-Tandem Mass Spectrometry Method for the Analysis of Illicit Drugs and Psychopharmaceuticals in Wastewater. *J. Chromatogr. A* **2022**, *1685*, 463562. https://doi.org/10.1016/j.chroma.2022.463562

(44) Shaaban, H.; Mostafa, A.; Go, T. Green Gas and Liquid Capillary Chromatography. In: Pena-Pereira, F., Tobiszewski, M. (Eds). *The Application of Green Solvents in Separation Process*. Elsevier, 2017, pp 453–482. https://doi.org/10.1016/B978-0-12-805297-6.00015-2

(45) Habib, A.; Mabrouk, M. M.; Fekry, M.; Mansour, F. R. Glycerol as a Novel Green Mobile Phase Modifier for Reversed Phase Liquid Chromatography. *Microchem. J.* **2021**, *169*, 106587. https://doi.org/10.1016/j.microc.2021.106587

(46) Keppel, T. R.; Jacques, M. E.; Wels, D. D. The Use of Acetone as a Substitute for Acetonitrile in Analysis of Peptides by Liqid Chromatography/Electrospray Ionization Mass Spectometry. *Rapid Commun. Mass Spectrom.* **2010**, *24*, 6–10. https://doi.org/10.1002/rcm

(47) Capriotti, A. L.; Cavaliere, C.; Foglia, P.; Samperi, R.; Stampachiacchiere, S.; Ventura, S.; Laganà, A. Ultra-High-Performance Liquid Chromatography-Tandem Mass Spectrometry for the Analysis of Free and Conjugated Natural Estrogens in Cow Milk without Deconjugation. *Anal. Bioanal. Chem.* **2015**, *407* (6), 1706–1719. https://doi.org/10.1007/s00216-014-8398-z

(48) Atapattu, S. N. Solvation Properties of Acetone-Water Mobile Phases in Reversed-Phase Liquid Chromatography. *J. Chromatogr. A* **2021**, *1650*, 462252. https://doi.org/10.1016/j.chroma.2021.462252

(49) Atapattu, S. N. Retention Properties of Acetone-Water Mobile Phases on a Biphenylsiloxane-Bonded Silica Stationary Phase in Reversed-Phase Liquid Chromatography. *J. Sep. Sci.* **2022**, *45* (9), 1487–1492. https://doi.org/10.1002/jssc.202200033

(50) Dogan, A.; Eylem, C. C.; Akduman, N. E. B. Application of Green Methodology to Pharmaceutical Analysis Using Eco-Friendly Ethanol-Water Mobile Phases. *Microchem. J.* **2020**, *157*, 104895. https://doi.org/10.1016/j.microc.2020.104895
(51) Vállez-gomis, V.; Peris-pastor, G.; Benedé, J. L.; Chisvert, A.; Salvador, A. Green Determination of Eight Water-Soluble B Vitamins in Cosmetic Products by Liquid Chromatography with Ultraviolet Detection. *J. Pharm. Biomed. Anal*. **2021**, *205*, 114308. https://doi.org/10.1016/j.jpba.2021.114308
(52) Nováková, L.; Grand-Guillaume Perrenoud, A.; Francois, I.; West, C.; Lesellier, E.; Guillarme, D. Modern Analytical Supercritical Fluid Chromatography Using Columns Packed with Sub-2μm Particles: A Tutorial. *Anal. Chim. Acta* **2014**, *824*, 18–35. https://doi.org/10.1016/j.aca.2014.03.034
(53) Lemasson, E.; Bertin, S.; West, C. Use and Practice of Achiral and Chiral Supercritical Fluid Chromatography in Pharmaceutical Analysis and Purification. *J. Sep. Sci.* **2016**, *39* (1), 212–233. https://doi.org/10.1002/jssc.201501062
(54) Lu, X.; Du, N.; Zhang, D.; Zhou, X.; Li, X.; Ju, J. Efficient , Green , and Rapid Strategy for Separating Actinomycin D and X 2 Using Supercritical Fluid Chromatography. *J. Pharm. Biomed. Anal*. **2021**, *195*, 113835. https://doi.org/10.1016/j.jpba.2020.113835
(55) Ramezani, A. M.; Absalan, G.; Ahmadi, R. Green-Modified Micellar Liquid Chromatography for Isocratic Isolation of Some Cardiovascular Drugs with Different Polarities through Experimental Design Approach. *Anal. Chim. Acta* **2018**, *1010*, 76–85. https://doi.org/10.1016/j.aca.2017.12.021
(56) Ramezani, A. M.; Absalan, G. Employment of a Natural Deep Eutectic Solvent as a Sustainable Mobile Phase Additive for Improving the Isolation of Four Crucial Cardiovascular Drugs by Micellar Liquid Chromatography. *J. Pharm. Biomed. Anal.* **2020**, *186*, 113259. https://doi.org/10.1016/j.jpba.2020.113259
(57) Bhamdare, H.; Pahade, P.; Bose, D.; Durgbanshi, A.; Carda-Broch, S.; Peris-Vicente, J. Detection of Most Commonly Used Pesticides in Green Leafy Vegetables from Sagar, India Using Direct Injection Hybrid Micellar Liquid Chromatography. *Advances in Sample Preparation* **2022**, *2*, 100015. https://doi.org/10.1016/j.sampre.2022.100015
(58) Ramezani, A. M.; Ahmadi, R.; Absalan, G. Designing a Sustainable Mobile Phase Composition for Melamine Monitoring in Milk Samples Based on Micellar Liquid Chromatography and Natural Deep Eutectic Solvent. *J. Chromatogr. A* **2020**, *1610*, 460563. https://doi.org/10.1016/j.chroma.2019.460563
(59) Al-Shaalan, N. H.; Jeehan Nasr, J.; Shalan, S.; El-Mahdy, A. M. Use of Green-Modified Micellar Liquid Chromatography for the Determination of Imidocarb Dipropionate Residues in Food Samples. *Microchem. J.* **2022**, *178*, 107316. https://doi.org/10.1016/j.microc.2022.107316
(60) Prebihalo, S. E.; Berrier, K. L.; Freye, C. E.; Bahaghighat, H. D.; Moore, N. R.; Pinkerton, D. K.; Synovec, R. E. Multidimensional Gas Chromatography: Advances in Instrumentation, Chemometrics, and Applications. *Anal. Chem.* **2018**, *90* (1), 505–532. https://doi.org/10.1021/acs.analchem.7b04226
(61) Krupčík, J.; Gorovenko, R.; Špánik, I.; Sandra, P.; Giardina, M. Comparison of the Performance of Forward Fill/Flush and Reverse Fill/Flush Flow Modulation in Comprehensive Two-Dimensional Gas Chromatography. *J. Chromatogr. A* **2016**, *1466*, 113–128. https://doi.org/10.1016/j.chroma.2016.08.032
(62) Garrigues, S.; de la Guardia, M. (Eds.) *Challenges in Green Analytical Chemistry*, 2nd edition. Royal Society of Chemistry, 2020.
(63) Crucello, J.; Pierone, D. V.; Hantao, L. W. Simple and Cost-Effective Determination of Polychlorinated Biphenyls in Insulating Oils Using an Ionic Liquid-Based Stationary Phase and Flow Modulated Comprehensive Two-Dimensional Gas Chromatography with Electron Capture Detection. *J. Chromatogr. A* **2020**, *1610*, 460530. https://doi.org/10.1016/j.chroma.2019.460530
(64) Pérez-Cova, M.; Tauler, R.; Jaumot, J. Chemometrics in Comprehensive Two-Dimensional Liquid Chromatography: A Study of the Data Structure and Its Multilinear Behavior. *Chemom. Intell. Lab. Syst.* **2020**, *201*, 104009. https://doi.org/10.1016/j.chemolab.2020.104009

(65) Stoll, D. R.; Carr, P. W. Two-Dimensional Liquid Chromatography: A State of the Art Tutorial. *Anal. Chem.* **2017**, *89* (1), 519–531. https://doi.org/10.1021/acs.analchem.6b03506
(66) Li, M. W. H.; Huang, X.; Zhu, H.; Kurabayashi, K.; Fan, X. Microfabricated Ionic Liquid Column for Separations in Dry Air. *J. Chromatogr. A* **2020**, *1620*, 461002. https://doi.org/10.1016/j.chroma.2020.461002
(67) Agrawal, A.; Keçili, R.; Ghorbani-bidkorbeh, F. Green miniaturized technologies in analytical and bioanalytical chemistry. *TrAC, Trends Anal. Chem.* **2021**, *143*, 116383. https://doi.org/10.1016/j.trac.2021.116383
(68) Regmi, B. P.; Agah, M. Micro Gas Chromatography: An Overview of Critical Components and Their Integration. *Anal. Chem.* **2018**, *90* (22), 13133–13150. https://doi.org/10.1021/acs.analchem.8b01461
(69) Hsieh, H. C.; Kim, H. A Miniature Closed-Loop Gas Chromatography System. *Lab on a Chip* **2016**, *16* (6), 1002–1012. https://doi.org/10.1039/c5lc01553g
(70) Whiting, J. J.; Myers, E.; Manginell, R. P.; Moorman, M. W.; Anderson, J.; Fix, C. S.; Washburn, C.; Staton, A.; Porter, D.; Graf, D.; Wheeler, D. R.; Howell, S.; Richards, J.; Monteith, H.; Achyuthan, K. E.; Roukes, M.; Simonson, R. J. A High-Speed, High-Performance, Microfabricated Comprehensive Two-Dimensional Gas Chromatograph. *Lab on a Chip* **2019**, *19* (9), 1633–1643. https://doi.org/10.1039/c9lc00027e
(71) Fialkov, A. B.; Lehotay, S. J.; Amirav, A. Less than One Minute Low-Pressure Gas Chromatography - Mass Spectrometry. *J. Chromatogr. A* **2020**, *1612*. https://doi.org/10.1016/j.chroma.2019.460691
(72) Peretzki, A. J.; Belder, D. On-Chip Integration of Normal Phase High-Performance Liquid Chromatography and Droplet Microfluidics Introducing Ethylene Glycol as Polar Continuous Phase for the Compartmentalization of n-Heptane Eluents. *J. Chromatogr. A* **2020**, *1612*, 460653. https://doi.org/10.1016/j.chroma.2019.460653

Brazilian Journal of Analytical Chemistry
2023, Volume 10, Issue 40, pp 35-53
doi: 10.30744/brjac.2179-3425.RV-136-2022

BrJAC

REVIEW

Fundamentals and Analytical Strategies for Metabolomics Workflow: *An Overview and Microbial Applications*

Hanna C. de Sá, Emile K. P. dos Santos, Samara C. dos Santos, Rafaela S. Nunes, Gisele A. B. Canuto*

Departamento de Química Analítica, Instituto de Química, Universidade Federal da Bahia, Rua Barão de Jeremoabo, 147, Salvador, BA, 40170-115, Brazil

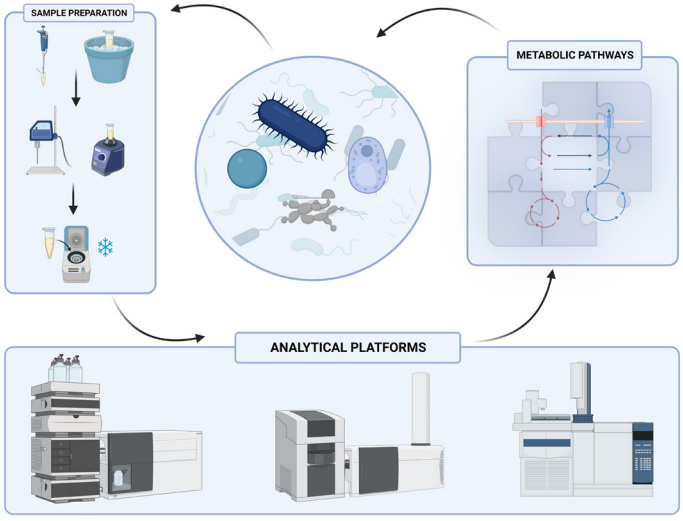

Metabolomics has become a prominent area within the omics sciences and allows an understanding of complex biological systems. Among several areas of knowledge, the study of microorganisms (microbial metabolomics) has received attention. Due to the many species of microorganisms and their high metabolic complexity, many challenges are involved in metabolomics workflow. Careful experimental design and execution of the experiments will provide reliable results, allowing correct biological interpretation. This review presents the fundamentals of metabolomics and workflow, focusing on the description of the steps and analytical strategies applied to microbial sample preparation, highlighting the current challenges in sample handling. In addition, the state of the art of analytical technologies based on separation techniques hyphenated to mass spectrometry and applications in microbial metabolomics are presented.

Keywords: sample preparation, mass spectrometry, chromatography, capillary electrophoresis, microbial metabolomics

INTRODUCTION

Metabolomics is a post-genomic approach used to determine alterations in metabolite levels, which are the end product of metabolism. The term metabolomics appeared for the first time in 2001,[1] and since then, it has been used in works that aim to understand biological processes. The determination of biochemical changes is performed by comparing sample groups with different environmental influences, genetics, or external interventions (drug treatment, diet, etc.). Therefore, this bioanalytical strategy combines careful sample preparation, high-throughput analytical instruments, bioinformatics, and chemometrics. Thus, metabolomics presents itself as a powerful phenotyping tool.[2,3]

Cite: de Sá, H. C.; dos Santos, E. K. P.; dos Santos, S. C.; Nunes, R. S.; Canuto, G. A. B. Fundamentals and Analytical Strategies for Metabolomics Workflow: *An Overview and Microbial Applications. Braz. J. Anal. Chem.* 2023, *10* (40), pp 35-53. http://dx.doi.org/10.30744/brjac.2179-3425.RV-136-2022

Submitted 09 December 2022, Resubmitted 02 March 2023, Accepted 27 April 2023, Available online 19 May 2023.

The analysis strategies involve two complementary approaches, named untargeted and targeted metabolomics. Untargeted metabolomics is a hypothesis-generated approach in which as many as possible metabolites are semi-quantitatively determined to obtain global information about the biological organism. In contrast, targeted studies, a hypothesis-driven strategy, quantify specific metabolites or chemical classes selected according to the prior knowledge of the organism under investigation.[4]

The applications of metabolomics permeate different areas of knowledge, from clinical studies using biological fluids (to understanding diseases for diagnostic and prognostic purposes),[5-8] in the analysis of plants,[9,10] foods,[11] and even cellular metabolism focused on different microorganisms,[12-15] denominated microbial metabolomics. This review presents some fundamentals and discussion of analytical strategies employed in metabolomics, emphasizing the technical aspects and challenges applied to microbial metabolomics.

MICROBIAL METABOLOMICS

Metabolomics of microorganisms (MO) is one of the growing areas of study within the omics sciences, given its wide application in biotechnology and microbiology fields. This is observed by the linear increase of published works in the last years (Figure 1). Such publications comprise mainly studies on microbiota (gut microbiota), given the physiological effects on health, disease prevention, and immune system improvement due to the colonization of microorganisms in the human body. Other applications include understanding cellular metabolism, identifying MO species, and regulatory metabolic pathways.[16]

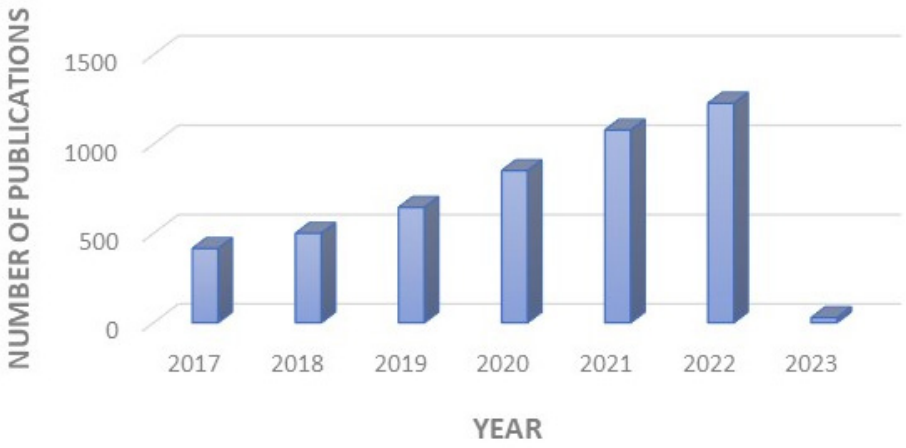

Figure 1. Literature inspection related to “microbial metabolomics” in the title, abstract, or keywords from 2017 to 2022 on PubMed database.

Challenges in microbial metabolomics encompass the difficulty of developing standardized methodologies for sample preparation. The differentiation between exometabolome (extracellular metabolites) and endometabolome (intracellular metabolites) is laborious and time-consuming, making it necessary to optimize the extraction step due to the large number of existing species and different cell membrane compositions. Another bottleneck in such investigations is the extensive amount of metabolites present in these organisms. This makes it difficult the metabolite assignment, being necessary to classify them as “unknown metabolites”, and important biological information is lost.[16,17]

METABOLOMICS WORKFLOW

The metabolomics workflow involves several steps, from experimental design to the determination of altered metabolites and biological interpretation (Figure 2). Biological problem definition and decisions about the type and number of samples, study groups, and sample collection are the initial steps of this workflow. An appropriate experimental design is crucial and will define the analytical procedures applied,

especially considering the type of approach (if targeted or untargeted metabolomics) and the analytical platforms used. The following steps include sample preparation and data acquisition by different analytical platforms, whose theoretical and practical aspects will be discussed in the following sections of this review.

Metabolomics raw data are complex and require dedicated software for processing and generating the data matrix (2D). Methods and advances in metabolomics data processing have been recently revised.[18,19] Altogether, processing steps involve the detection of analytical signals, background removal, alignment, clustering, and normalization. Different tools, from instrumental vendors to open-access software, are applied for this purpose.[4] It is important to emphasize the need for extra attention in processing methods, to maintain the integrity of biological information and accuracy in interpreting metabolic changes. Subsequently, chemometric methods and univariate statistical analysis are used to find differentiation between the groups under investigation. Several review articles bring fundamentals and methods of statistical analysis commonly applied to metabolomics studies.[20-22]

Metabolite assignation is another critical step in the metabolomics workflow and has been considered challenging, requiring sophisticated instrumentation, authentic analytical standards, and database inspection. The assignation of analytical signals can be performed in two ways: by annotation or identification. Metabolite annotation (also called putative annotation) is a tentative assignment based on the search of the mass (*m/z*) in different libraries or databases (such as METLIN, HMDB, LipidMaps, PubChem, etc.). On the other hand, metabolite identification is more accurate, requiring experiments based on tandem mass spectrometry (MS/MS or MS^n) analysis followed by comparing spectral fragmentation patterns and retention time with authentic analytical standards are performed.[23] Ultimately, the metabolomics workflow encompasses the raising of hypotheses and the elucidation of the biological question. Thus, pathway enrichment analyses have been applied to help understand the metabolic alterations.[24] Finally, the results can be validated using new cohorts and performing novel metabolomics experiments.

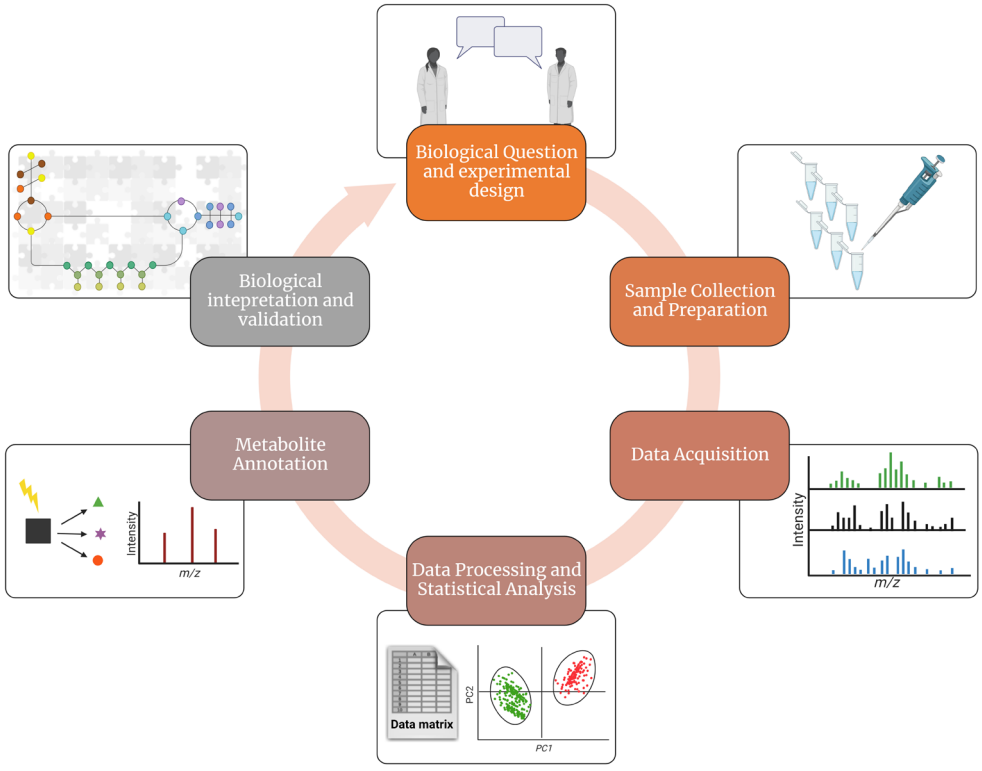

Figure 2. General metabolomics workflow. Created with “BioRender.com”.

Sample Preparation

Sample preparation is a crucial step in the workflow and reflects the success of a metabolomics study. Rapid conversion of metabolites (generally 1-2 s), cell degradation, metabolite leakage, extraction efficiency (in the face of large chemical variability), and reproducibility are considered the major challenges in this step.[16,25] Regarding cellular analysis, in addition to the basic quenching and extraction steps, other factors must be considered, such as preparation of the culture medium, number of passages, and sample harvesting. Therefore, every experiment must be carefully designed. In the case of microorganisms, due to the different growth conditions and cell wall composition, it is recommended to optimize all stages, from cell inoculation and maintenance to metabolite extraction.[26] Furthermore, accurate results are achieved after an appropriate choice of procedures, depending on the metabolomics approach (targeted or untargeted) and analytical platform.[27]

The reproducibility of cell growth is obtained with the establishment of controlled conditions, such as pH, light, temperature, medium composition, and dissolved gases. Usually, MOs are grown in bioreactors, which can operate under fixed nutrient conditions (fed-batch) or with a renewal of culture medium and biomass (chemostat).[28] Sample collection should be rapid and avoid metabolite turnover rates. In order to perform that, the inactivation of enzymes by quenching methods is necessary.[29]

Metabolic quenching is a continuous process within sample preparation in which enzymes are rapidly deactivated, and cells must maintain their integrity.[17,29] Different protocols are found in the literature[30] and include exposing samples to extreme temperature and pH conditions. Cold organic solvents (methanol or acetonitrile, for example), pure or in saline mixtures, have been applied for quenching of several MO species, such as *Pichia pastoris,*[15] *Lactobacillus plantarum,*[31] and *Corynebacterium glutamicum.*[32] Other methods include liquid nitrogen[33,34] and fast filtration.[35,36] However, due to the formation of ice crystals, the promotion of metabolite leakage, and fast turnover rates of some classes of metabolites these methods are less used. Alternative quenching procedures involve the application of a glycerol-saline[37] or acid/alkaline solutions.[29,30] Often, these methods culminate in metabolite leakage by the high susceptibility of the cell membrane, causing significant loss of metabolic information and interference by the glycerol solution.[30] Thus, there is no consensus regarding the best quenching protocol, but it is known that it is organism-dependent. The application of the quenching step must take into account the effectiveness of the process and reproducibility. For this reason, methods must be continuously optimized for each organism under study.

A complete understanding of the metabolism of microorganisms is obtained after analyzing the extracellular and intracellular portions. In order to perform that, pellet separation from the culture medium is carried out by centrifugation or fast filtration.[25] For intracellular analysis, however, a washing step is necessary before extracting the metabolites to completely remove interferents from the culture medium or compounds secreted by the MO. Usually, NaCl saline solutions[38,39] or phosphate-buffered saline solution (PBS)[12,40,41] are applied. It is important to highlight that these solutions must be used at low temperatures, to maintain the inactivation of the enzymes.

Intracellular extraction combines membrane disruption methods with the extractor solvent.[27] Cell lysis can be performed mechanically, with instruments such as sonicators, tissuelyzers, vibration mills, etc., or even by freezing-thawing cycles.[42] Methanol, ethanol, acetonitrile, and chloroform (pure and mixtures) have been frequently employed to access the endometabolome in different MO.[30] Aqueous methanol and acetonitrile solutions have been the most applied in microbial metabolomics. Such extractants combined with ultrasound bath and vortex mixing were used to extract intracellular metabolites from bacteria[12,13,36] and fungus.[15,35] The choice of the type of lysis and solvent extractor is closely related to the analytical technique used and, consequently, metabolite physicochemical properties. In addition, the ease of permeability of the cellular membrane is also a factor that influences lysis.[27] It is known that gram-positive bacteria, for example, have high concentrations of peptidoglycan in their membranes, providing greater mechanical resistance compared to gram-negative, which are essentially composed of lipopolysaccharides.[43] In this sense, several works focus on optimizing intracellular extraction,[32,36,44] highlighting the importance of systematic evaluations in the study of MO.

Sample preparation for extracellular metabolomics compared to intracellular is quite simple. The quenching step is not necessary, since there is no enzymatic activity in the culture medium.[27,45] Extracellular metabolites come from cellular secretion processes, the composition of the culture medium, or even cell leakage. Thus, any changes in the exometabolome composition result from external factors associated with the cell growth environment (such as pH, temperature, and nutrients).[28,46] Culture medium supernatants are usually subjected to simple dilution, deproteinization, desalting, preconcentration, or evaporation.[17] Such procedures are carried out in order to remove interferences such as sugars, proteins, salts, and lipids present in high concentrations in the culture medium. These species can cause malfunctions in the analytical instruments through the precipitation and consequent obstruction of the chromatographic system. In addition, problems with ionization suppression and sensitivity decrease are frequently observed.[27,46] Different protein precipitation and salt removal methods require large solution volumes, resulting in low recovery of metabolites.[46] Alternative methods for extraction and preconcentration, such as solid phase extraction (SPE) and solid phase microextraction (SPME), have shown good results when applied to microbial metabolomics. Despite the great advantage of using a reduced volume of toxic solvents and still determining low concentrations of analytes (parts per trillion, ppt to parts per million, ppm), such methods are expensive and selective, being applied more frequently in targeted studies.[46,47]

This topic provides an overview and challenges of the methods applied to sample preparation for microbial metabolomics. More details can be found in recently published review articles[27] focusing on intracellular,[30] extracellular,[46] and bacterial metabolomics.[25] Due to the increased interest in the study of microorganisms and the lack of universal sample preparation methods, optimizations, and the establishment of protocols are encouraged in order to improve extraction efficiency and, consequently, the generation of reliable and reproducible results.

Analytical Platforms

The most applied technologies in metabolomics studies are based on mass spectrometry (MS) and nuclear magnetic resonance (NMR). The former is often coupled with chromatographic techniques (liquid, LC, and gas chromatography, GC) or capillary electrophoresis (CE). Such couplings provide better sensitivity and selectivity in detecting the thousands of metabolites that comprise the metabolome.[48] Ye and co-workers[17] recently reviewed the technological novelties applied to microbial metabolomics. A careful survey of the literature showed the growing application of MS and hyphenated platforms (GC-MS, LC-MS, and CE-MS), comprising more than 57% of publications versus 31% of NMR in the last 22 years. Table I presents an overview comparison of the advantages and disadvantages of separation techniques hyphenated to mass spectrometry (LC-MS, GC-MS, and CE-MS) applied to metabolomics studies. Another highlight is the use of more than one analytical platform, especially in the last ten years, comprising around 11% of the works. It is known that no analytical technique is capable of covering the entire metabolome due to the great diversity of metabolites with variable concentration ranges. In this sense, the use of more than one platform has been recommended in the study of MO. Thus, given the relevance and scope of separation techniques coupled to MS, the general aspects and some applications in microbial metabolomics are presented in the following subsections.

Table I. Advantages and disadvantages of the separation techniques hyphenated to mass spectrometry applied to metabolomics studies

Analytical Platform	Advantages	Disadvantages
GC-MS	✓ Good repeatability ✓ Robustness ✓ High resolution ✓ High detectability ✓ Detection of volatile compounds ✓ Available libraries/databases	✓ Time-consuming sample preparation ✓ Non-derivatized samples (outliers) ✓ Moderate metabolic coverage ✓ Difficult to identify novel compounds
LC-MS	✓ Versatility ✓ Good repeatability ✓ High resolution ✓ Wide metabolic coverage	✓ Identification requires analytical standards and MS/MS analysis ✓ Different columns and separation modes to cover metabolome ✓ Lower reproducibility than GC-MS
CE-MS	✓ Low sample volume ✓ Simple sample pretreatment ✓ High resolution	✓ Identification requires analytical standards and MS/MS analysis ✓ Low repeatability than LC-MS and GC-MS ✓ Low sensitivity (dilution by sheath liquid)

GC-MS

Gas Chromatography coupled to Mass Spectrometry (GC-MS) is one of the analytical techniques most applied to metabolomics studies and has been gaining prominence in microbiology.[48] This technique has been used to characterize the volatile metabolome since it has excellent resolving power in the separation of non-polar and volatile or chemically volatilizable metabolites.[49] Overall, analyte separation is conducted in bore fused-silica capillaries filled with non-polar stationary phases, such as 5%(diphenyl)-polydimethylsiloxane (PDMS).[48] Recently, the use of 2D GCxGC, using columns with more polar phases (with higher % of diphenyl-PDMS and cyanopropylphenyl-PDMS, for example), has increased the selectivity and coverage of the metabolome by improving the separation of isomers.[50] In microbial metabolomics, GCxGC was applied to analyze the volatile exometabolome of *Candida albicans*, *Candida tropicalis*, and *Candida glabrata*. The methodology provided an annotation of 126 metabolites, including acids, alcohols, ketones, terpenes, aldehydes, among others. This chemical characterization of species can provide insights into clinical diagnosis, guiding pharmacological interventions.[14] Another interesting work used two-dimensional analysis to assess metabolic changes mediated by ozone stress in *Cobetia marina*, model bacteria for biofouling. The untargeted analysis using the non-polar and mid-polar chromatography column allowed the observation of a reduction in the content of fatty acids and amino acids by increasing ozone concentration.[51]

The GC-MS coupling provides fast, sensitive, and selective analyses allowing the separation and quantification of hundreds of metabolites, due to the high sensitivity and resolving power, especially when using time of flight (ToF) analyzers.[52] In addition to these advantages, the almost universal use of electron ionization (EI), typically operating at -70 eV, causes the high energy supplied to molecules to produce ion fragments. The highly reproducible fragmentation pattern, characteristic of each molecule, allows the application of several spectral libraries (NIST or online databases) for metabolite assignment and annotation. In order to improve the level of confidence in metabolite identification by combining information on retention time and mass spectra, it is recommended to build own libraries using authentic analytical standards or by co-injection of labeled compounds.[48,50]

Metabolome coverage by GC-MS is limited to the analysis of volatiles. Thus, in order to improve the detectability and metabolite volatility, and stability at working temperatures, chemical derivatization reactions are required.[16,48] Derivatization aims to make the metabolites volatile and thermally stable. Several methods have been applied in metabolomics studies, but the two-step oximation and silylation are the most frequently used. This method consists primarily of adding O-methoxyamine to completely dried extracts, aiming to protect carbonyl groups and prevent the cyclization of reducing sugars. The volatility reduction by the following silylation step is performed by the replacement of active hydrogens by trimethylsilylate (TMS) group.[52] Despite using well-established and extensively studied methods, this additional sample preparation step is often performed manually. It is time-consuming and influences analytical performance, especially by the loss of metabolites due to its volatility.[25] Online derivatization using automated systems has been used to improve the reproducibility of generated data. This robotic system was applied in the derivatization of intracellular metabolites of *Candida albicans*, reducing the total reaction time to a few hours.[33]

An automated system that analyzes volatile compounds without requiring derivatization is based on solid-phase microextraction combined with headspace (HS-SPME). In this solvent-free method, the analytes are collected in the headspace after volatilization in a highly reproducible way and short time.[30] HS-SPME has been successfully applied in the search for volatile biomarkers discriminating between seven different species of mycobacteria responsible for causing diseases such as leprosy and tuberculosis.[53] Another study sought the determination of volatile organic compounds (VOC) by HS-SPME-GC-MS in yeast strains for the biocontrol of post-harvest diseases caused by contamination by harmful mycotoxins.[54]

LC-MS

Hyphenated liquid chromatography with mass spectrometry (LC-MS) has been the most applied analytical platform in metabolomics studies.[55] The chromatographic separation is based on the partition difference between the analyte (metabolite) and the stationary and mobile phases, according to their physicochemical characteristics of polarity, charge, and size.[56] Gradient elution is often used to analyze complex samples such as cells and biological fluids. This elution improves the resolution between chemical species and is especially interesting for untargeted approaches.

One of the main advantages of LC is its versatility in terms of the metabolites classes that this technique can separate. This is achieved due to different separation modes. Metabolomics studies are generally restricted to reverse-phase liquid chromatography (RPLC) and hydrophilic interaction liquid chromatography (HILIC) analyses. RPLC uses a non-polar separation column and a more polar mobile phase, facilitating the separation of non-polar and moderately polar metabolites. HILIC, on the other hand, presents a polar stationary phase and a mobile phase containing an initial mixture of organic solvent and low % water, with a progressive increase in the aqueous portion throughout the chromatographic run. Thus, HILIC is interesting for separating highly polar substances, complementing RPLC.[57,58] Recent advances in this separation technique include the development of columns with smaller particle sizes, in addition to porous (sub-3 µm and sub-2 µm) or fused-core particles for faster and more efficient separation. High-pressure liquid chromatography (HPLC) and ultra-high-performance liquid chromatography (UHPLC) instruments, the latter capable of withstanding pressures greater than 10,000 psi, have been widely used in metabolomics.[56] Interesting compilations encompassing the fundamentals, optimization strategies of separation methods, and applications in metabolomics are found in the literature.[56,58,59]

LC can be coupled to MS using different ionization sources, in which electrospray (ESI) in positive and negative modes being the most applied. ESI has been shown to be very efficient in the ionization of large biomolecules and small metabolites, such as sugars, sterols, steroids, amino acids, phospholipids, fatty acids, among others. LC-MS combines the high robustness, resolving power, and selectivity of LC with the high sensitivity of MS, and no need for chemical derivatization, allowing a wide range of metabolome coverage. The prior separation of chemical species reduces the complexity of the matrix, reducing ionization suppression problems, which are often encountered in direct MS analysis methods.[60] Advances in MS

systems include the development of fast data acquisition rate, mass accuracy, and sensitivity for a wide range of *m/z*.[61] Different mass analyzers provide valuable information to assist in one of the most challenging steps of the metabolomics workflow: accurate metabolite annotation. Triple quadrupole (QqQ), quadrupole time of fight (QToF), and Orbitrap (OT) instruments are used. These analyzers allow the performance of tandem-MS (MS^n) analyses, which enable the accurate structural elucidation of metabolites based on the search for fragments generated in spectral libraries or using authentic analytical standards.[56]

The possibility of applying different analysis strategies is especially interesting regarding microbial metabolomics due to the high complexity of metabolites from interactions in microbiomes.[50] A method based on HILIC-MS using an OT-MS was used to understand the mechanisms involved in combining different treatments against *Pseudomonas aeruginosa*.[38] RPLC-MS and HILIC-MS were used to understand the influence of probiotics on the growth and biotransformation of four *Lactobacillus* strains, demonstrating different profiles of cellular adaptation to the environment.[62] Another interesting work developed a new approach using two zwitterionic columns in HILIC-MS analysis to quantify microbial boundary fluxes. This new strategy, focusing on the *Staphylococcus aureus* exometabolome, determined of almost 400 metabolites in less than 5 min of analysis. This method demonstrated high precision for more than 1000 injections, allowing the identification of microbial species in different clinical conditions.[63]

CE-MS

Compared to the chromatographic separation techniques, capillary electrophoresis mass spectrometry (CE-MS) has been the least applied analytical technique in metabolomics investigations. The separation mechanism involved in CE differs slightly from LC and GC and is based on the differentiated migration of ionic or ionizable solutes under an electric field.[64] Different separation modes are used, such as capillary zone electrophoresis (CZE) for small and large ionic molecules; micellar electrokinetic chromatography (MEKC) for neutral species; capillary isotachophoresis (CITP) for small ionic molecules; capillary gel electrophoresis (CGE) for large biomolecules and polymers; among others.[65] Due to its versatility, this orthogonal technique is suitable for the determination of the polar and ionic portion of the metabolome, with the advantage of not requiring derivatization. Furthermore, CE combines high resolving power and separation efficiency, achieved by the planar electroosmotic flow (EOF) profile formed inside the capillary and the small volumes of sample injected. It was a very interesting technique for application in biological studies, especially with sample volume restriction.[48,66] Sample handling can be minimal, including cell lysis, dilution, and protein removal.[48] Compared to LC, CE has the advantage of not requiring large volumes of organic solvents for solute elution and shorter analysis times. On the other hand, its presents lower sensitivity since it works with a small volume of injected sample (nL) and poor migration time reproducibility due to fluctuations of EOF.[64]

The CE-MS coupling, generally performed via electrospray (ESI), emerged in the late 1980s and proved advantageous for its sensitivity and selectivity, with lower limits of detection (LODs) when compared to the frequently used UV-Vis methods. However, CE-MS coupling is not as simple as LC-MS and GC-MS due to the high electric field and low eluent flow rates (low EOF), which maintain unstable electrospray formation.[66] Two CE-MS interface configurations are found: coaxial sheath liquid and sheathless interface. The first has a system configured for continuous pumping of a sheath liquid (SHL), composed of mixtures of organic solvents (acetonitrile, methanol, or isopropanol) with acidified aqueous solutions (formic or acetic acid) and volatile additives (ammonium salts). The SHL is mixed with the CE eluent in order to improve the ionization of the analytes, promoting the stability of the spray formed in the ESI. Optimizations of the composition of the background (BGE) and the SHL are critical and must be performed together to obtain the maximum ionization of the analytes for both positive and negative ionization modes.[67]

Despite being widely applied, the SHL interface considerably reduces the detection sensitivity by diluting the eluent. In order to circumvent such compromise, a technology based on a sheathless interface was developed by Moini.[68] In this configuration, the coated (metal or polymeric) porous tip of the capillary improves spray formation and mass transfer by directly inserting eluent from the CE into the MS system by

applying a voltage at the capillary outlet. This configuration was applied in metabolomics for the first time in 2012 to characterize the metabolic profile of human urine[69] and has since been used in cellular,[70] tissue samples,[71] and body fluids (urine, plasma, and cerebrospinal fluid),[72] among other studies. Configuration changes and improvements in the prototypes, such as the incorporation of a nanocapillary electrophoresis-MS (nanoCESI), allowed pre-concentrations and increased system sensitivity.[73] However, some limitations must still be considered, such as short capillary lifetime, variation in EOF, and low repeatability and robustness.[65]

The development of new CE-MS interfaces and technologies for volume-restricted investigations have increased their use in metabolomics in the last ten years (about 30-40%, according to PubMed search using *"metabolomics"* and *"CE-MS"* keywords). Despite the challenges and limitations, the conventional interface (co-axial sheath liquid) is still been the most applied. Compared with other analytical platforms, CE-MS is also considered a limited technique, attributed to the difficulty of establishing standard protocols, low reproducibility, and the lack of experts in the field.[74] Regarding microbial metabolomics, its application is even more incipient. A recent work evaluated the metabolic profile of the response of *Schefersomyces stipitis* to N-acetyl-d-glucosamine (GlcNAc), an amino sugar used as an abundant renewable carbon source. Intracellular analysis by CE-ToF-MS allowed a better understanding of fungal metabolism, demonstrated by the increase in nitrogen-containing metabolites known for biological and pharmacological properties.[75] Another interesting investigation using CE-MS and LC-MS was performed by Yamamoto and collaborators,[76] showing differences between small and large intestinal metabolic profiles between specific pathogen-free and germ-free mice. The findings suggested that differences in the functions of each part of the intestinal tract are associated with the colonization of different microbial species, resulting in specific metabolites related to inflammatory processes. Understanding interactions and associations with inflammation can help improve health promotion.

APPLICATIONS OF CLINICAL MICROBIAL METABOLOMICS

Microbial metabolomics has been a prominent area within the omics sciences, given the importance of MO for understanding cellular mechanisms. As previously mentioned, research articles in microbial metabolomics have increased linearly in the last years (Figure 1). Some revisions including methods and new findings have been published recently.[16,25,77] Among these, some works involving the discovery of new drugs, resistance to antibiotics, intestinal microbial metabolism comprehension, metabolic engineering, and biotechnological processes (such as fermentation) have been the focus of researchers in the field.[17] Clinical applications involving the understanding of pathologies associated with MO and the development of diagnostic tools and new treatments have also been of interest. An untargeted investigation by GC-MS evaluated the metabolic alterations provoked by the biofilm community of *Candida albicans* and *Klebsiella pneumoniae*. The analysis of the endometabolic profile of individual and dual biofilms showed marked differences (Figure 3), in which 40 metabolites with significant alterations were identified. Such compounds were associated with the maturation of biofilms. They could be an important starting point for developing strategies to combat infections caused by these opportunistic MOs, promoting quality of life and reducing mortality in hospitalized patients.[78] The metabolic response of *Escherichia coli* was evaluated in a multi-omics, polar metabolomics, and lipidomics study to understand adaptations to acid stress and amino acid supplementation in environments such as the stomach and intestine. *E. coli* is an opportunistic pathogen responsible for severe urinary tract and intestinal infections. The results indicated a coordinated correlation between amino acid-dependent mechanisms for acid resistance and lipidomics modulations, emphasizing lipid synthesis routes and metabolite transport changes. According to the authors, complementary studies need to be carried out to understand the mechanism and acid resistance to the gut environment. However, the initial findings help elucidate this MO's adaptation to develop new treatments for pathogenic organisms.[79] Table II presents a compilation of selected applications, described throughout this review, including the objectives and brief descriptions of the analytical methods used.

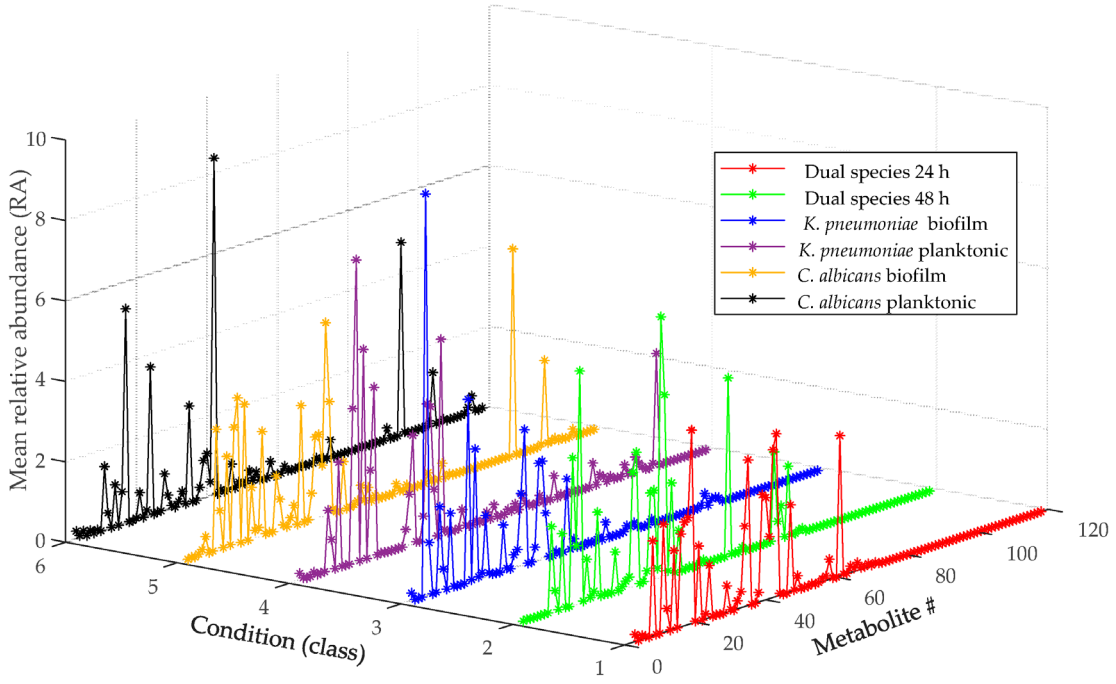

Figure 3. Extracellular metabolic profiling analyzed by GC-MS of the six conditions studied in the biofilms of *Candida albicans* and *Klebsiella pneumoniae*.

[Reprinted under the terms and conditions of the Creative Commons Attribution (CC BY) license (https://creativecommons.org/licenses/by/4.0/) from reference No. 78: Galdiero, E.; Salvatore, M. M.; Maione, A.; de Alteriis, E.; Andolfi, A.; Salvatore, F.; Guida, M. GC-MS-Based Metabolomics Study of Single- and Dual-Species Biofilms of *Candida albicans* and *Klebsiella pneumonia*. *Int. J. Mol. Sci.* **2021**, *22* (7), 3496. http://dx.doi.org/10.3390/ijms22073496.]

Table II. Selected applications and analytical methods used in mass spectrometry-based microbial metabolomics

Microorganism (Sample type)	Aim	Quenching	Extraction Methods	Analytical Platform (Ionization modes)	Ref.
Aphanizomenon flos-aquae and *Microcystis aeruginosa* (cell pellet)	To understand the effect of *Microcystis aeruginosa* on *Aphanizomenon flos-aquae* growth.	Liquid N_2	Cellular extraction by homogenization at 35 Hz (4 min) with MeOH/H_2O (3:1, v/v), followed by sonication (5 min) in an ice-water bath (procedure repeated twice).	RPLC-MS/MS (positive and negative)	12
Azospirillum brasilense (cell pellet)	To evaluate the effect of growth of wild-type and mutant *Azospirillum brasilense* under low and high nitrogen.	Liquid N_2	Cellular extraction with MeOH 80% and sonication for 60 min. Dried extracts were derivatized by methoxyamination (50 ºC until residue resuspension) and silylation (60 min at 50 ºC).	GC-MS	13
Candida albicans, Candida glabrata, and *Candida tropicalis* (culture medium)	To differentiate *Candida* spp. by exometabolomics strategy.	**	SPME extraction using a fused silica fiber (divinylbenzene/carboxen/ polydimethylsiloxane). The headspace extraction occurred under agitation (350 rpm) at 50 °C for 30 min.	GC-MS	14
Bacillus licheniformis (cell pellet)	Optimization of sample preparation of *Bacillus licheniformis* for GC-MS untargeted metabolomics.	60% MeOH 0.9% NH_4HCO_3	Cell disruption with bead-milling and MeOH 70% solution (at -40 °C). Dried extracts were derivatized by methoxyamination (30 ºC for 90 min) and silylation (37 ºC for 120 min).	GC-MS	31
Corynebacterium glutamicum (cell pellet)	Optimization of sample preparation of *Corynebacterium glutamicum* for LC-MS untargeted metabolomics.	40% MeOH (-20 ºC)	Extraction with EtOH/H_2O (3:1, v/v) at 100 °C, incubation in boiling-water bath (15 min) and disruption in a grinder system (5 M/s, 30 s, 5 cycles) (2x). Dried extracts resuspended in ACN/H_2O (1:1, v/v, with 0.1% F.A.).	HILIC-MS (negative)	32
Candida albicans (cell pellet)	To study the mechanism of action of basil essential oil in *Candida albicans.*	Liquid N_2	Cell homogenization with 50% (v/v) cold MeOH and incubated at -20 ºC (30 min) and re-extraction with MeOH/$CHCl_3$ (3:1, v/v). Combined organic phases were dried and derivatized by methoxyamination and silylation, both performed at 37 ºC for 120 min.	GC-MS	33
Escherichia coli (cell pellet)	To evaluate the mechanism of colistin resistance mcr-1-mediated in *Escherichia coli.*	Liquid N_2	Pure MeOH (at -20 ºC) vortexed for 1 min. Cell lyse by freeze-thaw cycles in liquid N_2 (3x). Re-extraction with same conditions. Combined supernatants were dried and resuspended in ACN/H_2O (50/50 v/v, with 0.1% F.A.).	RPLC-MS (positive and negative)	34

(continues on the next page)

Table II. Selected applications and analytical methods used in mass spectrometry-based microbial metabolomics (continuation)

Microorganism (Sample type)	Aim	Quenching	Extraction Methods	Analytical Platform (Ionization modes)	Ref.
Saccharomyces cerevisiae (cell pellet)	Optimization of sample preparation of *Saccharomyces cerevisiae* for GC-MS untargeted metabolomics.	Fast filtration	Cells were extracted with ACN/H_2O (1:1, v/v) and glass beads by vortexing for 3 min. Dried extracts were derivatized by methoxyamination (30 ºC for 90 min and 200 rpm) and silylation (37 ºC for 30 min and 200 rpm).	GC-MS	35
Pseudomonas fluorescens, Streptomyces coelicolor, and *Saccharomyces cerevisiae* (cell pellet)	Optimization of quenching method for microbial metabolomics.	Glycerol/NaCl solution (13.5 g L^{-1}) (3:2, v/v)	Cell homogenization with 50% (v/v) of MeOH/H_2O (3:2, v/v, at -30 ºC) by vortexing (1 min), followed by freeze-thaw cycles (3x). The residual pellet was re-extracted with the same MeOH/H_2O solution by vortexing. Combined extracts were resuspended in NaCl (1 mol L^{-1}), MeOH, and pyridine, followed by derivatization with methyl chloroformate.	GC-MS	37
Pseudomonas aeruginosa (cell pellet)	To understand the mechanism of action of combined antibiotics (polymyxin and amikacin) against susceptible and resistant *Pseudomonas aeruginosa.*	ND	Freeze-thaw cycles (3x) in combination with $CHCl_3$/MeOH/H_2O (1:3:1, v/v/v) were used for intracellular extraction.	HILIC-MS (positive and negative)	38
Acinetobacter baumannii (cell pellet and culture medium)	To understand the mechanism of action of combined antibiotics (colistin and doripenem) against *Acinetobacter baumannii.*	Dry ice/EtOH bath	Freeze-thaw cycles (3x) in combination with $CHCl_3$/MeOH/H_2O (1:3:1, v/v/v, at -80 ºC) were used for intracellular extraction. Culture supernatant were mixed with $CHCl_3$/MeOH/H_2O (1:3:1, v/v/v) solution for extracellular extraction.	HILIC-MS (positive and negative)	39
Staphylococcus aureus (cell pellet)	To detect altered metabolites in *Staphylococcus aureus* using targeted metabolomics.	ND	Pure cold MeOH was vortexed with the pellets (~ 1 min). The mixture was maintained at -20 ºC (20 min). Supernatants were dried and resuspended in ACN/H_2O (1:1, v/v).	HILIC-MS (positive and negative)	41
Cobetia marina (cell pellet)	To understand metabolic changes in *Cobetia marina* under ozone stress.	Aqueous NaCl (0.85%, v/v) frosted into ice bulks, followed by storage at -80 ºC (3 min)	Cell disruption in a speed homogenization system (1 min) with 50% $CHCl_3$/ 50% MeOH/H_2O (21:79, v/v). Procedure repeated twice. Upper phases were combined and dried, followed by derivatization by methoxyamination and silylation, both performed at 60 ºC (60 min).	GC-MS	51

(continues on the next page)

Table II. Selected applications and analytical methods used in mass spectrometry-based microbial metabolomics (continuation)

Microorganism (Sample type)	Aim	Quenching	Extraction Methods	Analytical Platform (Ionization modes)	Ref.
Mycobacterium spp. (cell pellet)	To investigate potential volatile organic biomarkers that differentiate mycobacteria.	Ice bath	Samples were incubated for 15 min under 250 rpm and exposed to a SPME fiber (polydimethylsiloxane/carboxen/ divinylbenzene) for 20 min at 37 ºC.	GC-MS	53
Aspergillus carbonarius and *Aspergillus ochraceus* (cell suspension)	To understand the alterations in volatile organic compounds by the mycotoxin (ochratoxin A) contamination in *Aspergillus*.	ND	Samples were equilibrated for 30 min at 50ºC under agitation and exposed to a SPME fiber (polydimethylsiloxane) for 30 min.	GC-MS	54
Staphylococcus aureus (cell pellet)	To optimize an HILIC-MS method for quantification of microbial boundary fluxes.	Cold MeOH and -80 ºC storage	Supernatants from quenched samples were diluted with 50% MeOH at 1:10 (v/v).	HILIC-MS (positive and negative)	63
Scheffersomyces stipites (cell pellet)	To understand metabolic effects of *N*-acetyl-d-glucosamine as carbon and nitrogen source in *Schefersomyces stipites.*	MeOH (-40 ºC)	Boiling EtOH 75% (v/v) was added to the pellets and extraction was performed in a water bath at 95 °C. Samples were dried and resuspended in ultrapure H_2O.	CE-MS (positive and negative)	75
Not specified (mice intestinal tissue)	To investigate differences into the metabolome of intestinal luminal and correlate with commensal microbiota in mice.	Storage at -80 °C	Pure MeOH and zirconia beads were vortexed with the sample tissues, containing PBS (0.957 mmol L^{-1}). After protein precipitation, supernatants were concentrated and dissolved in H_2O.	CE-MS (positive and negative), and LC-MS (negative)	76
Candida albicans and *Klebsiella pneumoniae* (culture medium)	To investigate the metabolic changes in single- and dual-species biofilm development.	**	Supernatants were dried and derivatized by silylation, in which rotated samples were exposed to a stream of air (50-120 ºC).	GC-MS	78
Escherichia coli (cell pellet and culture medium)	To characterize the *Escherichia coli* adaptations to acid stress.	ND	Cold MeOH were vortexed with the pellets and culture medium supernatants. Samples were maintained at -20 ºC (20 min) to precipitation and further analysis of supernatants.	LC-MS (positive and negative)	79

ACN, acetonitrile; EtOH, ethanol; F.A., formic acid; MeOH, methanol; ND, not described.
**Extracellular metabolomics does not require quenching step.

CONCLUSIONS

Given the increased interest in understanding the metabolic relationships and interactions between microorganisms and hosts, metabolomics appears to be an appropriate study tool. The great complexity of the metabolome of microorganisms makes such studies challenging, especially in the analytical aspects of sample preparation and data acquisition. Sample harvesting and metabolic quenching must be carefully planned according to the studied organism. Cellular metabolism disruption without metabolite leakage or degradation during quenching requires optimization. The analysis of intracellular metabolome also demonstrates a lack of standard methods. Systematized studies of extractor solvent composition and cell membrane rupture methods are encouraged. The variable chemical diversity in microorganisms means that more than one analytical technique is required for broad metabolome coverage. The use of separation techniques coupled with mass spectrometry has provided excellent results, given the high versatility and separation power, combined with the detectability and sensitivity of the MS. LC-MS has undoubtedly been the most applied platform, using different elution modes. GC-MS arises as the gold standard for elucidation of the volatile metabolome. Despite requiring an additional step of derivatization in sample preparation, methods based on microextraction are used efficiently. Finally, despite being little explored, CE-MS requires little sample volume and proves useful for highly polar and ionic metabolites, complementing the information on the metabolic profile obtained by the other analytical platforms.

Thus, with the chemical complexity of the studied organisms and recent technological advances, the analytical chemistry field occupies an important niche within metabolomics, including investigations in microbial metabolomics, in which new optimizations and methods developments are often needed.

Conflicts of interest

The authors declare no financial conflicts of interest.

Acknowledgements

H.C.S. and R.S.N. are thankful to the “Conselho Nacional de Desenvolvimento Científico e Tecnológico” (PIBIC-CNPq), and S.C.S. is thankful to the “Fundação de Amparo a Pesquisa do Estado da Bahia” (PIBIC-FAPESB) for the undergraduate research fellowships.

REFERENCES

(1) Fiehn, O. Combining genomics, metabolome analysis, and biochemical modelling to understand metabolic networks. *Comp. Funct. Genomics* **2001**, *2* (3), 155–68. http://dx.doi.org/10.1002/cfg.82

(2) Zhang, X.; Li, Q.; Xu, Z.; Dou, J. Mass spectrometry-based metabolomics in health and medical science: a systematic review. *RSC Adv*. **2020**, *10* (6), 3092-3104. http://dx.doi.org/10.1039/c9ra08985c

(3) Klassen, A.; Faccio, A. T.; Canuto, G. A. B.; da Cruz, P. L. R.; Ribeiro, H. C.; Tavares, M. F. M.; Sussulini, A. Metabolomics: Definitions and Significance in Systems Biology. In: Sussulini, A. (Ed.) *Metabolomics: From Fundamentals to Clinical Applications*, 1st ed.; Springer International Publishing AG, 2017, pp 3-17. https://doi.org/10.1007/978-3-319-47656-8_1

(4) Canuto, G. A. B.; da Costa, J. L.; da Cruz, P. L. R.; de Souza, A. R. L.; Faccio, A. T.; Klassen, A.; Rodrigues, K. T.; Tavares, M. F. M. Metabolômica: definições, estado-da-arte e aplicações representativas. *Quím. Nova* **2018**, *41* (1), 75-91. http://dx.doi.org/10.21577/0100-4042.20170134

(5) Nunes, E. C.; de Filippis, A. M. B.; Pereira, T. E. S.; Faria, N. R. C.; Salgado, A.; Santos, C. S.; Carvalho, T. C. P. X.; Calcagno, J. I.; Chalhoub, F. L. L.; Brown, D.; Giovanetti, M.; Alcantara, L. C. J.; Barreto, F. K.; de Siqueira, I. C.; Canuto, G. A. B. Untargeted Metabolomics Insights into Newborns with Congenital Zika Infection. *Pathogens* **2021**, *10* (4), 468. http://dx.doi.org/10.3390/pathogens10040468

(6) Santos, A. L. M.; Vitório, J. G.; de Paiva, M. J. N.; Porto, B. L. S.; Guimarães, H. C.; Canuto, G. A. B.; Carvalho, M. G.; de Souza, L. C.; de Toledo, J. S.; Caramelli, P.; Duarte-Andrade, F. F.; Gomes, K. B. Frontotemporal dementia: Plasma metabolomic signature using gas chromatography-mass spectrometry. *J. Pharm. Biomed. Anal*. **2020**, *189*, 113424. http://dx.doi.org/10.1016/j.jpba.2020.113424

(7) Dudzik, D.; Platas, I. I.; Renau, M. I.; Esponera, C. B.; Mendoza, B. R. H.; Lerin, C.; Ramón-Krauel, M.; Barbas, C. Plasma Metabolome Alterations Associated with Extrauterine Growth Restriction. *Nutrients* **2020**, *12* (4), 1188. http://dx.doi.org/10.3390/nu12041188

(8) Jacob, M.; Lopata, A. L.; Dasouki, M.; Rahman, A. M. A. Metabolomics toward personalized medicine. *Mass Spectrom. Rev*. **2019**, *38* (3), 221-238. http://dx.doi.org/10.1002/mas.21548

(9) Neto, J. C. R.; Vieira, L. R.; Ribeiro, J. A. A.; de Sousa, A. C. F.; Júnior, M. T. S.; Abdelnur, P. V. Metabolic effect of drought stress on the leaves of young oil palm (*Elaeis guineensis*) plants using UHPLC-MS and multivariate analysis. *Sci. Rep*. **2021**, *11* (1), 18271. http://dx.doi.org/10.1038/s41598-021-97835-x

(10) Hooshmand, K.; Kudjordjie, E. N.; Nicolaisen, M.; Fiehn, O.; Fomsgaard, I. S. Mass Spectrometry-Based Metabolomics Reveals a Concurrent Action of Several Chemical Mechanisms in Arabidopsis-Fusarium oxysporum Compatible and Incompatible Interactions. *J. Agric. Food Chem*. **2020**, *68* (51), 15335-15334. http://dx.doi.org/10.1021/acs.jafc.0c05144

(11) Ballesteros-Vivas, D.; Alvarez-Rivera, G.; León, C.; Morantes, S. J.; Ibánez, E.; Parada-Alfonso, F.; Cifuentes, A.; Valdés, A. Foodomics evaluation of the anti-proliferative potential of Passiflora mollissima seeds. *Food Res. Int*. **2020**, *130*, 108938. http://dx.doi.org/10.1016/j.foodres.2019.108938

(12) Jin, H.; Ma, H.; Gan, N.; Wang, H.; Li, Y.; Wang, L.; Song, L. Non-targeted metabolomic profiling of filamentous cyanobacteria Aphanizomenon flos-aquae exposed to a concentrated culture filtrate of Microcystis aeruginosa. *Harmful Algae* **2022**, *111*, 102170. http://dx.doi.org/10.1016/j.hal.2021.102170

(13) Kukolj, C.; Pedrosa, F. O.; de Souza, G. A.; Sumner, L. W.; Lei, Z.; Sumner, B.; do Amaral, F. P.; Juexin, W.; Trupti, J.; Huergo, L. F.; Monteiro, R. A.; Valdameri, G.; Stacey, G.; de Souza, E. M. Proteomic and Metabolomic Analysis of Azospirillum brasilense ntrCMutant under High and Low Nitrogen Conditions. *J. Proteome Res*. **2020**, *19* (1), 92-105. http://dx.doi.org/10.1021/acs.jproteome.9b00397

(14) Costa, C. P.; Bezerra, A. R.; Almeida, A.; Roch, S. M. Candida Species (Volatile) Metabotyping through Advanced Comprehensive Two-Dimensional Gas Chromatography. *Microorganisms* **2020**, *8* (12), 1911. http://dx.doi.org/10.3390/microorganisms8121911

(15) Tredwell, G. D.; Aw, R.; Edwards-Jones, B.; Leak, D. J.; Bundy, J. G. Rapid screening of cellular stress responses in recombinant Pichia pastoris strains using metabolite profiling. *J. Ind. Microbiol. Biotechnol*. **2017**, *44* (3), 413-417. http://dx.doi.org/10.1007/s10295-017-1904-5

(16) Belinato J. R.; Bazioli, J. M.; Sussulini, A.; Augusto, F.; Fill, T. P. Metabolômica microbiana: inovações e aplicações. *Quím. Nova* **2019**, *42* (5), 546-559. http://dx.doi.org/10.21577/0100-4042.20170324

(17) Ye, D.; Li, X.; Shen, J.; Xia, X. Microbial metabolomics: From novel technologies to diversified applications. *TrAC, Trends Anal. Chem*. **2022**, *148*, 1165-1140. http://dx.doi.org/10.1016/j.trac.2022.116540

(18) Peraldo-Molina, Á.; Solà-Santos, P.; Perera-Lluna, A.; Chicano-Gálvez, E. Data Processing and Analysis in Mass Spectrometry-Based Metabolomics. *Methods Mol. Biol*. **2023**, *2571*, 207-239. http://dx.doi.org/10.1007/978-1-0716-2699-3_20

(19) Hu, B.; Canon, S.; Eloe-Fadrosh, E. A.; Anubhav; Babinski, M.; Corilo, Y.; Davenport, K.; Duncan, W. D.; Fagnan, K.; Flynn, M.; Foster, B.; Hays, D.; Huntemann, M.; Jackson, E. K. P.; Kelliher, J.; Li, P. E.; Lo, C. C.; Mans, D.; McCue, L. A.; Mouncey, N.; Mungall, C. J.; Piehowski, P. D.; Purvine, S. O.; Smith, M.; Varghese, N. J.; Winston, D.; Xu, Y.; Chain, P. S. G. Challenges in Bioinformatics Workflows for Processing Microbiome Omics Data at Scale. *Front Bioinform*. **2022**, *1*, 826370. http://dx.doi.org/10.3389/fbinf.2021.826370

(20) Barnes, S. Overview of Experimental Methods and Study Design in Metabolomics, and Statistical and Pathway Considerations. In: Li, S. (Ed.) *Computational Methods and Data Analysis for Metabolomics*, 1st ed.; Humana, 2020, pp 1-10. https://doi.org/10.1007/978-1-0716-0239-3_1
(21) Yi, L.; Dong, N.; Yun, Y.; Deng, B.; Ren, D.; Liu, S.; Liang, Y. Chemometric methods in data processing of mass spectrometry-based metabolomics: A review. *Anal. Chim. Acta* **2016**, *914*, 17-34. https://doi.org/10.1016/j.aca.2016.02.001
(22) Gromski, P. S.; Muhamadali, H.; Ellis, D. I.; Xu, Y.; Correa, E.; Turner, M. L.; Goodacre, R. A tutorial review: Metabolomics and partial least squares-discriminant analysis--a marriage of convenience or a shotgun wedding. *Anal. Chim. Acta* **2015**, *879*, 10-23. https://doi.org/10.1016/j.aca.2015.02.012
(23) Gil-de-la-Fuente, A.; Armitage, E. G.; Otero, A.; Barbas, C.; Godzien, J. Differentiating signals to make biological sense - A guide through databases for MS-based non-targeted metabolomics. *Electrophoresis* **2017**, *38* (18), 2242-2256. http://dx.doi.org/10.1002/elps.201700070
(24) Karnovsky, A.; Li, S. Pathway Analysis for Targeted and Untargeted Metabolomics. In: Li, S. (Ed.) *Computational Methods and Data Analysis for Metabolomics*, 1st ed.; Humana, 2020, pp 387-400. https://doi.org/10.1007/978-1-0716-0239-3_19
(25) Kamal, K. M.; Maifiah, M. H. M.; Rahim, N. A.; Hashim, Y. Z. H-Y.; Sani, M. S. A.; Azizan, K. A. Bacterial Metabolomics: Sample Preparation Methods. *Biochem. Res. Int*. **2022**, 9186536. http://dx.doi.org/10.1155/2022/9186536
(26) Chetwynd, A. J.; Dunn, W. B.; Rodriguez-Blanco, G. Collection and Preparation of Clinical Samples for Metabolomics. In: Sussulini, A. (Ed.) *Metabolomics: From Fundamentals to Clinical Applications*, 1st ed. Springer International Publishing AG, 2017, pp 19-44. https://doi.org/10.1007/978-3-319-47656-8_2
(27) Patejko, M.; Jacyna, J.; Markuszewski, M. J. Sample preparation procedures utilized in microbial metabolomics: An overview. *J. Chromatogr. B* **2017,** *1043*, 150-157. http://dx.doi.org/10.1016/j.jchromb.2016.09.029
(28) Mashego, M. R.; Rumbold, K.; De Mey, M.; Vandamme, E.; Soetaert, W.; Heijnen, J. J. Microbial metabolomics: past, present and future methodologies. *Biotechnol. Lett*. **2007**, *29* (1), 1-16. http://dx.doi.org/10.1007/s10529-006-9218-0
(29) Álvarez-Sánchez, B.; Priego-Capote, F.; de Castro, M. D. L. Metabolomics analysis II: Preparation of biological samples prior to detection. *TrAC, Trends Anal. Chem*. **2010**, *29*, 120-127. http://dx.doi.org/10.1016/j.trac.2009.12.004
(30) Pinu, F. R.; Villas-Boas, S. G.; Aggio, R. Analysis of Intracellular Metabolites from Microorganisms: Quenching and Extraction Protocols. *Metabolites* **2017**, *7* (4), 53. http://dx.doi.org/10.3390/metabo7040053
(31) Wang, H. B.; Feng, Y. R.; Gui, S. Q.; Zhang, Y.; Lu, F. P. A sample pretreatment method to suit the metabolomic analysis of Bacillus licheniformis based on GC-MS. *Anal. Methods* **2017**, *9*, 2299. http://dx.doi.org/10.1039/C7AY00008A
(32) Zhang, Q.; Zheng, X.; Wang, Y.; Yu, J.; Zhang, Z.; Dele-Osibanjo, T.; Zheng, P.; Sun, J.; Jia, S.; Ma, Y. Comprehensive optimization of the metabolomic methodology for metabolite profiling of Corynebacterium glutamicum. *Appl. Microbiol. Biotechnol*. **2018**, *102* (16), 7113–7121. http://dx.doi.org/10.1007/s00253-018-9095-1
(33) Miao, Q.; Zhao. L.; Wang, Y.; Hao, F.; Sun, P.; He, P.; Liu, Y.; Huang, J.; Liu, X.; Liu, X.; Deng, G.; Li, H.; Li, L.; Tang, Y.; Wang, L.; Feng, M.; Jia, W. Microbial metabolomics and network analysis reveal fungistatic effect of basil (*Ocimum basilicum*) oil on Candida albicans. *J. Ethnopharmacol*. **2020**, *260*, 113002. http://dx.doi.org/10.1016/j.jep.2020.113002
(34) Li, H.; Wang, Y.; Meng, Q.; Wang, Y.; Xia, G.; Xia, X.; Shen, J. Comprehensive proteomic and metabolomic profiling of mcr-1-mediated colistin resistance in Escherichia coli. *Int. J. Antimicrob. Agents* **2019**, *53* (6), 795-804. http://dx.doi.org/10.1016/j.ijantimicag.2019.02.014

(35) Yun, E. J.; Seo, S. O.; Kwak, S.; Oh, E. J.; Lee, S. H.; Jin, Y. S.; Kim, K. H. Fast filtration with a vacuum manifold system as a rapid and robust metabolome sampling method for Saccharomyces cerevisiae. *Process Biochem*. **2021**, *110*, 195-200. http://dx.doi.org/10.1016/j.procbio.2021.08.012
(36) Liu, T.; Jin, Z.; Wang, Z.; Chen, J.; Wei, L. J.; Hua, Q. Metabolomics analysis of Actinosynnema pretiosum with improved AP-3production by enhancing UDP-glucose biosynthesis. *J. Biosci. Bioeng*. **2020**, *130* (1), 36-47. http://dx.doi.org/10.1016/j.jbiosc.2020.02.013
(37) Villas-Boas, S. G.; Bruheim, P. Cold glycerol-saline: The promising quenching solution for accurate intracellular metabolite analysis of microbial cells. *Anal. Biochem*. **2007**, *370*, 87–97. http://dx.doi.org/10.1016/j.ab.2007.06.028
(38) Hussein, M.; Han, M. L.; Zhu, Y.; Zhou, Q.; Lin, Y. W.; Hancock, R. E. W.; Hoyer, D.; Creek, D. J.; Li, J.; Velkov, T. Metabolomics Study of the Synergistic Killing of Polymyxin Bin Combination with Amikacin against Polymyxin-Susceptible and -Resistant *Pseudomonas aeruginosa*. *Antimicrob. Agents Chemother*. **2020**, *64* (1), e01587-19. http://dx.doi.org/10.1128/AAC.01587-19
(39) Maifiah, M. H. M.; Creek, D. J.; Nation, R. L.; Forrest, A.; Tsuji, B. T.; Velkov, T.; Li, J. Untargeted metabolomics analysis reveals key pathways responsible for the synergistic killing of colistin and doripenem combination against *Acinetobacter baumannii*. *Sci. Rep*. **2017**, *7*, 45527. http://dx.doi.org/10.1038/srep45527
(40) Kuang, E.; Marney, M.; Cuevas, D.; Edwards, R. A.; Forsberg, E. M. Towards Predicting Gut Microbial Metabolism: Integration of Flux Balance Analysis and Untargeted Metabolomics. *Metabolites* **2020**, *10* (4), 156. http://dx.doi.org/10.3390/metabo10040156
(41) Schelli, K.; Rutowski, J.; Roubidoux, J.; Zhu, J. Staphylococcus aureus methicillin resistance detected by HPLC-MS/MS targeted metabolic profiling. *J. Chromatogr. B* **2017**, *1047*, 124-130. http://dx.doi.org/10.1016/j.jchromb.2016.05.052
(42) Gomes, T. A.; Zanette, C. M.; Spier, M. R. An overview of cell disruption methods for intracellular biomolecules recovery. *Prep. Biochem. Biotechnol*. **2020**, *50* (7), 635-654. http://dx.doi.org/10.1080/10826068.2020.1728696
(43) Mielko, K. A.; Jabłoński, S. J.; Łukaszewicz, M.; Młynarz, P. Comparison of bacteria disintegration methods and their influence on data analysis in metabolomics. *Sci. Rep*. **2021**, *11* (1), 20859. http://dx.doi.org/10.1038/s41598-021-99873-x
(44) Yang, Q.; Tao, R.; Yang, B.; Zhang, H.; Chen, Y. Q.; Chen, H.; Chen, W. Optimization of the quenching and extraction procedures for a metabolomic analysis of Lactobacillus plantarum. *Anal. Biochem*. **2018**, *557*, 62-68. http://dx.doi.org/10.1016/j.ab.2017.12.005
(45) Horak, I.; Engelbrecht, G.; Jansen van Resburg, P. J.; Claassens, S. Microbial metabolomics: essential definitions and the importance of cultivation conditions for utilizing Bacillus species as bionematicides. *J. Appl. Microbiol*. **2019**, *127* (2), 326-343. http://dx.doi.org/10.1111/jam.14218
(46) Pinu, F. R.; Villas-Boas, S. G. Extracellular Microbial Metabolomics: The State of the Art. *Metabolites* **2017**, *7* (3), 43. http://dx.doi.org/10.3390/metabo7030043
(47) Dettmer, K.; Aronov, P. A.; Hammock, B. D. Mass spectrometry-based metabolomics. *Mass Spectrom. Rev.* **2007**, *26* (1), 51-78. http://dx.doi.org/10.1002/mas.20108
(48) Kuehnbaum, N. L.; Britz-McKibbin, P. New advances in separation science for metabolomics: resolving chemical diversity in a post-genomic era. *Chem Rev*. **2013**, *113* (4), 2437–2468. http://dx.doi.org/10.1021/cr300484s
(49) Lopes, A. S.; Santa Cruz, E. C.; Sussulini, A.; Klassen, A. Metabolomic Strategies Involving Mass Spectrometry Combined with Liquid and Gas Chromatography. In: Sussulini, A. (Ed.) *Metabolomics: From Fundamentals to Clinical Applications,* 1st ed.; Springer International Publishing AG, 2017; pp 77-98. https://doi.org/10.1007/978-3-319-47656-8_4
(50) Bauermeister, A.; Mannochio-Russo, H.; Costa-Lotufo, L. V.; Jarmusch, A. K.; Dorrestein, P. C. Mass spectrometry-based metabolomics in microbiome investigations. *Nat. Rev*. **2022**, *20* (3), 143-160. http://dx.doi.org/10.1038/s41579-021-00621-9

(51) Li, J.; Rumancev, C.; Lutze, H. V.; Schmidt, T. C.; Rosenhahn, A.; Schimitz, O. J. Effect of ozone stress on the intracellular metabolites from Cobetia marina. *Anal. Bioanal. Chem*. **2020**, *412* (23), 5853-5861. http://dx.doi.org/10.1007/s00216-020-02810-6
(52) Mastrangelo, A.; Ferrarini, A.; Rey-Stolle, F.; García, A.; Barbas, C. From sample treatment to biomarker discovery: A tutorial for untargeted metabolomics based on GC-(EI)-Q-MS. *Anal. Chim. Acta*. **2015**, *900*, 21-35. http://dx.doi.org/10.1016/j.aca.2015.10.001
(53) Beccaria, M.; Franchina, F. A.; Nasir, M.; Mellors, T.; Hill, J. E.; Purcaro, G. Investigating Bacterial Volatilome for the Classification and Identification of Mycobacterial Species by HS-SPME-GC-MS and Machine Learning. *Molecules* **2021**, *26* (15), 4600. http://dx.doi.org/10.3390/molecules26154600
(54) Farbo, M. G.; Urgeghe, P. P.; Fiori, S.; Marcello, A.; Oggiano, S.; Balmas, V.; Hassan, Z. U.; Jaoua, S.; Migheli, Q. Effect of yeast volatile organic compounds on ochratoxin A-producing *Aspergillus carbonarius* and *A. ochraceus*. *Int. J. Food Microbiol*. **2018**, *284*, 1-10. http://dx.doi.org/10.1016/j.ijfoodmicro.2018.06.023
(55) Gika, H.; Virgiliou, C.; Theodoridis, G.; Plumb, R. S.; Wilson, I. D. Untargeted LC/MS-based metabolic phenotyping (metabonomics/metabo-lomics): the state of the art. *J. Chromatogr. B* **2019**, *1117*, 136–147. http://dx.doi.org/10.1016/j.jchromb.2019.04.009
(56) Furlani, I. L.; Nunes, E. C.; Canuto, G. A. B.; Macedo, A. N.; Oliveira, R. V. Liquid Chromatography-Mass Spectrometry for Clinical Metabolomics: An Overview. In: Colnaghi, S. A. V. (Ed.) *Separation Techniques Applied to Omics Sciences*, 1st ed.; Springer Nature Switzerland, 2021; pp 179-213. https://doi.org/10.1007/978-3-030-77252-9_10
(57) Tang, D. Q.; Zou, L.; Yin, X. X.; Ong, C. N. HILIC-MS for metabolomics: an attractive and complementary approach to RPLC-MS. *Mass Spectrom. Rev.* **2016**, *35* (5), 574–600. http://dx.doi.org/10.1002/mas.21445
(58) Rojo, D.; Barbas, C.; Rupérez, F. J. LC-MS metabolomics of polar compounds. *Bioanalysis* **2012**, *4* (10), 1235–1243. http://dx.doi.org/10.4155/bio.12.100
(59) Zhou, B.; Xiao, J. F.; Tuli, L.; Ressom, H. W. LC-MS-based metabolomics. *Mol. BioSyst*. **2012**, *8* (2), 470-481. http://dx.doi.org/10.1039/c1mb05350g
(60) Ortmayr, K.; Causon, T. J.; Hann, S.; Koellensperger, G. Increasing selectivity and coverage in LC-MS based metabolome analysis. *TrAC, Trends Anal. Chem*. **2016**, *82*, 358–366. http://dx.doi.org/10.1016/j.trac.2016.06.011
(61) Cui, L.; Lu, H.; Lee, Y. H. Challenges and emergent solutions for LC-MS/MS based untargeted metabolomics in diseases. *Mass Spectrom. Rev*. **2018**, *37* (6), 772-792. http://dx.doi.org/10.1002/mas.21562
(62) Chamberlain, M.; O'Flaherty, S.; Cobián, N.; Barrangou, R. Metabolomic Analysis of Lactobacillus acidophilus, L. gasseri, L. crispatus, and Lacticaseibacillus rhamnosus Strains in the Presence of Pomegranate Extract. *Font. Microbiol*. **2022**, *13*, 863228. http://dx.doi.org/10.3389/fmicb.2022.863228
(63) Groves, R. A.; Mapar, M.; Aburashed, R.; Ponce, L. F.; Bishop, S. L.; Rydzak, T.; Drikic, M.; Bihan, D. G.; Benediktsson, H.; Clement, F.; Gregson, D. B.; Lewis, I. A. Methods for Quantifying the Metabolic Boundary Fluxes of Cell Cultures in Large Cohorts by High-Resolution Hydrophilic Liquid Chromatography Mass Spectrometry. *Anal. Chem*. **2022**, *94* (25), 8874-8882. http://dx.doi.org/10.1021/acs.analchem.2c00078
(64) Tavares, M. F. M. Eletroforese capilar: conceitos básicos. *Quím. Nova* **1996**, *19* (2), 173-181.
(65) Rodrigues, K. T.; Cieslarová, Z.; Tavares, M. F. M.; Simionato, A. V. C. Strategies Involving Mass Spectrometry Combined with Capillary Electrophoresis in Metabolomics. In: Sussulini, A. (Ed.) *Metabolomics: From Fundamentals to Clinical Applications*, 1st ed.; Springer International Publishing AG, 2017; pp 99-141. https://doi.org/10.1007/978-3-319-47656-8_5
(66) Ramautar, R.; Demirci, A.; de Jong, G. J. Capillary electrophoresis in metabolomics. *TrAC, Trends Anal. Chem*. **2006**, *25* (5), 455-466. http://dx.doi.org/10.1016/j.trac.2006.02.004

(67) Drouin, N.; Ramautar, R. Capillary Electrophoresis-Mass Spectrometry for Metabolomics: Possibilities and Perspectives. In: Simionato, A. V. C. (Ed.) *Separation Techniques Applied to Omics Sciences*, 1st ed.; Springer Nature Switzerland AG, 2021, pp 159-178. https://doi.org/10.1007/978-3-030-77252-9
(68) Moini, M. Simplifying CE-MS operation. 2. Interfacing low-flow separation techniques to mass spectrometry using a porous tip. *Anal. Chem*. **2007**, *79* (11), 4241–4246. http://dx.doi.org/10.1021/ac0704560
(69) Ramautar, R.; Busnel, J. M.; Deelder, A. M.; Mayboroda, A. Enhancing the coverage of the urinary metabolome by Sheathless capillary electrophoresis-mass spectrometry. *Anal. Chem*. **2012**, *84* (2), 885–892. http://dx.doi.org/10.1021/ac202407v
(70) Canuto, G. A. B.; Castilho-Martins, E. A.; Tavares, M.; López-Gonzável, Á.; Rivas, L.; Barbas, C. CE-ESI-MS metabolic fingerprinting of Leishmania resistance to antimony treatment. *Electrophoresis* **2012**, *33* (12), 1901-1910. http://dx.doi.org/10.1002/elps.201200007
(71) Sanchez-Lopez, E.; Kammeijer, G. S. M.; Crego, A. L.; Marina, M. L.; Ramautar, R.; Peters, D. J. M.; Mayboroda, O. A. Sheathless CE-MS based metabolic profiling of kidney tissue section samples from a mouse model of Polycystic Kidney Disease. *Sci. Rep*. **2019**, *9* (1), 806. http://dx.doi.org/10.1038/s41598-018-37512-8
(72) Ramautar, R.; Shyti, R.; Schoenmaker, B.; de Groote, L.; Derks, R. J. E.; Ferrari, M. D.; van der Maagdenberg, A. M. J. M.; Deelder, A. M.; Mayboroda, O. A. Metabolic profiling of mouse cerebrospinal fluid by sheathless CE-MS. *Anal. Bioanal. Chem*. **2012**, *404* (10), 2895-2900. http://dx.doi.org/10.1007/s00216-012-6431-7
(73) Kawai, T.; Ota, N.; Okada, K.; Imasato, A.; Owa, Y.; Morita, M.; Tada, M.; Tanaka, Y. Ultrasensitive Single Cell Metabolomics by Capillary Electrophoresis-Mass Spectrometry with a Thin-Walled Tapered Emitter and Large-Volume Dual Sample Preconcentration. *Anal. Chem*. **2019**, *91* (16), 10564–10572. http://dx.doi.org/10.1021/acs.analchem.9b01578
(74) Zhang, W.; Ramautar, R. CE-MS for metabolomics: Developments and applications in the period 2018–2020. *Electrophoresis* **2019**, *42* (4), 381-401. http://dx.doi.org/10.1002/elps.202000203
(75) Inokuma, K.; Matsuda, M.; Sasaki, D.; Hasunuma, T.; Kondo, A. Widespread effect of N-acetyl-d-glucosamine assimilation on the metabolisms of amino acids, purines, and pyrimidines in *Schefersomyces stipites*. *Microb. Cell Fact*. **2018**, *17*, 153. http://dx.doi.org/10.1186/s12934-018-0998-4
(76) Yamamoto, Y.; Nakanishi, Y.; Murakami, S.; Aw, W.; Tsukimi, T.; Nozu, R.; Ueno, M.; Hioki, K.; Nakahigashi, K.; Hirayama, A.; Sugimoto, M.; Soga, T.; Ito, M.; Tomita, M.; Fukuda, S. A Metabolomic-Based Evaluation of the Role of Commensal Microbiota throughout the Gastrointestinal Tract in Mice. *Microorganisms* **2018**, *6* (4), 101. http://dx.doi.org/10.3390/microorganisms6040101
(77) Li, G.; Jian, T.; Liu, X.; Lv, Q.; Zhang, G.; Ling, J. Application of Metabolomics in Fungal Research. *Molecules* **2022**, *27* (21), 7365. http://dx.doi.org/10.3390/molecules27217365
(78) Galdiero, E.; Salvatore, M. M.; Maione, A.; de Alteriis, E.; Andolfi, A.; Salvatore, F.; Guida, M. GC-MS-Based Metabolomics Study of Single- and Dual-Species Biofilms of Candida albicans and Klebsiella pneumonia. *Int. J. Mol. Sci*. **2021**, *22* (7), 3496. http://dx.doi.org/10.3390/ijms22073496
(79) Gold, A.; Chen, L.; Zhu, J. More than Meets the Eye: Untargeted Metabolomics and Lipidomics Reveal Complex Pathways Spurred by Activation of Acid Resistance Mechanisms in *Escherichia coli*. *J. Proteome Res*. **2022**, *21* (12), 2958-2968. https://doi.org/10.1021/acs.jproteome.2c00459

Brazilian Journal of Analytical Chemistry
2023, Volume 10, Issue 40, pp 54-64
doi: 10.30744/brjac.2179-3425.RV-07-2023

BrJAC

REVIEW

The Emerging of Microplastic and Nanoplastic as Pollutants and their Characterization and Analysis

Lilian Rodrigues Rosa Souza

Departamento de Química, FFCLRP, Universidade de São Paulo, 14040-901 Ribeirão Preto, SP, Brazil

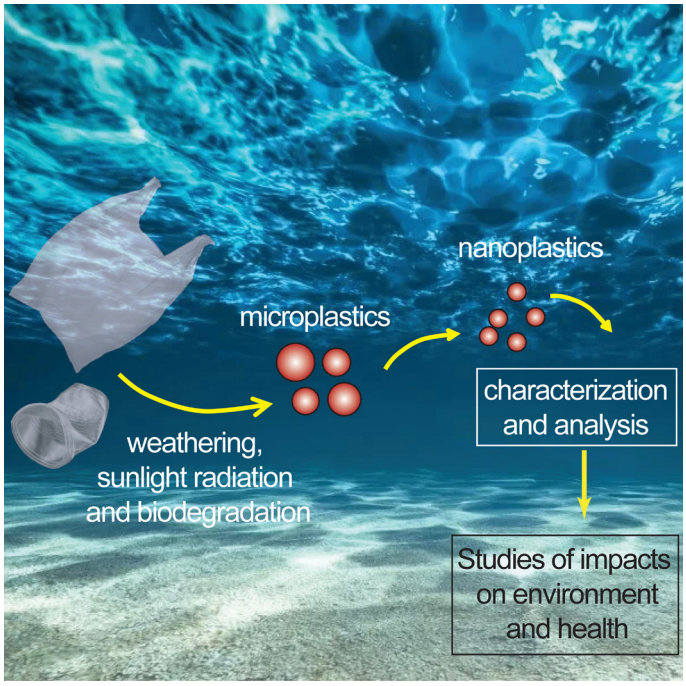

Global plastic pollution is a serious problem that is increasing over the years since millions of tons of plastics end up in the environment. These plastics are fragmented due to sunlight radiation, biodegradation, and other environmental factors leading to small debris which can be transformed into microplastics and nanoplastics. Due to their small size and high surface area, these materials can be easily absorbed by organisms besides being able to adsorb toxic pollutants. Considering these issues, studies about their toxicity and fate in the environment are of great importance, however, the success of these studies depends on the methods of sampling, sample preparation, and also analysis, which need to be developed and improved. Thus, the current review proposes an integrated approach of methodologies of sampling, sample preparation, and analysis of solid and aqueous samples with microplastics and nanoplastics besides discussing the challenges and new methodologies for microplastics and nanoplastics analysis.

Keywords: microplastic, nanoplastic, environmental pollution, nanoplastic analysis, sample preparation

INTRODUCTION

Over the past decades, Earth is polluted with plastic waste since its production has been massively employed for a wide range of applications in order to improve life quality, however, this extensive use of plastics has resulted in severe environmental pollution which is getting concerned of the scientific community.[1] Plastic pollution achieved alarming levels in the environment and it is estimated that this pollution on land and in freshwater could be many times greater than the estimated 4.8 to 12.7 million tonnes.[2] Consequently, the large plastic debris is like to break down into small debris due to weathering, sunlight radiation, and biodegradation: the microplastics (MP) and even the nanoplastics (NP) (Figure 1).[1]

Cite: Souza, L. R. R. The Emerging of Microplastic and Nanoplastic as Pollutants and their Characterization and Analysis. *Braz. J. Anal. Chem.* 2023, *10* (40), pp 54-64. http://dx.doi.org/10.30744/brjac.2179-3425.RV-07-2023

Submitted 23 January 2023, Resubmitted 19 March 2023, Accepted 30 April 2023, Available online 15 May 2023.

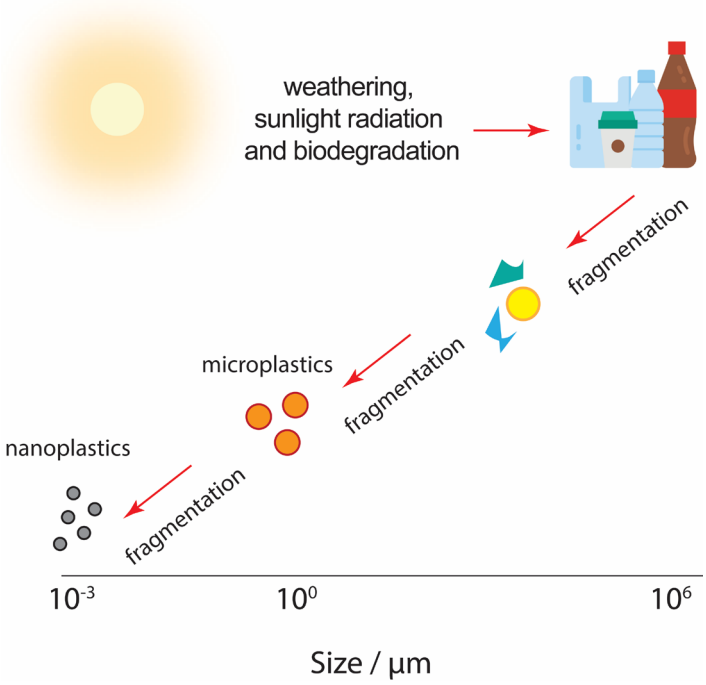

Figure 1. Schematic representation of the fragmentation of plastics and nanoplastic formation.

Since this is an emerging issue in the environment, some distinctions are necessary to be made for these terminologies. Firstly, it is common the association of polymers and plastics, and consequently the association of nanopolymers as NPs. However, it must be taken into account that all plastics are polymer-based, however, not all polymers are plastics and consequently, there is a distinction between NPs and nanopolymers.[2] The second consideration is about the size and characteristics of these materials since the properties and behavior of nanomaterials cannot be extrapolated for a bulk counterpart, and due to this, it can be made a separation of NPs and MPs regardless of the size range.[2] With these considerations in mind and the inaccuracy in the definition, it can be assumed that MPs can be further degraded to NPs, which have a particle size between 1 nm and 100 nm.[3] These characteristics enable MPs and NPs to escape from the wastewater treatment process and enter the environment (aquatic ecosystem, soil, and sediments)[3] and also in the food chain.

The reach of MPs and NPs achieved alarming consequences since studies have demonstrated that these materials can be translocated across the placenta into the fetal kidney, heart, lung, liver, and brain in the late-stage of pregnancy, besides these materials have also been found in breast milk.[4]

Furthermore, some studies have demonstrated that MPs and NPs are able to bind toxic metals such as Pb and Cu,[5,6] which can enhance the problem of toxicity of these metals since they can be spread in different environments and contaminate them.

Although these studies about nano and microplastics are getting attention, compared with the vast literature about nanoparticles (toxicity, analysis, and characterization), the MPs and NPs investigation is at the infancy stage (Figure 2), and protocols are still under development.[1]

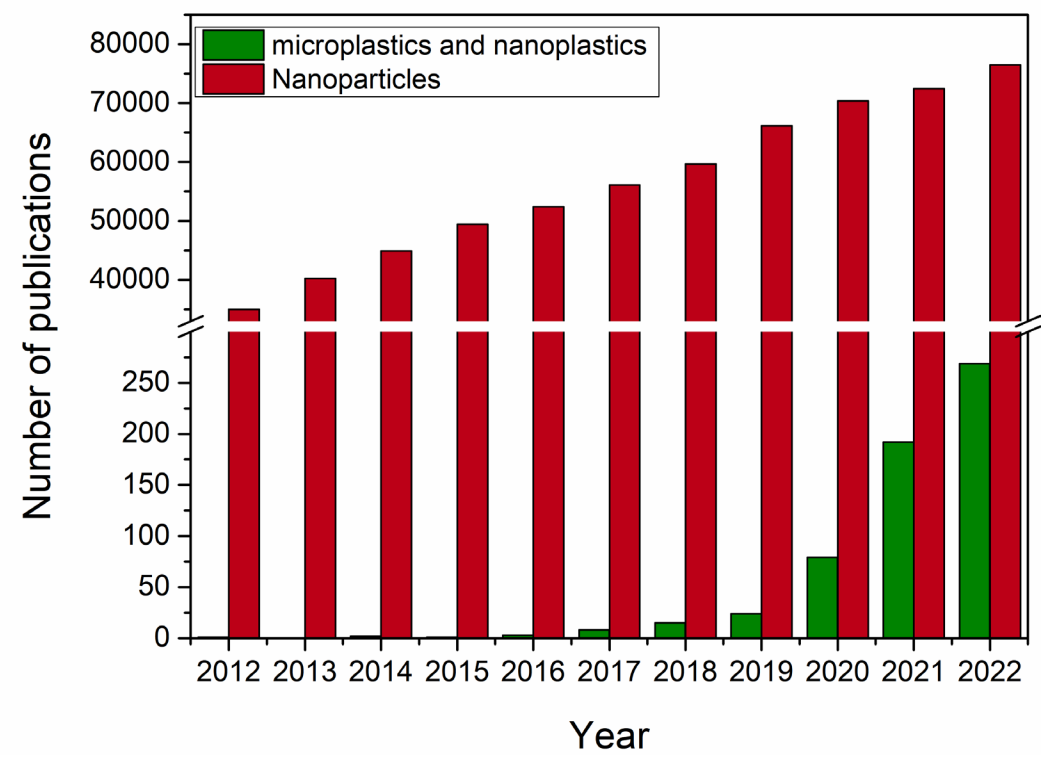

Figure 2. Comparison of the number of publications between microplastics and nanoplastics and nanoparticles (source: Scopus)

The success of studies about the toxicity of MPs and NPs as well as their fate in the environment depends on the methods of sampling, sample treatments, separation, and analysis, therefore the development of these methodologies is undoubtedly of great importance.

Considering this challenge, this review aims to provide a recent overview of the methods for the determination of micro and nanoplastics and also the methods of sample treatments considering the challenges that have to be overcome.

SAMPLING AND SAMPLE TREATMENT

The sampling and processing methods for water samples are similar for both fresh and saltwater, although differences can be noted in the distribution of MPs since it is influenced by density (since generally, MPs will be deeper in freshwater) and hydrodynamic profile of the samples.[7] The water samples are collected directly from the area in which the study will be performed and nets are frequently used to collect MPs from water samples. Different nets can be employed according to the deep and also the pore diameters (for example, for superficial collection, neuston or manta can be employed with approximately 333 μm). Pumps are also used for sampling since it is possible to obtain several cubic meters of water per hour and is used for a specific depth where extraction is guaranteed.[8] Crew and co-workers employed specific bottles for water sampling in which the 4 L plastic jugs were acid-washed and used to collect water at a depth of 0-5 cm. This procedure was repeated 25 times to filter 100 L of water sample through a piece of 100 mm nylon mesh.[9]

The sampling of soil and sediment samples depends on the distribution of MPs and NPs which is influenced by different factors such as meteorological, temporal, and dependent on the sampling area and can compromise the reproducibility of the results.[7] The collection of MPs on beaches is easy to implement by using forceps, and sieving and allows the collection of large volumes of the sample or replicates while the collection of samples from seabed requires the use of specialized equipment such as box corer and

grab samples, furthermore, since the deep is an important factor, the number of replicates can vary in order to ensure the representativity.[7] The collection of soil can correspond to the uppermost horizon (0-10 cm, organo-mineral horizon) and can be collected using stainless steel shovel, stainless steel corer, and Lenz sampler. Due to the heterogeneous matrix, soil samples are easily affected by human interaction and making it difficult to obtain representative samples. It is also important that the sampling amount of soil should exceed the amount essential for the analysis of MPs allowing additional repetitions when needed.[10,11] As MPs particles are particulates with a wide range of size, their distribution in soil also can be significantly variable.[12] In order to overcome this problem, some authors[13,14] employed composite samples taken from defined subunits within a sampling site to get a representative sample from the contaminated site.

Different sample preparation can be employed for aqueous samples such as seawater, river water, or other aqueous sources. Filtration is commonly the first step that concentrates the MPs and NPs and enables an increase in the quality of analysis. The sieving is another treatment that differs from filtration by the use of a sieve (usually with a mesh size between 0.038 and 4.750 mm) to separate the MPs.[8] The preconcentration treatments is a tool to improve the limit of detection (LOD) and limit of quantification (LOQ) of analysis and different methodologies can be employed in this step such as ultrafiltration,[15–17] crossflow ultrafiltration,[15,17] ultracentrifugation,[17] and cloud point extraction.[1,18–20] In ultrafiltration, is employed a porous membrane ranging from 10 to 100 kDa of molecular weight cutoff where the solution penetrates by an applied pressure.[17] The ultracentrifugation uses faster spinning speeds able to collect dispersed particles, and since MPs and NPs are insoluble, they can be sedimented. However, this technique may damage the MPs, thus if the composition of MPs is the only information required, this will not be a problem.[17] Cai et al. employed ultracentrifugation for separation and enrichment in river water samples and they reported that NPs fragments were successfully separated and enriched by a factor of nearly 50 times with a high recovery rate (87.1%).[21] Cloud point extraction is a technique based on the formation of micelles from a nonionic surfactant abbe to bind and concentrate the analyte or particle of interest when they are heated above its cloud point temperature.[18]

For solid samples such as sediments and soil, the extraction procedure is one of the most employed methodologies for sample preparation. Wahl and co-workers performed a water-soil extraction with ultrapure water added to soil at a soil/water ratio of 1:4 and stirred at 300 r min^{-1} for 72 h and after, samples were filtered to 0.8 mm (Sartorius filters).[10] Junhao et al. recommend that drying made easier the separation of MP from the soil, however, the temperature must be moderate in order to avoid MPs degradation, therefore, it is suggested that drying takes place at a temperature close to 60 ºC.[17] Crew and co-workers employed sieving (in order to separate in 8 different sediment size fractions) and also dried the sediment samples in order to perform the extraction of microplastics.[9] In the density separation, the soil is treated using ultrasonic, and after is added a saturated solution of zinc chloride, calcium chloride, sodium bromide, or zinc bromide is for the suspension medium. After, stirring and sedimentation of the mixture, the supernatant with MPs is filtered.[17] Recently, Schütze and co-workers performed a systematic study of the different solutions (NaBr, H_2O, NaCl, and sodium hexametaphosphate) with different densities in order to separate a mixture of microplastics, polyethylene (PE), polypropylene (PP), polyvinyl chloride (PVC), polyethylene terephthalate, and three biodegradable polymers (PLA, PBS, MB), achieving recovery rates of 87.3–100.3% for conventional polymers, and 38.2–78.2% for biodegradable polymers for NaBr solution.[22] Electrostatic separation is a dry processing technique and can be employed since the soil constituents are electrically conductive and MPs and NPs are not this method has the advantage to be quick, simple and up to 99% of the original mass can be removed without the loss of MPs.[17] The digestion of organic matter is sometimes desired (if the proposal of the study is not to investigate the interaction of MPs and organic matter in the environment) since it can affect the accurate identification and quantification of MPs and NPs. Different digestion methods can be used for this proposal such as digestion with acid (commonly with HNO_3 and/or HCl), alkali (commonly with KOH and NaOH), H_2O_2, and enzyme which is the least aggressive method with low impact on MPs.[17] The combination of density separation and removal

of organic matter was also employed by Hurley et al.[23] to separate the microplastics from a complex solid matrix. Oxidation methods using H_2O_2, Fenton's reagent (identified as the optimum protocol), and alkaline digestion with NaOH and KOH were employed to remove the organic matter, and water and NaI were employed for density separation of the microplastics.[23]

The different sample treatments for solid and liquid samples are summarized in Table I.

Table I. Some methodologies for sample treatment for MPs and NPs analysis

Methodology	Characteristic	Reference
	Liquid samples	
Filtration	Large volumes of water can be filtered and the particles are directly concentrated during the sampling	24
Sieving	Simple and employs sieves with a mesh size between 0.038 and 4.750 mm	8
Preconcentration	Different methodologies such as ultrafiltration, crossflow ultrafiltration, ultracentrifugation, and cloud point extraction.	1,15–20
	Solid samples	
Digestion	Can be performed with acid and alkali solutions, H_2O_2, and enzymes	17
Electrostatic separation	High separation efficiency, quick, and simple	17
Density separation	Simple, different salt solutions can be employed	17
Extraction	Simple, can employ different solutions and solvents such as water	10
Drying	Avoiding temperatures above 60 ºC	17

Another technique for MPs and NPs separation has been widely used: field flow fractionation (FFF). The FFF is a fluid-assisted hydrodynamic separation method that is used to separate macromolecular particles (proteins, nanomaterials) from colloidal particles. The principle of the method is based on the distinct diffusivity of the particles in which when the particles pass through the FFF, a perpendicular field is applied and the particles stay at different distances from the channel wall and present different retention times, enabling the fractionation of the particles in the sample.[25] The most used FFF for MPs and NPs is the asymmetrical flow field-flow fractionation (AF4).[1] In this mode, the sample sorting is achieved by sample circulation in the channel, where the particles stabilize at different heights, according to the difference in diameters, after introducing two opposite flow streams.[25] Pashaei et al. employed the AF4 for the characterization and determination of NPs and MPs in hypersaline lakes and they found that MPs and NPs have different transport mechanisms in this environment and fate compared to lake and ocean.[26] Correia and Loeschner coupled multi-angle light scattering (MALS) with AF4 for the detection of NPs in food and reported that although polystyrene NPs could be detected and characterized, the determination and characterization of polyethylene NPs in fish samples were not possible and consequently new methodologies need to be developed to improve this determination.[27] Recently, Müller and co-workers employed the AF4 to investigate the impact of MPs and NPs presented in paints on *Daphnia magna* and on the murine cell line which was strongly affected by the polymers of MPs and NPs.[28]

ANALYSIS OF MICROPLASTICS AND NANOPLASTICS

Identification and quantification of microplastics can be made by spectroscopy methods, microscopy images, and also by visual analysis. Plastics with a size ranging from centimeters and millimeters are

easy to be detected by the naked eye after the collection of samples. Optical microscopes (OMs) are widely employed as an identification tool for smaller plastic particles especially when they are colored. However, the determination of smaller microplastics with no color or specific shape is difficult.[29] Given this, the scanning electron microscope (SEM) can overcome this problem, since it is possible to visualize at nanometer size. Furthermore, SEM equipped with energy-dispersive X-ray (SEM/EDX) also can provide information about the composition and surface structure of the MPs and NPs which is a useful tool for the identification of the MPs and NPs.[29] The SEM/EDX can identify some MPs and NPs due to the elemental signatures. In view of this, Wang et al. easily identified PVC MPs due to the unique elemental signature pf PVC including chlorine.[30] Besides the identification of the type of MPs due to the elemental signature, it is also possible to evaluate the aging of the MP in the environment. This was observed by Tiwari et al., the authors observed characteristics cracks in MPs surfaces, suggesting polymer aging, mechanical and oxidative weathering.[31]

Vibrational techniques such as Fourier-transform infrared (FT-IR) and Raman spectroscopy are widely used for identifying the chemical composition of MPs and NPs, since they can provide information about the functional groups and molecular structure besides the information about size, size distribution, and morphology.[29,32,33]

The micro-FTIR spectroscopy (μ-(FT)IR spectroscopy) is the most employed method for MPs analysis, in which the FTIR spectrometer is coupled to an optical microscope and can be performed in reflectance or transmission mode. The reflectance mode allows an investigation of the particle surface MPs modifications due to aging effects, however, this mode can suffer undesired light-scattering effects on the particle surface that decrease the spectral quality. The transmission mode presents high-quality spectra, however, the thickness or color of MPs influences the analysis since it may lead to total absorption causing unidentifiable spectra due to the convergence of the bands.[33] A small size of MPs (20 μm) present in bottled drinking water was identified using using FTIR microscope as reported by Zainuddin and Syuhada.[34]

Raman microspectroscopy (RM), a non-destructive method based on the effect of inelastic light scattering on molecules, can also be coupled with confocal optical microscopy. This configuration provides a resolution lower than 1 μm, which is better than μ-(FT)IR spectroscopy (with a resolution of about 10 μm). This technique allows analysis of MPs in aqueous and wet samples since it is insensitive to water, however, it may suffer interference due to fluorescence of inorganic and organic impurities in the samples.[33] The surface-enhanced Raman spectroscopy (SERS) is also a technique employed for MPs and NPs characterization. This technique amplifies the Raman signal using a laser source combining the advantages of both plasmonics and Raman scattering.[35] Hu et al. employed this technique in order to analyze polystyrene NP and they reported a high sensitivity (detection limit of 6.25 μg/mL for 100 nm PS NP), interference resistance, good repeatability, and quantitative analysis ability ($R2 > 0.970$).[36] Furthermore, the combination of preconcentration methods and these techniques for analysis can enhance the limits of detection improving the analysis. According to Yang et al, the combination of bifunctional Ag nanowire membranes was employed to enrich NPs and enhance the surface-enhanced Raman spectroscopy (SERS) spectra. Good retention rates (86.7% for 50 nm and approximately 95.0% for 100–1000 nm) and high sensitivity (down to 10–7 g/L for 50–1000 nm and up to 105 SERS enhancement factor) of standard polystyrene (PS) NPs were achieved.[37]

In contrast to spectroscopic methods, thermoanalytical methods are destructive techniques such as thermogravimetric analysis (TGA), differential scanning calorimetry (DSC), and pyrolysis-gas chromatography-mass spectrometry, and the sample is thermally decomposed under defined conditions.[38] The TGA measures the mass change as a function of thermolysis temperature and although it is a useful tool, it can be a challenge to quantify the fraction of different types of plastics in a mixture.[29] TGA has long been used in the investigation of the thermal properties of plastics since it is an easy and quick technique, moreover, when combined with FTIR and CG-MS the characterization of polymers based on the gaseous decomposition products can be improved.[39] Dümichen et al. compared the polyethylene MPs analysis from TGA and pyrolyze gas chromatography-mass spectrometry and reported that high sample masses in TGA

(200 times higher than used in the chromatography technique) were able to be analyzed from complex non-homogenous matrices.[40] The combination of TGA and FTIR could distinguish and also quantify MPs of PVC and PS in mussels and seawater samples as reported by Yu et al.[41]

Differential scanning calorimetry (DSC) is another thermal analysis that measures the amount of energy required to increase the temperature of the sample as a function of temperature, and the identification of the type of plastic can be made using established libraries of the thermal degradation patterns.[29] This technique requires reference materials to identify the polymer and due to this, it is useful for identifying primary MPs.[42] According to Shabaka et al., this technique was able to reveal the presence of ten polymers ranging from 0.5 mm to 5 mm and with a variety of shapes and colors in seawater and shoreline sediments.[43] Chialanza and co-workers coupled optical microscopy with image analysis (IA) and DSC and these combined techniques provided particle characterization and counting procedures based on image analysis chemical identification of MPs based on DSC signal processing.[44]

Pyrolysis-gas chromatography-mass spectrometry has been one of the techniques employed to explore the characteristics of MPs and NPs since non or minimum pretreatment is needed, it has high sensitivity, it can analyze mixtures of different polymers, it is a fast technique, and also it is possible to analyze the samples quantitatively.[45] The quantification and detection of MPs and NPs are accomplished by characteristic pyrolysis products and their respective indicator ions.[38] Blancho and co-workers employed this technique to analyze polypropylene and polystyrene NP in suspensions and also explored different matrix effects by spiking the NP in different organic matter suspensions (i.e., algae, soil natural organic matter, and soil humic acid). They reported that polypropylene NP identification was validated while polystyrene NP requires preliminary treatment.[46] Coupling the tandem mass spectrometry to pyrolysis-gas chromatography, the detection of MPs was improved according to Albignac et al. since besides this method was employed to analyze MPs from 500 µm down to 0.7 µm, the quantification of six common polymers was possible in one run.[47]

Table II. The most employed techniques for MPs and NPs analysis

Technique	Characteristic	Reference
Optical microscope	Determination of smaller microplastics with no color or specific shape is difficult	29
SEM	Possibility to visualize at nanometer-size	29
SEM/EDX	Provide information about the composition and surface structure	29
Raman microspectroscopy	Allows analysis of MPs in aqueous and wet samples, may suffer interferences due to fluorescence	33
Micro-FTIR spectroscopy	Resolution limited to approximately 10 µm, performed in reflectance or transmission mode	33
Thermogravimetric analysis	Easy and quick technique, difficult to analyze mixtures of plastics	29,39
Differential scanning calorimetry	Requires a reference material to identify the polymer	42
Pyrolysis-gas chromatography-mass spectrometry	High sensitivity, possibility to analyze mixtures of different polymers, and analyze the samples quantitatively	45

These techniques can be combined to provide more accurate information about the MPs and NPs in samples. The FTIR, AFM-IR and Pyr-GC/MS were employed by Li et al. for the characterization of NPs in tap water samples which were polyolefins, polystyrene, polyvinyl chloride, polyamide, and some plastic additives. Furthermore, besides the identification of the polymer present in MPs samples, the size was also identified: the abundance of NPs with the most frequent particle sizes in a range of 58–255 nm was 1.67–2.08 μg L^{-1} in tap water.[48]

FUTURE PERSPECTIVES

Considering that there is a lack of information about the toxic effects and fate of MPs and NPs, the development of these studies needs improvements in the sample preparation and mostly in the analysis of the samples. A new strategy of the methodology of analysis is emerging which is the use of Single Particle Inductively Coupled Plasma Mass Spectrometry (SP-ICP-MS). According to Jiménez-Lamana, the possibility to associate metals such as nanoparticles (gold nanoparticles) in NPs and MPs make the analysis possible since the adsorbed Au produced a SP-ICP-MS signal allows the counting of individual NPs particles, and hence their accurate quantification.[49] This possibility of analysis can be an important tool for the investigation of metals adsorbed in MPs and NPs, allowing their direct characterization.

Although this new possibility of analysis emerged, there are challenges to be overcome such as (i) ensuring the sampling is representative as possible, since representative MPs and NPs samples are essential for the interpretation of the analysis, and also the consequences of the presence of these materials in the environment. In view of this, the improvement of the sampling technique considering the spatial and temporal variation is critical. (ii) Understand the complex composition of NPs and MPs, since in the environment, these materials can be associated with toxic metals (and other compounds) and also organic matter and these compositions can affect the fate and toxicity of these materials. (iii) Improve the techniques of sampling and analysis of small NPs to avoid loss of these materials and obtain more complete information about the presence of these materials in the environment.[50,51]

Furthermore, compared with the studies about nanoparticles, the investigation of MPs and NPs is in the beginning and due to this, this is a wide field of study to be explored.

Conflicts of interest

No conflicts to declare.

Acknowledgements

The author thanks PRP-USP PIPAE (2021.1.10424.1.9) for financial support.

REFERENCES

(1) Cai, H.; Xu, E. G.; Du, F.; Li, R.; Liu, J.; Shi, H. Analysis of Environmental Nanoplastics: Progress and Challenges. *Chem. Eng. J.* **2021**, *410*, 128208. https://doi.org/10.1016/J.CEJ.2020.128208

(2) Gigault, J.; El Hadri, H.; Nguyen, B.; Grassl, B.; Rowenczyk, L.; Tufenkji, N.; Feng, S.; Wiesner, M. Nanoplastics Are Neither Microplastics nor Engineered Nanoparticles. *Nat. Nanotechnol.* **2021**, *16* (5), 501–507. https://doi.org/10.1038/s41565-021-00886-4

(3) Shen, M.; Zhang, Y.; Zhu, Y.; Song, B.; Zeng, G.; Hu, D.; Wen, X.; Ren, X. Recent Advances in Toxicological Research of Nanoplastics in the Environment: A Review. *Environ. Pollut.* **2019**, *252*, 511–521. https://doi.org/10.1016/J.ENVPOL.2019.05.102

(4) Liu, S.; Lin, G.; Liu, X.; Yang, R.; Wang, H.; Sun, Y.; Chen, B.; Dong, R. Detection of Various Microplastics in Placentas, Meconium, Infant Feces, Breastmilk and Infant Formula: A Pilot Prospective Study. *Sci. Total Environ.* **2023**, *854*, 158699. https://doi.org/10.1016/J.SCITOTENV.2022.158699

(5) Davranche, M.; Veclin, C.; Pierson-Wickmann, A. C.; El Hadri, H.; Grassl, B.; Rowenczyk, L.; Dia, A.; Ter Halle, A.; Blancho, F.; Reynaud, S.; Gigault, J. Are Nanoplastics Able to Bind Significant Amount of Metals? The Lead Example. *Environ. Pollut.* **2019**, *249*, 940–948. https://doi.org/10.1016/j.envpol.2019.03.087

(6) Manickam, S.; Senthilkumar, R.; Saravanakumar, K.; Reddy Prasad, D. M.; Naveen Prasad, B. S. The Potential of Polyethylene Microplastics to Transport Copper in Aquatic Systems: Adsorption and Desorption Studies. *Water Environ. Res.* **2022**, No. July, 1–9. https://doi.org/10.1002/wer.10809
(7) Prata, J. C.; da Costa, J. P.; Duarte, A. C.; Rocha-Santos, T. Methods for Sampling and Detection of Microplastics in Water and Sediment: A Critical Review. *TrAC - Trends Anal. Chem.* **2019**, *110*, 150–159. https://doi.org/10.1016/J.TRAC.2018.10.029
(8) Tornero, Q.; Dzuila, M.-A.; Robert, D.; Keller, N.; Rodríguez-Chueca, J.; Garcia-Muñoz, P. Methods of Sampling and Sample Preparation for Detection of Microplastics and Nanoplastics in the Environment. In: Tyagi, R. D.; Pandey, A.; Drogui, P.; Yadav, B.; Pilli, S. (Eds.). *Current Developments in Biotechnology and Bioengineering*; Elsevier, 2023. Chapter 4, pp 79–97. https://doi.org/10.1016/B978-0-323-99908-3.00004-X
(9) Crew, A.; Gregory-Eaves, I.; Ricciardi, A. Distribution, Abundance, and Diversity of Microplastics in the Upper St. Lawrence River. *Environ. Pollut.* **2020**, *260*. https://doi.org/10.1016/J.ENVPOL.2020.113994
(10) Wahl, A.; Le Juge, C.; Davranche, M.; El Hadri, H.; Grassl, B.; Reynaud, S.; Gigault, J. Nanoplastic Occurrence in a Soil Amended with Plastic Debris. *Chemosphere* **2021**, *262*. https://doi.org/10.1016/j.chemosphere.2020.127784
(11) Yang, L.; Zhang, Y.; Kang, S.; Wang, Z.; Wu, C. Microplastics in Soil: A Review on Methods, Occurrence, Sources, and Potential Risk. *Sci. Total Environ.* **2021**, *780*, 146546. https://doi.org/10.1016/J.SCITOTENV.2021.146546
(12) Möller, J. N.; Löder, M. G. J.; Laforsch, C. Finding Microplastics in Soils: A Review of Analytical Methods. *Environ. Sci. Technol.* **2020**, *54* (4), 2078–2090. https://doi.org/10.1021/acs.est.9b04618
(13) Zhang, G. S.; Liu, Y. F. The Distribution of Microplastics in Soil Aggregate Fractions in Southwestern China. *Sci. Total Environ.* **2018**, *642*, 12–20. https://doi.org/10.1016/J.SCITOTENV.2018.06.004
(14) Scheurer, M.; Bigalke, M. Microplastics in Swiss Floodplain Soils. *Environ. Sci. Technol.* **2018**, *52*, 3591–3598. https://doi.org/10.1021/acs.est.7b06003
(15) Mintenig, S. M.; Bäuerlein, P. S.; Koelmans, A. A.; Dekker, S. C.; van Wezel, A. P. Closing the Gap between Small and Smaller: Towards a Framework to Analyse Nano- and Microplastics in Aqueous Environmental Samples. *Environ. Sci. Nano* **2018**, *5*, 1640–1649. https://doi.org/10.1039/C8EN00186C
(16) Estahbanati, M. R. K.; Kiendrebeogo, M.; Mostafazadeh, A. K.; Drogui, P.; Tyagi, R. D. Treatment Processes for Microplastics and Nanoplastics in Waters: State-of-the-Art Review. *Mar. Pollut. Bull.* **2021**, *168*, 112374. https://doi.org/10.1016/J.MARPOLBUL.2021.112374
(17) Junhao, C.; Xining, Z.; Xiaodong, G.; Li, Z.; Qi, H.; Siddique, K. H. M. Extraction and Identification Methods of Microplastics and Nanoplastics in Agricultural Soil: A Review. *J. Environ. Manage.* **2021**, *294*, 112997. https://doi.org/10.1016/J.JENVMAN.2021.112997
(18) Zhou, X. X.; Hao, L. T.; Wang, H. Y. Z.; Li, Y. J.; Liu, J. F. Cloud-Point Extraction Combined with Thermal Degradation for Nanoplastic Analysis Using Pyrolysis Gas Chromatography-Mass Spectrometry. *Anal. Chem.* **2019**, *91* (3), 1785–1790. https://doi.org/10.1021/acs.analchem.8b04729
(19) Picó, Y.; Barceló, D. Pyrolysis Gas Chromatography-Mass Spectrometry in Environmental Analysis: Focus on Organic Matter and Microplastics. *TrAC Trends Anal. Chem.* **2020**, *130*, 115964. https://doi.org/10.1016/J.TRAC.2020.115964
(20) Ivleva, N. P. Chemical Analysis of Microplastics and Nanoplastics: Challenges, Advanced Methods, and Perspectives. *Chem. Rev.* **2021**, *121* (19), 11886–11936. https://doi.org/10.1021/acs.chemrev.1c00178
(21) Cai, H.; Chen, M.; Du, F.; Matthews, S.; Shi, H. Separation and Enrichment of Nanoplastics in Environmental Water Samples via Ultracentrifugation. *Water Res.* **2021**, *203*, 117509. https://doi.org/10.1016/J.WATRES.2021.117509
(22) Schütze, B.; Thomas, D.; Kraft, M.; Brunotte, J.; Kreuzig, · Robert. Comparison of Different Salt Solutions for Density Separation of Conventional and Biodegradable Microplastic from Solid Sample Matrices. *Environ. Sci. Pollut. Res.* https://doi.org/10.1007/s11356-022-21474-6

(23) Hurley, R. R.; Lusher, A. L.; Olsen, M.; Nizzetto, L. Validation of a Method for Extracting Microplastics from Complex, Organic-Rich, Environmental Matrices. *Environ. Sci. Technol*. **2018**, *52* (13), 7409–7417. https://doi.org/10.1021/acs.est.8b01517
(24) Stock, F.; Kochleus, C.; Bänsch-Baltruschat, B.; Brennholt, N.; Reifferscheid, G. Sampling Techniques and Preparation Methods for Microplastic Analyses in the Aquatic Environment – A Review. *TrAC Trends Anal. Chem.* **2019**, *113*, 84–92. https://doi.org/10.1016/J.TRAC.2019.01.014
(25) Zhao, K.; Wei, Y.; Dong, J.; Zhao, P.; Wang, Y.; Pan, X.; Wang, J. Separation and Characterization of Microplastic and Nanoplastic Particles in Marine Environment. *Environ. Pollut.* **2022**, *297*, 118773. https://doi.org/10.1016/J.ENVPOL.2021.118773
(26) Pashaei, R.; Loiselle, S. A.; Leone, G.; Tamasi, G.; Dzingelevičienė, R.; Kowalkowski, T.; Gholizadeh, M.; Consumi, M.; Abbasi, S.; Sabaliauskaitė, V.; Buszewski, B. Determination of Nano and Microplastic Particles in Hypersaline Lakes by Multiple Methods. *Environ. Monit. Assess.* **2021**, *193* (10), 1–15. https://doi.org/10.1007/s10661-021-09470-8
(27) Correia, M.; Loeschner, K. Detection of Nanoplastics in Food by Asymmetric Flow Field-Flow Fractionation Coupled to Multi-Angle Light Scattering: Possibilities, Challenges and Analytical Limitations. *Anal. Bioanal. Chem.* **2018**, *410* (22), 5603–5615. https://doi.org/10.1007/s00216-018-0919-8
(28) Müller, A. K.; Brehm, J.; Völkl, M.; Jérôme, V.; Laforsch, C.; Freitag, R.; Greiner, A. Disentangling Biological Effects of Primary Nanoplastics from Dispersion Paints' Additional Compounds. *Ecotoxicol. Environ. Saf.* **2022**, *242*, 113877. https://doi.org/10.1016/j.ecoenv.2022.113877
(29) Jung, S.; Cho, S. H.; Kim, K. H.; Kwon, E. E. Progress in Quantitative Analysis of Microplastics in the Environment: A Review. *Chem. Eng. J.* **2021**, *422*, 130154. https://doi.org/10.1016/J.CEJ.2021.130154
(30) Wang, Z. M.; Wagner, J.; Ghosal, S.; Bedi, G.; Wall, S. SEM/EDS and Optical Microscopy Analyses of Microplastics in Ocean Trawl and Fish Guts. *Sci. Total Environ.* **2017**, *603–604*, 616–626. https://doi.org/10.1016/J.SCITOTENV.2017.06.047
(31) Tiwari, M.; Rathod, T. D.; Ajmal, P. Y.; Bhangare, R. C.; Sahu, S. K. Distribution and Characterization of Microplastics in Beach Sand from Three Different Indian Coastal Environments. *Mar. Pollut. Bull.* **2019**, *140*, 262–273. https://doi.org/10.1016/J.MARPOLBUL.2019.01.055
(32) Picó, Y.; Barceló, D. Analysis of Microplastics and Nanoplastics: How Green Are the Methodologies Used? *Curr. Opin. Green Sustain. Chem.* **2021**, *31*, 100503. https://doi.org/10.1016/J.COGSC.2021.100503
(33) Schymanski, D.; Oßmann, B. E.; Benismail, N.; Boukerma, K.; Dallmann, G.; von der Esch, E.; Fischer, D.; Fischer, F.; Gilliland, D.; Glas, K.; Hofmann, T.; Käppler, A.; Lacorte, S.; Marco, J.; Rakwe, M. EL; Weisser, J.; Witzig, C.; Zumbülte, N.; Ivleva, N. P. Analysis of Microplastics in Drinking Water and Other Clean Water Samples with Micro-Raman and Micro-Infrared Spectroscopy: Minimum Requirements and Best Practice Guidelines. *Anal. Bioanal. Chem.* **2021**, *413*, 5969–5994. https://doi.org/10.1007/s00216-021-03498-y
(34) Zainuddin, Z.; Syuhada. Study of Analysis Method on Microplastic Identification in Bottled Drinking Water. *Macromol. Symp.* **2020**, *391*, 1–8. https://doi.org/10.1002/masy.201900195
(35) Dey, T. Microplastic Pollutant Detection by Surface Enhanced Raman Spectroscopy (SERS): A Mini-Review. *Nanotechnol. Environ. Eng.* **2023**, *8*, 41–48. https://doi.org/10.1007/s41204-022-00223-7
(36) Hu, R.; Zhang, K.; Wang, W.; Wei, L.; Lai, Y. Quantitative and Sensitive Analysis of Polystyrene Nanoplastics down to 50 Nm by Surface-Enhanced Raman Spectroscopy in Water. *J. Hazard. Mater.* **2022**, *429*. https://doi.org/10.1016/J.JHAZMAT.2022.128388
(37) Yang, Q.; Zhang, S.; Su, J.; Li, S.; Lv, X.; Chen, J.; Lai, Y.; Zhan, J. Identification of Trace Polystyrene Nanoplastics Down to 50 Nm by the Hyphenated Method of Filtration and Surface-Enhanced Raman Spectroscopy Based on Silver Nanowire Membranes. *Cite This Environ. Sci. Technol* **2022**, *2022*. https://doi.org/10.1021/acs.est.2c02584

(38) Primpke, S.; Fischer, M.; Lorenz, C.; Gerdts, G.; Scholz-Böttcher, B. M. Comparison of Pyrolysis Gas Chromatography/Mass Spectrometry and Hyperspectral FTIR Imaging Spectroscopy for the Analysis of Microplastics. *Anal. Bioanal. Chem.* **2020**, *412* (30), 8283–8298. https://doi.org/10.1007/S00216-020-02979-W
(39) Mansa, R.; Zou, S. Thermogravimetric Analysis of Microplastics: A Mini Review. *Environ. Adv.* **2021**, *5*, 100117. https://doi.org/10.1016/J.ENVADV.2021.100117
(40) Dümichen, E.; Barthel, A. K.; Braun, U.; Bannick, C. G.; Brand, K.; Jekel, M.; Senz, R. Analysis of Polyethylene Microplastics in Environmental Samples, Using a Thermal Decomposition Method. *Water Res.* **2015**, *85*, 451–457. https://doi.org/10.1016/J.WATRES.2015.09.002
(41) Yu, J.; Wang, P.; Ni, F.; Cizdziel, J.; Wu, D.; Zhao, Q.; Zhou, Y. Characterization of Microplastics in Environment by Thermal Gravimetric Analysis Coupled with Fourier Transform Infrared Spectroscopy. *Mar. Pollut. Bull.* **2019**, *145*, 153–160. https://doi.org/10.1016/J.MARPOLBUL.2019.05.037
(42) Shim, a, W. J.; Honga, S. H.; Eo. S. The Method Requires Reference Materials to Identify Polymer Types Because Each Plastic Product Has Different Characteristics in DSC. DSC Can Be Useful for Identifying Specific Primary Microplastics, Such as Polyethylene Microbeads, for Which Reference Mat. *Anal. Methods* **2017**, *9*, 1384–1391. https://doi.org/10.1039/C6AY02558G
(43) Shabaka, S. H.; Ghobashy, M.; Marey, R. S. Identification of Marine Microplastics in Eastern Harbor, Mediterranean Coast of Egypt, Using Differential Scanning Calorimetry. *Mar. Pollut. Bull.* **2019**, *142*, 494–503. https://doi.org/10.1016/J.MARPOLBUL.2019.03.062
(44) Chialanza, M. R.; Sierra, I.; Pérez Parada, A.; Fornaro, L. Identification and Quantitation of Semi-Crystalline Microplastics Using Image Analysis and Differential Scanning Calorimetry. *Environ. Sci. Pollut. Res*. **2018**, *25*, 16767–16775.https://doi.org/10.1007/s11356-018-1846-0
(45) Ainali, N. M.; Bikiaris, D. N.; Lambropoulou, D. A. Aging Effects on Low- and High-Density Polyethylene, Polypropylene and Polystyrene under UV Irradiation: An Insight into Decomposition Mechanism by Py-GC/MS for Microplastic Analysis. *J. Anal. Appl. Pyrolysis* **2021**, *158*, 105207. https://doi.org/10.1016/J.JAAP.2021.105207
(46) Blancho, F.; Davranche, M.; Hadri, E.; Grassl, B.; Gigault, J. Nanoplastics Identification in Complex Environmental Matrices: Strategies for Polystyrene and Polypropylene. *Environ. Sci. Technol* **2021**, *55*, 8759. https://doi.org/10.1021/acs.est.1c01351
(47) Albignac, M.; Ghiglione, J. F.; Labrune, C.; ter Halle, A. Determination of the Microplastic Content in Mediterranean Benthic Macrofauna by Pyrolysis-Gas Chromatography-Tandem Mass Spectrometry. *Mar. Pollut. Bull.* **2022**, *181*, 113882. https://doi.org/10.1016/J.MARPOLBUL.2022.113882
(48) Li, Y.; Wang, Z.; Guan, B. Separation and Identification of Nanoplastics in Tap Water. *Environ. Res.* **2022**, *204*, 112134. https://doi.org/10.1016/J.ENVRES.2021.112134
(49) Jiménez-Lamana, J.; Marigliano, L.; Allouche, J.; Grassl, B.; Szpunar, J.; Reynaud, S. S. A Novel Strategy for the Detection and Quantification of Nanoplastics by Single Particle Inductively Coupled Plasma Mass Spectrometry (ICP-MS). *Anal. Chem.* **2020**, *92* (17), 11664–11672. https://doi.org/10.1021/acs.analchem.0c01536
(50) Meng, Y.; Kelly, F. J.; Wright, S. L. Advances and Challenges of Microplastic Pollution in Freshwater Ecosystems: A UK Perspective. *Environ. Pollut.* **2020**, *256*, 113445. https://doi.org/10.1016/J.ENVPOL.2019.113445
(51) Hale, R. C.; Seeley, M. E.; La Guardia, M. J.; Mai, L.; Zeng, E. Y. A Global Perspective on Microplastics. *J. Geophys. Res. Ocean.* **2020**, *125* (1), e2018JC014719. https://doi.org/10.1029/2018JC014719

Brazilian Journal of Analytical Chemistry
2023, Volume 10, Issue 40, pp 65-75
doi: 10.30744/brjac.2179-3425.AR-93-2022

BrJAC

ARTICLE

Development of an Electrochemical Sensor Modified with Dealuminated Zeolite with Citric Acid for Hydroxyzine Determination by BIA-Amperometry

Fabiana da Silva Felix[1], Matheus Julien Ferreira Bazzana[1], Letícia Cristina Assis[1], Bethânia Leite Mansur[1], Sara Silveira Vieira[2], Zuy Maria Magriotis[2], Leonardo Luiz Okumura[3], Adelir Aparecida Saczk[1]*

[1]Depto. de Química, Universidade Federal de Lavras (UFLA), CP 3037, CEP 37200-900, Lavras, MG, Brazil
[2]Depto. de Engenharia, Universidade Federal de Lavras (UFLA), CP 3037, CEP 37200-900, Lavras, MG, Brazil
[3]Depto. de Química, Universidade Federal de Viçosa (UFV), CP 36570-900, Viçosa, MG, Brazil

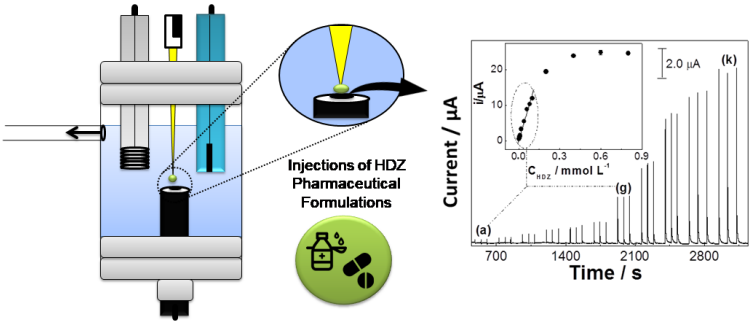

An electrochemical sensor modified with zeolite dealuminated with citric acid was developed for the determination of hydroxyzine in pharmaceutical products during BIA-amperometry experiments. The modified electrochemical sensor was prepared by mixing powdered graphite with zeolite treated with citric acid homogenized with hexane and mineral oil (60:20:20% w/w/w respectively). The developed sensor showed reproducible amperometric responses in a linear range of $1.0x10^{-6}$ – $2.0x10^{-5}$ mol L^{-1} in +1,28 V (vs. Ag/AgCl). The detection limit and detection limit found were $3.10x10^{-7}$ mol L^{-1} e $1.04x10^{-6}$ mol L^{-1}, respectively. The method developed by BIA-amperometry was applied for the determination of the analyte in tablets and commercial syrups and the results found agreement with the nominal values of the commercial samples.

Keywords: batch Injection analysis, amperometric sensor, carbon paste electrodes, hydroxyzine, zeolite

INTRODUCTION

The need to carry out quality control of medicines, foods and other products intended for human consumption in a fast and effective way has contributed to advances in the development of automated analytical systems. These systems have promising characteristics that contribute to the performance of a large number of analyzes in a short time with the sensitivity and selectivity required in the development of

Cite: Felix, F. S.; Bazzana, M. J. F.; Assis, L. C.; Mansur, B. L.; Vieira, S. S.; Magriotis, Z. M.; Okumura, L. L.; Saczk, A. A. Development of an Electrochemical Sensor Modified with Dealuminated Zeolite with Citric Acid for Hydroxyzine Determination by BIA-Amperometry. *Braz. J. Anal. Chem.* 2023, *10* (40), pp 65-75. http://dx.doi.org/10.30744/brjac.2179-3425.AR-93-2022

Submitted 23 September 2022, Resubmitted 20 December 2022, 2nd time Resubmitted 23 January 2023, Accepted 10 March 2023, Available online 03 March 2023.

analytical methods.[1,2] Flow injection analysis (FIA) was the first automated analytical system, developed in 1975 by Ružička and Hansen.[3] FIA systems have advantages related to high analytical frequency, analysis speed, precision and reproducibility, being used in the analysis of food, drugs and chemical contaminants.[3–6] However, the consumption of a large amount of regents and the use of complex systems with pumps and valves make the analysis in FIA unfeasible and disadvantageous.[1,7]

As an alternative to FIA analysis, batch injection analysis (BIA) was developed by Wang and Taha in 1991.[8] It is a tool which has been explored by some research groups as an alternative to perform quick analysis in a very simplified way. BIA analysis consists of the direct injection of small volumes of samples on the center of the detector immersed in a solution in the absence of the analyte through a motorized micropipette.[1,7,9] Electrochemical detectors are widely combined with BIA, mainly amperometric ones, for the development of sensors capable of performing the determination of a wide range of electroactive analytes.[1]

To improve the sensitivity and selectivity of electrochemical sensors, different materials have been used to modify their surfaces. Generally, these materials give the electrochemical sensor a high surface area and good electronic conductivity.[10] Traditionally, materials such as graphene, carbon nanotubes, metallic nanoparticles and other nanomaterials are used as excellent modifiers.[11–14] Recently, sensors modified with zeolites have been reported in the literature due to high surface area and appreciable physicochemical properties sensors.[15,16] A specific case is dealuminated zeolite with citric acid, which produces changes in the outer layer of zeolite material, conferring a large volume of mesopores to this material.[17] In this perspective, the present work aimed to develop an electrochemical sensor modified with dealuminated zeolite with citric acid for the determination of hydroxyzine (HDZ).[18] During amperometric experiments, this sensor modified with zeolite was associated with a BIA configuration for analyses of pharmaceutical samples.

MATERIALS AND METHODS

Reagents and solutions

Hydroxyzine Hydrochoride (99,5%) was kindly provided by Medquímica Industria Farmaceutica LTDA., Juiz de Fora, MG, Brazil. Acetic acid, phosphoric acid and boric acid were purchased from Sigma Aldrich (St. Louis, MO, USA). Hexane and dichloromethane were purchased from Merk (Darmstadt, Germany). Acetonitrile was purchased from LiChrosolv (Germany). Powder graphite was purchased from Synth (Brazil). HZSM-5 zeolite (MFI structure) used in this work was supplied by Zeochem (reference n V1148.4) with a Si/Al ratio of 14 and modified with citric acid (CA) by Vieira et al.[17] Zeolite modified with CA will be presented in this paper as MZCA.

The solutions were prepared with ultrapure water from Milli-Q purification system with resistivity 18.2 MΩ cm (Millipore, Bedford, USA). The stock solution of HDZ in the concentration of 0.10 mol L^{-1} was prepared by dissolving the solid salt in ultrapure water and stored in a dark flask under refrigeration.

The standard solutions of the analyte were properly diluted with supporting electrolyte just before the measurements. Britton-Robinson (BR) 0.1 mol L^{-1} buffers, at different pH values (2.0 – 6.0), were prepared by mixing 0.5 mol L^{-1} acetic acid solution to 0.5 mol L^{-1} phosphoric acid solution and 0.5 mol L^{-1} boric acid solution. A 1.0 mol L^{-1} sodium hydroxide solution was used to adjust the desired pH value. The pharmaceutical formulations of the syrup and the pills were purchased in a local drugstore.

Instrumentation

Cyclic voltammetry and amperometry

All measurements were performed using a potentiostat μ-AutoLab Type III (Metrohm). Cyclic voltammetry studies were carried out using a conventional electrochemical cell of 10 mL. The working electrode body was made of 7.0 cm long Teflon® coated rod with a small hole 3.0 mm in diameter and depth of 2.0 mm as well as the electric contact was made of a copper wire which was connected to the back of the Teflon®. Then, it was filled with carbon paste modified with zeolite. The reference electrode was the $Ag/AgCl_{(KClsat)}$

built in our lab,[19] and the auxiliary was of platinum wire. The BIA-amperometry experiments were performed in a wall-jet cell capable of 25 mL as shown in Figure 1.

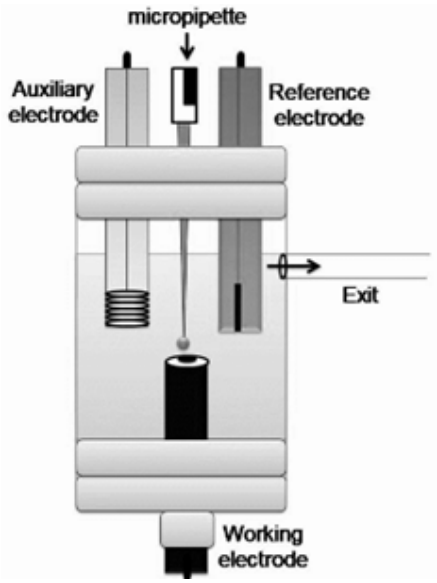

Figure 1. Representation of wall-jet cell (length of 6.5 cm and diameter of 3.0 cm).

HDZ standard solutions and drug samples were injected into the system by an automatic electronic micropipette (E4 XLS, model SE4-100XLS+ – Rainin, USA) with the tip centered at 2.0 mm of the working electrode surface.

Preparation of the modified electrode with zeolite

The preparation of carbon paste modified with zeolite was adapted from the method described by Wang and Walcarius (1996).[15] The zeolite was mixed with the powdered graphite in the proportion of interest and suspended in an organic solvent (10.0 mL of solvent to 1.0 g of the solid mixture). The system was homogenized in a magnetic stirrer at a temperature of 100 °C until complete evaporation of the organic solvent. Mineral oil was added in the desired proportion to the homogeneous solid composed of zeolite and graphite powder to obtain modified carbon paste. In this study, the solvents dichloromethane and hexane were evaluated. Experiments were also carried out without the solvent homogenization step proposed by the method described as a comparison criterion.

Sample preparation

For HDZ voltammetric analysis, aliquots of 1.50 mL of the syrup of HDZ 2.0 mg mL^{-1} were transferred to a volumetric flask of 1.0 L and completed with 0.1 mol L^{-1} of phosphate buffer (pH = 4.0).

For the analysis of tablets of HDZ the average mass of 3 tablets was calculated. The tablets were macerated in a pestle mortar. A suitable mass of the homogenized powder was weighed and homogenized with 10 mL of 0.1 mol L^{-1} of phosphate buffer (pH = 4.0) and the excipients were removed by filtration. The filtered solution was transferred to a volumetric flask of 25 mL and completed with 0.1 mol L^{-1} of phosphate buffer (pH = 4.0). Appropriate aliquots of HDZ were added to the electrochemical cell containing 10 mL of electrolyte solution.

For the performance of HPLC/DAD the syrup and tablet samples were diluted in order to obtain a solution whose hydrozixine concentration was 100 µg mL^{-1} based on methodology described by Brandão and collaborators (2011).[20] First, a tablet was diluted in ultrapure water in a 10 mL volumetric flask, thus obtaining a concentration of 100 µg mL^{-1} hydroxyzine solution. In the case of liquid samples, about 250 µL of each syrup sample were diluted in ultrapure water in 5 mL flasks (with calibrated flask volume) to obtain a 100 µg mL^{-1} hydroxyzine solution. The solutions were stored in amber vials and kept under refrigeration.

Comparison technique

Comparative HDZ analysis was performed in a high-pressure liquid chromatograph (HPLC) (model HP 1100, Germany) equipped with quaternary pump, autosampler, temperature-controlled column compartment and diode array detector (DAD). The software for the operation of the analysis and manipulation of the chromatograms was the ChemStation version Rev.03.2.B. The column used was a Zorbax Elypse Plus C18 (5 µm, 250 x 4.6 mm, Agilent, USA). The chromatographic method was adapted from Brandão and collaborators (2011)[20] and consisted of maintaining the column temperature at 58 °C, wavelength 232 nm, flow rate 0.8 mL/min and acidified mobile phase (pH 4.0) composed of acetonitrile:water (4:6). The analysis time was 9 min and the injected volume of sample and standard was 20 µL.

For the analytical curve, a stock solution of hydroxyzine (3.74 mg mL^{-1}) was prepared by diluting the standard in BR buffer (pH = 4.0) and from this, the working solutions were prepared for curve construction (0.80 to 0.120 mg mL^{-1}). After the optimization of the method, the curve was made in triplicate and the samples were injected in sextuplicate. The hydroxyzine content in commercial samples was determined from the peak areas corresponding to the analyte of interest in the samples and the linear regression obtained from the calibration curve.

RESULTS AND DISCUSSION

Characterization of zeolite modified with citric acid

The MZCA zeolite used as modifier in this work was a HZSM-5 dealuminated with citric acid (CA) in a concentration of 1.0 mol L^{-1} under the temperature of 80 ºC.[17] Figure 2 shows the adsorption isotherms for HZSM-5 and MZCA zeolites. These isotherms show the simultaneous presence of mesopores that can be evidenced by the presence of a hysteresis loop at higher P/P0 (close to 1) and micropores (high initial N2 uptake at P/P0 < 0.1). Usually, this observation occurs for materials that possess non-rigid slit-shaped pores and has been attributed to the presence of interparticle mesopores created by agglomeration of small crystallites.[21] The adsorption sites may be located on the surface of these mesopores.[17]

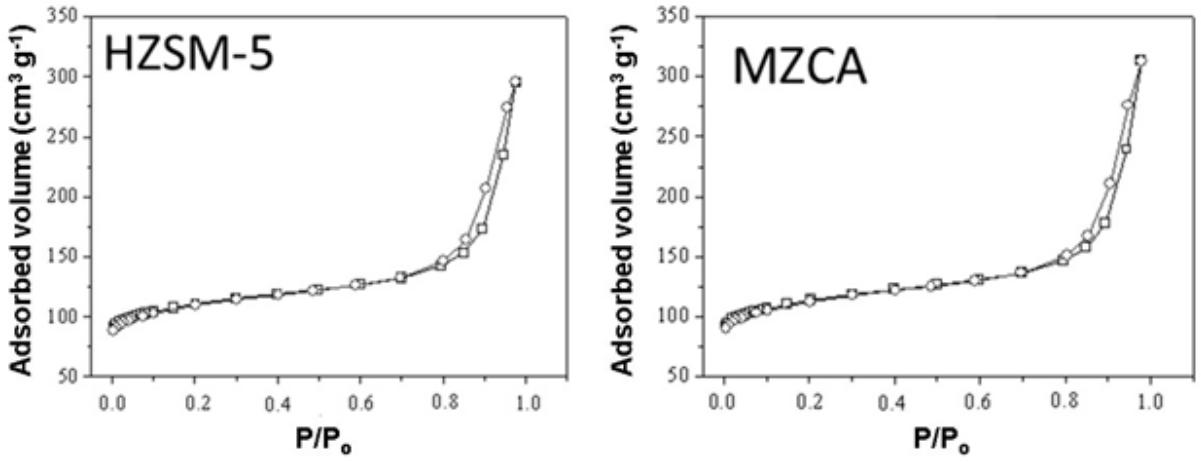

Figure 2. N_2 adsorption–desorption isotherm obtained for parent HZSM-5 e MZCA sample: being -□- adsorption isotherm and -○- desorption isotherm.

The results obtained in Figure 2 were treated using the t-plot method to determine the external area (S_{ext}), micropore volume (V_{micro}) and pore volume (V_{pore}). They indicated that MZCA material has a large V_{micro} (0.15 $cm^3\,g^{-1}$) and V_{pore} (0.49 $cm^3\,g^{-1}$) and S_{ext} (73.0 $m^2\,g^{-1}$).

The FTIR data from both materials (Figure 2) indicates the presence of a band in the region of 798 cm^{-1} referring to the symmetrical stretching of the Si-O-Si bond of the zeolite lattice structure. The HZSM-5 zeolite has a characteristic absorption band observed in the region between 550 cm^{-1} and which can be attributed to the vibrations of the five-membered double rings that make up its structure. For the MCZA material, this band was observed in the region of 547 cm^{-1}. Dealumination can cause not only a shift in

the FTIR spectrum bands, but also a thinning of the same, and the small shift in these bands was due to the low dealumination that the citric acid treatment caused.[17] In addition, this treatment decreased the intensity of the band at 3608 cm^{-1}, attributed to the Si(OH)-Al groups that are adsorption sites (acidic sites), as well as the OH bands related to extra-framework Al species (3662 and 3780 cm^{-1}). It was also observed that Al content (Si/Al ratio) decreased with CA treatment. These results mentioned were published by our research group in 2015.[17]

Anyhow this CA dealumination improved the electronic transfer and the MCZA zeolite was used as modifying agent during construction of working electrode.

Voltammetric studies of hydroxyzine using the CPE modified with zeolites

The electrochemical behavior of HDZ was investigated in carbon paste electrode (CPE) modified with MZCA and CPE in the absence of this zeolite. The voltammetric experiments were performed with $5.0x10^{-4}$ mol L^{-1} of the analyte in 0.10 mol L^{-1} of BR buffer solution (pH 4.0) and are presented in Figure 3. The electrolyte was initially chosen due to the hydroxyzine oxidation-reduction reaction, which takes place preferentially in an acidic medium, according to the work developed by Lourençao et al. (2017).[22]

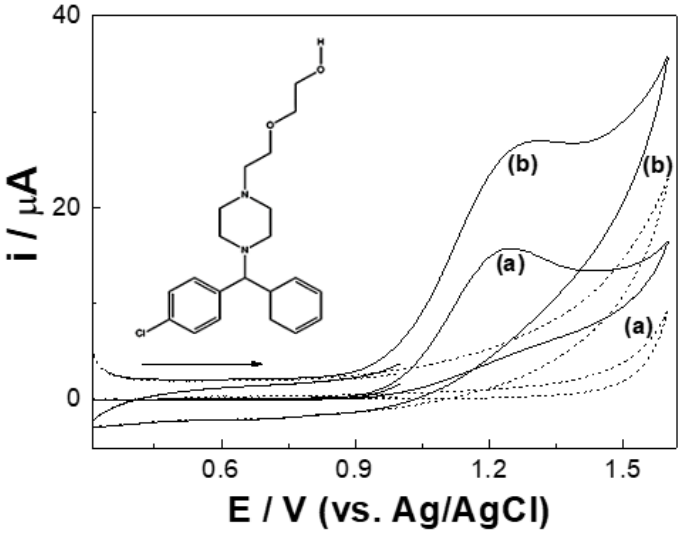

Figure 3. Cyclic voltammograms recorded for (a) CPE and (b) CPE + MZCA, both prepared in hexane, in 0.1 mol L^{-1} BR buffer solution, pH 4.0 (dashed line) and 5.0 $x10^{-4}$ mol L^{-1} HDZ solution (solid line). The inset shows the chemical structure of hydroxyzine (HDZ).

The process presented in Figure 3 for both cases (CPE with or without MZCA) corresponds to irreversible electrooxidation (E_{pa} = +1.28 V vs. Ag/AgCl) of the hydroxyl group located on the aliphatic part of the analyte molecule (HDZ or 2-[2-[4-[(4-chlorophenyl)-phenylmethyl]piperazin-1-yl]ethoxy]ethanol).[22,23] No other peaks were observed in the reverse scan direction (considering a potential region from 0.3 to 1.6 V vs. Ag/AgCl), which indicated the irreversible nature of the reaction. The increase in anodic peak current (I_{pa}) found in voltammograms b, is related to the presence of MZCA. This material has a large volume of micropore (V_{micro} = 0.15 $cm^3\ g^{-1}$) and pore (V_{pore} = 0.49 $cm^3\ g^{-1}$) in addition to high external area (S_{ext} = 73.0 $m^2\ g^{-1}$) that favor the HDZ multilayer adsorption mechanism on the external surface of the working electrode. The high external area of the MZCA can be attributed to the external acidity (40 µmol g^{-1}) obtained from the dealumination of the zeolite with the incorporation of CA.[17] Thus, the CPE with MZCA (CPE/MZCA) was selected for further analysis due to the significant increase of approximately 36.0% in I_{pa} when compared to the CPE.

The CPE/MZCA was evaluated under different conditions of paste preparation, according to the method proposed by Wang and Walcarius (1996),[15] in which the zeolite was homogenized in graphite by the addition of an organic solvent.[15] The method initially proposed uses dichloromethane as a solvent for the homogenization of graphite with zeolite. Based on the principles of green chemistry, which implies

a reduction in the consumption of toxic organic solvents, clean technology, and reduction at source, the hexane solvent was tested as a less toxic.[24] Analyzes were performed with 5.0x10^{-4} mol L^{-1} of the analyte in 0.10 mol L^{-1} of BR buffer solution (pH 4.0). In this study, the voltammograms of CPE/MZCA (a) and CPE (b) in the absence solvent, CPE/MZCA in the presence of dichloromethane (c) and CPE/MZCA in the presence of hexane (d) are compared in Figure 4.

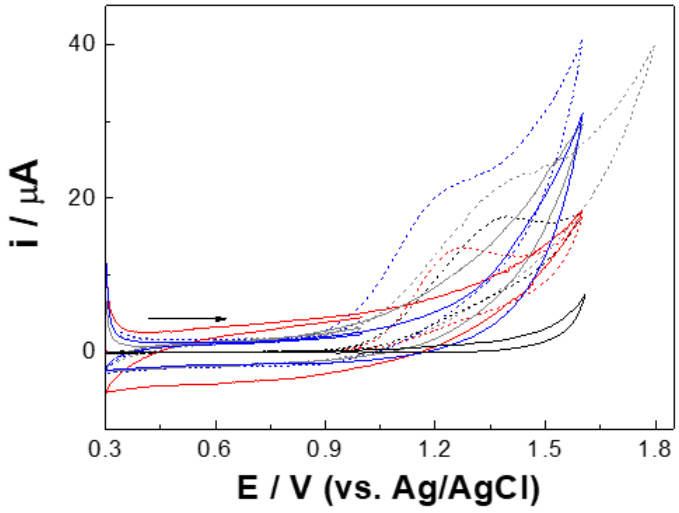

Figure 4. Cyclic voltammograms of 5.0 x 10^{-4} mol L^{-1} HDZ in 0.1 mol L^{-1} BR buffer solution (pH 4.0) (dashed line) and only electrolyte (solid line), under different working electrode preparation conditions: (red line) CPE/MZCA and (black line) CPE in absence of solvent, (gray line) CPE/MZCA in dichloromethane and (blue line) CPE/ MZCA in hexane.

The results obtained (Figure 4) demonstrate a significant increase in I_{pa} when CPE/MZCA is found in the presence of solvents such as dichloromethane and hexane, (gray and blue lines, respectively). Due to the lower toxicity and the significant increase in I_{pa}, hexane was selected as the homogenizing solvent in the preparation of the working electrode. Thus, subsequent experiments were carried out with CPE/ MZCA in the presence of hexane (CPE/MZCA-Hex).

The CPE/MZCA-Hex was evaluated in different proportions of graphite (80 – 50%), zeolite MZCA-Hex (10 – 30%) and mineral oil (20 – 50%). The results indicated that in the proportion of 60:20:20% w/w/w for construction of working electrode, the I_{pa} presented the significantly increased when compared to the other proportions.

Other voltammetric studies (not presented in this work) were also performed with the solution 0.10 mol L^{-1} of BR buffer solution and varying the pH over a range from 2.0 to 6.0. The pH range was evaluated in this range, since at pH above 6.0 there is a decrease in I_{pa}.[22] The results show that increasing the pH value improves the intensity of I_{pa} up to pH 4.0. At higher pH, I_{pa} remains constant and the peak shifts to more positive potentials. Similar results are reported in the work developed by Lourencao and collaborators (2017).[22] In this sense, the 0.1 mol L^{-1} of BR buffer solution pH 4.0 was selected for further analysis.

The apparent electroactive surface area of the CPE/MZCA-Hex was evaluated by cyclic voltammetry at different scan rates and using the Randles-Sevcik Equation (Equation 1).

$$i_p = (2{,}69x10^{-5}).n^{2/3}.AD_0.^{1/2}\,\upsilon^{1/2}C_0 \qquad \text{Equation 1}$$

where n is the number of electrons, A is the electrode area (cm^2), C_0 is the concentration of the electroactive species (mol cm^{-3}), D_0 is the diffusion coefficient (cm^3 s^{-1}) and υ is the sweep speed (V s^{-1}).

The voltammetric experiments were performed with 0.1 mol L^{-1} $K_3[Fe(CN)_6]$ solution in 0.1 mol L^{-1} KCl as supporting electrolyte. The scan speed was varied from 50 mV s^{-1} to 900 mV s^{-1} and the active surface area found for the modified working electrode was of 0.1041 cm^2.

It still takes into account the cyclic voltammetric experiments, it was possible to observe in the inset of Figure 5 that after successive additions of HDZ (from 2.0 x 10^{-4} to 1.0 x 10^{-3} mol L^{-1}) in 0.10 mol L^{-1} of BR buffer solution, pH 4.0, the current signals were very stable and reproducible with r = 0.996 (scan rate of 100 mV s^{-1}).

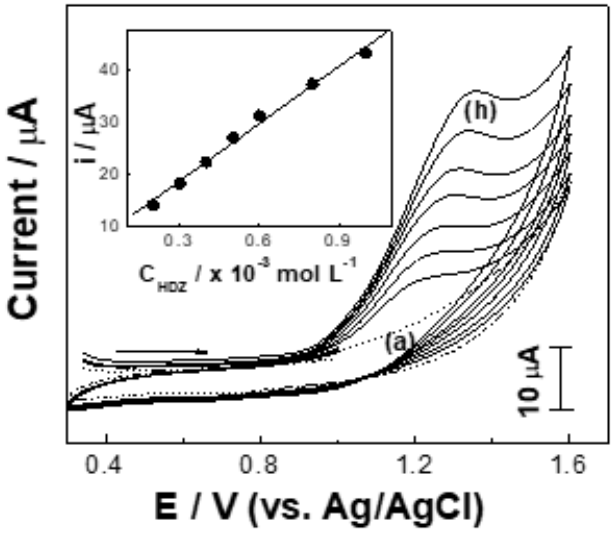

Figure 5. Voltammograms of HDZ standard solutions in 0.1 mol L^{-1} BR buffer solution (pH 4.0), using a working electrode constructed from carbon paste + MZCA-Hex + mineral oil (60:20:20%, w/w/w): (a) electrolyte; (b) 2.0; (c) 3.0; (d) 4.0; (e) 5.0; (f) 6.0; (g) 8.0 x 10^{-4} and (h) 1.0 x 10^{-3} mol L^{-1}. Scan rate: 100 mV s^{-1}. Apparent electroactive surface area of 0.1041 cm^2.

Amperometry Bath Injection Analysis (BIA-Amperometry)

To establish the best conditions for amperometry in association with bath injection analysis (BIA) in the determination of HDZ, main parameters (distance between the micropipette and the electrode surface, working potential, sample injection volume and injection speed) were investigated using 1.0x10^{-5} mol L^{-1} of the analyte in 0.1 mol L^{-1} BR buffer solution (pH = 4.0). Amperometric studies under hydrodynamic conditions were performed to obtain the best distance between the micropipette and the electrode surface (from 1.0 to 3.0 mm) as well as the best work potential (from 0.5 to 1.5 V vs. Ag/AgCl). The optimal distance between CPE/MZCA-Hex and the micropipette tip was found to be 2.0 mm, as well as the most favorable work potential was 1.3 V (vs. Ag/AgCl).

The effect of the volume of the sample injected into the system was evaluated from 10 to 100 μL. The experiments showed an increase in I_{pa} with the increase in sample volume up to 80 μL. For larger volumes, the increase was less significant and the time required for each analysis also increased. In this sense, the volume chosen for carrying out the subsequent experiments was 80 μL.

The effect of injection speed was also evaluated in a range from 22.5 to 126.6 μL s^{-1}, considering a working potential of 1.3 V and a sample volume of 80 μL. It was possible to observe that I_{pa} significantly increased up to a velocity of 80 μL s^{-1}. At higher speeds, the increase was negligible. For this experiment, the best injection speed selected was of 80 μL s^{-1}.

Figure 6 indicates that throughout the investigated range of analyte concentration (from 1.0 x 10^{-6} to 1.0 x 10^{-4} mol L^{-1}), the behavior of I_{pa} was only reproducible and linear in 1.0 x 10^{-6} – 2.0 x 10^{-5} mol L^{-1}. In higher concentration ranges (from 4.0x10^{-5} to 1.0x10^{-4} mol L^{-1}) there is a deviation from linearity. The analytical curve constructed in the linear range presented a slope of 0.13035 ± 0.0013 μA mol L^{-1} and an intercept of 1.2841x10^{-7} ± 1.247 μA, with a correlation coefficient of 0.992. The estimated detection limit (LOD) was 2.57x10^{-7} mol L^{-1} and the calculated quantification limit (LOQ) was 8.55x10^{-7} mol L^{-1}.[19]

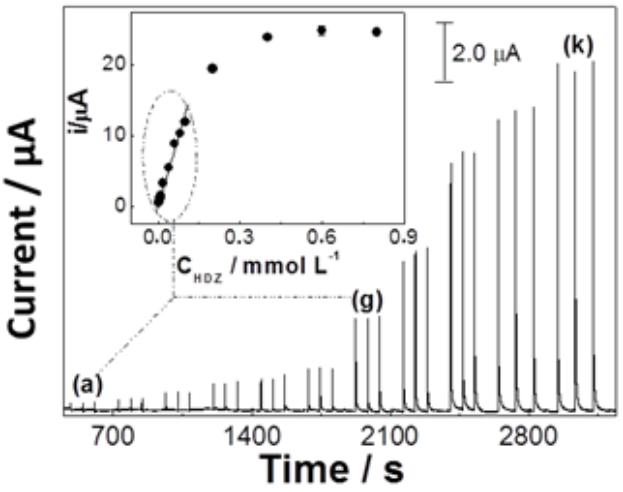

Figure 6. BIA -Amperometric responses of the PCE modified with zeolite for increasing HDZ concentrations in 0.1 mol L^{-1} BR buffer solution, pH 4.0: (a) 1.0; (b) 2.0; (c) 4.0; (d) 6.0; (e) 8.0 x 10^{-6}; (f) 1.0; (g) 2.0; (h) 4.0; (i) 6.0; (j) 8.0 x 10^{-5} and (k) 1.0x10^{-4} mol L^{-1}. Working potential: +1.3 V (vs. Ag/AgCl), injected volume: 80 µL and injection speed: 80 µL s^{-1}. The detail shows the analytical curve (a-g).

In the work carried out by Lourencao and collaborators,[22] the method applying square-wave adsorptive anodic stripping voltammetry (SWAdASV) presented LOD of 1.0x10^{-7} mol L^{-1}. The work developed by Beltagi et al. a SWAdASV procedure has been developed, presenting LOD of 1,5x10^{8} mol L^{-1}. When compared to the developed method, the LOD of the mentioned works are smaller, however in both cases an adsorption process is used that can improve the LOD, however, it makes the analysis more time consuming.[22,23] Figure 7 shows the responses of 25 successive additions of standard solution at the concentration of 8.0x10^{-6} mol L^{-1} of HDZ in 0.1 mol L^{-1} BR buffer solution, pH 4.0. A good repeatability of the analytical signal is observed throughout the experiment, with a relative standard deviation equal to 2.60%. The injection frequency found was 121 per hour.

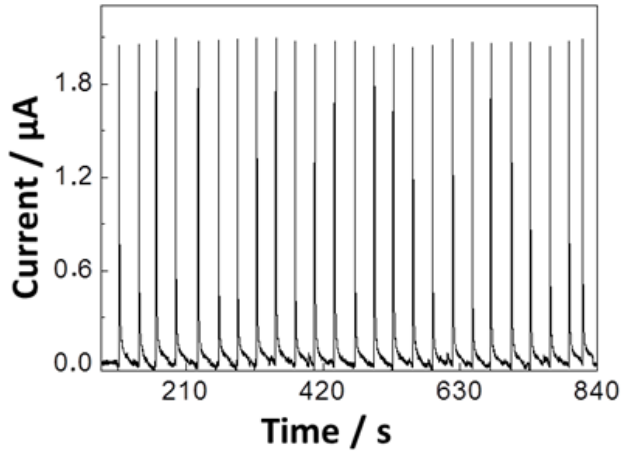

Figure 7. 25 injections of 8.0x10^{-6} mol L^{-1} HDZ in 0.1 mol L^{-1} BR buffer solution (pH 4.0) and using PCE modified with zeolite. Working potential: +1.3 V (vs. Ag/AgCl), injected volume: 80 µL and injection speed: 80 µL s^{-1}.

Figure 8 shows the results obtained in the BIA-amperometry system for pharmaceutical samples which is preceded by a series of additions of standard HDZ solutions in a range from 1.0x10^{-6} to 2.0x10^{-5} mol L^{-1}. In this experiment, a linear relationship between I_{pa} and analyte concentration was also observed, as can be seen in the analytical curve (inset of Figure 8).

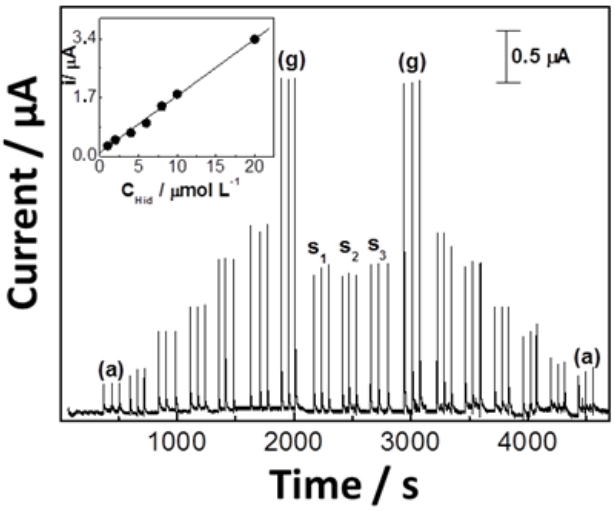

Figure 8. BIA-Amperometric responses of the PCE modified with zeolite for increasing HDZ concentrations in 0.1 mol L^{-1} BR buffer solution (pH 4.0): (a) 1.0; (b) 2.0; (c) 4.0; (d) 6.0; (e) $8.0x10^{-6}$; (f) 1.0; (g) $2.0x10^{-5}$ mol L^{-1} and pharmaceutical samples (S_1-S_3). Working potential: +1.3 V (vs. Ag/AgCl), injected volume: 80 µL and injection speed: 80 µL s^{-1}. The detail shows the analytical curve (a-g).

The performance of the developed electroanalytical method was compared with the HPLC/UV-Vis proposed by Brandao and collaborators (2011).[20] Table I presents these results accompanied by the corresponding standard deviations calculated from three independent measurements for each sample.

Table I. Results obtained for the analysis of hydroxyzine dihydrochloride in 3 pharmaceutical formulations using the proposed BIA-amperometry and HPLC method[20]

Sample	Composition	Nominal value (mg)	Amperometry ± S.D.[a] (mg)	HPLC ± S.D.[a]
S_1	Sodium benzoate, potassium sorbate, carmellose, sodium cyclamate, sodium saccharin, glycerol, cherry and raspberry essences	2.0	2.10 ± 0.02	1.64 ± 0.02
S_2	sodium benzoate, potassium sorbate, sorbitol, glycerol, cherry flavor, raspberry essence, povidone, propylene glycol, sucralose, hydrochloric acid, sodium hydroxide	2.0	2.07 ± 0.02	1.81 ± 0.01
S_3	Starch, lactose monohydrate, copovidone, talc, magnesium stearate	25.0	25.3 ± 0.1	21.34 ± 0.16

[a] n=3

The results obtained by the method proposed using CPE/MZCA-Hex as the working electrode are close to the nominal values of samples (S_1, S_2 and S_3) with a percentage difference of 5.0%, 3.5% and 1.2%, respectively, indicating a good performance of the proposed method. The greatest differences are observed in the results obtained by HPLC/UV-Vis (18.0%, 10.0% and 15.0% for S_1, S_2 and S_3 samples)

compared with labelled values. These results attest that the BIA-amperometry method proved to be more effective due to minor differences in relation to the nominal value.

CONCLUSIONS

In this study, an BIA-amperometry methodology was developed using a modified carbon paste electrode. The results obtained indicated a good applicability of CPE/MZCA-Hex in the amperometric determination of HDZ in pharmaceutical formulations. The BIA-amprometry method showed reproducible and stable responses during the execution of the experiments. The modification of the working electrode with CPE/MZCA-Hex may have facilitated the oxidation process of HDZ, improving the sensitivity of the method when compared to the electrode without modification (36.0% increase in anodic current value). The proposed method presents a linear response to HDZ concentration in a range of $1.0x10^{-6}$ to $1.0x10^{-5}$ mol L^{-1}, with an LOD of $2.57x10^{-7}$ mol L^{-1} and a differentiated sampling rate (121 injections per hour).

Conflicts of interest

The authors declare that there is no conflict of interest.

Acknowledgements

The authors are grateful for the "Coordenação de Aperfeiçoamento de Pessoal de Nível Superior" – Brazil (CAPES) – Financing Code 001, "Conselho Nacional de Desenvolvimento Científico e Tecnológico" (CNPq), "Fundação de Amparo à Pesquisa do Estado de Minas Gerais" (FAPEMIG), Embrapa Café (code 10.18.20.043.00.02).

REFERENCES

(1) Haššo, M.; Švorc, Ľ. Batch Injection Analysis in Tandem with Electrochemical Detection: The Recent Trends and an Overview of the Latest Applications (2015–2020). *Monatshefte fur Chemie* **2022**. https://doi.org/10.1007/s00706-022-02898-9

(2) Squissato, A. L.; Munoz, R. A. A.; Banks, C. E.; Richter, E. M. An Overview of Recent Electroanalytical Applications Utilizing Screen-Printed Electrodes Within Flow Systems. *ChemElectroChem* **2020**, *7* (10), 2211–2221. https://doi.org/10.1002/celc.202000175

(3) Ŗužička, J.; Hansen, E. H. Flow Injection Analyses: Part I. A New Concept of Fast Continuous Flow Analysis. *Anal. Chim. Acta* **1975**, *78* (1), 145–157. https://doi.org/https://doi.org/10.1016/S0003-2670(01)84761-9

(4) Shaidarova, L. G.; Gedmina, A. V; Poadnyak, A. A.; Chelnokova, I. A.; Budnikov, H. C. Selective Voltammetric and Flow-Injection Amperometric Determination of Acyclovir and Valacyclovir on an Electrode with a Reduced Graphene Oxide–Polyglycine Film Composite. *J. Anal. Chem.* **2022**, *77* (6), 681–687. https://doi.org/10.1134/S1061934822060156

(5) Vandeput, M.; Rodríguez-Gómez, R.; Izere, A.-M.; Zafra-Gómez, A.; De Braekeleer, K.; Delporte, C.; Van Antwerpen, P.; Kauffmann, J.-M. Electrochemical Studies of Ethoxyquin and Its Determination in Salmon Samples by Flow Injection Analysis with an Amperometric Dual Detector. *Electroanalysis* **2018**, *30* (7), 1293–1302. https://doi.org/10.1002/elan.201700611

(6) Mentana, A.; Palermo, C.; Iammarino, M.; Chiaravalle, A. E.; Centonze, D. Electroanalytical Characterisation of Nitrosamines in Different Mobile Phases as Supporting Electrolytes. *Microchem. J.* **2021**, *171*. https://doi.org/10.1016/j.microc.2021.106885

(7) Quintino, M. S. M.; Angnes, L. Batch Injection Analysis: An Almost Unexplored Powerful Tool. *Electroanalysis* **2004**, *16* (7), 513–523. https://doi.org/10.1002/elan.200302878

(8) Wang, J.; Taha, Z. Batch Injection Analysis. *Anal. Chem.* **1991**, *63* (10), 1053–1056. https://doi.org/10.1021/ac00010a025

(9) Wang, J.; Taha, Z. Batch Injection with Potentiometric Detection. *Anal. Chim. Acta* **1991**, *252* (1), 215–221. https://doi.org/https://doi.org/10.1016/0003-2670(91)87218-V

(10) Lan, L.; Yao, Y.; Ping, J.; Ying, Y. Recent Advances in Nanomaterial-Based Biosensors for Antibiotics Detection. *Biosens. Bioelectron.* **2017**, *91*, 504–514. https://doi.org/10.1016/j.bios.2017.01.007
(11) Baig, N.; Sajid, M.; Saleh, T. A. Recent Trends in Nanomaterial-Modified Electrodes for Electroanalytical Applications. *TrAC - Trends Anal. Chem.* **2019**, *111*, 47–61. https://doi.org/10.1016/j.trac.2018.11.044
(12) Torrinha, Á.; Oliveira, T. M. B. F.; Ribeiro, F. W. P.; Correia, A. N.; Lima-Neto, P.; Morais, S. Application of Nanostructured Carbon-Based Electrochemical (Bio)Sensors for Screening of Emerging Pharmaceutical Pollutants in Waters and Aquatic Species: A Review. *Nanomaterials* **2020**, *10* (7), 1–29. https://doi.org/10.3390/nano10071268
(13) Katz, E.; Willner, I. Biomolecule-Functionalized Carbon Nanotubes: Applications in Nanobioelectronics. *ChemPhysChem* **2004**, *5* (8), 1084–1104. https://doi.org/10.1002/cphc.200400193
(14) Ehtesabi, H. Carbon Nanomaterials for Salivary-Based Biosensors: A Review. *Mater. Today Chem.* **2020**, *17*. https://doi.org/10.1016/j.mtchem.2020.100342
(15) Wang, J.; Walcarius, A. Zeolite-Modified Carbon Paste Electrode for Selective Monitoring of Dopamine. *J. Electroanal. Chem.* **1996**, *407* (1–2), 183–187. https://doi.org/10.1016/0022-0728(95)04488-4
(16) Jendrlin, M.; Radu, A.; Zholobenko, V.; Kirsanov, D. Performance Modelling of Zeolite-Based Potentiometric Sensors. *Sensors Actuators B Chem.* **2022**, *356*. https://doi.org/10.1016/j.snb.2021.131343
(17) Vieira, S. S.; Magriotis, Z. M.; Ribeiro, M. F.; Graça, I.; Fernandes, A.; Lopes, J. M. F. M.; Coelho, S. M.; Santos, N. A. V; Saczk, A. A. Use of HZSM-5 Modified with Citric Acid as Acid Heterogeneous Catalyst for Biodiesel Production via Esterification of Oleic Acid. *Microporous Mesoporous Mater.* **2015**, *201* (C), 160–168. https://doi.org/10.1016/j.micromeso.2014.09.015
(18) Zayed, S. I. M.; Al-Talhi, A. A. H.; Thagafi, A. E. A. Determination of Hydroxyzine by Differential Pulse Anodic Voltammetry Using Carbon Paste Electrode. *J. Chil. Chem. Soc.* **2018**, *63* (3), 4064–4067. https://doi.org/10.4067/s0717-97072018000304064
(19) Felix, F. S.; Daniel, D.; Matos, J. R.; do Lago, C. L.; Angnes, L. Fast Analysis of Terbutaline in Pharmaceuticals Using Multi-Walled Nanotubes Modified Electrodes from Recordable Compact Disc. *Anal. Chim. Acta* **2016**, *928*, 32–38. https://doi.org/10.1016/j.aca.2016.04.045
(20) Brandão, M. A. F.; Nascimento, L. G. B.; Polonini, H. C.; Fonseca, R. G.; Montesano, G.; Vaz, U. P.; Raposo, N. R. B.; Grossi, L. N.; Ferreira, A. O. A High Performance Liquid Chromatography Method for Determination of Hydroxyzine Hydrochloride in Syrup. *Lat. Am. J. Pharm.* **2011**, *30* (9), 1798–1802.
(21) Rouquerol, J.; Rouquerol, F.; Llewellyn, P.; Maurin, G.; Sing, K. S. W. *Adsorption by Powders and Porous Solids: Principles, Methodology and Applications* (2nd Ed.). Elsevier Inc., 2013. https://doi.org/10.1016/C2010-0-66232-8
(22) Lourencao, B. C.; Silva, T. A.; da Silva Santos, M.; Ferreira, A. G.; Fatibello-Filho, O. Sensitive Voltammetric Determination of Hydroxyzine and Its Main Metabolite Cetirizine and Identification of Oxidation Products by Nuclear Magnetic Resonance Spectroscopy. *J. Electroanal. Chem.* **2017**, *807*, 187–195. https://doi.org/10.1016/j.jelechem.2017.11.013
(23) Beltagi, A. M.; Abdallah, O. M.; Ghoneim, M. M. Development of a Voltammetric Procedure for Assay of the Antihistamine Drug Hydroxyzine at a Glassy Carbon Electrode: Quantification and Pharmacokinetic Studies. *Talanta* **2008**, *74* (4), 851–859. https://doi.org/10.1016/j.talanta.2007.07.009
(24) Zimmerman, J. B.; Anastas, P. T.; Erythropel, H. C.; Leitner, W. Designing for a Green Chemistry Future. *Science* **2020**, *367* (6476), 397–400. https://doi.org/10.1126/science.aay3060

Brazilian Journal of Analytical Chemistry
2023, Volume 10, Issue 40, pp 76-89
doi: 10.30744/brjac.2179-3425.AR-106-2022

BrJAC

ARTICLE

Extraction of Non-Volatile Chemical Compounds in High-Quality and Traditional Coffee

Gabriela M. R. N. Alcantara[1], Giovanna B. F. Spíndola[2], Wanessa R. Melchert[2]*

[1]*Centro de Energia Nuclear na Agricultura, Universidade de São Paulo, Av. Centenário, 303, São Dimas, 13400-970, Piracicaba, SP, Brazil*

[2]*Escola Superior de Agricultura Luiz de Queiroz, Universidade de São Paulo, Av. Pádua Dias, 11 – Agronomia, 13418-900, Piracicaba, SP, Brazil*

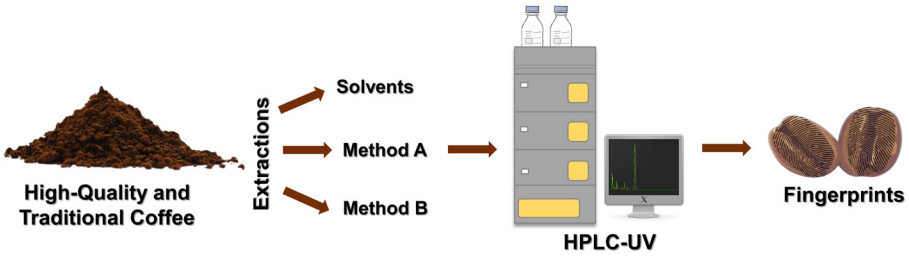

Coffee contains different volatile and non-volatile compounds, which are responsible for its characteristic flavor and aroma attributes. The extraction of non-volatile compounds from high-quality and traditional coffee by different methods was evaluated to determine the chemical compounds that discriminate between coffee types. Standard methods of preparing the coffee drink by consumers were evaluated. Method A corresponded to boiling water with coffee, and method B to the strained coffee method. Extraction with different solvents did not distinguish the compounds chosen as markers for coffees. In addition to being non-toxic and low-cost, water was the most suitable solvent, conforming to the principles of green chemistry while enabling direct comparison with sensory analysis. The total dissolved solids, percentage extraction, and non-volatile compounds were quantified to select the most satisfactory extraction method. The TDS value ranged from 1.7 to 3 between methods and coffee types, and the extraction percentage ranged from 25 to 45%. Significant differences in the extracts obtained using methods A and B high-quality versus traditional coffees were detected using the Student's *t*-test. Although method A extracted the chemical compounds in more substantial amounts, method B was also efficient in extracting the compounds and was easily executed given its similarity to the usual way of preparing coffee beverages used by consumers. The evaluated non-volatile compounds were identified in both high-quality and traditional coffee samples. In the chosen extraction method (method B), the average concentrations in mg 100 g^{-1} of the sample found for the compounds were: 5-hydroxymethylfurfural (11±0.5), 3,4-hydroxybenzoic acid (62±4), catechin (58±5), 4-hydroxybenzoic acid (58±2), caffeine (1152±44), chlorogenic acid (598±23), caffeic acid (0.7±0.1), and gallic acid (3±0.2).

Keywords: coffees, extraction, non-volatile compounds

Cite: Alcantara, G. M. R. N.; Spíndola, G. B. F.; Melchert, W. R. Extraction of Non-Volatile Chemical Compounds in High-Quality and Traditional Coffee. *Braz. J. Anal. Chem.* 2023, *10* (40), pp 76-89. http://dx.doi.org/10.30744/brjac.2179-3425.AR-106-2022

Submitted 04 November 2022, Resubmitted 24 January 2023, 2nd time Resubmitted 13 March 2023, 3rd time Resubmitted 05 May 2023, Accepted 13 May 2023, Available online 25 May 2023.

INTRODUCTION

Coffee is the second most widely consumed beverage worldwide and has high economic importance, being one of Brazil's main export products. There are more than 100 species of the genus L. (*Rubiacea*e); thus most types of coffee in this class are *Coffea arabica* and *Coffea canephora*, also called 'robusta' of the cultivar 'conilon'.[1] The coffee drinks made from these two varieties are significantly different in aroma and flavor because the arabica species have better sensorial properties than the robusta species,[2,3] providing the highest value and most consumer appreciation. In general, commercially available coffee drinks are produced from arabica coffee, robusta, or mixtures of these species.[4]

Coffee blends are a common practice in the coffee industry to standardize sensory properties such as bitterness, flavor, and aroma.[5] According to the Brazilian Coffee Industry Association (ABIC), roasted and ground coffees can be classified into three categories: Traditional (arabica blended with conilon up to a limit of 30%), Superior (blend with up to 15% conilon), and Gourmet (arabica only).[6] This classification considers the different proportions of conilon coffee and the maximum percentage of defects and sensory analysis scores, associated with the final quality.[7]

Sensory analysis is widely used in classifying coffee worldwide, but can still be seen as subjective. Therefore, analysis of the physicochemical and chemical composition is a complementary resource because the constituents of each species can be directly related to the attributes of the coffee beverage.[8,9] Thus, the chemical compounds in roasted coffee grains confer a series of attributes that give coffee its flavor and peculiar aromas.[10,11] In roasted coffee, these chemical components can be grouped into volatile substances, responsible for the aroma, and non-volatile substances, for the acidity sensations, bitterness, and astringency.[12]

Phenolic compounds contribute to the flavor and aroma of coffee drinks due to their high concentration in coffee and their physiological and pharmacological properties.[13] These compounds are characterized by one or more aromatic rings attached to at least one hydroxyl radical and/or other substitutents. Furthermore, they can be divided according to the number of phenolic rings and the structures to which they are attached.[14] The main phenolic compounds in coffee are phenolic acids, such as hydroxybenzoic (gallic, vinylic, and syringic) and hydroxycinnamic (caffeic, ferulic, sinapic, and *p*-coumaric). Esterified quinic acid, tartaric acid, or carbohydrates and their derivatives can also be found in most foods.[14–16]

Phenolic compounds represent a significant fraction of the coffee composition and can be used as chemical descriptors and markers of the authenticity of foods.[17] These compounds can be extracted with water, organic solvents, or polar organic solvent mixtures. The polar solvents used most frequently in the extraction of these compounds from food are methanol, ethanol, and acetone, often mixed with water in ratios of 80:20 (v/v) or 50:50 (v/v).[18]

Brewing is an essential step in preparing coffee beverages to achieve maximum extraction of the constituent compounds and to ensure aroma and flavor characteristics. The extraction efficiency is the ratio between the mass of ground coffee powder that passes through the cup and the total amount of ground coffee used.[19] In this context, coffee shops have introduced instruments to ensure quality control of the extraction process. Thus, baristas and coffee enthusiasts worldwide have started using scales, gauges, proportions, and control charts to prepare better-quality coffee.

Refractometers are used to evaluate the percentage of coffee extraction by determining the total dissolved solids (TDS) in brewed coffee, where the percentage of coffee extracted by a given extraction method can be estimated.[20] The TDS can be determined from the Brix degree (°Bx), which is a measurement of the refractive index. Due to the linear correlation between the °Bx and TDS, it is possible to convert the °Bx to the TDS through the mathematical equation: %TDS = 0.85 × % °Bx given that refractometers are usually more accessible than TDS meters.[20] The TDS measurement can be used to calculate the percentage coffee extraction (PE) through the correlation: Extraction = TDS × Beverage/Dosage. The TDS value is the same as found from the °Bx conversion; thus, the TDS of drink corresponds to the amount of water, and the 'Dosage' represents the serving in grams of coffee.

Although there are works in the literature that evaluate different extraction methods, the TDS and percentage of extraction in evaluating these methods as a parameter of quality and efficiency are still little

explored. Still, many of the methods investigated address coffee preparation methods such as espresso, mocha, V60, cold brew, and french press,[19] which use water as an extractor solvent since it is a drink for consumption is capable of extracting the compounds that represent characteristics sensory the drink. On the other hand, when looking for non-volatile markers, it is necessary to investigate other solvents in the extraction. There is a hypothesis that possible classification markers for coffees are extracted by solvents other than water due to the difference in polarity of the bioactive compounds present in coffee. There may still be varying effects when different solvents are used in the extraction, increasing the chances of observing important spectral changes.[21]

Liquid chromatography (LC) is one of the most commonly employed chromatographic fingerprinting methodologies. It has been widely applied to identify, classify and evaluate the quality of different types of foods. Furthermore, several classes of food solutions, in polar and non-polar solvents, can be directly and quickly analyzed by LC without the need for derivatization. Finally, the versatility of the chromatographic methods allows the interaction both in the separation steps and in the measurement ones to acquire an analytical signal with the maximum of useful information. These methods are excellent candidates for obtaining fingerprints for food identification, classification, and authentication.[22]

Thus, this exploratory study aims to evaluate the efficacy of different solvents and processes in extracting the characteristic compounds that discriminate high-quality and traditional coffee types using an High-performance liquid chromatography (HPLC) method with UV detection.

MATERIALS AND METHODS

Reagents, equipment, and accessories

All solutions and extracts were prepared using deionized water (18.2 MΩ cm at 25 °C) and analytical-grade reagents. The following analytical standards were used: 5-hydroxymethylfurfural (5-HMF), 3,4-hydroxybenzoic, catechin, 4-hydroxybenzoic, caffeine, chlorogenic acid (CGA), caffeic acid, and gallic acid from Sigma Aldrich.

The stock solutions of the standards were prepared at known concentrations: 3,4-hydroxybenzoic, catechin, and 4-hydroxybenzoic at 6250 mg L^{-1}; caffeine 12500 mg L^{-1}; gallic acid 2510 mg L^{-1}; CGA 5000 mg L^{-1}; caffeic acid 126 mg L^{-1} and 5-HMF 508 mg L^{-1}.

Chromatographic separation was achieved using HPLC (Agilent, model 1100 series) in reverse phase, equipped with a pre-column and C18 column (4.6 × 250 mm – 5 µm), at a flow rate of 0.8 mL min^{-1}.

Coffee samples and extract preparation

Samples of 100% arabica coffee were analyzed from the Alta Mogiana region (*Gourmet* Coffee) and a traditional coffee sample acquired in a local market in the city of Piracicaba, SP, Brazil. The ground coffee grains of the samples were passed through a granulometric sieve (20 mesh) for standardization, stored in a Falcon tube®, and protected from light until extraction.

Extraction procedure

The extracts were filtered through conventional filter paper and a syringe filter (hydrophilic PTFE membrane; filter diameter and pore of 13 mm and 0.45 µm, respectively) before chromatographic injection. Extraction methods A and B were performed in triplicate.

Extraction employing different solvents

In a 50 mL Falcon tube®, 1.0 g of sample and the volume of solvent (totaling 15 mL) were added as described in the experimental design (Table I), followed by agitation for 30 min at 150 rpm on an orbital table (Quimis, SP, Brazil; Model Q225M). Thereafter ethanol, ethyl acetate, acetone, water, and combinations of the organic solvents with water 50:50 (v/v) were evaluated as extraction solvents.

Table I. Experimental design for extraction employing different solvents

Extracts	Water (%)	Ethanol (%)	Ethyl acetate (%)	Acetone (%)
1	0	100	0	0
2	0	0	100	0
3	0	50	50	0
4	0	0	0	100
5	0	50	0	50
6	0	0	50	50
7	0	33.3	33.3	33.3
8	100	0	0	0
9	50	50	0	0
10	50	0	50	0
11	50	0	0	50
12	100	0	0	0

Extraction methods

Method A: The sample (10 g) and 150 mL of water were heated at 90 °C in a beaker for 2 min.

Method B: On a commercial support, 10 g of sample was added to filter paper, and 150 mL of water at 90 °C was poured onto the coffee.

Separation and quantification of non-volatile compounds

The non-volatile compounds were separated under the following chromatographic conditions: mobile phase: 95% (A) 5% of acetic acid in water (v/v), and 5% (B) acetonitrile; injected sample volume: 30 µL; run time: 55 min, with UV detection at 280 and 320 nm, adapted the Alves et al. and Alcantara, Melchert, and Dresch.[1,23]

The chromatographic profiles of the analytical standards were obtained under the same chromatographic conditions and used to identify the compounds by UV detection at: 280 nm for 5-HMF, 3,4-hydroxybenzoic, catechin, 4-hydroxybenzoic, caffeine, and gallic acid and 320 nm for CGA and caffeic acid.

The reference solutions 3,4-hydroxybenzoic, catechin, and 4-hydroxybenzoic, were prepared by dissolving 62.5 mg of each standard in 10 mL of deionized water; gallic acid was prepared by dissolving 25.1 mg in 10 mL of deionized water. The 5-HMF and caffeic acid reference solutions were prepared by dissolving 50.8 and 12.6 mg, respectively, in 100 mL of deionized water. The caffeine and CGA reference solutions were prepared by dissolving 312.5 and 125.0 mg, respectively, in 25 mL of deionized water.

5-HMF, 3,4-hydroxybenzoic, catechin, 4-hydroxybenzoic, caffeine, gallic acid, CGA, and caffeic acid were identified and quantified from the calibration curve through triplicate measurements based on the peak areas. Table II presents the linear equations obtained from the calibration curve of each compound. The limit of detection (LOD) was estimated through the parameters of the analytical curve, being expressed by the equation $LOD = 3{,}3 \times s/a$, where $\boldsymbol{s}$ is the standard deviation of the linear coefficient and $\boldsymbol{a}$ is the value of the angular coefficient. The concentrations of these compounds found in the coffee samples are expressed in mg 100 g^{-1} of ground-roasted coffee.

Table II. Calibration curves of the compounds identified in the coffee samples

Compound	Concentration (mg 100 g^{-1})	Straight equation	R^2	LOD (mg 100 g^{-1})	Retention time (min)
Gallic acid	0.05 – 0.75	Area = 0.48 + 103.46 C	0.999	0.002	4.5
5-HMF	0.2 – 4	Area = 33.19 + 263.80 C	0.999	0.036	6.4
3,4- Hydroxybenzoic	1.25 – 20	Area = -11.13 + 57.17 C	0.999	0.091	7.1
Catequina	2.5 – 25	Area = 0.90 + 23.43 C	0.999	0.346	10.5
4- Hydroxybenzoic	2.5 – 20	Area = -291.19 + 87.85 C	0.997	0.766	12.5
Caffeine	50 – 175	Area = 6352.75 + 83.60 C	0.998	5.015	20.7
CGA	10 – 125	Area = -117.77 + 61.23 C	0.999	0.966	12.5
Caffeic acid	0.0125 – 0.25	Area = 7.38 + 120.20 C	0.999	0.003	18.3

°Bx, TDS, and PE

The TDS and PE were calculated from the °Bx of all the extracts prepared with water by using a portable refractometer and conversion equations (1) and (2).

$$TDS = 0.85 \times \% \text{ °Bx} \quad (1)$$

$$PE = TDS \times \text{Drink/Dosage} \quad (2)$$

The beverage value corresponds to the amount of water, and the 'Dosage' represents the serving (g) of coffee.

Statistical analysis

The Student's *t*-test was performed at a significance level of 95% ($\alpha = 0.05$) to evaluate the difference between the extraction methods and coffee types. OriginPro 2022 software (Student Version 9.9.0.220) was used for the statistical analysis and construction of the figures.

RESULTS AND DISCUSSION

Screening solvents for discrimination of high-quality and traditional coffees

To maximize the extraction efficiency, different parameters such as the solvent, agitation, extraction time, solute/solvent ratio, temperature, and mass transfer efficiency[16] should be evaluated, permitting determination of the chemical markers that distinguish different coffees. The evaluated solvents were selected according to the guidelines of Bunzel and Schendel[18] who analyzed solvents for extracting phenolic compounds from foods, including water, polar organic solvents, or a mixture of polar organic solvents. The frequently used polar solvents include methanol, ethanol, and acetone (polarity index 5.1, 4.3, and 5.1, respectively) and less polar ethyl acetate (polarity index 4.4).[24] Moreover, detection at 280 and 320 nm was used for identification and quantification, as an essential method for analyzing the phenolic compounds in coffee. Caffeine and phenolic compounds such as CGA and caffeic acid are abundant compounds in coffee that carry out characteristics responsible for its flavor, aroma, and nutritional characteristics.[5,25] In the literature, the absorption spectrum of CGA presents a band at 300 nm, with a maximum of 326 nm. This absorption band can be attributed to organic foods and lipids.[26] For methylxanthines (caffeine, theobromine, and theophylline) extracted with water, the maximum absorption wavelength reported in the literature is between 270 and 280 nm.[27] Furthermore, phenolic compounds present in their organic

structure groups, usually unsaturated, called chromophores, absorb electromagnetic radiation in the UV-Vis regions,[28] thus allowing the detection of these compounds in this spectrum region.

The wavelength for the detection of the compounds was chosen after a previous study of the maximum absorption wavelengths of each compound, and monitoring the wavelengths between 280 and 320 nm allowed the simultaneous detection of important compounds for the characterization of coffee.

The proportion of the extraction solvent can be determined through statistical mixture design to optimize the quantity and variety of extracted metabolites. The statistical mixture design was applied using ethanol, ethyl acetate, acetone, and water (Table I); the chromatographic profiles are shown in Figure 1.

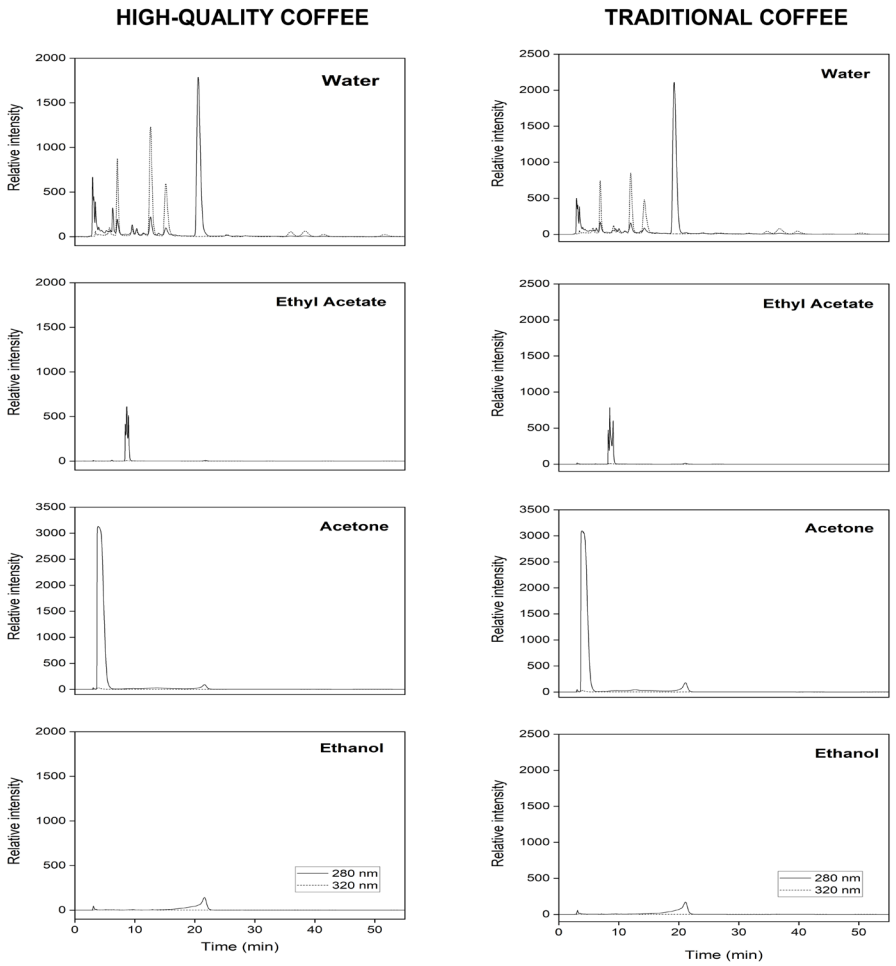

Figure 1. Chromatographic profiles in 280 and 320 nm for analysis of high-quality and traditional coffee using water, ethyl acetate, acetone, and ethanol as extractor solvent (100%). Chromatographic conditions: mobile phase consisting of 95% (A) 5% acetic acid in water (v/v) and 5% (B) acetonitrile; injection volume: 30 µL; and flow rate: 0.8 mL min^{-1}.

The profiles obtained at 280 and 320 nm, it was found that water enabled the extraction of a wider variety of compounds than the other solvents used in this study (Figure 1). Still showed a resolution value equal to 2.54 and 2.35 for neighboring peaks (6 min and 7 min) at 280 nm for the high-quality and traditional coffee, respectively, and a resolution equal to 3.62 and 2.93 for neighboring peaks (12 min and 15 min) at 320 nm for high-quality and traditional coffee respectively. As resolution values were more significant than 1.5, baseline separation was achieved.[28] Furthermore, depending on the solvent used, there was less extraction and separation of the compounds, baseline resolution was not achieved, and

the different peaks that appear in the chromatographic profiles refer to the solvent evaluated. Hence, using water as an extraction solvent proved advantageous for, extracting more compounds, conforming to the guidelines of green chemistry, and allowing direct comparison with the sensory analysis of coffee, while being inexpensive. The effectiveness of water as a solvent is expected due to the polarity of water (polarity index 10.2) and the compounds present in coffee, which are easily solubilized in the water, such as trigonelline, caffeine, and CGA.[29]

Furthermore, Abreu et al.[26] evaluated the effect of water, ethanol, and dichloromethane on the extraction of secondary metabolites from special and traditional coffees through blend planning, where water was the most effective extraction solvent. Thus, water enable the best discrimination between high-quality and traditional coffees and enabled corroboration with the results found in this work.

The interaction of solvents and water in the extraction (50:50 v/v) was evaluated as described in the experimental design (Table I); the chromatographic profiles are shown in Figures 2 and 3. The compounds found in the water were also extracted with a solvent and water mixture by evaluating the chromatographic profiles obtained.

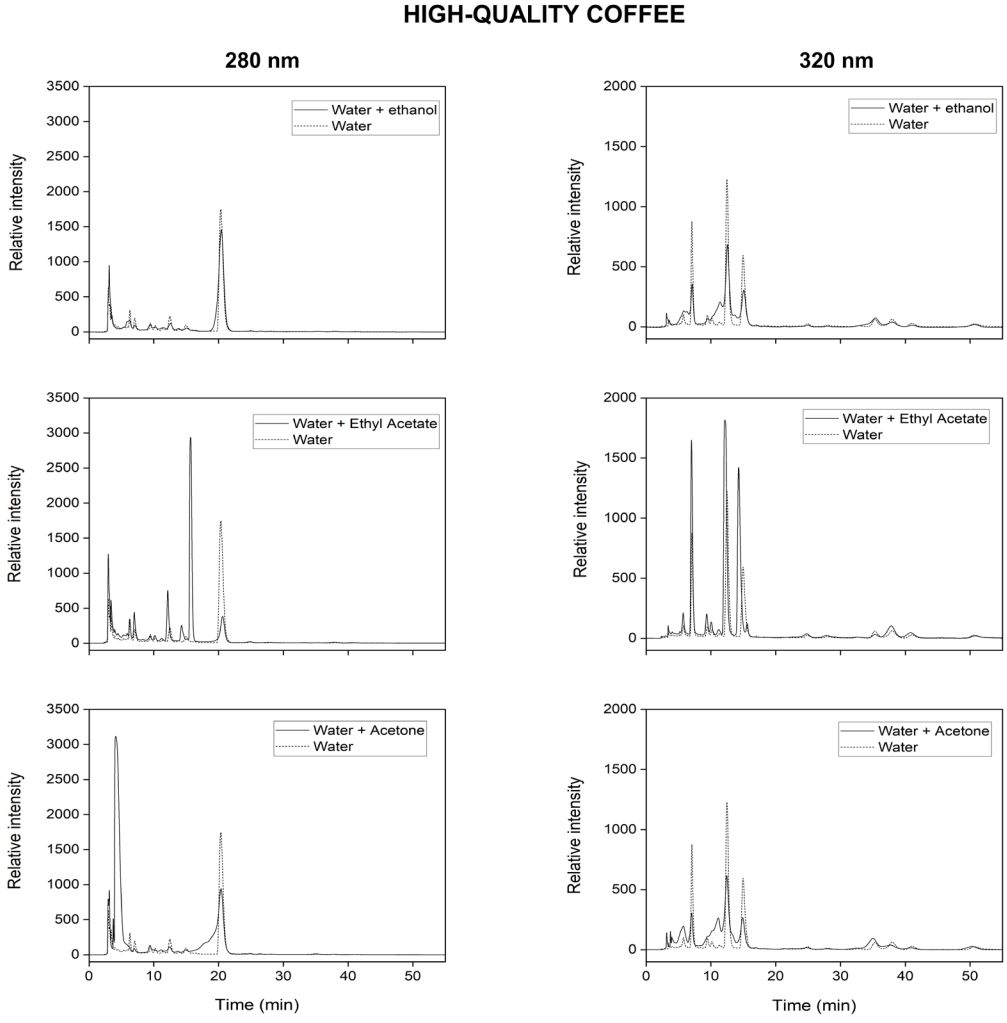

Figure 2. Chromatographic profiles obtained at 280 and 320 nm for high-quality coffee employing water and solvent mixture (50:50 v/v) as extractant. Chromatographic conditions: mobile phase consisting of 95% (A) 5% acetic acid in water (v/v) and 5% (B) acetonitrile; injection volume: 30 µL; flow rate: 0.8 mL min^{-1}.

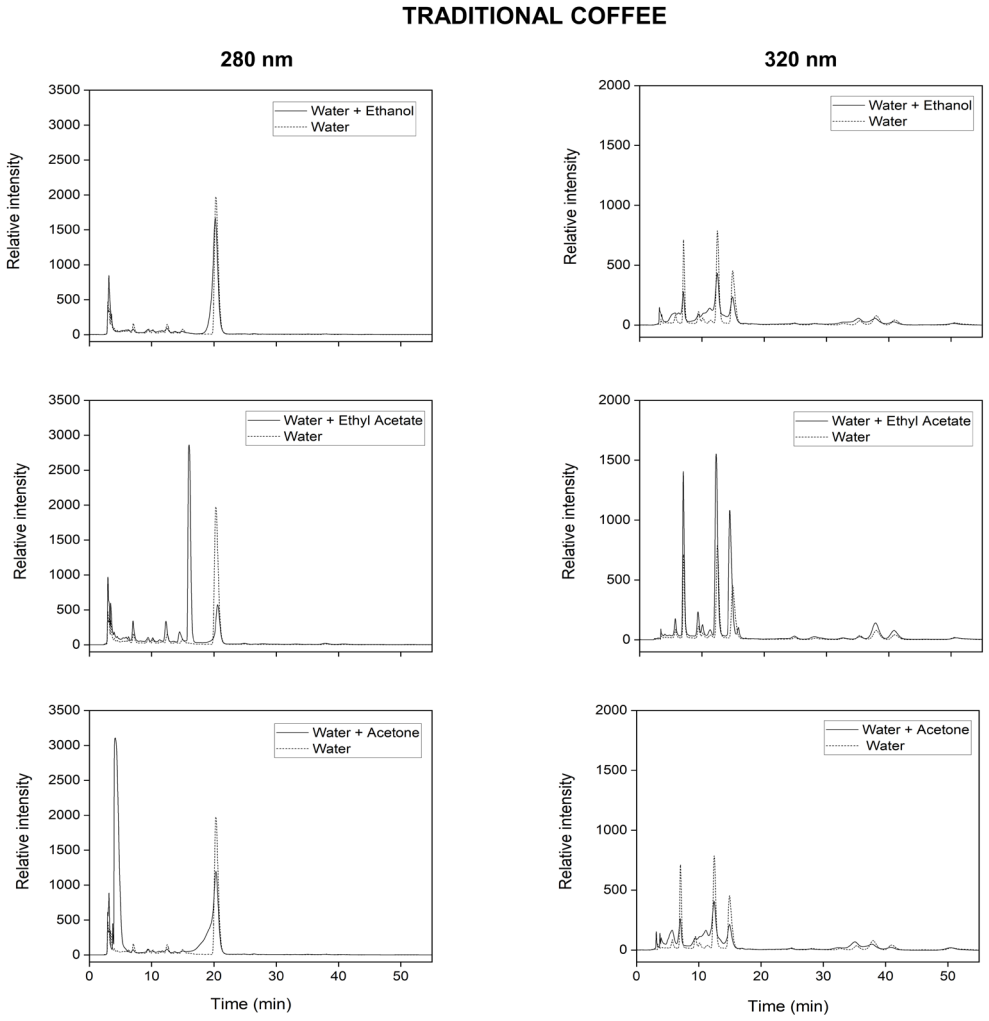

Figure 3. Chromatographic profiles obtained at 280 and 320 nm for traditional coffee employing solvent extraction using water and solvent (50:50 v/v). Chromatographic conditions: mobile phase consisting of 95% (A) 5% acetic acid in water (v/v) and 5% (B) acetonitrile; injection volume: 30 µL; flow rate: 0.8 mL min^{-1}.

In the literature, methanol was also cited as a solvent for coffee extraction. However, the chromatographic profiles were similar to those obtained with the other solvents, where no different compounds were extracted compared to those obtained by extraction with water.

The comparative exploratory evaluation of the chromatographic profiles obtained made it possible to judge the efficiency of solvent extraction for the work. Applying the experimental design (Table I) was an effective tool for optimizing the extraction conditions. It is possible to evaluate the solvents individually and their interactions using the experimental design. However, the different assessed solvents in the extraction in this work did not allow the discrimination of chemical compounds between the coffees. However, the differentiation between the types of coffee samples can be made by quantifying these compounds. So, choosing the method and the solvent is crucial, and the maximum extraction was achieved when using water as the extraction solvent.

Discrimination between high-quality and traditional coffees via extraction using methods A and B

Coffee preparation is a solid-liquid extraction process that involves three steps: (1) water absorption by ground coffee; (2) mass transfer of the soluble solids from the ground coffee to hot water; and (3) separation of the extract from the spent solids. Several variables can modify the quality of coffee beverages, such as

the contact time between the water and ground coffee, extraction time, ratio between ground coffee and water, water temperature and pressure, filter type, and boiling process.[25]

This work evaluated two extraction methods aiming at maximum extraction and the search for discriminating compounds between coffee types for high-quality and traditional coffee according to the comparison of the analysis of chromatographic profiles, as presented in Figure 4.

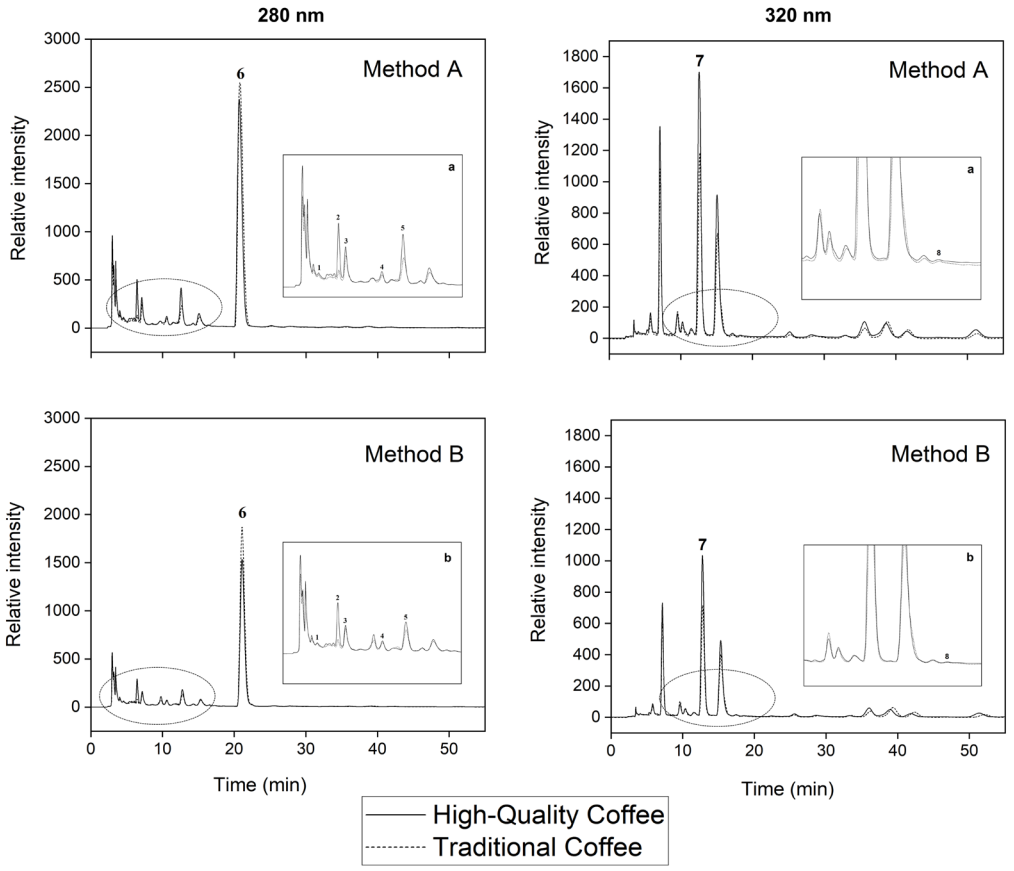

Figure 4. Chromatographic profiles of high-quality and traditional coffee, obtained at 280 and 320 nm. Images *a* and *b* are magnifications of the circulated parts. The compounds are (1) gallic acid, (2) 5-HMF, (3) 3,4-hydroxybenzoic, (4) catechin, (5) 4-hydroxybenzoic, (6) caffeine, (7) CGA, and (8) caffeic acid. Chromatographic conditions: mobile phase consisting of 95% (A) 5% acetic acid in water (v/v) and 5% (B) acetonitrile; injection volume: 30 µL; flow rate: 0.8 mL min^{-1}.

Evaluation of the chromatographic profiles at the two wavelengths (280 and 320 nm) verified the similarity between the extraction methods (Figure 4).

There were no significant differences in the chromatographic profiles of the high-quality and traditional coffee samples. Nonetheless, eight (5-HMF, 3,4-hydroxybenzoic, catechin, 4-hydroxybenzoic, caffeine, CGA, caffeic acid, and gallic acid) non-volatile compounds were identified and quantified in the high-quality and traditional coffee samples. The concentrations of these substances are presented in Table III.

Table III. Quantity of compounds in high-quality and traditional coffees extracted by methods A and B

Compound	mg 100 g^{-1} of sample			
	High-quality coffee		Traditional coffee	
	Method A	Method B	Method A	Method B
Gallic acid	4 ± 1^{aA}	3 ± 0.3^{bA}	3 ± 0.1^{aB}	2 ± 0.1^{cC}
5-HMF	33 ± 0.3^{aA}	18 ± 1^{cB}	5 ± 0.2^{bC}	3 ± 0.1^{dD}
3,4- Hydroxybenzoic	124 ± 1^{aA}	61 ± 4^{cB}	101 ± 4^{bC}	62 ± 4^{cD}
Catechin	97 ± 2^{aA}	58 ± 7^{cB}	89 ± 2^{bC}	58 ± 2^{cD}
4- Hydroxybenzoic	150 ± 3^{aA}	69 ± 3^{cB}	79 ± 2^{bC}	47 ± 1^{dD}
Caffeine	1799 ± 12^{aA}	962 ± 39^{cB}	2108 ± 29^{bC}	1342 ± 49^{dD}
CGA	1289 ± 5^{aA}	695 ± 30^{cB}	816 ± 15^{bC}	501 ± 16^{dD}
Caffeic acid	2 ± 0.1^{aA}	0.5 ± 0.1^{cB}	2 ± 0.1^{bC}	0.9 ± 0.1^{dD}

*Averages followed by the same letter, lowercase (comparison between classification) and uppercase (comparison between methods) in the line do not differ from each other, by Student's *t*-test, at a significance level of 95% (α = 0.05).

Different levels of the same compounds were found in the high-quality and traditional coffees, as presented in Table III. There was no significant difference in the content of gallic acid in the high-quality coffee samples extracted using methods A and B, according to the Student's *t*-test at the 95% confidence level. However, there were significant differences in the contents of 5-HMF, 3,4-hydroxybenzoic, catechin, 4-hydroxybenzoic, caffeine, CGA, and caffeic acid. Furthermore, the content of these compounds in high-quality and traditional coffees can be used as a marker, except for gallic acid, catechin, and 3,4-hydroxybenzoic for which there was no significant difference at the 95% confidence level.

From comparison of the extracts of the high-quality and traditional samples prepared using methods A and B, the concentrations of 5-HMF (33±0.3 mg 100 g^{-1} in the sample obtained by method A and 18±1 mg 100 g^{-1} in the sample obtained by method B) and CGA (1289±5 mg 100 g^{-1} in the sample obtained by method A and 695±30 mg 100 g^{-1} in the sample obtained by method B) were higher for high-quality coffee than traditional coffee. Thus, the content of these compounds is associated with the type of roast used and the sensory characteristics of higher-quality coffee.[23]

The highest caffeine content was found in traditional coffee. This result can be correlated to the coffees classified because blends between arabica and canephora species[5,30] constitute the traditional coffees.

Table IV presents some concentrations of CGA, caffeine, caffeic acid, and 5-HMF compounds found in the literature for different samples of roasted coffee.

Table IV. Contents of compounds quantified in different samples of the coffee

Description	Compounds				Ref.
	mg 100 g^{-1} of sample				
	CGA	Caffeine	Caffeic acid	5-HMF	
Gourmet	270 - 1200	990 - 1290	-	-	7
Traditional	140 - 690	1070 - 1790	-	-	
High-quality	2110	3440	790	100	23
Traditional	860	4890	300	-	

(continues on the next page)

Table IV. Contents of compounds quantified in different samples of the coffee (continuation)

Arabica	220 - 5960	4700	-	< 230	27
Robusta	130 - 6190	7200	-	< 40	

Comparing the concentrations found in this work (Table III) with those found by Souza et al.[7] (Table IV), the caffeine concentration was higher for the traditional classification coffee, and the CGA concentration was higher for the gourmet coffee. The concentration values were similar between the works. In work by Alcantara et al.,[23] 5-HMF was not detected for traditional coffee. The values found by the authors were higher than those found in this work for caffeine, caffeic acid, and 5-HMF, which may be linked to the coffee characteristics and the extraction method used by the authors. In the literature, levels of up to 230 mg 100 g^{-1} of 5-HMF were found for Arabica coffee and 40 mg 100 g^{-1} for Robusta coffee, with a marked decrease of the compound being observed in coffees with roasting.[27]

For works that investigated different conditions of extraction and concentration of chemical compounds in coffees, among these compounds caffeine and CGA, the results show differences in the concentrations of the compounds according to the extraction condition.[19,25] The concentrations of the compounds increase with temperature, regardless of the extraction method, flow rate, or contact time. Table V presents some concentrations of CGA and caffeine compounds found in the literature for different extraction conditions.

Table V. Contents of compounds quantified in different conditions of extraction

Description	**Compounds** mg mL^{-1}		**Ref.**
	CGA*	**Caffeine**	
Cold Drip	0.45 ± 0.04	1.27 ± 0.15	25
Cold Brew	0.35 ± 0.04	0.97 ± 0.12	
French Press	0.40 ± 0.03	1.09 ± 0.11	
Espresso Caffè Firenze	1.56 ± 0.17	1.43 ± 0.07	19
Espresso high-quality	4.80 ± 0.30	4.20 ± 0.09	
Espresso classical	4.46 ± 0.10	4.10 ± 0.16	
V60	0.80 ± 0.08	0.74 ± 0.09	
Cold Brew	1.39 ± 0.15	1.25 ± 0.12	
Aeropress	0.72 ± 0.11	0.78 ± 0.09	
French Press	0.53 ± 0.07	0.52 ± 0.06	
Moka	1.22 ± 0.18	1.28 ± 0.04	
Method A High-quality coffee	0.86 ± 0.01	1.20 ± 0.01	This study
Method B High-quality coffee	0.46 ± 0.02	0.64 ± 0.03	
Method A Traditional coffee	0.54 ± 0.01	1.41 ± 0.02	
Method B Traditional coffee	0.33 ± 0.01	0.89 ± 0.03	

*The CGA contents shown refer to 5-caffeoylquinic acid (5-CQA).

Despite the different extraction conditions presented in Table V, comparing the concentrations of CGA and caffeine, were found similar concentration values among the works.[19,25]

The same non-volatile compounds were identified in both extracts evaluated and significantly differed in the Student's *t*-test between methods (A and B) and the coffee type (high-quality and traditional). Although method A extracted a greater quantity of the compounds, method B was chosen due to its ease of execution compared to method A. The method chosen also had an efficient method for extracting compounds chosen as possible markers and is the method most similar to the usual method used by consumers in preparing the coffee beverage.

Total dissolved solids and extraction percentage

The °Bx of the coffee extracts prepared by methods A and B was evaluated. The TDS and PE were 3 and 45% and 1.7 and 25% for high-quality coffee extracted using methods A and B, respectively. For traditional coffee, the TDS and PE obtained with methods A and B were 3 and 39% and 1.8 and 26%, respectively.

The extraction percentage was higher for both coffees when method A was used (45 and 39%, respectively, for high-quality and traditional coffee). With method B, the average PE was 26%, which is closer to the ideal extraction value (18 and 22%), representing Lockart's quality and pleasant drink sensory characteristics proposed in 1957 in the Coffee Preparation Control Chart.[31]

Angeloni et al.,[19] when investigating eight different coffee beverage preparation methods, found a TDS variation from 1.35 ± 0.03 to 8.44 ± 0.38, and the range for PE was 28.60 ± 1.03 to 13.46 ± 1.56. The highest PE was found for the Mocha method and the lowest for the Espresso Caffè Firenze method.

Methods A and B both afforded superior extraction of coffee (PE > 22%), which is advantageous for quantifying the compounds. However, the coffee beverage may present notes of bitterness and astringency.

Despite being widely used by baristas and recommended by the Association of Specialty Coffees for evaluating the correct degree of extraction,[25] there are few studies on the TDS of coffees in the literature. In this study, a relationship between the highest extraction percentage and the highest levels of compounds quantified by method A was found.

CONCLUSIONS

Different extraction methods and variables were evaluated in the preparation of coffee extract. The TDS and PE results contributed to the choice of the extraction method. In addition to being non-toxic and low-cost, water was the optimal solvent for conforming to the principles of green chemistry and allowing direct comparison with sensory analysis. Among the extraction methods, method A enable the extraction of the largest amount of non-volatile compounds. Method B also showed satisfactory results for extracting the compounds of interest, with a PE closer to the ideal value (18 and 22%). This extraction method was chosen for further studies due to its ease of execution and similarity to the usual way of preparing coffee beverages used by consumers. Furthermore, the contents of the compounds can be used to discriminate between different coffees, where 5-HMF, 4-hydroxybenzoic, CGA, and caffeic acid can be used as possible markers.

Conflicts of interest

The authors declare that they have no conflict of interest.

Acknowledgements

The authors appreciate the financial support of the National Council for Scientific and Technological Development (grant number 142474/2020-7), Coordination of Improvement of Higher Education Personnel (CAPES) and São Paulo Research Foundation (FAPESP).

REFERENCES

(1) Alves, S. T.; Dias, R. C. E.; Benassi, M. de T.; Scholz, M. B. dos S. Metodologia para Análise Simultânea de Ácido Nicotínico, Trigonelina, Ácido Clorogênico e Cafeína Em Café Torrado por Cromatografia Líquida de Alta Eficiência. *Quim. Nova* **2006**, *29* (6), 1164–1168. https://doi.org/10.1590/s0100-40422006000600003

(2) Barbin, D. F.; Felicio, A. L. S. M.; Sun, D.-W.; Nixdorf, S. L.; Heirooka, E. Y. Application of Infrared Spectral Techniques on Quality and Compositional Attributes of Coffee: An Overview. *Food Res. Int.* **2014**, *61*, 23–32. https://doi.org/10.1016/j.foodres.2014.01.005

(3) Assis, C.; Pereira, H. V.; Amador, V. S.; Augusti, R.; de Oliveira, L. S.; Sena, M. M. Combining Mid Infrared Spectroscopy and Paper Spray Mass Spectrometry in a Data Fusion Model to Predict the Composition of Coffee Blends. *Food Chem.* **2019**, *281*, 71–77. https://doi.org/10.1016/j.foodchem.2018.12.044

(4) Esteban-Díez, I.; González-Sáiz, J. M.; Pizarro, C. An Evaluation of Orthogonal Signal Correction Methods for the Characterisation of Arabica and Robusta Coffee Varieties by NIRS. *Anal. Chim. Acta* **2004**, *514* (1), 57–67. https://doi.org/10.1016/j.aca.2004.03.022

(5) Monteiro, P. I.; Santos, J. S.; Rodionova, O. Y.; Pomerantsev, A.; Chaves, E. S.; Rosso, N. D.; Granato, D. Chemometric Authentication of Brazilian Coffees Based on Chemical Profiling. *J. Food Sci.* **2019**, *84* (11), 3099–3108. https://doi.org/10.1111/1750-3841.14815

(6) Associação Brasileira da Indústria do Café. *Categorias de qualidade do café: recomendações técnicas ABIC*. https://www.abic.com.br/recomendacoes-tecnicas/categorias-de-qualidade-do-cafe/ (accessed 2020-03-12).

(7) Souza, R. M. N.; Canuto, G. A. B.; Dias, R. C. E.; Benassi, M. de T. Teores de Compostos Bioativos Em Cafés Torrados e Moídos Comerciais. *Quim. Nova* **2010**, *33* (4), 885–890. https://doi.org/10.1590/S0100-40422010000400002

(8) Agnoletti, B. Z.; Oliveira, E. C. da S.; Pinheiro, P. F.; Saraiva, S. H. Discriminação de Café Arábica e Conilon Utilizando Propriedades Físico-Químicas Aliadas à Quimiometria. *Rev. Virtual Quim.* **2019**, *11* (3), 785–805. https://doi.org/10.21577/1984-6835.20190057

(9) Pereira, L. L.; Cardoso, W. S.; Guarçoni, R. C.; da Fonseca, A. F. A.; Moreira, T. R.; ten Caten, C. S. The Consistency in the Sensory Analysis of Coffees Using Q-Graders. *Eur. Food Res. Technol.* **2017**, *243* (9), 1545–1554. https://doi.org/10.1007/s00217-017-2863-9

(10) Malta, M. R.; Nogueira, F. D.; Guimarães, P. T. G. Composição Química, Produção e Qualidade Do Café Fertilizado Com Diferentes Fontes e Doses de Nitrogênio. *Ciência e Agrotecnologia* **2003**, *27* (6), 1246–1252. https://doi.org/10.1590/S1413-70542003000600006

(11) Ribeiro, F. C.; Figueiredo, L. P.; Giomo, G. S.; Isquierdo, E. P.; Ferreira, I. T.; Borém, F. M. Qualidade de Bebida, Condutividade Elétrica e Lixiviação de Potássio de Grãos de Café (*Coffea arabica* L.) Submetidos a Diferentes Métodos de Degomagem Biológica. Work presented at the *VI Simpósio de Pesquisa dos Cafés do Brasil* (SPCB), Vitória, ES, BRA, 2009, p 4. http://www.sbicafe.ufv.br/handle/123456789/2902

(12) Buffo, R. A.; Cardelli-freire, C. Coffee Flavour : An Overview. *Flavour Fragr. J.* **2004**, *19*, 99–104. https://doi.org/10.1002/ffj.1325

(13) Abrahão, S. A.; Pereira, R. G. F. A.; Duarte, S. M. da S.; Lima, A. R.; Alvarenga, D. J.; Ferreira, E. B. Compostos Bioativos e Atividade Antioxidante Do Café (*Coffea arabica* L.). *Ciência e Agrotecnologia* **2010**, *34* (2), 414–420. https://doi.org/10.1590/S1413-70542010000200020

(14) Oliveira, D. M.; Bastos, D. H. M. Biodisponibilidade de Ácidos Fenólicos. *Quim. Nova* **2011**, *34* (6), 1051–1056. https://doi.org/10.1590/S0100-40422011000600023

(15) Farah, A.; Donangelo, C. M. Phenolic Compounds in Coffee - Minireview. *Braz. J. Plant Physiol.* **2006**, *18* (1), 23–36. https://doi.org/10.1590/S1677-04202006000100003

(16) Haminiuk, C. W. I.; Maciel, G. M.; Plata-Oviedo, M. S. V.; Peralta, R. M. Phenolic Compounds in Fruits - an Overview. *Int. J. Food Sci. Technol.* **2012**, *47* (10), 2023–2044. https://doi.org/10.1111/j.1365-2621.2012.03067.x

(17) Schieber, A. *Introduction to Food Authentication*, 2nd ed.; Elsevier Inc., 2018. https://doi.org/10.1016/B978-0-12-814264-6.00001-3
(18) Bunzel, M.; Schendel, R. R. Determination of (Total) Phenolics and Antioxidant Capacity in Food and Ingredients. In: Nielsen, S. S. (Ed.) *Food Analysis*. Springer International Publishing: Indiana/USA, 2017, pp 455–468. https://doi.org/10.1007/978-3-319-45776-5_25
(19) Angeloni, G.; Guerrini, L.; Masella, P.; Bellumori, M.; Daluiso, S.; Parenti, A.; Innocenti, M. What Kind of Coffee Do You Drink? An Investigation on Effects of Eight Different Extraction Methods. *Food Res. Int*. **2019**, *116*, 1327–1335. https://doi.org/10.1016/j.foodres.2018.10.022
(20) Gómez, O. S. Converting Brix to TDS – An Independent Study. **2019**, 1–28. https://doi.org/10.13140/RG.2.2.10679.27040
(21) Terrile, A. E.; Marcheafave, G. G.; Oliveira, G. S.; Rakocevic, M.; Bruns, R. E.; Scarminio, I. S. Chemometric Analysis of UV Characteristic Profile and Infrared Fingerprint Variations of Coffea arabica Green Beans under Different Space Management Treatments. *J. Braz. Chem. Soc.* **2016**, *27* (7), 1254–1263. https://doi.org/10.5935/0103-5053.20160022
(22) Cuadros-Rodríguez, L.; Ruiz-Samblás, C.; Valverde-Som, L.; Pérez-Castaño, E.; González-Casado, A. Chromatographic Fingerprinting: An Innovative Approach for Food "identitation" and Food Authentication – A Tutorial. *Anal. Chim. Acta* **2016**, *909*, 9–23. https://doi.org/10.1016/J.ACA.2015.12.042
(23) Alcantara, G. M. R. N.; Dresch, D.; Melchert, W. R. Use of Non-Volatile Compounds for the Classification of Specialty and Traditional Brazilian Coffees Using Principal Component Analysis. *Food Chem.* **2021**, *360*, 130088. https://doi.org/10.1016/j.foodchem.2021.130088
(24) Snyder, L. R. Classification of the Solvent Properties of Common Liquids. *J. Chromatogr. Sci.* **1978**, *16* (6), 223–234. https://doi.org/10.1093/chromsci/16.6.223
(25) Angeloni, G.; Guerrini, L.; Masella, P.; Innocenti, M.; Bellumori, M.; Parenti, A. Characterization and Comparison of Cold Brew and Cold Drip Coffee Extraction Methods. *J. Sci. Food Agric.* **2018**, *99* (1), 391–399. https://doi.org/10.1002/jsfa.9200
(26) Abreu, M. B.; Marcheafave, G. G.; Bruns, R. E.; Scarminio, I. S.; Zeraik, M. L. Spectroscopic and Chromatographic Fingerprints for Discrimination of Specialty and Traditional Coffees by Integrated Chemometric Methods. *Food Anal. Methods* **2020**, *13* (12), 2204–2212. https://doi.org/10.1007/s12161-020-01832-1
(27) Vignoli, J. A.; Viegas, M. C.; Bassoli, D. G.; Benassi, M. T. Roasting Process Affects Differently the Bioactive Compounds and the Antioxidant Activity of Arabica and Robusta Coffees. *Food Res. Int.* **2014**, *61*, 279–285. https://doi.org/10.1016/J.FOODRES.2013.06.006
(28) Harris, D. C. *Análise Química Quantitativa*, (6th ed.). LTC-Livros Técnicos e Científicos Editora S.A., Rio de Janeiro, 2005.
(29) Nogueira, M.; Trugo, L. C. Distribuição de Isômeros de Ácido Clorogênico e Teores de Cafeína e Trigonelina em Cafés Solúveis Brasileiros. *Food Sci. Technol.* **2003**, *23* (2), 296–299. https://doi.org/10.1590/S0101-20612003000200033
(30) Vignoli, J. A.; Bassoli, D. G.; Benassi, M. T. Antioxidant Activity, Polyphenols, Caffeine and Melanoidins in Soluble Coffee: The Influence of Processing Conditions and Raw Material. *Food Chem.* **2011**, *124* (3), 863–868. https://doi.org/10.1016/j.foodchem.2010.07.008
(31) Specialty Coffee Association. *Towards a New Brewing Chart*. https://sca.coffee/sca-news/25/issue-13/towards-a-new-brewing-chart#_ftnref1 (accessed 2022-05-02).

Brazilian Journal of Analytical Chemistry
2023, Volume 10, Issue 40, pp 90-98
doi: 10.30744/brjac.2179-3425.AR-108-2022

BrJAC

ARTICLE

Iridium Oxides Based Potentiometric Sensor for pH Monitoring in Biological Samples

Jessica Soares Guimaraes Selva, Mauro Bertotti*

Departamento de Química Fundamental, Instituto de Química, Universidade de São Paulo, Av. Professor Lineu Prestes, 748, 05508-000, São Paulo, SP, Brazil

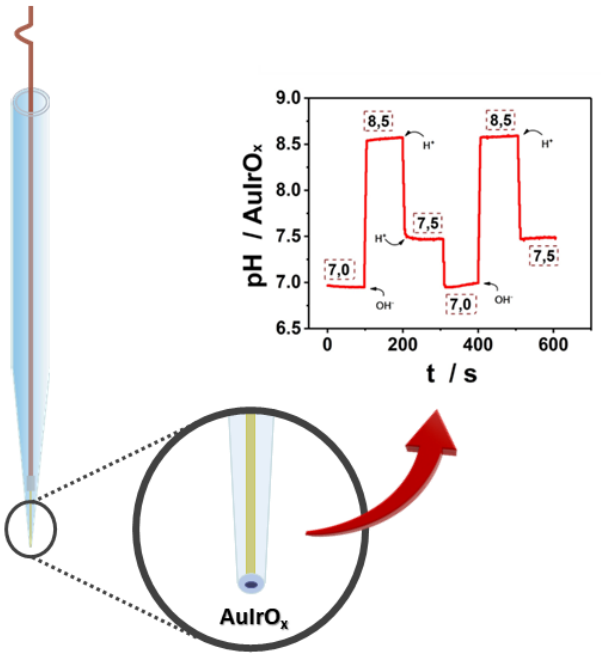

The fabrication and long-term application of a pH Au microelectrode based on an iridium oxide film are reported. A uniform iridium oxide film with a typical thickness of around 1 µm was coated on the microelectrode surface through a 2-step procedure involving electrodeposition at constant potential and further continuous voltammetric scans. A super-Nernstian slope of around 77 mV per pH unit was found from open circuit potential measurements in a broad pH range (2 to 10) in 0.01 mol L^{-1} phosphate buffer. It was demonstrated experimentally that the short-term pH precision of the IrO_x sensor is ± 0.1 pH. The response stability was maintained in the physiological pH range, and the sensor exhibited excellent reproducibility, long-term stability, and a short response time of < 10 s. The results reported in this work confirmed that iridium oxide showed very promising pH sensing performance and can serve as an electrode material for detecting local pH changes in samples of increased complexity, such as juice fruits, culture medium, synthetic urine, and blood.

Keywords: Potentiometric sensor, iridium oxides, pH sensor, microelectrodes, biological samples

INTRODUCTION

The original glass electrode probe is the most employed sensor for pH measurements because of its reliability, accuracy, and lifetime. However, there is a continuous interest in developing pH sensors on a miniature scale. Accordingly, efforts have been devoted in the last years to fabricate pH sensors that are relatively easy to miniaturize by using several solid-state metal oxides, including PtO_2, IrO_x, RuO_2, OsO_2, Ta_2O_5, RhO_2, TiO_2, and SnO_2.[1]

Iridium oxide (IrO_x)-modified electrodes have received particular attention, mainly for applications towards sensing different molecules of biological relevance.[2] Such material has also been extensively used in fabricating potentiometric pH sensors because of the formation of hydroxide groups on the oxide

Cite: Selva, J. S. G.; Bertotti, M. Iridium Oxides Based Potentiometric Sensor for pH Monitoring in Biological Samples. *Braz. J. Anal. Chem.* 2023, *10* (40), pp 90-98. http://dx.doi.org/10.30744/brjac.2179-3425.AR-108-2022

Submitted 09 November 2022, Resubmitted 23 January 2023, Accepted 01 March 2023, Available online 17 March 2023.

surface. The potential of the interface is determined by the ratio of the Ir(III) and Ir(IV) species, which in turn depends on the proton exchange capacity facilitated by the OH^- groups on the surface.[3,4]

pH potentiometric sensors based on IrO_x films are quite attractive because they present some interesting features such as potential stability, relationship between potential and pH over a wide range, fast response, and response immunity from the interference of redox species.[5–8] The pH sensing using iridium oxide materials has mainly been explored in different fields, i.e., to get information on pH in biological medium and corrosion studies, as well as for *in situ* measurements and in microscopic environments.[9–18]

The electrodeposition of iridium oxide films onto electrode surfaces has been conducted by different approaches. Among them, galvanostatic deposition proved to be the least indicated since it can provide fragile films which can be easily damaged. Potentiostatic electrodeposition provides more reproducible films, but they remain brittle. Elsen *et al*.[19] observed that films produced by cyclic voltammetry and constant applied potential are more compact and durable. Santos et al.[15] reported that more robust and reproducible iridium oxide films were obtained through a two-step procedure based on potentiostatic polarization for a certain time and subsequent recording of a few voltammetric cycles.

In previous work, we have fabricated a miniaturized Au microelectrode containing an iridium oxide film to get information on the role of transporters and pumps in larva midgut through pH determinations.[20] Our goal now is to enhance some features of such a microsensor aiming at getting more sensitive pH measurements with enhanced stability and short response time. This was achieved by changing some conditions in the protocol employed for the film preparation. We have demonstrated that such a miniaturized sensor shows favorable sensing performance and can be successfully applied to measure pH in biological samples.

MATERIALS AND METHODS

Chemicals

All chemicals and reagents were analytical grade and used without any further purification. All aqueous solutions were prepared using ultrapure water (Barnstead Nanopure Systems, 18 MΩ cm).

Instrumentation

The electrochemical experiments were performed using an Autolab PGSTAT128 potentiostat (Metrohm, Utrecht, Netherlands), interfaced with NOVA 1.11 software for data acquisition. Cyclic voltammograms (CVs) were recorded in a three-electrode configuration, using a gold microelectrode, $Ag|AgCl|KCl_{(sat)}$, and platinum wire as the working, reference, and auxiliary electrodes, respectively. Open circuit potential (OCP) measurements were conducted with the $AuIrO_x$ sensor as the indicator electrode and a $Ag|AgCl|KCl_{(sat)}$ as the reference.

$AuIrO_x$ Sensor preparation

A $AuIrO_x$ sensor was manufactured from a gold microfiber (99.99%, hard, 0.025 mm, Goodfellow®) sealed into a borosilicate capillary (O.D. 1 mm, I.D. 0.5 mm e 10 cm long, Sutter Instrument Company®) using a micropipette puller P2000. An $[Ir(COO)_2(OH)_4]^{2-}$ solution was used for the electrodeposition of the IrO_x film onto the electrode surface. The solution is prepared from $[IrCl_6]^{2-}$, H_2O_2 30% (w/w) and $C_2H_2O_4$, and the pH is adjusted to 10.5 using K_2CO_3, as previously reported by Santos[15] and Yamanaka[21]. The electrodeposition was accomplished according to a 2-step procedure:

i) A constant potential was applied for 600 s (0.8 V vs. $Ag|AgCl|KCl_{(sat)}$).

ii) 50 voltammetric cycles were recorded at scan rate = 100 mV s^{-1} from 0 to 1 V vs. $Ag|AgCl|KCl_{(sat)}$,

The sensor´s electrochemical behavior was examined through cyclic voltammetry in a 0.01 mol L^{-1} phosphate buffer solution (pH 7.0), which was also employed to calibrate the the $AuIrO_x$ sensor at different pH values.

Biological application

The $AuIrO_x$ sensor was employed to follow pH changes through OCP measurements. Before use, the device was calibrated adequately in a phosphate buffer solution in a pH range from 2 to 10. The sensor was placed in the solution during the measurements, and the potential was recorded for 60 s. The pH of all samples was measured with a commercial glass electrode for comparison, except for the blood sample, whose pH was measured through the arterial blood gas technique.[22,23]

RESULTS AND DISCUSSION

Figure 1 shows the CVs obtained after the potentiostatic step (E = 0.8 V vs. $Ag|AgCl|KCl_{(sat)}$ for 600 s), where an IrO_x film was electrodeposited. In the forward scans the peaks around 0.4 V and 0.8 V correspond to the oxidation of Ir (II) to Ir (III) and then to Ir (IV), respectively. In the reverse scans, the peaks around 0.55 V and 0.3 V correspond to the inverse processes. The electron transfer processes involving the iridium oxides lead to a continuous current increase as a consequence of the material accumulated onto the electrode surface during the CVs recording. Such a procedure leads to the growth of a mixed film of Ir(IV)/Ir(III) oxides with greater crystallinity and stability, which is sensitive to changes in the pH.[15,24] The number of potential cycles determines the amount of material electrodeposited on the electrode surface, as well as its distribution.

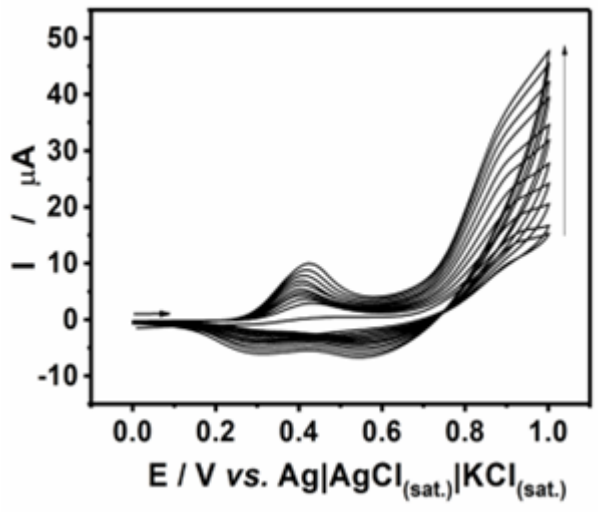

Figure 1. Cyclic voltammograms recorded with a Au microelectrode (r = 2.5 μm) in the iridium complex solution (pH 10.5) after the electrodeposition step. v = 100 mV s^{-1}. Here are presented the first CV and, after that, one every five measurements.

Although the mechanism for the film formation is still not well established in the literature, the most accepted reaction can be described by Equation 1[15,18,21]:

$$[Ir(COO)_2(OH)_4]^{2-}_{(aq)} \rightarrow IrO_{2(s)} + 2CO_{2(g)} + 2H_2O + 2e^- \qquad \text{Equation 1}$$

According to this reaction, the deposition of a hydrated iridium oxide film and the parallel formation of CO_2 take place.

To confirm the oxide layer electrodeposition, voltammograms were recorded in phosphate buffer solution (pH 7.0) before and after the 2-step procedure. By inspection of the CV shown in Figure 2 (red curve), the modification of the microelectrode surface is clearly confirmed. For instance, a voltammetric curve that resembles those obtained in a solution containing the iridium complex (Figure 1) is noticed in the 0.0 to 0.5 V potential range. Such electron transfer processes correspond to the Ir(III) oxide oxidation and concurrent reverse process (reduction of Ir(IV) oxide). The thickness of the film oxide layer was calculated by taking into account the charge under the cathodic peak and considering that a 1 μm thick iridium oxide film contains ca. 7.8 x 10^{-7} mol cm^{-2}, hence the film thickness was found to be 0.91 μm.[15]

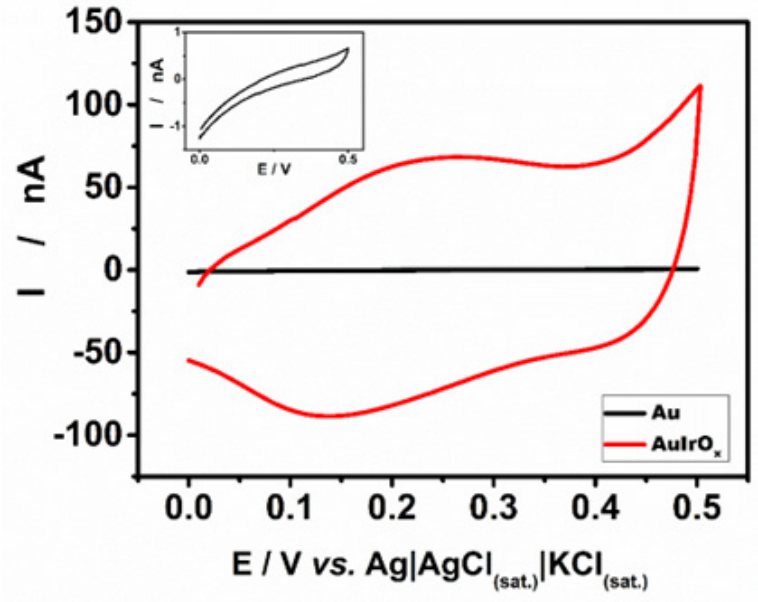

Figure 2. Cyclic voltammograms recorded in 0.01 mol L^{-1} PBS (pH 7.0), before and after the gold surface modification. v = 100 mV s^{-1}. Inset: Cyclic voltammogram recorded at the gold surface before the modification rescaled.

The sensitivity of the fabricated IrO_x sensor to pH was examined through open circuit potential measurements in 0.01 mol L^{-1} phosphate solution at different pH values, and Figure 3 displays the results. A linear correlation between potential values and solution pH is observed, and this dependence is based on the electron transfer reaction that governs the pH-sensitive properties of the $AuIrO_x$ sensor, given by Equation 2:[15,25,26]

$$2[IrO_2(OH)_{2-X}(2+x)\ H_2O]^{(2-X)-} + (3-2x)H^+ + 2e^- \rightleftharpoons [Ir_2O_3(OH)_3.3H_2O]^{3-} + 3H_2O \quad \text{Equation 2}$$

Therefore, the redox potential can be expressed as indicated by Equation 3:

$$E = E^0 - \frac{2.303RT\ (3-2x)}{2F}\ pH\ = E^0 - \frac{59\ (3-2x)}{2}\ pH \quad \text{Equation 3}$$

where: E = redox potential (mV); E° = standard electrode potential (mV); R = universal ideal gas constant (8.314 J K^{-1} mol^{-1}); T = temperature (K); F = Faraday constant (96485 C mol^{-1}); x = a value between 0 and 2.[18]

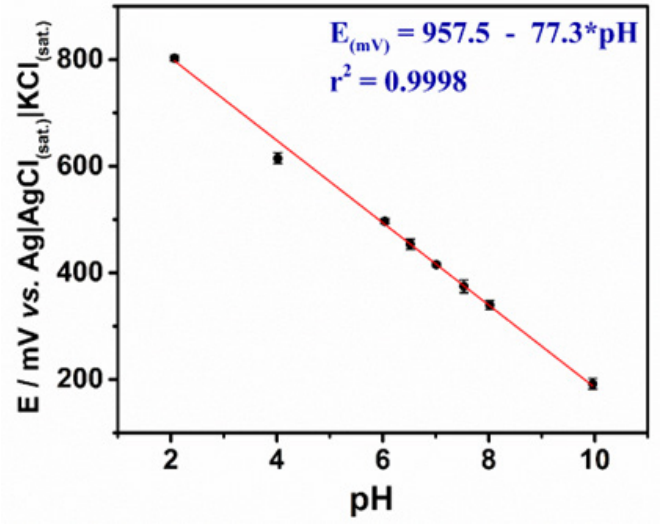

Figure 3. Potential values measured with the $AuIrO_x$ sensor as a function of pH.

It is easily deducible from Equation 3 that the slope value is 59 mV pH^{-1} when x = 0.5, the typical case where the number of electrons transferred in Equation 2 is equivalent to the number of protons. Likewise, for x = 0, the slope is 88.5 mV pH^{-1}, and a ratio of 3 protons to 2 electrons is expected. Hence, the difference in sensitivity is attributed to a mixed potential of two different oxyhydroxide states regarding the iridium oxide films.

A super-Nernstian response in an extensive pH range is exhibited in Figure 3. Such a behavior is usual for $AuIrO_x$ electrodes, for which slopes can vary up to -90 mV per pH unit.[15,27] The relative acidity of both iridium oxides involved in Equation 2[28,29] determines the pH response and justifies slopes higher than 60 mV per pH unit.[30,31]

A potentiometric titration was performed in order to evaluate the response time of the $AuIrO_x$ sensor to changes in pH, as well as the device's ability to detect slight variations in the solution pH. Measurements with the $AuIrO_x$ sensor were performed in the 6.5 to 7.5 pH range, and a parallel study was also conducted with a commercial pHmeter. Figure 4A displays the results, and one can conclude that the fabricated $AuIrO_x$ sensor responded quite adequately to changes in pH, providing quick and stable responses. Furthermore, the pH values provided by the $AuIrO_x$ sensor are in excellent agreement with those obtained with the pHmeter, as shown in Figure 4B.

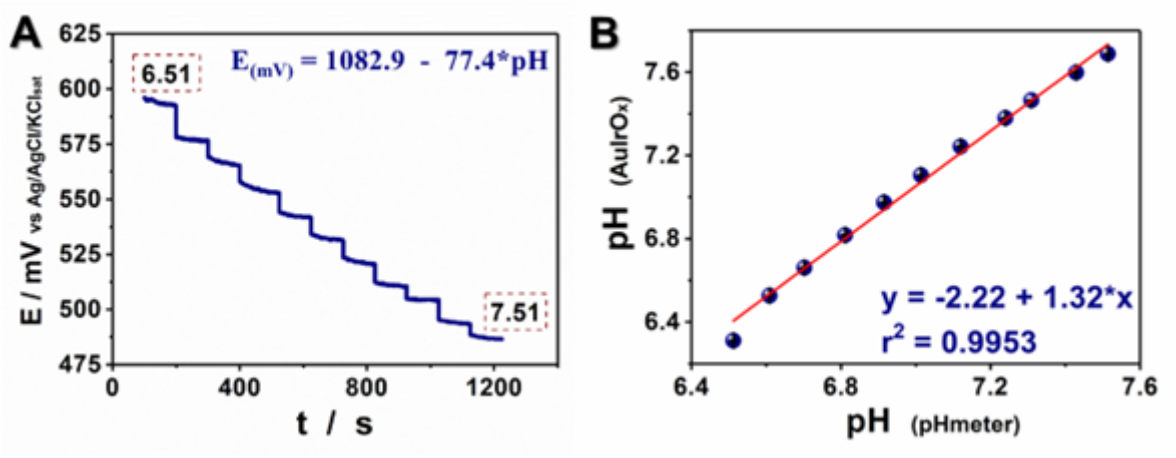

Figure 4. A) Dependence of OCP measurements recorded with the $AuIrO_x$ sensor on the pH. Values presented in the boxes correspond to those measured with the pHmeter. **B)** Correlation plot of pH values measured with the pHmeter and the AuIrOx sensor.

The fabricated sensor was applied to get the pH information in more complex samples such as synthetic urine, lemon juice, DMEM (Dulbecco's modified Eagle's medium), and blood. Table I shows that the $AuIrO_x$ sensor presented satisfactory results compared with the reference values. In order to check whether there was a difference between the results, a paired t test was performed, where it was found that there is no significant difference between the methods with a 95% confidence level.

Table I. Comparison between pH values of different samples measured with a glass electrode or by gasometry (blood) and those obtained with the $AuIrO_x$ sensor (n=3)

Sample	pH (Reference)	pH ($AuIrO_x$ Sensor)
Lemon juice	2.37	2.50 (± 0.08)
Synthetic urine	6.06	5.76 (± 0.02)
Synthetic urine + NaOH	6.73	6.38 (± 0.03)

(continues on the next page)

Table I. Comparison between pH values of different samples measured with a glass electrode or by gasometry (blood) and those obtained with the $AuIrO_x$ sensor (n=3) (continuation)

Sample	pH (Reference)	pH ($AuIrO_x$ Sensor)
DMEM	8.49	8.76 (± 0.07)
DMEN + CH_3COOH	4.17	4.63 (± 0.09)
Blood	6.88	7.1 (± 0.1)

The response time of the proposed sensor was assessed through measurements in a complex sample matrix. Accordingly, a synthetic urine solution´s pH was monitored after adding small volumes of 0.1 mol L^{-1} NaOH and 0.5 mol L^{-1} H_2SO_4 solutions. Measurements were performed under stirring using the $AuIrO_x$ sensor and a glass electrode during the entire process. A similar experiment was also performed using a DMEM solution, and Figure 5 presents the results. It is observed that, despite the slight difference between the absolute pH values, the sensor follows the solutions pH changes in both experiments. Moreover, no memory effect was observed, even in complex media such as synthetic urine and DMEM solution.

The results shown in Figure 5 also indicate that the response time of the $AuIrO_x$ sensor was very short. For instance, after adding acid or base solutions, a potential stabilization was achieved after around 5 s, which is considered relatively fast for pH sensing devices based on oxide films. In the literature,[5,27,32,33] it appears that, on average, sensors based on electrodeposited iridium oxide films (EIROF's) exhibit response times greater than 10 s. This shows that the developed sensor is quite efficient for real-time pH monitoring.

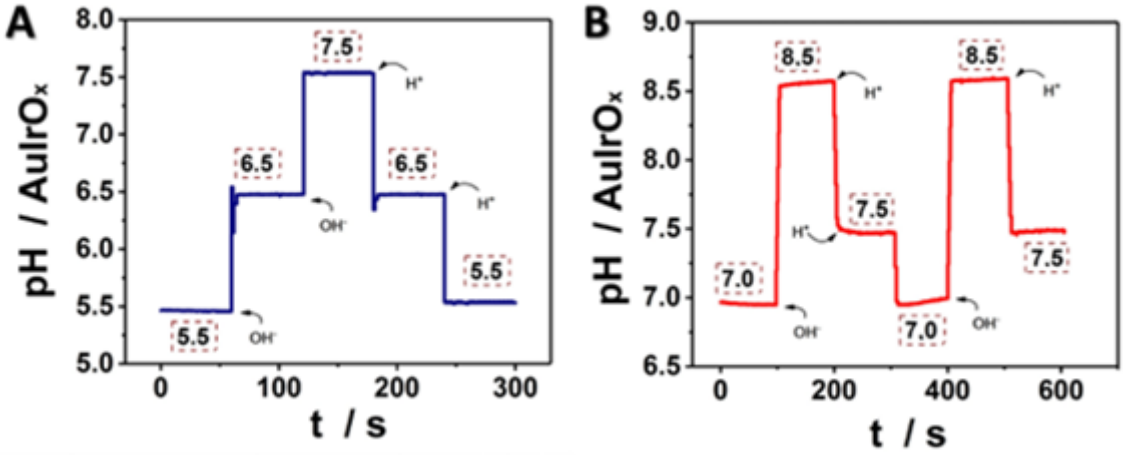

Figure 5. pH monitoring obtained with the AuIrOx sensor in: **A)** synthetic urine; **B)** DMEM during addition of 0.1 mol L^{-1} NaOH and 0.5 mol L^{-1} H_2SO_4 solutions. The boxes show the pH values measured with the pHmeter.

CONCLUSIONS

By coating the surface of a Au microelectrode with a layer of IrO_x, a potentiometric pH sensor was fabricated. The film was electrodeposited from an iridium complex solution by applying 0.8 V vs. $Ag|AgCl|KCl_{(sat)}$ for 600 s, followed by recording 50 cyclic voltammograms. This methodology allowed obtaining robust, stable, and sensitive IrO_x films to monitor reliably pH changes in solutions with a complex composition such as blood, synthetic urine, and DMEM culture medium. In addition, the device presented a wide working range (from pH 2 to 10) and fast response (< 10 s), allowing stable and sensitive pH measurements (0.1 unit).

In conclusion, the proposed $AuIrO_x$ sensor showed extremely promising attributes for getting real-time pH, having the potential to be an important tool in the study of complex systems such as biological medium. It should also be pointed out that such a sensor can be easily miniaturized, hence chemical information can be obtained in microscopic environments such as single cells.

Conflicts of interest

There are not conflicts to declare.

Acknowledgements

The authors would like to thank the financial support from the São Paulo State Research Foundation (FAPESP 2018/08782-1), and the National Council for Scientific and Technological Development (CNPq 141866/2016-0).

REFERENCES

(1) Manjakkal, L.; Szwagierczak, D.; Dahiya, R. Metal Oxides Based Electrochemical pH Sensors: Current Progress and Future Perspectives. *Prog. Mater. Sci.* **2020**, *109*, 100635. https://doi.org/10.1016/j.pmatsci.2019.100635

(2) Dong, Q.; Sun, X.; He, S. Iridium Oxide Enabled Sensors Applications. *Catalysts* **2021**, *11* (10), 1164. https://doi.org/10.3390/catal11101164

(3) Hitchman, M. L.; Ramanathan, S. Considerations of the pH Dependence of Hydrous Oxide Films Formed on Iridium by Voltammetric Cycling. *Electroanalysis* **1992**, *4* (3), 291–297. https://doi.org/10.1002/elan.1140040306

(4) Olthuis, W.; Robben, M. A. M.; Bergveld, P.; Bos, M.; van der Linden, W. E. pH Sensor Properties of Electrochemically Grown Iridium Oxide. *Sens. Actuators, B* **1990**, *2* (4), 247-256. https://doi.org/10.1016/0925-4005(90)80150-X

(5) Marzouk, S. A. M.; Ufer, S.; Buck, R. P.; Johnson, T. A.; Dunlap, L. A.; Cascio, W. E. Electrodeposited Iridium Oxide pH Electrode for Measurement of Extracellular Myocardial Acidosis during Acute Ischemia. *Anal Chem* **1998**, *70* (23), 5054–5061. https://doi.org/10.1021/ac980608e

(6) Papeschi, G.; Bordi, S.; Carla, M.; Criscione, L.; Ledda, F. An Iridium-Iridium Oxide Electrode for in Vivo Monitoring of Blood pH Changes. *J. Med. Eng. Technol*. **2009**, *5* (2), 86-87. https://doi.org/10.3109/03091908109042445

(7) Fog, A. Electronic Semiconducting Oxides as pH Sensors. *Sens. Actuators* **1984**, *5*, 13–20.

(8) Kinlen, P. J.; Heider, J. E.; Hubbard, D. E. A Solid-State pH Sensor Based on a Nafion-Coated Iridium Oxide Indicator Electrode and a Polymer-Based Silver Chloride Reference Electrode. *Sens. Actuators, B* **1994**, *22* (1), 13-25. https://doi.org/10.1016/0925-4005(94)01254-7

(9) O'Hare, D.; Parker, K. H.; Winlove, C. P. Metal-Metal Oxide pH Sensors for Physiological Application. *Med. Eng. Phys.* **2006**, *28* (10), 982–988. https://doi.org/10.1016/j.medengphy.2006.05.003

(10) Gláb, S.; Hulanicki, A.; Edwall, G.; Folke, F.; Ingman, I.; Koch, W. F. Metal-Metal Oxide and Metal Oxide Electrodes as pH Sensors. *Crit. Rev. Anal. Chem.* **1989**. https://doi.org/10.1080/10408348908048815

(11) Smiechowski, M. F.; Lvovich, V. F. Iridium Oxide Sensors for Acidity and Basicity Detection in Industrial Lubricants. *Sens. Actuators, B* **2003**, *96* (1–2), 261–267. https://doi.org/10.1016/S0925-4005(03)00542-2

(12) Kakooei, S.; Ismaila, M. C.; Ari-Wahjoedia, B. Electrodeposition of Iridium Oxide by Cyclic Voltammetry: Application of Response Surface Methodology. *MATEC Web Conf.* **2014**, *13*, 04024. https://doi.org/10.1051/matecconf/20141304024

(13) Nguyen, C. M.; Rao, S.; Seo, Y.-S.; Schadt, K.; Hao, Y.; Chiao, J.-C. Micro pH Sensors Based on Iridium Oxide Nanotubes. *IEEE Trans. Nanotechnol.* **2014**, *13* (5), 945–953. https://doi.org/10.1109/TNANO.2014.2332871

(14) Yang, J.; Kwak, T. J.; Zhang, X.; McClain, R.; Chang, W. J.; Gunasekaran, S. Digital pH Test Strips for In-Field pH Monitoring Using Iridium Oxide-Reduced Graphene Oxide Hybrid Thin Films. *ACS Sens.* **2016**, *1* (10), 1235–1243. https://doi.org/10.1021/ACSSENSORS.6B00385/ASSET/IMAGES/SE-2016-00385M_M009.GIF
(15) Santos, C. S.; Lima, A. S.; Battistel, D.; Daniele, S.; Bertotti, M. Fabrication and Use of Dual-Function Iridium Oxide Coated Gold SECM Tips. An application to pH Monitoring above a Copper Electrode Surface during Nitrate Reduction. *Electroanalysis* **2016**, *28* (7), 1441-1447. https://doi.org/10.1002/elan.201501082
(16) Rouhi, J. Development of Iridium Oxide Sensor for Surface pH Measurement of a Corroding Metal under Deposit. *Int. J. Electrochem. Sci.* **2017**, *12*, 9933–9943. https://doi.org/10.20964/2017.11.07
(17) Jović, M.; Hidalgo-Acosta, J. C.; Lesch, A.; Costa Bassetto, V.; Smirnov, E.; Cortés-Salazar, F.; Girault, H. H. Large-Scale Layer-by-Layer Inkjet Printing of Flexible Iridium-Oxide Based pH Sensors. *J. Electroanal. Chem.* **2018**, *819*, 384–390. https://doi.org/10.1016/j.jelechem.2017.11.032
(18) Zhu, Z.; Liu, X.; Ye, Z.; Zhang, J.; Cao, F.; Zhang, J. A Fabrication of Iridium Oxide Film pH Micro-Sensor on Pt Ultramicroelectrode and Its Application on in-Situ pH Distribution of 316L Stainless Steel Corrosion at Open Circuit Potential. *Sens. Actuators B Chem* **2018**, *255*, 1974–1982. https://doi.org/10.1016/j.snb.2017.08.219
(19) Elsen, H. A. Thermodynamic and Dynamic Investigations of Hydrated Iridium Oxide Potentiometric pH Micro-Sensors. PhD thesis, University of California Berkeley, 2007.
(20) Barroso, I. G.; Santos, C. S.; Bertotti, M.; Ferreira, C.; Terra, W. R. Molecular Mechanisms Associated with Acidification and Alkalization along the Larval Midgut of Musca Domestica. *Comp. Biochem. Physiol., Part A: Mol. Integr. Physiol.* **2019**, *237*, 110535. https://doi.org/10.1016/j.cbpa.2019.110535
(21) Yamanaka, K. Anodically Electrodeposited Iridium Oxide Films (AEIROF) from Alkaline Solutions for Electrochromic Display Devices. *Jpn. J. Appl. Phys.* **1989**, *28* (4R), 632–637. https://doi.org/10.1143/JJAP.28.632
(22) Williams, A. J. Assessing and Interpreting Arterial Blood Gases and Acid-Base Balance. *BMJ* **1998**, *317*, 1213–1216. https://doi.org/10.1136/bmj.317.7167.1213
(23) Viegas, C. A. A. Gasometria arterial. *J. Pneumol*. **2002**, *28* (Supl3), S233-S238.
(24) Steegstra, P.; Busch, M.; Panas, I.; Ahlberg, E. Revisiting the Redox Properties of Hydrous Iridium Oxide Films in the Context of Oxygen Evolution. *J. Phys. Chem. C* **2013**, *117* (40), 20975–20981. https://doi.org/10.1021/jp407030r
(25) Baur, J. E.; Spaine, T. W. Electrochemical Deposition of Iridium (IV) Oxide from Alkaline Solutions of Iridium(III) Oxide. *J. Electroanal. Chem.* **1998**, *443* (2), 208–216. https://doi.org/10.1016/S0022-0728(97)00532-9
(26) Burke, L. D.; Mulcahy, J. K.; Whelan, D. P. Preparation of an Oxidized Iridium Electrode and the Variation of Its Potential with pH. *J. Electroanal. Chem. Interfacial Electrochem.* **1984**, *163* (1–2), 117–128. https://doi.org/10.1016/S0022-0728(84)80045-5
(27) Elsen, H. A.; Monson, C. F.; Majda, M. Effects of Electrodeposition Conditions and Protocol on the Properties of Iridium Oxide pH Sensor Electrodes. *J. Electrochem. Soc.* **2009**, *156* (1), F1–F6. https://doi.org/Doi 10.1149/1.3001924
(28) Clausmeyer, J.; Masa, J.; Ventosa, E.; Öhl, D.; Schuhmann, W. Nanoelectrodes Reveal the Electrochemistry of Single Nickelhydroxide Nanoparticles. *Chem. Commun.* **2016**, *52* (11), 2408–2411. https://doi.org/10.1039/c5cc08796a
(29) Ying, Y.-L.; Ding, Z.; Zhan, D.; Long, Y.-T. Advanced Electroanalytical Chemistry at Nanoelectrodes. *Chem. Sci*. **2017**, *8*, 3338-3348. https://doi.org/10.1039/c7sc00433h
(30) Steegstra, P.; Ahlberg, E. In Situ pH Measurements with Hydrous Iridium Oxide in a Rotating Ring Disc Configuration. *J. Electroanal. Chem.* **2012**, *685*, 1–7. https://doi.org/10.1016/j.jelechem.2012.07.040

(31) El-Deen, E.; El-Giar, M.; Wipf, D. O. Microparticle-Based Iridium Oxide Ultramicroelectrodes for pH Sensing and Imaging. *J. Electroanal. Chem.* **2007**, *609* (2), 147-154. https://doi.org/10.1016/j.jelechem.2007.06.022
(32) Marzouk, S. A. M. Improved Electrodeposited Iridium Oxide pH Sensor Fabricated on Etched Titanium Substrates. *Anal. Chem.* **2003**, *75* (6), 1258–1266. https://doi.org/10.1021/ac0261404
(33) Debold, E. P.; Beck, S. E.; Warshaw, D. M. Effect of Low pH on Single Skeletal Muscle Myosin Mechanics and Kinetics. *American Journal of Physiology-Cell Physiology* **2008**, *295* (1), C173–C179. https://doi.org/10.1152/ajpcell.00172.2008

Brazilian Journal of Analytical Chemistry
2023, Volume 10, Issue 40, pp 99-111
doi: 10.30744/brjac.2179-3425.AR-112-2022

BrJAC

ARTICLE

The Importance of Sample Preparation for Omics Analysis: *Which Extraction Method is the Most Suited for my Biological Question?*

Mariana Silveira Marques[1], Patrick Cesar Ferreira[1], Thales Fernando Dias Pereira[1], Alessandra Sussulini*[1,2]

[1]*Laboratório de Bioanalítica e Ciências Ômicas Integradas (LaBIOmics), Instituto de Química, Universidade Estadual de Campinas (UNICAMP), Caixa Postal 6154, 13083-970, Campinas, SP, Brazil*

[2]*Instituto Nacional de Ciência e Tecnologia de Bioanalítica (INCTBio), Instituto de Química, Universidade Estadual de Campinas (UNICAMP), Caixa Postal 6154, 13083-970, Campinas, SP, Brazil*

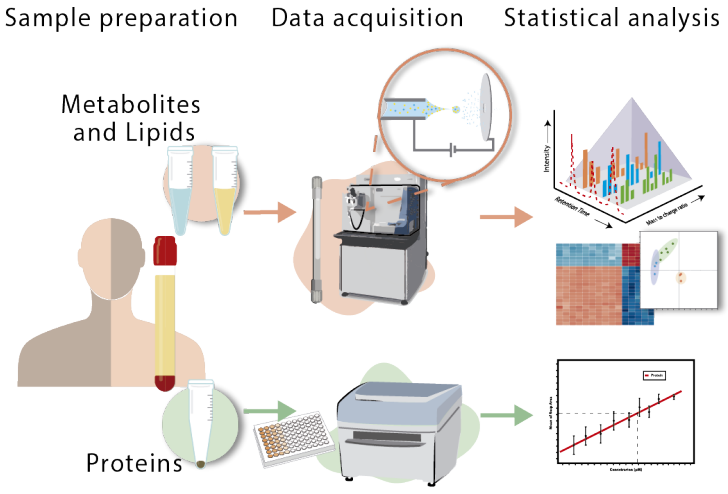

The instrumental aspect employed in metabolomic and lipidomic strategies has been well developed as of the past two decades, allowing large-scale analysis with high sensitivity and reproducibility, while statistical analysis and bioinformatics are emerging fields for omics data interpretation. Conversely, sample preparation is an important element that, if not optimized, has an impact on metabolome profiling and may result in erroneous and biased biological interpretation, remaining the bottleneck of the metabolomics workflow. Therefore, this work presents an evaluation of liquid-liquid extraction protocols for blood serum samples aiming at metabolomics and lipidomics analysis using liquid chromatography coupled to mass spectrometry (LC-MS). The Bligh & Dyer, Matyash and SIMPLEX protocols were investigated and the findings demonstrate that the composition of the solvents in each approach has a considerable impact on the putatively identified lipids, as well as the average concentration of extracted proteins. The study of the aqueous fraction, however, revealed no statistically significant variations in the identified metabolites. Hence, the optimization of the sample preparation step is crucial for biomolecules profiling and must be carefully considered in accordance with the objectives of the research and the chosen biological matrices.

Keywords: sample preparation, liquid-liquid extraction, metabolomics, lipidomics, mass spectrometry

Cite: Marques, M. S.; Ferreira, P. C.; Pereira, T. F. D.; Sussulini, A. The Importance of Sample Preparation for Omics Analysis: *Which Extraction Method is the Most Suited for my Biological Question? Braz. J. Anal. Chem.* 2023, *10* (40), pp 99-111. http://dx.doi.org/10.30744/brjac.2179-3425.AR-112-2022

Submitted 10 November 2022, Resubmitted 14 April 2023, 2nd time Resubmitted 27 April 2023, Accepted 02 May 2023, Available online 19 May 2023.

INTRODUCTION

Metabolomics and lipidomics are sophisticated bioanalytical approaches capable of identifying a wide range of metabolites (molecules with molecular mass below 1500 Da) present in biological systems.[1,2] These strategies have grown in prominence over the last two decades and are now employed to develop diagnosis and prognosis strategies, as well as to uncover novel biomarkers.[3,4] The core of this type of study is sample handling and preparation, data acquisition in analytical platforms, data pre-processing, statistical analysis and, lastly, biological interpretation.[5]

Particularly, sample preparation is a critical and frequently disregarded step that, when poorly planned and executed, may jeopardize all subsequent stages of the metabolomics workflow, resulting in biased and inaccurate biological interpretations.[6] Thus, it is fundamental to carefully optimize sample preparation to guarantee proper detection of metabolites and broad metabolome coverage.

When working with biological fluids, the matrix complexity, and the diversity of metabolites, as well as the concentration range of the compounds, are factors that must be considered while selecting sample preparation methods.[7] Particularly in the case of untargeted metabolomics analysis, these methods should not be class-specific, facilitating the extraction of metabolites with diverse physical-chemical characteristics. It is also critical that they are simple, quick, and reproducible, with as few steps as possible to reduce systematic errors during the operation. Finally, the extraction technique must remove or, at least, lessen interfering compounds such as proteins and other macromolecules that may influence the instrumental analysis.[7]

Despite several developments in metabolomics and lipidomics, no consensus on a standard metabolite/lipid extraction procedure has been reached. The most commonly used extraction procedure in liquid chromatography coupled to mass spectrometry (LC-MS) based metabolomics of blood serum samples is liquid-liquid extraction.[8] Bligh & Dyer, a classic procedure, employs a ternary solution of methanol, water, and chloroform.[9] The organic fraction (methanol and chloroform) is largely composed of low-polarity metabolites (lipids), whereas the aqueous fraction is composed of more polar metabolites and hydrophilic ions. Although this is a frequently reported technique, which provides variety in terms of metabolite range, the substitution of chloroform has been extensively addressed in the academic field due to the efforts to use cleaner and greener solvents.

Matyash *et al*. presented an alternative approach that uses methyltertbutyl ether (MTBE), a safer solvent with comparable efficiency to the Bligh & Dyer extraction method.[10] The Matyash method is already quite common for lipidomics research since the organic fraction is located on top, making aliquoting of this fraction straightforward. More recently, in 2016, Coman *et al.* established a methodology of simultaneous extraction of metabolites, proteins and lipids (SIMPLEX) and indicated its application in multi-omics research with similar sensitivity and repeatability to the Bligh & Dyer and Matyash methods.[11] The substitution of water with an aqueous solution of ammonium acetate lowers the miscibility of organic solvents in water and promotes phase separation. This phenomenon, known as salting out, allows for the presence of polar metabolites in the organic fraction.

It is evident that there is a demand for the development of robust strategies for preparing biological samples for metabolomic and lipidomic studies. The use of optimized and standardized protocols can certainly strengthen the maturity of these sciences and facilitate the comparison of results obtained among different research laboratories. In this context, the main objective of this study was to evaluate and compare the Bligh & Dyer, Matyash, and SIMPLEX methods for preparing human blood serum samples for subsequent LC-MS analyses.

Our study provides a comprehensive assessment of the advantages and limitations of these methods, both in terms of the polar metabolites and non-polar lipids obtained in each extraction. Additionally, we used two different chromatography columns based on reversed-phase liquid chromatography - RPLC - and hydrophilic interaction liquid chromatography - HILIC - that allow for a broad investigation of biomolecules present in this biological matrix. By comparing these three methods in detail, we aim to contribute to the existing knowledge of sample preparation methods for metabolomics and lipidomics and provide a more

comprehensive understanding of their effectiveness. The outcomes of this study can assist researchers in selecting the most suitable sample preparation method for their specific research needs.

MATERIALS AND METHODS

Sample collection

This study protocol was revised by the Ethics Committee of the University of Campinas (protocol number 775/2010). All subjects were previously informed of its purpose and written consent was obtained. Following venipuncture, blood samples were preserved in a dry tube without anticoagulants. After the clot formation in an ice bath for 1 h, the samples were centrifuged at 10000 *g* for 10 min at 4 ºC. The supernatant, namely the blood serum, was aliquoted in microtubes of 1500 µL, each containing 200 µL of the biological fluid and 0.05% (m/v) sodium azide. The samples were then stored in a biofreezer set at -80 ºC. The sample analysis was performed after thawing in an ice bath, in accordance with all biosafety standards for biological sample manipulation.

Sample preparation

For this study, three different extraction methods were used to fraction the blood serum into three phases – aqueous, organic and protein – for subsequent LC-MS analysis. For all extraction procedures, 40 µL of blood serum were used and quintuplicates were performed (Figure 1).

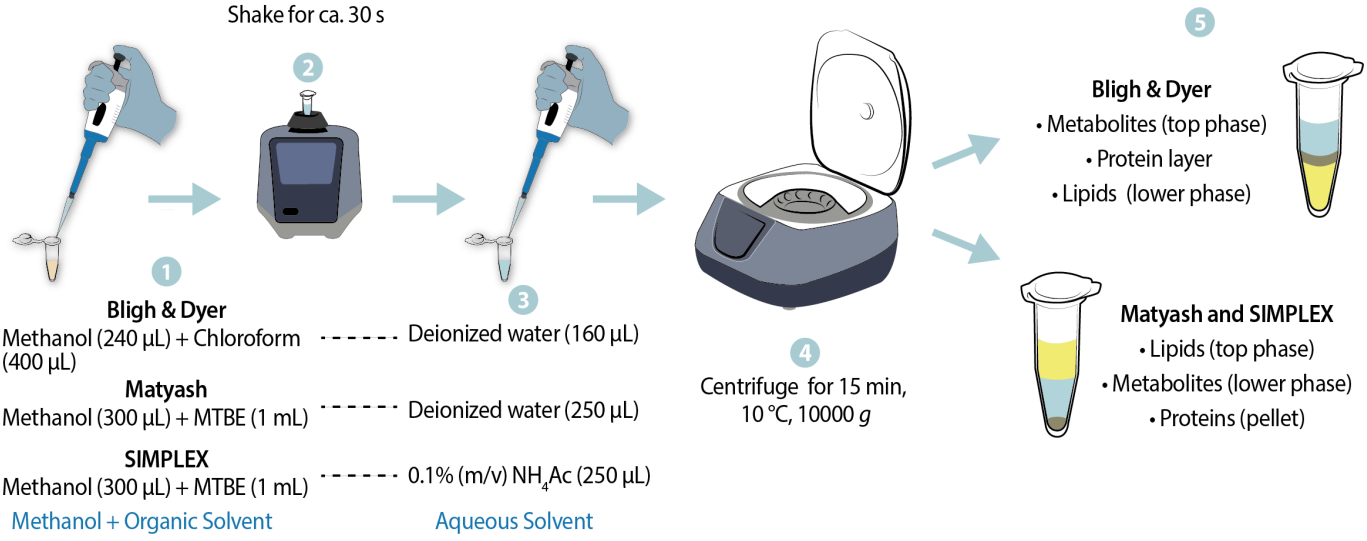

Figure 1. Schematic representation of the extraction replicated for the three tested methods. Text blocks (1) and (3) indicate the solvents and quantities used for each extraction method.

The aqueous and organic phases were dried in a vacuum concentrator (SpeedVac) in modes V-AQ and V-HV, respectively, and stored in a biofreezer until analysis. Before analyzing each phase, 400 µL of a solution composed by the mobile phase at the initial chromatography gradient condition was added and filtered using a polyvinylidene difluoride (PVDF) 0.22 µm filter.

To ensure total protein precipitation, 400 µL of acetone was added to the remaining pellet overnight and rinsed three times with isopropanol (IPA). For protein dilution with the purpose of total quantification, 400 µL of a resuspension solution composed of 0.2 mol L^{-1} triethylammonium bromide (TEAB), 0.02 mol L^{-1} Tris-HCl pH 8.8, 5.0 mmol L^{-1} ethylenediamine tetra acetic acid (EDTA) pH 8.8, and 6.0 mol L^{-1} urea was added to each tube.

Total protein quantification

The protein solutions were quantified using the bicinchoninic acid assay (BCA)[12] with an analytical curve of bovine serum albumin (BSA) standard ranging from 0 to 56 μg mL^{-1}. Aside from the 200 μL of BCA reagent, 2 μL of diluted protein and 25 μL of water were added to each well. The detection was performed using the EnSpire® Multimode Plate Reader with the wavelength set at 593 nm.

LC-MS analysis

The organic and aqueous phase were both analyzed in an Ultimate 3000 (Thermo) liquid chromatograph coupled to an Orbitrap QExactive (Thermo) mass spectrometer equipped with a heated electrospray ionization (HESI) source operating both in positive (ESI (+)) and negative (ESI (-)) modes using the full-scan mode followed by MS/MS analysis in the data dependent acquisition (DDA) method of the 5 most abundant peaks. The capillary voltage was established at 3.5 V, the drying gas flow at 10 L min^{-1} and the gas temperature at 300 ºC for the RPLC analysis and 350 ºC for the HILIC analysis. A full scan was performed with a resolution of 70000 and *m/z* range of 100 to 1500, 1 spectrum was acquired by minute for MS/MS with collision energy of 40 eV. The sampler temperature was set to 10 °C and the column oven temperature was set to 45 °C.

For the organic phase, a Sigma-Aldrich Titan™ C18 (particle size 1.9 μm, 2.1 x 100 mm) column was used; the mobile phase A was a solution of acetonitrile (ACN):H_2O (40:60 v/v) with 10 mmol L^{-1} ammonium acetate, while the mobile phase B was a solution of ACN:IPA (10:90 v/v) with 10 mmol L^{-1} ammonium acetate. The elution gradient started with 40% B from minutes 0-2, 50% B from minutes 3-6, 70% B from minutes 6.1-8, 100% B from minutes 9-11, and from minutes 12-14 the column was stabilized for the following run. For the aqueous phase, an ACQUITY BEH HILIC (particle size 1.7 μm, 2.1 x 150 mm) column was used, and the chromatography gradient was performed according to Sun *et al*.[13]

To verify instrumental and data stability, three quality control samples (QC) were injected at the start of the batch and one after each set of five samples and a blank sample.

Data pre-treatment

After LC-MS analysis, the raw data was converted to .mzML using Proteowizard MSConverter. MS-DIAL (version 4.9)[14] was used to align the spectra and identify features with the LipidBlast[15] database for lipidomics and MassBank of North America (MoNA)[16] for metabolomics. The alignment parameters were as follows: MS^1 tolerance of 0.02 Da, MS^2 tolerance of 0.06 Da, minimum peak height of 1000 and MS/MS abundance cutoff 30.

The statistical analysis was carried out utilizing the statistical analysis [one factor] functionality of on-line software MetaboAnalyst.[17] Considering that each dataset behaves uniquely, it is advised to visually observe which normalization, transformation and scaling methods are better suited to each individual dataset. In this situation, it was observed that the filtering of data prior to normalization compromised the quality of statistical analysis, hence all data was normalized before the filtering of features by the relative standard deviation (RSD < 30%).

RESULTS AND DISCUSSION

Protein quantification

An analytical curve with coefficient of determination (R^2) = 0.9577 and a linear equation of y = 0.0034x + 0.1238 was obtained by BCA. The average concentration, standard deviation, and coefficient of variation were calculated using that information and the values of absorbance from the diluted protein samples (Table I).

Table I. Average concentration (AC), standard deviation (SD) and coefficient of variation (CV) obtained from total protein concentration for the group of samples in each method

Extraction method	Replicate	Concentration µg mL^{-1}	AC µg mL^{-1}	SD µg mL^{-1}	CV %
Bligh & Dyer	1	93	81	14	17
	2	87			
	3	80			
	4	89			
	5	58			
Matyash	1	58	60	15	25
	2	84			
	3	64			
	4	52			
	5	44			
SIMPLEX	1	116	105	22	21
	2	95			
	3	84			
	4	93			
	5	138			

Analysis of variance (ANOVA) test was performed and returned a *p*-value < 0.05; therefore, the differentiation among the tested methods is of statistical relevance. As such, it is feasible to establish that SIMPLEX performed better for protein extraction, whereas Matyash had a lower average protein concentration. The extraction of proteins, especially for metabolomics and lipidomics analysis using LC-MS, must not interfere with the global metabolome analysis as stated by Want *et al.*[18] Since this work in 2006, we have not found any other original comparisons of the impact of protein extraction on metabolomics and lipidomics of serum samples; however, as previously mentioned,[7] the more proteins are depleted, the less interferences for these omic strategies.

Organic phase

Both ESI (+) and ESI (-) data were normalized using quantile normalization followed by filtering of features, logarithmic transformation and Pareto scaling. In order to categorize and identify the most important features for the differentiation of extraction methods, partial least squares discriminant analysis (PLS-DA) and one-way ANOVA were used to obtain variable importance projection (VIP) scores and *p*-values, respectively. Principal component analysis (PCA) was also a key statistical tool to define how the data of the three tested groups behave (Figure 2 and Figure 3).

According to the PCA scores plots, for both negative (Figure 2B) and positive (Figure 3B) ionization modes, the Bligh & Dyer sample group presents a strong distinction in general, while the Matyash and SIMPLEX sample groups are superposed.

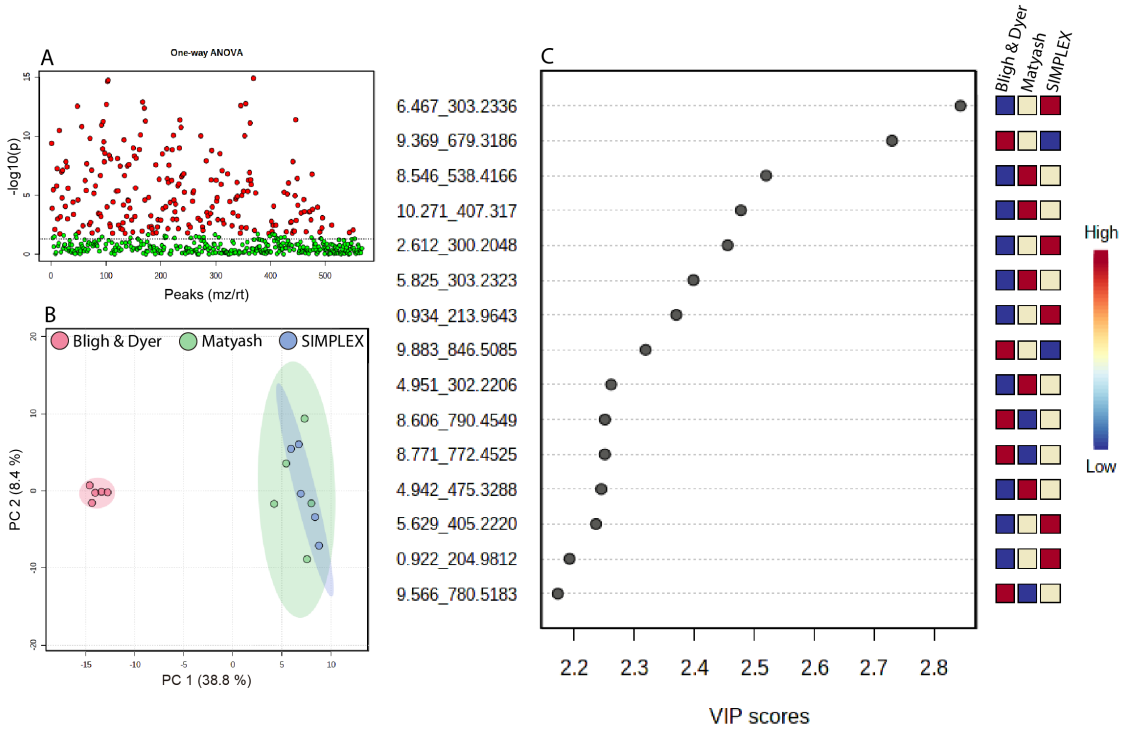

Figure 2. ESI (-) data. (A) Relevant ions identified by ANOVA with *p*-value < 0.05. (B) PCA scores plot. (C) Representation of the most important features according to the VIP scores obtained from PLS-DA; the colored boxes to the right indicate the concentration level of each metabolite in the sample groups.

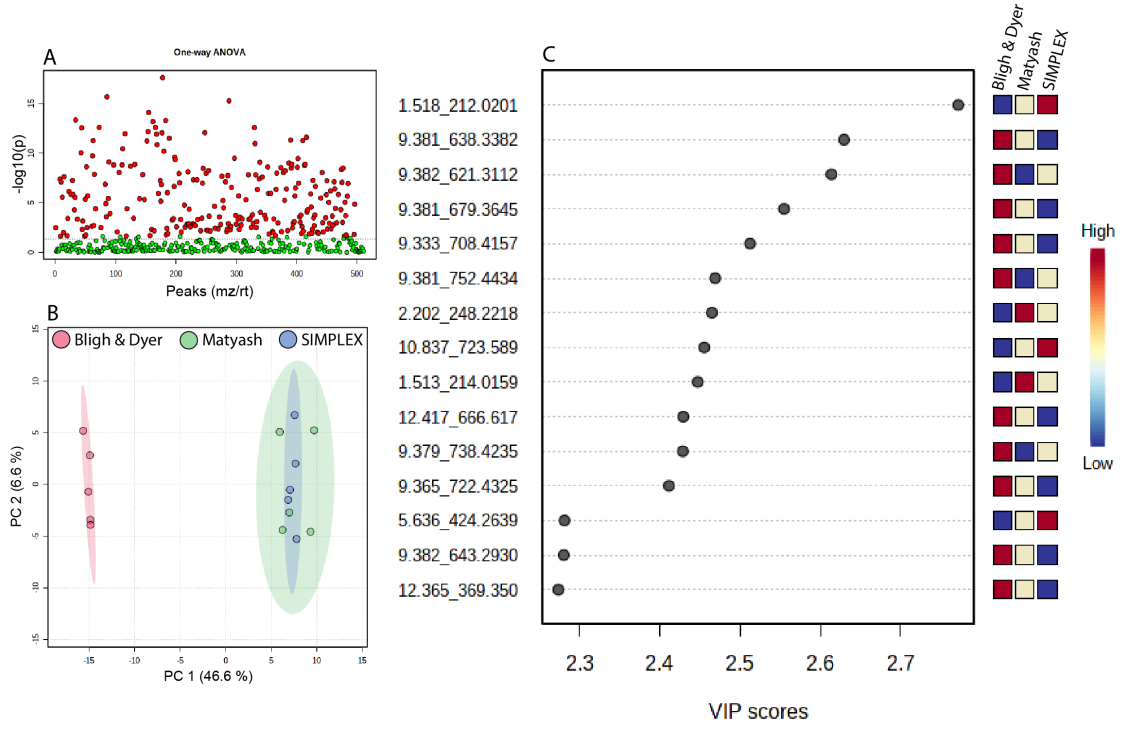

Figure 3. ESI (+) data. (A) Relevant ions identified by ANOVA with *p*-value < 0.05. (B) PCA scores plot. (C) Representation of the most important features according to the VIP scores obtained from PLS-DA; the colored boxes to the right indicate the concentration level of each metabolite in the sample groups.

The differential features were selected by *p*-value < 0.05 and VIP score > 1 and were later putatively identified according to the information provided by the LipidBlast database. Considering those exclusion criteria, 60 relevant features were presented for ESI (-) and 50 for ESI (+) as depicted in Figure 4 and annotated in Table S1 (Supplementary Material). This information allows evaluating which lipid classes present a greater influence in the methods differentiation.

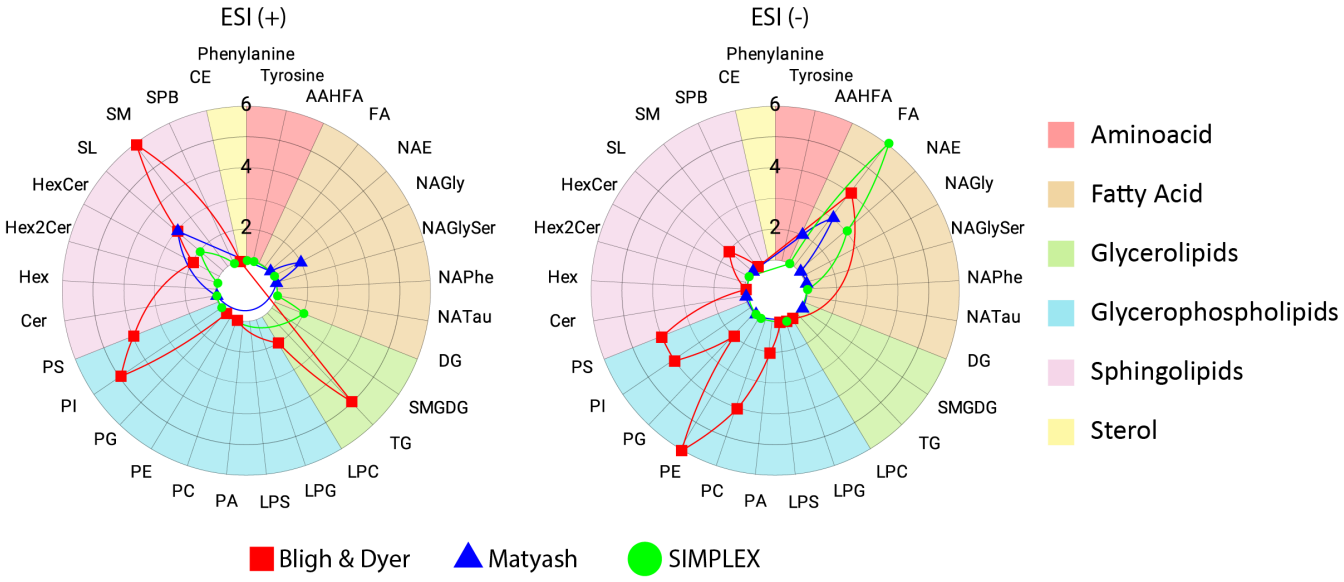

Figure 4. Differential lipids and their respective classes for both ESI (+) and ESI (-) modes. Their influence in the differentiation was considered by observing which of the extraction methods had a higher relative intensity of each feature according to PLS-DA. AAHFA: acyl alpha-hydroxyl fatty acid, CE: cholesterol esters, Cer: ceramides, DG: diacylglycerol, Hex: hexoside, Hex2Cer: dihexosylceramide, HexCer: hexosylceramide, LPC: lysophosphatidylcholine, LPG: lysophosphatidylglycerol, LPS: lysophosphatidylserine, NAE: N-acyl glycine, NAGly: N-acyl glycine, NAGlySer: N-acyl glycyl serine, NAPhe: N-acyl phenylalanine, NATau: N-acyl taurine, PA: phosphatidic acid, PC: phosphatidylcholine, PE: phosphatidylethanolamine, PG: phosphatidylglycerol, PI: phosphatidylinositol, PS: phosphatidylserine, SL: sulfonolipid, SMGDG: semino lipid, SPB: sphingosine, TG: triacylglycerol.

Figure 4 depicts the relative quantification of lipid subclasses for each sample extraction procedure and the symbols used to illustrate the various extraction processes are described. Lipid subclasses are specified outside of the outer circle, whereas lipid classes are marked with distinct colors within the circle. The distance of a node from the center of the graph indicates the number of times that the lipid subclass was designated as statistically significant. These graphs demonstrate that the selection of an extraction method can have an impact on the profile of lipids identified. The purpose of this analysis is to emphasize that the choice of extraction method can lead to different interpretations.

Bligh & Dyer and SIMPLEX methods, identified by red squares and green circles, respectively, present potential use for preliminary studies of lipidomic profiles. However, SIMPLEX is technically more convenient, since the lipid fraction is located on the upper phase. In addition, Bligh & Dyer presents a more biased and intense signalization for glycerophospholipids, especially in the negative ionization mode. On the other hand, SIMPLEX offers a more balanced representation of most lipid subclasses, while exhibiting an enhanced performance for some fatty acids.

In contrast, the Matyash method exhibited inferior performance when compared to SIMPLEX and Bligh & Dyer in terms of lipidomic coverage. Specifically, only seventeen lipids in total were both statistically significant and putatively identified using the Matyash method, while Bligh & Dyer identified 63 and SIMPLEX identified 26. In terms of lipid class, the Matyash method presented a slightly better indication of fatty acids, which is consistent with the results obtained using its derived method, SIMPLEX.

For studies in their preliminary stages or for multi-omic approaches, the possibility of a broad variety of lipids identified is very beneficial.[7] Ribeiro *et al*., with the use of Bligh & Dyer extraction method in blood serum samples, indicated glycerophospholipids such as phosphatidylinositols (PI) and phosphatidylethanolamines (PE), as relevant in the differentiation of bipolar disorder type I subjects in comparison to healthy controls.[19] Likewise, Delafiori *et al*., using human plasma extracted with a similar method to the one described by Matyash (instead of using MTBE, uses THF), researched about COVID-19 and, in this case, glycerophospholipids (GP), glycerolipids (GL), sphingolipids (SP) and sterols (ST) presented altered levels, being essential for the automated diagnosis and risk assessment of this disease.[20] This corroborates with our results in the sense that the choice of extraction procedure reflects on lipidome coverage, since both articles employ similar biological samples.

Aqueous phase

For the ESI (+) data, normalization was performed by sum, logarithmic transformation and centered by autoscaling, while for ESI (-) data, normalization was performed by quantile and centered by autoscaling (no transformation).

After further evaluation of PCA, PLS-DA and one-way ANOVA results, it was observed that there was no significant statistical distinction among the three extraction methods, so a two-way analysis was performed for the pairings Bligh & Dyer-Matyash, Bligh & Dyer-SIMPLEX and Matyash-SIMPLEX to assess the differential features. For both the positive and negative ESI modes, there were no identifiable features distinguishing these analyses. Therefore, the sample preparation method does not influence the metabolomics results when only more polar metabolites are evaluated.

Data interpretation

In addition to multivariate statistical analysis, Qual Browser (Thermo) was used to acquire the total ion count (TIC) and peak intensity for both positive and negative ESI modes on all chromatograms. This enabled the determination of which extraction method presents a better ionization and less interference during chromatographic runs and posterior MS/MS analysis (Table II).

From two-factor ANOVA with replication, the *p*-value for the columns and ionization modes (HILIC-ESI(+/-)-MS and C18-ESI(+/-)-MS), as well as the extraction methods (Bligh & Dyer, Matyash and SIMPLEX) were smaller than 0.05, showing the relevance of the variation of these parameters when it comes to TIC.

It was previously reported by Radulović *et al.* that the TIC of biological samples and plant extracts, when analyzed using multivariate techniques, can facilitate assessment of the metabolome profile of such complex mixtures for GC-MS analysis. Furthermore, it is mentioned in the same article that this method may also be suitable for LC-MS based analysis and, given the homogeneity of our dataset (CV < 15%), it is safe to assume that this hypothesis is supported by our results.[21]

The results display a higher TIC for samples analyzed with HILIC-ESI(-)-MS, similarly as pointed out by Boudah *et al*. in a study comparing the performance of three types of chromatographic stationary phases (HILIC and C18 included) for metabolome coverage. In this study, it is also concluded that different types of chromatographic systems provide a better knowledge and identification of the whole metabolome, since different stationary phases are complementary to one another in an analytical sense, which corroborates with the results presented in Table II and the performed statistical analysis.[22]

Table II. Total ion count values for each sample obtained from raw data using Qual Browser software. Average value was calculated for each group and all datasets are homogeneous (CV < 15%). The higher average ion count is highlighted in bold

Extraction method	Replicate	HILIC-ESI(+)	HILIC-ESI(-)	C18-ESI(+)	C18-ESI(-)
Bligh & Dyer	1	408850	441256	289517	335189
	2	398889	442713	287149	332972
	3	409640	446584	287467	336576
	4	398721	450633	288442	335850
	5	395587	448903	289596	334134
	Average	**402337**	**446018**	**288434**	**334944**
Matyash	1	402391	443852	282873	334988
	2	396079	443485	280509	333868
	3	393151	443354	278585	331019
	4	396866	446335	283394	333467
	5	398637	443563	282376	334612
	Average	397425	444118	281547	333591
SIMPLEX	1	393743	444356	282210	334703
	2	395887	446602	282764	337339
	3	392145	445813	283288	333953
	4	392584	439641	279187	332098
	5	402511	447100	278113	332417
	Average	395374	444702	281112	334102

CONCLUSIONS

Overall, the results presented in this study suggest that the Bligh & Dyer method is more robust than the other approaches for blood serum lipidomics, both for untargeted and targeted analysis, due to a greater range of detected metabolites and extraction of specific lipid classes. The aqueous phase was analyzed using HILIC coupled to mass spectrometry and, in this case, there were no significant differences between the three extraction methods tested.

The SIMPLEX extraction method has a better performance in protein extraction from the other phases (aqueous and organic), a fact that indicates less interference of those proteins in lipidomics and metabolomics LC-MS analysis. The lipidomics analysis strongly indicated that the Bligh & Dyer method was adequate both for targeted analysis of glycerophospholipids, as well as for untargeted (global) analysis, but it is important to highlight that the SIMPLEX method, even with a smaller lipid relative concentration when compared to Bligh & Dyer, is also suitable for untargeted analysis.

Regarding the metabolomic profiling, there is no evidence as of this work that any extraction method individually is more adequate or presents a better profiling of any metabolite classes, although Bligh & Dyer has demonstrated a higher value of TIC, both for lipidomics and metabolomics.

Considering the environmental impact of using chloroform in laboratory studies, it is advised that the Bligh & Dyer method be chosen with caution for small scale studies. For untargeted analysis, SIMPLEX has presented a similar result, being able to uncover the profile with high accuracy and efficiency while also using a more environmentally friendly solvent.

Conflicts of interest

The authors declare no conflicts of interest.

Acknowledgments

The authors would like to thank FAPESP (grant number 2021/14599-8), CAPES, CNPq (grant number 306662/2022-1), FAEPEX and INCTBio (FAPESP 2014/50867-3 and CNPq 465389/2014-7 grant numbers) for financial support and Diego Campaci de Andrade (Institutional Laboratory of Mass Spectrometry - LIEM, Institute of Chemistry, UNICAMP) for technical support.

REFERENCES

(1) Klassen, A.; Faccio, A. T.; Canuto, G. A. B.; da Cruz, P. L. R.; Ribeiro, H. C.; Tavares, M. F. M.; Sussulini, A. Metabolomics: Definitions and Significance in Systems Biology. In: Sussulini, A. (Ed.) *Metabolomics: From Fundamentals to Clinical Applications*; Sussulini, A., Ed.; Advances in Experimental Medicine and Biology; Springer International Publishing: Cham, 2017, pp 3–17. https://doi.org/10.1007/978-3-319-47656-8_1

(2) Wang, J.; Wang, C.; Han, X. Tutorial on Lipidomics. *Anal. Chim. Acta* **2019**, *1061*, 28–41. https://doi.org/10.1016/j.aca.2019.01.043

(3) Lima, N. M.; Fernandes, B. L. M.; Alves, G. F.; de Souza, J. C. Q.; Siqueira, M. M.; Patrícia do Nascimento, M.; Moreira, O. B. O.; Sussulini, A.; de Oliveira, M. A. L. Mass Spectrometry Applied to Diagnosis, Prognosis, and Therapeutic Targets Identification for the Novel Coronavirus SARS-CoV-2: A Review. *Anal. Chim. Acta* **2022**, *1195*, 339385. https://doi.org/10.1016/j.aca.2021.339385

(4) Beyoğlu, D.; Idle, J. R. Metabolomic and Lipidomic Biomarkers for Premalignant Liver Disease Diagnosis and Therapy. *Metabolites* **2020**, *10* (2), 50. https://doi.org/10.3390/metabo10020050

(5) Blaise, B. J.; Correia, G. D. S.; Haggart, G. A.; Surowiec, I.; Sands, C.; Lewis, M. R.; Pearce, J. T. M.; Trygg, J.; Nicholson, J. K.; Holmes, E.; Ebbels, T. M. D. Statistical Analysis in Metabolic Phenotyping. *Nat. Protoc.* **2021**, *16* (9), 4299–4326. https://doi.org/10.1038/s41596-021-00579-1

(6) Roca, M.; Alcoriza, M. I.; Garcia-Cañaveras, J. C.; Lahoz, A. Reviewing the Metabolome Coverage Provided by LC-MS: Focus on Sample Preparation and Chromatography-A Tutorial. *Anal. Chim. Acta* **2021**, *1147*, 38–55. https://doi.org/10.1016/j.aca.2020.12.025

(7) Salem, M. A.; de Souza, L. P.; Serag, A.; Fernie, A. R.; Farag, M. A.; Ezzat, S. M.; Alseekh, S. Metabolomics in the Context of Plant Natural Products Research: From Sample Preparation to Metabolite Analysis. *Metabolites* **2020**, *10* (1), 37. https://doi.org/10.3390/metabo10010037

(8) Burato, J. S. S.; Medina, D. A. V.; de Toffoli, A. L.; Maciel, E. V. S.; Lanças, F. M. Recent Advances and Trends in Miniaturized Sample Preparation Techniques. *J. Sep. Sci.* **2020**, *43* (1), 202–225. https://doi.org/10.1002/jssc.201900776

(9) Bligh, E. G.; Dyer, W. J. A Rapid Method of Total Lipid Extraction and Purification. *Can. J. Biochem. Physiol.* **1959**, *37* (8), 911-917. https://doi.org/10.1139/o59-099

(10) Matyash, V.; Liebisch, G.; Kurzchalia, T. V.; Shevchenko, A.; Schwudke, D. Lipid Extraction by Methyl-Tert-Butyl Ether for High-Throughput Lipidomics. *J. Lipid Res.* **2008**, *49* (5), 1137–1146. https://doi.org/10.1194/jlr.D700041-JLR200

(11) Coman, C.; Solari, F. A.; Hentschel, A.; Sickmann, A.; Zahedi, R. P.; Ahrends, R. Simultaneous Metabolite, Protein, Lipid Extraction (SIMPLEX): A Combinatorial Multimolecular Omics Approach for Systems Biology. *Mol. Cell. Proteomics* **2016**, *15* (4), 1435–1466. https://doi.org/10.1074/mcp.M115.053702

(12) Walker, J. M. The Bicinchoninic Acid (BCA) Assay for Protein Quantitation. In: Walker, J.M. (Ed.) *The Protein Protocols Handbook*; Walker, J. M., Ed.; Humana Press, Totowa, NJ, 2009, pp 11–15. https://doi.org/10.1007/978-1-59745-198-7_3

(13) New, L.-S.; Chan, E. C. Y. Evaluation of BEH C18, BEH HILIC, and HSS T3 (C18) Column Chemistries for the UPLC-MS-MS Analysis of Glutathione, Glutathione Disulfide, and Ophthalmic Acid in Mouse Liver and Human Plasma. *J. Chromatogr. Sci.* **2008**, *46* (3), 209–214. https://doi.org/10.1093/chromsci/46.3.209

(14) Tsugawa, H.; Ikeda, K.; Takahashi, M.; Satoh, A.; Mori, Y.; Uchino, H.; Okahashi, N.; Yamada, Y.; Tada, I.; Bonini, P.; Higashi, Y.; Okazaki, Y.; Zhou, Z.; Zhu, Z.-J.; Koelmel, J.; Cajka, T.; Fiehn, O.; Saito, K.; Arita, M.; Arita, M. A Lipidome Atlas in MS-DIAL 4. *Nat. Biotechnol.* **2020**, *38* (10), 1159–1163. https://doi.org/10.1038/s41587-020-0531-2

(15) Kind, T.; Liu, K.; Lee, D. Y.; Defelice, B.; Meissen, J. K.; Fiehn, O. LipidBlast in Silico Tandem Mass Spectrometry Database for Lipid Identification. *Nat. Methods* **2013**, *10* (8), 755–758. https://doi.org/10.1038/nmeth.2551

(16) Horai, H.; Arita, M.; Kanaya, S.; Nihei, Y.; Ikeda, T.; Suwa, K.; Ojima, Y.; Tanaka, K.; Tanaka, S.; Aoshima, K.; Oda, Y.; Kakazu, Y.; Kusano, M.; Tohge, T.; Matsuda, F.; Sawada, Y.; Hirai, M. Y.; Nakanishi, H.; Ikeda, K.; Akimoto, N.; Maoka, T.; Takahashi, H.; Ara, T.; Sakurai, N.; Suzuki, H.; Shibata, D.; Neumann, S.; Iida, T.; Tanaka, K.; Funatsu, K.; Matsuura, F.; Soga, T.; Taguchi, R.; Saito, K.; Nishioka, T. MassBank: A Public Repository for Sharing Mass Spectral Data for Life Sciences. *J. Mass Spectrom.* **2010**, *45* (7), 703–714. https://doi.org/10.1002/jms.1777

(17) Pang, Z.; Zhou, G.; Ewald, J.; Chang, L.; Hacariz, O.; Basu, N.; Xia, J. Using MetaboAnalyst 5.0 for LC–HRMS Spectra Processing, Multi-Omics Integration and Covariate Adjustment of Global Metabolomics Data. *Nat. Protoc.* **2022**, *17* (8), 1735–1761. https://doi.org/10.1038/s41596-022-00710-w

(18) Want, E. J.; O'Maille, G.; Smith, C. A.; Brandon, T. R.; Uritboonthai, W.; Qin, C.; Trauger, S. A.; Siuzdak, G. Solvent-Dependent Metabolite Distribution, Clustering, and Protein Extraction for Serum Profiling with Mass Spectrometry. *Anal. Chem.* **2006**, *78* (3), 743–752. https://doi.org/10.1021/ac051312t

(19) Ribeiro, H. C.; Klassen, A.; Pedrini, M.; Carvalho, M. S.; Rizzo, L. B.; Noto, M. N.; Zeni-Graiff, M.; Sethi, S.; Fonseca, F. A. H.; Tasic, L.; Hayashi, M. A. F.; Cordeiro, Q.; Brietzke, E.; Sussulini, A. A Preliminary Study of Bipolar Disorder Type I by Mass Spectrometry-Based Serum Lipidomics. *Psychiatry Res.* **2017**, *258*, 268–273. https://doi.org/10.1016/j.psychres.2017.08.039

(20) Delafiori, J.; Navarro, L. C.; Siciliano, R. F.; de Melo, G. C.; Busanello, E. N. B.; Nicolau, J. C.; Sales, G. M.; de Oliveira, A. N.; Val, F. F. A.; de Oliveira, D. N.; Eguti, A.; dos Santos, L. A.; Dalçóquio, T. F.; Bertolin, A. J.; Abreu-Netto, R. L.; Salsoso, R.; Baía-da-Silva, D.; Marcondes-Braga, F. G.; Sampaio, V. S.; Judice, C. C.; Costa, F. T. M.; Durán, N.; Perroud, M. W.; Sabino, E. C.; Lacerda, M. V. G.; Reis, L. O.; Fávaro, W. J.; Monteiro, W. M.; Rocha, A. R.; Catharino, R. R. Covid-19 Automated Diagnosis and Risk Assessment through Metabolomics and Machine Learning. *Anal. Chem.* **2021**, *93* (4), 2471–2479. https://doi.org/10.1021/acs.analchem.0c04497

(21) Radulović, N. S.; Blagojević, P. D.; Skropeta, D. Average Mass Scan of the Total Ion Chromatogram versus Percentage Chemical Composition in Multivariate Statistical Comparison of Complex Volatile Mixtures. *J. Braz. Chem. Soc.* **2010**, *21* (12), 2319-2326. https://doi.org/10.1590/S0103-50532010001200020

(22) Boudah, S.; Olivier, M.-F.; Aros-Calt, S.; Oliveira, L.; Fenaille, F.; Tabet, J.-C.; Junot, C. Annotation of the Human Serum Metabolome by Coupling Three Liquid Chromatography Methods to High-Resolution Mass Spectrometry. *J. Chromatogr. B* **2014**, *966*, 34–47. https://doi.org/10.1016/j.jchromb.2014.04.025

SUPPLEMENTARY MATERIAL

Table S1. List of significant features with higher relative concentration in each of the tested extraction methods. FA: Fatty Acyl; SP: Sphingolipid; GL: Glycerolipid; GP: Glycerophospholipid; ST: Sterol.

SIMPLEX		Bligh & Dyer		Matyash	
Experimental *m/z*	**Class**	**Experimental m/z**	**Class**	**Experimental *m/z***	**Class**
182.08142	Amino acid	**199.17055**	FA	**244.22766**	FA
279.23297	FA	**241.21709**	FA	**300.21723**	FA
290.26840	SP	**281.17392**	FA	**301.21762**	FA
300.20483	FA	**291.23282**	FA	**301.21768**	FA
301.21774	FA	**413.19739**	GP	**302.22061**	FA
302.24194	FA	**414.19919**	GP	**303.23239**	FA
303.23367	FA	**474.28601**	SP	**407.31738**	FA
305.24866	FA	**476.19254**	GP	**439.27182**	FA
341.26910	FA	**508.28290**	GP	**468.44153**	SP
342.27286	FA	**564.34442**	SP	**469.44604**	FA
357.30005	FA	**580.33856**	GP	**538.41669**	SP
409.31128	FA	**596.33405**	GP	**587.32898**	GP
424.26395	FA	**616.40839**	SP	**604.36938**	SP
440.27557	FA	**632.33344**	GP	**624.47095**	SP
455.26706	GP	**646.34875**	GP	**709.52600**	FA
461.34894	FA	**653.30157**	GP	**745.55518**	SP
540.42548	SP	**654.30438**	GP	**809.54926**	GL
572.39526	SP	**666.61755**	ST		
586.43750	FA	**671.46753**	GP		
601.39117	GL	**679.31866**	GP		
723.58954	GL	**692.44183**	SP		
731.47791	GP	**695.38074**	GP		
778.51581	SP	**695.41125**	GP		
822.46191	GP	**736.40955**	GP		

(continues on the next page)

Table S1. List of significant features with higher relative concentration in each of the tested extraction methods. FA: Fatty Acyl; SP: Sphingolipid; GL: Glycerolipid; GP: Glycerophospholipid; ST: Sterol. (continuation)

SIMPLEX		Bligh & Dyer		Matyash	
Experimental *m/z*	**Class**	**Experimental m/z**	**Class**	**Experimental *m/z***	**Class**
862.62531	SP	**738.42352**	GP		
880.59003	GP	**744.46588**	GP		
		745.48792	SP		
		749.48608	SP		
		752.44342	GP		
		762.42474	GP		
		763.42456	GP		
		772.45496	GP		
		780.51831	GP		
		786.46912	GP		
		790.45496	GP		
		805.44153	GP		
		818.48822	SP		
		828.49091	GP		
		842.57800	SP		
		845.46991	GP		
		845.50519	GP		
		846.50854	GP		
		870.75256	GL		
		872.77197	GL		
		879.74152	GL		
		903.72260	SP		

Brazilian Journal of Analytical Chemistry
2023, Volume 10, Issue 40, pp 112-122
doi: 10.30744/brjac.2179-3425.AR-121-2022

BrJAC

ARTICLE

Multi-Techniques for Iodine Determination and Dose Uniformity Assays in Iodized Mineral Dietary Supplements

Marcia Foster Mesko*, **Rodrigo Mendes Pereira**, **Natalia Jorge Bielemann**, **Filipe Soares Rondan**, **Diogo La Rosa Novo**

Centro de Ciências Químicas, Farmacêuticas e de Alimentos, Universidade Federal de Pelotas, 96010-610, Capão do Leão, RS, Brazil

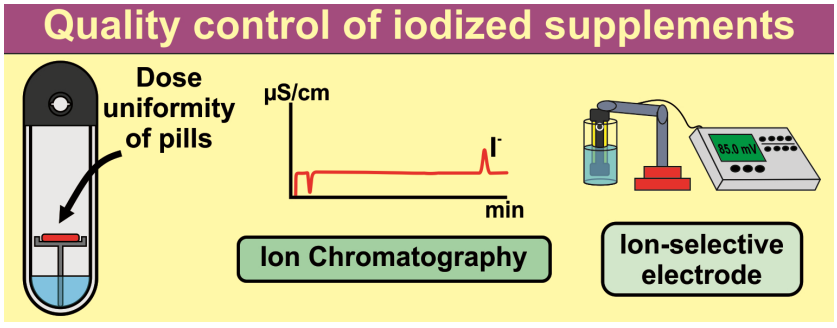

The determination of iodine in iodized mineral dietary supplements is considered a challenge, especially in view of the variety in the sample composition and the analyte concentration. Thus, in this work, microwave-induced combustion (MIC) was combined with ion chromatography (IC) and ion-selective electrode potentiometry (ISE) for iodine determination and dose uniformity assays in mineral dietary supplements. Sample masses up to 800 mg were efficiently digested and only a diluted alkaline solution (200 mmol L^{-1} NH_4OH) was necessary to absorb the analyte for further determination step. The final digest was fully compatible with multi-technique detection usually available in routine analysis laboratories. Recoveries ranging from 94% to 106% was achieved and relative standard deviations for repeatability and intermediate precision were always lower than 8%. Limits of quantification were 4 µg g^{-1} and 10 µg g^{-1}, respectively, by using IC and ISE. The analytical method was applied for iodine determination in mineral dietary supplements from four brands with different iodine dosages (from 100 to 1250 µg g^{-1}, according to the manufacturers) and for uniformity assay evaluation using individual tablets/capsules of mineral dietary supplements. Non-compliance regarding label information for some samples was reported, drawing the attention of supervisory institutions. The analytical strategies presented in the present study can be successfully used in routine analysis of the quality control of mineral dietary supplements.

Keywords: dietary supplements, iodine determination, microwave-induced combustion, ion chromatography, ion-selective electrode

INTRODUCTION

Iodine is an indispensable nutrient for human health and an essential substrate for thyroid hormone syntheses - triiodothyronine (T_3) and thyroxine (T_4).[1] These hormones are involved in several important

Cite: Mesko, M. F.; Pereira, R. M.; Bielemann, N. J.; Rondan, F. S.; Novo, D. L. R. Multi-Techniques for Iodine Determination and Dose Uniformity Assays in Iodized Mineral Dietary Supplements. *Braz. J. Anal. Chem.* 2023, *10* (40), pp 112-122. http://dx.doi.org/10.30744/brjac.2179-3425.AR-121-2022

Submitted 16 November 2022, Resubmitted 12 January 2023, Accepted 23 January 2023, Available online 10 February 2023.

biological roles as the development of the central nervous system, skeletal growth, and multiple organ regulation.[2] However, iodine can cause several disorders in unsuitable concentrations as hypothyroidism and hyperthyroidism.[2] Iodine absence is more common than excess in humans, in addition to hypothyroidism, causing damage to brain development, endemic cretinism, delayed physical development, spastic diplegia, and infant mortality.[3] To overcome the iodine absence growing public, institutions such as United Nations Children's Fund (UNICEF), International Council for Control of Iodine Deficiency Disorders (ICCIDD), and World Health Organization (WHO) have recommended iodine addition in cooking salt ranging from 15 to 45 μg g^{-1}.[4] Even so, other iodine sources have been recommended as mineral dietary supplements.

Mineral dietary supplements have also been commonly used to supply iodine deficiency in human organisms. These products are relatively inexpensive and easily purchased in several markets without prescription from healthcare professionals. The quality control of capsules/tablets used for supplementation has been established in official compendiums such as British and United States Pharmacopoeia.[5,6] However, the use of wet digestion with concentrated acids or fusion methods can lead iodine to losses by volatilization. Classical volumetric techniques have been recommended for iodine quantification, and even an important classical method, these techniques are extremely dependent on analyst visual acuity and are not very sensitive, making difficult quantification at low concentrations.[5-10] Nowadays, sensitive and selective instrumental analytical techniques have been included in some Pharmacopoeias given the disadvantages of classical methods. Atomic absorption spectrometry (AAS),[11] high-resolution continuum source molecular absorption spectrometry (HR-CS-MAS),[12] ion-selective electrode potentiometry (ISE),[13] neutron activation analysis (NAA),[14] inductively coupled plasma-mass spectrometry (ICP-MS),[15,16] and ion chromatography (IC)[17,18] have been proposed for iodine determination in several matrices including raw materials and pharmaceutical products.

Among sensitive and selective instrumental analytical techniques, IC and ISE stand out because they present several advantages for routine analyses as suitable sensitivity, selectivity, and lower acquisition and maintenance costs than others.[13,18] These techniques are interesting alternatives for iodine quantification in mineral dietary supplements in routine analysis. However, they require the sample in a solution form to be analyzed. Thus, a suitable sample preparation method is fundamental to the success of the analysis. The sample preparation step can be considered a challenge for further iodine determination in solid samples. Digestion methods using concentrated acids during the sample preparation, to convert the solid sample in an aqueous solution, are not suitable for further iodine determination considering the formation of volatile compounds – HI or I_2 – and non-quantitative recoveries are consequences of this carelessness.[13] Concentrated acids in the final solution are not adequate for using analytical techniques such as IC and ISE.

Thus, microwave-induced combustion (MIC) can be an excellent alternative as a sample preparation method for mineral dietary supplements for further iodine determination by IC and ISE.[19,20] Microwave-induced combustion is performed in closed vessels, minimizing losses by volatilization, presenting high sample throughput compared to other combustion methods in closed vessels, and allowing to choose a suitable absorbing solution for the analyte and the determination technique. This method still allows a reflux step to wash the vessel wall and ensure a quantitative recovery of the analyte. Microwave-induced combustion has been employed for the digestion of different matrices such as foods, biological materials, polymers, and drugs, aiming for the subsequent iodine determination by several analytical techniques.[21-27] Recently, MIC was reported as a suitable sample preparation method for subsequent halogen determination in Brazilian Pharmacopeia,[28] but still not optimized for subsequent determination of iodine in mineral dietary supplements.

Thus, considering the relevance of iodine determination in mineral dietary supplements, the main objective of this study was to propose two analytical alternatives for iodine determination in mineral dietary supplements using MIC as a sample preparation method and IC or ISE as a determination technique. Accuracy was evaluated by recovery tests in two levels using standard solutions and by comparison of the results. Precision was evaluated by repeatability and intermediate precision. Proposed analytical methods

were applied for iodine determination in mineral dietary supplements from four brands with different iodine dosages (from 100 to 1250 μg g^{-1}, according to the manufacturers). Moreover, proposed analytical methods were applied for iodine dose uniformity assays considering each tablet/capsule of mineral dietary supplements.

MATERIALS AND METHODS

Instrumentation

A microwave oven (Multiwave 3000™, Anton Paar, Austria), equipped with eight high-pressure quartz vessels with an internal volume of 80 mL (maximum pressure and temperature of 80 bar and 280 °C, respectively), was used for the sample preparation method by MIC. Quartz holders were used to supporting the samples and the filter paper inside the vessels. An ion chromatograph (861 Advanced Compact IC, Metrohm, Switzerland), equipped with a chemical suppression system, a conductivity detector, an anion-exchange column (250 mm x 4 mm i. d.) based on polyvinylalcohol with quaternary amine groups (Metrosep A Supp5, Metrohm), and a 20 μL sampling loop were used for iodine determination by IC. A potentiometer (HI 3221 pH/ORP/ISE meter, HANNA Instruments, USA) equipped with an electrode of iodide (HI 4111, HANNA Instruments, USA) was used for iodine determination by ISE. A hot plate with agitation (RH Basic, IKA, USA) was used for sample homogenization.

Reagents

All solutions were prepared using ultrapure water (18 MΩ cm) obtained from a purification system (Mega Up, MegaPurity, South Korea). Reagents were of analytical grade or higher purity. Water, $(NH_4)_2CO_3$ (concentrations of 25, 50, and 100 mmol L^{-1}), and NH_4OH (concentrations of 25, 50, and 200 mmol L^{-1}) were evaluated as absorbing solutions in the MIC method. The solution of 27% NH_4OH (Synth, Brazil) and $(NH_4)_2CO_3$ solid reagent (Merck) were used to prepare the evaluated absorbing solutions. Ammonium nitrate (6 mol L^{-1}) was used as a combustion igniter, which was prepared by the dissolution of the solid reagent (Merck) in water.

Small discs (12 mg, 15 mm in diameter) of filter paper (Qualy, J Prolab, Brazil) were used as a combustion aid, and polyethylene (PE) films were used to wrap the samples for digestion by MIC. Before combustion, the discs of filter paper and PE films were cleaned by immersion in 10% (v v^{-1}) HNO_3 (Vetec, Brazil) for 20 min in an ultrasonic bath (USC-1800 A, Unique, 40 kHz, 155 W, Brazil), subsequently rinsed with ethanol (Synth, Brazil) and ultrapure water, and dried in a class – 100 laminar bench (CSLH-12, Veco, Brazil). Oxygen (99.5%, Linde, Brazil) was used for the pressurization of the vessels in the MIC method. Quartz vessels and holders were cleaned with 6 mL of 14.4 mol L^{-1} HNO_3 (Vetec) using a microwave heating program set at 1000 W for 10 min (heating step) and 0 W for 20 min (cooling step). After that, the same procedure was repeated using 6 mL of water to decrease the blank values and eliminate the traces of acid.

The standard solutions used for the iodine determination by IC and by ISE were prepared by the dilution of a stock standard solution (100 μg mL^{-1}) obtained by the dissolution of KI salt (Merck) in water. Mixtures containing Na_2CO_3 and $NaHCO_3$ solutions were evaluated as eluent in IC analysis, prepared by dissolution of the respective salts (Merck) (recommended by the manufacturer). HPLC-grade acetonitrile (JT Baker, Phillipsburg, USA) was evaluated as an organic modifier in the mobile phase. Ionic strength adjusters (ISA, HI 4000-00, HANNA Instruments, USA) were used in iodine determination by ISE.

Samples of mineral dietary supplements

Samples of mineral dietary supplements, composed mostly of organic excipients, containing different dosages of iodine (according to the manufacturers – 100 μg g^{-1}, 260 μg g^{-1}, 870 μg g^{-1}, and 1250 μg g^{-1}, respectively) were labeled as A, B, C, and D. Around 100 g of each sample, regardless of their presentation, were homogenized and dried in an oven (400/2ND, DeLeo, Brazil) for about 4 h at 60 ± 5 ºC before the start of the experiments. Dietary supplements in tablet form were homogenized in porcelain mortar and pestle until obtaining a fine powder (less than 80 mesh or 180 μm) and subjected to a sieving step to guarantee

the homogeneity of all samples. Dietary supplements in capsule form had their contents removed. The samples (30 capsules/tablets of each one) were also digested individually, according to the United States Pharmacopoeia, to evaluate the test uniformity of dosage units.[6]

Proposed mineral dietary supplement sample preparation by microwave-induced combustion

Initial studies were performed using an arbitrarily selected sample of mineral dietary supplement labeled as sample "DS-A". Initially, sample masses (400 to 1000 mg) were weighed and wrapped in PE films (8 x 8 cm), and the PE films were sealed by heating, resulting in small wraps. The wrap of PE containing the sample was placed under a small disc of filter paper, moistened with an NH_4NO_3 solution (50 µL, 6 mol L^{-1}), on the base of a quartz holder. The quartz holders were transferred into quartz vessels, previously charged with 6 mL of absorbing solution (water, 25, 50, and 100 mmol L^{-1} $(NH_4)_2CO_3$ or 25, 50, 100, and 200 mmol L^{-1} NH_4OH). After closing, the vessels were positioned in the rotor, pressurized with 20 bar of oxygen, and the combustion process was carried out. The heating program used for combustion was as follows: *i)* 50 s at 1400 W (ignition step); *ii)* 1 min at 0 W (combustion step); *iii)* 5 min at 1400 W (reflux step) and *iv)* 20 min at 0 W (cooling step). After digestion, the pressure of each vessel was released, and the digests were transferred to volumetric flasks and diluted with ultrapure water up to 25 mL for subsequent iodine determination by IC and ISE.

The accuracy of the proposed method was evaluated by analyte recovery tests. A reference solution containing 2000 µg mL^{-1} of iodine was added at two concentration levels (50% and 75% of the concentration in the solution present in the sample before digestion by MIC). All iodine species (organic and other inorganic species) are converted to iodide after combustion step.[13,27] The precision was evaluated using the relative standard deviations (RSDs) of the measurements at repeatability (intra-day precision) and intermediate precision (inter-day precision) according to Eurachem guidelines.[29] The maximum variation in conditions between the runs was performed by the analysis of mineral dietary supplements on different days and by different analysts. All results were statistically evaluated using GraphPad InStat version 3.00 computer software package (GraphPad, San Diego, USA). The limit of detection (LOD) and limit of quantification (LOQ) were calculated from the mean of the blank values plus three times (for LOD) or ten times (for LOQ) the standard deviation obtained for ten replicates of blank, according to the instructions described in the protocols of the Instituto Nacional de Metrologia, Qualidade e Tecnologia (INMETRO).[30]

RESULTS AND DISCUSSION

Evaluation of the eluent for iodine determination by ion chromatography

During the sample preparation by MIC, the total iodine concentration present in the sample (bonded to organic compounds or in iodate form) is converted to iodide.[13] Thus, total iodine is determined as iodide by IC. Initially, a relatively high time of analysis is required for iodine determination (retention time of iodide is around 45 min because of its high interaction with anion-exchange column based on polyvinylalcohol with quaternary amine groups) using the eluent recommended by the manufacturer (a mixture containing 3.2 mmol L^{-1} Na_2CO_3 and 1.0 mmol L^{-1} $NaHCO_3$) and the peak resolution for iodide was considered insufficient ($R < 1.5$).[29] Thus, a mixture of 9 mmol L^{-1} Na_2CO_3 and 3 mmol L^{-1} $NaHCO_3$ was evaluated to reduce the IC analysis time and to improve the peak resolution. Although the retention time for iodide has been reduced to approximately 25 min, noise and drift in baseline, considered unsuitable for analysis, were observed, probably related to the high concentration of the eluent. Thus, a mixture containing 6 mmol L^{-1} Na_2CO_3 and 2 mmol L^{-1} $NaHCO_3$ was evaluated, and the retention time for iodide was approximately 30 min. Using this solution as an eluent, the noise was reduced, the drift was eliminated, and the peak resolution was considered suitable ($R \geq 1.5$).

Organic solvents can change the retention characteristics of the column packing toward the analyte and alter retention order, peak efficiency, and resolution to optimize the separation.[31,32] Thus, the eluent of 6 mmol L^{-1} Na_2CO_3 and 2 mmol L^{-1} $NaHCO_3$ in 10% (v v^{-1}) acetonitrile medium was studied. Acetonitrile

was used as an organic modifier in the mobile phase to facilitate the elution of analytes in a strong interaction with the ion exchange sites of the chromatographic column.[33] Retention time of iodide was decreased to approximately 24 min, which represents a reduction time of around 50% compared to the eluent recommended by the manufacturer. A larger amount of acetonitrile was not evaluated to avoid excessive system pressure increase. Thus, the mixture of 6 mmol L^{-1} Na_2CO_3 and 2 mmol L^{-1} $NaHCO_3$ in 10% (v v^{-1}) acetonitrile medium was selected as the eluent, and the final chromatograms with the established conditions are shown in Figure 1.

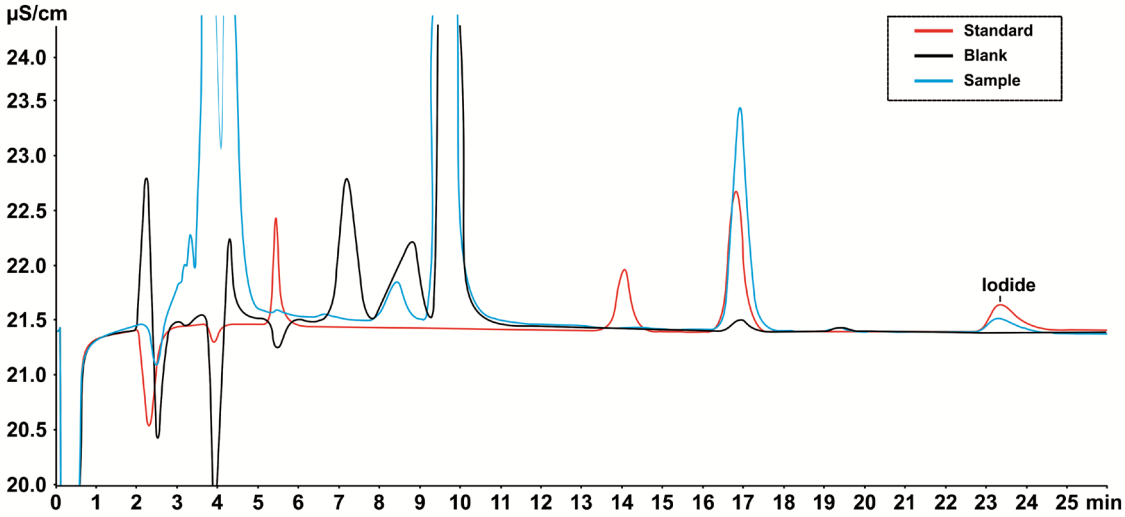

Figure 1. Chromatograms for iodine determination by IC for (—) standard containing 1 µg mL^{-1}, (—) blank after MIC method, and (—) mineral dietary supplements after MIC method.

Evaluation of microwave-induced combustion on the sample preparation of mineral dietary supplements for subsequent iodine determination

Sample mass and absorbing solution during sample preparation by MIC were carefully evaluated for further iodine determination in mineral dietary supplements by IC and ISE. Initially, sample mass was evaluated considering the pressure reached in the quartz vessel and the final aspects of the digests at the end of the combustion process. The aspects of the resulting solutions from the combustion of sample masses, ranging from 400 to 1000 mg, are shown in Figure 2. As can be observed, from 400 mg to 800 mg (Figures 2A to 2E), the aspect of the solutions was clear, suggesting a complete combustion reaction. Combustion of 900 mg (Figure 2F) and 1000 mg (Figure 2G) lead to yellowish color with particulate residues final solution. However, sample masses up to 800 mg (Figure 2E) resulted in a colorless solution without residue presence. Thus, 800 mg of sample mass was chosen for further evaluation. The maximum pressure of the system reached about 50% of the maximum pressure (80 bar) recommended as safe by the manufacturer.

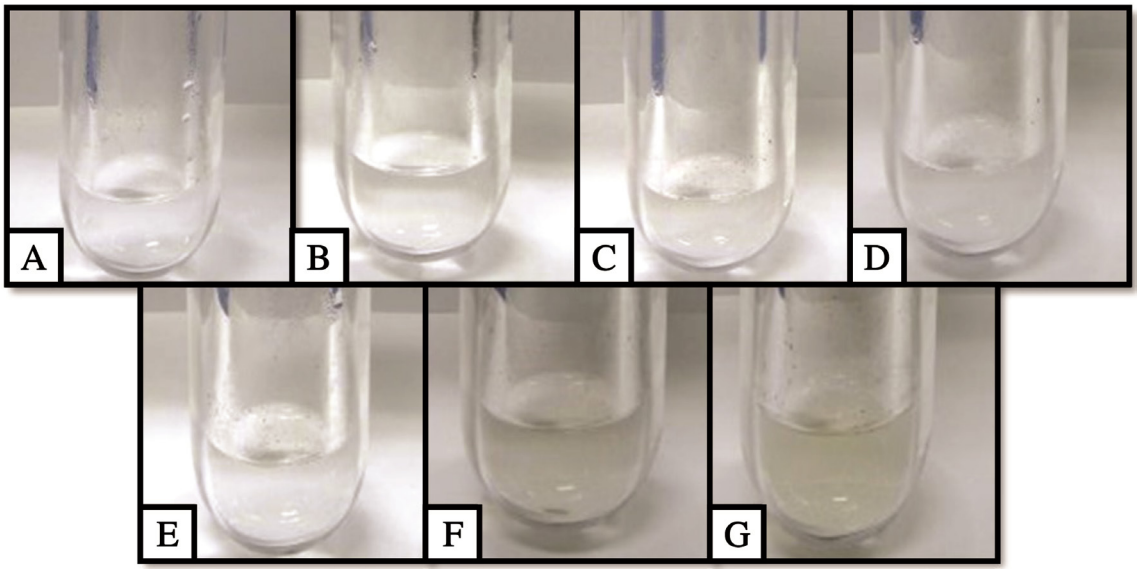

Figure 2. Aspects of solutions obtained after digestion by MIC using (A) 400 mg; (B) 500 mg; (C) 600 mg; (D) 700 mg; (E) 800 mg; (F) 900 mg and (G) 1000 mg of mineral dietary supplement.

The most suitable solution for iodine absorption after mineral dietary supplement combustion was also optimized. Water, $(NH_4)_2CO_3$ (25, 50, and 100 mmol L^{-1}), and NH_4OH (25, 50, and 100 mmol L^{-1}) were initially evaluated according to previous studies presented in the literature.[34,35] Iodine concentrations after combustion of 800 mg of mineral dietary supplement using different absorbing solutions are shown in Figure 3. Ion chromatography was used as a determination technique. As shown in Figure 3, iodine concentration using water as the absorbing solution was always lower than those using alkaline absorbing solutions, which is probably related to its instability in the final solution at low pH (around 3).[13] This pH value may be related to iodine volatile species.[36] Additionally, the precision of the measurements for the repeatability using water as the absorbing solution was considerably high (RSD ≤ 19%). No statistical differences were observed for iodine concentration using $(NH_4)_2CO_3$ or NH_4OH as absorbing solutions. Thus, 100 mmol L^{-1} NH_4OH was chosen as the absorbing solution considering better results for repeatability (RSD < 6%).

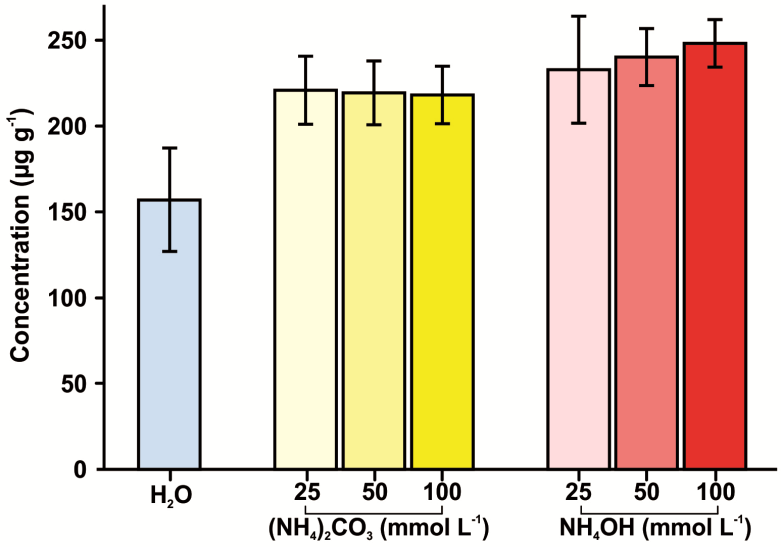

Figure 3. Iodine concentration obtained after digestion of 800 mg of the mineral dietary supplement "DS-A" by MIC using water or different concentrations of $(NH_4)_2CO_3$ or NH_4OH solutions, and iodine determination by IC (n = 5).

Feasibility of the proposed MIC method for iodine determination by ion chromatography and potentiometric ion-selective electrode

The feasibility of the proposed MIC method for further iodine determination by IC and ISE was evaluated by comparison of the results obtained for the sample DS-A. Iodine determination was performed indirectly through the determination of iodide by IC and ISE. The results for iodine in the sample DS-A after the MIC method obtained by IC (244 ± 20 μg g^{-1}) did not present a statistical difference from those obtained by ISE (250 ± 23 μg g^{-1}). Calibration curves of both determination techniques were performed ranging from 0.1 to 1.0 μg mL^{-1}. Limits of detection and quantification using IC (2 μg g^{-1} and 4 μg g^{-1}, respectively) were quite similar to those using ISE (4 μg g^{-1} and 10 μg g^{-1}, respectively). Thus, both determination techniques can be considered suitable for routine analysis. The high digestion efficiency of the MIC method provides a suitable solution for an accurate and precise total iodine determination using IC and ISE.

Analytical figure of merit

For accuracy evaluation of the proposed MIC method and further iodine determination by IC and ISE, spikes in two levels of concentration (corresponding to 50% and 75% of the iodine concentration in solution after sample preparation of DS-A sample by MIC using the selected conditions) were carried out. For the first level of the spike (50%), iodine recoveries ranged from 95 to 103%; however, for the second level of the spike (75%), recoveries for iodine were always less than 70%. Thus, considering the high iodine concentration in the mineral dietary supplement, 200 mmol L^{-1} NH_4OH was also evaluated as the absorbing solution, and thus, recoveries ranging from 94 to 106% were obtained. Additionally, the RSDs for repeatability were always lower than 2%, and 200 mmol L^{-1} NH_4OH was chosen as the absorbing solution of the method. Intermediate precision was also evaluated, and the RSD was always lower than 8%. Therefore, the proposed MIC sample preparation method using 800 mg of sample mass and 200 mmol L^{-1} NH_4OH as absorbing solution presents suitable accuracy and precision for iodine determination by IC and ISE in a wide range of concentrations, which is essential for the quality control of mineral dietary supplements.

Determination of iodine in mineral dietary supplements and dose uniformity assays

The proposed analytical strategies were applied for iodine determination in iodized mineral dietary supplements from four manufacturers containing different dosages of iodine. Results obtained from homogenized tablets/capsules of each sample are shown in Table I.

Table I. Iodine concentration in iodized mineral dietary supplements after sample preparation by MIC and determination by IC and ISE (mean ± standard deviation, n = 5)

Samples	Reported concentration (μg g^{-1})	Obtained concentration (μg g^{-1})	
		IC	ISE
DS-A	260	244 ± 20	250 ± 23
DS-B	100	773 ± 54	750 ± 30
DS-C	870	741 ± 20	761 ± 32
DS-D	1250	1209 ± 44	1218 ± 48

As shown in Table I, iodine concentration in DS-A, DS-C, and DS-D did not present significant differences (Student's *t*-test, confidence level of 90%, $p > 0.10$) when compared with the values informed on the labels. On the other hand, iodine concentration in DS-B presents a significant difference (Student's *t*-test, confidence level of 90%, $p > 0.10$) when compared with the value informed on the label. This is indicative

of the unreliability of the value reported on the label and the importance of quality control of these products using accurate and precise analytical tools. An additional study was performed based on the uniformity dosage units assessment of the United States Pharmacopeia.[6] This test has been also a demand by the pharmaceutical industry for routine analysis. Considering an official demand recommended by Pharmacopoeias, new analytical strategies are being proposed,[13,37-39] presenting results in agreement and disagreement with the limits established by Pharmacopoeias. United States Pharmacopeia establishes that each tablet must contain between 90% and 110% of the amount of active substance declared by the manufacturer. The individual tablets/capsules of mineral dietary supplements were digested using the proposed MIC method and iodine was determined by IC and ISE. The results are presented in Table II.

Table II. Iodine concentration in mineral dietary supplements obtained by IC and ISE after digestion of samples in commercial form (30 tablets or capsules) by MIC (mean ± standard deviation, n = 5)

Sample	Reported value (μg g^{-1})	Obtained concentration (μg g^{-1})	
		IC	ISE
DS-A	260	251 ± 32	231 ± 24
DS-B	100	596 ± 460	571 ± 510
DS-C	870	631 ± 132	651 ± 122
DS-D	1250	1206 ± 56	1226 ± 44

Similarly, iodine concentration in DS-A, DS-B, and DS-D did not present significant differences (Student's *t*-test, confidence level of 90%, $p > 0.10$) when compared with the values informed on the labels. On the other hand, the concentration of iodine in the DS-C sample units presented significant differences (Student's *t*-test, confidence level of 90%, $p > 0.10$) when compared with the values informed on the labels. In addition, iodine concentration in samples DS-B and DS-C presented a high RSD (77% and 21%, respectively), which demonstrates problems in the uniformity of doses and reinforces the importance of effective quality control of dietary supplements. The iodine concentration obtained for sample DS-B in the uniformity of dosage units test and homogenized sample (Table I) was higher than the values reported by the manufacturer, while the iodine concentration obtained for sample DS-C in the uniformity of dosage units test and homogenized sample (Table I) were lower than values reported by the manufacturer.

The determination of uniformity was performed using the recommendations of the United States Pharmacopoeia. This uniformity results in disagreement with United States Pharmacopoeia can be associated with several factors during medication production. Inspection of regulatory agencies that supervise the production of the supplements is quite flawed and there is a significant demand presented through analytical studies. While the consumption of a product with concentrations above those reported on the label may cause health problems due to continued exposure, such as hyperthyroidism, the products with concentrations below those described on labels may be ineffective for suitable supplementation. These results indicate a need for a suitable analytical method for the quality control of this kind of product and the proposed method is an excellent alternative for the quality control of mineral dietary supplements.

CONCLUSIONS

The proposed MIC sample preparation method was feasible and suitable for the digestion of mineral dietary supplements for the subsequent iodine determination by IC or ISE. The use of the proposed analytical strategies allows efficient sample digestion using a suitable absorbing solution according to green chemistry for the iodine, in addition to being compatible with IC and ISE. Moreover, the proposed analytical tools presented high throughput, suitable sensitivity and selectivity, and accuracy and precision. The high

digestion efficiency of the proposed MIC method also allowed accurate and precise iodine determination by IC and ISE, which are interesting alternatives for routine analysis because they present low acquisition and maintenance costs when compared to other determination techniques. The proposed method was also suitable for uniformity of dosage units test – a requested test from the pharmaceutical industry for routine analysis - and it can be also an excellent tool for this purpose. In this sense, the proposed analytical methods may be promising alternatives for mineral dietary supplement quality control, considering the importance of controlling the concentration of iodine in this type of sample.

Conflicts of interest

The authors declare no conflicts of interest.

Acknowledgements

This study was financed in part by the "Coordenação de Aperfeiçoamento de Pessoal de Nível Superior" (CAPES), Finance Code 001, Brazil. The authors are also grateful to "Conselho Nacional de Desenvolvimento Científico e Tecnológico" (CNPq), Code 409357/2016-2 and 312843/2020-8, Brazil, "Instituto Nacional de Ciência e Tecnologia em Bioanalítica" (INCTBio - 573672/2008-3), and "Fundação de Amparo à Pesquisa do Estado do Rio Grande do Sul" (FAPERGS), Code 16/2551-0000-516-8 and 19/2551-0001866-5, Brazil, for supporting this study.

REFERENCES

(1) Pearce, E. N. Iodine nutrition: recent research and unanswered questions. Eur. *J. Clin. Nutr*. **2018**, *72*, 1226-1228. https://doi.org/10.1038/s41430-018-0226-7

(2) Moran, C.; Schoenmakers, N.; Visser, W. E.; Schoenmakers, E.; Agostini, M.; Chatterjee, K. Genetic disorders of thyroid development, hormone biosynthesis and signalling. *Clin. Endocrinol.* **2022**, *97* (4), 502-514. https://doi.org/10.1111/cen.14817

(3) Uthayaseelan, K.; Kadari, M.; Subhan, M.; Parel, N. S.; Krishna, P. V.; Gupta, A.; Uthayaseelan, K. Congenital Anomalies in Infant with Congenital Hypothyroidism: A Review of Pathogenesis, Diagnostic Options, and Management Protocols. *Cureus* **2022**, *14* (5), 1-9. https://doi.org/10.7759/cureus.24669

(4) Agência Nacional de Vigilância Sanitária – Anvisa. Resultado do monitoramento do teor de iodo no sal para consumo humano. Relatório Ano: 2014. Available at: https://www.gov.br/anvisa/pt-br/centraisdeconteudo/publicacoes/alimentos/relatorio-pro-iodo-2014.pdf/view (accessed in November, 2022)

(5) British Pharmacopoeia 2013. The Stationery Office, London, 2013.

(6) The United States Pharmacopoeia (USP 30). The National Formulary (NF 25). United States Pharmacopoeia Convention Inc., Rockville, 2007.

(7) Wang, C. Y.; Tarter, J. G. Determination of halogens in organic compounds by ion chromatography after sodium fusion. *Anal. Chem.* **1983**, *55* (11), 1775-1778. https://doi.org/10.1021/ac00261a029

(8) Gorbunova, M. O.; Baulina, A. A.; Kulyaginova, M. S.; Apyari, V. V.; Furletov, A. A.; Garshev, A. V.; Dmitrienko, S. G. Determination of iodide based on dynamic gas extraction and colorimetric detection by paper modified with silver triangular nanoplates. *Microchem. J*. **2019**, *145*, 729-736. https://doi.org/10.1016/j.microc.2018.11.046

(9) Binnerts, W. T. Determination of iodine in milk. *Anal. Chim. Acta*. **1954**, *10*, 78-80. https://doi.org/10.1016/S0003-2670(00)89625-7

(10) AOAC Official Method 932.21, Iodine in Drugs. The Association of Official Analytical Chemists, Gaithersburg, MD, USA.

(11) Yebra, M. C.; Bollaín, M. H. A simple indirect automatic method to determine total iodine in milk products by flame atomic absorption spectrometry. *Talanta* **2010**, *82*, 828-833. https://doi.org/10.1016/j.talanta.2010.05.067

(12) Schneider, M.; Welz, B.; Huang, M.; Becker-Ross, H.; Okruss, M.; Carasek, E. Iodine determination by high-resolution continuum source molecular absorption spectrometry – A comparison between potential molecules. *Spectrochim. Acta B* **2019**, *153*, 42-49. https://doi.org/10.1016/j.sab.2019.01.006
(13) Mesko, M. F.; Teotonio, A. C.; Oliveira, D. T. T.; Novo, D. L. R.; Costa, V. C. A feasible method for indirect quantification of L-T_4 in drugs by iodine determination. *Talanta* **2017**, *166*, 223-227. https://doi.org/10.1016/j.talanta.2017.01.039
(14) Norman, B. R.; Iyengar, V. The application of preirradiation combustion and neutron activation analysis technique for the determination of iodine in food and environmental reference materials. *Biol. Trace Elem. Res*. **1998**, *63* (3), 221-229. https://doi.org/10.1007/BF02778940
(15) Reksten, A. M.; Ho, Q. T.; Nostbakken, O. J.; Markhus, M. W.; Kjellevold, M.; Bokevoll, A.; Hannisdal, R.; Froyland, L.; Madsen, L.; Dahl, L. Temporal variations in the nutrient content of Norwegian farmed Atlantic salmon (Salmo salar), 2005–2020. *Food Chem*. **2022**, *373*, 131445. https://doi.org/10.1016/j.foodchem.2021.131445
(16) Nascimento, M. S.; Druzian, G. T.; Pereira, L. S. F.; Mesko, M. F.; Picoloto, R. S.; Mello, P. A.; Flores, E. M. M. Microwave-assisted extraction for further Cl, Br, and I determination in medicinal plants by ICP-MS: a study of carbon interferences. *J. Anal. Atom. Spectrom*. **2022**, *37* (3), 535-543. https://doi.org/10.1039/D1JA00429H
(17) Moraes, D. P.; Pereira, J. S.; Diehl, L. O.; Mesko, M. F.; Dressler, V. L.; Paniz, J. N. G.; Knapp, G.; Flores, E. M. M. Evaluation of sample preparation methods for elastomer digestion for further halogens determination. *Anal. Bioanal. Chem*. **2010**, *397* (2), 563-570. https://doi.org/10.1007/s00216-010-3478-1
(18) Coelho Junior, G. S.; Rondan, F. S.; Hartwig, C. A.; Santos, R. F.; Mello, P. A.; Mesko, M. F. Determination of Halogens by Ion Chromatography in Edible Mushrooms after Microwave-Induced Combustion for Sample Preparation. *J. Anal. Methods Chem*. **2021**, *2021*, 1-9. https://doi.org/10.1155/2021/6005481
(19) Taflik, T.; Duarte, F. A.; Flores, É. L.; Antes, F. G.; Paniz, J. N.; Flores, É. M. M.; Dressler, V. L. Determination of bromine, fluorine and iodine in mineral supplements using pyrohydrolysis for sample preparation. *J. Braz. Chem. Soc*. **2012**, *23* (3), 488-495. https://doi.org/10.1590/S0103-50532012000300016
(20) Flores, E. M. M. Microwave-assisted sample preparation for trace element determination, Elsevier, Amsterdam, **2014**.
(21) Mello, J. E.; Novo, D. L. R.; Coelho Junior, G. S.; Scaglioni, P. T.; Mesko, M. F. A Green Analytical Method for the Multielemental Determination of Halogens and Sulfur in Pet Food. *Food Anal. Methods* **2020**, *13*, 131-139. https://doi.org/10.1007/s12161-019-01549-w
(22) Mesko, M. F.; Toralles, I. G.; Coelho Junior, G. S.; Rondan, F. S.; Costa, V. C.; Hartwig, C. A.; Scaglioni, P. T. Ion chromatography coupled to mass spectrometry as a powerful technique for halogens and sulfur determination in egg powder and its fractions. *Rapid Commun. Mass Spectrom*. **2020**, S3, *34*, e8775. https://doi.org/10.1002/rcm.8775
(23) Novo, D. L. R.; Henn, A. S.; Flores, E. M. M.; Mesko, M. F. Feasibility of microwave-induced combustion combined with inductively coupled plasma mass spectrometry for bromine and iodine determination in human nail. *Rapid Commun. Mass Spectrom*. **2020**, S3, *34*, e8675. https://doi.org/10.1002/rcm.8675
(24) Novo, D. L. R.; Mello, J. E.; Rondan, F. S.; Henn, A. S.; Mello, P. A.; Mesko, M. F. Bromine and iodine determination in human saliva: Challenges in the development of an accurate method. *Talanta* **2019**, *191*, 415-421. https://doi.org/10.1016/j.talanta.2018.08.081
(25) Mesko, M. F.; Balbinot, F. P.; Scaglioni, P. T.; Nascimento, M. S.; Picoloto, R. S.; Costa, V. C. Determination of halogens and sulfur in honey: a green analytical method using a single analysis. *Anal. Bioanal. Chem*. **2020**, *412*, 6475-6484. https://doi.org/10.1007/s00216-020-02636-2

(26) Toralles, I. G.; Coelho Jr, G. S.; Costa, V. C.; Cruz, S. M.; Flores, E. M. M.; Mesko, M. F. A fast and feasible method for Br and I determination in whole egg powder and its fractions by ICP-MS. *Food Chem*. **2017**, *221*, 877-883. https://doi.org/10.1016/j.foodchem.2016.11.081
(27) Muller, A. L. H.; Mello, P. A.; Mesko, M. F.; Duarte, F. A.; Dressler, V. L.; Muller, E. I.; Flores, E. M. M. Bromine and iodine determination in active pharmaceutical ingredients by ICP-MS. *J. Anal. Atom. Spectrom*. **2012**, *27*, 1889-1894. https://doi.org/10.1039/C2JA30212H
(28) Farmacopeia Brasileira. Agência Nacional de Vigilância Sanitária (ANVISA), Brasília, **2010**.
(29) Magnusson, B. The fitness for purpose of analytical methods: a laboratory guide to method validation and related topics. Eurachem, 2014.
(30) Instituto Nacional de Metrologia, Qualidade e Tecnologia (INMETRO). Orientação sobre Validação de Métodos Analíticos. Available at: http://www.inmetro.gov.br/Sidoq/Arquivos/CGCRE/DOQ/DOQ-CGCRE-8_05.pdf (accessed in November, 2022).
(31) Bliesner, D. M. *Validating chromatographic methods: A Practical Guide*. John Wiley & Sons, New Jersey, USA, 2006.
(32) Weiss, J. *Handbook of Ion Chromatography*. 4th ed.; John Wiley & Sons, New Jersey, USA, 2016.
(33) Rabin, S.; Stillian, J. Practical aspects on the use of organic solvents in ion chromatography. *J. Chromatogr. A* **1994**, *671* (1-2), 63-71. https://doi.org/10.1016/0021-9673(94)80222-X
(34) Rondan, F. S.; Hartwig, C. A.; Novo, D. L. R.; Moraes, D. P.; Cruz, S. M.; Mello, P. A.; Mesko, M. F. Ultra-trace determination of bromine and iodine in rice by ICP-MS after microwave-induced combustion. *J. Food Compos. Anal*. **2018**, *66*, 199-204. https://doi.org/10.1016/j.jfca.2017.12.023
(35) Mesko, M. F.; Costa, V. C.; Picoloto, R. S.; Bizzi, C. A.; Mello, P. A. Halogen determination in food and biological materials using plasma-based techniques: challenges and trends of sample preparation. *J. Anal. Atom. Spectrom*. **2016**, *6* (31), 1243-1261. https://doi.org/10.1039/C5JA00488H
(36) Cook, M. K.; Dial, A. R.; Hendy, I. L. Iodine stability as a function of pH and its implications for simultaneous multi-element ICP-MS analysis of marine carbonates for paleoenvironmental reconstructions. *Marine Chem*. **2022**, *245*, 104148. https://doi.org/10.1016/j.marchem.2022.104148
(37) Gregorini, A.; Ruiz, M. E.; Volonté, M. G. A derivative UV spectrophotometric method for the determination of levothyroxine sodium in tablets. *J. Anal. Chem*. **2013**, *68*, 510-515. https://doi.org/10.1134/S1061934813060075
(38) Nora, F. M. D.; Oliveira, A. S.; Lucas, B. N.; Ferreira, D. F.; Duarte, F. A.; Costa, A. B.; Silva, F. E. B.; Barin, J. S. A Novel Thermal Infrared Enthalpimetric Method for Fast, High-Throughput Determination of the Content Uniformity of Captopril Tablets. *J. Braz. Chem. Soc.* **2019**, *30* (5), 1082-1088. https://doi.org/10.21577/0103-5053.20180240
(39) Ahmad, N. R.; Omar, F. K.; Yusif, A. W. *Iraqi National Journal of Chemistry*. **2018**, *18* (2), 85-92.

Brazilian Journal of Analytical Chemistry
2023, Volume 10, Issue 40, pp 123-131
doi: 10.30744/brjac.2179-3425.AR-122-2022

BrJAC

ARTICLE

Bioaccessibility of Ca, Fe, Mg, and Mn in Brazilian Propolis

Lana P. B. Pereira, Robson Carlos M. Brito, Kelly das Graças Fernandes Dantas*

Faculdade de Química, Universidade Federal do Pará, Rua Augusto Corrêa, nº 1, Guamá, Belém, 66075-110, PA, Brazil

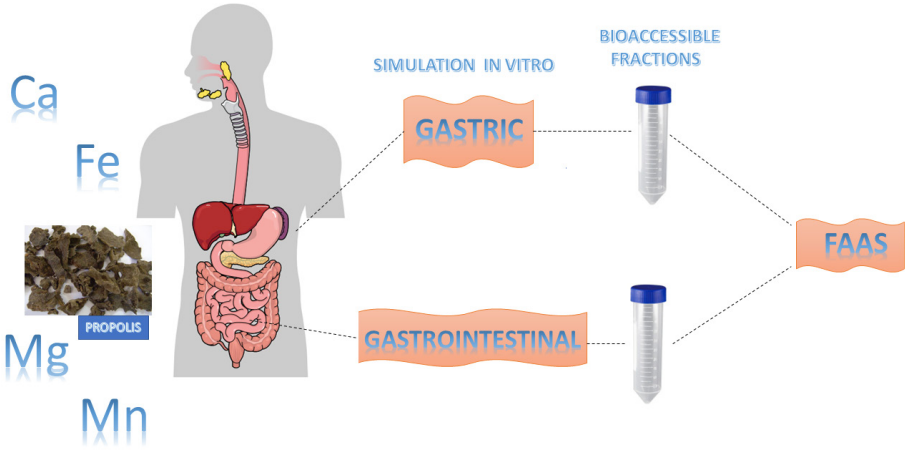

The objective of this study was to determine and evaluate the bioaccessibility of Ca, Fe, Mg, and Mn in *Apis mellifera* and Melipona propolis samples. Flame atomic absorption spectrometry was used for the determination of total Ca, Fe, Mg, and Mn in digested propolis, and of the bioaccessible fractions. The levels of Ca, Fe, Mg, and Mn obtained after digestion ranged from 423.43 – 4368.42, 3.85 – 814.92, 139.02 – 1170.68, and 14.28 – 67.29 mg kg^{-1}, respectively. The bioaccessible contents after simulated gastric digestion of Ca, Fe, Mg, and Mn ranged from 17.62 – 63.35, 0.12 – 1.64, 26.06 – 86.34, and 12.08 – 83.05%, respectively. In the simulation of the gastrointestinal tract, the concentrations ranged from 3.05 – 73.08% for Ca, 0.63 – 2.45% for Fe, 0.16 – 43.26% for Mg, and 1.47 – 8.45% for Mn. In general, the simulation showed higher bioaccessible contents after gastric, compared to gastrointestinal digestion.

Keywords: propolis, inorganic elements, gastric digestion, bioaccessibility

INTRODUCTION

An increasing demand for healthy lifestyle habits has been observed, as well as for the consumption of food with functional properties. In this context, apiculture products have aroused the interest of both consumers and researchers, thanks to their chemical composition. Propolis, in particular, stands out for its therapeutic properties (antimicrobial, anti-inflammatory, healing, and anesthetic) that can be used in the pharmaceutical industry and food.[1]

Propolis is a generic term used to describe the complex mixture of softwood, gummy and balsamic substances collected by bees from buds, flowers, and plant exudates, to which the bees add salivary

Cite: Pereira, L. P. B.; Brito, R. C. M.; Dantas, K. G. F. Bioaccessibility of Ca, Fe, Mg, and Mn in Brazilian Propolis. *Braz. J. Anal. Chem.* 2023, *10* (40), pp123-131. http://dx.doi.org/10.30744/brjac.2179-3425.AR-122-2022

Submitted 16 November 2022, Resubmitted 11 March 2023, 2nd time Resubmitted 07 June 2023, Accepted 12 June 2023, Available online 19 June 2023.

secretions, wax, and pollen to produce the final material. It is also called ‘‘Bee-glue” which is a natural resin substance present in bee hives, and used by Honey bees as a cementing material to close open spaces in their hives.[2,3]

The beneficial use of propolis has prompted an investigation of its chemical composition because propolis contains polyphenols (flavonoids, phenolic acids, and esters), phenolic aldehydes, and others.[2,3] The flavonoids are affected by the source and ecological botanical environment where the bee lives.[2] In propolis can be found micro and macro elements like Mn, Fe, Si, Mg, Se, Ca, Na and, vitamins B1, B2, B6, C, and E.[3,4]

Bioaccessibility has been defined as the fraction of a component that is released from the matrix in the gastrointestinal tract, making it available for intestinal absorption, it can be measured via several experimental models, such as in vitro digestion.[5] On the other hand, no study has reported on the bioaccessibility of inorganic elements in propolis samples. The bioaccessible fractions show more accurately the contribution after consumption of these inorganic elements present in food.

Many studies have been conducted on the bioaccessibility of inorganic elements in different samples. Khouzam, Pohl & Lobinski (2011),[5] determined the bioaccessibility of essential micronutrients in samples of cheese, bread, fruit and vegetables by DF-SP-ICP-MS. Peixoto, Mazon & Cadore (2013),[6] studied the bioaccessibility of metals in samples of chocolate milk by ICP-OES and GFAAS. Kulkarni, Acharya & Rajurkar (2007),[7] evaluated the bioaccessibility of some essential elements in samples of grass of wheat by INAA. Dutta, Maharia, Acharya & Reddy (2014),[8] estimated the bioaccessibility of trace elements in plants by INAA and ICP-MS. Bossu, Menezes & Nogueira (2020)[9] determined the bioaccessibility of zinc, calcium and phosphorus in milk by ICP OES. Jacobs et al. (2021)[10] studied the bioaccessibility of metals in samples of grape skins by MIP OES. Alves, Nunes & Dantas (2017),[11] evaluated the bioaccessibility of copper, iron and manganese in amazonian fruits by GF AAS. Mingroni et al. (2019)[12] estimated the bioaccessibility of calcium, cooper and mangnesium in fresh and dried fruits by FAAS.

The goal this study was evaluate the bioaccessibility of calcium, iron, magnesium, and manganese in *Apis mellifera* and Melipona propolis samples by flame atomic absorption spectrometry (FAAS).

MATERIALS AND METHODS

Instrumentation

A flame atomic absorption spectrometer (model Thermo iCE 3300, Cambridge, UK) was used for determination of Ca, Fe, Mg, and Mn in digested propolis samples, and bioaccessible fractions. The wavelength, and hollow-cathode lamp current used for Ca, Fe, Mg, and Mn were 422.7, 248.4, 285.2, and 279.5 nm, and 5, 6, 4, and 5 mA, respectively.

A cryogenic mill (Model 6770, SPEX CertPrep) was used to grind the samples.

A microwave oven (Start E, Milestone, Sorisole, Italy) was used to digest the samples.

A thermostatic bath (Model Q226M, Quimis, Brazil) was used in the gastric and gastrointestinal tract simulation tests.

A centrifuge (Quimis, São Paulo, Brazil) was used to separate the bioaccessible fractions.

Reagents, solutions, and samples

All reagents used were of analytical grade. All dilutions and solution preparations were performed with ultrapure water from a Synergy-UV water purification system (Millipore, Bedford, MA, USA).

The Ca, Fe, Mg, and Mn reference solutions were prepared at a concentration of 1000 mg L^{-1} (Sigma, USA).

Lanthanum oxide (Spectron, Brazil) and concentrated hydrochloric acid (Isofar, Brazil) were used to prepare the solution of lanthanum chloride (1%, m v^{-1}) for determination of Ca and Mg in samples, and bioaccessible fractions by FAAS.

Microwave digestion of the samples used 30% (w w^{-1}) H_2O_2 (Impex, Brazil), and 14.0 mol L^{-1} HNO_3 (Sigma, Brazil).

Sodium chloride and hydrochloric acid (both from Synth, São Paulo, Brazil), sodium bicarbonate (CRQ, Brazil), pepsin (Sigma-Aldrich, cat. no. P7012, São Paulo, Brazil), pancreatin (Sigma-Aldrich, cat. no. P1750, São Paulo, Brazil), and bile salts (Sigma-Aldrich, cat. no. 48305, St. Louis, MO, USA) were used in the simulated gastric, and gastrointestinal digestion.

The samples were obtained in different locations from Pará State, where seven samples of bee species *Apis mellifera* (PNT: Nova Timboteua city, PCo: Colares city, POu: Ourém city, PCP: Capitão Poço city, PBr: Bragança city, PVi: Vigia city and PSA: Santo Antônio do Tauá city), one sample of bee species Scaptotrigona sp (PBel 2: Belterra city) and one sample of bee Friseomellita varia (PBel 1: Belterra city) were collected.

Total determination

The samples were first ground in a cryogenic mill. An amount of each sample was weighed (0.25 g, n = 3) into digestion flasks. A volume of 4.0 mL of 14.0 mol L^{-1} HNO_3, and 4.0 mL of 30% w/w H_2O_2 were added, and the samples were digested in the microwave oven cavity. The heating program was performed in three steps: the first step (ramp) was performed for 10 min at 200 ºC (800 W); the second step (hold) was performed for 20 min at 200 ºC (800 W), and the third step cooled the system through forced ventilation for a period of 50 min. The solutions obtained after digestion were transferred to volumetric flasks and diluted to 14 mL with ultrapure water, and digested Ca, Fe, Mg, and Mn were determined by FAAS.

Bioaccessible fractions determination

The procedure was performed in two stages, one for determining gastric digestion and the other for gastrointestinal digestion. The procedure of gastric digestion and gastrointestinal digestion used in this study was adapted from Khouzam et al. (2011),[5] Kulkarni et al. (2007),[7] Stelmach, Pohl & Szymczycha-Madeja (2014),[13] and Moreda-Piñeiro et al. (2012),[14] as the simulation process conditions being most suitable for propolis samples.

Simulated gastric digestion

The in vitro gastric digestion process was performed in triplicate (n = 3), where 1.0 g of each sample was weighed into volumetric flask, and then 10 mL gastric fluid (10 g L^{-1} of pepsin in 0.15 mol L^{-1} NaCl with pH adjusted to 2.5 with 2 mol L^{-1} HCl) was added. The solution was stirred for 1 min. The volumetric flasks were placed in a thermostatic bath at 37 °C for 4 h with constant agitation. After agitation, the flasks were placed in an ice bath for 30 min, and then centrifuged for 20 min at 4000 rpm. The supernatants were filtered using 0.45 µ membrane cellulose filters (Millipore, Bedford, MA, USA), and then acidified with HNO_3 for a final acid concentration of 5.0% (v/v). The solutions obtained were analyzed by FAAS.

Simulated gastrointestinal digestion

The gastrointestinal digestion procedure was performed after the gastric digestion. The solutions obtained after the gastric digestion procedure were adjusted to pH 7.0 with 0.1 mol L^{-1} $NaHCO_3$, and then 10 mL of intestinal fluid (0.5 g pancreatin and 0.25 g of bile salts were made up to a final volume of 100 mL with 0.1 mol L^{-1} $NaHCO_3$) was added. The solutions were agitated for 1 min and placed in a thermostatic bath at 37 °C for 4 h with constant agitation. After agitation, the volumetric flasks were placed in an ice bath for 30 min and then centrifuged for 20 min at 4000 rpm. The supernatants were filtered using 0.45 µ membrane cellulose filters (Millipore, Bedford, MA, USA), and then acidified with HNO_3 for a final acid concentration of 5.0% (v/v). The solutions obtained were analyzed by FAAS.

Evaluation of the methods

The evaluation of measurements by FAAS was evaluated by the method of addition and recovery, where known concentrations of Ca (0.5, 1.0, 1.5, and 2.0 mg L^{-1}), Fe (3.0, 5.0, 7.0, and 9.0 mg L^{-1}), Mg (0.1, 0.3, 0.5, and 0.7 mg L^{-1}), and Mn (0.5, 1.5, 2.5, and 3.5 mg L^{-1}) were added to four digested samples and four

bioaccessible fractions for further analysis by FAAS. The certified reference material (GBW 07604, Poplar leaves) (*n* = 3) was also used for evaluating the measures by FAAS.

The efficiency of the sample preparation procedure was evaluated by adding known concentrations of Ca, Fe, Mg, and Mn to the samples for further microwave digestion and analysis by FAAS.

RESULTS AND DISCUSSION

Evaluation of sample preparation and analysis procedures

The accuracy of the measurements by FAAS was evaluated by the method of addition and recovery of analyte. The digested and bioaccessible fractions were spiked with four different concentration levels, and the resulting solutions analyzed by FAAS. Recoveries found for Ca, Fe, Mg, and Mn were 107.4 – 119.4%, 86.7 – 116.5%, 80.0 – 106.3%, and 89.6 – 114.3%, respectively. The results obtained of the certified reference material (GBW 07604 – Poplar leaves) indicated that the concentrations of elements determined by FAAS method are in agreement with the certified value (Ca: 110.0%; Fe: 87%; Mg: 95%; Mn: 90%) at a 95% confidence level (Student's *t* test; $t_{critical}$= 4.30).

The accuracy of the sample preparation was also evaluated. The recoveries obtained for Ca, Fe, Mg, and Mn were 94.9 – 103.9%, 88.6 – 108.8%, 83.3 – 97.4%, and 107.4 – 118.5%, respectively.

Table I shows the figures of merit obtained in the determination of Ca, Fe, Mg, and Mn in digested and bioaccessible fractions of propolis by FAAS.

Table I. Figures of merit

Parameters	Ca	Fe	Mg	Mn
LOD (mg kg^{-1})	3.82	0.29	0.09	0.56
LOQ (mg kg^{-1})	12.74	0.98	0.32	1.88
C_o	0.3137	0.0567	0.9976	0.9976
R^2	0.9998	0.9961	0.9976	0.9976

LOD: Detection limit; LOQ: Quantification limit; C_o: Characteristic concentration; R^2: Correlation coefficient.

Total and bioaccessible contents

Table II presents the total and bioaccessible fraction concentrations of Ca, Fe, Mg, and Mn in propolis by FAAS.

Table II. Total and bioaccessible contents (mg kg^{-1}) in propolis

	Ca (mg kg^{-1})			Fe (mg kg^{-1})			Mg (mg kg^{-1})			Mn (mg kg^{-1})		
Samples	**Total**	**DG[a]**	**DGI[b]**	**Total**	**DG[a]**	**DGI[b]**	**Total**	**DG[a]**	**DGI[b]**	**Total**	**DG[a]**	**DGI[b]**
PBel 1	423.43 ± 26.23	268.25 ± 7.86 (63.35)	309.43 ± 13.17 (73.08)	167.65 ± 17.91	2.76 ± 0.004 (1.64)	1.68 ± 0.01 (1)	139.02 ± 4.15	120.03 ± 1.01 (86.34)	43.25 ± 1.41 (31.11)	39.4 ± 0.76	8.84 ± 0.06 (22.44)	1.19 ± 0.13 (3.02)
PBel 2	4368.42 ± 139.78	2286.65 ± 4.28 (52.34)	1407.06 ± 50.56 (32.21)	366.66 ± 3.48	1.41 ± 0.01 (0.38)	9.00 ± 0.44 (2.45)	823.27 ± 7.02	537.66 ± 6.94 (65.31)	356.19 ± 1.68 (43.26)	52.41 ± 1.40	13.91 ± 0.28 (26.54)	1.61 ± 0.06 (3.07)
PNT	2081.87 ± 18.71	650.37 ± 17.77 (31.24)	239.25 ± 50.56 (11.49)	280.91 ± 10.31	< LOD	2.15 ± 0.20 (0.76)	1040.06 ± 30.69	475.44 ± 5.66 (45.71)	269.68 ± 1.68 (25.93)	48.26 ± 1.96	40.08 ± 1.17 (83.05)	4.08 ± 0.26 (8.45)
PBr	2262.89 ± 100.28	398.87 ± 36.15 (17.62)	69.06 ± 10.16 (3.05)	714.92 ± 83.51	0.89 ± 0.01 (0.12)	4.54 ± 0.08 (0.63)	539.49 ± 49.20	253.87 ± 6.18 (47.06)	73.68 ± 2.74 (13.66)	63.92 ± 3.80	7.77 ± 0.24 (12.15)	1.06 ± 0.05 (1.66)
PCo	1902.11 ± 75.33	489.72 ± 1.02 (25.75)	311.56 ± 21.30 (16.38)	247.66 ± 20.15	1.84 ± 0.12 (0.74)	4.15 ± 0.19 (1.67)	428.75 ± 24.05	116.5 ± 8.48 (27.17)	33.75 ± 1.06 (7.87)	67.29 ± 1.40	15.37 ± 0.10 (22.84)	1.69 ± 0.08 (2.51)
POu	2711.75 ± 43.13	1136.34 ± 43.88 (41.90)	1638.12 ± 20.50 (60.4)	814.57 ± 27.87	5.83 ± 0.46 (0.71)	6.20 ± 0.15 (0.76)	616.49 ± 7.42	452.22 ± 3.40 (73.35)	136.25 ± 0.53 (22.10)	50.58 ± 0.49	12.32 ± 0.11 (24.36)	0.81 ± 0.06 (1.60)
PSA	1747.48 ± 43.16	759.63 ± 29.69 (43.47)	64.06 ± 8.22 (3.66)	< LOD	< LOD	< LOD	368.41 ± 9.80	253.31 ± 12.64 (68.76)	30.87 ± 0.11 (8.37)	28.57 ± 0.25	3.45 ± 0.09 (12.08)	0.42 ± 0.02 (1.47)
PCP	2973.60 ± 27.71	611.84 ± 20.90 (20.57)	328.54 ± 38.90 (11.04)	47.61 ± 0.57	< LOD	< LOD	1170.68 ± 57.81	305.06 ± 0.97 (26.06)	8.00 ± 1.50 (0.68)	14.28 ± 0.12	7.40 ± 0.11 (51.82)	0.37 ± 0.02 (2.59)
PVi	1358.56 ± 60.18	692.97 ± 8.35 (51)	197.62 ± 22.98 (14.54)	3.85 ± 0.57	< LOD	< LOD	392.84 ± 0.99	188.34 ± 6.05 (47.94)	0.63 ± 0.01 (0.16)	50.37 ± 0.35	7.91 ± 0.06 (15.70)	1.28 ± 0.05 (2.54)

[a]Gastric digestion; [b]Gastrointestinal digestion; The values between parentheses are the percentages of the values of bioaccessibility.

Determination of the total element concentrations in propolis

Nutrients such as vitamins and minerals even in small amounts are essential for the body. Ca, Fe, Mg, and Mn are important in the body development, and they are present in the teeth, bones, and some play a fundament role as a structural part in many enzymes.[15]

The total content of Ca, Fe, Mg, and Mn in propolis samples is presented in Table II. The results obtained showed high concentrations of essential elements in the samples.

The levels of Ca obtained in digested propolis samples ranged from 423.4 – 4368.4 mg kg^{-1}. The samples from Belterra city presented different values of Ca. Lower levels of Ca were found in PBel 1 compared to those in PBel 2. The Ca concentrations found in propolis by Finger et al. (2014)[16] were lower (1660 mg kg^{-1}) compared to the values obtained for most of the samples studied.

The levels of Fe (648.2 – 852.4 mg kg^{-1}) found in propolis from Argentina by Cantarelli et al. (2011),[17] and level of Fe (49.17 mg kg^{-1}) found in propolis by Matuszewska et al (2021)[18] were similar to the values obtained in this study.

Mg content in propolis ranged from 139.0 to 1170.7 mg kg^{-1}. PCP presented the highest levels of Mg in all samples. The lowest concentrations were found in PBel 1. This study obtained concentrations of Mg similar to the values (328.0 – 971 mg kg^{-1}) obtained by Bonvehí & Bermejo (2013)[19] in propolis from Southern Spain.

The Mn concentrations found in samples ranged from 14.3 to 67.3 mg kg^{-1}. PCo presented the highest concentrations of Mn among the studied samples while PCP presented the lowest. Matuszewska et al. (2021)[18] found the concentration of Mn (7.2 mg kg^{-1}) in propolis samples were lower compared to the values obtained for most of the samples studied.

Bioaccessibility of elements in propolis samples

The total element concentration is very important but it is not sufficient to evaluate the risk or benefit related to the intake of elements in food. Bioaccessibility tests can be estimated the fractions released into the gastrointestinal tract during digestion[20]. The results of bioaccessibility in propolis are shown in Table I.

The Ca contents obtained in the bioaccessible fractions of propolis ranged between 17.6 and 63.4% for simulated gastric digestion, and between 3.1 and 73.1% for simulation gastrointestinal digestion. respectively. The highest level of bioaccessible Ca was found in PBel 1 (propolis of stingless bees). Machado. Silva, Fanchiotti & Costa (2001)[21] reported that 30% of ingested Ca is absorbed by the body. Most samples presented bioaccessible levels during gastrointestinal simulation below that absorbed by the body.

The levels of Fe found in the gastric and gastrointestinal fractions ranged from 0.1 to 1.6% and 0.63 to 2.5%, respectively. PBel 1 presented the highest levels of bioaccessible Fe in simulated gastric digestion (1.6%) while PBel 2 showed the highest contents of bioaccessible Fe in simulated gastrointestinal digestion (2.5%). Higher levels of bioaccessible iron were obtained in the gastrointestinal digestion of most samples studied. All samples showed bioaccessible levels below the iron absorption level. According to Germano & Canniatti-Brazaca (2002)[22] the iron absorption is 10%.

The levels bioaccessible of Mg found in the gastric and gastrointestinal simulations ranged from 26.1 to 86.3% and from 0.2 to 43.3%, respectively. PBel 1 showed the highest levels of bioaccessible Mg in the gastric simulation (86.3%), and PBel 2 presented the higher levels of bioaccessible Mg in the gastrointestinal simulation. All samples presented bioaccessible levels below the value of absorption of Mg in gastrointestinal simulation. which according to Monteiro & Vannucchi (2010)[23] is 45% of the total ingested.

The bioaccessible Mn contents found in the simulated gastric, and gastrointestinal digestions ranged from 12.1 to 83.1%, and from 1.5 to 8.5%, respectively. The highest concentrations of Mn available for absorption were found in PNT. According Fairweather-Tait (1992),[24] the daily absorption of Mn by the body is 3 – 4% of the total ingested. In the gastrointestinal simulation, most of the samples presented levels similar to the percentage of Mn absorbed per day.

The results shown that in most of the samples, the bioaccessible fraction was higher in the gastric phase than in the gastrointestinal phase (Figure 1).

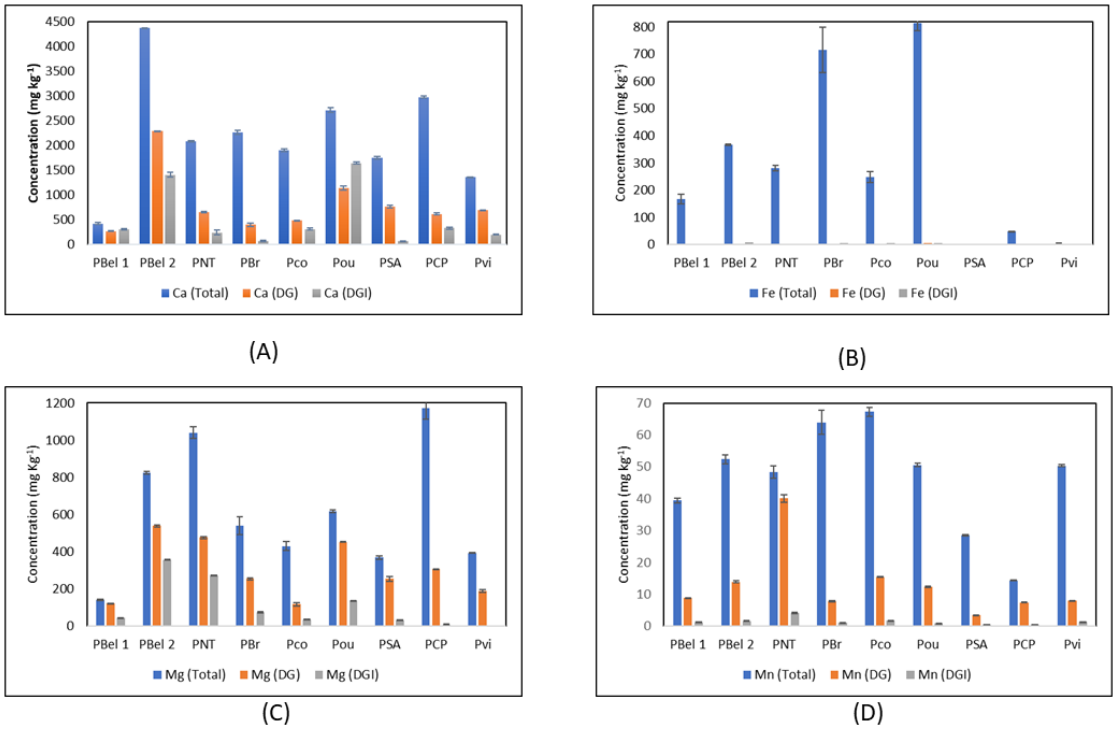

Figure 1. Total and bioaccessible contents (mg kg^{-1}) of calcium (A), iron (B), magnesium (C), and manganese (D) in propolis.

This was probably because of the gastric phase the low pH of the gastric fluid can increase the solubility of metal and precipitation can occur in the gastrointestinal phase.[20] Furthermore, the elevated presence of compounds such as phytates, oxalates, fibers, and other compounds can reduce the bioaccessibility of elements during gastrointestinal digestion because increases the likelihood of such compounds undergoing complexation reactions with elements present in the samples.[12, 20]

CONCLUSIONS

The bioaccessibility levels of Ca, Fe, Mg, and Mn found in propolis by gastric and gastrointestinal simulation showed that these inorganic elements are available for absorption in the body. The study of the bioaccessibility of inorganic constituents in propolis is an important contribution to the development of studies on this product, in addition to achieving a better chemical characterization of *Apis mellifera* and Melipona propolis samples.

Conflicts of interest

The authors declare that they have no conflict of interest.

Acknowledgements

The authors are grateful to “Coordenação de Aperfeiçoamento de Pessoal de Nível Superior” (CAPES) by fellowships.

REFERENCES

(1) Mello, B. C. B. S.; Petrus, J. C. C.; Humbinger, M. D. Desempenho do processo de concentração de extratos de própolis por nanofiltração. *Food Sci. Technol*. **2010**, *30* (1), 166-172. https://doi.org/10.1590/S0101-20612010000100025

(2) Almuhayawi. M. S. Propolis as a novel antibacterial agent. *Saudi J. Biol. Sci*. **2020**, *27*, 3079–3086. https://doi.org/10.1016/j.sjbs.2020.09.016

(3) Anjum, S. I.; Ullah, A.; Khan, K. A.; Attaullah, M.; Khan, H.; Ali, H.; Bashir, M. A.; Tahir, M.; Ansari, M. J.; Ghramh, H. A.; Adgaba, N.; Dash, C. K. Composition and functional properties of propolis (bee glue): A review. *Saudi J. Biol. Sci*. **2019**, *26*, 1695 – 1703. https://doi.org/10.1016/j.sjbs.2018.08.013

(4) Przybyłek, I.; Karpinski, T. M. Antibacterial Properties of Propolis. *Molecules* **2019**, *24*, 1-17. https://doi.org/10.3390/molecules24112047

(5) Khouzam, R. B.; Pohl, P.; Lobinski, R. Bioaccessibility of essential elements from White cheese, bread, fruit and vegetables. *Talanta* **2011**, *86*, 425-428. https://doi.org/10.1016/j.talanta.2011.08.049

(6) Peixoto, R. R. A.; Mazon, E. A. M.; Cadore, S. Estimation of the Bioacessibility of Matallic Elements in chocolate drink poder using an in vitro digestion method and spectrometric techniques. *J. Braz. Chem. Soc*. **2013**, *24*, 884-890. https://doi.org/10.5935/0103-5053.20130111

(7) Kulkarni, S. D.; Acharya, R.; Rajurkar, N. S.; Reddy, A. V. R. Evaluation of bioaccessibility of some essential elements from wheatgrass (*Triticum aestivum* L.) by in vitro digestion method. *Food Chem*. **2007**, *103*, 681–688. https://doi.org/10.1016/j.foodchem.2006.07.057

(8) Dutta, R. K.; Maharia, R. S.; Acharya, R.; Reddy, A. V. R. Analysis of bioaccessible concentration of trace elements in plant based edible materials by INAA and ICPMS methods. *J. Radioanal. Nucl. Chem*. **2014**, *300*, 185-189. https://doi.org/10.1007/s10967-014-3013-5

(9) Bossu, C. M.; Menezes, E. A.; Nogueira, A. R. A. Bioacessibilidade de zinco. cálcio e fósforo em extrato de soja e amostras de leite bovino. caprino e ovino. *Quim. Nova* **2020**, *43* (6), 718-722. http://dx.doi.org/10.21577/0100-4042.20170544

(10) Jacobs, B.; Bonemann, D. H.; Pereira, C. C.; De Souza, A. O.; Luckow, A. C. B.; Lisboa, M. T.; Ribeiro, A. S.; Cadore, S.; Nunes, A. M. Avaliação da concentração total e da fração bioacessível de metais em amostras de casca de uva de cultivares tannat e cabernet sauvignon por MIP OES. *Quim. Nova* **2021**, *44* (5), 547-552. http://dx.doi.org/10.21577/0100-4042.20170709

(11) Alves, B. S. F.; Nunes, P. O.; Dantas, K. G. F. Evaluation of in vitro Bioaccessibility of Copper. Iron and Manganese in Amazonian Fruits. *Rev. Virtual Quim*. **2017**, *9* (6), 2288-2298. http://dx.doi.org/10.21577/1984-6835.20170136

(12) Mingroni, T. T.; Hamada, J.; Xavier, A. D. S.; Cavalcante, C.; Do Nascimento, A. N. In vitro Evaluation of Ca, Cu, and Mg Bioaccessibility in Fresh and Dried Fruits. *J. Braz. Chem. Soc*. **2019**, *30* (1), 108–115. http://dx.doi.org/10.21577/0103-5053.20180159

(13) Stelmach, E.; Pohl, P.; Szymczycha-Madeja, A. Evaluation of the Bioaccessability of Ca, Fe, Mg and Mn in Ground Coffee Infusions by in vitro Gastrointestinal Digestion. *J. Braz. Chem. Soc*. **2014**, *25*, 1993-1999. https://doi.org/10.5935/0103-5053.20140183

(14) Moreda-Piñero, J.; Moreda-Piñero, A.; Romaris-Horta, V.; Dominguez-Gonzales, R.; Alonso-Rodriguez, E.; Lópes-Mahía, P.; Muniategui-Lorenzo, S.; Prada-Rodriguez, D.; Bermejo-Barrera, P. Trace metals in marine foodstuff: Bioavailability estimation and effect of major food constituents. *Food Chem*. **2012**, *134*, 339-345. https://doi.org/10.1016/j.foodchem.2012.02.165

(15) Gharibzahedi, S. M. T.; Jafari, S. M. The importance of minerals in human nutrition: Bioavailability. food fortification. processing effects and nanoencapsulation. *Trends in Food Sci. & Technol*. **2017**, *62*, 119-132. https://doi.org/10.1016/j.tifs.2017.02.017

(16) Finger, D.; Kelte Filho, I.; Torres, Y. R.; Quináia, S. P. Propolis as an indicator of environmental contamination by metals. *Bull. Environ. Contam. Toxicol*. **2014**, *92*, 259-264. https://doi.org/10.1007/s00128-014-1199-4

(17) Cantarelli, M. A.; Camiña, J. M.; Pettenati, E. M.; Marchevsky, E. J.; Pellerano, R. G. Trace mineral content of Argentinean raw propolis by neutron activation analysis (NAA): Assessment of geographical provenance by chemometrics. *LWT-Food Science Tecnol*. **2011**, *44*, 256-260. https://doi.org/10.1016/j.lwt.2010.06.031
(18) Matuszewska, E.; Klupczynska, A.; Maciołek, K.; Kokot, Z. J.; Matysiak, J. Multielemental Analysis of Bee Pollen. Propolis. and Royal Jelly Collected in West-Central Poland. *Molecules* **2021**, *26*, 1-18. https://doi.org/10.3390/molecules26092415
(19) Bonvehí, J. S.; Bermejo, F. J. O. Element content of propolis collected from different areas of South Spain. *Environ. Monit. Assess*. **2013**, *185*, 6035-6047. https://doi.org/10.1007/s10661-012-3004-3
(20) Souza, L. A.; Souza, T. L.; Santana, F. B.; Araujo, R. G. O.; Teixeira, L. S. G.; Santos, D. C. M. B.; Korn, M. G. Determination and in vitro bioaccessibility evaluation of Ca, Cu, Fe, K, Mg, Mn, Mo, Na, P and Zn in linseed and sesame. *Microchem. J*. **2018**, *137*, 8-14. https://doi.org/10.1016/j.microc.2017.09.010
(21) Machado, D. F.; Silva, R.; Fanchiotti, F. E.; Costa, N. M. B. Probióticos, prebióticos e simbióticos e seus efeitos na biodisponibilidade de cálcio. *Nutrire Rev. Soc. Bras. Aliment. Nutr*. **2001**, *22*, 73-83.
(22) Germano, R. M. A.; Canniatti-Brazaca, S. G. Importância do ferro em nutrição humana. *Rev. Soc. Bras. Alim*. **2002**, *24*, 85-104.
(23) Monteiro, T. H.; Vannuchi, H. Funções plenamente reconhecidas de nutrientes: Magnésio, Vol16. International Life Sciences Institute (ILSI) Brasil, São Paulo, 2010.
(24) Fairweather-Tati, S. J. Bioavailability of trace elements. *Food Chem*. **1992**, *43*, 213-217. https://doi.org/10.1079/NRR19960016

Brazilian Journal of Analytical Chemistry
2023, Volume 10, Issue 40, pp 132-157
doi: 10.30744/brjac.2179-3425.AR-129-2022

BrJAC

ARTICLE

Determination of Essential and Non-Essential Elements in Dietary Supplements by Microwave-Induced Plasma Optical Emission Spectrometry: *Method Development and Study of Non-Spectral Interferences*

Paola de Azevedo Mello*, Gustavo Rossato Bitencourt, Thaís dos Santos Berón, Aline Lima Hermes Müller

Departamento de Química, Universidade Federal de Santa Maria, 97105-900, Santa Maria, RS, Brazil

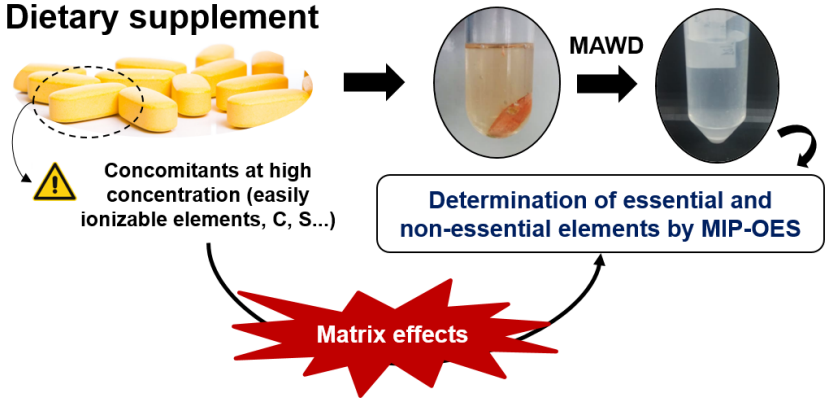

Dietary supplements have been used to overcome nutritional deficiencies and the knowledge concerning essential and non-essential elements is an important issue. In this work the suitability of microwave-induced plasma optical emission spectrometry (MIP OES) for the determination of essential and non-essential elements in dietary supplements was evaluated. Twelve dietary supplement samples of several classifications (vitamins/minerals, minerals, amino acids, and botanicals) were digested in their whole form for determination of essential (Ca, Co, Cu, Fe, K, Mg, Mn, Mo, Na, and Zn) and non-essential (Ag, Al, B, Ba, Be, Cd, Cr, La, Li, Ni, Pb, Sr, and V) elements by MIP OES. Potential non-spectral interferences by common concomitants (C, S, K, Na, and Ca) were evaluated, as well as those by residual acidity of digests. The study of non-spectral interferences showed that a signal suppression effect is observed with higher concentrations of Ca, Na, and K. Relatively good robustness was observed considering the presence of C and S, as well as residual HNO_3. The limits of quantification (LOQs) were dependent on the sample mass used for decomposition (from 0.6 to 1.6 g in the commercial product) and on the minimum dilution factor. From the results, there was a prevalence of essential and non-essential elements in vitamins and minerals, minerals, and botanicals-based dietary supplements, whereas lower concentrations were found in the dietary supplements based on amino acids. All elements were in a concentration below the recommended dietary allowances (RDAs), exception for those with the concentration intentionally higher. Accuracy of results by

Cite: Mello, P. A.; Bitencourt, G. R.; Berón, T. S.; Müller, A. L. H. Determination of Essential and Non-Essential Elements in Dietary Supplements by Microwave-Induced Plasma Optical Emission Spectrometry: *Method Development and Study of Non-Spectral Interferences*. *Braz. J. Anal. Chem.* 2023, *10* (40), pp 132-157. http://dx.doi.org/10.30744/brjac.2179-3425.AR-129-2022

Submitted 01 December 2022, Resubmitted 14 February 2023, Accepted 24 April 2023, Available online 15 May 2023.

MIP OES was evaluated by using standard reference materials (SRM) NIST 1572 and NIST 1575a. In addition, results showed no statistical difference by comparison with those by ICP OES. MIP OES proved to be a suitable technique for the determination of metals in dietary supplements, being a feasible alternative for the quality control of these products.

Keywords: dietary supplements, essential elements, non-essential elements, MIP OES, bioanalytical chemistry

INTRODUCTION

Several essential nutrients are required for the healthy functioning of the human body, such as proteins, vitamins, and minerals. Nowadays, due to the large consumption of processed foodstuffs and the lack of essential nutrients in these ones, people have been suffering from nutritional deficiencies and, consequently, from related diseases.[1] In order to overcome these nutritional deficiencies the use of dietary supplements has grown, associated with other factors, such as the carefulness of people with health care and the higher consumption by athletes and bodybuilding exercise practitioners, among others.[1,2]

The elements required by humans and provided by dietary supplements can be divided into essential and non-essential elements, depending on their known or unknown/uncertain role in the physiological system of humans, respectively.[3] In addition to those elements added to supply, both essential and non-essential elements can be introduced as contaminants, from raw materials, manufacturing, transport, and storage of the final products, moreover those introduced into botanicals-based from the environment.[2,4] In this sense, the contamination of several classes of dietary supplements by these elements has been reported.[5–7] In view of this, for monitoring the concentration of essential and non-essential elements added as a supplier in dietary supplements, as well as present as elemental contaminant, several analytical techniques have been used, with emphasis to the plasma-based spectrometric techniques, such as optical emission spectrometry (ICP OES) and mass spectrometry (ICP-MS).[2] Among these, microwave-induced plasma optical emission spectrometry (MIP OES) can be also an alternative, promoting suitable limits of detection (LOD) for quality control of essential and non-essential elements in dietary supplements, similar with those by ICP OES. However, so far, MIP OES was few explored and only one report was found for the determination of Al, Ba, Ca, Cd, Cr, Cu, Fe, K, Mg, Mn, Na, Ni, P, V, and Zn in Spirulina dietary supplements.[8]

Elemental determination by MIP OES tends to be prone to matrix effects more than ICP OES due to the use of nitrogen as plasma gas on the current MIP OES instrumentation. This results in lower plasma temperatures compared to that achieved by argon plasma-based (about 5000 K for nitrogen-based against 10000 K for argon-based plasmas).[9] This characteristic makes essential to evaluate the non-spectral interferences in the analysis by N_2-MIP OES. However, to date, there are few studies reported about this on the current MIP OES instruments, mostly focused on non-spectral interferences caused by easily ionizable elements (EIEs, e.g. Na and K).[10–13] Either signal suppression or enhancement have been related to the high concentrations of EIEs, mainly due to changes in the physical properties of the plasma, such as excitation temperature and ionization equilibrium.[12,14] Moreover, the excitation/ionization energy of the element line also impact on the interference phenomena. Serrano et al.[12] reported that atomic lines with excitation energy below 3.26 eV had a signal enhancement with a 0.5% w w^{-1} calcium nitrate solution, while ionic lines (higher excitation/ionization energy) had a signal suppression. This same work is the only one reporting the influence of carbon and sulfur on the determination by MIP OES, despite the well-studied effects demonstrated by ICP OES.[15–17] Operating with 0.5% w w^{-1} glycerol or sulfuric acid solutions, lower effects were observed by MIP OES when compared with ICP OES. In that case, the plasma temperature was considered beneficial to reduce the physical effects caused by carbon and sulfur on the measurements by MIP OES.[12]

Thus, the purpose of this work was to evaluate the suitability of MIP OES for the determination of essential and non-essential elements in dietary supplements, aiming a method for the quality control of

elements added as a supplier, as well as those present as contaminants. For this, in order to develop a reliable method, a study of non-spectral interferences was carried out, comprising common concomitant elements present in dietary supplements (C, S, Na, K, and Ca). Moreover, non-spectral interferences caused by residual HNO_3 acidity remained from sample preparation were also investigated.

MATERIALS AND METHODS

Samples and standard reference materials

Twelve dietary supplements from different brands were purchased in the local and electronic market, originating from Brazil and the USA, in the form of tablets, capsules, and powders. The samples were coded as vitamins and minerals (VM), minerals (MN), amino acids (AM), and botanicals (BT). The characteristics of each sample are shown in Table S1 (Supplementary Material). Whole samples were used for sample digestion, without any pre-treatment procedure, by inserting the tablets, capsules, or powders directly into the digestion vessel.

The accuracy of the proposed method was evaluated using two standard reference materials (SRM): 1572 (Citrus Leaves) and 1575a (Trace Elements in Pine Needles), both from the National Institute of Standards and Technology (NIST, USA).

Instrumental

A microwave-induced plasma optical emission spectrometer (4210 MP AES, Agilent Technologies, USA) equipped with a N_2 generator (model 4107, Agilent Technologies, USA), a five-channel peristaltic pump and an inert concentric nebulizer (OneNeb® series 2, Agilent Technologies, USA) was used. Operational conditions for measurements by MIP OES are shown in Table I. The nebulizer gas flow-rate and the plasma observation position of each element were optimized automatically by the instrument software (MP Expert, Agilent Technologies, USA).

Sample preparation was performed in a microwave-assisted single reaction chamber system (Ultrawave™, Milestone, Italy). The system is composed by five quartz vessels with a capacity of 40 mL, which are placed in a rack and into a modified polytetrafluoroethylene (PTFE-TFM) vessel. The vessel is inserted in the microwave cavity chamber (1 L), which is sealed and pressurized with 40 bar of Ar (99.5%, White Martins, Brazil) before microwave irradiation. The system was set to operate at a maximum power, temperature, and pressure of 1500 W, 270 °C, and 160 bar, respectively.

Reference values for elements were obtained using an inductively coupled plasma optical emission spectrometer (Spectro Ciros CCD, Spectro Analytical Instruments, Germany). Carbon and sulfur content in digests were also determined by ICP OES. The operational conditions for the determination by ICP OES are shown in Table S2 (Supplementary Material). Argon (99.998%, White Martins, Brazil) was used as plasma, auxiliary, and nebulizer gas in ICP OES.

Determination of residual acidity in digests was performed by an automatic titration system (836, Metrohm, Switzerland) equipped with a module of automatic stirring (803 Ti Stand, Metrohm) and a combined pH electrode (6.0262.100, Metrohm).

All statistical calculations were performed using GraphPad InStat software (GraphPad InStart Inc, Version 3.06, 2007) with a confidence level of 95%.

Table I. Operational conditions for elemental determination by N_2-MIP OES

Parameter	MIP OES
Microwave frequency (MHz)	2450
Plasma power (kW)	1.0
Plasma gas flow-rate (L min^{-1})	20
Auxiliary gas flow-rate (L min^{-1})	1.0

(continues on the next page)

Table I. Operational conditions for elemental determination by N_2-MIP OES (continuation)

Parameter	**MIP OES**	
Background correction	Auto	
Replicates	3	
Read time (s)	3	
Stabilization time (s)	15	
Peristaltic pump rotation	15	
Analytes (wavelength, nm)	Nebulizer gas flow-rate (L min^{-1})	Plasma observation position
Ag(I) (328.068)	0.70	50
Al(I) (394.401)	0.35	-130
B(I) (249.677)	0.40	10
Ba(II) (493.408)	0.75	0
Be(I) (234.861)	0.50	0
Ca(II) (396.847)	0.65	-10
Cd(I) (228.802)	0.45	-10
Co(I) (340.512)	0.60	80
Cr(I) (357.868)	0.90	0
Cu(I) (324.754)	0.80	10
Fe(II) (259.940)	0.50	50
K(I) (766.461)	1.00	10
La(II) (433.374)	0.55	-10
Li(I) (670.784)	1.00	10
Mg(II) (280.271)	0.55	-10
Mn(I) (403.307)	1.00	-10
Mo(I) (386.410)	0.75	-10
Na(I) (589.592)	1.00	10
Ni(I) (341.476)	0.30	40
Pb(I) (363.957)	0.55	-10
Sr(II) (407.771)	0.60	0
V(I) (437.923)	0.95	-10
Zn(I) (213.857)	0.55	-40

(I) Atomic emission line; (II) Ionic emission line.

Reagents and standards

Water was ultra-purified in a Milli-Q system (18.2 MΩ cm, Merck Millipore, USA) and was used for the preparation of all standards, solutions, and dilutions, as well as for cleaning and washing materials.

Nitric acid (65%, Merck, Germany) and hydrochloric acid (37%, Merck) were sub-boiling distilled (DuoPur, Milestone, Italy) before use for sample digestion.

For elemental determination by MIP OES and ICP OES, analytical standards ranging from 1 to 100 μg L^{-1} were prepared by dilution of a multielement stock reference solution (SCP33MS, SCP Science, 10 mg L^{-1}, Canada) in 5% v v^{-1} HNO_3. Moreover, for the determination of analytes at higher concentration, analytical standards from 0.25 to 5 mg L^{-1} were prepared by dilution of a multielement stock reference solution (Merck IV, Merck, 1000 mg L^{-1}) in 5% v v^{-1} HNO_3. For the determination of dissolved carbon in digests by ICP OES, analytical standards (25 to 500 mg L^{-1}) were prepared by dilution of a 10 g L^{-1} stock solution, prepared with citric acid (Dinâmica, Brazil) in ultrapure water. Ytrium (Assurance, Spex CertiPrep®, 1001.5 ± 3 mg L^{-1} in 0.28 mol L^{-1} HNO_3, USA) was used as internal standard for the determination of carbon by ICP OES, being 1 mg L^{-1} added to all analytical standards, blanks, and samples. Sulfur was determined by ICP OES and analytical standards (0.25 to 5 mg L^{-1}) were prepared by dilution of a stock reference solution (Assurance, Spex CertiPrep®, 1003 ± 3 mg L^{-1}, USA) in 5% v v^{-1} HNO_3.

For the study of non-spectral interferences by MIP OES, spiked solutions containing 100 μg L^{-1} of all analytes were prepared in synthetic matrices containing 25, 250, and 5000 mg L^{-1} of C, S, Na, K, and Ca in 5% v v^{-1} HNO_3. A 10 g L^{-1} stock solution of each interferent was prepared by dissolution/dilution of citric acid, calcium nitrate (Dinâmica, Brazil), sulfuric acid (97%, Sigma Aldrich, USA), sodium nitrate (Cinética Química, Brazil), and potassium nitrate (Êxodo Científica, Brazil). Moreover, non-spectral interferences by residual HNO_3 acidity (10 to 50% v v^{-1}) were also evaluated.

Sample preparation

The procedure used for the decomposition of dietary supplements was based on previous works.[18,19] Whole samples with sample masses ranging from 0.5 to 1.6 g for tablet or capsules were used. For the powdered samples, 0.5 g was weighed and inserted into the digestion vessel. Samples were weighed directly into the digestion vessels, and then 10 mL of HNO_3:HCl (8:2) solution was added. The digestion vessels were placed in the instrument rack, which was inserted into the single reaction chamber system (lined with PTFE-TFM, containing 130 mL of water and 5 mL of HNO_3). The system was then sealed and pressurized with 40 bar or Ar. All digestions were carried out using maximum temperature, pressure, and microwave power of 270 °C, 160 bar, and 1500 W, respectively. Heating program used was: 10 min of ramp and holding for 20 min at 270 °C. After digestion, the obtained digests were transferred to volumetric flasks and made up to 25 mL with ultrapure water for further elemental determination by MIP OES, ICP OES, and ICP-MS.

Elemental determination by MIP OES and study of non-spectral interferences

The interferences caused by common concomitant elements (C, S, Na, K, and Ca) on the determination by MIP OES were evaluated. Solutions containing 100 μg L^{-1} of all analytes were spiked with 25, 250, or 5000 mg L^{-1} of each concomitant. In addition, the influence of the residual HNO_3 acidity in the digests was also evaluated, and the spiked solutions of all analytes were prepared in 10, 20, 30, 40, and 50% v v^{-1} HNO_3. Reference values for the study of non-spectral interferences were considered those for a solution containing 100 μg L^{-1} of all analytes in 5% v v^{-1} HNO_3.

In this study, acceptable spike recoveries were based on the repeatability uncertainty. In this sense, 10 replicates of a standard solution containing 100 μg L^{-1} of all analytes in 5% v v^{-1} HNO_3 were measured, and a relative standard deviation (RSD) of 4.8% was obtained. Then, an expanded uncertainty equal to 11% was estimated, which was calculated using the standard uncertainty (4.8%), multiplied by the coverage factor (k=2.2).[20] Thus, the acceptable recoveries were in the range of 89–111% and it was used for all optimizations carried out in this study.

In addition to consider spike recoveries, non-spectral interferences were also related to the E_{sum} (i.e., the sum of the excitation and ionization energy) of the lines determined by MIP OES (Table S3, Supplementary Material).

RESULTS AND DISCUSSION

Considering the complex matrices of the dietary supplements, that can come from materials from several origins and can have a mixture of matrices in their compositions and taking into account the interferences that can arise from digests in the lower temperature MIP, non-spectral interferences caused by the common concomitant elements (C, S, Na, K, and Ca) were evaluated. Moreover, non-spectral interferences from residual HNO_3 acidity remained from sample preparation were also investigated.

Study of non-spectral interferences by MIP OES

Carbon and sulfur-based non-spectral interferences by MIP OES

Dietary supplements, mainly vitamins and botanicals-based, can contain a relatively high concentration of carbon, which can cause interferences on the measurements by MIP OES. Carbon-related matrix effects on spectroscopic techniques have been widely studied.[15,21] For optical-emission techniques, such as MIP OES, effects on the signals can be induced by changes in the analyte transport and plasma ionization equilibrium.[16]

Carbon can be present in solutions as a consequence of partial digestion. In view of this, carbon-based matrix effects on the determinations by MIP OES were evaluated. Citric acid is a non-volatile carbon compound that has been normally used for carbon-based interferences studies.[18,22] Spiked solutions at 100 µg L^{-1} containing 25, 250, and 5000 mg L^{-1} C (as citric acid) were evaluated.

As the carbon content as well as the amount digested was different for each sample, dissolved carbon remained in digests ranged from 11.1 to 179 mg L^{-1} (Table S4, Supplementary Material). Spike recoveries for essential and non-essential elements are presented in Figure S1 (Supplementary Material).

The results demonstrated good robustness of MIP OES even operating with high concentration of carbon. Signal suppression for Co and Mo was observed, but at relatively high carbon concentration (5000 mg L^{-1}). It is important to note that, considering the E_{sum} of lines (Figure 1A), both Co and Mo have lower E_{sum} (3.21 and 4.05 eV, respectively) (dots between dashed lines indicate no matrix effect). Signal suppression effect by carbon have been related to lines with excitation energy lower than 6 eV, probably due to the inactivation of the excited state of the analyte by collisions with carbon atoms or radicals.[16] In another study,[12] MIP OES demonstrated to be more robust than ICP OES for the presence of 5% w w^{-1} glycerol (ca. 20 g L^{-1} of carbon), and no effects related to carbon were observed for the determination of As, Co, Cu, Mg, Mn, Mo, Sc, Se, Sr, and Zn. In general, the results in this work agree with those previous reports demonstrating a relatively suitable robustness of MIP OES to high concentrations of carbon which can be related to the lower plasma temperature that minimizes the effects (***e.g.,*** charge transfer reaction) caused by carbon in the plasma.[12]

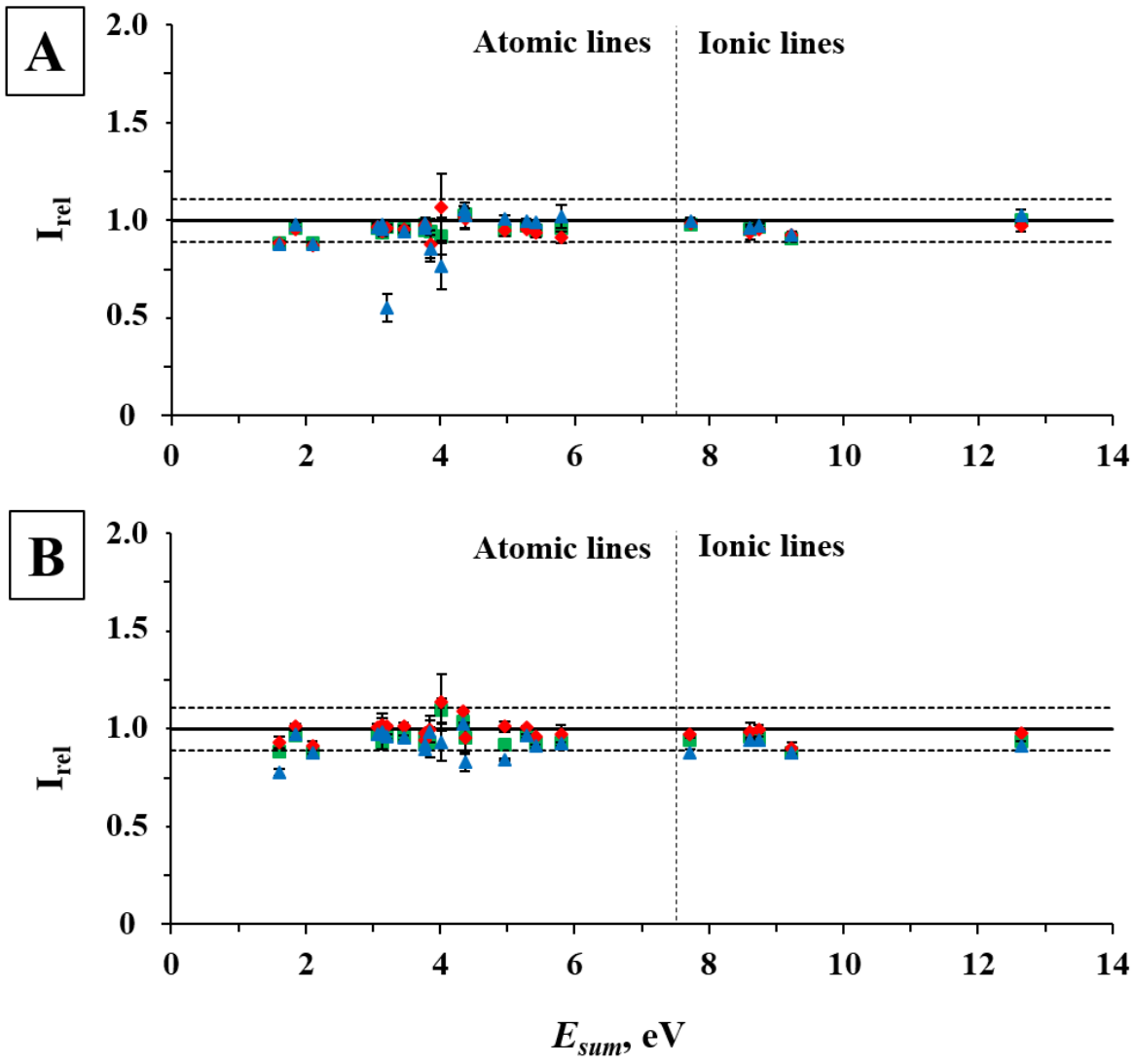

Figure 1. Relative signal intensity (I_{rel}) for lines according to E_{sum} values influenced by A) carbon (as citric acid) and B) sulfur (as sulfuric acid), with concentrations of 25 (■), 250 (◆), and 5000 (▲) mg L^{-1} by MIP OES. Continuous and dashed lines represent the 5% v v^{-1} HNO_3 reference solution value and the expanded uncertainty, respectively.

Sulfur can induce effects similar to carbon on the properties of the plasma (*i.e.*, ionization equilibrium, charge transfer reaction, etc.).[17] Due to matrix composition, sulfur content can be relatively high for some samples. As can be seen in Table S4, sulfur concentration in dietary supplements samples were in the range of 13.3 to 307 mg L^{-1}. The effect of sulfur on the determination by MIP OES was evaluated using spiked solutions containing different concentrations of sulfur (as sulfuric acid). Just as noted for carbon, low effects by sulfur were observed (Figure S2, Supplementary Material), since only the signal of K was suppressed with a relatively high sulfur concentration (5000 mg L^{-1}). It can be explained, possibly, by the lower E_{sum} of the line used for K (1.61 eV, Figure 1B) and the effect on of the excited state of elements with lower excitation energy caused by sulfur at high concentrations. As reported,[12] the poor matrix effects induced by sulfur in MIP OES were explained by the similar plasma temperatures even using a 5% w w^{-1} H_2SO_4 (ca. 16 g L^{-1} of S) solution compared to that using 1% w w^{-1} HNO_3 solution, and by the minimized physical interferences using the OneNeb® nebulizer (the same employed in this work).

Sodium-, potassium-, and calcium-based non-spectral interferences by MIP OES

High concentration of EIEs, such as sodium and potassium, induce a lower temperature and a higher electronic density in the plasma, causing changes in the ionization equilibrium.[23] Non-spectral interferences by sodium have been reported from 300 mg L^{-1}.[11] Despite fewer effects are expected for calcium due to the higher ionization energy (6.11 eV against 5.14 eV for sodium, for example), significant consequences can be observed in the presence of higher concentrations of calcium (the case of many dietary supplements).[14] For the samples investigated on this work, Na, K, and Ca concentrations were in the range of 6.27 to 128, 0.046 to 532, and 0.215 to 15851 mg L^{-1}, respectively (Table S4).

Non-spectral interferences promoted by sodium (as sodium nitrate), potassium (as potassium nitrate), and calcium (as calcium nitrate) on the determination by MIP OES were evaluated using spiked solutions containing crescent concentrations of these elements. As can be observed by spike recoveries (Figures S3 and S4, Supplementary Material), similar effects on signals were observed by both sodium and potassium, being those by sodium more significant. No interference for 25 mg L^{-1} of sodium and potassium was observed (except for Ca, which suffer a signal suppression in the presence of sodium). Absence of interferences were also observed by Baranyai et al.[11] in the determination of Ca, Cu, Fe, K, Mg, and Zn with about 30 mg L^{-1} of sodium in human blood serum. More pronounced effects were observed from 250 mg L^{-1} of sodium and potassium. Signal suppression for Ba, La, Ni, Pb, and Sr at 250 mg L^{-1} was observed. At least 20% suppression occurred for most of the analytes for 5000 mg L^{-1} of potassium and/or sodium, including total signal suppression of La, Ni, and Pb with sodium.

Regarding interferences by calcium, no effects with 25 mg L^{-1} were observed (Figure S5, Supplementary Material). From 250 mg L^{-1}, the effect of signal suppression was milder than those by sodium and potassium, and a total signal suppression for Mg and Pb occurred with 5000 mg L^{-1}. On the other hand, on the contrary of that observed for sodium and potassium, signal enhancement of some elements with lower E_{sum} (K, Li, Mo, Na, and V) was observed in the presence of higher concentration of calcium, reaching an enhancement of 130% for Na at 5000 mg L^{-1}.

As can be observed in Figure 2A and Figure 2B, atomic lines with lower E_{sum} had their signals more impacted by higher concentrations of sodium and potassium (from 5000 mg L^{-1}). However, signal suppression of ionic lines can be observed even with a concentration of 25 mg L^{-1}, which can be explained by higher energy required for the ionic lines.[14] On the other hand, different behavior occurred in the presence of calcium (Figure 2C). Whereas a signal enhancement for atomic lines with E_{sum} lower than 3.21 eV was observed (except for Al), atomic/ionic lines with E_{sum} higher than 3.46 eV had their signals suppressed. This same behavior was observed for the presence of 0.5% w w^{-1} of calcium nitrate (ca. 1.2 g L^{-1} of calcium).[12]

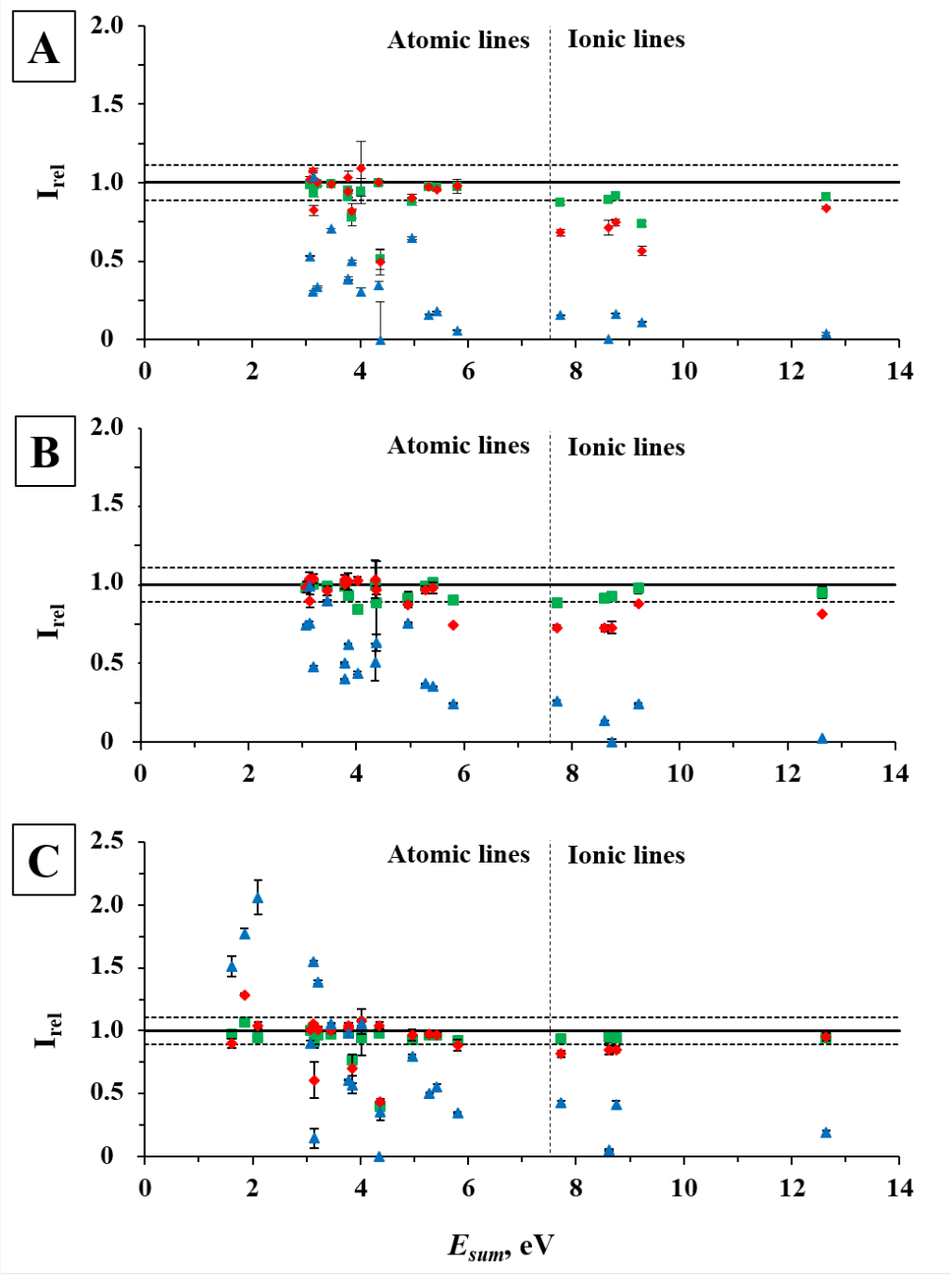

Figure 2. Relative signal intensity (Irel) for lines according to E_{sum} values influenced by A) sodium (as sodium nitrate), B) potassium (as potassium nitrate) and C) calcium (as calcium nitrate), with concentrations of 25 (■), 250 (◆), and 5000 (▲) mg L^{-1} by MIP OES. Continuous and dashed lines represent the 5% v v^{-1} HNO_3 reference solution value and the expanded uncertainty, respectively.

Influence of the residual HNO_3 acidity

It is well known that high residual acidity remained from sample preparation can induce physical non-spectral interferences on measurements by plasma-based spectrometric techniques. Changes in the analyte transport to the plasma, as well as effect in the thermal characteristics are reported.[24] However, so far, there is no study demonstrating the influence of the residual HNO_3 acidity on the determinations by MIP OES.

Thus, for this evaluation, spiked solutions containing all analytes were prepared to contain HNO_3 concentrations at 10, 20, 30, 40, and 50% v v^{-1}. The spike recoveries can be seen in Figure S6 (Supplementary Material). In general, MIP OES demonstrated a good tolerance at high HNO_3 concentrations, since the signal for most of the analytes was not damaged even when operating with a 50% v v^{-1} HNO_3 solution. On the other hand, Al, Co, K, and Pb had their signals suppressed for a 30% v v^{-1} HNO_3 solution, which is similar to the effects of residual HNO_3 acidity observed by ICP OES.[24] In this point, it is important to mention that digests of all samples, even using a powerful digestion system, presented a residual acidity in solution from 15 to 29%, except for AM-1 and AM-2 samples, in which the residual acidity was about 60% (probably due to acid hydrolysis of amino acids present), suggesting that care must be taken. Based on the results, if acidity higher than 30% is observed, a proper dilution must be performed previous to analysis.

Determination of common concomitants in dietary supplements

As observed in the study of non-spectral interferences, EIEs, such as sodium, potassium, and calcium, as well as carbon, sulfur, and residual HNO_3 acidity can bring several interferences on the determinations by MIP OES. Given this, the concentration of Na, K, Ca, S, and dissolved carbon in digests were determined by ICP OES. In addition, the residual acidity was determined by potentiometric titration. The results can be seen in Table S4.

Carbon dissolved in digests and sulfur concentration was not higher than 130 and 307 mg L^{-1}, respectively. From the study of non-spectral interferences, it is not expected interferences caused by carbon or sulfur for a concentration below 5000 mg L^{-1}. On the other hand, the maximum concentrations of sodium, potassium, and calcium in the samples were 128, 532, and 15851 mg L^{-1}, respectively. Based on the study of non-spectral interference, these concentrations interfere on several elements, mainly if synergic effects are considered. Because of this, a minimum dilution factor must be defined to the determinations by MIP OES, considering the concentration of at least sodium, potassium, and calcium. The dilutions factors employed were 10-fold for BT-2, 20-fold for VM-1 and 50-fold for VM-3, VM-4, MN-1, and MN-2 samples. Moreover, a minimum dilution factor of 4-fold was defined for samples AM-1 and AM-2 due to residual acidity, which was higher than 30%, to avoid signal suppression. Finally, it is important to emphasize that the LOQs of the method were impacted by the minimum dilution factor required, which will be further discussed.

Determination of essential and non-essential elements in dietary supplements by MIP OES after digestion by MAWD-SRC

Quality control of essential and non-essential elements added as supplier or as elemental impurities in dietary supplements is crucial. However, exception for As, Cd, Hg, and Pb, which have maximum concentrations in dietary supplements established by United States Pharmacopoeia (USP) General Chapter 2232[25] and by EC 629/2008 (except As),[26] there are not a regulation neither to other essential or non-essential elements in dietary supplements. Despite dietary supplements are not regulated as pharmaceutical products, the Q3D guideline on the elemental impurities of the International Council for Harmonization of Technical Requirements for Pharmaceuticals for Human Use (ICH-Q3D)[27] can be used as a reference for the maximum concentrations of some elements. The ICH-Q3D classified the elements in three classes, depending on their toxicity and uptake route: Class 1 (As, Cd, Hg, and Pb), Class 2A (Co, Ni, and V), Class 2B (Ag, Au, Ir, Os, Pd, Pt, Rh, Ru, Se, and Tl), and Class 3 (Ba, Cr, Cu, Li, Mo, Sb, and Sn). In addition, the recommended dietary allowance (RDA) of the elements also can be used as a limit for some essential elements (such as Ca, Fe, Zn, among others).

The concentrations of essential and non-essential elements determined in dietary supplements by MIP OES after digestion are shown in Table II. Considering the high concentration of concomitants in samples and the undesirable effects previously discussed on the study of non-spectral interferences, a minimum dilution factor was required for some samples. The LOQs obtained, related to samples masses and to minimum dilution factors are shown in Table S5 (Supplementary Material). The LOQs were estimated as

$10s + \bar{x}$, where $\bar{x}$ is the mean and *s* is the standard deviation of ten measurements of a blank.[28] The higher concentration of elements, as Na, K, and Ca required dilution that impaired the LOQs and results for Ag, Be, Co, La, Ni, and Pb were lower than the LOQ. It is noteworthy that most of the LOQs obtained for Cd and Pb not attend the maximum concentration established by USP General Chapter 2232 (0.5 μg g^{-1} for both) or EC 629/2008 (1.0 and 3.0 μg g^{-1}, respectively), except those achieved for Cd for samples without a minimum dilution factor (VM-2, AM-3, AM-4, and BT-1, LOQ was 0.290 μg g^{-1}).

As expected, essential elements are the majority in the vitamins and/or minerals dietary supplements, as well as for those botanical-based. Calcium, Fe, Na, Mg, and Zn are the elements with higher concentrations. On the other hand, lower concentrations of both essential and non-essential elements are found in amino acids dietary supplements, probably due to the few number of ingredients used in the formulation of these ones. With regard to non-essential elements in vitamins and/or minerals and botanical-based dietary supplements, Al was the element at higher concentration.

The concentration of all essential and non-essential elements determined in dietary supplements samples are below their RDAs (data not presented), except for those which concentration intentionally exceed the RDA and are labeled, cases of Cu in VM-3, Mg in MN-2, and Mn, Mo, and Zn in VM-3 and MN-2. In addition, taking into account the ICH-Q3D, the concentrations obtained were lower than that limited for V (Class 2A, 10 μg g^{-1}), Ag (Class 2B, 15 μg g^{-1}), Li, Ba, Mo, and Cr (Class 3, 55, 140, 300, and 1100 μg g^{-1}, respectively). However, the concentration of Cu (Class 3) exceed the limit established (300 μg g^{-1}) for VM-1 and VM-3 samples (442 and 1332 μg g^{-1}, respectively).

Table II. Results for essential and non-essential elements in different classes of dietary supplements after digestion and determination by MIP OES (mean ± standard deviation, n = 3)

Element	Vitamins and minerals				Minerals		Amino acids				Botanicals	
	VM-1	VM-2	VM-3	VM-4	MN-1	MN-2	AM-1	AM-2	AM-3	AM-4	BT-1	BT-2
Essential elements												
Ca, mg g^{-1}	136 ± 12	0.720 ± 0.026	159 ± 4	271 ± 18	307 ± 9	224 ± 20	< 0.044	0.094 ± 0.004	0.113 ± 0.006	< 0.037	0.386 ± 0.013	111 ± 12
Cu, µg g^{-1}	442 ± 15	< 0.455	1332 ± 67	< 22.7	< 10.5	110 ± 11	< 2.18	< 2.18	< 0.455	< 0.455	2.56 ± 0.12	14.5 ± 0.5
Fe, µg g^{-1}	178 ± 10	16202 ± 1682	11709 ± 721	293 ± 29	106 ± 8	176 ± 10	< 4.84	< 4.84	1.54 ± 0.10	14.0 ± 0.7	184 ± 11	511 ± 32
K, mg g^{-1}	< 0.173	0.054 ± 0.006	< 0.216	< 0.576	< 0.266	12.1 ± 0.9	< 0.055	< 0.055	< 0.011	0.616 ± 0.041	5.53 ± 0.22	12.6 ± 0.8
Mg, mg g^{-1}	70.9 ± 1.3	0.473 ± 0.032	62.7 ± 0.7	49.4 ± 4.4	105 ± 7	107 ± 8	< 0.010	< 0.010	0.024 ± 0.002	0.010 ± 0.001	5.66 ± 0.26	4.87 ± 0.09
Mn, µg g^{-1}	1440 ± 117	3482 ± 55	2710 ± 41	30.3 ± 0.9	40.4 ± 1.1	792 ± 23	< 0.203	0.326 ± 0.016	< 0.042	< 0.042	65.2 ± 2.6	39.5 ± 2.1
Mo, µg g^{-1}	34.3 ± 2.3	< 0.535	63.8 ± 2.4	< 26.8	< 12.4	< 12.4	< 2.57	< 2.57	< 0.535	< 0.535	< 0.535	< 5.35
Na, µg g^{-1}	562 ± 52	390 ± 28	977 ± 33	3027 ± 312	1510 ± 170	416 ± 22	357 ± 24	791 ± 15	614 ± 56	523 ± 18	1172 ± 79	306 ± 23
Zn, mg g^{-1}	9.96 ± 0.62	3.45 ± 0.18	10.8 ± 0.2	1.61 ± 0.12	4.47 ± 0.31	3.12 ± 0.17	< 0.013	< 0.013	< 0.003	< 0.003	0.020 ± 0.001	0.030 ± 0.001
Non-essential elements												
Al, µg g^{-1}	233 ± 20	73.5 ± 2.1	103 ± 7	107 ± 16	92.5 ± 9.7	73.4 ± 5.5	< 63.2	< 63.2	< 13.1	56.3 ± 1.9	316 ± 22	511 ± 32
B, µg g^{-1}	90.3 ± 6.6	< 0.826	106 ± 8	57.8 ± 4.3	7.11 ± 0.48	221 ± 18	< 3.97	< 3.97	< 0.826	< 0.826	2.13 ± 0.07	19.0 ± 0.7
Ba, µg g^{-1}	20.3 ± 1.6	0.292 ± 0.018	1.45 ± 0.13	8.46 ± 0.77	1.45 ± 0.12	18.1 ± 1.1	< 0.576	< 0.576	1.69 ± 0.11	3.75 ± 0.15	1.11 ± 0.05	20.7 ± 1.6
Cr, µg g^{-1}	18.3 ± 1.2	< 0.165	84.5 ± 4.2	1.73 ± 0.31	3.13 ± 0.07	11.4 ± 0.6	< 0.791	< 0.791	< 0.165	< 0.165	0.429 ± 0.007	3.20 ± 0.27
Li, µg g^{-1}	0.374 ± 0.015	< 0.074	0.464 ± 0.012	1.18 ± 0.08	0.509 ± 0.006	0.610 ± 0.007	< 0.357	< 0.357	< 0.074	< 0.074	0.248 ± 0.009	1.81 ± 0.12
Sr, µg g^{-1}	537 ± 24	< 0.338	28.4 ± 2.1	1058 ± 83	52.1 ± 3.9	66.7 ± 3.1	< 1.62	< 1.62	< 0.338	< 0.338	1.75 ± 0.12	53.0 ± 3.0
V, µg g^{-1}	1.35 ± 0.09	< 0.022	1.08 ± 0.09	< 1.12	0.960 ± 0.098	11.1 ± 0.6	< 0.107	< 0.107	< 0.022	< 0.022	0.219 ± 0.021	0.831 ± 0.075

Accuracy

The accuracy of the results obtained for essential and non-essential elements by MIP OES was evaluated by the digestion of two botanical SRMs (NIST 1572 and NIST 1575a) and further elemental determination by MIP OES. The results obtained are in Table III. No statistical differences (*t*-test, confidence level of 95%) were observed between found and certified values.

Table III. Results obtained for SRMs by MIP OES after wet digestion (mean ± standard deviation, n = 3)

Element	NIST 1572		NIST 1575a	
	Found value	Certified value	Found value	Certified value
Al, μg g^{-1}	96 ± 4	92 ± 15	630 ± 35	580 ± 30
B, μg g^{-1}	54.4 ± 2.4	n.i.	9.2 ± 0.3	9.6 ± 0.2
Ba, μg g^{-1}	17 ± 2	21 ± 3	5.7 ± 0.2	6.0 ± 0.2
Ca, % m m^{-1}	2.85 ± 0.19	3.15 ± 0.10	0.26 ± 0.02	0.25 ± 0.01
Cd, μg g^{-1}	< 0.14	0.03 ± 0.01	0.226 ± 0.022	0.233 ± 0.004
Co, μg g^{-1}	< 2.00	0.02[a]	< 2.00	0.061 ± 0.001
Cr, μg g^{-1}	0.5 ± 0.1	0.8 ± 0.2	< 0.4	0.3 – 0.5[a]
Cu, μg g^{-1}	15.5 ± 0.8	16.5 ± 1.0	2.5 ± 0.2	2.8 ± 0.2
Fe, μg g^{-1}	95 ± 18	90 ± 10	44 ± 2	46 ± 2
K, % m m^{-1}	1.53 ± 0.30	1.82 ± 0.06	0.425 ± 0.020	0.417 ± 0.007
Mg, % m m^{-1}	0.53 ± 0.04	0.58 ± 0.03	0.101 ± 0.011	0.106 ± 0.017
Mn, μg g^{-1}	21 ± 2	23 ± 2	442 ± 40	488 ± 12
Mo, μg g^{-1}	< 0.26	0.17 ± 0.09	0.300 ± 0.052	n.i.
Na, μg g^{-1}	134 ± 15	160 ± 20	65 ± 3	63 ± 1
Ni, μg g^{-1}	< 3.7	0.6 ± 0.3	< 3.73	1.47 ± 0.10
Pb, μg g^{-1}	12.0 ± 3.1	13.3 ± 2.4	< 2.20	0.167 ± 0.015
Sr, μg g^{-1}	88 ± 19	100 ± 2	6.01 ± 0.22	n.i.
Zn, μg g^{-1}	28 ± 2	29 ± 2	42 ± 2	38 ± 2

n.i. = not informed.

In addition, the accuracy was evaluated by comparing the results obtained for essential and non-essential elements in dietary supplements by MIP OES with those by ICP OES. The results obtained for one sample of each dietary supplement class analyzed are shown in Table S6 (Supplementary Material), and it is possible to see that they presented no statistical differences (*t*-test, confidence level of 95%). It is important to mention that the minimum dilution factor performed by MIP OES was the same used for ICP OES, impairing the LOQ.

CONCLUSIONS

In this work, the suitability of MIP OES for the determination of essential and non-essential elements in dietary supplements was evaluated. The study of non-spectral interferences demonstrated relatively

good robustness of MIP OES for elevated concentrations of carbon and sulfur since few elements were impacted and in this case for relatively high concentration of interferent (5000 mg L^{-1}). On the other hand, the study showed the great influence of EIEs on the measurements by MIP-OES. Signal suppression or enhancement effects were observed for several elements operating with a concentration from 250 mg L^{-1} of sodium, potassium, or calcium. Taking into account the high concentration of these elements normally found in dietary supplements, a minimum dilution factor should be employed to guarantee a free-interference response and reliable results by MIP OES. This directly impacts the LOQs, making difficult the determination of elements with lower concentrations.

Based on this study, it was possible to determine several essential and non-essential elements in dietary supplements by MIP OES. The accuracy was demonstrated using SRMs, and no statistical difference was observed between found and certified values (*t*-test). Thereby, the results demonstrated the feasibility of MIP OES for the quality control of metals, added as a supplier or present as elemental contaminants in dietary supplements.

Conflicts of interest

The authors declare that there is no conflict of interest regarding the publication of this article.

Acknowledgements

The authors are grateful to “Coordenação de Aperfeiçoamento de Pessoal de Nível Superior” (CAPES, Gustavo R. Bitencourt Process 88887.319221/2019-00) (Finance code 001), “Conselho Nacional de Desenvolvimento Científico e Tecnológico” (CNPq, Thaís S. Berón Process 130092/2021-5), Chemical Abstract Service (CAS) and Chemical & Engineering News (C&EN) (Brazilian Women in Chemistry and Related Sciences Award 2020 – Paola A. Mello) for supporting this study.

REFERENCES

(1) Camire, M. E.; Kantor, M. A. Dietary Supplements: Nutritional and Legal Considerations. *Food Technol.* **1999**, *53* (7), 87–96. https://www.ift.org/news-and-publications/food-technology-magazine/issues/1999/july/features/scientific-status-summary (accessed in 2022-03-15).

(2) Smichowski, P.; Londonio, A. The Role of Analytical Techniques in the Determination of Metals and Metalloids in Dietary Supplements: A Review. *Microchem. J.* **2018**, *136*, 113–120. https://doi.org/10.1016/j.microc.2016.11.007

(3) Chellan, P.; Sadler, P. J. The Elements of Life and Medicines. *Philos. Trans. R. Soc. A Math. Phys. Eng. Sci.* **2015**, *373* (2037). https://doi.org/10.1098/rsta.2014.0182

(4) Costa, J. G.; Vidovic, B.; Saraiva, N.; do Céu Costa, M.; Del Favero, G.; Marko, D.; Oliveira, N. G.; Fernandes, A. S. Contaminants: A Dark Side of Food Supplements? *Free Radic. Res.* **2019**, *53*, 1113–1135. https://doi.org/10.1080/10715762.2019.1636045

(5) Krejčová, A.; Kahoun, D.; Černohorský, T.; Pouzar, M. Determination of Macro and Trace Element in Multivitamins Preparations by Inductively Coupled Plasma Optical Emission Spectrometry with Slurry Sample Introduction. *Food Chem.* **2006**, *98* (1), 171–178. https://doi.org/10.1016/j.foodchem.2005.06.022

(6) Pereira, R. M.; Crizel, M. G.; La Rosa Novo, D.; dos Santos, C. M. M.; Mesko, M. F. Multitechnique Determination of Metals and Non-Metals in Sports Supplements after Microwave-Assisted Digestion Using Diluted Acid. *Microchem. J.* **2019**, *145*, 235–241. https://doi.org/10.1016/j.microc.2018.10.043

(7) Rzymski, P.; Budzulak, J.; Niedzielski, P.; Klimaszyk, P.; Proch, J.; Kozak, L.; Poniedziałek, B. Essential and Toxic Elements in Commercial Microalgal Food Supplements. *J. Appl. Phycol.* **2019**, *31* (6), 3567–3579. https://doi.org/10.1007/s10811-018-1681-1

(8) Neher, B. D.; Azcarate, S. M.; Camiña, J. M.; Savio, M. Nutritional Analysis of Spirulina Dietary Supplements: Optimization Procedure of Ultrasound-Assisted Digestion for Multielemental Determination. *Food Chem.* **2018**, *257*, 295–301. https://doi.org/10.1016/j.foodchem.2018.03.011

(9) Müller, A.; Pozebon, D.; Dressler, V. L. Advances of Nitrogen Microwave Plasma for Optical Emission Spectrometry and Applications in Elemental Analysis: A Review. *J. Anal. At. Spectrom.* **2020**, *35* (10), 2113–2131. https://doi.org/10.1039/d0ja00272k
(10) Berg, I.; Karlsson, S. Validation of MP-AES at the Quantification of Trace Metals in Heavy Matrices with Comparison of Performance to ICP-MS. Bachelor Diploma, Örebro University. School of Science and Technology. **2015**.
(11) Baranyai, E.; Tóth, C. N.; Fábián, I. Elemental Analysis of Human Blood Serum by Microwave Plasma—Investigation of the Matrix Effects Caused by Sodium Using Model Solutions. *Biol. Trace Elem. Res.* **2020**, *194* (1), 13–23. https://doi.org/10.1007/s12011-019-01743-1
(12) Serrano, R.; Grindlay, G.; Gras, L.; Mora, J. Evaluation of Calcium-, Carbon- and Sulfur-Based Non-Spectral Interferences in High-Power MIP-OES: Comparison with ICP-OES. *J. Anal. At. Spectrom.* **2019**, *34* (8), 1611–1617. https://doi.org/10.1039/c9ja00148d
(13) Fontoura, B. M.; Jofré, F. C.; Williams, T.; Savio, M.; Donati, G. L.; Nóbrega, J. A. Is MIP-OES a Suitable Alternative to ICP-OES for Trace Element Analysis? *J. Anal. At. Spectrom.* **2022**, *37* (5), 966–984. https://doi.org/10.1039/D1JA00375E
(14) Zhang, Z.; Wagatsuma, K. Matrix Effects of Easily Ionizable Elements and Nitric Acid in High-Power Microwave-Induced Nitrogen Plasma Atomic Emission Spectrometry. *Spectrochim. Acta - Part B At. Spectrosc.* **2002**, *57* (8), 1247–1257. https://doi.org/10.1016/S0584-8547(02)00049-6
(15) Serrano, R.; Grindlay, G.; Gras, L.; Mora, J. Insight into the Origin of Carbon Matrix Effects on the Emission Signal of Atomic Lines in Inductively Coupled Plasma Optical Emission Spectrometry. *Spectrochim. Acta - Part B At. Spectrosc.* **2021**, *177*, 106070. https://doi.org/10.1016/j.sab.2021.106070
(16) Grindlay, G.; Gras, L.; Mora, J.; de Loos-Vollebregt, M. T. C. Carbon-Related Matrix Effects in Inductively Coupled Plasma Atomic Emission Spectrometry. *Spectrochim. Acta Part B At. Spectrosc.* **2008**, *63* (2), 234–243. https://doi.org/10.1016/j.sab.2007.11.024
(17) Grindlay, G.; Gras, L.; Mora, J.; de Loos-Vollebregt, M. T. C. Carbon-, Sulfur-, and Phosphorus-Based Charge Transfer Reactions in Inductively Coupled Plasma–Atomic Emission Spectrometry. *Spectrochim. Acta Part B At. Spectrosc.* **2016**, *115*, 8–15. https://doi.org/10.1016/j.sab.2015.10.010
(18) Muller, A. L. H.; Oliveira, J. S. S.; Mello, P. A.; Muller, E. I.; Flores, E. M. M. Study and Determination of Elemental Impurities by ICP-MS in Active Pharmaceutical Ingredients Using Single Reaction Chamber Digestion in Compliance with USP Requirements. *Talanta* **2015**, *136*, 161–169. https://doi.org/10.1016/j.talanta.2014.12.023
(19) Avula, B.; Wang, Y. H.; Smillie, T. J.; Duzgoren-Aydin, N. S.; Khan, I. A. Quantitative Determination of Multiple Elements in Botanicals and Dietary Supplements Using ICP-MS. *J. Agric. Food Chem.* **2010**, *58* (16), 8887–8894. https://doi.org/10.1021/jf101598g
(20) JGCM. Evaluation of Measurement Data — Guide to the Expression of Uncertainty in Measurement; JGCM 100:2008; Bureau International Des Poids et Mesures. **2008**. https://www.bipm.org/documents/20126/2071204/JCGM_100_2008_E.pdf/cb0ef43f-baa5-11cf-3f85-4dcd86f77bd6 (accessed in 2022-04-21).
(21) Agatemor, C.; Beauchemin, D. Matrix Effects in Inductively Coupled Plasma Mass Spectrometry: A Review. *Anal. Chim. Acta* **2011**, *706* (1), 66–83. https://doi.org/10.1016/j.aca.2011.08.027
(22) Grindlay, G.; Mora, J.; de Loos-Vollebregt, M.; Vanhaecke, F. A Systematic Study on the Influence of Carbon on the Behavior of Hard-to-Ionize Elements in Inductively Coupled Plasma–Mass Spectrometry. *Spectrochim. Acta Part B At. Spectrosc.* **2013**, *86*, 42–49. https://doi.org/10.1016/j.sab.2013.05.002
(23) Chan, G. C.-Y.; Chan, W.-T. Plasma-Related Matrix Effects in Inductively Coupled Plasma—Atomic Emission Spectrometry by Group I and Group II Matrix-Elements. *Spectrochim. Acta Part B At. Spectrosc.* **2003**, *58* (7), 1301–1317. https://doi.org/10.1016/S0584-8547(03)00055-7

(24) Todolí, J.-L.; Mermet, J.-M. Acid Interferences in Atomic Spectrometry: Analyte Signal Effects and Subsequent Reduction. *Spectrochim. Acta Part B At. Spectrosc.* **1999**, *54* (6), 895–929. https://doi.org/10.1016/S0584-8547(99)00041-5
(25) U. S. Pharmacopeia (USP) General Chapter <2232> Elemental Contaminants in Dietary Supplements. **2012**. https://www.uspnf.com/sites/default/files/usp_pdf/EN/USPNF/elemental_contaminants_in_dietary_supplements_m5291_3-26-2012.pdf (accessed in 2022-03-27).
(26) E. U. Comission Regulation (EC) No 629/2008. Amending Regulation (EC) No 1881/2006 Setting Maximum Levels for Certain Contaminants in Foodstuffs. Official Journal of the European Union. **2008**. https://eur-lex.europa.eu/legal-content/EN/TXT/PDF/?uri=CELEX:32008R0629&from=EN (accessed in 2022-03-27).
(27) ICH. ICH Guideline Q3D (R1): Guideline for Elemental Impurities. **2019**. https://www.ich.org/fileadmin/Public_Web_Site/ICH_Products/Guidelines/Quality/Q3D/Q3D-R1EWG_Document_Step4_Guideline_2019_0322.pdf (accessed in 2022-08-15).
(28) IUPAC. IUPAC Compendium on Analytical Nomenclature, Definitive Rules 1997. **1998**. https://media.iupac.org/publications/analytical_compendium/ (accessed in 2022-08-15).

SUPPLEMENTARY MATERIAL

Table S1. Classification, sample code, dosage form, active ingredients, and origin of dietary supplements used in this study

Classification	Sample code	Dosage form	Active ingredientes	Origin
Vitamins and minerals	VM-1	Tablet	Vitamins A, B1, B2, B3, B5, B6, B7, B9, B12, C, D3, and K, MgO, Cr, Cu, Mb, Mn, Se, and Zn	Brazil
Vitamins and minerals	VM-2	Tablet	Vitamins A, B1, B2, B3, B6, B9, B12, C, and D, $FeSO_4$, $ZnSO_4$, $MnSO_4$, and calcium D-pantothenate	Brazil
Vitamins and minerals	VM-3	Tablet	Vitamins A, B1, B2, B5, B6, B7, B9, B12, C, D3, E, and K, $CaCO_3$, $C_4H_2FeO_4$, KI, MgO, ZnO, Na_2Se, $CuSO_4$, $MgSO_4$, $CrCl_3$, and Na_2MoO_4	USA
Vitamins and minerals	VM-4	Capsule	Vitamins D3 and E, oyster shell $CaCO_3$, $C_4H_8N_2MgO_4$, $Zn(C_2H_4NO_2)_2$, $C_5H_{11}NO_2Se$, and SiO_2	Brazil
Minerals	MN-1	Tablet	$CaCO_3$, MgO, $ZnSO_4$, $C_8H_9NaO_7$, $C_{18}H_{36}O_2$, TiO_2, and $MgSiO_3$	USA
Minerals	MN-2	Capsule	Calcium amino acid chelate, KH_2PO_4, KI, magnesium amino acid chelate, zinc amino acid chelate, $C_5H_{11}NO_2Se$, copper amino acid chelate, manganese amino acid chelate, $Cr(C_6H_4NO_2)_3$, Mo, KCl, H_3BO_3, vanadium amino acid chelate, glutamic acid, rice protein, parsley leaf, alfalfa leaf, horsetail, watercress, dandelion root, yellow dock root, and chamomile	USA
Amino acids	AM-1	Powder	Creatine monohydrate	Brazil
Amino acids	AM-2	Powder	Taurine, vitamins B6, B12, and PP, Beta-5 (*beta vulgaris L.*, powdered beet, and vitamin B5), NO2Drive (watermelon pulp, vitamin B2, vitamin B3, and calcium L-ascorbate), glucuronolactone, and caffeine	Brazil
Amino acids	AM-3	Capsule	L-leucine, L-isoleucine, and L-valine	Brazil
Amino acids	AM-4	Capsule	L-theanine	USA
Botanicals	BT-1	Capsule	Ginseng extract (*panax ginseng*), rice bran, and oat fiber	USA
Botanicals	BT-2	Capsule	Guarana (*paullinia cupana*) and açaí (*euterpe oleracea*) flavoring, catuaba (*anemopaegma mirandum*), cocoa (*theobroma cacao*), and ginseng (*panax ginseng*) extracts, vitamins A, B1, B2, B3, B5, B6, B9, B12, C, E and K2, Cu, Fe, Cr, Mn, Mo, Se, and Zn	Brazil

Table S2. Operational conditions for elemental determination by ICP OES

Parameter	ICP OES
RF power (W)	1400
Plasma gas flow-rate (L min^{-1})	15
Auxiliary gas flow-rate (L min^{-1})	0.2
Nebulizer gas flow-rate (L min^{-1})	0.7
Spray chamber, type	Cyclonic double-pass (Scott)
Nebulizer, type	Cross-flow
Analytes	Wavelength (nm)
Ag	328.068 (I)
Al	167.078 (II)
B	249.677 (I)
Ba	233.527 (II)
Be	234.861 (I)
C	193.030 (I)
Ca	396.847 (II)
Cd	228.802 (I)
Co	238.892 (II)
Cr	205.552 (II)
Cu	327.396 (I)
Fe	259.941 (II)
K	766.491 (I)
La	408.672 (II)
Li	670.780 (I)
Mg	280.270 (II)
Mn	259.373 (II)
Mo	202.095 (II)
Na	589.592 (I)
Ni	231.604 (II)
Pb	220.353 (II)
S	182.034 (I)
Sr	407.771 (II)
V	292.464 (II)
Y[a]	371.029 (II)
Zn	213.856 (I)

[a]Used as internal standard for the determination of C.

(I) Atomic emission line; (II) Ionic emission line.

Table S3. Wavelength and excitation + ionization energy (E_{sum}) values of the lines determined by MIP OES in this study

Element	Wavelength, nm	E_{sum}[a], eV
K	769.897 (I)	1.61
Li	670.784 (I)	1.85
Na	589.592 (I)	2.10
Mn	403.307 (I)	3.07
V	437.923 (I)	3.13
Al	396.152 (I)	3.14
Mo	386.410 (I)	3.21
Cr	357.868 (I)	3.46
Ag	328.068 (I)	3.78
Cu	327.395 (I)	3.78
Ni	361.939 (I)	3.85
Co	345.351 (I)	4.02
Mg	285.213 (I)	4.35
Pb	283.305 (I)	4.37
B	249.772 (I)	4.96
Be	234.861 (I)	5.28
Cd	228.802 (I)	5.42
Zn	213.857 (I)	5.80
Ba	493.408 (II)	7.72
La	433.374 (II)	8.61
Sr	407.771 (II)	8.74
Ca	396.847 (II)	9.23
Fe	259.940 (II)	12.64

[a]E_{sum} = excitation + ionization energy.

Table S4. Determination of common concomitants in dietary supplements by MIP OES (mean ± standard deviation, n = 3)

Samples	C[a], mg L^{-1}	S[a], mg L^{-1}	Na[a], mg L^{-1}	K[a], mg L^{-1}	Ca[a], mg L^{-1}	Residual acidity[b], %
VM-1	124 ± 23	51.2 ± 2.7	22.6 ± 0.3	8.64 ± 0.26	4224 ± 219	30 ± 1
VM-2	179 ± 6	300 ± 27	11.7 ± 0.3	1.27 ± 0.16	19.3 ± 0.7	26 ± 1
VM-3	129 ± 15	189 ± 2	90.5 ± 0.4	9.03 ± 0.07	11049 ± 12	15 ± 1
VM-4	16.6 ± 0.3	28.2 ± 1.0	111 ± 14	3.08 ± 0.37	8775 ± 905	29 ± 1
MN-1	11.1 ± 2.4	128 ± 7	128 ± 7	13.7 ± 0.6	15851 ± 589	15 ± 4
MN-2	16.9 ± 4.4	34.6 ± 2.6	28.3 ± 6.0	532 ± 12	11143 ± 750	17 ± 3
AM-1	50.6 ± 3.3	< 0.510	6.27 ± 0.11	0.046 ± 0.001	0.733 ± 0.008	60 ± 1
AM-2	50.3 ± 2.6	307 ± 25	15.5 ± 0.2	0.416 ± 0.007	2.02 ± 0.03	59 ± 1
AM-3	44.0 ± 4.0	13.3 ± 0.3	13.8 ± 0.4	0.120 ± 0.005	3.03 ± 0.05	24 ± 1
AM-4	50.8 ± 7.8	4.33 ± 0.07	9.44 ± 0.14	13.2 ± 0.1	0.215 ± 0.021	27 ± 2
BT-1	53.7 ± 2.0	17.5 ± 0.5	24.9 ± 1.4	122 ± 4	9.03 ± 0.25	27 ± 2
BT-2	43.5 ± 3.6	34.0 ± 1.9	7.75 ± 0.54	239 ± 38	2369 ± 364	29 ± 3

Determined by [a]ICP OES and [b]potentiometric titration.

Table S5. Limits of quantification (LOQs) obtained by MIP OES in this work

Element, μg g^{-1}	Vitamins and minerals				Minerals		Amino acids		Botanicals	
	VM-1	VM-2	VM-3	VM-4	MN-1	MN-2	AM-1 and AM-2	AM-3 and AM-4	BT-1	BT-2
Sample mass	800	600	1600	600	1300	1300	500	600	600	600
Minimum dilution factor	20	no	50	50	50	50	4	no	no	10
Ag	3.13	0.208	3.91	10.4	4.81	4.81	1.00	0.208	0.208	2.08
Al	198	13.1	247	658	304	304	63.2	13.1	13.1	132
B	12.4	0.826	15.5	41.3	19.1	19.1	3.97	0.826	0.826	8.26
Ba	1.80	0.120	2.25	6.00	2.77	2.77	0.576	0.120	0.120	1.20
Be	0.356	0.024	0.445	1.19	0.547	0.547	0.114	0.024	0.024	0.240
Ca	555	37.0	694	1850	854	854	178	37.0	37.0	370
Cd	4.36	0.290	5.45	14.5	6.70	6.70	1.39	0.290	0.290	2.90
Co	62.6	4.17	78.2	209	96.2	96.2	20.0	4.17	4.17	41.7
Cr	2.47	0.165	3.09	8.24	3.80	3.80	0.791	0.165	0.165	1.65
Cu	6.82	0.455	8.53	22.7	10.5	10.5	2.18	0.455	0.455	4.55
Fe	15.1	1.01	18.9	50.4	23.3	23.3	4.84	1.01	1.01	10.1
K	173	11.5	216	576	266	266	55.3	11.5	11.5	115
La	0.552	0.037	0.690	1.84	0.850	0.850	0.177	0.037	0.037	0.370
Li	1.12	0.074	1.40	3.72	1.72	1.72	0.357	0.074	0.074	0.740
Mg	32.0	2.13	40.0	107	49.2	49.2	10.2	2.13	2.13	21.3
Mn	0.636	0.042	0.795	2.12	0.978	0.978	0.203	0.042	0.042	0.420
Mo	8.03	0.535	10.0	26.8	12.4	12.4	2.57	0.535	0.535	5.35
Na	103	6.88	129	344	159	159	33.0	6.88	6.88	68.8
Ni	116	7.76	146	388	179	179	37.3	7.76	7.76	77.6
Pb	68.9	4.59	86.1	230	106	106	22.0	4.59	4.59	45.9
Sr	5.06	0.338	6.33	16.9	7.79	7.79	1.62	0.338	0.338	3.38
V	0.335	0.022	0.419	1.12	0.516	0.516	0.107	0.022	0.022	0.220
Zn	40.5	2.70	50.6	135	62.3	62.3	13.0	2.70	2.70	27.0

Table S6. Results for VM-2, MN-2, AM-2, and BT-1 samples by MIP OES and ICP OES (mean ± standard deviation, n = 3)

Element	VM-2		MN-2		AM-2		BT-1	
	MIP OES	ICP OES	MIP OES	ICP OES	MIP OES	ICP OES	MIP OES	ICP OES
Ag, μg g^{-1}	< 0.208	< 0.115	< 4.81	< 2.65	< 1.00	< 0.551	< 0.208	< 0.115
Al, mg g^{-1}	0.073 ± 0.002	0.071 ± 0.001	0.073 ± 0.005	0.064 ± 0.004	< 63.2	< 91.1	316 ± 22	274 ± 19
B, μg g^{-1}	< 0.826	< 1.06	221 ± 18	264 ± 21	< 3.97	< 5.08	2.13 ± 0.07	2.04 ± 0.05
Ba, μg g^{-1}	0.292 ± 0.018	0.262 ± 0.013	18.1 ± 1.1	20.6 ± 1.3	< 0.576	< 0.426	1.11 ± 0.05	1.12 ± 0.06
Be, μg g^{-1}	< 0.024	< 0.025	< 0.547	< 0.587	< 0.114	< 0.122	< 0.024	< 0.025
Ca, mg g^{-1}	0.720 ± 0.026	0.763 ± 0.021	224 ± 20	226 ± 8	94.5 ± 3.7	101 ± 4	0.386 ± 0.013	0.378 ± 0.019
Cd, μg g^{-1}	< 0.290	< 0.161	< 6.70	< 3.72	< 1.39	< 0.774	< 0.290	< 0.161
Co, μg g^{-1}	< 4.17	3.48 ± 0.11	< 96.2	< 5.11	< 20.0	< 1.06	< 4.17	0.239 ± 0.007
Cr, μg g^{-1}	< 0.165	< 0.278	11.4 ± 0.6	11.6 ± 0.4	< 0.791	< 1.34	0.429 ± 0.007	0.417 ± 0.040
Cu, μg g^{-1}	< 0.455	< 0.278	110 ± 11	129 ± 7	< 2.18	< 1.69	2.56 ± 0.12	2.77 ± 0.21
Fe, mg g^{-1}	162 ± 1.7	158 ± 10	0.176 ± 0.010	0.170 ± 0.003	< 4.84	< 11.5	184 ± 11	192 ± 9
K, mg g^{-1}	0.054 ± 0.006	0.049 ± 0.007	12.1 ± 0.9	10.8 ± 0.4	< 55.3	20.8 ± 0.3	5.53 ± 0.22	5.11 ± 0.23
La, μg g^{-1}	< 0.037	< 0.075	< 0.850	< 1.73	< 0.177	< 0.359	< 0.037	< 0.075
Li, μg g^{-1}	< 0.074	< 1.50	0.610 ± 0.007	< 34.7	< 0.357	< 7.21	0.248 ± 0.009	< 1.50
Mg, mg g^{-1}	0.473 ± 0.032	0.512 ± 0.018	107 ± 8	111 ± 3	9.23 ± 0.70	8.44 ± 0.50	5.66 ± 0.26	5.56 ± 0.20
Mn, mg g^{-1}	3.49 ± 0.05	3.54 ± 0.03	0.792 ± 0.023	0.829 ± 0.027	0.326 ± 0.016	0.358 ± 0.024	65.2 ± 2.6	63.5 ± 2.6
Mo, μg g^{-1}	< 0.535	< 0.498	< 12.4	10.9 ± 0.9	< 2.57	< 2.39	< 0.535	< 0.498
Na, mg g^{-1}	0.390 ± 0.028	0.415 ± 0.031	0.416 ± 0.022	0.413 ± 0.011	791 ± 15	777 ± 22	1172 ± 79	1040 ± 67
Ni, μg g^{-1}	< 7.76	5.36 ± 0.57	< 179	< 51.2	< 37.3	< 10.6	< 7.76	< 2.22
Pb, μg g^{-1}	< 4.59	< 3.92	< 106	< 90.5	< 22.0	< 18.8	< 4.59	< 3.92
Sr, μg g^{-1}	< 0.338	< 0.349	66.7 ± 3.1	69.9 ± 4.4	< 1.62	< 1.68	1.75 ± 0.12	1.96 ± 0.10
V, μg g^{-1}	< 0.022	< 0.366	11.1 ± 0.6	12.3 ± 1.5	< 0.107	< 1.76	0.219 ± 0.021	< 0.366
Zn, mg g^{-1}	3.45 ± 0.18	3.22 ± 0.12	3.12 ± 0.17	3.21 ± 0.16	< 13.0	< 11.8	20.2 ± 0.6	21.3 ± 0.9

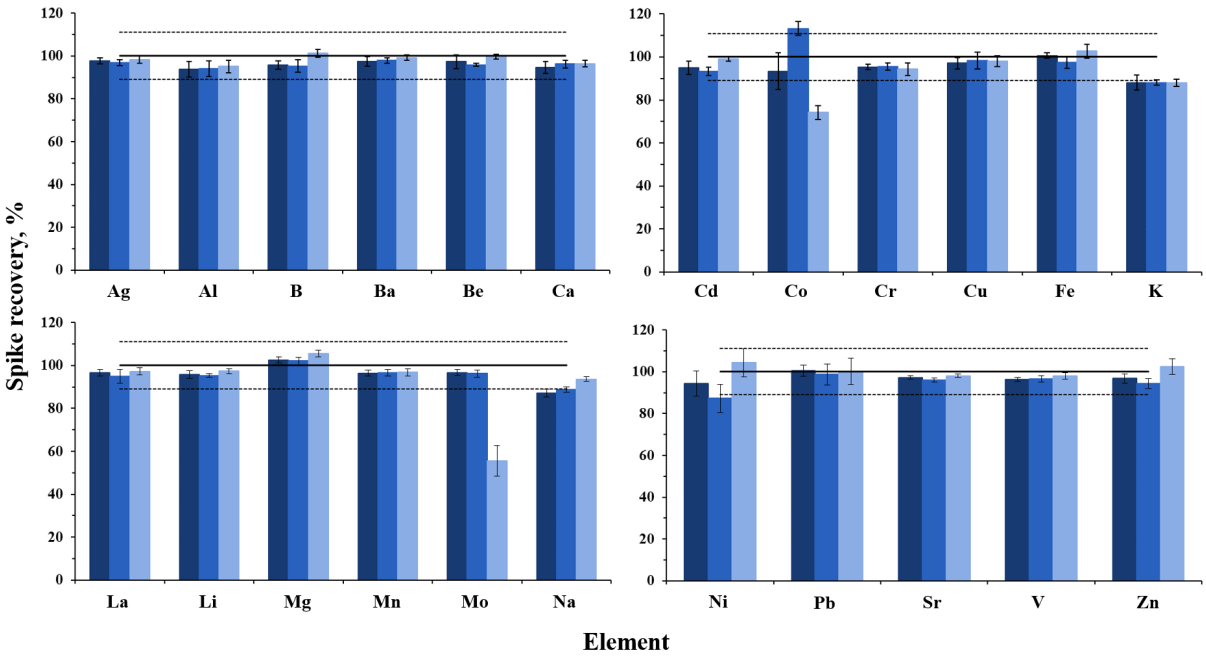

Figure S1. Spike recoveries obtained for metals (100 µg L^{-1}) with 25 (■), 250 (■), and 5000 mg L^{-1} (■) of carbon (as citric acid) by MIP OES. Continuous and dashed lines represents the reference value (100%) and the expanded uncertainty, respectively.

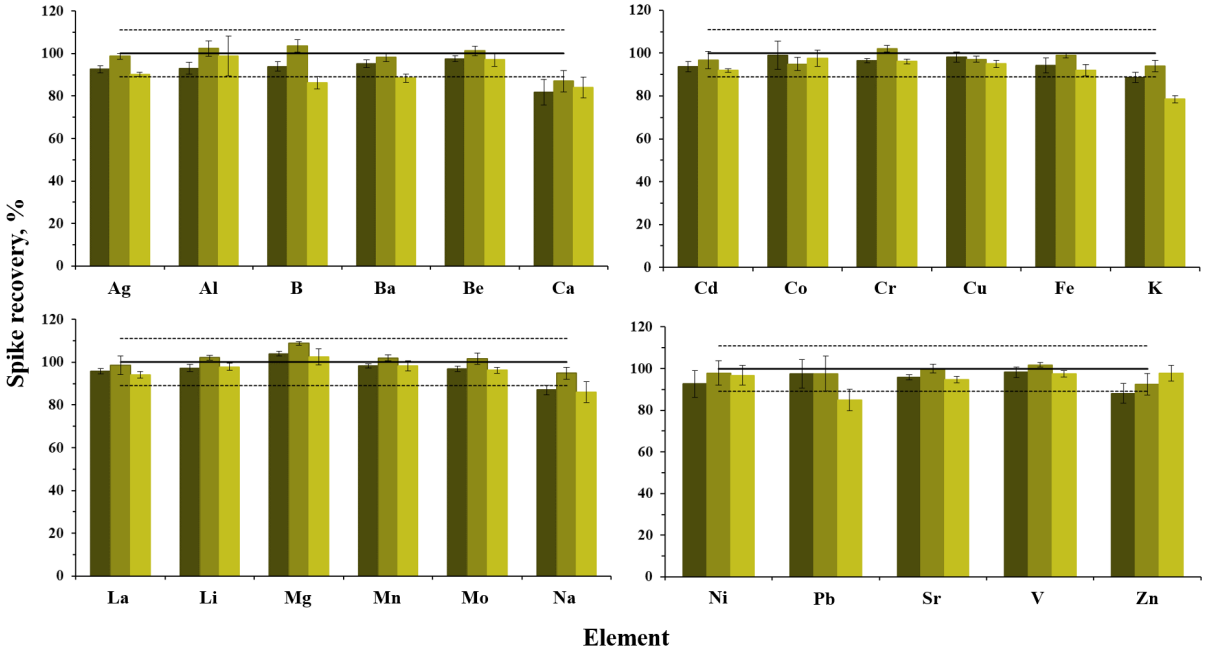

Figure S2. Spike recoveries obtained for metals (100 µg L^{-1}) with 25 (■), 250 (■), and 5000 mg L^{-1} (■) of sulfur (as sulfuric acid) by MIP OES. Continuous and dashed lines represents the reference value (100%) and the expanded uncertainty, respectively.

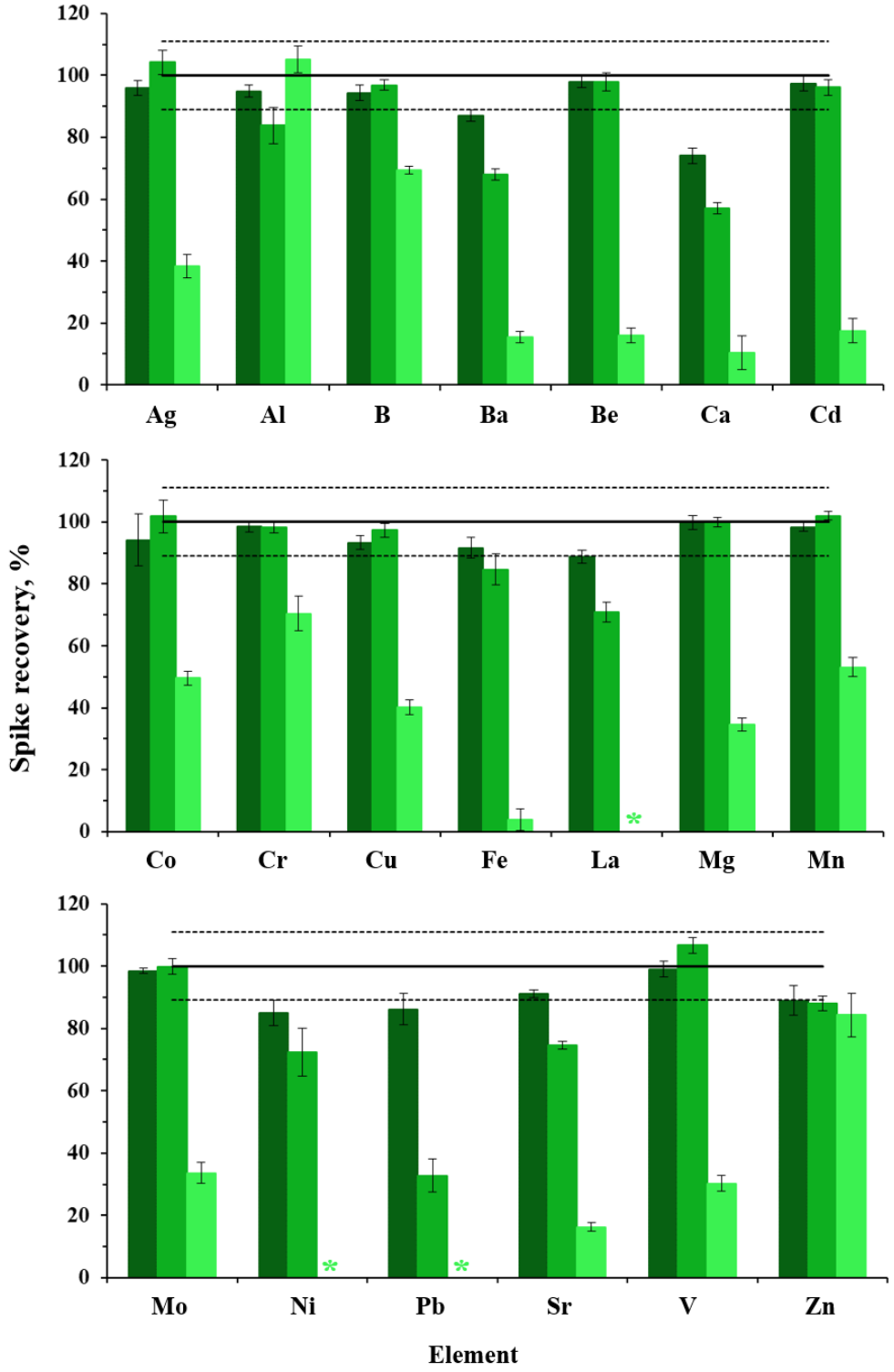

Figure S3. Spike recoveries obtained for metals (100 µg L^{-1}) with 25 (■), 250 (■), and 5000 mg L^{-1} (■) of sodium (as sodium nitrate) by MIP OES. Continuous and dashed lines represents the reference value (100%) and the expanded uncertainty, respectively. *Total signal suppression.

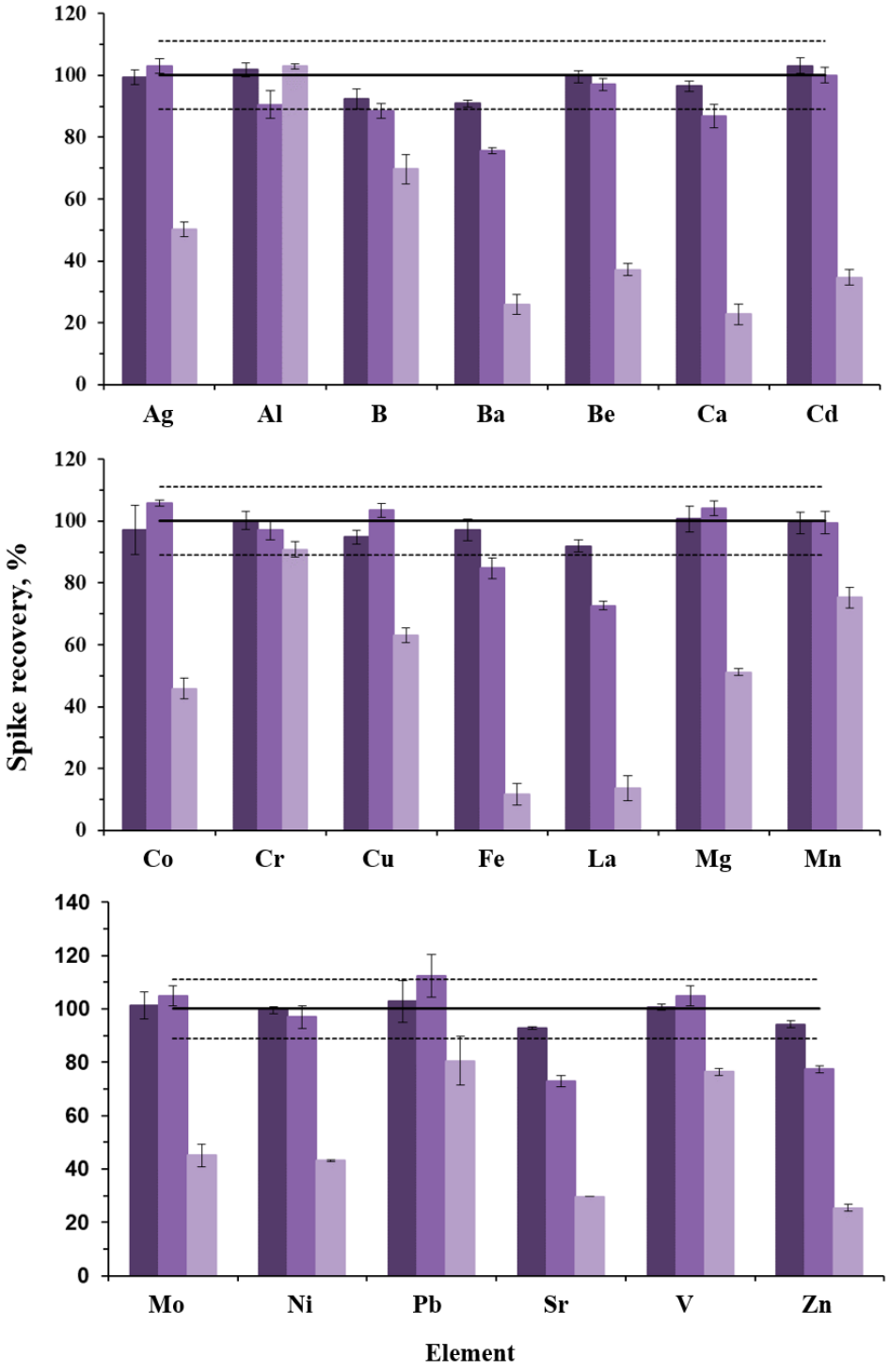

Figure S4. Spike recoveries obtained for metals (100 µg L^{-1}) with of 25 (■), 250 (■), and 5000 mg L^{-1} (■) of potassium (as potassium nitrate) by MIP OES. Continuous and dashed lines represents the reference value (100%) and the expanded uncertainty, respectively.

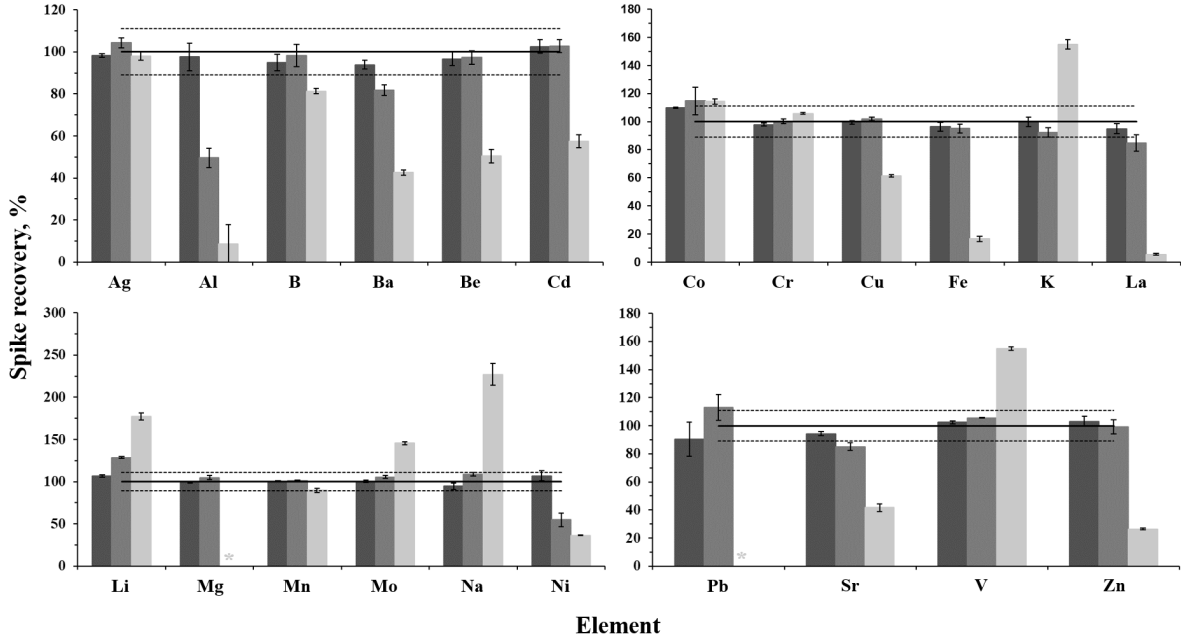

Figure S5. Spike recoveries obtained for metals (100 µg L^{-1}) with 25 (■), 250 (■), and 5000 mg L^{-1} (■) of calcium (as calcium nitrate) by MIP OES. Continuous and dashed lines represents the reference value (100%) and the expanded uncertainty, respectively. *Total signal suppression.

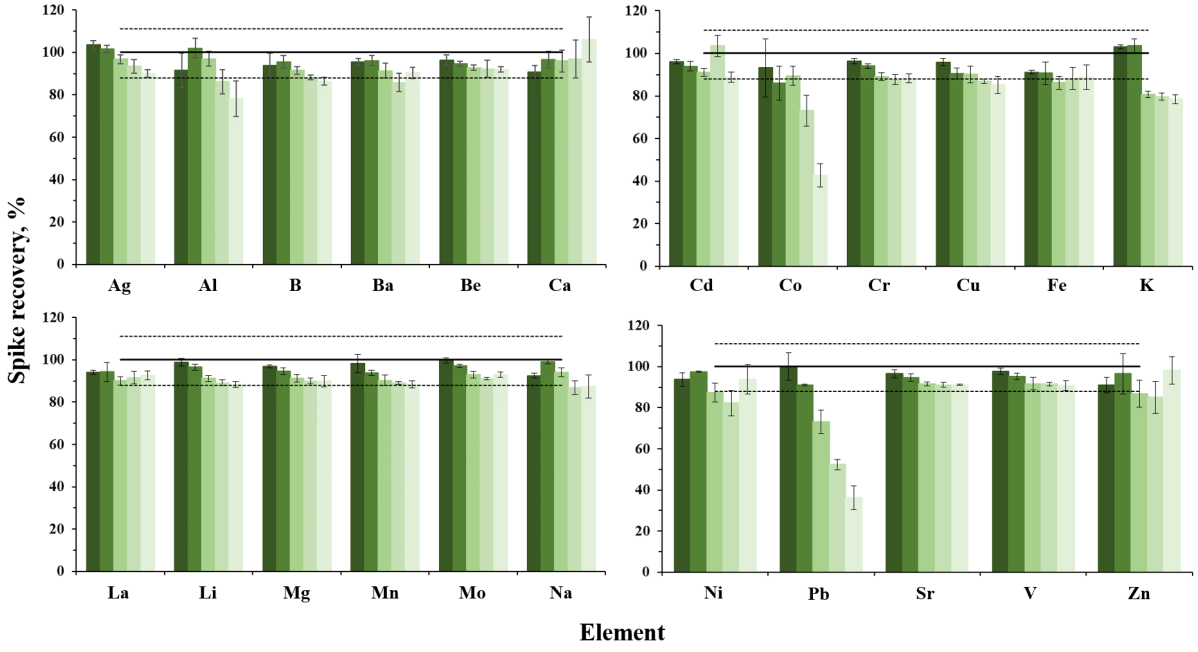

Figure S6. Spike recoveries obtained for metals (100 µg L^{-1}) with residual HNO_3 acidity at 10 (■), 20 (■), 30 (■), 40 (■), and 50% v v^{-1} HNO_3 (■) by MIP OES. Continuous and dashed lines represents the reference value (100%) and the expanded uncertainty, respectively.

Brazilian Journal of Analytical Chemistry
2023, Volume 10, Issue 40, pp 158-169
doi: 10.30744/brjac.2179-3425.AR-130-2022

BrJAC

ARTICLE

In Vitro Bioaccessibility of Cd, Cu, Fe and Zn in Basil (*Ocimum basilicum* L. Grecco a palla) after Cadmium Intoxication

Sofia da S. Martins[1], Giselle V. de Sousa[1,2], Vânia de Lourdes G. Teles[1,3], Letícia M. Costa*[1]

[1]LEAQUAA, Universidade Federal de Minas Gerais, Instituto de Ciências Exatas, Departamento de Química, Av. Presidente Antônio Carlos, 6627, Pampulha, PO Box 702, CEP 31270-901, Belo Horizonte, MG, Brazil.
[2]LASP, Instituto de Ciências Biológicas, Universidade Federal de Viçosa, 35570-00, Florestal, MG, Brazil
[3]Centro de Tecnologia da Universidade Federal de Alagoas, Av. Lourival Melo Mota, S/N,Tabuleiro do Martins Maceió, AL, Brazil

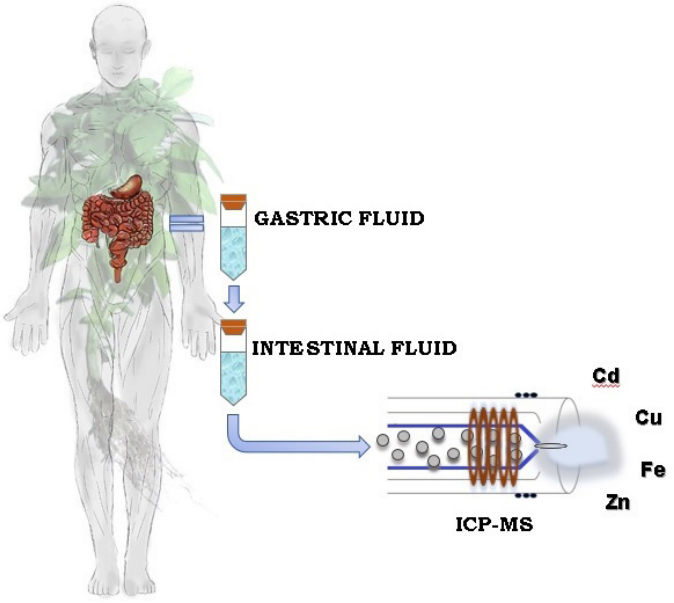

Cadmium is a toxic element which can be accumulated in the edible parts of plants compromising an entire food chain with serious damage to the living organisms, presenting synergistic and antagonistic effects with the elemental bioaccessibility. In this work, a simulated gastrointestinal digestion was performed to assess the *in vitro* bioaccessibility of Cd, Cu, Fe and Zn in basil samples after Cd intoxication. The hydroponic cultivation was made in a Hoagland solution at different concentrations (0, 1.5 and 3.0 μmol L^{-1}). Elemental concentration was achieved using a microwave-assisted acid digestion after the growing up of the plants in vermiculite pots by 15 days. The *in vitro* gastrointestinal procedure was applied in fresh and lyophilized leaves followed by a clean-up step in a sonoreactor cup horn using 1 mL of the extract, 100 μL of HNO_3 and 500 μL of H_2O_2 by 5 minutes. The results showed that Cd bioaccessibility was statistically different at 95% confidence level ($p < 0.05$) for the lyophilized and fresh leaves samples. The *in vitro* bioaccessibility increased with concentration in the contamination treatment. Moreover, a high positive correlation was observed between Cd-Fe and Cu-Zn, and a negative correlation between Cd-Zn and Fe-Zn in lyophilized and fresh leaves, respectively, suggesting that the absorption of essential elements was affected by Cd.

Cite: Martins, S. S.; de Sousa, G. V.; Teles, V. L. G.; Costa, L. M. *In Vitro* Bioaccessibility of Cd, Cu, Fe and Zn in Basil (*Ocimum basilicum* L. Grecco a palla) after Cadmium Intoxication. *Braz. J. Anal. Chem.* 2023, *10* (40), pp 158-169. http://dx.doi.org/10.30744/brjac.2179-3425.AR-130-2022

Submitted 16 January 2023, Resubmitted 24 March 2023, Accepted 27 April 2023, Available online 02 June 2023.

Keywords: gastrointestinal digestion, toxic metal, hydroponic cultivation, basil leaves

INTRODUCTION

Cadmium is the third major contaminant in the environment, after Hg and Pb. It can be accumulated in edible parts of plants, and its bioaccumulation in the food chain is highly dangerous to all living organisms with negative long-time effects on human health.[1–3] Some foodstuffs, such as green leaves vegetables, fish and meat, may accumulate different levels of cadmium,[4] which is mainly reabsorbed in the human body by gastrointestinal, pulmonary and dermal systems.[1]

In plant tissues, several metal transporters and channels are involved into Cd reaching the root cells until its final accumulation in the edible parts, even when the element is present at low concentration.[3,5-7] Basil can uptake Cd from soil and water through their root cells, translocate and accumulate in the aerial part that contains edible parts for animals and humans.[6,8] Despite the fact that Cd is a non-essential element for plants, it can influence the uptake of nutrients.

Aerial parts of *Ocimum basilicum* L. are employed as a vegetable source for human consumption given their nutritional value in terms of natural minerals, trace elements and several characteristics of the herb, such as antioxidant, anti-aging, anti-inflammatory, anticarcinogenic, antimicrobial, cardiovascular, among others.[9] The economic relevance and global spread of basil is due to its multiple uses in cooking of different countries, both in its natural and dehydrated form, and in folk medicine and as essential oil in the cosmetic industry.[10–12]

Only a fraction of the mineral present in the food matrix is bioaccessible and can be absorbed by the human body.[13] Bioaccessibility is defined as the soluble fraction of a mineral that is released from its matrix food into the gastrointestinal tract, and refers to the maximum bioavailability and proportion of a contaminant ingested with food that is absorbed by the intestine, entering the systemic circulation with toxic effects.[14] It is typically evaluated by a sequential analysis with simulation digestion using artificial gastric and intestinal juices.[14,15] Recently, several studies have evaluated the bioaccessibility of mineral and trace elements by simulated gastrointestinal digestion in different food matrices, such as vegetables,[16–18] rice,[19,20] fruits,[21] yerba mate tea[22] and in rice.[23] The knowledge of the in vitro bioaccessibility of metals in vegetables is relevant for nutritional information and health risk assessment. The release of minerals in the gastrointestinal digestion process depends on different factors since in the aqueous solutions minerals with chemical similarities can compete for transport proteins or other uptake mechanisms, as well as for chelating organic substances, facilitating or hindering absorption.[24]

Therefore, it is pertinent to evaluate how bioaccessibility of toxic elements interfere with the absorption of nutrients by the human body during simulation of the gastrointestinal digestion. In this sense, the aim of this study was to investigate the influence of the lyophilized and fresh leaves of basil on the in vitro bioaccessibility of Cd, Cu, Fe and Zn, and the correlations established with Cd and these nutrients.

MATERIALS AND METHODS

Sample

Basil seeds (*Ocimum basilicum* Grecco a palla), purchased at a local market of Belo Horizonte, MG, Brazil, were germinated on Germitest paper for three days. Aluminium foil sheets with holes spaced at 2 cm were adapted into 1,000 mL pots to allocate the rootlets, which were cultivated in 5% v v^{-1} Hoagland nutrient solution.[25] Each pot contained thirteen seedlings, and their solutions were supplemented with 1, 1.5 and 3.0 µmol L^{-1} of Cd (as $Cd(NO_3)_2.4H_2O$) in triplicate. A control experiment was also performed without Cd supplementation. The nutrient solution and Cd supplementation were changed every 3 days, and after 15 days of hydroponic cultivation, the plants were transferred to vermiculite pots, irrigated daily with ultrapure water and kept on this substrate for another 15 days. Then, the leaves were harvested after 30 days of the beginning of the cultivation. Fresh leaves were split in two parts: one was used immediately while the other part was separated for freeze-drying.

Chemicals, materials and instrumentation

Reagents were of analytical grade, and all the solutions were prepared using ultrapure water (resistivity > 18.2 MΩ cm) obtained by a Direct-Q system (Millipore, SAS-67120, Malssheim, France). All glassware, plastic bottles and microwave vessels were cleaned overnight with 10% v v^{-1} HNO_3 and then washed with deionized water. Nitric acid (65% m m^{-1}) purified by a DuoPUR system (Milestone, Sorisole, Italy), and hydrogen peroxide (30% m m^{-1}) (Merck, Darmstadt, Germany) were used for the microwave digestion and ultrasound extraction. Hydrochloric acid (37% m m^{-1}, (Merck, Darmstadt, Germany), pepsin, pancreatin, bile salts, and sodium bicarbonate ($NaHCO_3$) employed in the in vitro gastrointestinal digestion were provided by Sigma- Aldrich.

A Milestone Ethos 1 − Advanced Microwave Digestion System oven (Sorisole, Italy) was employed for the basil leaves acid digestion. The leaves were frozen in a 0222E24, MODULYOD-230 Thermo Electron Corporation freeze-dryer (Asheville, USA) at 600 W. A thermostatic bath Dubnoff Quimis® (model 0226M2) and shaking table (model TS-2000ª VDRL SHAKER) were used in the in vitro gastrointestinal digestion procedure (IVG). All samples of IVG were pre-treated in a cup-horn ultrasonic processor (VCX 505, Sonic& Materials INC, USA), operating at 500W and 20 kHz before introduction in the ICP-MS.

An inductively coupled plasma mass spectrometer 7700 (Agilent Technology, Tokyo, Japan) was used for determination of Cd, Cu, Fe and Zn. A collision cell (He gas) was employed to correct isobaric interference and the instrumental parameters were: RF power 1.55 kW, plasma gas flow 15 L min^{-1}, auxiliar gas flow 1 L min^{-1}, nebulization gas flow 1.05 L min^{-1}, He flow rate in the collision cell 1.2 L min^{-1}, Micro-Mist nebulizer and Scott type – double pass nebulization chamber. The measurements were performed in He mode at an integration time, sweeps, replicates and resolution equal to 0.3 s, 100, 3 and <1, respectively. The monitored isotopes were ^{111}Cd, ^{63}Cu, ^{56}Fe and ^{66}Zn. Reference Cd, Cu, Fe and Zn solutions were prepared daily by an adequate dilution from a 10 µg mL^{-1} multi-element standard solution (ESI, M1-ICPMSE-100, USA). The calibration curve was prepared with six levels from 0 to 100 µg L^{-1} and 0 to 75 µg L^{-1} for microwave-assisted digestion and IVG, respectively.

Sample preparation

Fresh leaves from each plant were washed and dried on paper towels. For the total sample obtained for each Cd treatment (0, 1.5 and 3.0 µmol L^{-1}), 200 mg of fresh leaves were immediately subjected to IVG and the rest was frozen and lyophilized for at least 24 h. The lyophilized samples were weighed, macerated with mortar and pestle, and stored for the IVG and microwave-assisted acid digestion procedures.

Microwave-assisted acid digestion was used to determine the total concentration of the elements. A mass of 15 mg of leaves was weighed into PTFE-vessels in triplicate for each Cd treatment (0, 1.5 and 3.0 µmol L^{-1}). Volumes of 3.5 mL of HNO_3, 3.5 mL of H_2O and 1.0 mL of H_2O_2 were added separately to each vessel, which was submitted to a heating program in the microwave oven: 10 min until reached 165 °C, 20 min at 165 °C following by 30 min ventilation. Final volume was adjusted to 10 mL and the quantification was done by ICP-MS.

Determination of Cd, Cu, Fe and Zn bioaccessibility after the in vitro gastrointestinal digestion

The IVG simulation was developed according to the procedure described by the US Pharmacopeia.[26] The simulated gastric and intestinal solutions were daily prepared. The simulated gastric fluid was prepared by solubilization of 0.2 g of NaCl and 0.32 g of pepsin in deionized water, with subsequent addition of 0.7 mL of concentrated hydrochloric acid. The volume was filled up to 100 mL and the pH adjusted to 1.2.[15,27] The intestinal fluid was prepared by diluting 0.68 g of K_2HPO_4, 1 g of pancreatin, 1.25 g of bile salts and addition of 7.7 mL of NaOH 0.2 mol L^{-1}. Final volume was completed to 100 mL and the pH adjusted to 6.8 - 7.0 using 3% m v^{-1} $NaHCO_3$.[27]

3.5 mL of gastric fluid was added in 200 or 15 mg of fresh and lyophilized leaves, respectively. The mixture was submitted to slow stirring (approximately 60 rpm) at 37 °C in a thermostatic bath for 2 hours. Then, the tubes were transferred to an ice bath for 5 minutes in order to stop the enzymatic activity.

Subsequently, for intestinal digestion, 0.4 mL of $NaHCO_3$ + 3 mL of intestinal fluid was added to the gastric digest. Again, the solution was stirred in a thermostatic bath for 2 h at 37 °C, with constant stirring. [27]

Each assay was performed in triplicate (including blanks), and the final volume was adjusted to 10 mL using ultrapure water following centrifuged for 10 minutes at 10000 rpm at 4 °C. The clean-up step at sonoreactor cup horn was performed with 1 mL digested, 100 µL HNO_3 and 500 µL H_2O_2 by 5 minutes. Final volume was filled up to 2 mL with ultrapure water and the samples were centrifuged for 5 min at 12,000 rpm to prevent clogging of the ICP-MS nebulization system.

The following formula described by Leufroy (2012)[28] was adopted to obtain the percentage (%) of bioaccessibility of the elements:

$$\%\text{Bioaccessibility} = \left(\frac{\text{Fraction of element released}}{\text{Total element concentration}}\right) \text{x } 100$$

in which the fraction of the element released in the simulated digestion is compared to the total amount of the element.

Data treatment

The differences between bioaccessible fraction in lyophilized and fresh leaves for each Cd treatment were tested by a *t*-test ($p < 0.05$) using GraphPad Prism 5.01. The correlation plot for total concentration of elements in leaves and bioaccessibility were calculated by the software R[28] applying Pearson test with significance of regression for $p < 0.05$.

RESULTS AND DISCUSSION

The evaluated Cd concentrations (0, 1.5 and 3.0 µmol L^{-1}) were below the effective concentration that inhibits 50% of basil roots enhancement (EC_{50} = 3.6 µmol L^{-1} of Cd), as reported by Teles et al. (2022).[6] Previous studies reported bioaccumulation of Cd preferentially in the root, but the element can also be translocated until the leaves.[5,6,8]

To obtain samples with healthy aspects which would not be rejected by consumers, the samples were grown in vermiculite, an inert substrate, to complete the development cycle, after 15 days of hydroponic culture with Cd supplementation. Figure 1 (A, B and C) shows the seedlings at the end of 15 days in the hydroponic cultivation, while Figure 2 presents the samples after 30 days grown in vermiculite, respectively.

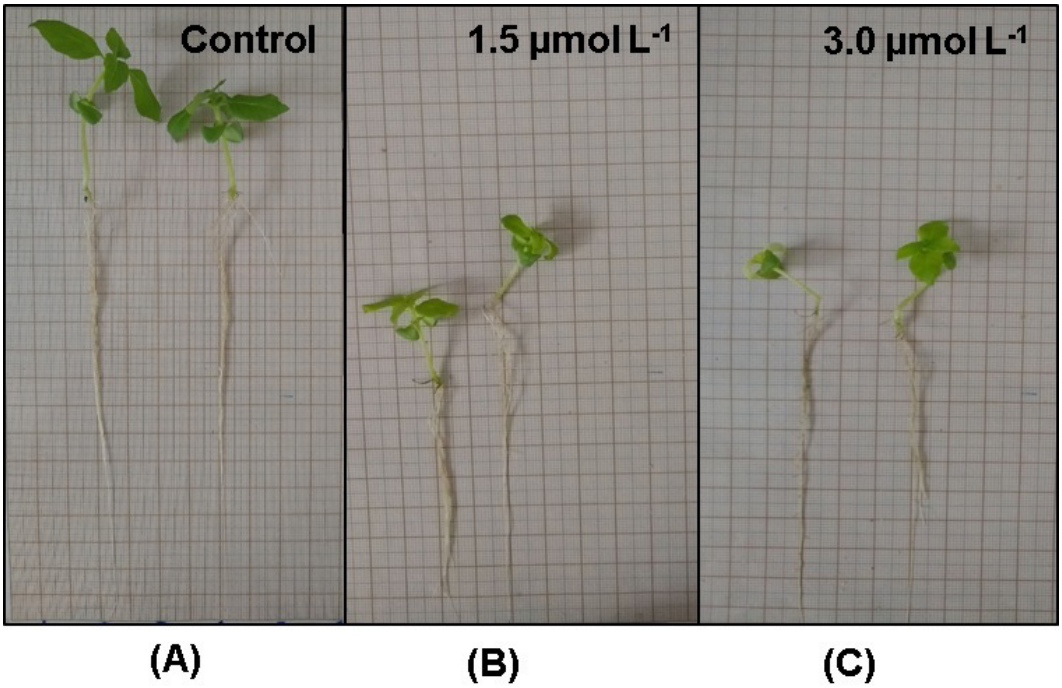

Figure 1. Basil samples after 15 days of hydroponic cultivation in Hoagland's solution and Cd supplementation at different concentrations 0 µmol L^{-1} - control (A), 1.0 µmol L^{-1} (B) and 3.0 µmol L^{-1} (C) for immediate transplanting into vermiculite substrate.

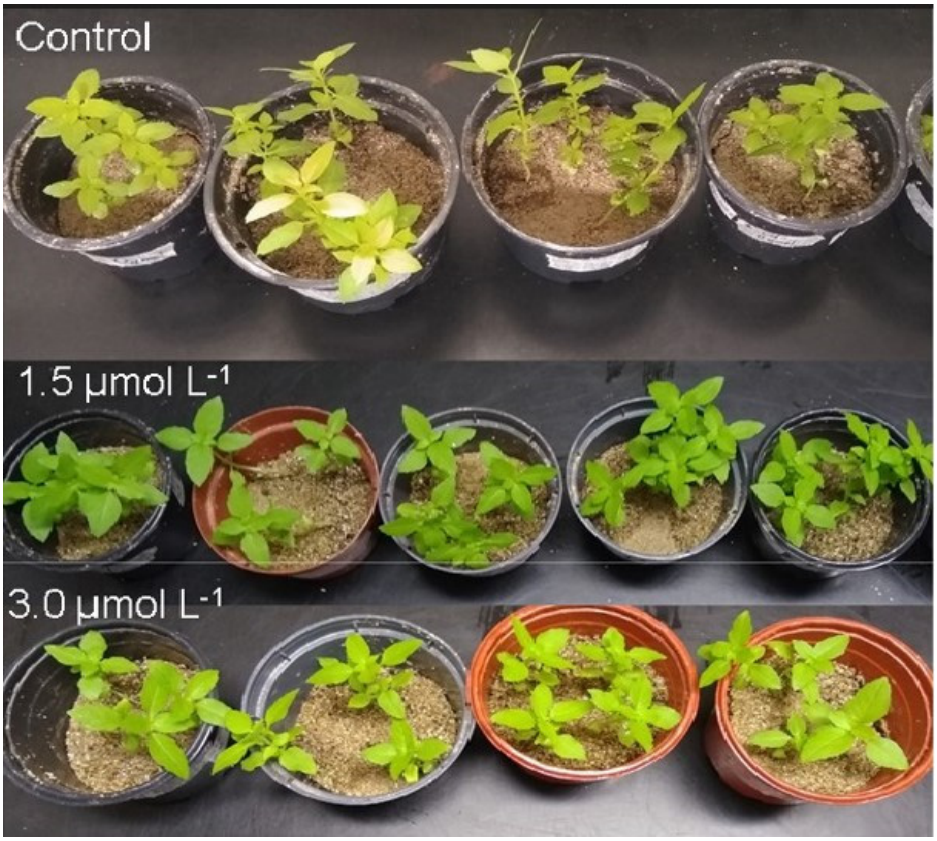

Figure 2. Basil samples after 30 days cultivation (15 days of hydroponic cultivation and 15 days in vermiculite substrate).

Some important characteristics were identified in the basil seedlings exposed to Cd (Figure 1) such as chlorosis on the leaves, stunting and reduced root length and number/size of leaves, which corroborate with the effects of Cd on plants reported in the literature.[3,10,29] These results justified the transplanting to vermiculite substrate to promote the development of the basil seedlings (Figure 2). Increasing Cd concentration compromised the accumulation of biomass in basil leaves. The biomasses in leaves cultivated with 1.0 and 3.0 μmol L^{-1} of Cd were on average 83% and 41% lower than that of control plants, respectively. Cd toxicity can be related to the stunted plant growth, negatively affecting water and nutrient uptake and translocation, photosynthesis, carbon and nitrogen assimilation, and oxidative stress.[3]

Bioaccessible fractions of minerals and their correlations

The limit of detection (LOD) and quantification (LOQ) of microwave-assisted acid digestion and IVG digestion procedures for Cd, Cu, Fe and Zn are presented in Table I. The LOD and LOQ are defined as $3.3*s/m$ and $10*s/m$, respectively, where s is the standard deviation corresponding to 10 analytical blanks and m is the slope of the calibration curve.[31] The analytical blanks of the gastrointestinal digestion have also undergone the clean-up procedure.

Table I. Limit of detection (LOD) and quantification (LOQ) of Cd, Cu, Fe and Zn in basil leaves after microwave-assisted acid digestion (MW) and gastrointestinal digestion procedures

Elements	Microwave-assisted acid digestion (MW)		Gastrointestinal digestion	
	LOD (μg kg^{-1})	LOQ (μg kg^{-1})	LOD (μg kg^{-1})	LOQ (μg kg^{-1})
Cd	0.071	0.230	0.288	0.951
Cu	0.602	2.00	7.95	26.2
Fe	10.7	35.3	11.4	37.8
Zn	8.44	27.9	0.989	3.26

Table II displays the total concentration (μg g^{-1}) of Cd, Cu, Fe and Zn after microwave-assisted acid digestion (MW) and bioaccessible fraction. Cadmium content in basil leaves is directly proportional to the exposure concentration during cultivation. Total concentration of Cu and Zn also increased proportionally with Cd intoxication while for Fe it was observed a decreased of its concentration. According to the Brazilian legislation,[32] Cd concentrations in leafy vegetables must be lower than 0.20 mg kg^{-1}. The humidity content in the basil leaves was around 94.8 ± 0.2%. So, MW total concentration for Cd treatments of 1.5 and 3.0 μmol L^{-1} in wet weight is around 1.2 and 2.3 mg kg^{-1}, respectively with both values exceeding the legislation. However, the total amount of the elements present in food does not reflect the amount absorbed and metabolized by the human body. In fact, *in vitro* experiments may elucidate the mechanism of absorption and correlation with other essential nutrients present in the physiological concentrations that can be absorbed by the human body.

In this study, the IVG digestion was performed according to Bertin et al. (2016)[15] and Nascimento (2011)[27] with the addition of the clean-up step by sonication of the extracts in the cup horn reactor in order to prevent clogging of the ICP-MS nebulization system. The results showed that the Cd bioaccessible fraction differed statistically ($p < 0.05$) in lyophilized and fresh leaves and as well as contamination level (1.5 μmol L^{-1} and 3.0 μmol L^{-1}). The bioaccessible fraction in lyophilized leaves is higher than in fresh ones and directly proportional to the Cd concentration.

The bioaccessibility of Cd in samples was approximately 51% and 45% in the contaminated leaves at 1.5 μmol L^{-1} and 3.0 μmol L^{-1}, respectively (Table II). No significant difference (*t* test: $t_{experimental} < t_{critical}$, $p < 0.05$) was found in the bioaccessible Cd concentration for the gastrointestinal extracts when comparing lyophilized and fresh samples with the increase of Cd concentration. This result showed that the treatment

with 3 μmol L^{-1} of Cd was not statistically different from those obtained with 1.5 μmol L^{-1}, even increasing twice the concentration level.

The Cd daily intake for lyophilized and fresh leaves at 1.5 μmol L^{-1} was calculate as 0.2 and 0.095 μg kg^{-1}, respectively, using the bioaccessible fraction related to the body weight of an adult (60 kg) that regularly consumes 1 g of basil leaves (aromatic herb added to food), as described by Schmite et al. (2019)[22]. Similarly, for lyophilized and fresh leaves at 3.0 μmol L^{-1} of Cd were 0.35 and 0.2 μg kg^{-1}, respectively. Considering that the acceptable monthly dose of Cd is 25 μg kg^{-1} (60 kg body weight),[22] the values of consumption per adult were 0.145 and 0.07 μg kg^{-1} and 0.262 and 0.142 μg kg^{-1} for lyophilized and fresh leaves at 1.5 and 3.0 μmol L^{-1}, respectively. These values indicated that basil leaves obtained under this condition are a food-safe product, representing only 0.29−0.60 and 0.57–1.05% for leaves contaminated at 1.5 and 3.0 μmol L^{-1}, respectively. These results were similar to those obtained by Schmite et al.[22]

Several factors can increase Cd uptake through the human gastrointestinal, such as low intakes of vitamin D, Ca and trace elements as Cu and Zn.[1] Several trace elements, such as Fe, Zn and Cu are components of enzymes, and should be supplied to the human body, preferably from the diet.[13] Our findings showed that bioaccessible fractions of elements also depend on how the samples are consumed (lyophilized or fresh leaves) as they differ statistically at 95% confidence (*t*-test, $t_{experimental} < t_{crit}$), except for Cu in the 1.5 μmol L^{-1} contaminated leaf and Fe in all samples ($p < 0.05$, Table II). The total Cu bioaccessible fraction concentration ranged from 7.4 to 16 μg g^{-1} and 12 to 39 to lyophilized and fresh leaves, respectively. The Recommended Daily Allowance (RDA) as published by U.S. Food and Drugs Administration of Cu is 0.9 mg day^{-1}.[33] Total Cu concentration ranged from 0.013 to 0.049 mg g^{-1}, showing that 1 g of basil presented 1.4 to 5.1% of RDA considering the daily intake of an adult (60 Kg). The bioaccessibility was greater in the fresh leaves when compared to the lyophilized. The total Fe bioaccessible fraction concentration ranged from 237 to 240 μg $g^{-1}$and from 262 to 313 μg g^{-1} for the lyophilized and fresh leaves, respectively. The RDA to Fe is 18 mg day^{-1} and the total concentration ranged from 0.405 to 0.759 mg g^{-1}, showing that 1 g of basil presented 2.2 to 4.2% of RDA. The Fe bioaccessible was greater in the fresh leaves (daily intake for 60 Kg adult).

For Zn, the bioaccessible fraction concentration varied from 70 to 158 μg g^{-1} and 37 to 53 μg g^{-1} for the lyophilized and fresh leaves, respectively. The Zn bioaccessibility in the lyophilized leaves was higher than that obtained for fresh leaves (*t* test $p < 0.05$) at all levels of Cd contamination. The RDA of Zn is 11 mg day^{-1} and the total concentration ranged from 0.074 to 0.234 mg g^{-1}, showing that 1 g of basil presented 0.67 to 2.13% of RDA. On the other hand, the bioaccessible fraction was smaller to fresh leaves when compared to the lyophilized (daily intake for 60 kg adult) (Table II).

Previous studies showed that Cd interferes with the uptake and translocation of different nutrients and positive correlations between Cd-Fe and Cd-Cu and weak negative correlations between Cd-Zn were observed to basil leaves.[6] Then, Pearson correlation (Figures 3 A and B) of the bioaccessibility in lyophilized and fresh leaves was used to find out which elements positively correlated with one another (blue) and those elements that showed negative correlations with each other (red).

Table II. Total concentration (μg g^{-1}) of Cd, Cu, Fe and Zn after microwave acid digestion (MW) and bioaccessibility (%) in the lyophilized and fresh leaves after *in vitro* gastrointestinal digestion (n = 3) ± sd

Cd treatment (μmol L^{-1})	Elements	MW total concentration (μg g^{-1})	Lyophilized leaves		Fresh leaves		Daily intake* μg kg^{-1} (body weight)	
			Bioaccessible fraction (μg g^{-1})	Bioaccessibility (%)	Bioaccessible fraction (μg g^{-1})	Bioaccessibility (%)	Lyophilized leaves	Fresh leaves
0	Cd	<LOQ	<LOQ	-	-	-	-	-
	Cu	12.6 ± 1.0	7.38 ± 0.46	58.6 ± 5.9	11.8 ± 2.3	93.6 ± 19.7	0.123	0.197
	Fe	759 ± 46	250 ± 7 [a]	32.9 ± 2.2	262 ± 10 [a]	34.5 ± 2.5	4.17	4.37
	Zn	74.3 ± 5.3	70.3 ± 2.3	94.9 ± 7.5	36.6 ± 16.0	49.5 ± 2.1	1.17	0.610
1.5	Cd	23.3 ± 1.2	11.9 ± 0.7	51.3 ± 4.0	5.7 ± 0.6	24.7 ± 2.9	0.198	0.095
	Cu	20.4 ± 2.3	15.6 ± 1.8 [b]	76.4 ± 12.2	20.2 ± 4.8 [b]	99.2 ± 26.3	0.260	0.337
	Fe	428 ± 27	240 ± 11 [c]	56.0 ± 4.4	276 ± 69 [c]	64.5 ± 16.6	4.00	4.60
	Zn	123 ± 16	98.3 ± 12.6	79.7 ± 14.6	42.5 ± 0.46	34.4 ± 4.5	1.64	0.708
3.0	Cd	46.3 ± 1.9	21.0 ± 0.9	45.4 ± 2.7	11.4 ± 1.2	24.6 ± 2.7	0.350	0.190
	Cu	49.0 ± 5.3	13.9 ± 1.0	28.4 ± 3.7	38.7 ± 8.4	78.9 ± 19	0.232	0.645
	Fe	405 ± 27	237 ± 29 [d]	58.4 ± 8.1	313 ± 64 [d]	77.2 ± 17	3.95	5.22
	Zn	234 ± 16	158 ± 38	67.7 ± 16.7	53.2 ± 5.0	14.6 ± 2.2	2.63	0.89

*Based on the bioaccessible fraction of element to calculate the intake dose by an adult of 60 kg body weight who regularly consumes 1g of basil.
Equal letters to bioaccessible fraction indicate no significant difference by *t*-test ($p < 0.05$).

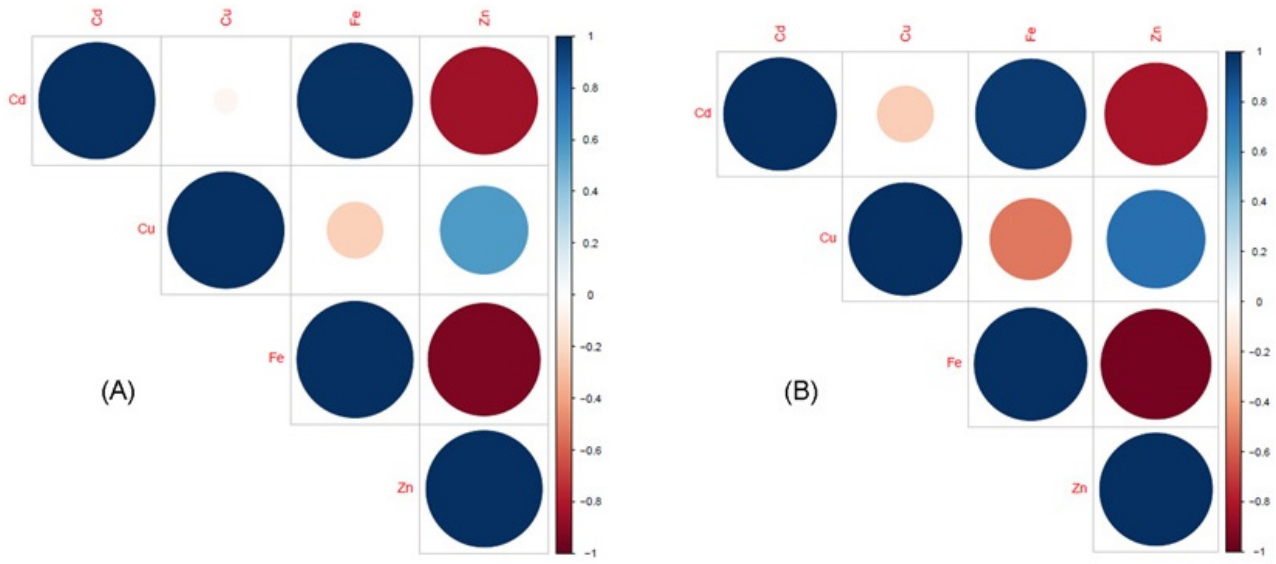

Figure 3. Correlogram matrix for bioaccessibility in basil samples, which grew at different Cd concentrations of 0, 1.5 and 3.0 µmol L^{-1} (A) lyophilized leaves (B) fresh leaves. Pearson's correlation analysis with the significance levels of $p < 0.05$.

In general, the correlograms presented similar correlations of both samples (Figure 3 A and B), demonstrating that the form of consumption did not affect bioaccessibility of elements, except for Cd-Cu ($r > -0.04$, Pearson test) in lyophilized leaves. However, a positive correlation between Cd-Fe and Cu-Zn and negative correlation between Cd-Zn and Fe-Zn were observed in lyophilized and fresh leaves, showing the strongest correlation attested by Pearson's ($r >$ than 0.75). Indeed, *in vitro* bioaccessibility is an estimation of the *in vivo* bioaccessibility and may not reflect the fraction that is available for gastrointestinal metal absorption, once *in vivo* involves a more complex metabolism of the elements in gastrointestinal digestion. According to Sun et al. (2019),[20] *in vivo* bioavailability tests are likely more physiologically relevant and, when possible, should be employed in risk assessments of human exposure to Cd *via* rice consumption.

Our findings showed that Cd in fresh leaves negatively affects the absorption of Cu, but the opposite happens with Fe, resulting probably in a negative correlation between Cu-Fe (Figure 3B). In human health, Cu is recognized as an essential trace element with function of cofactor of many redox enzymes and immune functions as well as involved in the Fe metabolism.[34,35]

Iron is a versatile, essential element in plant metabolism and human health with function related to the synthesis of haemoglobin and myoglobin, and plays a critical role in many metabolic processes such as oxygen transport, deoxyribonucleic acid (DNA) synthesis, and electron transportation.[34,35] People with low iron supplies present important metabolic parameter for cadmium uptake.[1] Our findings showed synergic effects of bioaccessibility of Cd and Fe.

Competition studies suggested that several other potentially toxic metals may share the iron intestinal absorption pathway, for example, Zn,[36] which may be related to the negative correlation between bioaccessibility of Fe-Zn in both samples of this study. In contrast to the synergistic effect of bioaccessibility of Cd with Fe, there is also an antagonistic effect between Cd-Zn. Concerning Zn, it is assumed that their molecular homology and divalent cation could be a reason for a compensatory higher Cd resorption.[1] After iron, zinc is the second most abundant metal ion in organisms[18] and it is an essential key nutrient for several biochemical activities, such as in human health. Zinc is essential for maintaining the structure and activity of many enzymes, besides playing a key role in the synthesis of nucleic acids and proteins.[34]

The results indicated that the presence of Cd causes synergic interferences with Fe and antagonic with Zn for both leaves, but antagonic with Cu to fresh leaves. In addition to the toxicity of Cd to human health, this toxic metal also influences the absorption of essential elements to the human body.

CONCLUSION

Cadmium contamination in basil samples provided a new insight for obtaining correlations of *in vitro* bioaccessibility with the essential elements Cu, Fe and Zn as a consequence of Cd uptake, absorption and translocation. In addition, it could be observed that Cd bioaccessible fraction in lyophilized leaves is greater than in fresh leaves and directly proportional to its concentration. It was also demonstrated that Cd *in vitro* bioaccessibility did not range with the increasing of its concentration in the intoxication treatments.

Conflicts of interest

The authors declare that they have no conflict of interest.

Acknowledgements

The authors are grateful to CAPES (Coordenação de Aperfeiçoamento de Pessoal de Nível Superior) and CNPq (Conselho Nacional de Desenvolvimento Científico e Tecnológico) for research funds and grants.

REFERENCES

(1) Godt, J.; Scheidig, F.; Grosse-Siestrup, C.; Esche, V.; Brandenburg, P.; Reich, A.; Groneberg, D. A. The Toxicity of Cadmium and Resulting Hazards for Human Health. *J. Occup. Med. Toxicol.* **2006**, *1* (1), 1–6. https://doi.org/10.1186/1745-6673-1-22

(2) Sanità di Toppi, L.; Gabbrielli, R. Response to Cadmium in Higher Plants. *Environ. Exp. Bot.* **1999**, *41* (2), 105–130. https://doi.org/10.1016/S0098-8472(98)00058-6

(3) Ismael, M. A.; Elyamine, A. M.; Moussa, M. G.; Cai, M.; Zhao, X.; Hu, C. Cadmium in Plants: Uptake, Toxicity, and Its Interactions with Selenium Fertilizers. *Metallomics* **2019**, *11* (2), 255–277. https://doi.org/10.1039/c8mt00247a

(4) Hayat, M. T.; Nauman, M.; Nazir, N.; Ali, S.; Bangash, N. Environmental Hazards of Cadmium: Past, Present, and Future. In: Hasanuzzaman, M.; Prasad, M. N. V.; Fujita, M. (Eds.). *Cadmium Toxicity and Tolerance in Plants*. Academic Press, 2019. Chapter 7, pp 163–183. https://doi.org/10.1016/B978-0-12-814864-8.00007-3

(5) Teles, V. de L. G.; Sousa, G. V.; Vendramini, P. H.; Augusti, R.; Costa, L. M. Identification of Metabolites in Basil Leaves by Desorption Electrospray Ionization Mass Spectrometry Imaging after Cd Contamination. *ACS Agric. Sci. Technol.* **2021**, *14* (5). https://doi.org/10.1021/acsagscitech.0c00038

(6) Teles, V. de L. G.; Sousa, G. V; Modolo, L. V; Augusti, R.; Costa, L. M. Ionomic Responses of Hydroponic-Grown Basil (*Ocimum basilicum* L.) to Cadmium Long-Time Exposure. *Metallomics* **2022**, *14* (5). https://doi.org/10.1093/MTOMCS/MFAC023

(7) Sousa, G. V.; Teles, V. L. G.; Pereira, E. G.; Modolo, L. V.; Costa, L. M. Interactions between As and Se upon Long Exposure Time and Effects on Nutrients Translocation in Golden Flaxseed Seedlings. *J. Hazard. Mater.* **2021**, *402*, 123565. https://doi.org/10.1016/j.jhazmat.2020.123565

(8) Alamo-Nole, L.; Su, Y. F. Translocation of Cadmium in *Ocimum basilicum* at Low Concentration of CdSSe Nanoparticles. *Appl. Mater. Today* **2017**, *9*, 314–318. https://doi.org/10.1016/j.apmt.2017.08.014

(9) Güez, C. M.; de Souza, R. O.; Fischer, P.; Leão, M. F. de M.; Duarte, J. A.; Boligon, A. A.; Athayde, M. L.; Zuravski, L.; de Oliveira, L. F. S.; Machado, M. M. Evaluation of Basil Extract (*Ocimum basilicum* L.) on Oxidative, Anti-Genotoxic and Anti-Inflammatory Effects in Human Leukocytes Cell Cultures Exposed to Challenging Agents. *Braz. J. Pharm. Sci.* **2017**, *53* (1). https://doi.org/10.1590/s2175-97902017000115098

(10) Zheljazkov, V. D.; Callahan, A.; Cantrell, C. L. Yield and Oil Composition of 38 Basil (*Ocimum basilicum* L.) Accessions Grown in Mississippi. *J. Agric. Food Chem.* **2008**, *56* (1), 241–245. https://doi.org/10.1021/jf072447y

(11) Zheljazkov, V. D.; Craker, L. E.; Xing, B. Effects of Cd, Pb, and Cu on Growth and Essential Oil Contents in Dill, Peppermint, and Basil. *Environ. Exp. Bot.* **2006**, *58* (1–3), 9–16. https://doi.org/10.1016/j.envexpbot.2005.06.008
(12) Güez, C. M.; de Souza, R. O.; Fischer, P.; Leão, M. F. de M.; Duarte, J. A.; Boligon, A. A.; Athayde, M. L.; Zuravski, L.; de Oliveira, L. F. S.; Machado, M. M. Evaluation of Basil Extract (*Ocimum basilicum* L.) on Oxidative, Anti-Genotoxic and Anti-Inflammatory Effects in Human Leukocytes Cell Cultures Exposed to Challenging Agents. *Braz. J. Pharm. Sci.* **2017**, *53* (1). https://doi.org/10.1590/s2175-97902017000115098
(13) Khouzam, R. B.; Pohl, P.; Lobinski, R. Bioaccessibility of Essential Elements from White Cheese, Bread, Fruit and Vegetables. *Talanta* **2011**, *86* (1), 425–428. https://doi.org/10.1016/j.talanta.2011.08.049
(14) He, M.; Ke, C. H.; Wang, W. X. Effects of Cooking and Subcellular Distribution on the Bioaccessibility of Trace Elements in Two Marine Fish Species. *J. Agric. Food Chem.* **2010**, *58* (6), 3517–3523. https://doi.org/10.1021/jf100227n
(15) Bertin, R. L.; Maltez, H. F.; Gois, J. S. de; Borges, D. L. G.; Borges, G. da S. C.; Gonzaga, L. V.; Fett, R. Mineral Composition and Bioaccessibility in Sarcocornia Ambigua Using ICP-MS. *J. Food Compos. Anal.* **2016**, *47*, 45–51. https://doi.org/10.1016/J.JFCA.2015.12.009
(16) Doniec, J.; Florkiewicz, A.; Duliński, R.; Filipiak-Florkiewicz, A. Impact of Hydrothermal Treatments on Nutritional Value and Mineral Bioaccessibility of Brussels Sprouts (*Brassica oleracea* Var. Gemmifera). *Molecules* **2022**, *27* (6). https://doi.org/10.3390/molecules27061861
(17) Ramírez-Ojeda, A. M.; Moreno-Rojas, R.; Cámara-Martos, F. Mineral and Trace Element Content in Legumes (Lentils, Chickpeas and Beans): Bioaccesibility and Probabilistic Assessment of the Dietary Intake. *J. Food Compos. Anal.* **2018**, *73* (January), 17–28. https://doi.org/10.1016/j.jfca.2018.07.007
(18) D'imperio, M.; Montesano, F. F.; Serio, F.; Santovito, E.; Parente, A. Mineral Composition and Bioaccessibility in Rocket and Purslane after Zn Biofortification Process. *Foods* **2022**, *11* (3). https://doi.org/10.3390/FOODS11030484
(19) Zhuang, P.; Sun, S.; Zhou, X.; Mao, P.; McBride, M. B.; Zhang, C.; Li, Y.; Xia, H.; Li, Z. Bioavailability and Bioaccessibility of Cadmium in Contaminated Rice by in Vivo and in Vitro Bioassays. *Sci. Total Environ.* **2020**, *719*, 137453. https://doi.org/10.1016/j.scitotenv.2020.137453
(20) Sun, S.; Zhou, X.; Li, Z.; Zhuang, P. In Vitro and in Vivo Testing to Determine Cd Bioaccessibility and Bioavailability in Contaminated Rice in Relation to Mouse Chow. *Int. J. Environ. Res. Public Health* **2019**, *16* (5). https://doi.org/10.3390/ijerph16050871
(21) Pupin, L.; Santos, V. da S.; dos Santos Neto, J. P.; De Fusco, D. O.; Teixeira, G. H. de A. Is the Bioaccessibility of Minerals Affected by the Processing Steps of Juçara Fruit (*Euterpe edulis* Mart.)? *LWT - Food Sci. Technol.* **2018**, *91*, 14–25. https://doi.org/10.1016/j.lwt.2018.01.024
(22) Schmite, B. de F. P.; Bitobrovec, A.; Hacke, A. C. M.; Pereira, R. P.; Weinert, P. L.; dos Anjos, V. E. In Vitro Bioaccessibility of Al, Cu, Cd, and Pb Following Simulated Gastro-Intestinal Digestion and Total Content of These Metals in Different Brazilian Brands of Yerba Mate Tea. *Food Chem.* **2019**, *281*, 285–293. https://doi.org/10.1016/j.foodchem.2018.12.102
(23) Liu, K.; Zheng, J.; Wang, X.; Chen, F. Effects of Household Cooking Processes on Mineral, Vitamin B, and Phytic Acid Contents and Mineral Bioaccessibility in Rice. *Food Chem.* **2019**, *280*, 59–64. https://doi.org/10.1016/j.foodchem.2018.12.053
(24) Sandström, B. Micronutrient Interactions: Effects on Absorption and Bioavailability. *Braz. J. Nutr.* **2001**, *85* (S2), S181. https://doi.org/10.1049/bjn2000312
(25) Water-culture, T. <CA Ag Experiment Station_Circular 347_1950.Pdf>. **1950**. Verificar se a referência correta é: Hoagland, D. R.; Arnon, D. I. *The Water-Culture Method for Growing Plants without Soil*. Agricultural Experiment Station, Circular 347. The College of Agriculture University of California, Berkeley, California, 1950. https://doi.org/citeulike-article-id:9455435 (este doi leva a uma mensagem de erro)
(26) US Pharmacopeia XXIV & National Formulary. Rockville: The United States Pharmacopeial Convention, v.19; 2000.

(27) Nascimento, A. N. *Especiação e Biodisponibilidade de Metaloproteínas de Ca, Cu, Fe, Mg e Zn Em Castanha de Caju*. PhD Thesis in Chemistry, Institute of Chemistry, University of São Paulo, São Paulo, SP, Brazil, 2011. https://doi.org/10.11606/T.46.2011.tde-07022012-082107
(28) Leufroy, A.; Noël, L.; Beauchemin, D.; Guérin, T. Use of a Continuous Leaching Method to Assess the Oral Bioaccessibility of Trace Elements in Seafood. *Food Chem*. **2012**, *135* (2), 623–633. https://doi.org/10.1016/j.foodchem.2012.03.119
(29) RStudio Team. *RStudio: Integrated Development Environment for R*. RStudio. PBC: Boston, MA, 2018.
(30) Clemens, S. Toxic Metal Accumulation, Responses to Exposure and Mechanisms of Tolerance in Plants. *Biochimie* **2006**, *88* (11), 1707–1719. https://doi.org/10.1016/j.biochi.2006.07.003
(31) Instituto Nacional de Metrologia, Normalização e Qualidade Industrial (INMETRO). *Orientação Sobre Validação de Métodos Analíticos DOQ-CGCRE-008*. Brazil, 2018.
(32) Agência Nacional de Vigilância Sanitária (ANVISA). Resolução RDC Nº 42, de 29 de agosto de 2013. *Inspeção de produtos vegetais. Dispõe sobre o regulamento técnico MERCOSUL sobre limites máximos de contaminantes inorgânicos em alimentos*. Ministério da Saúde do Brasil.
(33) U.S. Food & Drug Administration (FDA). *Daily Value and Percent Daily Value: Changes on the New Nutrition and Supplement Facts Labels*. March 2020, 1–6.
(34) Buturi, C. V.; Mauro, R. P.; Fogliano, V.; Leonardi, C.; Giuffrida, F. Mineral Biofortification of Vegetables as a Tool to Improve Human Diet. *Foods* **2021**, *10* (2). https://doi.org/10.3390/FOODS10020223
(35) Bost, M.; Houdart, S.; Oberli, M.; Kalonji, E.; Huneau, J. F.; Margaritis, I. Dietary Copper and Human Health: Current Evidence and Unresolved Issues. *J. Trace Elem. Med. Biol.* **2016**, *35*, 107–115. https://doi.org/10.1016/j.jtemb.2016.02.006
(36) Abbaspour, N.; Hurrell, R.; Kelishadi, R. Review on Iron and its Importance for Human Health. *J. Res. Med. Sci.* **2014**, *19* (2), 164–174.

Brazilian Journal of Analytical Chemistry
2023, Volume 10, Issue 40, pp 170-181
doi: 10.30744/brjac.2179-3425.TN-80-2022

BrJAC

TECHNICAL NOTE

Development and Validation of a High Performance Liquid Chromatography Ultraviolet Detection Method for the Quantitative Determination of Vancomycin Hydrochloride

Priscilla Sete de Carvalho Onofre[1], Daniele Porto Barros[1], Gabriela Trindade de Souza e Silva[2], Fernando Luiz Affonso Fonseca[3], Paulo César Pires Rosa[2], Mavilde da Luz Gonçalves Pedreira[1], Maria Angélica Sorgini Peterlini[1]

[1]*Departamento de Enfermagem Pediátrica, Universidade Federal de São Paulo, Campus São Paulo, Rua Napoleão de Barros, 754, CEP 04024-002, São Paulo, SP, Brazil*

[2]*Faculdade de Ciências Farmacêuticas, Universidade Estadual de Campinas, Campinas, SP, Brazil*

[3]*Instituto de Ciências Ambientais, Químicas e Farmacêuticas, Universidade Federal de São Paulo, Campus Diadema, Diadema, SP, Brazil*

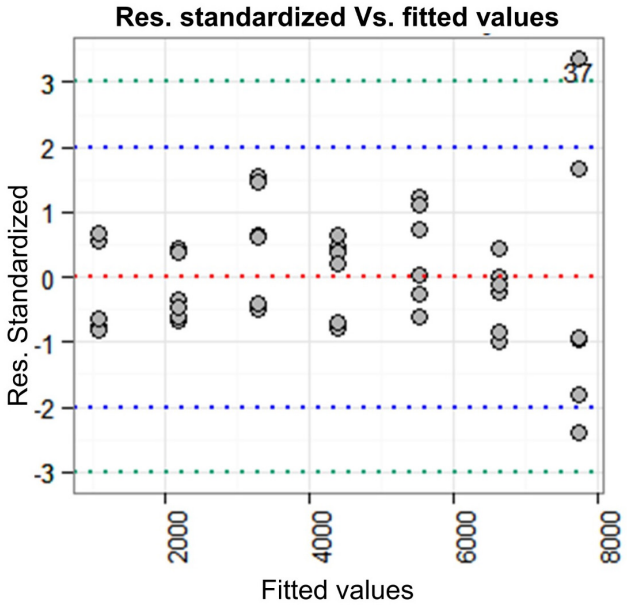

Vancomycin hydrochloride is a tricyclic glycopeptide that contains amino acids and sugars. This substance is indicated to treat serious infections caused by Gram-positive bacteria by intravenous infusion. The objective of this study was to develop and validate an analytical methodology by high performance liquid chromatography with ultraviolet detection (HPLC-UV) to determine vancomycin hydrochloride content by assessing the parameters of selectivity, linearity, working range, matrix effect, robustness, precision, and accuracy. The sample used was vancomycin hydrochloride in a vial and analyzes were carried out on HPLC-UV system with C18 reverse-phase column at 30 °C, pH=4 and diode-array detection (220 nm). The mobile phase was composed of acetonitrile and monobasic ammonium phosphate buffer (8:92 v/v), 1 mL min^{-1} flow rate, injection volume of 20 µL and 15 minute of run time. The method has been shown to be selective, free from mobile phase interference, diluent and other substances on vancomycin hydrochloride retention time; the method is linear in the range between 25 and 175 µg mL^{-1}; matrix effect showed parallelism between the lines, thus indicating the absence of interference of the matrix constituents in analysis of the

Cite: Onofre, P. S. C.; Barros, D. P.; Silva, G. T. S.; Fonseca, F. L. A.; Rosa, P. C. P.; Pedreira, M. L. G.; Peterlini, M. A. S. Development and Validation of a High Performance Liquid Chromatography Ultraviolet Detection Method for the Quantitative Determination of Vancomycin Hydrochloride. *Braz. J. Anal. Chem.* 2023, *10* (40), pp 170-181. http://dx.doi.org/10.30744/brjac.2179-3425.TN-80-2022

Submitted 28 August 2022, Resubmitted 07 February 2023, Accepted 11 February 2023, Available online 02 March 2023.

compound of interest; the method was robust with drug variations proportional to the deliberate changes caused by the change in the flow rate of the mobile phase and in the column temperature; the method showed accuracy at 25, 50, and 75 µg mL^{-1} concentrations, showing satisfactory recovery rate after addition of the standard. The analytical methodology described proved to be simple, fast, safe and was considered valid.

Keywords: validation studies, HPLC-UV, high performance liquid chromatography, vancomycin

INTRODUCTION

Vancomycin hydrochloride is a complex tricyclic glycopeptide drug that contains amino acids and sugars (Figure 1). This substance is indicated to treat serious infections caused by Gram-positive bacteria resistant to other lower potential antibiotics for both adults and child. This drug is mainly used to treat respiratory tract infections due to methicillin-resistant *Staphylococcus aureus* and *Staphylococcus epidermidis,* as well as prophylaxis in major cardiac surgeries.[1-3]

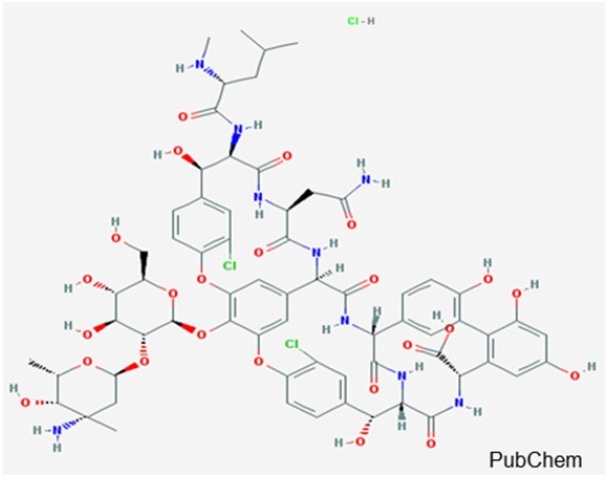

Figure 1. Chemical structure of vancomycin hydrochloride.

Analytical methods for the determination of vancomycin hydrochloride stability are described in several international compendiums using techniques such as high-performance liquid chromatography with ultraviolet detection (HPLC-UV), capillary electrophoresis, mass spectrometry, polarized immunofluorescence, radioimmunoassay, among others.[4-6]

The liquid chromatography is an appropriate method due to its relative low cost when compared with other techniques, and mainly due to the ease and speed in separating, identifying and quantifying the analyzed compounds. The HLPC has been used for both dosing this antibiotic in the product and in biological fluids.[4-6] Until now, this is the most widely used antimicrobial determination procedure, and it is even the official method for purity determination by the British Pharmacopeia and United States Pharmacopeia (USP).[7-9]

The choice for the appropriate analytical methodology is of fundamental importance for the quality control procedure of the active substance or pharmaceutical form. Thus, for the use of the analytical method or its adaptation, it is necessary to perform a validation study, to guarantee the efficiency in pharmacological analyses in routine uses, with reliable information about the sample.[10]

The validation of an analytical methodology produces evidence to confirm the proposed technique as reliable for what it applies, constituting a series of procedures, ensuring credibility to the measures obtained. The main purpose of this validation is to show that the analytical method is suitable for its purpose.[9-10]

The Brazilian Health Regulatory Agency (ANVISA), in the Collegiate Board Resolution (RDC) No. 166 of 2017,[11] defines the objective of validating active compounds as the demonstration that the method follows the analytical premises. The validation must ensure reliability in the results to which it is proposed, whether quantitative or qualitative determination of drugs.

The objective of this study was to develop and validate a fast and reliable analytical methodology by HPLC-UV, considering the parameters recommended by the RDC 166/2017 from ANVISA, to determine vancomycin hydrochloride content.

MATERIALS AND METHODS

Equipment and materials

The instruments and materials used in the experiment were: a high performance liquid chromatograph system with an ultraviolet detector (Agilent Technologies®-1260 Infinity Series HPLC Modular), an autosampler, a diode-array detector (DAD), a 4.6 x 250 mm C18 reverse-phase analytical column, particle size 5 µm (Waters®- Spherisorb ODS 2 Hypersil and Thermo Scientific®- ODS Hypersil), analytical balance (Shimadzu®- AUY220, Kyoto, Japan); 0.45 µm pore-coated polyvinylidene fluoride (PVDF) membrane (MF-Millipore®, type HAWP, Darmstadt, Germany); 13 mm diameter Nylonmembrane syringe filter with 0.45 µm pore size (Allcrom®-Membrane Solutions); Millipore filtration system for HA organic solvents, 0.45 µm; benchtop digital pH meter (Kasvi® K39-2014B, Curitiba, Brazil); magnetic stirrer (Warmnest® CJ-882A, Zhejiang, China); ultrasonic washer (Ultronique®—Eco-sonics, Indaiatuba, SP, Brazil); vacuum pump (Prismatec® 121-Type 2 VC, Itu, SP, Brazil) and type 1 ultrapure water purification system (Direct Q 3®-Merck Millipore®, Massachusetts, USA).

Reagents, drug, reference standard and solvents

The HPLC grade organic solvent acetonitrile (Carlo Erba®, Val-de-Reuil, France) was used to prepare the solutions; the following substances were also used: phosphoric acid 85.0% PA- ACS (Synth®, Diadema, SP, Brazil); monobasic ammonium phosphate (Sigma-Aldrich, Vetec®, Duque de Caxias, RJ, Brazil); Vancomycin hydrochloride equivalent to 500 mg in vial presentation as a lyophilized powder (Vancocina® CP - ABL Antibiotics from Brazil, Cosmópolis, SP, Brazil); distilled water (DA) in a 10 mL plastic ampoule (Isofarma Industrial Pharmaceutical Ltda, Eusébio, CE, Brazil); standard of vancomycin hydrochloride of USP considered a primary reference (USP, United States of America, 98.8% vancomycin content USP Catalog No. 1709007) and 0.9% Sodium Chloride (NaCl) (JP Indústria Farmacêutica SA, Ribeirão Preto, SP, Brazil).

Preparation of the mobile phase and standard solution

The mobile phase (MP) was prepared by combining monobasic ammonium phosphate (5 mg mL^{-1}) in deionized water and mixing this solution in a ratio of 92% to 8% of acetonitrile.

Subsequently, a 1 mg mL^{-1} solution of standard vancomycin hydrochloride solution in MP was prepared. The solution was homogenized and solubilized in an ultrasonic washer. Based on this solution, an aliquot for the preparation of 0.1 mg mL^{-1} solution was filtered and analyzed by chromatographic method.

Sample preparation

The drug vancomycin hydrochloride (500 mg) was reconstituted in 10 mL of DA (50 mg mL^{-1}) in the vial itself and then diluted in 0.9% NaCl solution at 5 mg mL^{-1}. Then this solution was diluted in a concentration of 0.1 mg mL^{-1}.

Chromatographic conditions

Chromatographic analyses were conducted in isocratic mode; with the column temperature set at 30 °C and DAD configured at 220 nm of wavelength, 1 mL min^{-1} flow rate, 20 µL injection volume and 15 min analytical run time. The quantification of vancomycin hydrochloride was performed by external standardization.

Parameter determination for method validation

The validation of the chromatographic method for the analysis of vancomycin hydrochloride concentrations was performed following the recommended guidelines for analytical methods regarding the selectivity, linearity, working range, matrix effect, robustness, precision and accuracy as required by the RDC 166/2017 of ANVISA.[11]

Selectivity

As for the assessment of the selectivity parameter, MP chromatograms, reference standard, vancomycin hydrochloride solution and sample diluent, consisting of 0.9% NaCl solution, were compared, as well as the purity signal.[11]

Matrix effect

In this study, five different concentrations were used in triplicate. Starting from the vancomycin hydrochloride solution prepared at 5,000 μg mL^{-1}, 0.2 mL aliquots were removed with micropipette and transferred to 10 mL volumetric flasks. Then the standard volumes were added to these flasks for the preparation of solutions in the range of 25–125 μL. The two resulting curves were compared and assessed by the *t*-test.

Linearity and linear range

The linearity was determined based on a mathematical relationship of the analyte average area for each aliquot and its respective theoretical concentration, thus obtaining an analytical curve by the linear equation y = ax + b, the coefficients a and b being estimated by linear regression. Therefore, three analytical curves were analyzed in the concentration range of 25–175 μg mL^{-1} (seven points) from a stock solution at 1 mg mL^{-1}, diluted with MP.

Area results were assessed visually at first, followed by the least squares method, preceded by the Cochran test, followed by residue analysis.[11]

Robustness

This test was elaborated to assess the ability of the chromatographic method to resist small changes in analytical parameters, thus the analytical column temperature of 28 °C and 32 °C and the MP flow of 0.8 mL min^{-1} and 1.2 mL min^{-1} were modified. In order to assess the impact of these changes, the following parameters were evaluated: peak purity of the compound of interest, retention factor (K) and resolution (RS).[9,11] Therefore, Equations 1 and 2 were used.

$$K = t\,c/t\,s \qquad \text{Equation 1}$$

where:
tc = time required by the sample components
ts = time required by the eluent

$$Rs = \frac{2(tr1 - tr2)}{w1 + w2} \qquad \text{Equation 2}$$

where:
tr1 = retention time of the sample
tr2 = retention time of the peak prior to the analyte of interest
w1 = peak width of the analyte of interest
w2 = peak width prior to the analyte of interest

Precision

In the intraday accuracy study, nine replicates of individually prepared a 100 µg mL^{-1} concentration were used. The samples were assessed under the same operating conditions, same analyst and same instrumentation, in a single analytical run.

In order to identify possible variations of the data collection site due to analyses performed on different days or by different analysts, the intermediate precision or reproducibility analysis was performed. In this test, different samples were assessed on different non-consecutive days.

Accuracy

The accuracy (recovery) test was performed by comparing the results achieved in the analysis of vancomycin hydrochloride solution samples with the results obtained by analyzing samples containing known standard concentrations.

The quantities of 25, 50 and 75 µg were added to the standard sample solution. These quantities are considered low, medium and high concentration measurements, respectively, and they were analyzed in three replicates of each level. The recovery factor (% R) was calculated by subtracting the concentration determined in the added sample (C_b) from the concentration determined in the non-added sample (C_a), then the result was divided by the added concentration (C_c), and finally the value was multiplied by 100, as shown in Equation 3.[11]

$$\%R = \frac{(Cb - Ca)x\ 100}{Cc} \qquad \text{Equation 3}$$

where:
C_a= concentration determined in the non-added sample
C_b= concentration determined in the added sample
C_c= added concentration

RESULTS AND DISCUSSION

This is an experimental study to develop and validate the analytical methodology for quantification of vancomycin hydrochloride.

The analytical strategy of validation and the analysis steps were conducted according to ANVISA RDC 166/2017[11] and the analytical performance parameters determined by experiments were: selectivity, linearity, working range, matrix effect, robustness, accuracy, and precision appropriate to the analysis.

The performance of the analysis tests provided satisfactory results in relation to the validation criteria of the proposed analytical methods.

The study was conducted at the Laboratory of Nursing Experiments (Laboratório de Experimentos de Enfermagem – LEEnf), Paulista Nursing School, Federal University of São Paulo, SP, Brazil.

In the selectivity or specificity test, no substances eluting near or at the same retention time of the test compound were detected. The compound peak was shown as high purity. Figure 2 shows the chromatograms analyzed.

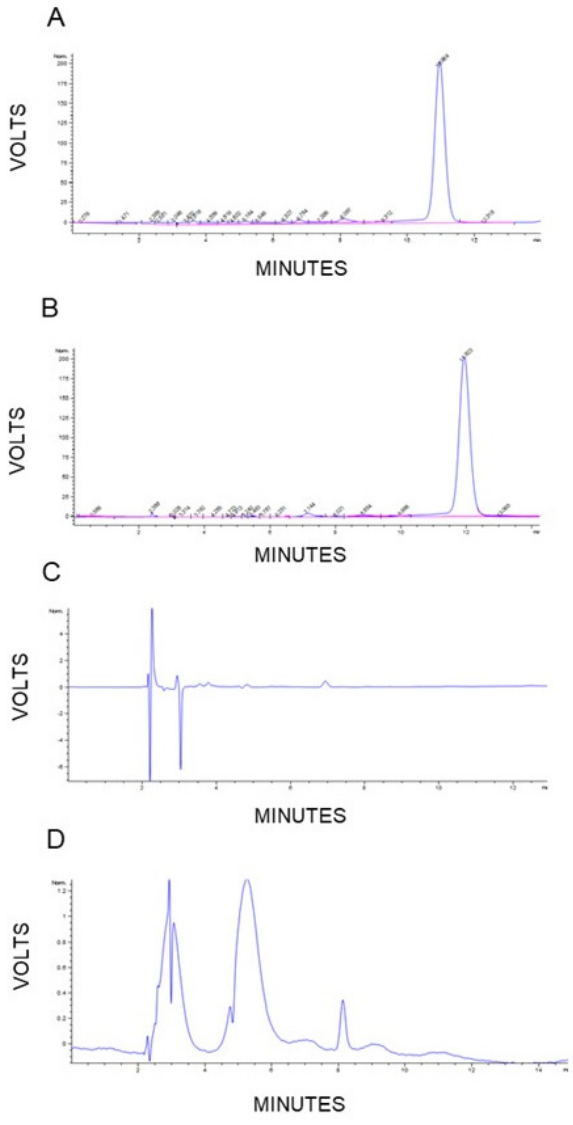

Figure 2. A. Chromatographic separation of vancomycin hydrochloride **sample**; **B.** Chromatographic separation of the vancomycin hydrochloride reference **standard**; **C.** Chromatographic analysis of diluent (0.9% sodium chloride solution) **D.** Mobile Phase chromatographic analysis report. Analyses performed in the isocratic mode method, C18 column at 30 °C, 220 nm wave, with Mobile Phase at a ratio of 92% buffer-solution and 8% acetonitrile, at a flow rate of 1 mL min^{-1} and 20 µL of injection volume.

The chromatograms in Figure 2 present that at the retention time of the vancomycin hydrochloride solution, no interfering substances were observed to elute at or near the standard time (Figure 2 C and D).

The investigation of selectivity conducted in this study was able to confirm that MP and diluent related to vancomycin hydrochloride standard do not have structurally similar components that could be present during the analyses at the same chromatographic peak. The presence of this peak was only verified in the drug solution.[11]

In the chromatograms analyzed, the vancomycin hydrochloride peak was unique in its retention time, with a gaussian distribution peak, and no other degradation or impurity peak was observed in the peak vicinity, therefore the method can be considered selective for the tested conditions.

Thus, seven duplicates of the vancomycin hydrochloride standard concentrations were analyzed for each of the three curves performed for the linearity assay. Table I shows the analytical curves of the method with the respective coefficients of determination (R^2) using the DAD ultraviolet detector in the concentration range 25–175 µg mL^{-1} (n=7 points).

Table I. Analytical curves (y=ax+b) for vancomycin hydrochloride determination by HPLC-UV in the linear range of 80% to 120%

Replicates	Analytical curves	R^2
Replicate 1	y = 45.544x – 147.66	0.9993
Replicate 2	y = 43.927x + 43.169	0.9997
Replicate 3	y = 43.983x – 12.339	0.9995
Resulting curve	y = 44.436x – 34.75	0.9999

Note: y = peak area of interest; x = concentration in μg mL^{-1}; R^2 = coefficient of determination.

Figure 3 shows the overlap of the curves obtained by the linearity study as well as the residual graph.

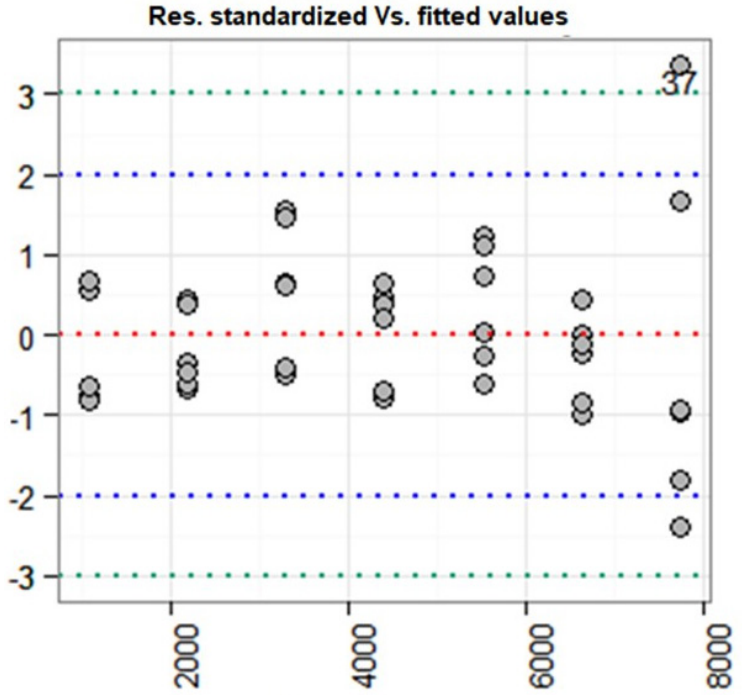

Figure 3. Graph of the residual *versus* adjusted values.

Linearity corresponds to the ability of the method to provide results directly proportional to the concentration of the analyzed substance. This linearity is obtained when the signal measured by each concentration of the analyte of interest is correlated, and the linear relationship is verified based on the mathematical treatment of the linear regression.[9,11] Thus, Cochran's test was carried out to assess the variance of experimental errors undergoing visual analysis of the residual graph (Figure 3). The calculated value for this test was smaller than the tabulated ones, then the variance of experimental errors (y values) are equal; the dataset therefore is homoscedastic. This observation coincides with the visual analysis of the graph, the variance seems constant, consequently, the dataset can be assessed by linear regression analysis.

Accordingly, in the mathematical model for linear regression analysis of the interval calibration curve proposed for the study, the R^2 was calculated (and it was shown within the acceptable value) proving

that the method is linear, as presented in Table I. Data corroborate ANVISA Resolution 166/2017,[11] which states that R^2 must be equal to or higher than 0.99; so, the method can be considered linear.

The matrix effect was measured by comparing the angular coefficients of the calibration curves and the fortified sample curve at five points of standard analysis (between 25–125 µg mL^{-1}) within the linear working range established by the linearity curve.

In Figure 4, parallelism between the lines can be observed, thus indicating the absence of interference of the matrix constituents in the analysis of the compound of interest.[11]

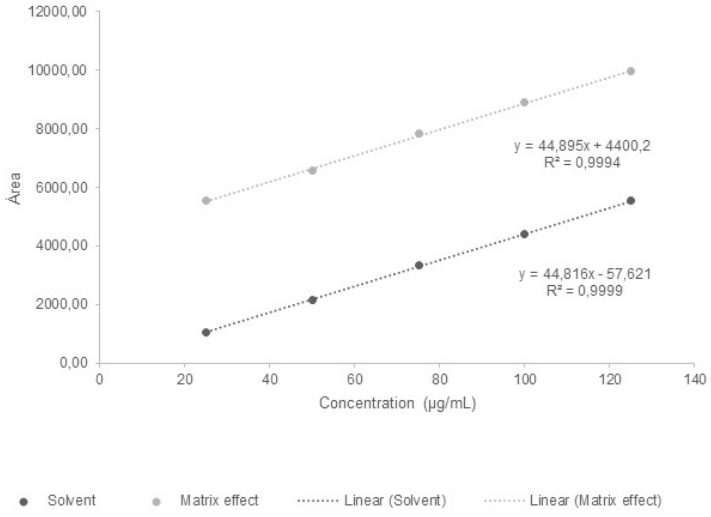

Figure 4. Curve obtained by the matrix effect in parallel to the linearity curve.

The robustness test was assessed by performing experiments with different chromatographic conditions by changing the MP flow rate and the column temperature. Those changes follow the recommendation of ANVISA RDC 166/2017.[11] Table II shows the results of the analyzed parameters.

Table II. Robustness of the vancomycin hydrochloride method according to variations in mobile phase flow and column temperature in relation to the original analysis conditions

Analysis parameter	Proposed method	MP flow rate 0.8 mL min^{-1}	MP flow rate 1.2 mL min^{-1}	Temperature 28 °C	Temperature 32 °C
Retention factor (K)	3.6	3.9	4.0	4.3	3.9
Previous Peak Resolution (RS)	2.3	3.0	2.1	2.6	2.3
Posterior Peak Resolution (RS)	4.0	4.7	4.0	3.5	2.8
Retention time (RT)	8.72	11.65	7.95	10.42	9.4
Purity	999.999	999.97	999.976	999.973	999.969

Note: MP = Mobile Phase.

The method is considered robust when the results of small deliberate changes caused by the analytical parameters of the method during the robustness test indicated that the sample varies proportionally with the programmed conditions and does not affect the performance of the analytical methodology.[9,11-12] In this

analysis, in the case of vancomycin hydrochloride, the K factor must present better resolution than the other peaks, with a value higher than 2. For the system under study was found based on Equation 1 the lowest K value equal to 3.9 (Table II).

The degree of separation quantification RS is considered robust when the value is higher than 2[9] corroborating the study under analysis, which presented RS of 2.1, calculated based on Equation 2, with a maximum retention time of 11.6 minutes. Thus, the mobile phase selected for validation even with the small modifications in the chromatographic conditions showed good resolution and within 15 minutes of running (Table II).

The purity of the peak was stable in relation to the purity presented in the proposed method (Table II). According to the robustness test premise, the small variations caused do not affect the analytical procedure.

In this study, in the precision test to verify the single-day repeatability, nine replicates at 100% of the test concentration individually prepared were used. The samples were assessed under the same operating conditions, single analyst and same instrumentation, in a single analytical run and with three injections each.[11]

The theoretical concentration was estimated based on the analytical curve equation and was expressed in μg mL^{-1}. The results obtained with this test are presented in Table III.

Table III. Intra-run accuracy test (intermediate test)

Replicates (sample)	Average sample areas (intermediate test)	Standard Deviation	CV (%)	Estimated theoretical concentration (μg mL^{-1})
1	4574.80	3.12	0.07	103.73
2	4574.80	3.12	0.07	103.73
3	4725.27	10.89	0.23	107.12
4	4451.54	34.18	0.77	100.96
5	4417.67	12.70	0.29	100.20
6	4442.59	40.34	0.91	100.76
7	4451.54	34.18	0.77	100.96
8	4417.67	12.70	0.29	100.20
9	4442.59	40.34	0.91	100.76
Overall average concentration				4499.8
Overall standard deviation				104.2
Relative standard deviation (%)				2.3

Note: CV = Coefficient of variation.

As to the intra-run accuracy, a satisfactory result expressed by CV 0.91% was obtained, remaining below the acceptable limit value of 5%. The relative standard deviation (RSD) value found in the experiment was below 5% (Table III), indicating the accuracy of the method, thus corroborating the limits expressed in compliance with the analytical validation rules of the ANVISA.[11]

Table IV. Inter-run accuracy test

Replicates (sample)	Average sample areas
1	4602.40
2	4504.50
3	4503.10
4	4498.00
5	4495.10
6	4496.20
7	4495.00
8	4501.50
9	4497.00
Overall average concentration	4510.31
Overall standard deviation	34.71
Relative Standard Deviation (%)	0.77

The intermediate precision was assessed by analyzing vancomycin hydrochloride solutions at a concentration of 100 μg mL^{-1}, on different and non-consecutive days, obtaining RSD of 0.8%. These results show that the method provides results with acceptable accuracy on different days of analysis and involving two distinct analysts (Table IV).

In the accuracy test for 25 μg mL^{-1}, 50 μg mL^{-1}, and 75 μg mL^{-1} concentrations, it was presented for each theoretical concentration: mean replica areas, relative standard deviation, and recovery (Table V).

Table V. Data obtained for accuracy test evaluation

Theoretical standard of vancomycin concentration added (μg mL^{-1})	Experimental vancomycin concentration (μg mL^{-1})	Mean of the area	Relative Standard Deviation	Recovery (%)
125	122.90	5535	0.107	99.9
150	145.13	6585	0.062	99.6
175	172.55	7829	0.284	101.3

The accuracy of the method was determined by studying the original matrix recovery by adding a known amount of the reference standard used for the study of vancomycin hydrochloride.

According to the ANVISA Resolution RDC 166/2017,[11] the standard deviation in the accuracy test should not exceed 15%, a premise met at the three concentrations studied, therefore, the accuracy of the method being validated was ensured.

The high percentages obtained in the recovery (near 100%) indicate the accuracy of the method. Regarding the RSD, the acceptable or true value is 5%, indicating that the assay is within the established recommendations (Table V).[11]

CONCLUSIONS

The method developed and validated according to ANVISA RDC 166/2017[11] parameters for the determination of vancomycin hydrochloride by HPLC-UV was simple, fast and efficient, and it can be safely applied to the analysis of solution containing vancomycin hydrochloride.

Conflicts of interest

The authors declare no conflicts of interest.

Acknowledgements

The researchers thank the members of the SEGTEC Group (Brazil) for their support during data collection, the “Coordenação de Aperfeiçoamento de Pessoal de Nível Superior” (CAPES) for providing the PhD scholarship to Priscilla Sete de Carvalho Onofre, and the “Conselho Nacional de Desenvolvimento Científico e Tecnológico” (CNPq), for granting research support [No. 462183/2014-9].

REFERENCES

(1) Costenaro, P.; Minotti, C.; Cuppini, E.; Barbieri, E.; Giaquinto, C.; Donà, D. Optimizing Antibiotic Treatment Strategies for Neonates and Children: Does Implementing Extended or Prolonged Infusion Provide any Advantage? *Antibiotics* **2020**, *9* (6), 329. https://doi.org/10.3390/antibiotics9060329

(2) Rybak, M. J.; Le, J.; Lodise, T. P.; Levine, D. P.; Bradley, J. S.; Liu, C.; Mueller, B. A.; Pai, M. P.; Wong-Beringer, A.; Rotschafer, J. C.; Rodvold, K. A.; Maples, H. D.; Lomaestro, B. M. Therapeutic monitoring of vancomycin for serious methicillin-resistant Staphylococcus aureus infections: A revised consensus guideline and review by the American Society of Health-System Pharmacists, the Infectious Diseases Society of America, the Pediatric Infectious Diseases Society, and the Society of Infectious Diseases Pharmacists. *Am. J. Health-Syst. Pharm*. **2020**, *77* (11), 835–864. https://doi.org/10.1093/ajhp/zxaa036

(3) McNeil, J. C.; Kaplan, S. L.; Vallejo, J. G. The Influence of the Route of Antibiotic Administration, Methicillin Susceptibility, Vancomycin Duration and Serum Trough Concentration on Outcomes of Pediatric Staphylococcus aureus Bacteremic Osteoarticular Infection. *The Pediatric Infectious Disease Journal* **2017**, *36* (6), 572–577. https://doi.org/10.1097/INF.0000000000001503

(4) Barco, S.; Mesini, A.; Barbagallo, L.; Maffia, A.; Tripodi, G.; Pea, F.; Saffioti, C.; Castagnola, E.; Cangemi, G. A liquid chromatography-tandem mass spectrometry platform for the routine therapeutic drug monitoring of 14 antibiotics: Application to critically ill pediatric patients. *J. Pharm. Biomed. Anal*. **2020**, *186*, 113273. https://doi.org/10.1016/j.jpba.2020.113273

(5) Lima, T. M.; Seba, K. S.; Gonçalves, J.; Cardoso, F.; Estrela, R. A Rapid and Simple HPLC Method for Therapeutic Monitoring of Vancomycin. *J. Chromatogr. Sci*. **2018**, *56* (2), 115–121. https://doi.org/10.1093/chromsci/bmx089

(6) Masse, M.; Genay, S.; Martin, M. A.; Carta, N.; Lannoy, D.; Barthélémy, C.; Décaudin, B.; Odou, P. Evaluation of the stability of vancomycin solutions at concentrations used in clinical services. *Eur. J. Hosp. Pharm*. **2020**, *27* (e1), e87–e92. https://doi.org/10.1136/ejhpharm-2019-002076

(7) Parker, S. L.; Guerra, V. Y. C.; Ordóñez, M. J. L.; Roger, C.; Lipman, J.; Roberts, J. A.; Wallis, S. C. An LC–MS/MS method to determine vancomycin in plasma (total and unbound), urine and renal replacement therapy effluent. *Bioanalysis* **2017**, *9*, 911-24. https://doi.org/10.4155/bio-2017-0019

(8) Zhang, M.; Moore, G. A.; Young, W. Determination of vancomycinin human plasma, bone and fat by liquid chromatography/tandem mass spectrometry. *J. Anal. Bioanal. Tech*. **2014**, *5*, 1-9. https://doi.org/10.4172/2155-9872.1000196

(9) United States Pharmacopeia Convention, 2019. The national formulary. USP 32nd Rev., NF 27th Ed. Rockville (MD). Available at: https://www.uspnf.com/official-text/proposal-statuscommentary/usp-32-nf-27 (accessed 2022-06-05).
(10) Ribani, M.; Bottoli, C. B. G.; Collins, C. H.; Jardim, I. C. S. F.; Melo, L. F. C. Validação em métodos cromatográficos e eletroforéticos. *Quim. Nova* **2004**, *27* (5), 771-80. https://doi.org/10.1590/S0100-40422004000500017
(11) Ministério da Saúde, Agência Nacional de Vigilância Sanitária. Resolução RDC No 166. Dispõe sobre a validação de métodos analíticos e dá outras providências. *Diário Oficial da União*, 25 de julho 2017. Available at: https://www.in.gov.br/materia/-/asset_publisher/Kujrw0TZC2Mb/content/id/19194581/do1-2017-07-25-resolucao-rdc-n-166-de-24-de-julho-de-2017-19194412 (accessed 2022-04-20).
(12) International Conference on Harmonisation (ICH). ICH Expert Working Group. Harmonised tripartite guideline. Validation of analytical procedures: text and methodology Q2(R1). In: International conference on harmonisation of technical requirements for registration of pharmaceuticals for human use. 2005 Nov. Geneva. https://database.ich.org/sites/default/files/Q2%28R1%29%20Guideline.pdf

Brazilian Journal of Analytical Chemistry
2023, Volume 10, Issue 40, pp 182-197
doi: 10.30744/brjac.2179-3425.TN-94-2022

BrJAC

TECHNICAL NOTE

Lanthanum Oxide Nanoparticles Distribution in Wistar Rats after Oral Exposure and Respective Effects

Graciela M. Heidrich[1], Vinicius M. Neves[1], Naiara Stefanello[1], Vanessa V. Miron[1], Thauan F. Lopes[1], Sindy R. Krzyzaniak[1], Paola de A. Mello[1], Maria Rosa C. Schetinger[1], Dirce Pozebon[2], Valderi L. Dressler[1]

[1]*Universidade Federal de Santa Maria, Avenida Roraima, 1000, Campus de Camobi, Santa Maria, RS, 97105-900, Brazil*

[2]*Universidade Federal do Rio Grande do Sul, Avenida Bento Gonçalves, 9500, Instituto de Química, 97501-970, Porto Alegre, RS, Brazil*

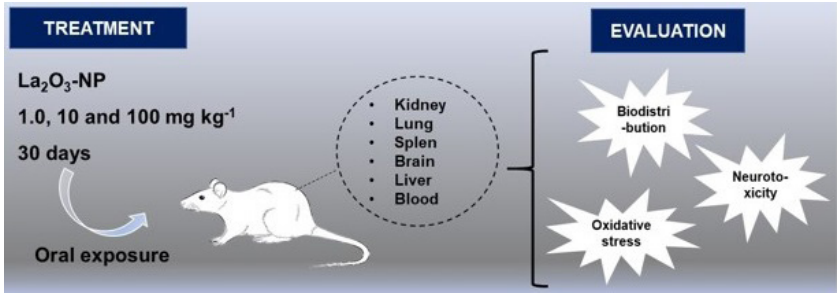

Adult Wistar rats were exposed to lanthanum oxide nanoparticles (La_2O_3-NPs). Animals were initially treated with single doses of La_2O_3-NPs suspensions at 5.0, 50, 300 and 2000 mg kg^{-1} per body weight (*bw*), which were orally administered. Behavior changes, symptoms of intoxication and mortality were not observed for individuals treated with the La_2O_3-NPs. However, the histological analysis of different organs of the treated rats revealed that 300 mg kg^{-1} and 2000 mg kg^{-1} *bw* La_2O_3-NPs caused hepatic lesions. Subsequently, 40 individuals were divided in four groups with 10 individuals in each group and daily treated with water only (control) and with 1.0, 10 and 100 mg kg^{-1} *bw* La_2O_3-NPs. After 30 days, it was observed that the La_2O_3-NPs did not affect the body weight and organs weight of the animals. The La_2O_3-NPs also did not change the levels of creatinine, urea, glutamyl transferase (γ-GT), alanine aminotransferase (ALT), aspartate aminotransferase (AST) and thiobarbituric acid reactive substances (TBARS) in blood serum. Neurotoxicity, evaluated by the acetylcholinesterase (AChE) activity, was not observed as well. An increase of reactive oxygen species (ROS) was found in kidney of rats treated with 100 mg kg^{-1} *bw* La_2O_3-NPs. Conversely, protein oxidation decreased in the liver of those animals. The catalase (CAT) activity was not affected by La_2O_3-NPs and that of superoxide dismutase (SOD) was in the liver of animals treated with 10 mg kg^{-1} *bw* La_2O_3-NPs. Lanthanum was determined in organs and blood of the treated animals. The element was not detected in the blood but was in the organs, in higher concentration in liver, kidneys, and heart. Lanthanum present in the form of NPs or as free ion could not be detected. As such, it is worth investigating possible transformation of La_2O_3-NPs in the organism, their elimination routes, and effects of longer exposure times.

Cite: Heidrich, G. M.; Neves, V. M.; Stefanello, N.; Miron, V. V.; Lopes, T. F.; Krzyzaniak, S. R.; Mello, P. A.; Schetinger, M. R. C.; Pozebon, D.; Dressler, V. L. Lanthanum Oxide Nanoparticles Distribution in Wistar Rats after Oral Exposure and Respective Effects. *Braz. J. Anal. Chem.* 2023, *10* (40), pp 182-197. http://dx.doi.org/10.30744/brjac.2179-3425.TN-94-2022

Submitted 28 September 2022, Resubmitted 14 December 2022, Accepted 20 December 2022, Available online 03 February 2023.

Keywords: La_2O_3 nanoparticles, bioanalytic, Wistar rats, Lanthanum accumulation, toxicity, ICP-MS

INTRODUCTION

Nanoparticles (NPs) has been increasingly used with the advance of science and technology. However, due to their nanometric dimension, NPs may lead to different biological effects when compared with macromolecular, and monoelemental species.[1] Therefore, studies concerning NPs toxicity are important. It is worth citing the NPs toxicity can be influenced by the pH and ionic strength of the physiological medium.[2-4]

The NPs effects in living organisms involves interactions with cellular components, membrane, organelles, and macromolecules present in the cell. Different NPs, treatment doses and exposure periods can induce different responses.[5] Silver nanoparticles (Ag-NPs), one of the most used and studied NPs, with spherical form and size ranging from 30 to 90 nm, has shown cytotoxic effect against breast cancer cell lines.[6,7] In addition, 20 nm Ag-NPs administered orally to rats for 30 days had negatively affected their memory and cognitive coordination.[8] Rare earth elements (REEs) have been increasingly used whereas beneficial or harmful effects of them to animals and humans have been observed. However, most studies have basically dealt with lanthanum (La) and cerium (Ce) in ionic form.[9-11] Lanthanum oxide nanoparticles (La_2O_3-NPs) have been used in semiconductors, fuel cells, optic devices, magnetic data storage, ceramics, catalyst, automobiles, biosensors, water treatment and biomedicine. Magnetic properties of La_2O_3-NPs were evaluated for field-controlled markers for drug release and as a contrast agent in nuclear magnetic resonance imaging.[12] La_2O_3-NPs have also been applied as antimicrobial and antiviral agent.[13,14] Therefore, the exposure of living organisms to La_2O_3-NPs have increased with the increasing use of La_2O_3-NPs. In a study conducted by Dressler et al. to verify La_2O_3-NPs deposition in bone, La_2O_3-NPs were administered orally to Wistar rats, and it was demonstrated that the NPs were present only on the surface of the bone.[15]

Distribution of NPs in organism regions and cells (biodistribution) can be used to detect the NPs fate.[16] For example, NPs can act as carriers of drugs and target specific cells, improving medical diagnosis and treatment.[17] The NPs biodistribution can be influenced by the route of administration (intravenous, oral, pulmonary, and dermal), physical (mainly size and shape) and chemical (reactivity) properties, besides the physiological environment in contact with the NPs. The absorption and distribution of NPs are also affected by the NPs coating material and surface charge.[1] One of the main routes of exposure of humans to NPs is through the consumption of products containing NPs in their composition. When ingested, NPs can be absorbed through the gastrointestinal tract and, in contact with the bloodstream, they can interact with proteins and other biomolecules.[2] In cases where NPs have protein-like dimensions of less than 40 nm and appropriate surface composition they can form complexes, which may lead to changes in proteins structure and even alter their functions and enzymatic activities.[18] For example, the enzymes alanine aminotransferase (ALT), aspartate transaminase (AST) and gamma-glutamyl transferase (γ-GT) present in liver can be altered when this organ is injured.[18] Thus, alteration of these enzymes in blood provides information about liver function and identifies possible hepatic lesions due to absorption of NPs. Renal damage can be identified by creatinine and urea alteration in blood serum.[19] Antioxidants are produced by the organism's metabolism system to inhibit the damage caused by the action of free radicals or non-radical reactive species. The relationship among oxidants and antioxidants is equilibrated in normal metabolism but the equilibrium can be affected by the increase of external agents (oxidants) that cause oxidative stress.[20, 21]

Despite the wide application of La_2O_3-NPs, little is known about their effects on animals. Therefore, the effect and distribution of La_2O_3-NPs in Wistar rats were studied in the present work. To this end, AST, ALT and γ-GT activities, uric acid, creatinine, antioxidant enzymes (catalase (CAT) and superoxide dismutase (SOD)), oxidative stress (through thiobarbituric acid reactive substances (TBARS)) protein oxidation, reactive oxygen species (ROS) and neurotoxicity were evaluated. Absorption of La_2O_3-NPs was evaluated through La determination in kidney, spleen, brain, pancreas, lung, and blood.

MATERIALS AND METHODS

Reagents and standards

Nanoparticles of La_2O_3 with a diameter of 15-30 nm, 99.9% purity and spherical morphology were purchased from Nanoamor (Houston, USA). These particles had been previously characterized, as reported by Nunes et al.[22] Nitric acid (65%, 1.4 kg L^{-1}, Sigma Aldrich, USA) was purified by sub-boiling distillation (in a duoPUR 2.01E system, Millestone, Sorisole, Italy) and then used in samples and solutions preparation. Water used throughout the work was distilled and purified (final resistivity of 18.2 MΩ cm) using a Milli-Q system (Millipore Corp., Bedford, USA). Other reagents and chemicals used were of analytical grade. Suspensions of La_2O_3-NPs were prepared in water and homogenized for 10 min in an ultrasound bath (Transsonic TI-H-5, Elma, Germany; 100 W, 25/45 kHz). Additional information about preparation of the La_2O_3-NPs suspensions can be found elsewhere.[22] Calibration solutions (ranging from 0.0 to 10.0 μg L^{-1} La) were prepared by dilution of a 10 mg L^{-1} multi-element solution (SCP33MS, SCP Science, Canada). The calibration solutions were prepared in 5% (v v^{-1}) nitric acid.

Animals

Sixty-day-old nulliparous and non-pregnant female Wistar rats, weighing 237-268 g each, were used in acute toxicity tests. Sixty-day-old male Wistar rats, weighing 251–322 g each, were used in subacute toxicity tests. The individuals were from the Central Animal House of the Federal University of Santa Maria (UFSM), Brazil. They were acclimated for seven days before starting the experiments. During the acclimation and experiments periods, the rats were housed in polycarbonate cages (five rats per cage) in a room with controlled temperature (23 °C ± 1) under 12 h light/dark cycle. Food and water were served *ad libitum*. The study was approved by the animal ethics committee of UFSM (protocol 4250170317).

Acute toxicity tests

The toxicity tests were carried out following the Guideline 425 from the Organization for Economic Co-operation and Development (OECD).[23] Doses of La_2O_3-NPs suspension were orally administered to the animals; the initial dose was 5.0 mg kg^{-1} *bw*. If the individual that had received this dose was still alive after 24 h, a second individual was treated with 50 mg kg^{-1} *bw* La_2O_3-NPs, followed by third and fourth individuals receiving 300 and 2000 mg kg^{-1} La_2O_3-NPs *bw*, respectively. One individual was treated with water only and used as control. The treated animals were observed for fourteen days, and symptoms associated with intoxication, like tremor, convulsion, diarrhoea and salivation were monitored. In the absence of mortality and intoxication signals, the animals were weighed, anesthetized with halothane (1-bromo-1-chloro-2,2,2-trifluoroethane) and euthanized. Then, their heart, spleen and liver were collected for histopathological analyses.

Subacute toxicity tests

In this case, 40 rats were divided in four groups with 10 individuals in each group, as follows: (*i*) control (individuals received water only), treated with (*ii*) 1.0, (*iii*) 10, and (*iv*) 100 mg kg^{-1} *bw* La_2O_3-NPs, respectively. The La_2O_3-NPs were administered orally (only with water in the case of the control animals), and each animal was daily treated at 5:00 pm. Following 30 days of treatment, the animals were weighed, anesthetized with halothane, and then euthanized. Their blood, brain, spleen, liver, lungs, heart, pancreas, and kidneys were removed and separated. The blood was collected through cardiac puncture and transferred to tubes containing ethylenediaminetetracetic acid (EDTA). The collected organs were separated, weighed, transferred to polypropylene tubes, which were maintained at -20 °C until analysis. The relative percentage of organ weight in relation to the body weight (*bw*) was calculated as Equation 1:

$$Relative\ organ\ weight\ (\%) = (organ\ weight\ \times 100)/b\,w \qquad \text{Equation 1}$$

Blood and organs analyses

The blood samples were centrifuged at 3500 *g* for 15 min, the precipitated discarded and the serum frozen at -20 °C for further analysis. AST, ALT and γ-GT activities were evaluated in duplicate using a semi-automatic analyzer (TP Analyzer Plus, Thermoplate, China) and commercial kits (Labtest Diagnostica, Brazil). Lipid peroxidation, ROS, protein oxidation, CAT and SOD activities were determined in liver and kidney tissues. For that purpose, separated parts of the organs were kept in 60 mmol L^{-1} Tris·HCl buffer (pH 7.4) in proportions of 1:10 (1 g of tissue in 10 mL of buffer), except for CAT and SOD. In this case, the proportion was 1:60 (1 g of tissue in 60 mL of buffer). Subsequently, the samples were homogenized and centrifuged at 2000 *g* for 10 min. Then, the supernatant was removed for analysis. Samples were always kept refrigerated during the analysis. The acetylcholinesterase (AChE) activity was measured in the cerebelum, estriatum, cerebral cortex and hippocampus. Absorbance was measured using an UV-1800 spectrometer (Shimadzu, Japan) or a SpectraMax i3 Molecular Device (LLC, USA).

Lipid peroxidation

The lipid peroxidation determination (with thiobarbituric acid – TBARS) in liver and kidney homogenates followed the method described by Olas et al.[24] In short, the sample placed in a 15 mL-tube was mixed with 15% (m/v) trichloroacetic acid in 0.25 mol L^{-1} HCl and 0.37% (m/v) thiobarbituric acid in 0.25 mol L^{-1} HCl. Subsequently, the tube containing the mixture was immersed in boiling water for 10 min. After cooling, the absorbance of the obtained solution was measured at 535 nm and the calculated results expressed as nmol malondialdehyde (MDA) mg^{-1} protein.

ROS determination

The ROS were determined by fluorimetry (QUIMIS Q798FIL, Brasil) according to Ali et al., whose method was adapted.[25] In this method, 2´,7´-dichlorofluorescein diacetate (DCFH-DA) is oxidized to fluorescent dichlorofluorescein (DCF) by intracellular ROS. The emission intensity was measured at 525 nm, after 30 min of adding the DCFH-DA. The calculated results were expressed as U DCF (unity of dichlorofluorescein) mg^{-1} protein.

Protein oxidation

The determination was based on the Levine method; the proteins oxidation occurs through reaction with 2,4-dinitrophenylhydrazine (DNPH) and the absorbance of the product is measured at 370 nm.[26] The results are expressed as nmol oxidized protein mg^{-1} protein.

Activities of CAT and SOD

The SOD and CAT activities in liver and kidney were measured according to methodologies recommended by Misra and Fridovich and Nelson and Kiesow, respectively.[27,28] The oxidation of epinephrine occurs at pH 10.5 to produce adrenochrome (of red color) whose absorbance is measured at 480 nm. The oxidation of epinephrine is inhibited by the addition of a sample containing SOD, decreasing the absorbance. The CAT activity was evaluated from the absorbance variation at 240 nm due to hydrogen peroxide decomposition in the sample at pH 8.5 and temperature of 37 °C, after 10 min. The results were expressed in μmol of SOD or CAT mg^{-1} protein.

Acetylcholinesterase activity

The acetylcholinesterase (AChE) activity in brain tissue was measured following an adapted method that had been developed by Ellman et al., as described by Rocha et al.[29,30] Thiocholine was mixed with 100 mmol L^{-1} potassium phosphate buffer (pH 7.5) and 1.0 mmol L^{-1} 5,5´-dithiobisnitrobenzoic acid (DTNB). The DTNB was reduced to thionitrobenzoic acid, producing a yellow-colored anion whose absorbance was measured at 412 nm. The calculated results were expressed as μmol AChE min^{-1} mg^{-1} protein.

Histological analysis

The spleen, heart, and liver of rats submitted to acute toxicity were removed and kept in 10% v v^{-1} buffered formalin. After dehydration, samples of these organs were embedded in paraffin and sectioned in 6 µm-thickness slices using a manual microtome. The slices were mounted on glass microscope slides, stained with hematoxylin-eosin and Masson/Goldner trichrome and visualised in a microscope (OLYMPUS CX21 microscope with an OLYMPUS camera).

Lanthanum determination

For La determination, liver, heart, kidney, pancreas, brain, spleen, and lung samples were decomposed in a microwave oven system (Speedwave 4, Berghof, Germany). The samples decomposition was carried out in trifluoromethyl-modified polytetrafluoroethylene (TFM-PTFE) flasks, where 4.0 mL of HNO_3 were added to 250 mg of sample and allowed to stand for 30 min at ambient temperature. Subsequently, the mixture was heated at 900 W for 40 min. After cooling, the digestate was transferred to a polypropylene flask (Sarstedt, Germany), where the sample solution volume was completed to 20 mL by adding water.

Lanthanum was determined by means of inductively coupled plasma-mass spectrometry (ICP-MS), being employed an Elan DRCII (PerkinElmer Sciex, Canada) instrument. This instrument was equipped with a concentric nebulizer (Meinhard Associates, USA), a baffled cyclonic spray chamber (from Glass Expansion) and a quartz torch fitted to a 2.0 mm internal diameter injector tube. Argon (99.996%, from Glass White Martins/Praxair, Brazil) was used as plasma, nebulizer, and auxiliary gas. The ICP-MS instrument was operated according to the manufacturer's recommendations. The conditions set are summarized in Table I.

Table I. Operating conditions set for lanthanum determination using ICP-MS

Parameter	Setting
Plasma power, W	1300
Plasma gas flow rate, L min^{-1}	15
Auxiliary gas flow rate, L min^{-1}	1.2
Nebulizer gas flow rate, L min^{-1}	1.16
Dwell time, ms	40
Readings	5
Readings per replicate	3
Replicates	3
m/z monitored	139

Accuracy, limits of detection and quantification

Accuracy was checked by analyzing the certified reference material (CRM) NIST 1566a (oyster tissue, from National Institute of Standards and Technology, USA). A *t*-test at 95% confidence level was applied to compare the La concentration found with that certified value. To check if the differences were significant in the other determinations, when appropriate, *t*-test or one-way ANOVA (analysis of variance) both at 95% confidence level were applied. The limits of detection (LOD) and quantification (LOQ) for La were calculated through $B + 3s$ (LOD) and $B + 10s$ (LOQ), respectively, where B is the blank concentration value and s is the standard deviation of 10 consecutive measurements of the blank. The LOD and LOQ were calculated following recommendations from the International Union of Pure and Applied Chemistry (IUPAC).

RESULTS AND DISCUSSION

Acute toxicity effects

Behavior alterations of the animals monitored for fourteen days after oral administration of 5, 50, 300, and 2000 mg kg^{-1} *bw* La_2O_3-NPs were not observed. They were weighed before and fourteen days after the La_2O_3-NPs administration and it was observed their weight had increased. Since the animals were in the growth phase, the weight increase was considered normal and not caused by the La_2O_3-NPs given to them. The ratio of the heart, spleen and liver weight to the body weight was not different for the different doses of La_2O_3-NPs – these organs and the animals were weighed before and 14 days after the La_2O_3-NPs administration. Figures 1, 2 and 3 show the histology of the liver, spleen and heart, respectively.

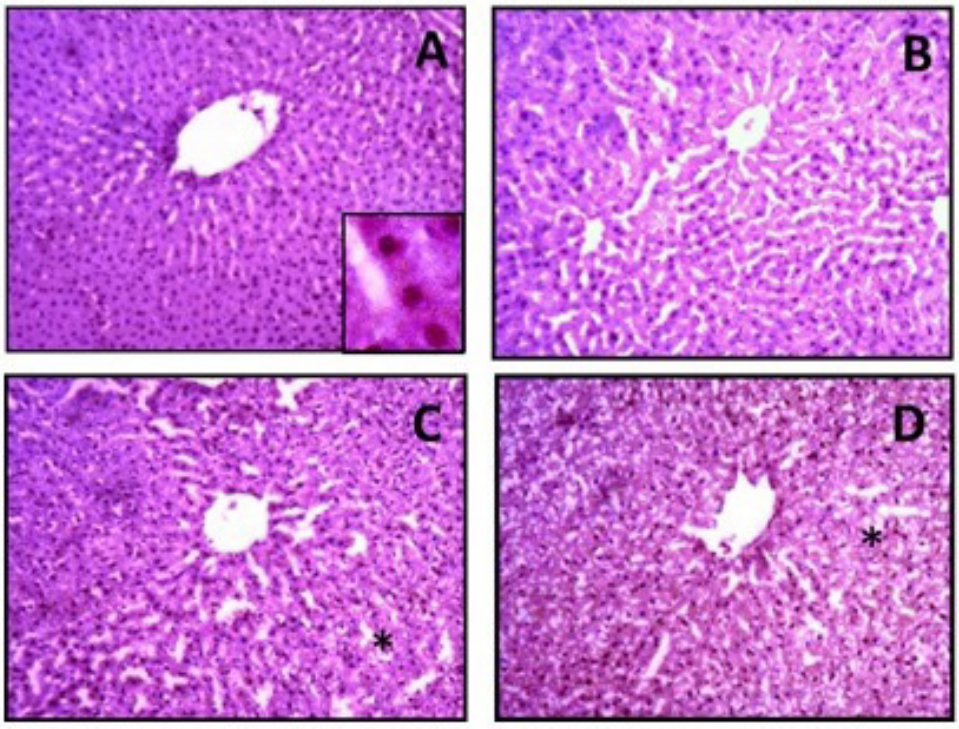

Figure 1. Histology of the rat's livers: control (A), treated with 5 (B), 300 (C), and 2000 (D) mg kg^{-1} *bw* La_2O_3-NPs. Magnification: 10x; 40x in the inset of Figure (A). * Denotes changes observed.

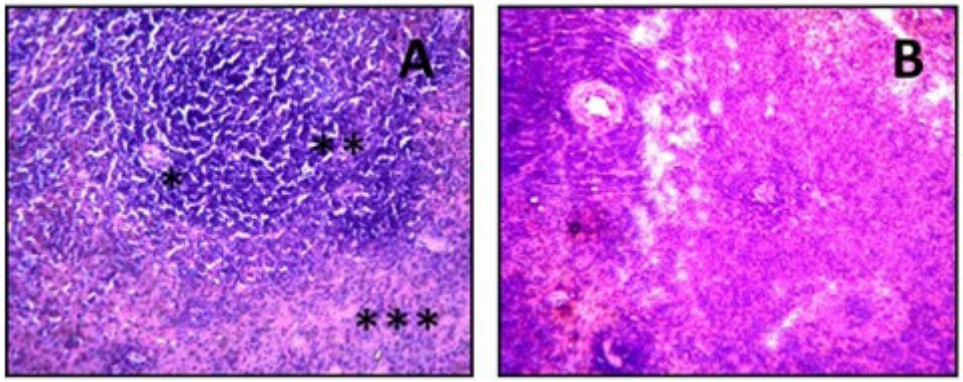

Figure 2. Spleen histology: control rat (A) and a rat treated with 2000 mg kg^{-1} *bw* La_2O_3-NPs (B). Magnification: 10x; * central arteriole; ** blank pulp; and *** red pulp.

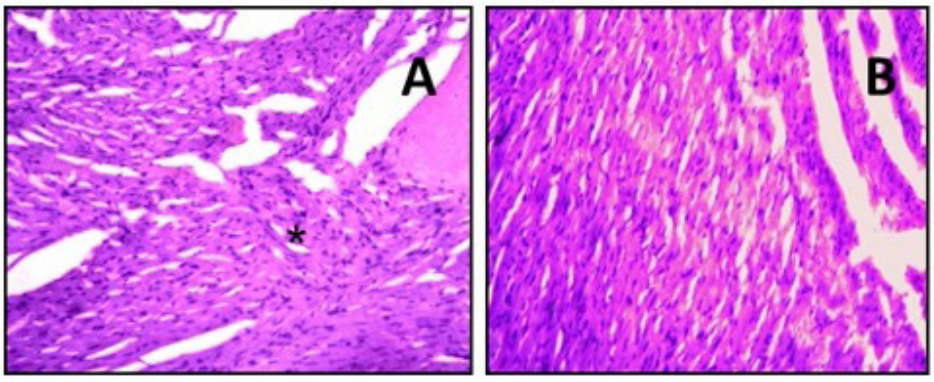

Figure 3. Heart histology: control rat (A) and a rat treated with 2000 mg kg^{-1} *bw* La_2O_3-NPs (B). Magnification: 10x (B); * muscle cells with central nuclei.

Normal histology with hepatocytes arranged radially from the central vein towards the periphery of the liver lobes was observed for the control animal (Figure 1A). Remarkable changes were not observed for the liver of an animal treated with 5 mg kg^{-1} *bw* La_2O_3-NPs (Figure 1B). On the other hand, treatment with 300 and 2000 mg kg^{-1} *bw* La_2O_3-NPs resulted in hydropic degeneration of the liver (Figures 1C and 1D), characterised by the presence of larger hepatocytes with a clear cytoplasm, small pale vacuoles and a normal nucleus. Any change was not observed in the spleen (Figures 2A and 2B) and heart (Figures 3A and 3B), even for the animals that had been treated with 2000 mg kg^{-1} *bw* La_2O_3-NPs (Figures 2B and 3B).

Subacute toxicity effects

The animals were daily observed and weekly weighed; physical modifications like hair loss, mucosal secretion, and weight loss were not detected during the treatment period (30 days) and all individuals survived. Figure 4 shows that the animals body weight increased, and according to ANOVA, there was not significant difference among the groups. As previously mentioned, the animals were in the growth phase and the weight increase was considered normal.

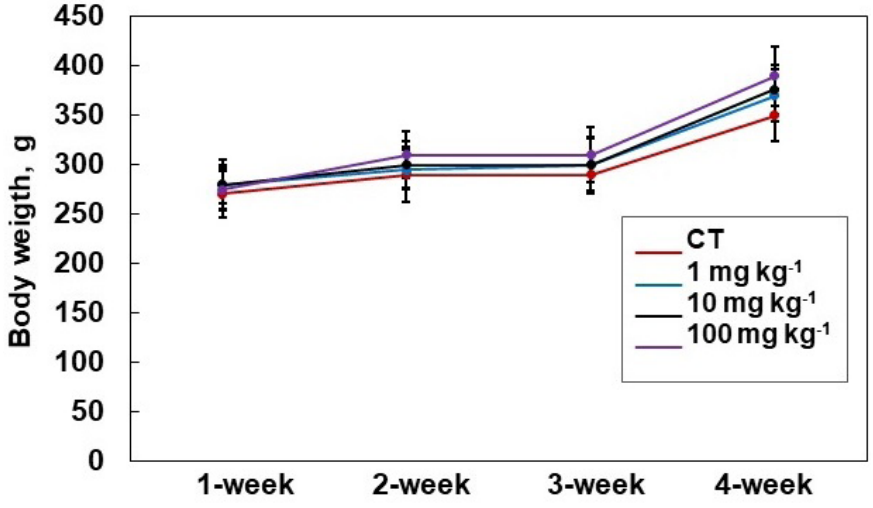

Figure 4. Body weight of the rats daily treated with La_2O_3-NPs for 30 days. The animals were weighed weekly. CT: control.

The animals were weighed and euthanized at the end of treatment period. Then, their organs were collected and weighed. The relative organ weigh (organ weight ×100)/*bw*) is given in Table II. According

to ANOVA, the relative organ weigh did not differ significantly among control rats and those treated with La_2O_3-NPs. However, a longer time exposure to La_2O_3-NPs would cause possible changes in the animals weight and must be studied em more details.

Table II. Relative organ weight for control rats (CT) and those treated with La_2O_3-NPs. Values are the mean ± standard deviation for 10 specimens or individuals.

	Relative organ weight, %			
Organ	**0.0 (CT)** (n = 10)	**1.0 mg kg^{-1} *bw*** (n = 10)	**10 mg kg^{-1} *bw*** (n = 10)	**100 mg kg^{-1} *bw*** (n = 10)
Brain	0.533 ± 0.038	0.539 ± 0.044	0.502 ± 0.182	0.536 ± 0.043
Liver	3.47 ± 0.11	3.66 ± 0.45	3.63 ± 1.29	3.80 ± 0.55
Left kidney	0.353 ± 0.150	0.357 ± 0.036	0.372 ± 0.036	0.368 ± 0.032
Right kidney	0.340 ± 0.144	0.351 ± 0.027	0.366 ± 0.038	0.362 ± 0.037
Spleen	0.177 ± 0.012	0.189 ± 0.016	0.182 ± 0.022	0.178 ± 0.015
Right lung	0.121 ± 0.018	0.124 ± 0.009	0.138 ± 0.024	0.135 ± 0.028
Heart	0.332 ± 0.031	0.340 ± 0.022	0.361 ± 0.054	0.337 ± 0.035
Pancreas	0.285 ± 0.027	0.245 ± 0.052	0.288 ± 0.031	0.255 ± 0.051
Body weight	359 ± 24	375 ± 19	386 ± 24	372 ± 18

Creatinine, urea, γ-GT, ALT and AST in blood serum

The creatinine, urea, γ-GT, ALT and AST levels found in blood serum of control rats and those treated with La_2O_3-NPs are given in Table III. The ANOVA revealed that levels were not statistically different.

Table III. Analysis of blood serum of control rats (CT) and those treated with La_2O_3-NPs. Values are the mean ± standard deviation for six individuals.

	Treated with La_2O_3-NPs, mg kg^{-1} *bw*			
Parameter	**0.0 (CT)** (n = 6)	**1.0** (n = 6)	**10** (n = 6)	**100** (n = 6)
Creatinine (mg dL^{-1})	0.4 ± 0.1	0.4 ± 0.1	0.4 ± 0.1	0.3 ± 0.1
Ureia (mg dL^{-1})	47 ± 7	52 ± 8	51 ± 8	48 ± 3
γ-GT (U L^{-1})	< 1	< 1	< 1	< 1
ALT (U L^{-1})	132 ± 35	157 ± 13	140 ± 41	161 ± 32
AST (U L^{-1})	48 ± 13	51 ± 6	49 ± 7	50 ± 8

Oxidative stress in kidney

Figure 5 illustrates the oxidative stress in kidney. According to Figure 5A, the ROS levels decreased in rats treated with 1.0 or 10 mg kg^{-1} *bw* La_2O_3-NPs and increased in those treated with 100 mg kg^{-1} *bw* La_2O_3-NPs. The ROS level for each group of animals treated with La_2O_3-NPs was significantly different when compared with the control group animals. Decreasing TBARS levels (Figure 5B) were observed for

all treatments but with significant differences for the groups of animals treated with 10 and 100 mg kg^{-1} *bw* La_2O_3-NPs when compared with the control group. On the other hand, significant difference was not observed in protein oxidation (Figure 5C), CAT (Figure 6A) and SOD (Figure 6B) levels.

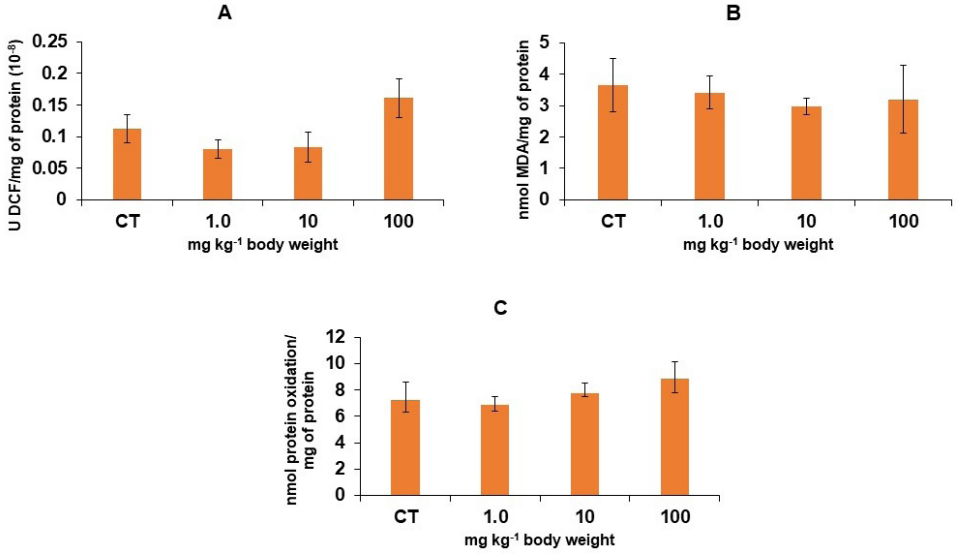

Figure 5. (A) Reactive oxygen species (ROS), (B) lipid peroxidation (as TBARS) and (C) protein oxidation levels in kidney of control rats and those treated with La_2O_3-NPs for 30 days. Each group comprised six individuals (*n* = 6).

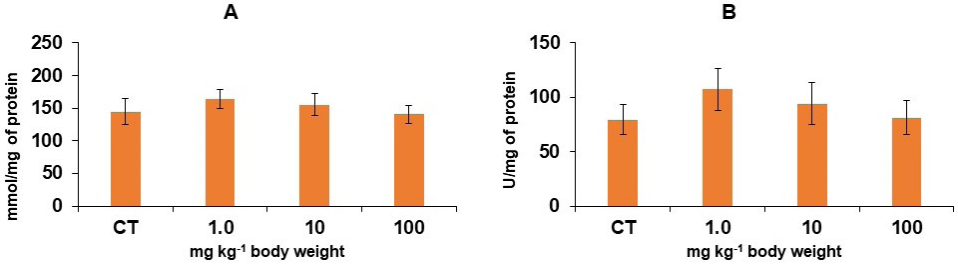

Figure 6. (A) Catalase and (B) superoxide dismutase activities in kidney of control rats and those treated with La_2O_3-NPs for 30 days. Each group comprised six individuals (*n* = 6).

Oxidative stress in liver

The oxidative stress in liver due to La_2O_3-NPs administration is depicted in Figure 7. The ROS levels in the liver (Figure 7A) of the control group animals and in those of the group treated with 10 mg kg^{-1} *bw* La_2O_3-NPs were significantly different. The difference was also significant for protein oxidation (Figure 7C) when the control group was compared with the group of rats treated with 100 mg kg^{-1} *bw* La_2O_3-NPs. However, for all groups the lipid peroxidation levels (Figure 7B) was not significantly different.

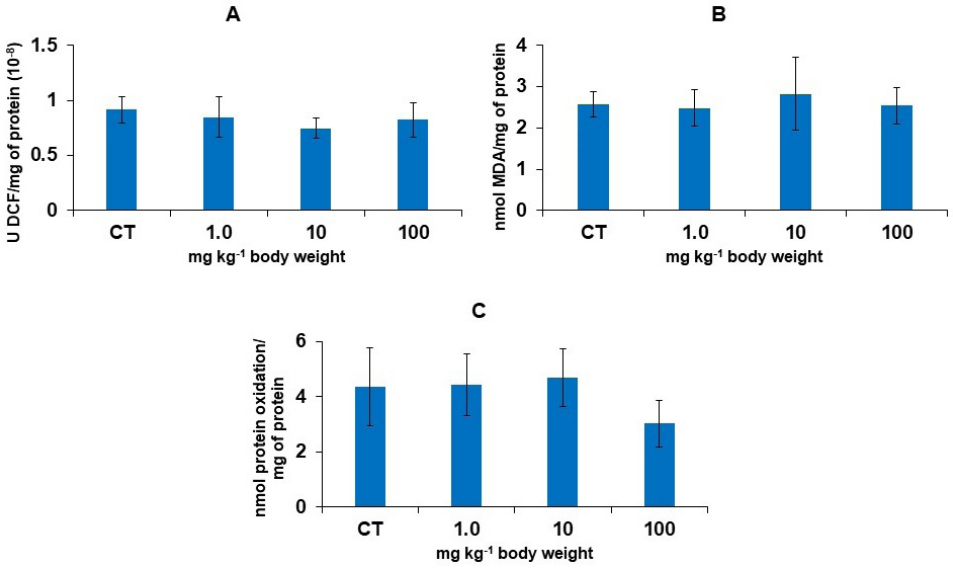

Figure 7. (A) reactive oxygen species, (B) lipid peroxidation, and (C) protein oxidation levels in liver homogenates of control rats and those treated with La_2O_3-NPs for 30 days. Each group comprised six individuals (n = 6).

The CAT and SOD activities were also not significantly different among the control and treated animal groups (Figure 8), excepting SOD for the group of animals treated with 10 mg kg^{-1} *bw* La_2O_3-NPs (Figure 8B).

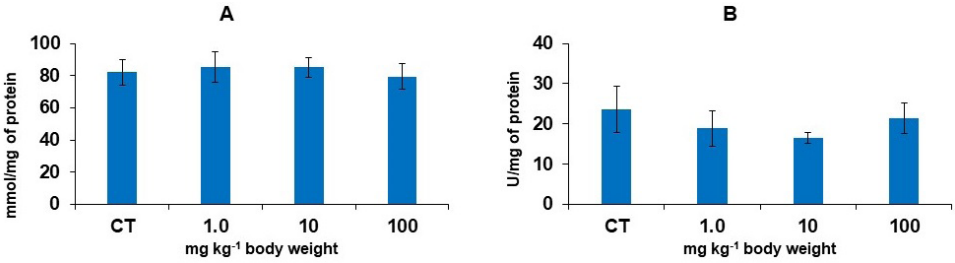

Figure 8. (A) catalase and (B) superoxide dismutase activities in liver homogenates of control rats and those treated with La_2O_3-NPs for 30 days. Each group comprised 6 individuals (n = 6) for CAT and 5 individuals for SOD (n = 5).

Acetylcholinesterase activity

Variation of the AChE activity was observed (Figure 9), but it was not significantly different for control and treated animals.

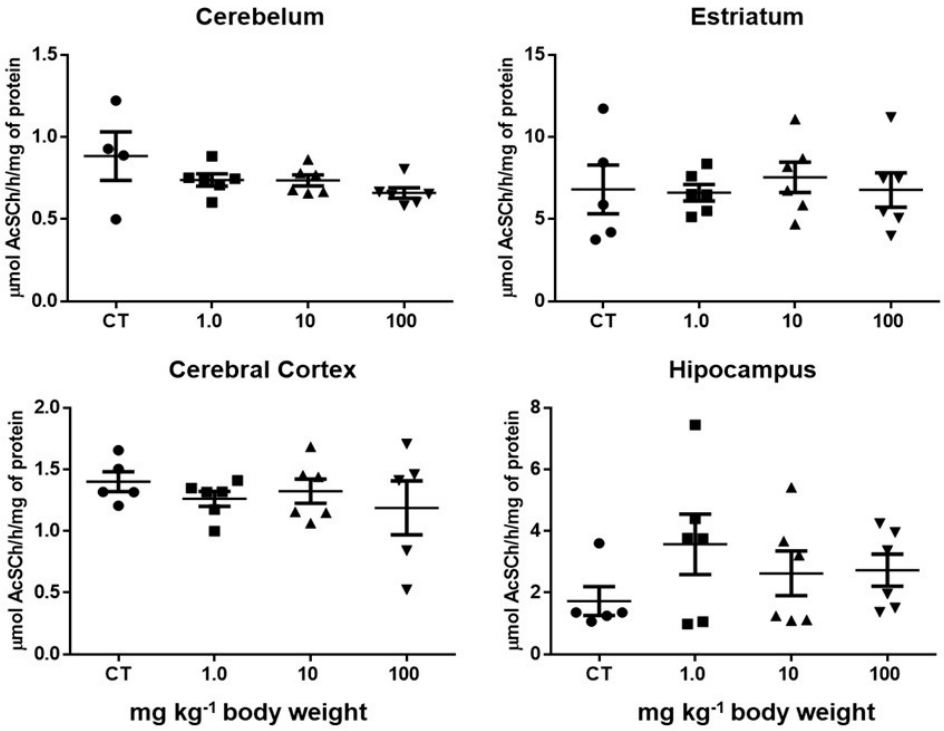

Figure 9. Acetylcholinesterase activity in brain of control rats and those treated with La_2O_3-NPs for 30 days. Each group comprised six individuals (n = 6).

Lanthanum determination

The La concentration in blood of control and treated animals were lower than LOQ, which was 10 ng g^{-1}. The LOD and LOQ for La in the organs were 1.0 ng g^{-1} and 3.0 ng g^{-1}, respectively. Lanthanum was detected in all analyzed organs, where higher concentration was found in liver, kidney, and heart (Figure 10). Accumulation of La in pancreas, brain, spleen, and lung in control animals and those treated with La_2O_3-NPs was not significantly different. Results for the more concentrated and diluted samples solutions were similar, which indicated there was not matrix interference. A CRM (NIST 1566a, Oyster Tissue) was analyzed in parallel. The La concentration found (0.28 ± 0.02 µg g^{-1}) agreed with that informed on the CRM certificate (0.3 µg g^{-1}), considering a t-test at 95% confidence level. In addition, possible matrix effect was checked by diluting the sample solution.

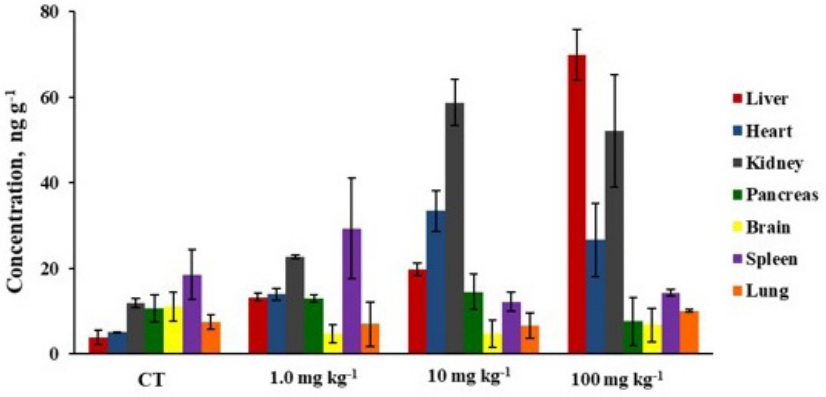

Figure 10. Lanthanum concentration found in organs of control (CT) rats and those treated with La_2O_3-NPs. Each bar represents the mean and standard deviation for three organs.

Discussion

Conditions as close as possible to those in real exposure should be considered in evaluating effects and toxicity of NPs, following *in vitro* and *in vivo* assay models. In the *in vitro* assay, cells are exposed to NPs of interest and parameters like inhibition of cell growth and respiration, free radicals production, lesions in DNA and other biochemical and cellular manifestations. *In vivo* assays use animal models, where growth, mortality, organs injury, enzymes activity, oxidation of proteins, production of ROS and other parameters are monitored.[31] Such parameters may indicate changes in normal body functioning due to the presence of NPs. Therefore, studies about the NPs toxicity are mandatory for a safer use of them. Possible effects of La_2O_3-NPs were investigated in the present study, considering physical and biochemical parameters and La bioaccumulation in different organs. Toxicity signals, body weight and ratio organ weight/body weight alterations were not induced by 5.0, 50, 300, and 2000 mg kg^{-1} *bw* La_2O_3-NPs. Histological analysis revealed that the spleen and heart of rats treated with La_2O_3-NPs at these concentrations were not affected. However, 300 and 2000 mg kg^{-1} *bw* La_2O_3-NPs injured the liver. As such, the investigation was continued, and the rats were treated with La_2O_3-NPs at concentration lower than 300 mg kg^{-1} *bw*; the welfare and safety of the animals were deemed in this case.

Although the body weight of the animals increased (Figure 3) during the treatment period (30 days), this was expected because they were 60-120 days old and still in the growth phase. The La concentration found in the analyzed rat organs (Figure 4) revealed the La_2O_3-NPs had accumulated in them. For each group, the La accumulation degree in the liver, kidney and heart ranged from 0.0002% to 0.005% of the administered La_2O_3-NPs amount in the period of treatment. These results are in accordance with the distribution degree of poorly soluble NPs reported by Geiser and Kreyling.[32] Similar distribution degree of administered nickel oxide NPs has been reported, with maximum accumulation of Ni in liver and kidney of rats.[33] Nevertheless, the NPs absorption is generally unfavorable. Agglomeration of the NPs may also difficult their absorption. The absorption of orally administered NPs can occur by specialized intestinal cells and accumulation in tissue might occur through the lymphatic system and blood circulation, as discussed by Silva et al. for titanium oxide NPs in humans.[34]

Lanthanum was not detected in blood probably because it was collected 24 h or more time after the last administration of La_2O_3-NPs. The accumulation of La in the liver can be explained by its cellular composition: it contains Kupffer cells, which are responsible for the removal of any “foreign” substance from blood in contact with the organ.[25] Perhaps this explains why greater accumulation of La occurred in the liver, and the La concentration in this organ increased with the La_2O_3-NPs concentration increase (see Figure 11). In previous studies, it has been demonstrated that La_2O_3-NPs can be incorporated in plants and bone.[22,15] Thus, it is possible that La_2O_3-NPs have been transported to the liver through the bloodstream and kept in the form of La_2O_3-NPs in the liver. Accumulation of La in the kidney may be related with the elimination of NPs through the urine, deeming that the renal system acts as a filter of impurities in the organism.[3] Accumulation of NPs in the heart remains unexplained. Park et al. observed accumulation of vanadium oxide-NPs in mice organs as follows: heart > liver > kidney > spleen.[35] These authors stated that additional studies were necessary to assess realistic causes and effects.

Creatinine, urea, γ-GT, ALT and AST increase may indicate toxicity effects of La_2O_3-NPs; creatinine and urea may indicate renal failure while γ-GT, ALT and AST indicate hepatic lesions. The creatinine, urea, γ-GT, ALT and AST levels (see Table III) in the blood of animals treated or not with La_2O_3-NPs were not different. Therefore, although La has accumulated in these organs, it can be affirmed that the La_2O_3-NPs administered did not damage the liver and kidneys during the treatment period (30 days). These findings corroborate those reported for organs of rats treated with copper oxide-NPs.[36] Exposure to metal oxide-NPs can induce excessive ROS generation, affects antioxidant enzymes and normal function of cell membrane due to imbalanced oxidant/antioxidant equilibrium.[37-39] An increase of ROS was found in kidney (Figure 5A) of rats treated with 100 mg kg^{-1} *bw* La_2O_3-NPs. Conversely, protein oxidation decreased in the liver of those animals (Figure 7C). Meanwhile, any significant effect of NPs on lipid peroxidation was not observed (Figure 7B).

The levels of ROS in the organism are controlled by protection mechanisms through the production of antioxidant enzymes like SOD and CAT for instance; SOD catalyzes reaction reduction of superoxide radicals to produce oxygen and hydrogen peroxide, while CAT catalyzes the hydrogen peroxide reduction to produce water and oxygen.[40,41] The CAT activity (Figure 8A) was not affected by La_2O_3-NPs and that of SOD (Figure 8B) was only in the liver of animals treated with 10 mg kg^{-1} *bw* La_2O_3-NPs.

Due to the small size of NPs they can cross the blood-brain barrier, interact with the central nervous system and induce neurotoxicity. The NPs can affect the AChE activity, the enzyme responsible for catabolizing acetylcholine, which is released into cholinergic synapses in the brain.[42] Inhibition of AChE induces acetylcholine accumulation and results in cholinergic toxicity and, therefore, the AChE activity is appropriate for evaluating the neurotoxicity of NPs.[43] For example, Canli et al. administered aluminum oxide-NPs (40 nm particles size) orally to rats (0, 0.5, 5 and 50 mg kg^{-1} *bw* NPs).[44] Significant decrease of the AChE activity in the brain of the animals was observed for all doses of NPs administered. Noor et al. observed reduction of AChE activity in the cortical and hippocampal brain regions in Wistar rats 24 h after receiving injection of gold-NPs (20 nm particles size).[45] However, in the present work the La_2O_3-NPs did not affect the AChE activity (Figure 9). The size of the administered La_2O_3-NPs was about 15-30 nm but these NPs can agglomerate, which would hinder their passage across the blood-brain barrier.[21] This is in accordance with the very low La concentration found the in brain (Figure 10), indicating that the NPs did not go into the brain easily.

The La concentration in blood of control and treated animals were lower than the LOQ. However, the La concentration was higher than the LOQ in the analyzed organs, at higher concentration in liver, kidney, and heart; the La concentration in liver, kidney and heart of animals treated with the NPs was higher than that in the organs of control animals. The accuracy was demonstrated through CRM analysis, revealing that interference were not insignificant since accurate results were obtained for La. Studies about La_2O_3-NPs transformation in the treated animals were not conducted. Nevertheless, in a previous study, NPs have been found on bones surface in rats treated with La_2O_3-NPs.[15] In this way, it can be inferred that La could also be present in the form of NPs in the analyzed organs.

CONCLUSIONS

Administration of La_2O_3-NPs at concentrations of 1.0, 10 and 100 mg kg^{-1} *bw* did not cause significant changes in biochemical parameters, body weight and organ weight of Wistar rats. Although the La concentration increased in liver, kidney and heart, oxidative stress and neurotoxicity were in general not induced by La_2O_3-NPs when administered at concentration lower than 100 mg kg^{-1} *bw* for 30 days.

Additional studies are necessary to demonstrate whether the La_2O_3-NPs are accumulated in the organs for longer period and if the toxicity will increase for longer time of exposure of the animals. It is also worth investigating possible agglomeration, solubilization or transformation of La_2O_3-NPs to free La (ionic form) during their metabolism in the organism.

Conflicts of interest

The authors declare that there is no conflict of interest.

Acknowledgments

This work was supported by “Conselho Nacional de Desenvolvimento Científico e Tecnológico” (CNPq Proc. Nr. 480929/2011-4 and 306052/2017-2).

REFERENCES

(1) de Matteis, V. Exposure to inorganic nanoparticles: Routes of entry, immune response, biodistribution and in vitro/in vivo toxicity evaluation. *Toxics* **2017**, *5*, 29. https://doi.org/10.3390/toxics5040029

(2) Kermanizadeh, A.; Balharry, D.; Wallin, H.; Loft, S.; Møller, P. Nanomaterial translocation-the biokinetics, tissue accumulation, toxicity and fate of materials in secondary organs - a review. *Crit. Rev. Toxicol*. **2015**, *45*, 837-872. https://doi.org/10.3109/10408444.2015.1058747

(3) Iavicoli, I.; Fontana, L.; Nordberg, G. The effects of nanoparticles on the renal system. *Crit. Rev. Toxicol*. **2016**, *46*, 490-560. https://doi.org/10.1080/10408444.2016.1181047
(4) Geppert, M.; Schwarz, A.; Stangassinger, L.M.; Wenger, S.; Wienerroither, L.M.; Ess, S.; Duschl, A.; Himly, M. Interactions of TiO_2 nanoparticles with ingredients from modern lifestyle products and their effects on human skin cells. *Crit. Rev. Toxicol*. **2020**, *33*, 1215-1225. https://doi.org/10.1021/acs.chemrestox.9b00428
(5) Panariti, A.; Miserocchi, G.; Rivolta, I. The effect of nanoparticle uptake on cellular behavior: disrupting or enabling functions? *Nanotechnol. Sci. Appl*. **2012**, *5*, 87-100. https://doi.org/10.2147/NSA.S25515
(6) Durán, N.; Rolim, W. R.; Durán, M.; Fávaro, W. J.; Seabra, A. B. Nanotoxicology of silver nanoparticles: toxicity in animals and humans. *Química Nova* **2019**, *42*, 206-213. https://doi.org/10.21577/0100-4042.20170318
(7) Sadat, N. A.; Salehzadeh, A. Green biosynthesise of silver nanoparticles using gracilaria gracilis extract and its effect on breast cancer line. *The Breast* **2019**, *48*, S72. https://doi.org/10.1016/S0960-9776(19)30745-3
(8) Węsierska, M.; Dziendzikowsk, K.; Gromadzka-Ostrowsk, J.; Dudek, J.; Polkowska-Motrenko, H.; Audinot, J. N.; Gutlebe, A. C.; Lankoff, A.; Kruszewski, M. Silver ions are responsible for memory impairment induced by oral administration of silver nanoparticles. *Toxicol. Lett.* **2018**, *290*, 133–144. https://doi.org/10.1016/j.toxlet.2018.03.019
(9) Abdelnour, S. A.; El-Hack M. E. A.; Khafaga, A. F.; Noreldin, A. E.; Arif, M.; Chaudhry, M. T.; Losaccog, C.; Abdeenh, A.; Abdel-Daim, M. M. Impacts of rare earth elements on animal health and production: Highlights of cerium and lanthanum. *Sci. Total Environ*. **2019**, *672*, 1021-1032. https://doi.org/10.1016/j.scitotenv.2019.02.270
(10) Pagano, G.; Aliberti, F.; Guida, M.; Oral, R.; Siciliano, A.; Trifuoggi, M.; Tommasi, F. Rare earth elements in human and animal health: State of art and research priorities. *Environ. Res*. **2015a**, *142*, 215-22. https://doi.org/10.1016/j.envres.2015.06.039
(11) Pagano, G.; Guida, M.; Tommasi, F.; Oral, R. Health effects and toxicity mechanisms of rare earth elements – Knowledge gaps and research prospects. *Ecotoxicol. Environ. Saf*. **2015b**, *115*, 40-48. https://doi.org/10.1016/j.ecoenv.2015.01.030
(12) Brabu, B. S.; Haribabu, M.; Revathy, S.; Anitha, M.; Thangapandiyan, K. R.; Navaneethakrishnan, C.; Gopalakrishnan, S. S.; Murugan, T. S. K. Biocompatibility studies on lanthanum oxide nanoparticles. *Toxicol. Res.* **2015**, *4* (4), 1037-1044. https://doi.org/10.1039/C4TX00198B
(13) Balusamy, B.; Kandhasamy, Y. G.; Senthamizhan, A.; Chandrasekaran, G.; Subramanian, M. S.; Kumarave, T. S. Characterization and bacterial toxicity of lanthanum oxide bulk and nanoparticles. *J. Rare Earths* **2012**, *30*, 1298-1302. https://doi.org/10.1016/S1002-0721(12)60224-5
(14) Liu, J.; Mei, W.; Li, Y.; Wang, E.; Ji, L.; Tao, P. Antiviral activity of mixed-valence rare earth borotungstate heteropoly blues against influeza virus in mice. *Antivir. Chem. Chemother.* **2000**, *11*, 367-372. https://doi.org/10.1177/095632020001100603
(15) Dressler, V. L.; Ogunmodede, O. T.; Heidrich, G. M.; Neves, V. M.; Schetinger, M. R. C.; Morsch, V. M. Investigative analysis of lanthanum oxide nanoparticles on elements in bone of wistar rats after 30 days of repeated oral administration. *Biol. Trace Elem. Res*. **2019**, *196*, 153-167. https://doi.org/10.1007/s12011-019-01907-z
(16) Sa, L. T. M.; Albernaz, M. S.; Patricio, B. F. C.; Falcão Jr., M. V.; Coelho, B. F.; Bordim, A.; Almeida, J. C.; Santos-Oliveira, R. Biodistribution of nanoparticles: initial considerations. *J. Pharm. Biomed. Anal.* **2012**, *70*, 602-604. https://doi.org/10.1016/j.jpba.2012.06.008
(17) Ocsoy, I.; Tasdemir, D.; Mazicioglu, S.; Celik, C.; Katı, A.; Ulgen, F. Biomolecules incorporated metallic nanoparticles synthesis and their biomedical applications. *Mater. Lett*. **2018**, *212*, 45-50. https://doi.org/10.1016/j.matlet.2017.10.068
(18) Ozer, J.; Ratner, M.; Shaw, M.; Bailey, W.; Schomaker, S. The current state of serum biomarkers of hepatotoxicity. *Toxicol*. **2008**, *245*, 194-205. https://doi.org/10.1016/j.tox.2007.11.021

(19) Hauck, T. S.; Anderson, R. E.; Fischer, H. C.; Newbigging, S.; Chan, W. C. In vivo quantum-dot toxicity assessment. *Small* **2010**, *6*, 138-144. https://doi.org/10.1002/smll.200900626
(20) Canli, E. G.; Ila, H. B.; Canli, M. Response of the antioxidant enzymes of rats following oral administration of metal-oxide nanoparticles (Al_2O_3, CuO, TiO_2). *Environ. Sci. Pollut. Res*. **2019a**, *26*, 938-945. https://doi.org/10.1007/s11356-018-3592-8
(21) Hauser-Davis, R. A.; Silva, J. A. N.; Rocha, R. C. C.; Saint'Pierre, T.; Ziolli, R. L., Arruda, M. A. Z. Acute selenium selenite exposure effects on oxidative stress biomarkers and essential metals and trace-elements in the model organism zebrafish (Danio rerio). *J. Trace Elem. Med. Biol*. **2016**, *33*, 68-72. https://doi.org/10.1016/j.jtemb.2015.09.001
(22) Neves, V. M.; Heidrich, G. M.; Rodrigues, E. S.; Enders, M. S. P.; Muller, E. I.; Nicoloso, F. T.; de Carvalho, H. W. P.; Dressler, V. L. La_2O_3 Nanoparticles: Study of Uptake and Distribution in *Pfaffia glomerata* (Spreng.) Pedersen by LA-ICP-MS and μ-XRF. *Environ. Sci. Technol.* **2019**, *53*, 10827-10834. https://doi.org/10.1021/acs.est.9b02868
(23) OECD, Acute oral toxicity: Up and down procedure, Guideline for Testing of Chemicals 425 OECD, **2008**, pp. 1-2. Available at: https://ntp.niehs.nih.gov/iccvam/suppdocs/feddocs/oecd/oecdtg425.pdf [Accessed in Dec. 2022].
(24) Olas, B.; Saluk-Juszczak, J.; Wachowicz, B. d-glucaro 1,4-lactone and resveratrol as antioxidants in blood platelets. *Cell Biol. Toxicol*. **2008**, *24*, 189–199. https://doi.org/10.1007/s10565-007-9028-8
(25) Ali, S. F.; LeBel, C. P.; Bondy, S. C. Reactive oxygen species formation as a biomarker of methylmercury and trimethyltin neurotoxicity. *Neurotoxicology* **1992**, *13*, 637–648. PMID: 1475065.
(26) Levine, R. L.; Garland, D.; Oliver, C. N.; Amici, A.; Climent, I.; Lenz, A. G.; Ahn, B. W.; Shaltiel, S.; Stadtman, E. R. Determination of carbonyl content in oxidatively modified proteins. *Meth. Enzymol*. **1990**, *186*, 464–478. https://doi.org/10.1016/0076-6879(90)86141-h
(27) Misra, H. P.; Fridovich, I. The role of superoxide anion in the autoxidation of epinephrine and a simple assay for superoxide dismutase. *J. Biol. Chem*. **1972**, *247*, 3170-3175. PMID: 4623845.
(28) Nelson, D. P.; Kiesow, L. A. Enthalpy of decomposition of hydrogen peroxide by catalase at 25 degrees C (with molar extinction coefficients of H_2O_2 solutions in the UV). *Anal. Biochem*. **1972**, *49*, 474-478. https://doi.org/10.1016/0003-2697(72)90451-4
(29) Ellman, G. L.; Courtney, K. D.; Andres Jr., V.; Feather-Stone, R. M. A new and rapid colorimetric determination of acetylcholinesterase activity. *Biochem. Pharmacol*. **1961**, *7*, 88-95. https://doi.org/10.1016/0006-2952(61)90145-9
(30) Rocha, J. B.; Emanuelli, T.; Pereira, M. E. Effects of early undernutrition on kinetic parameters of brain acetylcholinesterase from adult rats. *Acta Neurobiol. Exp.* **1993**, *53*, 431-437. PMID: 8249659.
(31) Hall, J. B.; Dobrovolskaia, M. A.; Patri, A. K.; McNeil, S. E. Characterization of nanoparticles for therapeutics. *Nanomedicine* **2007**, *2*, 789-803. https://doi.org/10.2217/17435889.2.6.789
(32) Geiser, M.; Kreyling, W. G. Deposition and biokinetics of inhaled nanoparticles. *Part. Fibre Toxicol*. **2010**, *7*, 1-17. https://doi.org/10.1186/1743-8977-7-2
(33) Dumala, N.; Mangalampalli, B.; Kamal, S. S. K.; Grover, P. Repeated oral dose toxicity study of nickel oxide nanoparticles in Wistar rats: a histological and biochemical perspective. *J. Appl. Toxicol.* **2019**, *39*, 1012–1029. https://doi.org/10.1002/jat.3790
(34) Silva, A. B.; Miniter, M.; Thom, W.; Hewitt, R. E.; Wills, J.; Jugdaohsingh, R.; Powell, J. J. Gastrointestinal absorption and toxicity of nanoparticles and microparticles: Myth, reality and pitfalls explored through titanium dioxide. *Curr. Opin. Toxicol.* **2020**, *19*, 112–120. https://doi.org/10.1016/j.cotox.2020.02.007
(35) Park, E. J.; Lee, G. H.; Yoon, C.; Kim, D. W. Comparison of distribution and toxicity following repeated oral dosing of different vanadium oxide nanoparticles in mice. *Environ. Res.* **2016**, *150*, 154-165. https://doi.org/10.1016/j.envres.2016.05.036
(36) Bugata, L. S. P.; Venkata, P. P.; Gundu, A. R.; Fazlur, R. M.; Reddy, U. A.; Kumar, J. M.; Mekala, V. R.; Bojja, S.; Mahboob, M. Acute and subacute oral toxicity of copper oxide nanoparticles in female albino Wistar rats. *J. Appl. Toxicol*. **2018**, *39*, 702-716. https://doi.org/10.1002/jat.3760

(37) Zhang, H.; Ji, Z.; Xia, T.; Meng, H.; Low-Kam, C.; Liu, R.; Pokhrel, S.; Lin, S.; Wang, X.; Liao, Y. P.; Wang, M.; Li, L.; Rallo, R.; Damoiseaux, R.; Telesca, D.; Mädler, L.; Cohen, Y.; Zink, J. I.; Nel, A. E. Use of metal oxide nanoparticle band gap to develop a predictive paradigm for oxidative stress and acute pulmonary inflammation. *ACS Nano.* **2012**, *6*, 4349-68. https://doi.org/10.1021/nn3010087

(38) Sarkar, A.; Ghosh, M.; Sil, P. C. Nanotoxicity: Oxidative Stress Mediated Toxicity of Metal and Metal Oxide Nanoparticles. *J. Nanosci. Nanotechnol.* **2014**, *14*, 730-43. https://doi.org/10.1166/jnn.2014.8752

(39) Lopaczyski, W.; Zeisel, S. H. Antioxidants, programmed cell death and cancer. *Nutr. J*. **2001**, *21*, 295–307. https://doi.org/10.1016/S0271-5317(00)00288-8

(40) Nita, M.; Grzybowski, A. The role of the reactive oxygen species and oxidative stress in the pathomechanism of the age-related ocular diseases and other pathologies of the anterior and posterior eye segments in adults. *Oxid. Med. Cell. Longevity* **2016**. https://doi.org/10.1155/2016/3164734

(41) Powers, S. K.; Jackson, M. J. Exercise-induced oxidative stress: cellular mechanisms and impact on muscle force production. *Physiol. Rev.* **2008**, *88*, 1243-1276. https://doi.org/10.1152/physrev.00031.2007

(42) Sinis, S. I.; Gourgoulianis, K. I.; Hatzoglou, C.; Zarogiannis, S. G. Mechanisms of engineered nanoparticle induced neurotoxicity in Caenorhabditis elegans. *Environ. Toxicol. Pharmacol*. **2019**, *67*, 29-34. https://doi.org/10.1016/j.etap.2019.01.010

(43) Sandahl, J. F.; Jenkins, J. J. Pacific steelhead (*Oncorhynchus mykiss*) exposed to chlorpyrifos: benchmark concentration estimates for acetylcholinesterase inhibition. *Environ. Toxicol. Chem.* **2002**, *21*, 2452-2458. https://doi.org/10.1002/etc.5620211126

(44) Canli, E. G.; Ila, H. B.; Canli, M. Responses of biomarkers belonging to different metabolic systems of rats following oral administration of aluminium nanoparticle. *Environ. Toxicol. Pharmacol.* **2019b,** *69*, 72-79. https://doi.org/10.1016/j.etap.2019.04.002

(45) Noor, N. A.; Fahmy, H. M.; Mourad, I. M. Evaluation of the potential neurotoxicity of gold nanoparticles in the different rat brain regions. *Int. J. Sci.: Basic Appl. Res*. **2016**, *30*, 114-129. ISSN 2307-4531.

Brazilian Journal of Analytical Chemistry
2023, Volume 10, Issue 40, pp 198-208
doi: 10.30744/brjac.2179-3425.TN-113-2022

BrJAC

TECHNICAL NOTE

Optimization of the Protein Sequential Extraction for Quantitative Determination of Albumins, Globulins, Prolamins and Glutelins in Edible Mushrooms

Saphire de Souza Lana Dias[1], Aline Pereira de Oliveira[1], Ivanise Gaubeur[2], Cassiana Seimi Nomura[3], Juliana Naozuka*[1]

[1]*Universidade Federal de São Paulo, Departamento de Química, Rua Prof. Artur Riedel, 275, 09972-270, Diadema, SP, Brazil*
[2]*Universidade Federal do ABC, Centro de Ciências Naturais e Humanas, Av. dos Estados, 5001, 09210-580, Santo André, SP, Brazil*
[3]*Universidade de São Paulo, Instituto de Química, Departamento de Química Fundamental, Av. Prof. Lineu Prestes, 748, 05508-900, São Paulo, SP, Brazil*

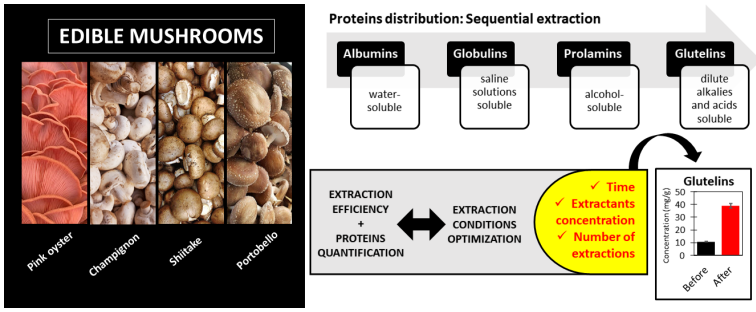

For physiological functions development and a healthy life maintenance, a balanced diet, containing carbohydrates, proteins, and lipids, should be practiced, and consumed. The proteins should be highlighted, since are essential macronutrients for cell growth and repair mechanisms in our body. There is an increase in the protein sources consumption, mainly by athletes, aiming an increase of muscle mass and to avoid muscle hypertrophy. Although animal proteins exhibit high digestibility, animal foods can not be accessible and widely consumed, due to high cost or lifestyle choice (vegetarians and vegans). In these sceneries, scientists and food industry are constantly searching for alternative proteins, such as plant and fungi proteins. In view of these information, extraction procedures are proposed to proteins fractionation. However, these procedures must be done to exhaustion to guarantee the acquisition of quantitative values. Therefore, the aims of this work were evaluated the protein distribution in edible mushrooms and optimized the sequential protein extraction procedure to obtain total concentration of albumin, globulin, prolamin and glutelin in edible mushrooms, evidencing the need to carry out extraction procedures until exhaustion to adequately attribute nutritional value to edible mushrooms (pink oyster, shiitake, portobello and champignon). The optimized extraction conditions (extractant, time, concentration, number of extractions) were as follows (H_2O, 30 min, ---, 3); (NaCl, 15 min, 0.25 mol L^{-1}, 1); (ethanol, 15 min, 50% (v v^{-1}), 1); (NaOH, 60 min, 0.25 mol L^{-1}, 8) for albumin, globulin, prolamin and glutelin

Cite: Dias, S. S. L.; Oliveira, A. P.; Gaubeur, I.; Nomura, C. S.; Naozuka, J. Optimization of the Protein Sequential Extraction for Quantitative Determination of Albumins, Globulins, Prolamins and Glutelins in Edible Mushrooms. *Braz. J. Anal. Chem.* 2023, *10* (40), pp 198-208. http://dx.doi.org/10.30744/brjac.2179-3425.TN-113-2022

Submitted 11 November 2022, Resubmitted 03 April 2023, Accepted 13 May 2023, Available online 25 May 2023.

extraction. The champignon mushrooms presented all protein group concentrations below LOD and LOQ. The portobello presented the lowest total proteins concentration. The pink oyster mushroom is the species with the highest concentration of albumin and glutelin as well as total protein concentration 4.7 times higher than shiitake mushroom, which is one of the most consumed mushroom species, showing that this exotic species can be promising mainly due to nutritional characteristics and protein source.

Keywords: edible mushrooms, protein distribution, sequential extraction, optimization

INTRODUCTION

For physiological functions development and a healthy life maintenance, a balanced diet, containing 45-55% carbohydrates, 20% proteins, and 25-30% lipids should be practiced and consumed.[1] Considering these chemical compounds, the proteins should be highlighted, since are essential macronutrients for cell growth and repair mechanisms in our body.[2,3] There is an increase in the protein sources consumption, mainly by athletes, aiming an increase of muscle mass and to avoid muscle hypertrophy.[1]

The protein effectiveness is evaluated by amino acids content and digestibility.[4,5] Of the total amino acids, there are eight essential for the body (leucine, isoleucine, methionine, valine, threonine, tryptophan, phenylalanine, and lysine).[1,5] It is important to point out that some amino acids are not synthesized by human body, being present in certain foods, such animal source. In animal proteins, there are essential amino acids, and they have high digestibility. However, the animal foods cannot be accessible and widely consumed, due to high cost or lifestyle choice (vegetarians and vegans).[1]

In these sceneries, scientists and food industry are constantly searching for alternative proteins. The research and the industrial products have shown that plant and fungi proteins are promising sources for consumers of a healthy life.[2,6] The protein value of mushrooms varies from 19 to 37% of dry weight and, depending on mushroom variety, 100 g of this food can cover from 29 to 66% of the Recommended Dietary Allowance (RDA) for men and from 36 to 80% for women.[5] It is worth mentioning that produce a large number of proteins and peptides with interesting biological activities, such as lectins, fungal immunomodulatory proteins, ribosome inactivating proteins, antimicrobial proteins, ribonucleases, and laccases.[7]

In addition to the protein content of the edible mushrooms, they attracted great interest from the medical and scientific community, due to their other nutrients, like carbohydrates, vitamins, calcium and iron.[8,9] Beside this, they can therapeutic and medicinal properties, presenting antitumor characteristics, modulate cholesterol levels, prevent platelet aggregation in the arteries, prevent cardiovascular disease, combat hepatitis C virus, and exert antioxidant and antibacterial properties.[10-12] In addition, studies have shown that edible mushrooms have the ability to modulate intestinal microbiota as well as immune system.[13]

Approximately 2,000 edible mushroom species are estimated to exist and around 30 of them are commercially grown worldwide.[14] In many countries, mushroom consumption has been growing significantly, due to the nutritional value and market availability, which makes the product more popular and affordable. *Agaricus bisporus* mushrooms are the most consumed and marketed, followed by *Lentinus edodes* (shitake mushrooms) and different species of the *Pleurotus* (oyster mushrooms) genus.[15] However, some exotic species can also be edible such as pink oyster mushrooms (*Pleurotus djamor*) which are exotic mushrooms with salmon color and fibrous texture. It is known that this species can be used to inhibit hepatoma cell proliferation and plays a vital role in antiviral, antitumor, and immunosuppressive biological activities.[16]

Considering the importance of the mushroom proteins, extraction procedures are proposed to proteins fractionation. However, these procedures must be done to exhaustion, or rather the optimization and repetition of the experimental steps must be performed to guarantee the acquisition of quantitative values. According to Christian,[17] the quantitative extraction is most efficiently carried out by performing multiple extraction with smaller portions of the same volume of solvent. Additionally, in the sequential extraction of the different protein types, the optimization of extraction with appropriated extractants is even more

imperative, since sequentially the extractants are capable to extract the species that are not extracted by the previous extractant, highlighting the NaOH that is the last extractant used in the sequential extraction, because it is not a selective protein extractant, being capable to extract any protein group and not just glutelins.[18,19] The use of sequential extraction procedure without optimization only provides qualitative information, resulting in only albumins, globulins, prolamins and glutelins distribution. In view of the protein importance and the fact that foods are protein sources for humans, it is essential to optimize the extraction steps to obtain quantitative results mainly aiming nutritional information on foods that are widely consumed but still little chemically characterized. Therefore, the aims of this work were evaluated the protein distribution in edible mushrooms and optimized the sequential protein extraction procedure to obtain total concentration of albumin, globulin, prolamin and glutelin in different species of edible mushrooms, evidencing the need to carry out extraction procedures until exhaustion to adequately attribute nutritional value to edible mushrooms.

MATERIALS AND METHODS

Instrumentation

Mushroom species were dried in a freeze dryer (Thermo Fisher Scientific, England) before of the sequential extraction. The mixture between dried sample and extractants was performed by constant agitation on orbital shaker (model 0225M, Quimis, Brazil). A centrifuge (Spectrafuge 6C Compact model, Labnet International, USA) was used for the phase separation.

The supernatants were analyzed by a spectrophotometer (model Q898DRM5, Quimis, Brazil) equipped with tungsten lamp and wavelength range of 325-1000 nm for protein quantification.

Reagents and samples

Four species of edible mushrooms (Pink oyster mushroom (*Pleurotus djamor*), champignon mushroom (*Agaricus bisporus*), shiitake (*Lentinula edodes*), and portobello (*Agaricus bisporus))* and, for each species, four packages of 200 g were purchased at a local market in Sao Paulo.

All solutions were prepared from analytical reagent grade chemicals and using high-purity deionized water obtained from a Milli-Q water purification system (Millipore, USA).

For the sequential extraction, the following reagents (Merck, Germany) were used: acetone, chloroform, ethanol, methanol, NaCl, and NaOH. The total protein concentration in the extracts was obtained using Bradford´s reagent (BioAgency, Brazil), which was diluted five times with deionized water before analysis. The analytical curve for quantification of proteins in the extracts was prepared with stock solution with 0.2 mg mL^{-1} of ovalbumin (BioAgency, Brazil).

Preliminary sample preparation

The four packages of 200 g of the same mushroom species were mixed and cleaned with deionized water. After that, mushrooms were dried by lyophilization (*ca.* 3 days) and grounded in decontaminated pestle and mortar. All grounded samples were stored in polypropylene tubes and kept frozen at -4 °C.

Grounded samples were submitted to sequential extraction procedures, aiming to quantify albumin, globulin, prolamin, and glutelin in different species of edible mushrooms.

Sequential extraction of proteins: proteins distribution

The protein screening was obtained only for pink oyster mushrooms, using sequential extraction procedure described by Naozuka & Oliveira (2007).[20] Sample mass of approximately 200 mg was submitted to sequential extraction, using 10 mL of different extractants: methanol/chloroform mixture (1:2 v v^{-1}), acetone (75 % v v^{-1}), deionized water, 0.5 mol L^{-1} NaCl, 70 % (v v^{-1}) ethanol, and 0.5 mol L^{-1} NaOH. The mixture methanol/chloroform and acetone were used to remove lipids and polyphenols, respectively. Subsequently, the extractants water, NaCl, ethanol, and NaOH were used, producing four supernatants containing albumins, globulins, prolamins, and glutelins, respectively. In Figure 1 is shown a schematic diagram of the sequential extraction experimental setup.

The mixture between samples and extractants were carried out using an orbital shaker at 1520 x g for 30 minutes. The supernatant separation was executed by centrifugation at 4000 rpm for 10 minutes. Protein determination was performed by the Bradford (1976) method.[21] Spectrophotometer calibration was performed using analytical reference solutions of 4, 6, 8, 10, 12, 16, and 20 µg of ovalbumin in 1.0 mL of Bradford reagent. Before analysis, water and NaOH supernatants were diluted with deionized water 2-20 times, while ethanol and NaCl supernatants were not diluted.

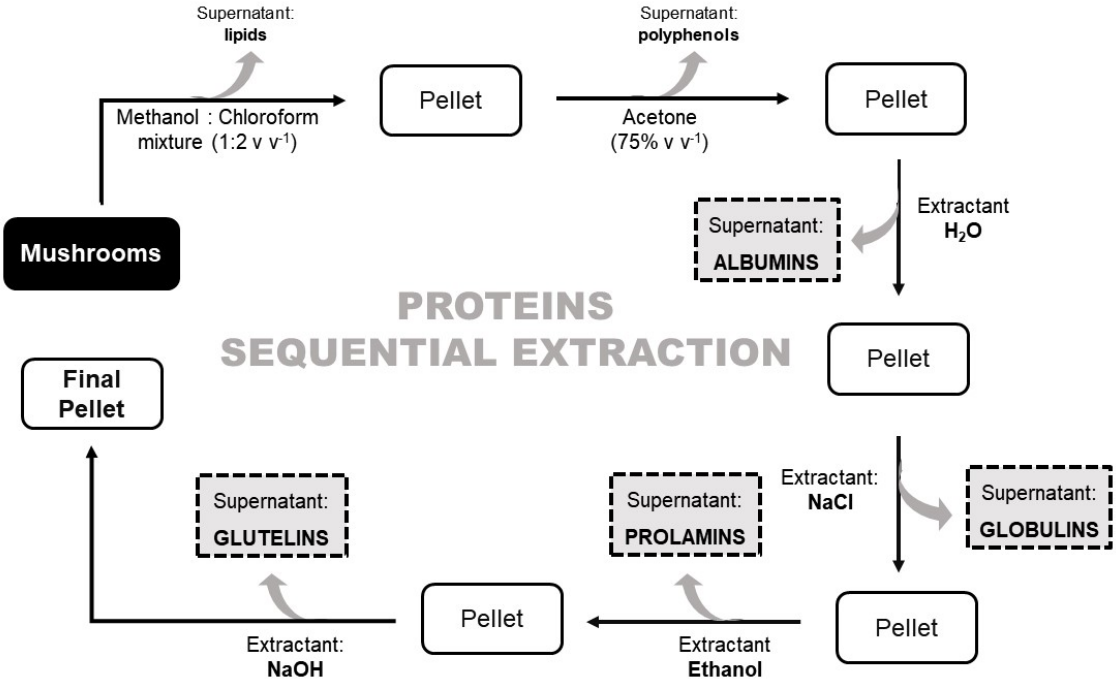

Figure 1. Schematic diagram of the protein sequential extraction experimental setup.

Sequential extraction of proteins: optimization

The sequential extraction optimization is important to obtain total albumins, globulins, prolamins and glutelins concentrations. Time, extractant concentrations and number of consecutives extraction were evaluated only for pink oyster mushrooms using the univariate analysis. Before sequential extraction, a sample mass of 200 mg was submitted to extraction with 10 mL of methanol/chloroform mixture (1:2 v v^{-1}) and acetone (75% v v^{-1}) to remove lipid and polyphenols, respectively.

The time (15, 30 and 60 min) of mixture between sample and extractants was firstly evaluated. The extractants used were deionized water, NaCl (0.5 mol L^{-1}), ethanol (70% v v^{-1}), and NaOH (0.5 mol L^{-1}). The separation of the solid phase was carried out by centrifugation at 1520 x g for 10 minutes. The best time was chosen based on the greatest extracted proteins concentration.

In the best time, the extractants concentration (0.25, 0.5 and 1.0 mol L^{-1} (NaCl and NaOH) and 50, 60, and 70% v v^{-1} (ethanol) was studied. Again, appropriated extractant concentration was chosen considering the greatest extracted proteins concentration.

Finally, with the optimal conditions of time and concentration kept fixed, the number of consecutive extractions was evaluated for each extractant. In each supernatant, proteins were quantified, and the number of consecutive extractions was obtained when the protein concentration was smaller than limit of detection (LOD).

The optimized conditions were applied to different species of edible mushrooms: pink oyster (*Pleurotus djamor*), champignon (*Agaricus bisporus*), shiitake (*Lentinula edodes*), and portobello (*Agaricus bisporus),* aiming the albumins, globulins, prolamins and glutelins determination.

Protein determination was performed by the Bradford (1976) method.[21] Spectrophotometer calibration was performed using analytical reference solutions of 4, 6, 8, 10, 12, 16, and 20 µg of ovalbumin in 1.0 mL of Bradford reagent. Before analysis, water and NaOH supernatants were diluted with deionized water 2-20 times, while ethanol and NaCl supernatants were not diluted.

RESULTS AND DISCUSSION

Proteins distribution in pink oyster mushroom

Protein quantification was carried out by Bradford method at 595 nm wavelength.[21] The Bradford method is commonly used for protein quantification in solutions, due to its simplicity, easy application, and high sensitivity providing satisfactory analytical response. This method consists of the non-covalent bond between the anionic form of Coomassie Blue Brilhant Blue (G-250) dye with proteins.[17] The dye reacts with the positively charged portion of the protein chain, usually arginine residues. Poor interactions are observed with basic (histidine and lysine) and aromatic (tyrosine, tryptophan and phenylalanine) residues. Thus, there is an equilibrium displacement of the dye to its ionic form, which corresponds to the species absorbing at 595 nm wavelength.[18,22] Furthermore, according to Zaia et al.,[23] there are few interferents substances in the Bradford method, which they can react with proteins or with the dye, increasing the absorbance. In food, possible interferents are lipids and polyphenols, [23] but in the proposed method, the initial extractions with methanol:chloroform and acetone (Figure 1) were capable to minimize the lipids and polyphenols presence. Considering the extractants (water, NaCl solution, ethanol, and NaOH solution), only NaCl solution above 1 mol L^{-1} can provide negative results in the Bradford method.[23] In view of this information, the interferences in the proposed method is strongly minimized, adding the fact that extracts are diluted, mainly globulins supernatant, before analysis.

The characteristic parameters of the analytical calibration curves (linear range, correlation coefficient (R^2) and sensibility), LOD and limits of quantification (LOQ) are shown in Table I. The LOD was calculated using the standard deviation of 10 measurements of the analytical blank sample ($3 \times \sigma_{blank}$, where σ is the standard deviation) and the LOQ was calculated as 3 × LOD. For the sequential extraction, the values were obtained in mg g^{-1}, considering a sample mass of 200 mg and a final volume of 10 mL.

Table I. Characteristic parameters of the analytical method

	Linear range (µg mL^{-1})	R^2	Sensibility	Analytical blank	LOD (mg g^{-1})	LOQ (mg g^{-1})
Sequential extraction	20–120	0.9791	0.0015	Water	0.6	1.7
				NaCl	0.3	0.9
				Ethanol	0.4	1.2
				NaOH	0.6	1.8

The separation of lipids and polyphenols was performed using a mixture of methanol/chloroform and acetone, respectively. In the absence of lipids and polyphenols, it was possible to separate different protein groups, applying the sequential extraction procedure.

Proteins are amino acids polymers, which are linked by peptide bonding. The amino acids can carboxyl and amino groups, besides non-protein parts. The amino acids composition with polar or non-polar groups influences the protein solubility. The charge arrangements in the proteins depends on acidic (*eg.* aspartyl and glutamyl) and basic (*eg*. histidyl, arginyl, and lysyl) amino acids. The non-protein parts (lipids, carbohydrates, and phosphates) can also alter the proteins solubility.[18] So, it is possible to separate different proteins groups, using appropriated solvents. According to the Osborne (1924) method, a sequential extraction with water, saline (*eg* NaCl) solutions, alcoholic (*eg* 70-80% v v^{-1} ethanol) solutions and acidic or alkaline (*eg* NaOH) solutions is capable to separate albumin, globulin, prolamin and glutelin, respectively.[20,24] The protein distribution in pink oyster mushrooms are shown in Table II.

According to Table II, it was verified that the highest protein concentration was found in the NaOH extract, corresponding to the glutelin group. The NaOH is the last extractant used in the sequential extraction, because it is not a selective protein extractant, being capable to extract any protein group.[18,19] In this way, high glutelin concentrations can occur when extractions with water, NaCl and ethanol are inefficient due to inadequate times, volumes and/or concentrations. Therefore, the sequential extraction procedure optimization should ensure complete proteins extraction from each protein group, allowing quantitative determination of albumin, globulin, prolamin, and glutelin in edible mushrooms.

Table II. Proteins distribution in pink oyster mushroom

Mushroom	Concentration (mg g^{-1}) ± standard deviation (n = 3)				
	Albumin	Globulin	Prolamin	Glutelin	Total*
Pink oyster	4.8 ± 0.2	< LOQ	< LOQ	10.7 ± 0.2	15.5 ± 0.3

*Concentration sum of each protein type.

Sequential protein extraction optimization

Protein distribution studies are important for a first investigation of different proteins present in the samples. Although protein distribution cannot provide the total concentrations of albumins, globulins, prolamins and glutelins, it contributes with important information about nutritional characteristics and potentialities. The value of the protein content in edible mushrooms requires the quantitative determination of albumin, globulin, prolamin, and glutelin, obtained after the sequential extraction optimization. For this, it was done an univariably optimization evaluating time, extractants concentrations, and number of consecutive extractions parameters.

Initially, the extraction time was varied and the obtained results for pink oyster mushroom are presented in Table III. Comparing the concentrations for each proteins group, the optimum time for the extraction were chosen considering the highest concentration obtained as well as standard deviation values. Therefore, 30 and 60 min for albumin and glutelin, respectively. For globulins and prolamins, it was maintained 15 min, since concentrations were below the LOQ for any extraction time.

At the fixed optimal time, the extractants concentrations were optimized, except for deionized water. The results are shown in the Table IV. The NaCl, ethanol and NaOH concentrations were, respectively, divided in three groups: minimum (0.25 mol L^{-1}, 50% (v v^{-1}) and 0.25 mol L^{-1}), intermediate (0.5 mol L^{-1}, 60% (v v^{-1}) and 0.5 mol L^{-1}) and maximum (1.0 mol L^{-1}, 70% (v v^{-1}) and 1.0 mol L^{-1}). For all protein types, the minimum extractant concentration (NaCl 0.25 mol L^{-1}, ethanol 50% v v^{-1}, and NaOH 0.25 mol L^{-1}) was more appropriate.

Table III. Concentration of albumin, globulin, prolamin and glutelin in pink oyster mushrooms at different extraction times

Extraction time	Protein concentration (mg g^{-1}) ± standard deviation (n = 3)			
	Albumin	Globulin	Prolamin	Glutelin
15 min	2.5 ± 0.5	< LOQ	< LOQ	8.8 ± 0.7
30 min	4.8 ± 0.2	< LOQ	< LOQ	11.1 ± 0.1
60 min	4.6 ± 0.2	< LOQ	< LOQ	15 ± 1

*Concentration sum of each protein type.

Table IV. Concentration of albumin, globulin, prolamin and glutelin in pink oyster mushrooms at different reagent concentrations

Extractant concentration	Protein concentration (mg g^{-1}) ± standard deviation (n = 3)				
	Albumin	Globulin	Prolamin	Glutelin	Total*
Minimum	4.6 ± 0.2	< LOQ	< LOQ	17 ± 4	22 ± 4
Intermediate	4.6 ± 0.2	< LOQ	< LOQ	15 ± 1	20 ± 1
Maximum	4.6 ± 0.2	< LOQ	< LOQ	15 ± 1	20 ± 1

*Concentration sum of each protein type.

After optimization of time and extractants concentrations, the extraction quantity with the same extractant was studied, being each sequential extraction step consecutively repeated until that protein determined concentrations were below the LOD and LOQ. This study was performed only for albumins and glutelins, because the globulin and prolamin concentrations were already below the LOD and LOQ. In the Figure 2 is shown the optimization results for the number of extractions. It is possible to observe that 3 (Figure 1A) and 8 (Figure 1B) consecutives extractions with water and NaOH solution completely extracted albumin and glutelin, respectively, considering the LOQ values presented previously in Table I. Considering 3 and 8 consecutives extractions with water and NaOH solution, respectively, the albumin and glutelin concentrations had an increase, when compared with results shown in the Table II (proteins distribution).

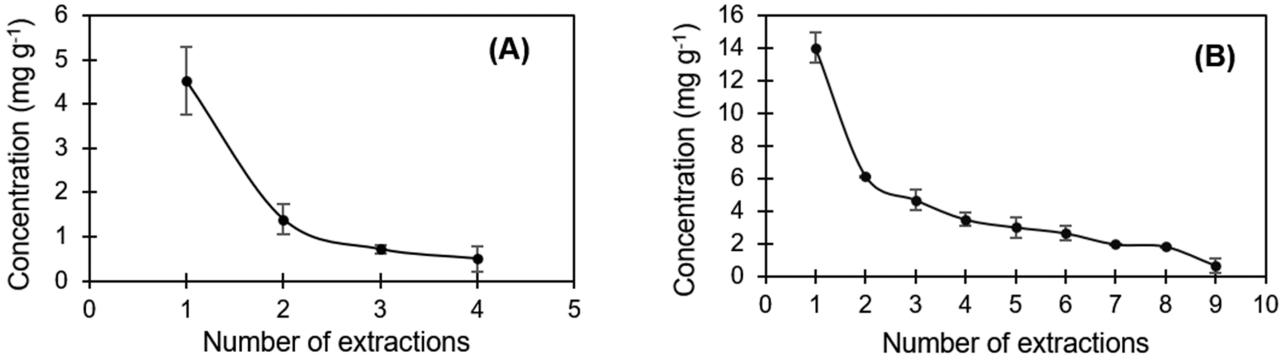

Figure 2. Concentration of albumin (A) and glutelin (B) in pink oyster mushrooms applying consecutive extractions

So, the quantitative extraction of albumins, globulins, prolamins and glutelins in mushrooms was accomplished using the optimized conditions summarized in the Table V.

Table V. Optimized parameters for sequential extraction of proteins

Parameters	Extractant			
	H_2O	NaCl	Ethanol	NaOH
Extraction time	30 min	15 min	15 min	60 min
Extractant concentration	--	0.25	50 % (v v^{-1})	0.25
Number of extractions	3	1	1	8

Protein quantitative determination in edible mushrooms

The albumin, globulin, prolamin, and glutelin concentrations in pink oyster, champignon, shiitake, and portobello mushrooms after sequential extraction using the optimized conditions are presented in Table VI.

Previous investigations determined the total protein concentrations in edible mushrooms[25,26], corresponding to 252, 234, 217, and 294 mg g^{-1} for pink oyster, champignon, shiitake, and portobelo, respectively. In this work, the total protein concentrations, Table VI, were obtained by the masses sum of all extracts, and comparing the literatures[25,26] and obtained results, it was possible to extract 18, 5 and 2% w/w for pink oyster, shiitake, and portobelo, respectively. For champignon, albumins, globulins, prolamins and glutelins were not found using the proposed method. Therefore, there are other protein groups in these edible mushrooms, and albumins, globulins, prolamins and glutelins are a small part of the whole proteins.

Table VI. Concentration of albumin, globulin, prolamin and glutelin in different mushroom species after optimized sequential extraction

Mushroom	Origin	Protein concentration (mg g^{-1}) ± standard deviation (n = 3)					DRV (%)
		Albumin	Globulin	Prolamin	Glutelin	Total[a]	
Pink oyster	Indoor growing	1.5 ± 0.1	0.9 ± 0.2	< LOQ	28 ± 2	30 ±2	0.40
Pink oyster	Commercial	7 ± 1	< LOQ	< LOQ	39 ± 2	46 ± 2	0.61
Champignon	Commercial	< LOQ	< LOQ	< LOQ	< LOQ	**n.d.	**n.d.
Shiitake	Commercial	0.7 ± 0.1	< LOQ	< LOQ	9.1 ± 0.2	9.8 ± 0.2	0.13
Portobello	Commercial	< LOQ	< LOQ	< LOQ	5.2 ± 0.1	5.2 ± 0.1	0.07

*%DRV refers to the percentage of the Daily Reference Value of each component supplied per 100 g portion of fresh mushroom in a 2000 kcal or 8,400 kJ diet, according to ANVISA RDC Resolution No. 360 December 23, 2003.[19]

**not determined (n.d.). [a]Total protein from sum of each protein type.

Comparing the proteins distribution (Table II) in pink oyster mushrooms with proteins concentrations obtained after sequential extraction conditions optimization, it is possible to observe that the albumins and glutelins concentrations suffered alteration (Table VI). Additionally, only pink oyster and shiitake mushrooms showed concentrations above the LOD and LOQ for albumin group while pink oyster mushroom was the species with the highest concentration of albumin and glutelin as well as total protein concentration 4.7 times higher than shiitake mushroom, which is one of the most consumed mushroom species, showing that this exotic species can be promising mainly due to nutritional characteristics and protein source.

The champignon mushrooms presented all protein group concentrations below LOD and LOQ. So, this proposed method was not capable to determine proteins in this mushroom and comparatively this mushroom species is not rich in proteins like pink oyster, portobello, and shiitake. Possibly, increasing the sample mass or decreasing the extractant volume, it would be possible to determine the albumin, globulin, prolamin and glutelin concentrations in champignon mushroom. The portobello can be considered the second mushroom species with the lowest total concentration of proteins, just showing glutelins group.

It is known that mushrooms can colonize different types of agricultural and agro-industrial waste such as sawdust, sugarcane bagasse, corn husk, and coffee pulp.[27,28] Therefore, it is important to point out that comparisons between published results for other authors are difficult, since cultivation conditions (climate and irrigation), substrate composition and maturation phase of the fruiting bodies mushrooms can promote variations in proteins distribution.[29-32] Besides that, extraction procedures differ notably from each other.

Although protein distribution is based on solubility differences and plays a fundamental biological role in uptake, digestion and absorption of proteins, there is still limited data provided on protein distribution for mushrooms.[33] A study published by Petrovska (2001) evaluated the albumin, globulins, prolamins, and glutelin distribution in mushrooms.[34] However, the extraction procedure showed difference when compared with proposed method, being the prolamins extraction performed with 55% v v^{-1} isopropyl alcohol, while for glutelin extraction, borate buffer (pH 10) with 0.6% v v^{-1} 2-mercaptoethanol and 0.5% w v^{-1} sodium dodecyl sulfate were used.

The results presented in Table VI are in agreement with those published by Helm et al. (2009) in which the *Pleurotus* mushrooms also presented the highest concentration of total proteins (37.51% (w w^{-1})) when compared to other mushrooms species.[35] On the other hand, in edible Macedonian and *Pleurotus eryngii* mushrooms, different results were obtained, since extraction procedures without optimization and different extractants for prolamins and glutelins were applied.[34,36] In Macedonian mushrooms, the abundance of protein fraction was as follow: albumins > glutelins > globulins > prolamins.[34] The total protein concentration presented in Table VI for champignon mushroom (*Agaricus bisporus*) was lower than 36.3% dry wt. of protein content in *A. bisporus* mushrooms reported earlier by Akyüz et al. (2010).[37]

Lastly, it was verified that pink oyster mushroom supplies 0.47% of the recommended daily protein intake (Daily Reference Values, DRV = 75.0 g) followed by shiitake mushroom (0.13%),[38] considering the daily intake of 100 g of fresh mushrooms with an average fresh edible mushrooms moisture of 90% and the total protein concentration the sum of albumin, prolamin, globulin and glutelin concentration.

CONCLUSIONS

For quantitative determination of different protein groups (albumin, globulin, prolamin and glutelin) in edible mushrooms, it is essential to optimization of sequential extraction procedure. It was observed that the optimization significantly altered the glutelin concentration in pink oyster mushroom.

The optimized sequential extraction was applied for pink oyster, shiitake, portobello and champignon mushrooms. The champignon mushrooms presented all protein group concentrations below LOD and LOQ. The portobello can be considered the second mushroom species with the lowest total concentration of proteins, just showing glutelins group. The pink oyster mushroom is the species with the highest concentration of albumin and glutelin as well as total protein concentration 4.7 times higher than shiitake mushroom, which is one of the most consumed mushroom species, showing that this exotic species can be promising mainly due to nutritional characteristics and protein source.

In this way, the evaluation of the quantitative protein distribution in different edible mushroom species can contribute with data capable of improving the nutritional information about the conscious use of these foods, since proteins play an essential role in the human organism and in the composition of the studied mushrooms.

Conflicts of interest

The authors declare that they have no conflict of interest.

This article does not contain any studies with human or animal subjects.

Acknowledgements

Saphire de Souza Lana Dias thanks the National Council for Scientific and Technological Development (CNPq) [grant number 800271/2018-1]. Aline Pereira de Oliveira [grant number 2017/05009-7 and 2019/00663-6], Cassiana Seimi Nomura [grant number 2021/14125-6] and Juliana Naozuka [grant numbers 2018/06332-9 and 2021/14125-6] thank the São Paulo Research Foundation (FAPESP) for the fellowship provided and financial support.

REFERENCES

(1) Bătrînu, A. M.; Tero-Vescan, A.; Miklos, A. Biochemical controversies regarding the use of vegetal proteins in performance athletes. *Acta Biologica Marisiensis* **2020**, *3* (2), 5-13. https://doi.org/10.2478/abmj-2020-0006

(2) Schweiggert-Weisz, U.; Eisner, P.; Bader-Mittermaier, S.; Osen, R. Food proteins from plants and fungi, *Curr. Opin. Food Sci.* **2020**, *32*, 156–162. https://doi.org/10.1016/j.cofs.2020.08.003

(3) Lehninger, A. L.; Nelson, D. L.; Cox, M. M., Cox, M. M. *Principles of biochemistry*. WH Freeman and Company, New York, NY, USA, 2005.

(4) Friedman, M. Nutritional Value of Proteins from Different Food Sources. A Review. *J. Agric. Food Chem.* **1996,** *44*, 6-29. https://doi.org/10.1021/jf9400167

(5) González, A.; Cruz, M.; Losoya, C.; Nobre, C.; Loredo, A.; Rodríguez, R.; Contreras, J.; Belmares, R. Edible mushrooms as a novel protein source for functional foods. *Food Funct.* **2020**, *11*, 7400–7414. https://doi.org/10.1039/D0FO01746A

(6) Ouzouni, P. K.; Petridis, D.; Koller, W. D.; Riganakos, K. A. Nutritional value and metal content of wild edible mushrooms collected from West Macedonia and Epirus, Greece. *Food Chem*. **2009**, *115* (4), 1575-1580. https://doi.org/10.1016/j.foodchem.2009.02.014

(7) Xu, X.; Yan, H.; Chen, J.; Zhang, X. Bioactive proteins from mushrooms. *Biotechnol. Adv.* **2011**, *29* (6), 667-674. https://doi.org/10.1016/j.biotechadv.2011.05.003

(8) Simões, M. G. *Desenvolvimento e crescimento da espécie de cogumelo Pleurotus ostreatus em garrafas de plástico reutilizado*. PhD thesis, Universidade dos Açores, Brazil, **2016**.

(9) Sudha, G.; Janardhanan, A.; Moorthy, A.; Chinnasamy, M.; Gunasekaran, S.; Thimmaraju, A.; Gopalan, J. Comparative study on the antioxidant activity of methanolic and aqueous extracts from the fruiting bodies of an edible mushroom *Pleurotus djamor*. *Food Sci. Biotechnol.* **2016**, *25* (2), 371-377. https://doi.org/10.1007/s10068-016-0052-4

(10) Sarangi, I.; Ghosh, D.; Bhutia, S. K.; Mallick, S. K.; Maiti, T. K. Anti-tumor and immunomodulating effects of *Pleurotus ostreatus* mycelia-derived proteoglycans. *Int. Immunopharmacol*. **2006**, *6* (8), 1287-1297. https://doi.org/10.1016/j.intimp.2006.04.002

(11) Guillamón, E.; García-Lafuente, A.; Lozano, M.; Rostagno, M. A.; Villares, A.; Martínez, J. A. Edible mushrooms: role in the prevention of cardiovascular diseases. *Fitoterapia* **2010**, *81* (7), 715-723. https://doi.org/10.1016/j.fitote.2010.06.005

(12) Muszyńska, B.; Grzywacz-Kisielewska, A.; Kała, K.; Gdula-Argasińska, J. Anti-inflammatory properties of edible mushrooms: A review. *Food Chem.* **2018**, *243*, 373-381. https://doi.org/10.1016/j.foodchem.2017.09.149

(13) Morales, D.; Shetty, S. A.; López-Plaza, B.; Gómez-Candela, C.; Smidt, H.; Marín, F. R.; Soler-Rivas, C. Modulation of human intestinal microbiota in a clinical trial by consumption of a β-d-glucan-enriched extract obtained from Lentinula edodes. *Eur. J. Nutr*. **2021**, *60*, 3249–3265. https://doi.org/10.1007/s00394-021-02504-4

(14) Silva, F. A. B.; Lucini, F.; Falcão, M. S.; Laindorf, B. L.; Maggio, L. P.; Putzke, J. Diversidade de cogumelos comestíveis em área de bioma pampa. *Anais do 10º Salão Internacional de Ensino, Pesquisa e Extensão da UNIPAMPA*. **2019**, *10* (2).

(15) Sande, D.; Oliveira, G. P.; Moura, M. A. F.; Martins, B. A.; Lima, M. T. N. S.; Takahashi, J. A. Edible mushrooms as a ubiquitous source of essential fatty acids. *Food Res. Int*. **2019**, *125*, 108524. https://doi.org/10.1016/j.foodres.2019.108524

(16) Dulay, R. M. R.; Miranda, L. A.; Malasaga, J. S.; Kalaw, S. P.; Reyes, R. G.; Hou, C. T. Antioxidant and antibacterial activities of acetonitrile and hexane extracts of *Lentinus tigrinus* and *Pleurotus djamour*. *Biocatal. Agric. Biotechnol*. **2017**, *9*, 141-144. https://doi.org/10.1016/j.bcab.2016.12.003

(17) Christian, G. D. Analytical Chemistry, 5th ed., John Wiley & Sons, Inc.,1994, Chapter 484.

(18) Chunhieng, T.; Pétritis, K.; Elfakir, C.; Brochier, J.; Goli, T.; Montet, D. Study of selenium distribution in the protein fractions of the Brazil nut, *Bertholletia excelsa*. *J. Agric. Food Chem*. **2004**, *52* (13), 4318-4322. https://doi.org/10.1021/jf049643e

(19) Kwon, K.; Park, K. H.; Rhee, K. C. Fractionation and characterization of proteins from coconut (*Cocos nucifera* L.). *J. Agric. Food Chem*. **1996**, *44* (7), 1741-1745. https://doi.org/10.1021/jf9504273
(20) Naozuka, J.; Oliveira, P. V. Cu, Fe, Mn and Zn distribution in protein fractions of Brazil-nut, cupuassu seed and coconut pulp by solid-liquid extraction and electrothermal atomic absorption spectrometry. *J. Braz. Chem. Soc*. **2007**, *18* (8), 1547-1553. https://dx.doi.org/10.1590/S0103-50532007000800015
(21) Bradford, M. M. A rapid and sensitive method for the quantitation of microgram quantities of protein utilizing the principle of protein-dye binding. *Anal. Biochem*. **1976**, *72* (1-2), 248-254. https://doi.org/10.1016/0003-2697(76)90527-3
(22) Naozuka, J.; Oliveira, P. V. Cooking effects on iron and proteins content of beans (Phaseolus vulgaris L.) by GF AAS and MALDI-TOF MS. *J. Braz. Chem. Soc*. **2012**, *23* (1), 156-162. https://dx.doi.org/10.1590/S0103-50532012000100022
(23) Zaia, D.M.S; Zaia, C. T. B. V.; Lichtig, J. Determinação de proteínas totais via espectrofometria: vantagens e desvantagens dos métodos existentes. *Quim. Nova* **1998**, *21* (6), 787-793.
(24) Osborne, T. B. *The Vegetable Proteins*, 2nd Ed. Green & Co, London, 1924.
(25) Hasan, M. T.; Khatun, M. H. A.; Sajib, M. A. M.; Rahman, M. M.; Rahman, M. S.; Roy, M.; Ahmed, K. U. Effect of wheat bran supplement with sugarcane bagasse on growth, yield and proximate composition of pink oyster mushroom (*Pleurotus djamor*). *A. J. Food Sci. Technol*, **2015**, *3* (6), 150-157. https://dx.doi.org/10.12691/ajfst-3-6-2
(26) Tabela de Composição Química dos Alimentos da Escola Paulista de Medicina, 2023. https://tabnut.dis.epm.br/ (accessed 2023-03-30).
(27) Moda, E. M.; Horii, J.; Spoto, M. H. F. Edible mushroom Pleurotus sajor-caju production on washed and supplemented sugarcane bagasse. *Scientia Agricola*. **2005**, *62* (2), 127-132.
(28) Silva, M. C.; Naozuka, J.; Luz, J. M. R.; Assunção, L. S.; Oliveira, P. V.; Vanetti, M. C.; Kasuya, M. C. Enrichment of *Pleurotus ostreatus* mushrooms with selenium in coffee husks. *Food Chem*. **2012**, *131* (2), 558-563. https://doi.org/10.1016/j.foodchem.2011.09.023
(29) Banik, S.; Nandi, R. Effect of supplementation of rice straw with biogas residual slurry manure on the yield, protein and mineral contents of oyster mushroom. *Ind. Crops Prod*. **2004**, *20* (3), 311-319. https://doi.org/10.1016/j.indcrop.2003.11.003
(30) Kalač, P. A review of chemical composition and nutritional value of wild-growing and cultivated mushrooms. *J. Sci. Food Agric*. **2013**, *93* (2), 209-218. https://doi.org/10.1002/jsfa.5960
(31) Kora, A. J. Nutritional and antioxidant significance of selenium-enriched mushrooms. *Bull. Natl. Res. Cent.* **2020**, *44* (34). https://doi.org/10.1186/s42269-020-00289-w
(32) Oliveira, A. P.; Naozuka, J. Preliminary results on the feasibility of producing selenium-enriched pink (*Pleurotus djamor*) and white (*Pleurotus ostreatus*) oyster mushrooms: Bioaccumulation, bioaccessibility, and Se-proteins distribution. *Microchem. J*. **2019**, *145*, 1143-1150. https://doi.org/10.1016/j.microc.2018.12.046
(33) Vetter, J. Biological values of cultivated mushrooms – A review. *Acta Aliment.* **2019**, *48 (2),* 229–240. https://doi.org/10.1556/066.2019.48.2.11
(34) Petrovska, B. B. Protein fraction in edible Macedonian mushrooms. *Eur. Food Res. Technol*. **2001**, *212* (4), 469-472. https://doi.org/10.1556/066.2019.48.2.11
(35) Helm, C. V.; Coradin, J. H.; Rigoni, D. Avaliação da composição química dos cogumelos comestíveis *Agaricus bisporus*, *Agaricus brasiliensis*, *Agaricus bisporus portobello*, *Lentinula edodes* e *Pleorotus ostreatus*. Comunicado Técnico 235 (INFOTECA-E), Embrapa Florestas, 2009.
(36) Krüzselyi, D.; Kovács, D.; Vetter, J. Chemical analysis of king oyster mushroom (Pleurotus eryngii) fruitbodies. *Acta Aliment*. **2016**, *45* (1), 20-27. https://doi.org/10.1556/066.2016.45.1.3
(37) Akyüz, M.; Kirbağ, S. Nutritive value of edible wild and cultured mushrooms. *Turk. J. Biol*. **2010**, *34* (1), 97-102. https://doi.org/10.3906/biy-0805-17

Brazilian Journal of Analytical Chemistry
2023, Volume 10, Issue 40, pp 209-210

FEATURE

Pittcon 2023: Philadelphia hosted the first in-person Pittcon post-COVID-19 pandemic

After a three-year hiatus due to the COVID-19 pandemic, Pittcon was held in Philadelphia March 18-22, 2023 at the Pennsylvania Convention Center.

Pittcon is a dynamic, transnational conference and exposition on laboratory science, a venue for presenting the latest advances in analytical research and scientific instrumentation, and a platform for continuing education and science-enhancing opportunity.

Pittcon is an event that has been going on for over 70 years. Photo: Pittcon

Pittcon is aimed at a wide range of people, from those who develop, buy and sell laboratory equipment to those who perform chemical and physical analysis, develop methods or manage scientists. No matter what your career position is, there is something for everyone.

Pittcon 2023 promoted scientific accomplishments by showcasing knowledge that will impact, enrich, and inspire the future of science. The event also offered many employment and networking opportunities, and social events for scientists to enjoy.

The mission of the Pittsburgh Conference is advancing and enriching scientific endeavor by connecting scientists worldwide, facilitating the exchange of research and ideas, showcasing the latest in laboratory innovation, and funding science education and outreach.

Joanna Aizenberg of Harvard University delivered the 2023 Wallace H. Coulter Lecture at Pittcon Conference. Dr. Aizenberg is a pioneer in the rapidly developing field of bio-inspired materials science and engineering. The title of her talk was “Venturing into Analytical Chemistry Using Photonic Crystals”.

The Pittcon 2023 conference was organized in eight different tracks: Bioanalytics and Life Sciences; Cannabis and Psychedelics; Energy and Environmental; Food Science and Agriculture; Forensics and Toxicology; Industry and Manufacturing; Nanotechnology and Materials Science; and Pharmaceutical.

The event also provided visitors with an exhibition with over 400 vendors. Visitors were given the opportunity to wander through a labyrinth of technical wonders and demonstrations, where highly specialized experts could answer questions about which tool is best to achieve impactful research or how certain laboratory equipment works.

Pittcon Exposition. Photo: Pittcon

Pittcon also had over 60 short courses that attendees could join for an extra fee. These short courses were divided into the same eight tracks as the rest of the conference. Additionally, there was the very popular Professional Skills Building track of courses that can help develop foundational knowledge that will be useful for decades to come.

Pittcon has a major philanthropic side: proceeds from every Pittcon conference help fund science education and outreach e divulgação científica.

In fact, over 90 percent of Pittcon’s net profit goes toward funding primary and secondary education, continuing education, scholarships, grants, laboratory improvements, and outreach activities.

The next Pittcon already has a date and venue: February 2024 in San Diego, California.

Find out more at: https://pittcon.org/

Source: Pittcon

Brazilian Journal of Analytical Chemistry
2023, Volume 10, Issue 40, pp 211-218

BrJAC

SPONSOR REPORT

PDF

This section is dedicated for sponsor responsibility articles.

Total Elemental Analysis in Clinical Research using the Thermo Scientific iCAP TQ ICP-MS

Tomoko Vincent
Applications Specialist at Thermo Fisher Scientific, Bremen, Germany

This report was extracted from the Thermo Scientific Technical Note 43283

INTRODUCTION

Trace element analysis of biological samples provides significant information to support clinical research and forensic toxicology. An interesting example of trace elemental analysis for clinical research purposes is exploring the degradation of titanium based orthopedic and dental implants in humans. Following recent research on the possible carcinogenic effects of titanium dioxide the fate of titanium in the human body has become a growing area of clinical research focus. To support this there is a need for the development of robust analytical methods for the identification and quantification of titanium in a range of samples such as human body fluids and organs. However, the development of such a method is challenging due to the low concentration of titanium in these types of samples and the potential isobaric interferences which single quadrupole ICP-MS cannot remove.

Advancements in ICP-MS technology have led to the development of triple quadrupole (TQ) ICP-MS instruments, which have the required sensitivity as well as the capability to resolve isobaric interferences resulting from polyatomic and isotopic species.

This technical note focuses on the development of a robust method for the analysis of titanium and other trace elements in human serum reference materials using the Thermo Scientific™ iCAP™ TQ ICP-MS.

Keywords: Clinical research, isobaric interferences, serum, titanium, trace elemental analysis, urine

Sample preparation

The certified reference materials (Seronorm™ Trace Elements in Serum L-1 and L-2, SERO, Norway) and volunteered human urine were gravimetrically diluted by a factor of ten in pre-cleaned (72 hours in 2% nitric acid, washed in ultra-pure water) polypropylene bottles with nitric acid (0.5% m/m Fisher Scientific) and tetramethylammonium hydroxide (TMAH, 2% m/m SIGMA-ALDRICH) in ultra-pure water (18 MΩ cm). A calibration blank, a series of standards and a Quality Control (QC) were prepared using the same procedure, replacing the certified reference material with single element standards (SPEX CertiPrep). The elements and final concentrations are shown in Table 1. All samples and standards were spiked with an internal standard mix (10 µg L^{-1} Ge, Y, Rh, Te and Bi).

Instrumentation

The iCAP TQ ICP-MS consists of three quadrupoles to improve interference removal compared to single quadrupole (SQ) ICP-MS. The first quadrupole (Q1) rejects all unwanted ions such as precursor species that may recombine in the collision / reaction cell (CRC) and subsequently interfere with the target analyte.

The second quadrupole (Q2) is used to selectively shift the interference or target analyte with an appropriate reaction gas.

The third quadrupole (Q3) isolates the product ion and removes any remaining interferences through a second stage of mass filtration allowing for interference free analysis of the analyte.

In this analytical method, TQ mass shift mode was used for the target element titanium (Figure 1). Titanium was reacted with ammonia gas (NH_3) to create the cluster ($^{48}Ti(NH_3)_3NH$) at *m/z* 114 in Q2.

Table 1. Elements analyzed and concentration of calibration standards and the QC

	Major STD1	Major STD2	Major STD3	Major STD4	QC CCVs
			(mg L^{-1})		
Ca	5	10	25	50	10
Fe	0.1	0.2	0.5	1	0.2
Mg	5	10	25	50	10
P	5	10	25	50	10
K	5	10	25	50	10
S	50	250	500	1000	100
Na	50	100	250	500	100
	Minor STD1	**Minor STD2**	**Minor STD3**	**Minor STD4**	**QC CCVs**
			(µg L^{-1})		
Sb	0.5	1	2.5	5	1
As	0.1	0.2	0.5	1	0.2
Ba	5	10	25	50	10
Cd	0.1	0.2	0.5	1	0.2
B	5	10	25	50	10
I	5	10	25	50	10
Pb	0.1	0.2	0.5	1	0.2
Li	500	1000	2500	5000	1000
Mo	0.1	0.2	0.5	1	0.2
Rb	0.5	1	2.5	5	1
Sr	5	10	25	50	10
Ti	0.5	1	2.5	5	1
U	0.005	0.01	0.025	0.05	0.01
V	0.1	0.2	0.5	1	0.2
Zn	50	100	250	500	100
Se	0.1	0.2	0.5	1	0.2
Al	50	100	250	500	100
Cr	0.5	1	2.5	5	1
Mn	5	10	25	50	10
Ni	5	10	25	50	10
Co	0.1	0.2	0.5	1	0.2

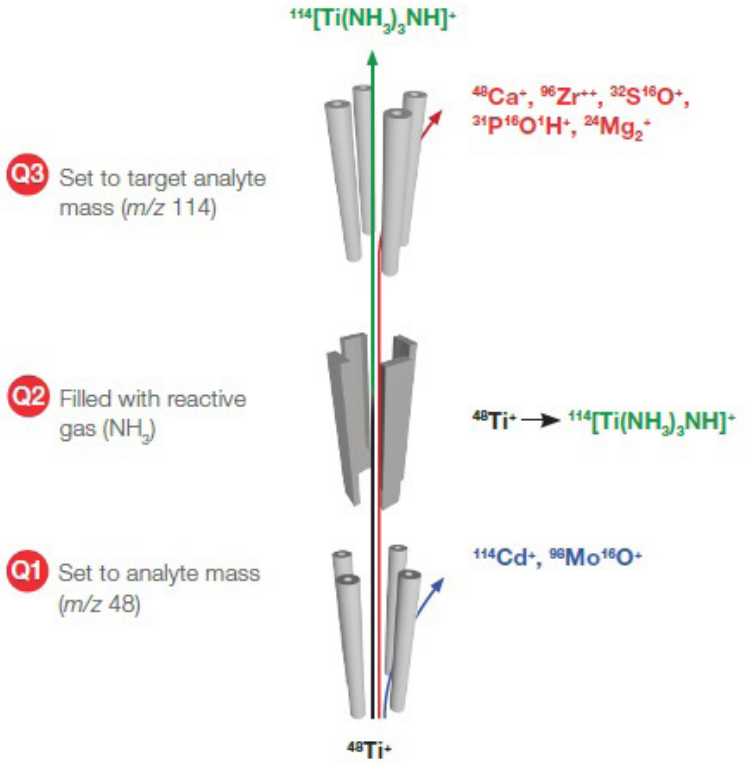

Figure 1. TQ mass shift mode for titanium.

The iCAP TQ ICP-MS also has the ability to operate in single quadrupole mode when advanced interference removal is not required. For many of the analytes in this analytical method, analysis using pure He as a collision gas and Kinetic Energy Discrimination (KED) mode is sufficient.

Method development and analysis

The sample introduction system used is detailed in Table 2. The operating parameters were optimized by the default autotune procedure in the Thermo Scientific™ Qtegra™ Intelligent Scientific Data System™ (ISDS) software that controls the iCAP TQ ICP-MS.

Table 2. Instrument configuration and operating parameters

Parameter	Value	
Nebulizer	PFA nebulizer 0.2 mL min^{-1}, pumped at 40 rpm	
Spraychamber	Quartz cyclonic spraychamber cooled at 3 °C	
Injector	2.5 mm Quartz	
Interface	High matrix (3.5 mm), Ni cones	
RF power	1550 W	
Nebulizer gas flow	1.001 L min^{-1}	
QCell setting	**SQ-KED**	**TQ-NH_3**
Gas flow	4.5 mL min^{-1}	0.29 mL min^{-1}
CR Bias	-21 V	-7.9 V
Q3 Bias	-18 V	-11 V
Dwell time	0.2 seconds per analyte, 5 sweeps	

The optimum measurement mode for each analyte was automatically selected by the Reaction Finder method development assistant within Qtegra ISDS Software. Additional measurement modes were selected for Ti to compare the efficiency of the interference removal in TQ mass shift mode:

SQ-KED – single quadrupole mode with CRC pressurized with He, KED applied, no filter on Q1 and Q3 set to mass 48

SQ-NH_3 – single quadrupole mode with CRC pressurized with NH_3, no filter on Q1 and Q3 set to product ion mass of 114

TQ-NH_3 – triple quadrupole mode with CRC pressurized with NH_3, Q1 set to mass 48 and Q3 set to product ion mass of 114

An internal standard was also associated with each analyte on a mass basis. Internal standard association and measurement modes for the final analysis are shown in Table 3.

Table 3. Measurement modes and internal standards used for each element

	Measurement mode	Analyte/Product Ion mass	Internal standard
Na	SQ-KED	23	^{74}Ge
Mg	SQ-KED	24	^{74}Ge
P	SQ-KED	31	^{74}Ge
S	SQ-KED	34	^{74}Ge
K	SQ-KED	39	^{74}Ge
Ca	SQ-KED	44	^{74}Ge
Fe	SQ-KED	56	^{74}Ge
Li	SQ-KED	7	^{74}Ge
B	SQ-KED	11	^{74}Ge
Al	SQ-KED	27	^{74}Ge
V	SQ-KED	51	^{74}Ge
Cr	SQ-KED	52	^{74}Ge
Mn	SQ-KED	55	^{74}Ge
Co	SQ-KED	59	^{74}Ge
Ni	SQ-KED	60	^{89}Y
Zn	SQ-KED	66	^{74}Ge
As	SQ-KED	75	^{89}Y
Se	SQ-KED	78	^{74}Ge
Rb	SQ-KED	85	^{89}Y
Sr	SQ-KED	88	^{89}Y
Mo	SQ-KED	95	^{103}Rh
Cd	SQ-KED	111	^{103}Rh
Ti	TQ-NH_3	114	$^{74}Ge^{14}N^{1}H_2$
Sb	SQ-KED	121	^{125}Te
I	SQ-KED	127	^{125}Te
Ba	SQ-KED	138	^{103}Rh
Pb	SQ-KED	208	^{209}Bi
U	SQ-KED	238	^{209}Bi

The sample analysis consisted of an external calibration curve followed by replicate analyses of the urine and serum samples. Continuous calibration verication (CCV) samples were analyzed every 10 samples and a total of 124 samples were measured during the analysis. All samples were presented for analysis using a Teledyne CETAC Technologies ASX-560 Autosampler. The rinse solution used on the autosampler between samples was the same as the diluent (0.5% HNO_3/2% TMAH).

RESULTS

Titanium in biological samples is particularly challenging due to the isobaric overlap of ^{48}Ca and polyatomic interferences from SO^+ and POH^+. To evaluate the efficiency of interference removal, three different measurement modes (SQ-KED, SQ-NH_3 or TQ-NH_3) were used to measure a certified reference material (CRM). The results for titanium quantification in both Serum L-1 and L-2 for each of the measurement modes are shown in Table 4. The result from the TQ-NH_3 is the most accurate when compared to the reported values for these materials. The Reaction Finder method development assistant automatically selects this mode for analysis.

To demonstrate the improved interference removal, the effect of the presence of cadmium in the sample was investigated. A ten-fold diluted serum sample and a10 mg L^{-1} cadmium standard were analyzed with TQ-NH_3 mode and spectra recorded. The ten-fold diluted serum sample shows a typical spectral fingerprint associated with the creation of $Ti(NH_3)_3X^+$ clusters (Figure 2). The 10 mg L^{-1} cadmium standard (Figure 3) measured with the same conditions and measurement mode, shows no presence of Cd in the spectra (only residual counts from the analysis of the serum), the Cd having been eliminated by Q1. This prevents any trace Cd in the sample from interfering with the analysis of Ti at *m/z* 114.

Table 4. Comparison of titanium results in the serum CRMs with different measurement modes

	Ti SQ-KED µg L^{-1}	Ti SQ-NH_3 µg L^{-1}	Ti TQ-NH_3 µg L^{-1}	Ti Reported Value µg L^{-1}
Serum L-1	167	1800	6.64	6.8
Serum L-2	262	1850	6.38	6.8

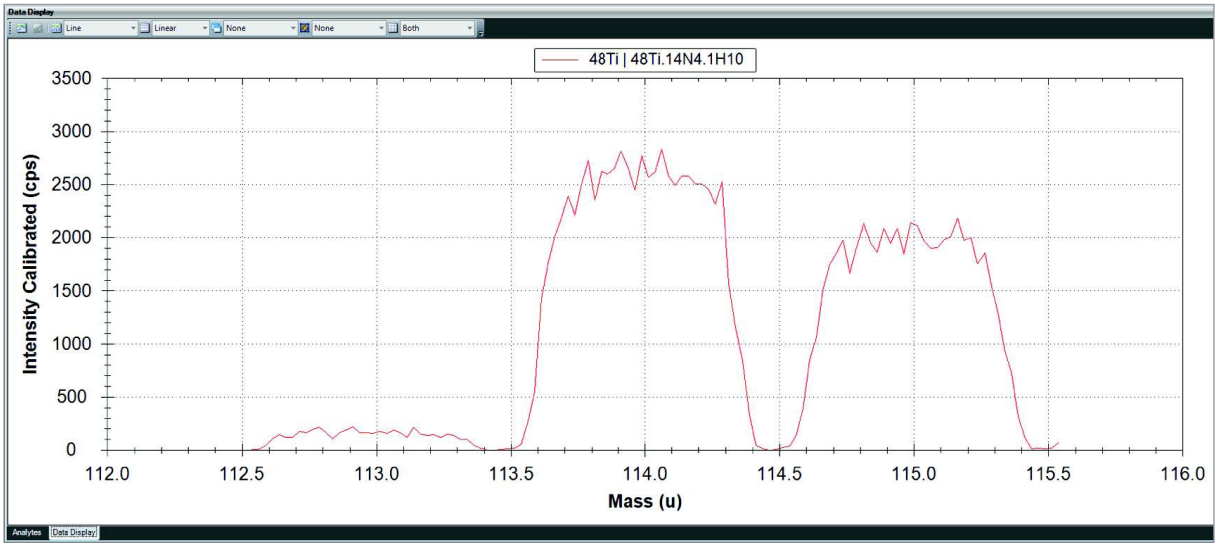

Figure 2. Spectra of serum sample (diluted 10-fold).

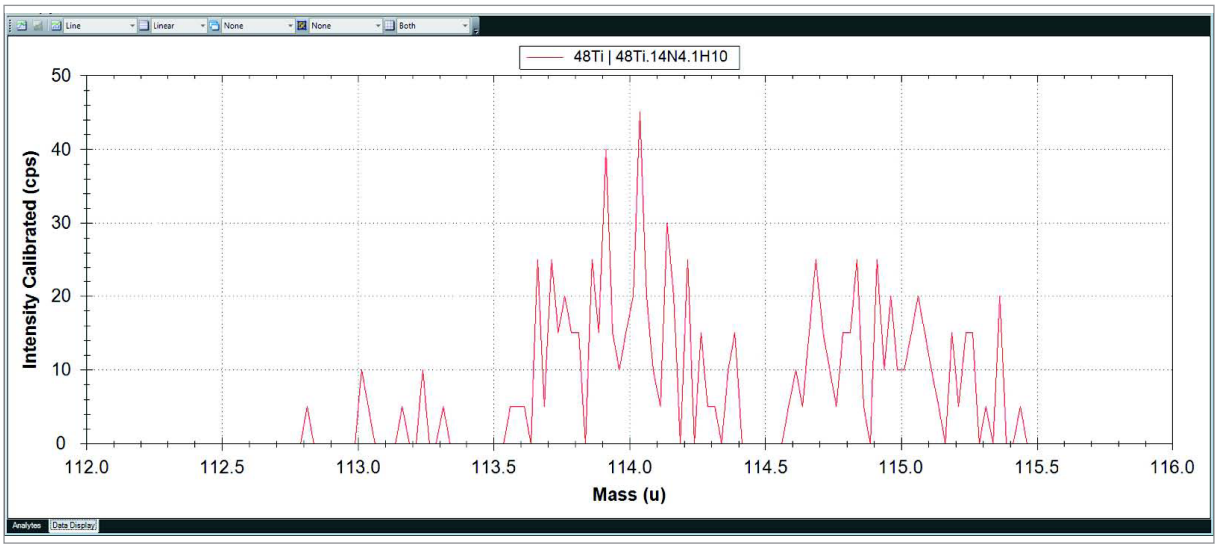

Figure 3. Spectra of 10 mg L^{-1} cadmium.

Selected calibrations for the multi-elemental analysis are shown in Figures 4 to 7. The calibration curve for the titanium with TQ mass shift mode (Figure 4) shows high sensitivity at 3903 cps/µg L^{-1} and excellent linearity with an R^2 value of 0.9998 for the calibration consisting of a blank and four standards (0, 0.5, 1, 2.5 and 5 µg L^{-1}).

All other elements analytes apart from Ti were analyzed using SQ-KED. When analyzing in this mode the first quadrupole simply acts as an ion guide. Calibration curves for arsenic and selenium using the SQ-KED mode are shown in Figures 5 and 6 respectively with the concentration range of 0.1 to 1 µg L^{-1}. The calibration curve for sulfur (Figure 7) is performed with the concentration range of 50 to 1000 mg L^{-1}. These are typical elements and typical concentration ranges expected in clinical research.

The results of the multi-elemental analysis of the serum CRMs are shown in Table 5. Measured values for the analytes in the reference materials are in good agreement with the reference or reported values. These values cover a wide concentration range from sub ppb to low % levels, demonstrating the importance of the dynamic range of the iCAP TQ ICP-MS. A urine sample, analyzed in the same analytical run, was found to contain typical elemental concentrations.

The detection limit (LOD) was determined based on three times the standard deviation of a ten-replicate measurement of the calibration blank. The method detection limits (MDL) for all of the elements analyzed were calculated by multiplying the LOD by the dilution factor (1:10) (Table 5). The LODs for all the elements of interest are well below the target levels required for clinical research sample analysis.

Table 5. Results for the serum CRMs and urine sample. The analyte labeled with a * are reported at mg L^{-1}, all other results are reported in µg L^{-1}.

	LOD	MDL	Serum L-1		Serum L-1		Urine
			Measured	Reference or reported value	Measured	Reference or reported value	Measured
Na*	0.0027	0.027	2743	2330-3504	3255	2820-4241	2977
Mg*	0.0001	0.0010	21.0	13.4-20.1	39.7	27.1-40.7	85.6
P*	0.0008	0.08	52.3	43.3-65.1	120	88-132	710
S*	0.145	1.3800	1100	1008	1495	1335	476
K*	0.0021	0.02	150	101-153	260	176-265	1946
Ca*	0.002	0.0200	90.1	69-104	124	95-143	99.8
Fe*	0.00002	0.00023	1.64	1.17-1.77	2.18	1.72-2.58	0.005

(continues on the next page)

Table 5. Results for the serum CRMs and urine sample. The analyte labeled with a * are reported at mg L^{-1}, all other results are reported in µg L^{-1}. (Continuation)

	LOD	MDL	Serum L-1		Serum L-1		Urine
			Measured	Reference or reported value	Measured	Reference or reported value	Measured
Li	1.13	11.2920	5778	4202-6320	10806	7739-11639	22.4
B	0.67	6.746	70.1	79.4	87	82.1	1548
Al	0.20	1.9670	54.2	25.2-75.7	122	96-144	13.7
V	0.002	0.022	1.04	1.10	1.26	1.10	0.229
Cr	0.008	0.0800	1.70	1.30-3.05	5.20	4.00-7.50	0.838
Mn	0.008	0.084	10.7	7.9-11.9	14.2	11.6-17.4	0.914
Co	0.0001	0.0010	1.38	0.67-1.57	2.16	2.13-3.97	0.027
Ni	0.006	0.055	6.26	3.38-7.9	9.41	7.9-11.9	1.45
Zn	0.051	0.5130	1052	844-1269	1527	1404-1831	359
As	0.002	0.018	0.383	0.400	0.374	0.380	1.31
Se	0.010	0.1000	80.8	51-120	124	95-176	7.31
Rb	0.004	0.035	4.20	4.40	8.70	8.70	812
Sr	0.006	0.0570	95.7	95.0	106	110	89.2
Mo	0.005	0.048	0.710	0.760	1.20	1.21	7.62
Cd	0.001	0.0100	0.130	0.130	0.140	0.140	0.229
Ti	0.002	0.02	6.64	6.80	6.38	6.80	0.151
Sb	0.006	0.0600	11.6	10.4	16.1	15.0	0.040
I	0.022	0.219	75.5	71.8	69.9	60.9	82.8
Ba	0.003	0.0300	172	190	133	139	2.09
Pb	0.0007	0.007	0.370	0.400	0.666	0.660	0.446
U	0.0001	0.0010	0.288	0.302	0.357	0.359	0.020

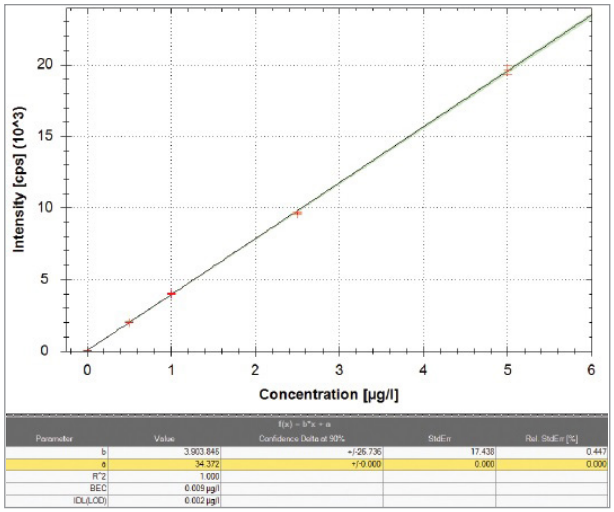

Figure 4. Calibration curve for titanium.

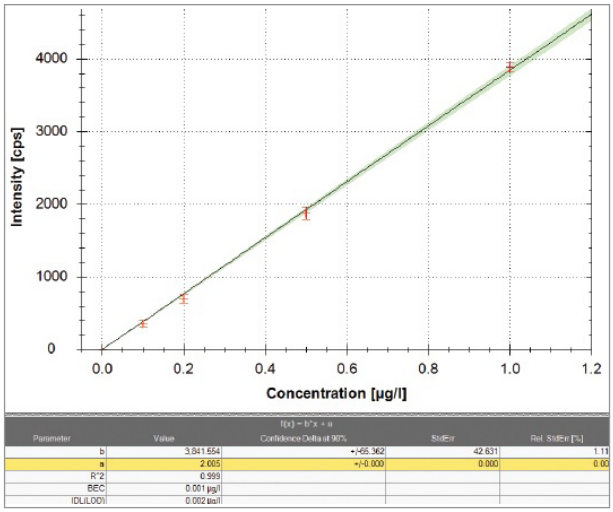

Figure 5. Calibration curve for arsenic.

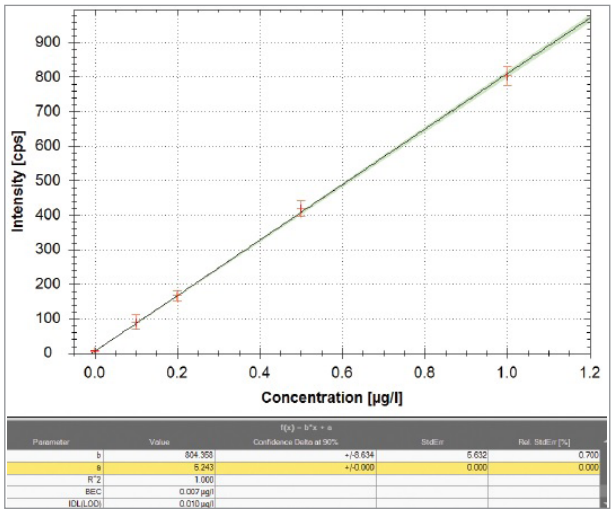

Figure 6. Calibration curve for selenium.

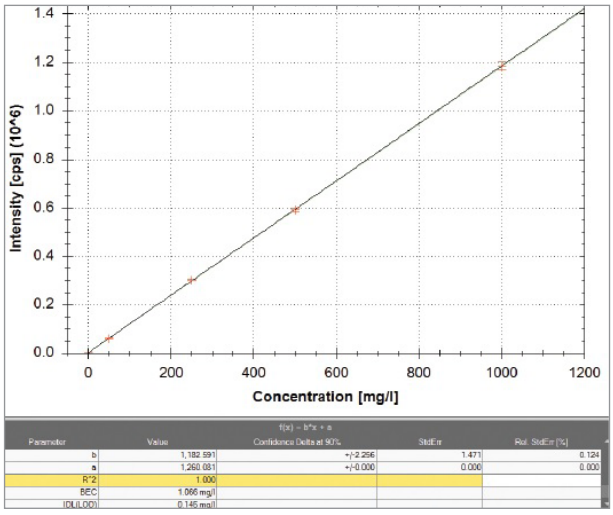

Figure 7. Calibration curve for sulfur.

The average results of the ongoing QC test over a period of eight hours (with a total of nine QC samples being measured) are shown in Figure 8. Average recoveries lie between 95 and 110% with standard deviations typically less than 2% (apart from B, As and Se where the SD was < 4% due to lower sensitivity). These results demonstrate the long term stability of the instrument when analyzing high matrix biological samples.

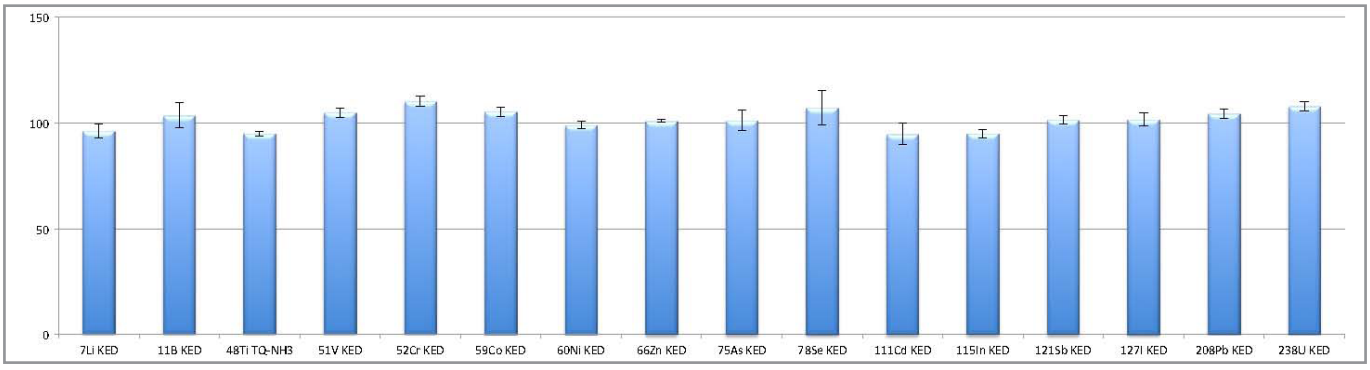

Figure 8. Calibration check verification standards (CCVs) measured during the analysis.

CONCLUSION

The Thermo Scientific iCAP TQ ICP-MS provides excellent performance for the determination of trace element analysis in biological samples making it ideal for clinical research. One key investigation is the degradation of metal-on-metal hip replacement implants, where Ti is often a component and where accurate analysis is problematic using SQ-ICP-MS.

With the iCAP TQ ICP-MS, powerful triple quadrupole technology provides the advanced performance required for the sensitive and accurate determination of Ti and other trace elements in complex samples, whilst the Reaction Finder tool allows for simple method setup by automatically selecting analytes of interest.

Find out more at thermofisher.com/TQ-ICP-MS

This Sponsor Report is the responsibility of Thermo Fisher Scientific.

Brazilian Journal of Analytical Chemistry
2023, Volume 10, Issue 40, pp 219-229

BrJAC

SPONSOR REPORT

PDF

This section is dedicated for sponsor responsibility articles.

Determination of Iodide in Multivitamin-Mineral Supplements using Ion Chromatography

Hua Yang and Jeffrey Rohrer

Thermo Fisher Scientific, Sunnyvale, CA, United States

This report was extracted from the Thermo Scientific Application Note 000069

Keywords: Food, nutrition, dietary supplements, electrochemical detection, Dionex IonPac AS20 column, RFIC system, pulsed amperometric detection (PAD), silver/silver chloride (Ag/AgCl) pH reference electrode, palladium hydrogen (PdH) reference electrode, silver working electrode

Goal

To develop a method for the determination of iodide in multivitamins using an ion chromatography (IC) system with a Thermo Scientific™ Dionex™ IonPac™ AS20 column and electrochemical detection

Introduction

Iodine is an essential mineral for the body. The thyroid gland uses iodine to produce thyroid hormones that regulate many important biochemical reactions and are metabolically critical. It is known that iodine deficiency can lead to varying degrees of growth and developmental abnormalities in children and adults.[1-3] Excess iodine can lead to thyroid disorders.[4] Therefore, an appropriate level of iodine is critical for the body to function properly. As the body does not produce iodine, it must be supplied by the diet (foods or dietary supplements). Multivitamin-mineral supplements containing iodine, usually in the form of potassium iodide or sodium iodide, are one of the common sources of dietary iodine.

In the United States, accurate measurements of nutrients are needed to ensure compliance with Food and Drug Administration (FDA) regulations on the Nutrition Facts and Supplement Facts labels. The percent daily value of iodine must be listed on the label if iodine is added to a food.[5] The current daily value for iodine is 150 µg for individuals aged ≥4 years. Determination of iodine in foods or dietary supplements is important and has been included in the National Institute of Standards and Technology (NIST) Dietary Supplement Laboratory Quality Assurance Program (DSQAP).[6]

Many analytical methods have been used for determining iodine in food matrices, including ion chromatography (IC) methods with electrochemical detection (ED).[7-9] A Thermo Scientific™ application note (AN) demonstrated the determination of iodide and iodate in infant formulas using acid digestion, and a 4 mm Thermo Scientific™ Dionex™ IonPac™ AG11/AS11 column set with manually prepared nitric acid eluent and ED.[7] This application note shows the development and validation of a different ED method with an alkaline eluent for the determination of iodide in multivitamin-mineral supplement samples. This ED method uses alkaline digestion and a 2 mm version of the Dionex IonPac AS20 column with electrolytically generated potassium hydroxide (KOH) eluent. Using an alkaline digestion sample preparation method and a dual channel IC system, the nutrient chlorine (as chloride) in the supplements can be determined by conductivity detection (CD) simultaneously, which will be reported in a different application document. Here we demonstrate using the CD channel to support ED method development. This document shows that the ED method is sensitive and accurate for determining iodide in multivitamin supplements for regulatory monitoring.

In addition, we also demonstrate using a palladium hydrogen (PdH) reference electrode rather than a silver/silver chloride (Ag/AgCl) reference electrode for iodide determination and compare its performance to that of the Ag/AgCl reference electrode. The PdH electrode is a solid-state reference electrode. It provides a more stable reference potential and offers other advantages, such as longer lifetime and less maintenance. Its value was previously demonstrated for carbohydrate determinations.[10]

Experimental

Equipment

- Thermo Scientific™ Dionex™ ICS-6000 Dual Channel HPIC™ system with RFIC™-EG module, conductivity and electrochemical detectors*
- Thermo Scientific™ Dionex™ AS-AP autosampler with 250 µL syringe and tray temperature control (P/N 074926)
- Thermo Scientific™ Dionex™ Chromeleon™ Chromatography Data System (CDS) software, version 7.2.10
- Thermo Scientific™ Dionex™ ICS-6000 ED Electrochemical Detector (P/N 072042) with Electrochemical Detector Cell (P/N 072044)

*For iodide determination, equivalent results can be achieved using a single-channel Thermo Scientific™ Dionex™ ICS-6000 system, Thermo Scientific™ Dionex™ ICS-5000+ system, or Thermo Scientific™ Dionex™ Integrion™ HPIC™ system with electrochemical detection.

Consumables

- Thermo Scientific™ Dionex™ EGC 500 KOH Potassium Hydroxide Eluent Generator Cartridge (P/N 075778)
- Thermo Scientific™ Dionex™ CR-ATC 600 Continuously Regenerated Anion Trap Column (P/N 088662)
- Thermo Scientific™ Dionex™ AS20 Analytical Column, 2 × 250 mm, (P/N 063065)
- Thermo Scientific™ Dionex™ AG20 Guard Column, 2 × 50 mm (P/N 063066)
- Thermo Scientific™ Dionex™ AS-AP Autosampler Vials 10 mL (P/N 074228)
- Thermo Scientific™ Dionex™ Electrochemical Detector Ag/AgCl pH Reference Electrode (P/N 061879)
- Thermo Scientific™ Dionex™ Electrochemical Detector Palladium Hydrogen (PdH) Reference Electrode (P/N 072075)**
- Thermo Scientific™ Dionex™ Electrochemical Detector Silver Disposable Electrode (P/N 063003). Package includes 6 electrodes and 6 gaskets (0.002 in.).
- Fisherbrand™ Polypropylene Centrifuge Tubes, 50 mL (Cat. No. 05-539-13)
- Thermo Scientific™ Nalgene™ Syringe Filter 0.2 µm PES (P/N 725-2520)

**Both reference electrodes were evaluated in this application note. Only one is needed to run this method.

Reagent and standards

- Degassed deionized (DI) water, 18 MΩ cm resistance or better
- Potassium iodide (>99.9%), A.C.S. reagent grade or better, for preparing iodide standards, Fisher Chemical™ (Fisher Scientific, P/N P410-100)
- Sodium hydroxide solution (50% w/w/Certified), Fisher Chemical™ (Fisher Scientific P/N SS254-500)

Samples

Four brands of multivitamin-products were purchased from local stores. The iodine contents (mg/kg) were calculated by the tablet weight and the label for each sample (Table 1).

Table 1. Sample details

Multivitamin	Information	Iodine on label (mcg*/tablet)	Weight of 3 tablets (g)	Label iodine (mg/kg)
Sample 1 (MV1)	Brand 1, Multivitamin for men	150	4.7254	95.2
Sample 2 (MV2)	Brand 2, Multivitamin for women	150	4.9449	91.0
Sample 3 (MV3)	Brand 3, Organic multivitamin	N/A	4.9000	N/A
Sample 4 (MV4)	Brand 4, Multivitamin	150	3.8324	117.4

*mcg = micrograms

IC setup and conditions

Figure 1 shows a schematic diagram of a Reagent-Free™ IC system for the determination of iodide. The dual channel setup used to develop the iodide method and measure chloride simultaneously on the second channel is shown in the Appendix. An autosampler with a diverter valve is used to serve both channels. For the determination of iodide, only one channel of the system with electrochemical detection, is required. In other words, only one pump of the DP or a single pump is used and the diverter valve is not needed for the AS-AP.

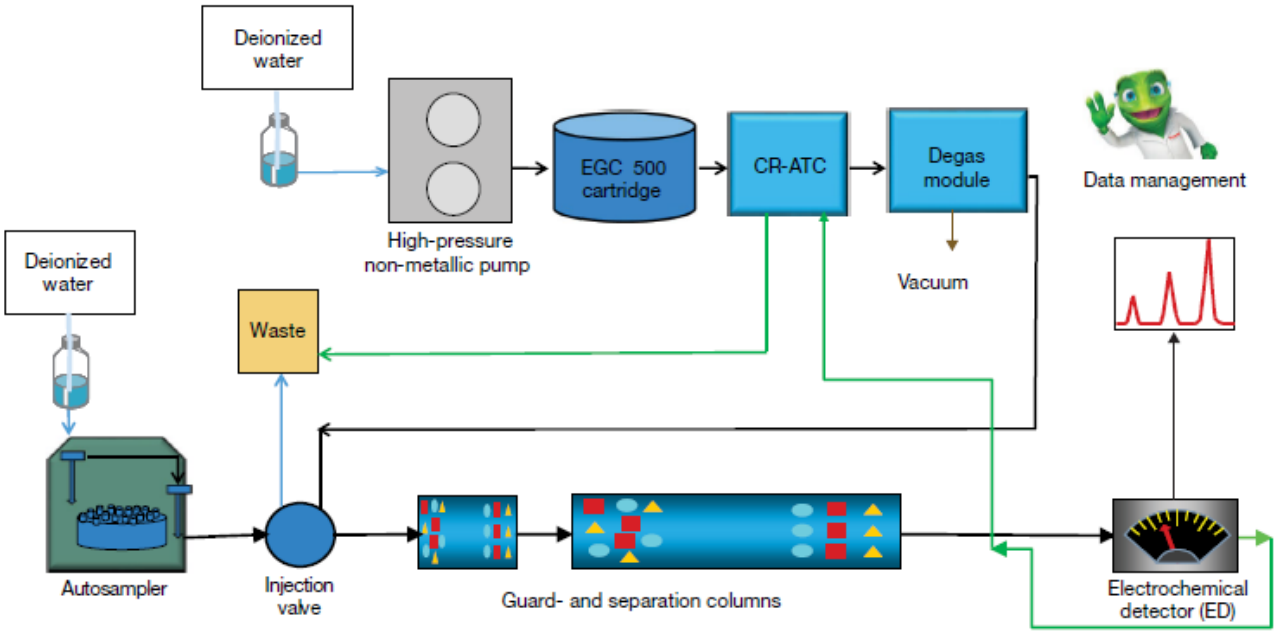

Figure 1. Schematic diagram of an RFIC system for the determination of iodide.

Table 2. Chromatography conditions

Parameter	Value
Columns	Dionex IonPac AS20 analytical column, 2 × 250 mm Dionex IonPac AG20 guard column, 2 × 50 mm
Eluent	30 mM potassium hydroxide (KOH)
Eluent source	Thermo Scientific™ Dionex™ EGC 500 KOH cartridge with Thermo Scientific™ Dionex™ CR-ATC 600 and high-pressure degasser
Flow rate	0.35 mL/min
Injection volume	25 µL (full loop)
Column temp.	30 °C
Sample tray temp.	4 °C
Detection	Electrochemical detection Pulsed amperometric detection (PAD) mode
Working electrode	Silver working electrode (disposable)
Reference electrode	Ag/AgCl pH reference electrode or PdH reference electrode
Run time	15 min

Waveform (when using Ag/AgCl reference electrode)	Silver, (Sulfide, Cyanide, Iodide, Thiosulfate)		
	Time (s)	Potential (V)	Integration
	0.00	-0.10	
	0.20	-0.10	Start
	0.90	-0.10	End
	0.91	-1.00	
	0.93	-0.30	
	1.00	-0.30	

Waveform (when using Palladium Hydrogen (PdH) reference electrode)	*Silver, (Sulfide, Cyanide, Iodide, Thiosulfate)		
	Time (s)	Potential (V)	Integration
	0.00	0.79	
	0.20	0.79	Start
	0.90	0.79	End
	0.91	-0.11	
	0.93	0.59	
	1.00	0.59	

Preparation of solutions and reagents

Iodide stock standard solutions (2,000 mg/L)

Iodide stock standard solution is prepared by dissolving 262.0 mg of dry potassium iodide salt in 100 mL of DI water. The stock standard is stable for at least six months when stored at 4 °C.

Calibration standards

Diluted calibration standard solutions are prepared from the 2,000 mg/L stock standard and DI water (Table 3).

Sample preparation

Extraction solution (0.02% (w/w) sodium hydroxide)

Mix 0.4 g of 50% w/w NaOH with 999.6 g DI water in a plastic bottle.

Sample powder

Grind >30 tablets and mix the resulting powder thoroughly. Store at room temperature if analyzed within 2 days. Otherwise, store at 4 °C.

Prepare sample

1. Weigh about 0.500 g of multivitamin sample into a 50 mL conical centrifuge tube and record the exact weight.
2. Add 20 mL (g) of the extraction solution into the tube, shake and mix well.
3. Place the tube in an ultrasonic bath and sonicate for >2 h.
4. Centrifuge at 6,000-7,000 rpm for 30 min.
5. Filter the sample solution through a 0.2 µm PES syringe filter, discarding the first couple drops of the effluent.
6. Dilute sample solution 1 to 20 with the extraction solution before IC analysis.

Prepare spiked sample

1. Weigh about 0.500 g of multivitamin sample into a 50 mL conical centrifuge tube and record the exact weight.
2. Add known amounts (approximately 30% to 70% of the label amount) of iodide standards into the solid multivitamin sample in the centrifuge tube.
3. Follow steps 2 to 6 above.

Table 3. Calibration standards (mg/L)

Analyte	Level 1*	Level 2	Level 3	Level 4	Level 5	Level 6	Level 7	Level 8
Iodide (mg/L)	0.001 (0.0025)	0.005	0.01	0.04	0.1	0.4	1.0	2.0

* Level 1 = 0.001 mg/L iodide when using a Ag/AgCl reference electrode; Level 1 = 0.0025 mg/L iodide when using a PdH reference electrode.

Results and discussion

Separation

The Dionex IonPac AS20 column is a hydroxide-selective, high-capacity anion-exchange column developed to determine anions that are strongly retained on other anionexchange columns. The selectivity for these highly retained anions, such as iodide, allows them to be determined with lower ionic strength eluents and in less time compared to other anion-exchange columns. Figure 2 shows the separation of a 0.4 mg/L iodide standard on a Dionex IonPac AS20 column set using a 30 mM KOH eluent and ED detection. Iodide elutes in less than 10 min and is well resolved from the void volume and the baseline dip, which is due to dissolved oxygen, at approximately 12 min. Figure 3 shows the separation of iodide in multivitamin sample 1. Most other anions in multivitamin samples retained by the Dionex IonPac AS20 column are not detected by ED. To ensure all anions elute and do not consume column capacity, multivitamin samples were analyzed using suppressed conductivity detection and the same separation conditions. That analysis (not shown) demonstrated that most anions elute well before iodide, with chloride eluting at approximately 3.3 min. Iodide elutes at 8.5 min and is well-resolved from other anions in the sample. The concentration of iodide in multivitamin sample 1 (MV1), however, is too low to be determined by suppressed conductivity detection.

Columns	Dionex IonPac AG20, 2 × 50 mm and Dionex IonPac AS20, 2 × 250 mm		
Eluent	Potassium hydroxide (KOH) 30 mM		
Eluent source	Dionex EGC 500 KOH Cartridge with Dionex CR-ATC 600 and Dionex high pressure degasser		
Flow rate	0.35 mL/min		
Inj. volume	25 µL (Full loop)		
Column temp.	30 °C		
Sampler temp.	4 °C		
Detection	Electrochemical detection (ED) with Ag/AgCl reference electrode and disposable silver working electrode		
		min	mg/L
Peak	1. Iodide	8.5	0.4

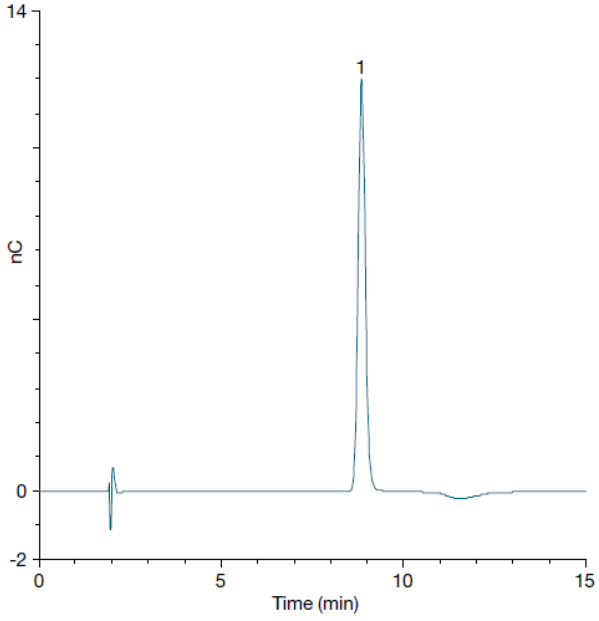

Figure 2. Chromatogram of 0.4 mg/L iodide.

Columns	Dionex IonPac AG20, 2 × 50 mm and Dionex IonPac AS20, 2 × 250 mm
Eluent	Potassium hydroxide (KOH) 30 mM
Eluent source	Dionex EGC 500 KOH Cartridge with Dionex CR-ATC 600 and Dionex high pressure degasser
Flow rate	0.35 mL/min
Inj. volume	25 µL (Full loop)
Column temp.	30 °C
Sampler temp.	4 °C
ED detection	Electrochemical detection (ED) with Ag/AgCl reference electrode and disposable silver working electrode
Sample	Multivitamin sample 1 (MV1)
Peak	1. Iodide

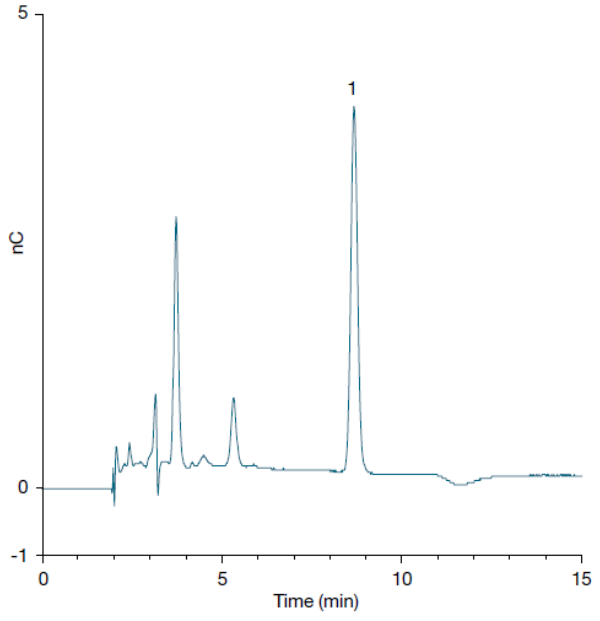

Figure 3. Chromatogram of multivitamin sample 1.

Table 4. Linearity and method detection limit for iodide determination using ED detection

Reference electrode	Analyte	Injection volume (µL)	Range (mg/L)	Coefficient of determination* (r^2)	Calculated** MDL (mg/L)
Ag/AgCl	Iodide	25	0.001–2	0.9995	0.0005
PdH	Iodide	25	0.0025–2	0.9991	0.0018

*Calibration type is linear and forced through the origin.

**MDL = (t) × (S)

Where t = Student's t value for a 99% confidence level and a standard deviation estimate with n-1 degrees of freedom (t = 3.14 for seven replicates); S = standard deviation of the replicate analyses.

Linearity and method detection limit

The method linearity was determined by triplicate injections of eight levels of calibration standards (Table 3). The method detection limit (MDL) was determined by performing seven replicate injections of the lowest level calibration standard, which is at a concentration of three to five times the estimated detection limit. Two different reference electrodes, a combination Ag/AgCl pH reference electrode for which we are using the Ag/AgCl half cell potential, and a PdH reference electrode, were studied for iodide determination. The results are shown in Table 4 and Figures 4 and 5. The study shows that peak area response is linear over the concentration ranges evaluated for each reference electrode with a coefficient of determination of 0.9995 for the Ag/AgCl reference electrode, and 0.9991 for the PdH reference electrode. The method is sensitive for the determination of iodide with MDL = 0.0005 mg/L when using the Ag/AgCl reference electrode and MDL = 0.0018 mg/L when using the PdH reference electrode.

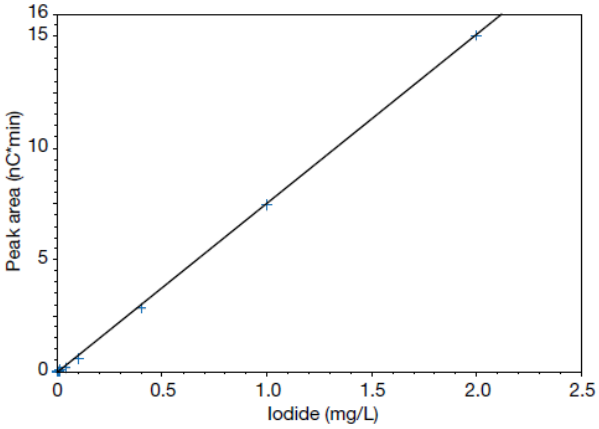

Figure 4. Calibration plot for iodide using a Ag/AgCl reference electrode with 25 µL injection volume.

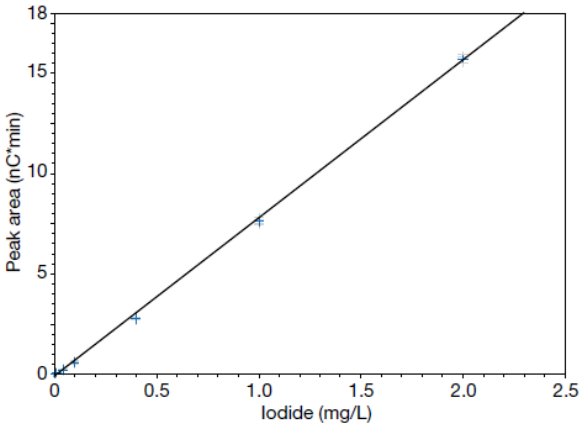

Figure 5. Calibration plot for iodide using a PdH reference electrode with 25 µL injection volume.

Precision and accuracy

The method precision was evaluated by measuring iodide in a multivitamin sample and expressed as the relative standard deviation (RSD) of the results (Table 5). Intraday precision was evaluated by four samples independently prepared on a single day with triplicate injections for each sample. Interday precision was evaluated by comparing the results over four days with new sample preparations each day. The method shows an intraday precision = 1.3%, and an interday precision = 1.6%.

Table 5. Reproducibility of determination of iodide in multivitamin sample 2*

Intraday (n=4)		Interday (Over 4 days)	
Iodide (mg/kg)	**RSD**	**Iodide (mg/kg)**	**RSD**
91.1 ± 1.2	1.3	90.1 ± 1.5	1.6

*Ag/AgCl reference electrode and 25 µL injection

The method accuracy was validated by recovery experiments. Spiked samples were analyzed together with non-spiked samples. The recovery percentages were calculated using the formula shown below:

% Recovery = (Total iodide in the spiked sample - Iodide in the sample before spiking*)/ Iodide added

*Calculated based on the result of non-spiked samples of 91.1 mg/kg.

Table 6 summarizes the recovery results. The method is accurate with recovery ranging from 94% to 101%.

Table 6. Spiked recovery of iodide in multivitamin at different spiked levels

Spiked in iodide/iodide in sample (%)	Sample weight (g)	Iodide added (mg)	Recovery (%)
30	0.50620	0.016	100
50	0.50361	0.024	94
70	0.50167	0.032	101

Determination of iodide in multivitamin preparations

To demonstrate the method's application for regulatory monitoring, four brands of multivitamin samples were tested using a Ag/AgCl reference electrode. Each multivitamin sample was tested at least three times (independently prepared samples on separate days). The results are listed in Table 7. The test results were consistent, with an RSD range from 0.9 to 2.5%. Multivitamin quality varied when judged by comparing results to the labeled values. Within the four brands tested, MV2's result agrees well with the label (99%), while MV4 is 47% higher than its claim. Determination of iodine in supplements is important and was included in NIST Dietary Supplement Laboratory Quality Assurance Program. This easy-to-use IC-ED method is suited for regulatory monitoring of iodine (as iodide) in these products.

Table 7. Determination of iodide in multivitamin samples

Multivitamin	Measured iodine* (mg/kg) (n≥3)	RSD	Label iodine (mg/kg)	Measured/label (%)
MV1	106 ± 1.4	1.3	95.2	111%
MV2	90.1 ± 1.5	1.6	91.0	99%
MV3	13.3 ± 0.1	0.9	N/A	N/A
MV4	173 ± 4.3	2.5	117.4	147%

*Data used Ag/AgCl reference electrode.

To compare Ag/AgCl and PdH reference electrodes, a set of samples was tested using both reference electrodes (Figures 6 and 7). The results were similar regardless of which reference electrode was used for iodide determination. While we did not run as many experiments with the PdH reference electrode as we did the Ag/AgCl reference, we believe that either reference electrode can be used for this application.

Columns	Dionex IonPac AG20, 2 × 50 mm and Dionex IonPac AS20, 2 × 250 mm	Columns	Dionex IonPac AG20, 2 x 50 mm and Dionex IonPac AS20, 2 x 250 mm
Eluent	Potassium hydroxide (KOH) 30 mM	Eluent	Potassium hydroxide (KOH) 30 mM
Eluent source	Dionex EGC 500 KOH Cartridge with Dionex CR-ATC 600 and Dionex high pressure degasser	Eluent source	Dionex EGC 500 KOH Cartridge with Dionex CR-ATC 600 and Dionex high pressure degasser
Flow rate	0.35 mL/min	Flow rate	0.35 mL/min

(continues on the next page)

Inj. volume	25 µL (Full loop)
Column temp.	30 °C
Sampler temp.	4 °C
Detection	Electrochemical detection (ED) with Ag/AgCl reference electrode and disposable silver working electrode
Samples	Four brands of multivitamin

	Iodine value (mg/kg)	
	Label	Measured
MV-1	95.2	106
MV-2	91.0	90.1
MV-3	N/A	13.3
MV-4	117.4	173

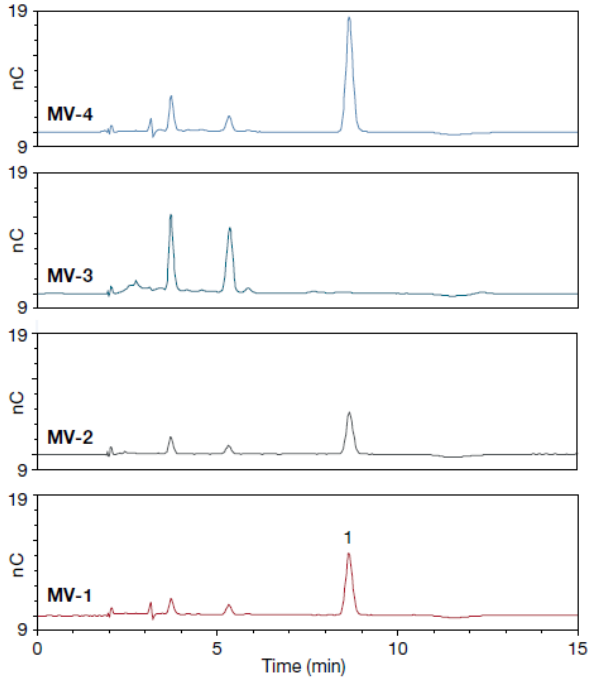

Figure 6. Chromatograms of multivitamin samples using a Ag/AgCl reference electrode.

Inj. volume	25 µL (Full loop)
Column temp.	30 °C
Sampler temp.	4 °C
Detection	Electrochemical detection (ED) with PdH reference electrode and disposable silver working electrode
Samples	Four brands of multivitamin

	Iodine value (mg/kg)	
	Label	Measured
MV-1	95.2	108
MV-2	91.0	92.3
MV-3	N/A	14.0
MV-4	117.4	171

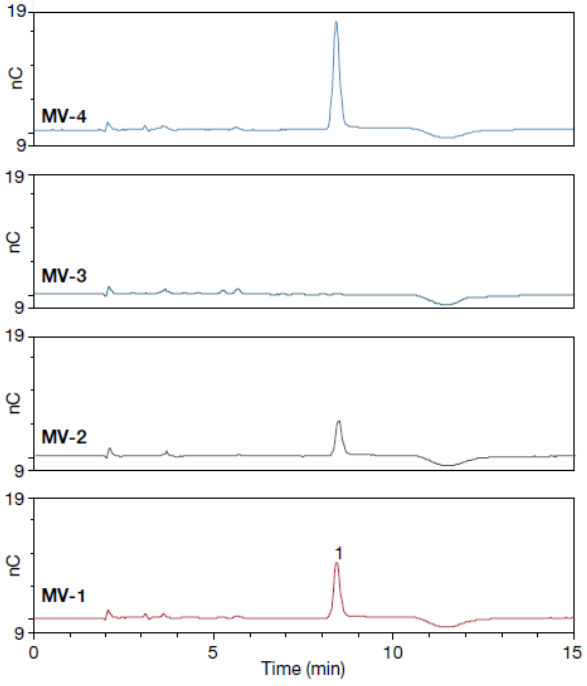

Figure 7. Chromatograms of multivitamin samples using a PdH reference electrode.

Conclusion

This application note demonstrates the development and validation of a 15 min IC-ED method for the determination of iodide in multivitamin products. The method uses a 2 mm Dionex IonPac AG20/AS20 column set with electrolytically generated potassium hydroxide (KOH) eluent and a disposable silver working electrode. Using this method, iodide is well separated and resolved from all common anions and organic acids found in the multivitamin samples. The method has a linear calibration, is sensitive, precise, and accurate. Four different multivitamin samples were tested, and the data show this IC-ED method can be used for the regulatory monitoring of iodine in multivitamins.

References

1. Iodine, Fact Sheet for Health Professionals, https://ods.od.nih.gov/factsheets/Iodine-HealthProfessional/ (Accessed April 8, 2021).
2. *Iodine, Fact Sheet for Consumers*, https://ods.od.nih.gov/factsheets/Iodine-Consumer/ (Accessed April 8, 2021).
3. Institute of Medicine, *Dietary Reference Intakes for Vitamin A, Vitamin K, Arsenic, Boron, Chromium, Copper, Iodine, Iron, Manganese, Molybdenum, Nickel, Silicon, Vanadium, and Zinc;* A Report of the Food and Nutrition Board, National Academic Press, Washington, DC, 2001.
4. Azizi, F.; Hedayati, M.; Rahmani, M.; Sheikloleslam, R.; Allahverdian, S.; Salarkia, N. Reappraisal of the Risk of Iodine-Induced Hyperthyroidism: An Epidemiological Population Survey. *J. Endocrinol. Invest*. **2005**, *28*, 23–29.
5. Trumbo, P.R. FDA regulations regarding iodine addition to foods and labeling of foods containing added iodine, *Am. J. Clin. Nutr*. **2016** Sep; *104*(Suppl 3), 864–867. https://www.ncbi.nlm.nih.gov/pmc/articles/PMC5004497/ (Accessed April 8, 2021).
6. *Dietary Supplement Laboratory Quality Assurance Program*, https://www.nist.gov/programs-projects/dietary-supplement-laboratory-quality-assurance-program (Accessed April 8, 2021).
7. Thermo Scientific Application Note 37: *Determination of Iodide and Iodate in Soy- and Milk-Based Infant Formulas*, Sunnyvale, CA, USA, 2016, https://appslab.thermofisher.com/App/1431/determination-iodide-infant-formula (Accessed April 8, 2021).
8. Liang, L.; Cai, Y.; Mou, S.; Cheng, J. Comparisons of Disposable and Conventional Silver Working Electrode for the Determination of Iodide Using High-Performance Anion-Exchange Chromatography with Pulsed Amperometric Detection. *J. Chromatogr. A* **2005**, *1085*, 37–41.
9. Chadha, R.K.; Lawrence, J.F. Determination of Iodide in Dairy Products and Table Salt by Ion Chromatography with Electrochemical Detection. *J. Chromatogr*. **1990**, *518*, 268–272.
10. Thermo Scientific Technical Note 73348: *Carbohydrate determinations by HPAE-PAD using a PdH reference electrode*, Sunnyvale, CA, USA, 2020, https://appslab.thermofisher.com/App/4378/a-pdh-reference-electrode-for-hpaepad (Accessed April 28, 2021).

Appendix

Dual channel IC system with RFIC-EG module, conductivity and electrochemical detections

Figure 8 shows the schematic of the setup used for this study. An autosampler with a diverter valve is used to serve both channels. The multivitamin samples are analyzed by CD and ED simultaneously. Besides the equipment and consumables for the ED channel, a diverter valve and suppressor are needed for the CD channel:

- Thermo Scientific™ Dionex™ AS-AP Autosampler with diverter valve (P/N 074123), 250 µL syringe, and tray temperature control
- Thermo Scientific™ Dionex™ ADRS 600 Anion Dynamically Regenerated Suppressor, 2 mm (P/N 088667)

Table 8. Chromatography conditions for the CD channel

Parameter	Value
Columns	Dionex IonPac AS20 analytical column, 2 × 250 mm Dionex IonPac AG20 guard column, 2 × 50 mm
Eluent	Isocratic, 30 mM potassium hydroxide (KOH)
Eluent source	Dionex EGC 500 KOH cartridge with CR-ATC 600 and Dionex high pressure degasser
Flow rate	0.35 mL/min

(continues on the next page)

Table 8. Chromatography conditions for the CD channel (continuation)

Parameter	Value
Injection volume	2.5 µL (full loop), 1/10 of ED channel
Column temperature	30 ˚C
Detection	Suppressed conductivity, Dionex ADRS 600 (2 mm) suppressor, recycle mode, 30 mA current
Detection temperature	25 °C
Sample tray temperature	4 ˚C
Run time	15 min

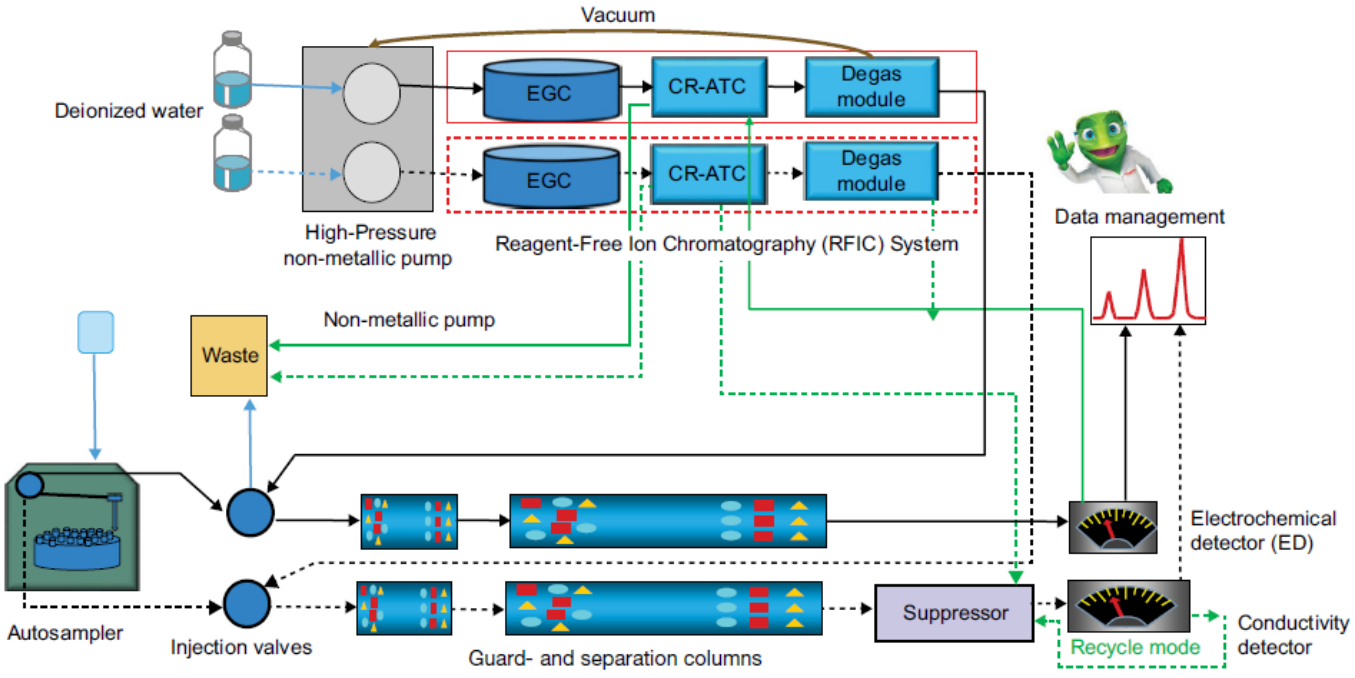

Figure 8. Illustration of the dual channel (ED+CD) RFIC system flow diagram.

Find out more at thermofisher.com

Brazilian Journal of Analytical Chemistry
2023, Volume 10, Issue 40, pp 230-237

BrJAC

SPONSOR REPORT

PDF

This section is dedicated for sponsor responsibility articles.

Simultaneous Digestion of Food Samples for Trace Element Analysis

Mixed-batch digestion of large sample amounts for high productivity and improved detection limits

This report was extracted from a Milestone Industry Report on ultraWAVE / FOOD

INTRODUCTION

Growing awareness and concern regarding food safety is reflected in the tightening of regulations governing toxic elements and compounds in food. Many toxic elements such as As, Hg, Cd, Pb etc. are routinely monitored, while minerals that are beneficial/essential to human health such as Se, Na, Mg, K, Ca, etc., are also measured. Traditional sample preparation techniques for food include hot block and closed-vessel microwave digestion.

Hot block digestions are time consuming, suffer from airborne contamination, poor digestion quality, and poor recovery of volatile compounds.

Closed-vessel microwave digestion has proven to be an effective technique with fast, complete digestions, a clean environment, and superior recovery of volatile compounds.

Milestone's innovative ultraWAVE with Single Reaction Chamber (SRC) technology further improves upon closed-vessel microwave digestion, by simplifying the sample preparation step, and providing fast, easy, effective, and the highest quality digestions of any food matrix with a single digestion method.

EXPERIMENTAL

In this industry report, a recovery study was performed on certified reference materials and pharmaceutical samples spiked with a multielement standard (impurities according to ICH Q3D) to demonstrate the efficacy of the ultraWAVE in the preparation of mixed samples from 0.5 g to 2 g in a single digestion program.

Instrumentation

The ultraWAVE is designed with a 1 Liter reactor, capable of operating at very high temperature and pressure (300 °C and 199 bar respectively). This capability ensures complete digestion of even the largest sample sizes (up to 3-5 g) as well as highly reactive and difficult-to-digest samples.

For the first time, a microwave digestion system ensures equal temperature and pressure conditions in all positions, even when different samples and/or chemistries are used. This results in superior digestion capabilities, higher productivity and better workflow for the lab.

The ultraWAVE's base load and positive pressure load prior to heating generates an equilibrium of temperature and pressure in each position, thus avoiding sample/elemental loss and cross contamination.

Samples can be weighed directly into disposable glass vials, eliminating the cleaning step. The easy handling of the vials and racks greatly reduces the operator time and associated labor costs.

Figure 1. Milestone's ultraWAVE.

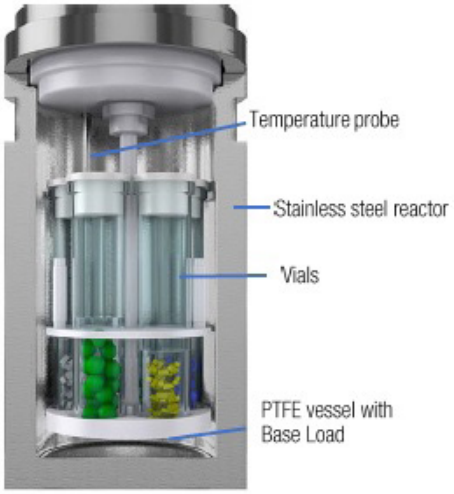

Figure 2. Schematic of the ultraWAVE's single reaction chamber (SRC).

Samples

Table 1. Acid used: 5 mL of HNO_3 67% and 0.5 mL of HCl 37%

Reference Material Code	Sample name
NIST 1567b	Wheat flour
NIST1568b	Rice Flour
NIST 1515	Apple Leaves
NIST 1573a	Tomato Leaves

Procedure and method

Sample weights up to 1.0 g for each of the flour CRMs (NIST 1567b, NIST 1568b) and up to 0.5 g for each of the other sample types (NIST 1515, NIST 1573a) were accurately weighed into PTFE vials (quartz and disposable glass vials are also available). Five mL of HNO_3 67% and 0.5 mL of HCl 37% (electronics (EL) grade acids, Kanto Chemicals) were added to the PTFE vials. A base load of 130 mL DI H_2O and 5 mL HNO_3 67% was added into the 1 Liter PTFE vessel. The analysis was performed with a Triple Quadrupole ICP-MS.

Table 2. UltraWAVE digestion heating programs for simultaneous digestion of four CRM food samples

Step	Time	Power (W)	Temp T1 (°C)	Temp T2 (°C)	Pressure (bar)
1	00:10:00	800	110	70	90
2	00:10:00	1200	180	70	90

(continues on the next page)

Table 2. UltraWAVE digestion heating programs for simultaneous digestion of four CRM food samples (continuation)

Step	Time	Power (W)	Temp T1 (°C)	Temp T2 (°C)	Pressure (bar)
3	00:10:00	1500	220	70	120
4	00:10:00	1500	220	70	120

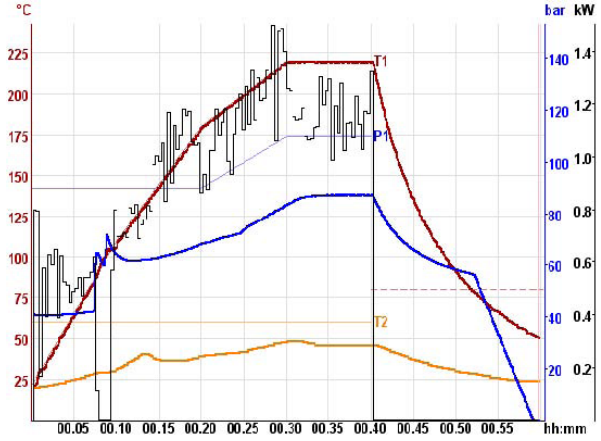

Figure 2. Internal temperature (red), external temperature (orange), pressure (blue) and power (black) graphs.

Table 3. Triple Quadrupole ICP-MS operating conditions

Parameter	Setting	
Cell mode	He mode	O_2 mode
Scan type	Single Quad	MS/MS
Plasma conditions	UHM-4	
RF power (W)	1600	
Sampling depth (mm)	10	
Carrier gas flow rate (L/min)	0.77	
Dilution gas flow rate (L/min)	0.15	
Extract 1 (V)	0	
Extract 2 (V)	-250	
Omega bias (V)	-140	
Omega lens (V)	8.8	
Cell gas flow (mL/min)	5.5	0.3 (20% of full scale)
KED (V)	5	-7

RESULTS AND DISCUSSION

The ultraWAVE system performed simultaneous digestion of four different reference materials with different sample amounts. The total time from weighing to analysis was less than one hour.

As shown in Figure 2, the system automatically adjusts the microwave power to follow the temperature profile.

Digestion of reactive samples such as oil, butter and other high fat content samples require precise, accurate and direct temperature control, which is especially important to control exothermic reactions and to ensure complete digestion.

The data shows excellent recoveries for all elements including volatiles, which is reflected in Tables 4 to 7 below.

Table 4. Results for NIST 1567b, Wheat flour, n=24

Element	Measured Solution Concentration (µg/L)	RSD (%)	Calculated Sample Concentration (mg/kg)	Certified Concentration (mg/kg)	Recovery (%)
23 Na	65.2	2.3	6.50±0.15	6.71±0.21	97
24 Mg	3842	1.6	383±6	398±12	96
27 Al	39	2.8	3.9±0.1	4.4±1.2	88
31->47 P	12936	2.0	1291±26	1333±36	97
32->48 S	15496	2.2	1546±34	1645±25	94
39 K	12700	2.3	1267±29	1325±20	96
44 Ca	1871	1.8	186.7±3.4	191.4±3.3	98
51 V	0.10	8.1	0.010±0.001	0.01*	100
55 Mn	86	1.7	8.54±0.14	9.00±0.78	95
56 Fe	142	1.6	14.20±0.22	14.11±0.33	101
63 Cu	19	1.6	1.94±0.03	2.03±0.14	96
66 Zn	112	1.9	11.17±0.21	11.61±0.26	96
75 As	0.047	16.5	0.0046±0.001	0.0048±0.0003	97
75->91 As	0.049	19.4	0.0049±0.001	0.0048±0.0003	101
78 Se	11.5	4.2	1.15±0.05	1.14±0.10	101
78->94 Se	11.8	1.9	1.17±0.02	1.14±0.10	103
85 Rb	6.54	1.8	0.652±0.012	0.671±0.012	97
95 Mo	4.60	2.1	0.459±0.009	0.464±0.034	99
111 Cd	0.239	5.7	0.0238±0.0014	0.0254±0.0009	94
118 Sn	0.0355	12.8	0.0035±0.0005	0.003*	118
202 Hg	0.0066	11.3	0.0007±0.0001	0.0005*	131
208 Pb	0.0937	4.4	0.0094±0.0004	0.0104±0.0024	90

*Reference value.

Table 5. Results for NIST 1568b Rice Flour, n = 24

Element	Measured Solution Concentration (µg/L)	RSD (%)	Calculated Sample Concentration(mg/kg)	Certified Concentration (mg/kg)	Recovery (%)
23 Na	65.6	3.2	6.54±0.28	6.74±0.19	97
24 Mg	5454	1.5	543±8	559±10	97
27 Al	40.3	3.3	4.01±0.13	4.21±0.34	95
31->47 P	15162	2.8	1510±43	1530±40	99
32->48 S	11369	2.5	1133±28	1200±10	94
39 K	12371	2.0	1233±24	1282±11	96
44 Ca	1158	2.1	115.3±2.5	118.4±3.1	97
51 V	182.3	1.0	18.2±0.2	19.2±1.8	95
55 Mn	75.4	1.0	7.51±0.08	7.42±0.44	101
56 Fe	0.173	1.7	0.0173±0.0003	0.0177±0.0005*	98
63 Cu	22.7	1.0	2.26±0.02	2.35±0.16	96
66 Zn	191.7	1.4	19.10±0.26	19.42±0.26	98
75 As	2.97	1.4	0.296±0.004	0.285±0.014	104
75->91 As	3.01	1.7	0.300±0.005	0.285±0.014	105
78 Se	3.4	8.9	0.341±0.030	0.365±0.029	93
78->94 Se	3.5	3.8	0.352±0.013	0.365±0.029	96
85 Rb	61.1	1.1	6.088±0.069	6.198±0.026	98
95 Mo	13.96	1.2	1.391±0.017	1.451±0.048	96
111 Cd	0.201	4.9	0.0201±0.0010	0.0224±0.0013	90
118 Sn	0.060	7.4	0.0060±0.0004	0.005±0.001*	121
202 Hg	0.0529	2.1	0.0053±0.0001	0.0059±0.0004	89
208 Pb	0.068	3.0	0.0068±0.0002	0.008±0.003*	85

*Reference value.

Table 6. Results for NIST 1515 Apple leaves, n=24

Element	Measured Solution Concentration (µg/L)	RSD (%)	Calculated Sample Concentration (mg/kg)	Certified Concentration (mg/kg)	Recovery (%)
11 B	141	2.9	28±0.8	27±2	104
23 Na	196	1.6	39.1±0.6	24.4±1.2	160*1
24 Mg	14083	1.3	2812±36	2710±80	104
27 Al	1458	1.6	291±5	286±9	102
31->47 P	8088	2.2	1615±35	1590*	102
32->48 S	9211	1.4	1839±26	1800*	102
39 K	80429	2.2	16057±361	16100±200	100
44 Ca	74060	1.2	14786±172	15260±1500	97
51 V	1.20	2.8	0.24±0.01	0.26±0.03	92
52 Cr	1.3	1.4	0.25±0.00	0.3*	85
55 Mn	265	1.0	53±1	54±3	98
56 Fe	379	0.8	76±1	80*	95
59 Co	0.44	1.5	0.088±0.001	0.09*	98
60 Ni	4.4	1.7	0.88±0.02	0.91±0.12	97
63 Cu	28.2	1.0	5.62±0.06	5.64±0.24	100
66 Zn	60.3	0.9	12.0±0.1	12.5±0.3	96
75->91 As	0.2	3.7	0.036±0.001	0.038±0.007	94
78-> 94 Se	0.271	13.8	0.054±0.008	0.050±0.009	108
85 Rb	46.3	0.9	9.2±0.1	9*	103
88 Sr	123.0	1.0	25±0	25±2	98
95 Mo	0.44	5.3	0.088±0.005	0.094±0.013	94
111 Cd	0.06	7.0	0.013±0.001	0.014*	91
121 Sb	0.06	4.6	0.011±0.001	0.013*	85
138 Ba	245	1.9	49±1	49±2	100
202 Hg	0.21	2.0	0.041±0.001	0.044±0.004	93
208 Pb	2.3	1.3	0.452±0.006	0.470±0.024	96
232 Th	0.14	2.2	0.028±0.001	0.03*	93
238 U	0.034	3.7	0.0068±0.0003	0.006*	113

*Reference value.

*[1]The measured Na result was high compared to the reference value; the same result was obtained from a repeated analysis of the same solution, so a spike recovery test was performed for confirmation. The spike recovery result was good (recovery: 99%), suggesting that the original sample had suffered Na contamination.

Table 7. Results for NIST 1573a Tomato Leaves, n = 24

Element	Measured Solution Concentration (µg/L)	RSD (%)	Calculated Sample Concentration (mg/kg)	Certified Concentration (mg/kg)	Recovery (%)
11 B	167	1.9	33.3±0.6	33.3±0.7	100
23 Na	613	2.5	122±3	136±4	90
24 Mg	57311	2.0	11412±225	12000*	95
27 Al	2573	2.4	512±12	598±12	86
31->47 P	10928	2.7	2176±59	2160±40	101
32-< 48 S	48387	1.4	9635±131	9600*	100
39 K	134250	2.2	26732±591	27000±500	99
44 Ca	243939	1.4	48574±671	50500±900	96
51 V	4.0	2.2	0.792±0.017	0.835±0.010	95
52 Cr	9.3	1.6	1.85±0.03	1.99±0.06	93
55 Mn	1236.5	1.5	246±4	246±8	100
56 Fe	1843.3	1.7	367±6	368±7	100
59 Co	2.8	1.4	0.55±0.01	0.57±0.02	96
60 Ni	7.9	1.9	1.56±0.03	1.59±0.07	98
63 Cu	23.7	1.5	4.71±0.07	4.70±0.14	100
66 Zn	149.4	1.5	29.8±0.5	30.9±0.7	96
75 As	0.7	2.3	0.141±0.003	0.112±0.004	126
75->91 As	0.6	1.7	0.112±0.002	0.112±0.004	100
78-> 94 Se	0.31	11.2	0.061±0.007	0.054±0.003	113
85 Rb	69.7	1.2	13.88±0.16	14.89±0.27	93
88 Sr	421.0	1.3	84±1	85*	99
95 Mo	2.1	2.8	0.42±0.01	0.46*	91
107 Ag	0.09	9.1	0.018±0.002	0.017*	104
111 Cd	7.4	1.4	1.47±0.02	1.52±0.04	97
121 Sb	0.28	3.4	0.055±0.002	0.063±0.006	88
138 Ba	302.8	2.1	60.3±1.3	63*	96
202Hg	0.15	2.4	0.030±0.001	0.034±0.004	88
232 Th	0.52	2.1	0.104±0.002	0.12*	87
238 U	0.14	2.3	0.029±0.001	0.035*	81

*Reference value.

CONCLUSION

The data illustrated in this industry report demonstrates the ultraWAVE's ability to provide full recovery of all elements, while avoiding cross contamination even when different samples and sample weights are digested in the same run. The ultraWAVE's ability to simultaneously digest different sample types, easy sample handling and superior throughput surpass the capabilities of hot blocks and traditional rotor-based microwave digestion systems. Its superior capabilities in terms of processing mixed samples, large sample amounts and ease of use provide unmatched productivity. The superior digestion quality achieved at high temperature and pressure maximizes the performance of the ICP-MS by reducing interferences, blanks and overall maintenance.

About Milestone

At Milestone we help chemists by providing the most innovative technology for metals analysis, direct mercury analysis and the application of microwave technology to extraction, ashing and synthesis. Since 1988 Milestone has helped chemists in their work to enhance food, pharmaceutical and consumer product safety, and to improve our world by controlling pollutants in the environment.

This Sponsor Report is the responsibility of Milestone.

26 – 28 September, 2023

São Paulo Expo, São Paulo , SP, Brazil

ANALITICA LATIN AMERICA IS CONSIDERED A GLOBAL MEETING POINT FOR THE ANALYTICAL CHEMICAL INDUSTRY AND THE MAIN LINK BETWEEN INDUSTRY AND ACADEMIA.

The event brings together suppliers, distributors, manufacturers and researchers in search of the latest innovations and trends in the sectors of laboratory technology, biotechnology, pharmaceuticals, cosmetics, food, agribusiness, among others. One of the great highlights of Analitica Latin America is the qualified and diversified content presented through the Analitica Congress.

WHY VISIT?

► + 400 brands present

► Only opportunity of the year to update yourself and network with the biggest companies in the sector

► Several attractions for your professional upgrade

I WANT TO VISIT

Testimonials from those who attended the last edition:

"I thought it was very important to participate in the fair to personally meet resellers, suppliers and get to know the manufacturers directly. Well organized fair and very attentive exhibitors."

★★★★★

Paula Fernanda Reolon

Purchasing Analyst at CBO Laboratory

THE 2022 EDITION BROKE ALL RECORDS

+6,500	+10 h	+14,000 m²	+400
Visitors	of Content	from Business Area	Exhibiting Brands present in the Last Edition

RELEASE

Redefining ICP-MS Triple Quadrupole Technology with Unique Ease of Use

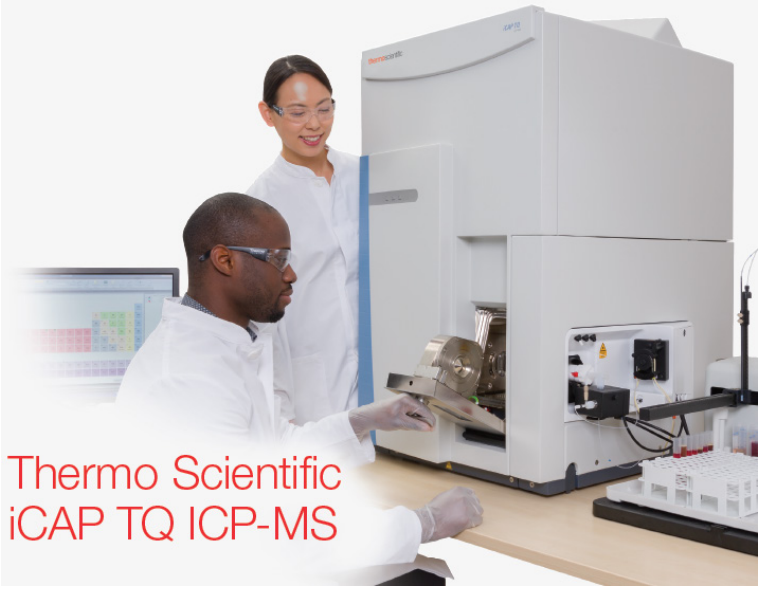

Empowering you with technology to achieve more today and be ready to master future challenges tomorrow, the Thermo Scientific iCAP™ TQ ICP-MS helps futureproof your laboratory against evolving legislation requirements, enables you to explore developing markets, and pushes the boundaries of your research.

Harness the power of Triple Quadrupole (TQ) ICP-MS with incredible accuracy and detection limits for the most challenging applications. Improved interference removal allows laboratories to tackle complex samples with ease and deliver data with the confidence of 'right first time' results.

Ease of use is the core concept behind the Thermo Scientific™ iCAP™ TQ ICP-MS, which has been designed for laboratories working in both routine and research applications. The system is based on a platform with an intuitive hardware design that simplifies the user experience. The operator-focused software streamlines workflows and integrates control of peripherals to automate sample handling.

Key features of the iCAP TQ ICP-MS

Unique ease-of-use

Combining user-inspired hardware with intelligent software, the iCAP TQ ICP-MS and the iCAP TQs ICP-MS both enable laboratories to effortlessly develop and maintain methods that ensure confidence in data quality. Reaction Finder, which is the systems' unique method development assistant, enables you to tackle challenging matrices without wasting time on complex method development.

Right-first-time results

Employ the power of triple quadrupole technology for uncomplicated analyses with superior accuracy during both research and routine applications. Thanks to the advanced interference removal capabilities of the iCAP TQ ICP-MS, analysis of samples with complex matrices can be performed with superior limits of detection for more accurate data.

Boundless capabilities

Fully integrated plugins for Thermo Scientific Qtegra Intelligent Scientific Data Solution (ISDS) Software enable the easy implementation of advanced applications, including automated sample handling, autodilution, speciation, nanoparticle analysis and laser ablation.

Find out more at https://www.thermofisher.com

thermo scientific

Thermo Scientific iCAP TQ ICP-MS

Delivering research level trace elemental analysis, combined with routine ease-of-use, the Thermo Scientific™ iCAP™ TQ ICP-MS is a high-performance, future-proof ICP-MS solution. Harness the power of Triple Quadropole (TQ) technology, in combination with a wide variety of reactive gases and experience, for uncomplicated analysis with incredible accuracy. Expand your applications and enhance your laboratory efficiency with breakthrough triple quadrupole technology that is so easy to use, any analyst can operate it.

Performance | Versatility | Operational Simplicity

VIDEO WEBSITE

ThermoFisher SCIENTIFIC

RELEASE

Dionex™ ICS-6000 Standard Bore and Microbore HPIC™ Systems

Get significant increases in resolution and throughput using the world's first modular ion chromatography (IC) system capable of operation up to 5000 psi

When solving ion analysis challenges, there are sometimes more questions than answers. The ability to develop and run different methods for a single sample or for different samples is increasingly important for analytical laboratories. A highly flexible ion chromatography (IC) system provides you with the freedom to develop, explore, and run different methods simultaneously.

The Thermo Scientific™ Dionex™ ICS-6000 HPIC™ system is a truly modular, highly configurable, high-performance system. The robust system design enables operation at up to 5000 psi and produces consistent, reliable results. As a top-of-the line ion chromatography system, it is designed for users who want to push the boundaries of what is possible in ion analysis.

Outstanding sensitivity plus convenience

- Excellent sensitivity, stability, and ease of use
- Enhanced baseline stability and sensitivity with top-of-the-line flow rate accuracy, eluent generator electronics stability, and conductivity cell temperature control

Optimized peak resolution with a choice of isocratic and electrolytic gradient separations

- Flexible support for microbore (1–3mm i.d.) and standard bore (3–7mm i.d.) columns
- Wide variety of Thermo Scientific standard and microbore columns
- Compatible with New 4µm Columns

Separations twice as fast without compromising resolution

- Significantly increased resolution from current methodologies at increased flow rates
- Higher resolution and dramatically better performance using smaller particle size (4µm) columns
- Faster run times with higher flow rates using 150mm columns, or higher resolution with standard flow rates using 250mm columns

Outstanding flexibility to configure the system you need

- Broad variety of modules and related products
- Flexible choice of detectors

Find out more at https://www.thermofisher.com

Thermo Scientific Dionex **ICS-6000** HPIC system

The freedom to explore!

When solving ion analysis challenges, there are sometimes more questions than answers. The ability to develop and run different methods for a single sample or for different samples is increasingly important for analytical laboratories. A highly flexible ion chromatography (IC) system provides you with the freedom to develop, explore, and run different methods simultaneously.

WEBSITE **VIDEO**

Find out more at **thermofisher.com/ICS6000**

ThermoFisher
SCIENTIFIC

RELEASE

ultraWAVE 3

Taking Productivity and Performance to New Heights

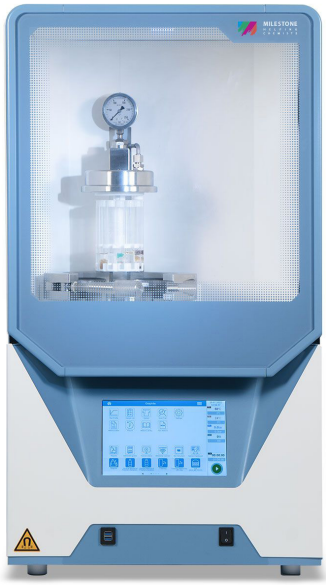

The new ultraWAVE 3 is the latest generation of SRC technology that further elevates the value of this technology for elemental analysis in terms of performance, time, workflow, and cost of ownership.

Single Reaction Chamber Technology

Updated construction that includes several technology advances further enhances the well-proven benefits of the SRC technology.

The new features of ultraWAVE 3 merge with those already intrinsic in the technology, so that labs will experience higher performance, greater productivity, and more streamlined workflow, providing them with improved competitiveness and a lower cost of ownership.

Thanks to its **superior digestion capabilities** that result from its **higher temperature and pressure features**, ultraWAVE's unique SRC technology provides greater digestion efficiency.

Several aspects of the system, such as **reduced handling and cleaning** and the ability **to process any samples simultaneously, reduce turnaround time** and increase lab efficiency.

BENEFITS

Rugged construction

Designed with all wetted components made of PTFE-TFM, fully compatible with any acid mixture and ensuring minimal maintenance to lower the cost of ownership.

High-pressure lines

Made of acid-resistant stainless steel, the two pressure lines, one for inlet and one for outlet, ensure high safety and lower blanks.

Racks

Available with racks of 7, 20, 27 and 40 vials to provide even higher throughput than previous generations.

easyTEMP Temperature control

True contactless temperature sensor to directly control the digestion of the samples from the inside out, without reading delays.

Advanced heating technology

The noiseless water-cooled magnetron ensures higher heating efficiency along with superior working conditions.

User interface

Equipped with the most up-to-date features to bring all digestion information within easy reach of the operator.

Find out more at milestonesrl.com

MILESTONE
HELPING CHEMISTS

ultraWAVE 3

Single Reaction Chamber Technology

Updated construction that includes several technology advances further enhances the well-proven benefits of the SRC technology.
The new features of **ultraWAVE 3** merge with those already intrinsic in the technology, so that labs will experience higher performance, greater productivity, and more streamlined workflow, providing them with improved competitiveness and a lower cost of ownership.
Thanks to its superior digestion capabilities that result from its higher temperature and pressure features, ultraWAVE's unique SRC technology provides greater digestion efficiency.
Several aspects of the system, such as reduced handling and cleaning and the ability to process any samples simultaneously, reduce turnaround time and increase lab efficiency.

VIDEO WEBSITE

www.milestonesrl.com/products/microwave-digestion/ultrawave-3

RELEASE

Pittcon Conference & Expo

Pittcon is a catalyst for the exchange of information, a showcase for the latest advances in laboratory science, and a venue for international connectivity.

Pittcon is a dynamic, transnational conference and exposition on laboratory science, a venue for presenting the latest advances in analytical research and scientific instrumentation, and a platform for continuing education and science-enhancing opportunity. Pittcon is for anyone who develops, buys, or sells laboratory equipment, performs physical or chemical analyses, develops analysis methods, or manages these scientists.

Pittcon Awards

Honoring scientists who have made outstanding contributions to Analytical Chemistry

Each year, Pittcon provides a venue where scientists who have made outstanding contributions to laboratory science, analytical chemistry, and applied spectroscopy are honored.

Among these awards is the **Pittcon Heritage Award** which honors those visionaries whose entrepreneurial careers shaped the instrumentation and laboratory supplies community and by doing so have transformed the scientific community at large.

The award has been presented jointly with Pittcon since 2002 and is given out each year at a special ceremony during the Pittcon Conference and Expo. The recipient's name and achievements are added to the Pittcon Hall of Fame, which conference attendees can visit at the show each year.

Pittcon 2024 – Conference on Analytical Chemistry and Applied Spectroscopy
February 24-28, 2024
San Diego, California, USA

Pittcon®
Conference and Exposition

Perfect weather, the wind in your hair, the tranquil tones of some far-off soft rock, and a gold rush of cool, quality science.

LEARN MORE

You asked... we listened.

Pittcon – the event made for scientific breakthroughs – will be collaborating on the US West Coast for the first time in our nearly 75-year history.

ATTEND

Create connections on the California coast.

Enter to win free dinner with the Pittcon Marketing Team if you attend Pittcon in 2024.

EXHIBIT

Take part in a Gold Rush of quality leads.

Enter to win a free floor plan logo advertisement for your company's registered 2024 booth.

Pittcon®
Conference and Exposition

RELEASE

SelectScience® Pioneers online Communication and Promotes Scientific Success

SelectScience® promotes scientists and their work, accelerating the communication of successful science. Through trusted lab product reviews, virtual events, thought-leading webinars, features on hot scientific topics, eBooks and more, independent online publisher SelectScience® provides scientists across the world with vital information about the best products and techniques to use in their work.

Some recent contributions from SelecScience® to the scientific community

Editorial Article by Mary Kay Bates, Senior Global Applications Scientist at Thermo Fisher Scientific:
Protecting against human error: Why documentation and data are important

Good documentation of lab processes and equipment is essential for safe and efficient projects. Good manufacturing practices (GMP) are a requirement of many laboratories, but there is no one way to do it. Bates explains why GMP needs to be planned and tailored for every process, “People new to this topic always want to say, ‘Just tell me how to do it. Just tell me how to comply and I'll do whatever.’ But there's no one prescriptive way to do that, and that's even more true in cell and gene therapy because every new process to produce a therapy is different”. Access **here**

The Scientists’ Channel
ASMS President, Prof. Susan Richardson, shares insights into the power of mass spectrometry for drinking water analysis

In this video, Prof. Susan Richardson, President of ASMS, and Professor in the Dept. of Chem&Biochem at the University of South Carolina, discusses the impact of pollen on disinfectant by-product formation in drinking water. Her team has found that presence of pollen can exacerbate the levels of disinfectant by-product in water and has developed a sensitive GC-MS analytical method that has allowed the quantification of about 70 target disinfection by-products at the low ppt level. Richardson also describes further technology that powers her research, how she’s identified previously unknown disinfection by-products that are formed through pollen precursors, and hints at what she’s excited for in the future of mass spectrometry. Access **here**

Women in Science Video
Needle in a haystack? Working with 3D data

In this presentation, Dr. Diane Turner FRSC, Senior Consultant & Director, Anthias Consulting Ltd., discusses how to make the most of your three-dimensional data in the field of analytical chemistry. This talk was presented at the SelectScience® Virtual Analytical Summit 2022. Access **here**

SelectScience® is the leading independent online publisher connecting scientists to the best laboratory products and applications.

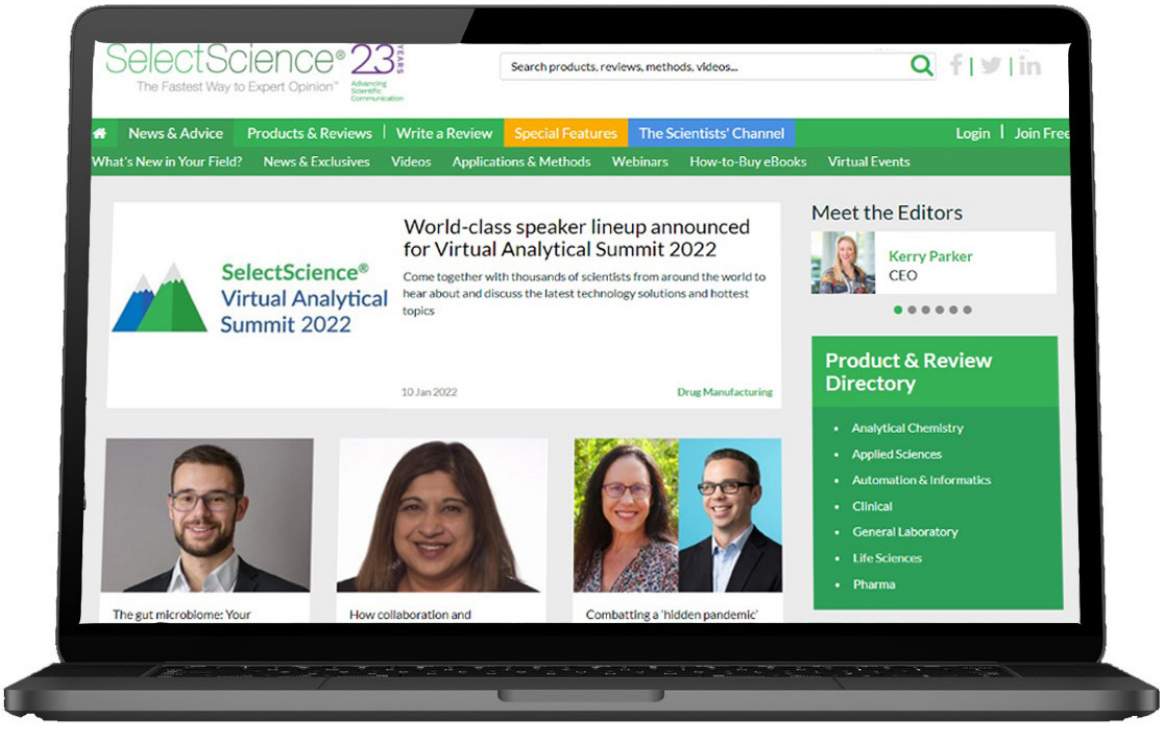

- Working with Scientists to Make the Future Healthier.
- Informing scientists about the best products and applications.
- Connecting manufacturers with their customers to develop, promote and sell technologies.

SelectScience®
The Fastest Way to Expert Opinion

RELEASE

CHROMacademy is the leading provider of eLearning for analytical science

CHROMacademy *helps scientific organizations acquire and maintain excellence in their laboratories*.

For over 10 years, CHROMacademy has increased knowledge, efficiency and productivity across all applications of chromatography. With a comprehensive library of learning resources, members can improve their skills and knowledge at a pace that suits them.

CHROMacademy covers all chromatographic applications – HPLC, GC, mass spec, sample preparation, basic lab skills, and bio chromatography. Each paradigm contains dozens of modules across theory, application, method development, troubleshooting, and more. Invest in analytical eLearning and supercharge your lab.

For more information, please visit www.chromacademy.com/

LC GC's CHROMacademy
powered by crawford scientific

CHROMacademy Lite members have access to less than 5% of our content. Premier members get so much more !

Video Training courses

Fundamental HPLC
Fundamental GC
Fundamental LCMS
Fundamental GCMS
HPLC Method Development
GC Method Development

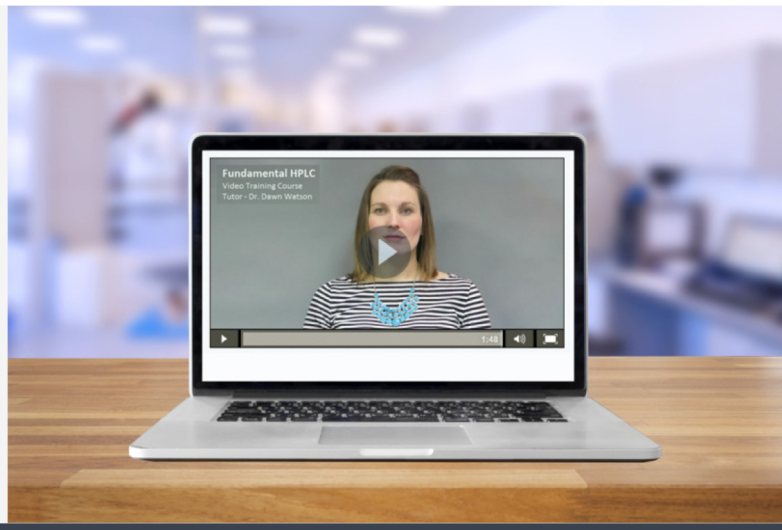

Ask the Expert

We are always on hand to help fix your instrument and chromatographic problems, offer advice on method development, help select a column for your application and more.

To find out more about Premier Membership contact:

Glen Murry: +1 732.346.3056 | Glen.Murry@ubm.com
Peter Romillo: +1 732.346.3074 | Peter.Romillo@ubm.com

www.chromacademy.com

The worlds largest e-Learning website for analytical scientists

NOTICES OF BOOKS

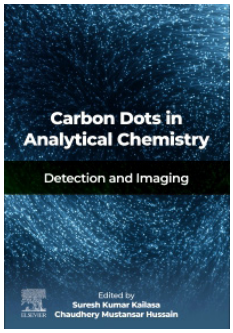

Carbon Dots in Analytical Chemistry: Detection and Imaging

Suresh Kumar Kailasa and Chaudhery Mustansar Hussain, Editors

August 30, 2022. Publisher: Elsevier

This book explores recent progress in the field of carbon dots synthesis and properties and their integration with various miniaturized analytical devices for the detection of chemical species and imaging of cells. It is dedicated to exploring the potential applications of carbon dots in analytical chemistry for clinical microbiology, pharmaceutical analysis and environmental analysis. Read more

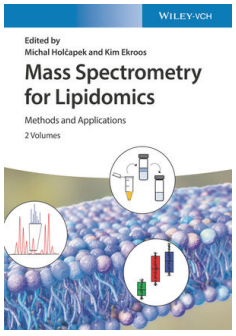

Mass Spectrometry for Lipidomics / Methods and Applications, Vols 1 and 2

Michal Holcapek and Kim Ekroos, Editors

February 2023. Publisher: Wiley-VCH

All-in-one guide to successful lipidomic analysis, combining the latest advances and best practices from academia, industry, and clinical research. This book presents a systematic overview of lipidomic analysis, covering established standards of lipid analysis, available technology, and key lipid classes, as well as applications in basic research, medicine, pharma, and the food industry. Read more

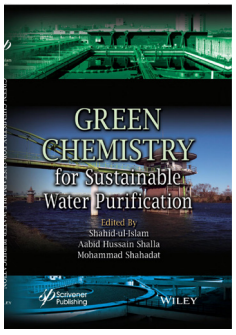

Green Chemistry for Sustainable Water Purification

Shahid-ul-Islam, Abid Hussain Shalla, Mohammad Shahadat, Editors

January 2023. Publisher: Wiley-VCH

This book provides systematic coverage of the most recent research and development in clean water treatment technologies based on green materials and nanocomposites. It discusses the different treatment technologies with a special focus on the green adsorption approach, using biological and hybrid biochemical treatment technologies to prevent water contamination and maintain the ecosystem. Read more

"Gestão da Qualidade em Laboratórios" / 5th Edition, Revised and Expanded

Igor Renato Bertoni Olivares, Author

May 2023. Publisher: Átomo

In the practical routine of laboratories, public or private — independent or located in large companies — we find different types of Quality Systems (ISO9001; ISO/IEC17025; BPL). The implementation of these systems requires specific professional qualification. In this scenario, this book presents in a simple and objective way, a comprehensive universe of application of Quality Systems, aiming to support those who work directly or indirectly in the area. Read more

PERIODICALS & WEBSITES

American Laboratory

American Laboratory® is a platform that addresses basic research, clinical diagnostics, drug discovery, environmental, food and beverage, forensics and other markets, and combines in-depth articles, news, and video to deliver the latest advances in their fields. **Featured Article:** ***Reducing Toxic Chemical Vapors in the Lab and the Basics of Proper Chemical Waste Storage.*** Implementing new chemical safety habits will result in important safety practices becoming part of the success of the scientists in the laboratory, their health and the progress of science. **Read more**

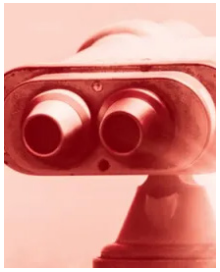

LCGC

Chromatographyonline delivers practical, nuts-and-bolts information to help scientists and lab managers become more proficient in the use of chromatographic techniques and instrumentation. **Point of View:** ***Are we Greenwashing Analytical Chemistry?*** Are analytical chemists really operating sustainable laboratories, or are they being too quick in marketing their “green” laboratory credentials? **Read more**

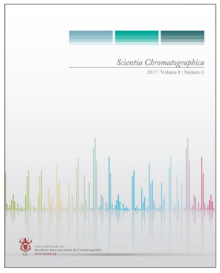

Scientia Chromatographica

Scientia Chromatographica is the first and to date the only Latin American scientific journal dedicated exclusively to Chromatographic and Related Techniques. With a highly qualified and internationally recognized Editorial Board, it covers all chromatography topics in all their formats, in addition to discussing related topics such as “The Pillars of Chromatography”, Quality Management, Troubleshooting, Hyphenation (GC-MS, LC-MS, SPE-LC-MS/MS) and others. It also provides columns containing general information, such as: calendar, meeting report, bookstore, etc. **Read more**

Select Science

SelectScience® has transformed global scientific communications and digital marketing over the last 23 years. Informing scientists about the best products and applications. Connecting manufacturers with their customers to develop, promote and sell technologies promotes scientists and their work, accelerating the communication of successful science. Scientists can make better decisions using independent, expert information and gain easy access to manufacturers. SelectScience® informs the global community through Editorial, Features, Video and Webinar programs. **Read more**

Spectroscopy

With the *Spectroscopy* journal, scientists, technicians, and lab managers gain proficiency through unbiased, peer-reviewed technical articles, trusted troubleshooting advice, and best-practice application solutions.
Feature article: ***Artificial Intelligence in Analytical Spectroscopy: Examples in Spectroscopy.*** A sample library of selected references discussing the application of artificial intelligence (AI) in analytical chemistry and molecular spectroscopy is presented. **Read more**

EVENTS in 2023

August 27 – 31
EuroAnalysis 2023
Geneva, Switzerland
https://www.euroanalysis2023.ch/

September 18 – 21
Latin American Symposium on Environmental Analytical Chemistry (XV LASEAC) & "Encontro Nacional de Química Ambiental" (X ENQAmb)
Ouro Preto, MG, Brazil
www.xvlaseac-xenqamb2023.com

September 26 – 28
Analitica Latin America Expo & Conference
São Paulo, SP, Brazil
https://www.analiticanet.com.br/

October 2 – 5
XXIV Simpósio Brasileiro de Eletroquímica e Eletroanalítica (SIBEE)
Universidade do Vale do Rio dos Sinos (UNISINOS), Porto Alegre, RS, Brazil
http://sociedade-sbee.org/eventos

October 8 – 13
SciX Conference
Nugget Casino Resort, Sparks, NV, USA
https://scixconference.org/

December 4 – 7
6th International Caparica Christmas Conference on Sample Preparation
Caparica, Portugal
https://www.sampletreatment2023.com/

AUTHOR GUIDELINES

Aims & Scope

Brazilian Journal of Analytical Chemistry is a double-blind peer-reviewed research journal dedicated to the diffusion of significant and original knowledge in all branches of Analytical and Bioanalytical Chemistry. It is addressed to professionals involved in science, technology, and innovation projects at universities, research centers and in industry. **BrJAC welcomes** the submission of research papers reporting studies devoted to new and significant analytical methodologies, putting in evidence the scientific novelty, the impact of the research and demonstrating the analytical or bioanalytical applicability. BrJAC **strongly discourages** those simple applications of routine analytical methodologies, or the extension of these methods to new sample matrices, unless the proposal contains substantial novelty and unpublished data, clearly demonstrating advantages over existing ones.

Additionally, there are other submission categories to BrJAC such as:

Reviews: They should be sufficiently broad in scope, but specific enough to permit an appropriate depth discussion, including critical analyses of the bibliographic references and conclusions. Manuscripts submitted for publication as Reviews must be original and unpublished. Reviews undergo double-blind full peer review and are handled by the Editor of Reviews.

Technical Notes: Concise descriptions of developments in analytical methods, new techniques, procedures, or equipment falling within the scope of the BrJAC. Technical notes also undergo double-blind full peer review.

Letters: Discussions, comments, and suggestions on issues related to Analytical Chemistry or Bioanalytical Chemistry. Letters are welcome and will be published at the discretion of the BrJAC Editor-in-Chief.

Point of View: This category is exclusively invited by the Editor-in-Chief.

See the next items for more information on the journal, the documents preparation, manuscript types, and how to prepare the submission.

Professional Ethics

Originality: manuscripts submitted for publication in BrJAC cannot have been previously published or be currently submitted for publication in another journal.

Preprint: BrJAC does not accept manuscripts that have been posted on preprint servers prior to the submission.

Integrity: the submitted manuscripts are the full responsibility of the authors. Manipulation/invention/omission of data, duplication of publications, the publication of papers under contract and confidentiality agreements, company data, material obtained from non-ethical experiments, publications without consent, the omission of authors, plagiarism, the publication of confidential data and undeclared conflicts of interests are considered serious ethical faults.
BrJAC discourages and restricts the practice of excessive self-citation by the authors.
BrJAC does not practice coercive citation, that is, it does not require authors to include references from BrJAC as a condition for achieving acceptance, purely to increase the number of citations to articles from BrJAC without any scientific justification.

Conflicts of interest: when submitting their manuscript for publication, the authors must include all potential sources of bias such as affiliations, funding sources and financial, management or personal relationships which may affect the work.

Copyright: will become the property of the Brazilian Journal of Analytical Chemistry, if and when a manuscript is accepted for publication. The copyright comprises exclusive rights of reproduction and distribution of the articles, including reprints, photographic reproductions, microfilms or any other reproductions similar in nature, including translations.

Request for permission to reuse figures and tables published in the BrJAC: researchers who want to reuse any document or part of a document published in the BrJAC should request reuse permission from the BrJAC Editor-in-Chief, even if they are the authors of such document. A template for requesting reuse permission can be downloaded **here**.

Misconduct will be treated according to the COPE's recommendations (https://publicationethics.org/) and the Council of Science Editors White Paper on Promoting Integrity in Scientific Journal Publications (https://www.councilscienceeditors.org/).

Manuscript submission

The BrJAC does not charge authors an article processing fee.

Manuscripts must be prepared according to the BrJAC manuscript template. Manuscripts in disagreement with the BrJAC guidelines are not accepted for revision.

The BrJAC uses an online manuscript manager system for the submission of manuscripts. This system guides authors stepwise through the entire submission process.

After the submitting author logs in to the system and enters his/her personal and affiliation details, the submission can be started.

All co-authors must be added to the Authors section.

Four documents are mandatorily uploaded by the submitting author: Cover letter, Title Page, Novelty Statement and the Manuscript. Templates for these documents are available for download **here**.

The four documents mentioned above must be uploaded as Word files. The manuscript Word file will be converted by the system to a PDF file which will be used in the double-blind peer review process.

All correspondence, including notification of the Editor’s decision and requests for revision, is sent by e-mail to the submitting author through the manuscript manager system.

Documents Preparation

It is highly recommended that authors download and use the templates to create their four mandatory documents to avoid the suspension of a submission that does not meet the BrJAC guidelines.

Cover Letter
The cover letter template should be downloaded and filled out carefully.
Any financial conflict of interest or lack thereof and agreement with BrJAC's copyright policy must be declared.
It is the duty of the submitting author to inform his/her collaborators about the submission of the manuscript and its eventual publication.
The Cover Letter must be signed by the corresponding author.

Title Page
The Title Page must contain information for each author: full name, affiliation and full international postal address, and information on the contribution of each author to the work. Acknowledgments must be entered on the Title Page. The submitting author must sign the Title Page.

Novelty Statement
The Novelty Statement must contain clear and succinct information about what is new and innovative in the study in relation to previously related works, including the works of the authors themselves.

Manuscript (all submission categories)

It is highly recommended that authors download the Manuscript template and create their manuscript in this template, keeping the layout of this file.

- **Language**: **English** is the language adopted by BrJAC. The correct use of English is of utmost importance. In case the Editors and Reviewers consider the manuscript to require an English revision, the authors will be required to send an English proofreading certificate before the final approval of the manuscript by BrJAC.
- **Required items**: the manuscript must include a title, abstract, keywords, and the following sections: Introduction, Materials and Methods, Results and Discussion, Conclusion, and References.
- **Identification of authors**: as the BrJAC adopts a double-blind review, the manuscript file must **NOT** contain the authors' names, affiliations nor acknowledgments. Full details of the authors and their acknowledgements should be on the Title Page.
- **Layout**: the lines in the manuscript must be numbered consecutively and double-spaced.
- **Graphics and Tables**: must appear close to the discussion about them in the manuscript. For **figures** use **Arabic** numbers, and for **tables** use **Roman** numbers.
- **Figure files:** when a manuscript is approved for publication, the BrJAC production team will contact the corresponding author to request separate files of each figure and a graphical abstract. These files must have **good resolution** and the extension **PNG or JPG**. The graphical abstract should preferably be created in landscape format. In the article diagrammed in the journal, the graphical abstract will occupy a space of 8 to 9 cm in length and 6 cm in height. Chemical structures must have always the same dimensions.
- **Permission to use content already published**: to use figures, graphs, diagrams, tables, etc. identical to others previously published in the literature, even if these materials have been published by the same submitting authors, a publication permission from the publisher or scientific society holding the copyrights must be requested by the submitting authors and included among the documents uploaded in the manuscript management system at the time of manuscript submission.
- **Chemical nomenclature, units and symbols**: should conform to the rules of the International Union of Pure and Applied Chemistry (IUPAC) and Chemical Abstracts Service. It is recommended that, whenever possible, the authors follow the International System of Units, the International Vocabulary of Metrology (VIM) and the NIST General Table of Units of Measurement. Abbreviations are not recommended except for those recognized by the International Bureau of Weights and Measures or those recorded and established in scientific publications. Use L for liters. Always use superscripts rather than /. For instance: use mg mL^{-1} and NOT mg/mL. Leave a space between numeric values and their units.
- **References throughout the manuscript:** the references must be cited as superscript numbers. It is recommended that references older than 5 (five) years be avoided, except in relevant cases. Include references that are accessible to readers.
- **References item:** This item must be thoroughly checked for errors by the authors before submission. From 2022, BrJAC is adopting the American Chemical Society's Style in the Reference item. Mendeley Reference Manager users will find the Journal of American Chemical Society citation style in the Mendeley View menu. Non-users of the Mendeley Reference Manager may refer to the ACS Reference Style Quick Guide DOI: https://doi.org/10.1021/acsguide.40303

Review process

Manuscripts submitted to the BrJAC undergo an initial check for compliance with all of the journal's guidelines. Submissions that do not meet the journal's guidelines will be suspended and an alert sent to the corresponding author. The authors will be able to resend the submission within 30 days. If the submission

according to the journal's guidelines is not made within 30 days, the submission will be withdrawn on the first subsequent day and an alert will be sent to the corresponding author.

Manuscripts that are in accordance with the journal's guidelines are submitted for the analysis of similarities by the iThenticate software.

The manuscript is then forwarded to the Editor-in-Chief who will check whether the manuscript is in accordance with the journal's scope and will analyze the similarity report issued by iThenticate.

If the manuscript passes the screening described above, it will be forwarded to an Associate Editor who will also analyze the iThenticate similarity report and invite reviewers.

Manuscripts are reviewed in double-blind mode by at least 2 reviewers. A larger number of reviewers may be used at the discretion of the Editor. As evaluation criteria, the reviewers employ originality, scientific quality, contribution to knowledge in the field of Analytical Chemistry, the theoretical foundation and bibliography, the presentation of relevant and consistent results, compliance with the BrJAC's guidelines, clarity of writing and presentation, and the use of grammatically correct English.

Note: In case the Editors and Reviewers consider the manuscript to require an English revision, the authors will be required to send an English proofreading certificate, by the ProofReading Service or equivalent service, before the final approval of the manuscript by the BrJAC.

The 1st-round review process usually takes around 5-6 weeks. If the manuscript is not rejected but requires corrections, the authors will have one month to submit a corrected version of the manuscript. In another 3-4 weeks, a new decision on the manuscript may be presented to the corresponding author.

The manuscripts accepted for publication are forwarded to the BrJAC production department. Minor changes to the manuscripts may be made, when necessary, to adapt them to BrJAC guidelines or to make them clearer in style, respecting the original content. The articles are sent to the authors for approval before publication. Once published online, a DOI number is assigned to the article.

Final Considerations

Whatever the nature of the submitted manuscript, it must be original in terms of methodology, information, interpretation or criticism.

With regard to the contents of published articles and advertisements, the sole responsibility belongs to the respective authors and advertisers; the BrJAC, its editors, editorial board, editorial office and collaborators are fully exempt from any responsibility for the data, opinions or unfounded statements.

Submit manuscripts at www.brjac.com.br